

# ORGANOMETALLICS

Volume 2, Number 2, February 1983

© Copyright 1983  
American Chemical Society

## He I and He II Photoelectron Studies of Bis(cyclopentadienyl)vanadium(III) Complexes

Jennifer C. Green\* and Martin P. Payne

*Inorganic Chemistry Laboratory, Oxford OX1 3QR, England*

Jan H. Teuben

*Department of Inorganic Chemistry, University of Groningen, Nijenborgh 16,  
9747 AG Groningen, The Netherlands*

Received June 10, 1982

He I and He II photoelectron spectra have been obtained for a series of bis( $\eta^5$ -cyclopentadienyl)vanadium(III) halides, alkyls, and aryls,  $V(\eta^5\text{-C}_5\text{H}_5)_2\text{X}$ , where X = Cl, Br, I, Me,  $\text{CH}_2\text{SiMe}_3$ ,  $\text{CH}_2\text{CMe}_3$ ,  $\text{C}_6\text{F}_5$ ,  $\text{C}_6\text{H}_5$ , *o*- $\text{C}_6\text{H}_4\text{Me}$ , *m*- $\text{C}_6\text{H}_4\text{Me}$ , and 2,6- $\text{C}_6\text{H}_3\text{Me}_2$ . Assignments are made principally on the basis of variations of band intensity with photon energy, ionization energy trends, and a generalized molecular orbital scheme. Evidence is presented for weak but significant  $\pi$  interactions between metal d and halogen p orbitals in the halide complexes and a  $\pi$ -donor effect in the alkyls.

### Introduction

The electronic structure of bent metallocene complexes had been extensively investigated in the last 10 years by a wide variety of techniques, including electron paramagnetic resonance (EPR) and photoelectron (PE) spectroscopy and X-ray crystallography, as well as by Fenske-Hall, SCF, and extended Hückel calculations.

The earliest bonding model for bent metallocenes was Ballhausen and Dahl's hybridization scheme<sup>1</sup> which employed equal contributions of the five ( $n-1$ )d, three  $np$ , and one  $ns$  orbitals to the metal-ligand bonding system and predicted for  $d^2$  systems, e.g.,  $\text{Mo}(\eta^5\text{-C}_5\text{H}_5)_2\text{H}_2$ , a lone-pair orbital directed between the two  $\sigma$ -bonded ligands. Crystallographic work, originally by Alcock,<sup>2</sup> but considerably extended by the systematic studies of Green, Prout et al.,<sup>3-5</sup> and Dahl<sup>6</sup> revealed that the L-M-L bond angle in  $d^2$   $M(\eta^5\text{-C}_5\text{H}_5)_2\text{X}_2$  complexes was too small to accommodate a lone pair between the X ligands, and furthermore the bond angle decreased with increasing number of d electrons,  $d^0$ - $d^2$ . Thus the crystallographic data supported a model in which the "lone-pair" orbital was

primarily directed normal to the plane bisecting the  $\text{ML}_2$  fragment.

EPR spectroscopy has enabled the electron distribution in the highest occupied molecular orbital (HOMO) of bent  $d^1$  metallocene complexes to be determined. Thus the single-crystal EPR studies of Peterson and Dahl<sup>7</sup> on the complexes  $V(\eta^5\text{-C}_5\text{H}_5)_2\text{S}_5$  and  $V(\eta^5\text{-C}_5\text{H}_4\text{Me})_2\text{Cl}_2$  revealed an  $A_1$  electronic ground state, with the unpaired electron residing in an orbital of ca. 80% d character, which is principally directed along the molecular  $z$  axis (using the coordinate system of Figure 1a) but has a small contribution along the  $x$  and  $y$  axes. If small ligand orbital contributions are neglected

$$\psi_{\text{HOMO}} = a|d_{z^2}\rangle + b|d_{x^2-y^2}\rangle$$

and  $a^2/b^2$  is 20 for  $V(\eta^5\text{-C}_5\text{H}_4\text{Me})_2\text{Cl}_2$  and 12.7 for  $V(\eta^5\text{-C}_5\text{H}_5)_2\text{S}_5$ . Comparison of calculated and observed spin polarization values ( $\chi$ ) showed that the HOMO had a negligibly small 4s contribution, illustrating a further difference between the observed and predicted electron distributions based on the Alcock or Ballhausen-Dahl models. These EPR results were conclusively supported by the nonparameterized Fenske-Hall molecular orbital (MO) calculations of the same authors,<sup>8</sup> who also showed previous EPR studies of related  $d^1$  complexes to have a

(1) Ballhausen, C. J.; Dahl, J. P. *Acta Chem. Scand.* 1961, 15, 1333.

(2) Alcock, N. W. *J. Chem. Soc. A* 1967, 2001.

(3) Green, J. C.; Green, M. L. H.; Prout, C. K. *J. Chem. Soc. Chem. Commun.* 1972, 421.

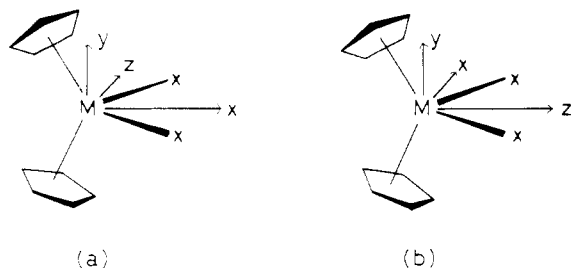
(4) Green, M. L. H. *Pure Appl. Chem.* 1972, 30, 373.

(5) Prout, C. K.; Cameron, T. S.; Critcheley, S. R.; Denton, B.; Rees, G. V. *Acta Crystallogr. Sect. B* 1974, B30, 2290.

(6) Dahl, L. F. 4th International Conference on Organometallic Chemistry, Bristol 1969.

(7) Petersen, J. L.; Dahl, L. F. *J. Am. Chem. Soc.* 1974, 96 2248; 1975, 97, 6416, 6422.

(8) Petersen, J. L.; Lichtenberger, D. L.; Fenske, R. F.; Dahl, L. F. *J. Am. Chem. Soc.* 1975, 97, 6433.



**Figure 1.** Structure and coordinate schemes for bent bis(cyclopentadienyl)metal complexes.

parallel interpretation. The frozen solution EPR work of Evans et al.<sup>9</sup> on the  $d^1$  complexes  $V(\eta\text{-C}_5\text{H}_5)_2\text{Et}_2$  and  $V(\eta\text{-C}_5\text{H}_5)_2(\text{CH}_2\text{SiMe}_3)_2$  gave very similar results, with  $a^2/b^2 = 17.4$  and  $14.1$ , respectively. More recent frozen solution EPR studies of  $\text{Ta}(\eta\text{-C}_5\text{H}_5)_2\text{Cl}_2$ <sup>10</sup> and  $\text{Ta}(\eta\text{-C}_5\text{H}_5)_2(\sigma\text{-C}_5\text{H}_5)_2$ <sup>11</sup> have yielded the very surprising result that the HOMO in these complexes has a metal contribution almost entirely described by  $d_{x^2-y^2}$  with  $a = 0.001$  and  $b = 0.999$ .

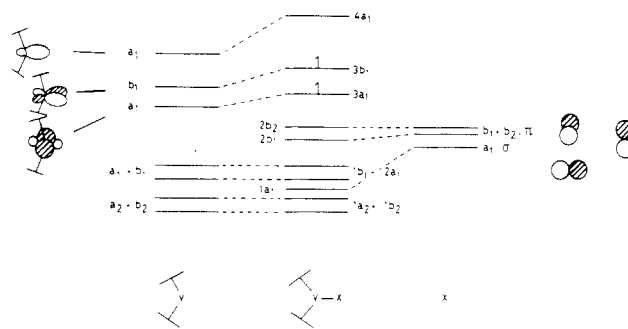
A qualitative molecular orbital bonding scheme for bent metallocenes was put forward by Green et al.,<sup>3,12</sup> this was obtained by bending the "straight"  $D_{5d}$  metallocene system to  $C_{2v}$  symmetry, the  $e_{2g}$ ,  $a_{1g}$ , and  $e_{1g}$  orbitals transforming as  $a_1 + b_1$ ,  $a_1$ , and  $a_2 + b_2$  orbitals respectively, using the coordinate scheme of Figure 1b. This approach was put on a more quantitative basis by the extended Hückel calculations of Hoffmann and Lauher<sup>13</sup> who examined the variation of metal orbital energies as a function of bending angle for the hypothetical  $[\text{Ti}(\eta\text{-C}_5\text{H}_5)_2]^+$  species. These authors calculated electron density distributions for all the predominantly metal orbitals.

$M(\eta\text{-C}_5\text{H}_5)_2X_n$  complexes have been extensively studied by PE spectroscopy.<sup>8,12,14-17</sup> In an account of bis(cyclopentadienyl)metal dihalides a classification of bonding type was proposed on the basis of the relative energies and extent of mixing of the halogen  $p\pi$  and cyclopentadienyl  $e_1$  orbitals, He I and He II intensities providing a criterion for determining orbital character. The relative energies of the halogen and cyclopentadienyl orbitals were found to be dependent on the metal as well as on the halogen (assuming differential relaxation effects to be minimal).

Bis(cyclopentadienyl)vanadium(III) halides, alkyls, and aryls were first synthesized by Fischer et al.<sup>18</sup> and de Liefde Meijer et al.<sup>19,20</sup> EPR,<sup>21,22</sup> magnetic measurements,<sup>23</sup> and more recently NMR studies<sup>24,25</sup> have demonstrated these

**Table I.** Measurement Conditions for Obtaining Photoelectron Spectra

compd	helium I		helium II	
	temp, °C	count rate, c/s	temp, °C	count rate, c/s
$V(\eta\text{-C}_5\text{H}_5)_2\text{Cl}$	118	1000	122	100
$V(\eta\text{-C}_5\text{H}_5)_2\text{Br}$	128	1000	132	100
$V(\eta\text{-C}_5\text{H}_5)_2\text{I}$	125	1000	129	100
$V(\eta\text{-C}_5\text{H}_5)_2(\text{C}_6\text{H}_5)$	95	1000	96	100
$V(\eta\text{-C}_5\text{H}_5)_2(2\text{-C}_2\text{H}_4\text{Me})$	84	1000	103	100
$V(\eta\text{-C}_5\text{H}_5)_2(3\text{-C}_6\text{H}_4\text{Me})$	90	1000	95	100
$V(\eta\text{-C}_5\text{H}_5)_2(2,6\text{-C}_6\text{H}_3\text{Me}_2)$	129	1000	119	80
$V(\eta\text{-C}_5\text{H}_5)_2(\text{C}_6\text{F}_5)$	123	1000	119	100
$V(\eta\text{-C}_5\text{H}_5)_2\text{Me}$	40	1400	51	100
$V(\eta\text{-C}_5\text{H}_5)_2\text{CH}_2\text{SiMe}_3$	59	800	62	200
$V(\eta\text{-C}_5\text{H}_5)_2\text{CH}_2\text{CMe}_3$	63	1000		



**Figure 2.** Qualitative energy level scheme for bis(cyclopentadienyl)vanadium halides.

complexes to have spin triplet ground states, and hence their  $d$  orbital configuration is  $1a_1^1 1b_1^1$ . We report below PE studies on a series of these molecules.

### Experimental Section

The compounds were prepared by literature methods.<sup>19,20,23</sup>

He I and He II spectra were obtained by using a Perkin-Elmer PS 16/18 spectrometer fitted with an Helectros lamp capable of supplying both He I and He II radiation. Measurement conditions are given in Table I and vertical ionization energies and some band intensity data in Table II.

The spectra were calibrated by admission of  $\text{N}_2$  and  $\text{Xe}$  and by reference to the He self-ionization band. This has an apparent IE (ionization energy) in the He I spectra of 4.99 eV (see Figure 3).

### Discussion

**Bis(cyclopentadienyl)vanadium(III) Halides.** A qualitative molecular orbital diagram for these halides may be constructed, by considering orbital interactions between a bent  $V(\eta\text{-C}_5\text{H}_5)_2^+$  unit and a halide ion,  $X^-$  (Figure 2). This MO diagram is similar to but more detailed than that proposed by Stucky and Fieselstein,<sup>24</sup> whose X-ray crystal study confirmed an approximate  $C_{2v}$  symmetry, the halogen atom residing symmetrically in the open face created by tilting the cyclopentadienyl rings, which themselves are in a staggered conformation. Figure 2 ignores the effects of spin-orbit coupling and excludes any cyclopentadienyl-halogen mixing.

The He I and He II PE spectra of the chloride, bromide, and iodide are illustrated in Figure 3 and vertical ionization energies (IE) band intensities and proposed assignments in Table II.1-3. For  $V(\eta\text{-C}_5\text{H}_5)_2\text{I}$  the intensity data are difficult to obtain accurately due to overlap of the second and third spectral bands. The spectra may be divided into

(25) Köhler, F. H.; Hoffmann, P.; Prössdorf, W. *J. Am. Chem. Soc.* 1981, 103, 6359.

(9) Evans, J. C.; Evans, A. G.; Espley, D. J. C.; Morgan, P. H.; Mortimer, J. *J. Chem. Soc., Dalton Trans.* 1978, 57.

(10) Al-Mowali, A. H.; Kuder, W. A. *J. Mol. Struct.* 1979, 57, 141.

(11) Al-Mowali, A. H. *J. Chem. Soc. Dalton Trans.* 1980, 426.

(12) Green, J. C.; Higginson, B.; Jackson, S. E. *J. Chem. Soc. Dalton Trans.* 1975, 403.

(13) Hoffman, R.; Lauher, J. W. *J. Am. Chem. Soc.* 1976, 98, 1729.

(14) Fragala, I.; Ciliberto, E.; Thomas, J. L. *J. Organomet. Chem.* 1979, 175 C25.

(15) Condorelli, G.; Fragala, I.; Centineo, A. *J. Organomet. Chem.* 1975, 87, 311.

(16) Clark, J. P.; Green, J. C. *J. Less-Common Met.* 1977, 31.

(17) Green, J. C.; Cauletti, C.; Clark, J. P.; Jackson, S. E.; Fragala, I. T.; Ciliberto E.; Coleman, A. W. *J. Electron Spectrosc. Relat. Phenom.* 1980, 18, 61.

(18) Fischer, E. O.; Vigoureaux, S.; Kuzel, P. *Chem. Ber.* 1960, 93, 701.

(19) de Liefde Meijer, H. J.; Janssen, M. J.; van der Kerk, G. J. M. *Recl. Trav. Chim. Pays-Bas* 1961, 80, 831.

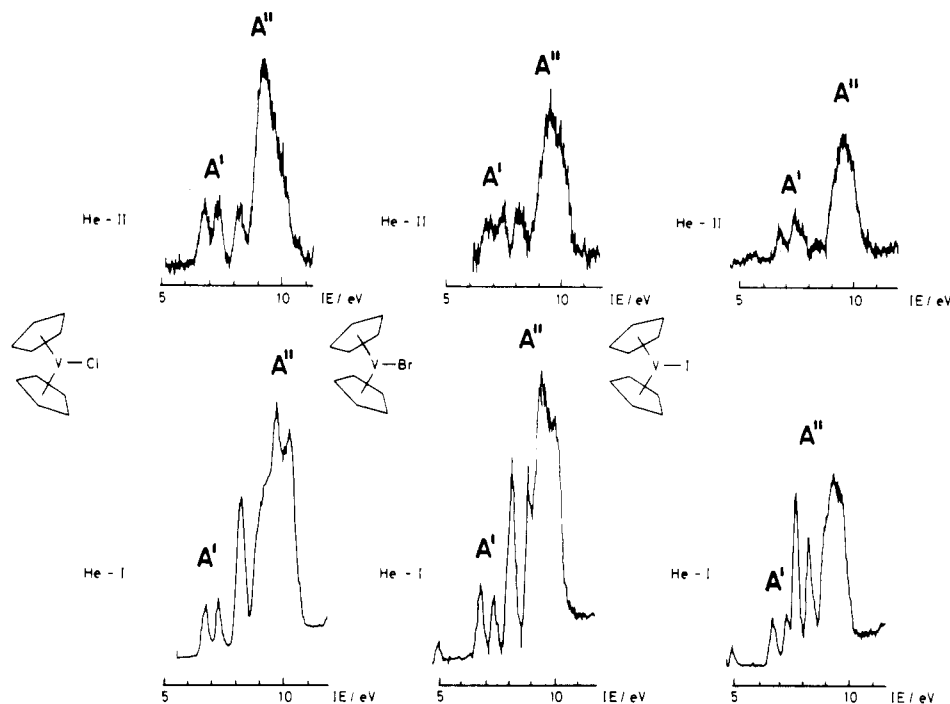
(20) de Liefde Meijer, H. J.; Janssen, M. J.; van der Kerk, G. J. M. *Chem. Ind. (London)* 1960, 119.

(21) Chien, J. C. W.; Boss, C. R. *J. Am. Chem. Soc.* 1961, 83, 3767.

(22) Dessy, R. E.; King, R. R.; Waldrop, M. J. *J. Am. Chem. Soc.* 1966, 88, 5112.

(23) Bouwman, H.; Teuben, J. H. *J. Organomet. Chem.* 1976, 110, 327.

(24) Fieselmann, B. F.; Stucky, G. D. *J. Organomet. Chem.* 1977, 137, 43.



**Figure 3.** He I and He II photoelectron spectra of  $V(\eta\text{-C}_5\text{H}_5)_2\text{Cl}$ ,  $V(\eta\text{-C}_5\text{H}_5)_2\text{Br}$ , and  $V(\eta\text{-C}_5\text{H}_5)_2\text{I}$ . Ionization bands at 4.99 eV are due to  $\text{He}(1s)^{-1}$  excited by He II radiation.

the following regions: A', 6–7.5 eV; A'', 7.5–11 eV;  $\beta$ , 11–16 eV; C, 16–20 eV, and D, >20 eV.

Above 11 eV the spectra are similar for all the halides, with a large amorphous band centered at  $\sim 13$  eV and a less intense one at  $\sim 17.5$  eV, resembling those of other metallocene systems,<sup>26,27</sup> and may be assigned to ionizations of the lowest  $\pi$  level and the  $\sigma$ -orbitals of the cyclopentadienyl rings.

A common feature of all PE spectra of the  $V(\eta\text{-C}_5\text{H}_5)_2\text{X}$  compounds is the presence of two relatively small narrow bands in region A' which become relatively more intense relative to the central band B on changing from He I to He II radiation. These bands are thereby assigned to ionizations of principally metal localized d orbitals. The first band however shows a smaller intensity increase than the second. In addition it is broader than the second and is more intense in the He I spectrum. These features are consistent with the first and second bands involving ionization from the metal-halogen antibonding  $3b_1$  orbital and the essentially nonbonding metal  $3a_1$  orbital respectively in agreement with the predictions of the MO diagram (Figure 2). The  $3b_1$  orbital ionization band gains intensity in the He I spectrum from its halogen content and gives rise to a broader band than the  $3a_1$  orbital as a result of its antibonding nature. As further support for  $b_1$  metal halogen  $\pi$  interactions we note that the separation of the first two bands is greater in the halides than in the aryls where the evidence suggests metal  $\pi$  interaction with the ring to be small.

On the basis of the characteristic decrease of halogen orbital ionization cross sections with increasing photon energy compared with C–C and C–H ionization bands, the subsequent bands at 8.29 eV for  $V(\eta\text{-C}_5\text{H}_5)_2\text{Cl}$ , 8.14 eV for  $V(\eta\text{-C}_5\text{H}_5)_2\text{Br}$ , and 7.69 and 8.30 eV for  $V(\eta\text{-C}_5\text{H}_5)_2\text{I}$  may be assigned to the halogen  $p\pi$  ( $2b_1 + 2b_2$ ) orbital ionizations. For the iodide two bands are observed due to the much larger spin-orbit coupling constant of iodine (0.63

eV) compared with bromine (0.305 eV) or chloride (0.073 eV). The splitting of the bands is very close to the atomic spin-orbit coupling constant of iodine, and the higher IE band is noticeably broader than the first as demonstrated by the half-width values quoted in Table II. This is consistent with a relatively weak interaction between the  $3b_1$  metal orbital and the  $2b_1$  halogen p orbital, as occurs for example in alkyl halides. Brogli and Heilbronner<sup>28</sup> showed that strong mesomeric interactions with bromine or iodine p orbitals, as occurs for example in aryl or vinyl halides, are required to increase the splitting of the p orbital energies much above the free atom values ( $\delta$ ). In further support of only a weak  $p\pi$  interaction, the  $\sim 0.3$ -eV increase in the energy of the  $3b_1$  orbital, calculated by comparison of the d orbital splittings of the halides and aryls, is small compared with the  $>1.0$ -eV lowering of the  $3b_1$  orbital energy found in bis(cyclopentadienyl)metal alkenes or carbonyl compounds<sup>12</sup> such as  $\text{Mo}(\eta\text{-C}_5\text{H}_5)_2\text{CO}$  or  $\text{W}(\eta\text{-C}_5\text{H}_5)_2(\eta\text{-C}_2\text{H}_4)$ , due to interaction with the high energy acceptor  $b_1\pi^*$  ligand orbitals. The very small He II/He I intensity ratios of the halogen p bands also indicate a small degree of metal-halogen  $\pi$  orbital mixing. Broadening of the bromine and chlorine  $p\pi$  bands relative to the two iodine  $p\pi$  bands, as demonstrated by their larger half-widths, is a result of the combined effect of spin-orbit coupling and mesomeric interactions with the metal.

Identification of the halogen  $p\sigma$  ( $1a_1$ ) ionization is more difficult. The broad band in the region 8.5–10.5 eV for all three halides, by analogy with the PE spectra of other bis(cyclopentadienyl) complexes,<sup>27</sup> must represent ionization of the cyclopentadienyl orbitals  $1a_2 + 1b_2 + 2a_1 + 1b_1$  in addition to the V–X  $1a_1$   $\sigma$  orbital ionization. The halogen character of this latter orbital should affect its band intensity sufficiently for it to be detected by changes in band profile with photon energy. For the chloride a significant change in band profile is observed. The low IE shoulder in the He I spectrum becomes the maximum of the band in the He II spectrum and is thereby assigned to cyclopentadienyl  $\pi$  ionizations. The peak at 10.35 eV

(26) Evans, S.; Green, M. L. H.; Jewitt, B.; Orchard, A. F.; Pygall, C. *F. J. Chem. Soc., Faraday Trans. 2* **1972**, *68*, 1847.

(27) Green, J. C. *Struct. Bonding (Berlin)* **1981**, *43*, 37.

(28) Heilbronner, E.; Brogli, F. *Helv. Chim. Acta* **1971**, *54*, 1423.

Table II. Vertical Ionization Energies, Relative Band Intensities, and Assignments for Bis( $\eta^5$ -cyclopentadienyl)vanadium(III) Halides, Alkyls, and Aryls

band	IE, eV	$w_{1/2}$	intensities		intensity ratio He I/He II	assignt
			He I	He II		
1. ( $\eta^5$ -Cp) <sub>2</sub> VCl						
A'	6.80	0.36	1.07	1.03	0.96	3b <sub>1</sub>
	7.42	0.28	0.93	0.97	1.04	3a <sub>1</sub>
A''	8.29	0.42	4.1	0.95	0.23	Cl p $\pi$
	9.47	}	22.4		0.41	Cp $\pi$ + Cl p $\sigma$
	9.81					
	10.35					
	10.35					
B	12.8	}	64	32.6	0.51	Cp $\sigma$ + Cp $\pi$
	13.2					
C	17.5					Cp $\sigma$
D	20.7					
	22.1					
2. ( $\eta^5$ -Cp) <sub>2</sub> VBr						
A'	6.81	0.33	1.08	0.89	0.82	3b <sub>1</sub>
	7.43	0.25	0.92	1.11	1.21	3a <sub>1</sub>
A''	8.14	0.37	3.9	1.3	0.34	Br p $\pi$
	8.90	}	16.3	9.9	0.61	Cp $\pi$ + Br p $\sigma$
	9.37					
	10.07					
	10.07					
B	12.9	}	47.6	28.5	0.55	Cp $\sigma$ + Cp $\pi$
	13.5					
C	17.6					Cp $\sigma$
3. ( $\eta^5$ -Cp) <sub>2</sub> VI						
A'	6.71	0.31	1.07	0.90	0.84	3b <sub>1</sub>
	7.33	0.21	0.93	1.10	1.17	3a <sub>1</sub>
A''	7.69	0.22	3.6	0.61	0.17	I p $\pi$ "2b <sub>2</sub> "
	8.30	0.28	3.1	0.37	0.12	I p $\pi$ "2b <sub>1</sub> "
	9.02	}	13.1	6.3	0.48	Cp $\pi$ + I p $\sigma$
	9.34					
	12.85					
	13.3					
B	13.3	}	49.8	36.4	0.73	Cp $\sigma$ + Cp $\pi$
	17.4					
C	17.4					Cp $\sigma$
D	21.1					
	23.3					
band	IE, eV	intensities		intensity ratio He II/He I	assignt	
		He I	He II			
4. ( $\eta^5$ -Cp) <sub>2</sub> VPh						
A'	6.52	0.86		~1	2b <sub>1</sub>	
	6.83	1.14		~1	4a <sub>1</sub>	
A'' <sub>1</sub>	7.67	3.19	2.49	0.78	V-C $\sigma$	
A'' <sub>2</sub>	8.53	}	16.9	13.9	0.82	Ar $\pi$
A'' <sub>3</sub>	9.13					
A'' <sub>4</sub>	11.02					
	11.02					
B	12.6	}	64.8	38.9	0.60	Ar $\sigma$ + Cp $\sigma$ + Cp $\pi$
	13.5					
C	17.55					Ar $\sigma$ + Cp $\sigma$
D	21.7					
5. ( $\eta^5$ -Cp) <sub>2</sub> V(2-MeC <sub>6</sub> H <sub>4</sub> )						
A'	6.51	0.84		~1	2b <sub>1</sub>	
	6.86	1.16		~1	4a <sub>1</sub>	
A <sub>1</sub> ''	7.55	3.25	2.45	0.75	V-C $\sigma$	
A <sub>2</sub> ''	8.23	6.0	4.1	0.68	Ar $\pi$	
A <sub>3</sub> ''	8.99	12.9	10.3	0.80	Cp $\pi$	
A <sub>4</sub> ''	10.83	8.4	5.3	0.63	Ar $\pi$ + Ar $\sigma$	
B	12.6	}	79	45		Ar $\sigma$ + Cp $\sigma$ + Cp $\pi$ + Me $\sigma$
	13.0					
C	15.4					Ar $\sigma$ + Cp $\sigma$ + Me $\sigma$
D	17.2					
	21.5					
6. ( $\eta^5$ -Cp) <sub>2</sub> V(3-MeC <sub>6</sub> H <sub>4</sub> )						
A'	6.52	0.69	0.71	1.03	2b <sub>1</sub>	
	6.83	1.31	1.29	0.98	4a <sub>1</sub>	
A <sub>1</sub> ''	7.56	2.7	2.0	0.74	V-C $\sigma$	
A <sub>2</sub> ''	8.18	5.5	3.1	0.57	Ar $\pi$	
A <sub>3</sub> ''	8.99	12.6	9.2	0.73	Cp $\pi$	
A <sub>4</sub> ''	10.83	8.0	4.4	0.55	Ar $\pi$ + Ar $\sigma$	
B	12.6	}	124	47	0.38	Ar $\sigma$ + Cp $\sigma$ + Cp $\pi$ + Me $\sigma$
B	13.1					
C	15.6					
	17.2					
D	21.4					Ar $\sigma$ + Cp $\sigma$ + Me $\sigma$
	22.1					

Table II (Continued)

band	IE, eV	intensities		intensity ratio He II/He I	assignt
		He I	He II		
7. $(\eta^5\text{-Cp})_2\text{V}(2,6\text{-Me}_2\text{C}_6\text{H}_3)$					
A'	6.51	0.84	0.83	0.99	2b <sub>1</sub>
	6.84	1.16	1.17	1.01	4a <sub>1</sub>
A <sub>1</sub> ''	7.55	3.32	3.15	0.95	V-C $\sigma$
A <sub>2</sub> ''	8.02	6.83	4.4	0.65	Ar $\pi$
A <sub>3</sub> ''	8.98	13.45	10.2	0.76	Cp $\pi$
A <sub>4</sub> ''	10.62	10.0	5.0	0.50	Ar $\pi$ + Cp $\pi$
B	12.6	151	53	0.35	Ar $\sigma$ + Cp $\sigma$ + Cp $\pi$ + Me $\sigma$
	13.25				
	14.9				
C	17.15				
D	20.6				
	21.9				
8. $(\eta^5\text{-Cp})_2\text{VC}_6\text{F}_5$					
A'	7.15	0.82	0.84	1.02	2b <sub>1</sub>
	7.43	1.18	1.16	0.98	4a <sub>1</sub>
A <sub>1</sub> ''	8.35	3.02			V-C $\sigma$
A <sub>2</sub> ''	9.39	18.5			Ar $\pi$ + Cp $\pi$
A <sub>3</sub> ''	9.93				
A <sub>4</sub> ''	11.65				
B	13.02	95.1			Ar $\sigma$ + Cp $\sigma$ + Cp $\pi$
	13.9				
	5.1				
C	16.35				
	17.3				
D	20.8				
9. $(\eta^5\text{-Cp})_2\text{VMe}$					
A'	6.42	0.99	0.89	0.89	
	6.85	1.01	1.11	1.10	
A''	8.14	14.4	9.9	0.69	V-C $\sigma$
	8.61				
	8.98				
B	11.68	5	2.3	0.46	Me $\sigma$
	12.4	77	34	0.44	Cp $\sigma$ + Cp $\pi$ + Me $\sigma$
	13.2				
C	17.1				
D	21.3				
	21.8				
	22.4				
10. $(\eta^5\text{-Cp})_2\text{VCH}_2\text{SiMe}_3$					
A'	6.32	0.91	0.85	0.93	
	6.82	1.09	1.15	1.06	
A''	7.90	2.27	0.81	0.36	V-C $\sigma$
	8.55	20.1	10.6	0.53	Cp $\pi$
	9.19				
	10.3				
B	13.3	98	34	0.35	Si-C $\sigma$
C	17.0				Cp $\sigma$ + Cp $\pi$ + CH <sub>2</sub> SiMe <sub>3</sub> $\sigma$
D	21.9				
	23.9				
11. $(\eta^5\text{-Cp})_2\text{VCH}_2\text{CMe}_3$					
A'	6.38	0.44	0.49	1.10	b <sub>1</sub>
A''	6.78	1.56	1.51	0.97	a <sub>1</sub>
	7.86	1.32	0.70		V-C $\sigma$
	8.38	8.09	6.3	0.78	Cp $\pi$
	8.84				
B	10.77				
	12.4	51.1	40.3	0.78	Cp $\sigma$ + Cp $\pi$ + alkyl $\sigma$
C	16.65				Cp $\sigma$ + alkyl $\sigma$

shows a large decrease in intensity in the He II spectrum, indicating predominantly halogen character; it is assigned to the 1a<sub>1</sub> V-Cl  $\sigma$  ionization. That the peak at 9.81 eV also suffers intensity loss at higher photon energies indicates that there is some mixing of cyclopentadienyl and halogen  $\pi$  orbitals, similar to that observed for Ta( $\eta^5\text{-C}_5\text{H}_5$ )<sub>2</sub>Cl<sub>2</sub>.<sup>17</sup>

For V( $\eta^5\text{-C}_5\text{H}_5$ )<sub>2</sub>Br and V( $\eta^5\text{-C}_5\text{H}_5$ )<sub>2</sub>I the 8.5–10.5-eV bands show a very similar profile in the He I and He II spectra, with the exception of the 8.9-eV peak in the spectrum of the bromide which shows a slight drop in intensity relative

to the rest of the band in the He II spectrum, suggesting its assignment to a V-Br  $\sigma$  orbital ionization. However, since it has been observed that metal-halogen  $\sigma$  ionization energies show a continuous decrease Cl > Br > I in most transition-metal complexes<sup>29</sup> and there is no band assignable to V-I  $\sigma$  orbital ionization below an IE of 8.9 eV in the spectrum of the iodide, this assignment is rather du-

bious and an alternative assignment as a cyclopentadienyl  $\pi$  orbital is more likely. In this context it should be recalled that the cyclopentadienyl  $\pi$  band of vanadocene shows exchange splitting, and owing to the open-shell nature of these compounds there is a possibility of similar structure in these vanadocene derivatives. The vanadium-halogen  $1a_1$   $\sigma$  orbital ionizations for the bromide and the iodide cannot therefore be assigned with certainty to a single peak but must lie under the 8.5–10.5-eV bands. Unlike the chloride, no evidence can be found from the He II/He I band profile comparisons for cyclopentadienyl-halogen orbital mixing in the bromide and iodide.

The mean ionization energies of the halogen p orbital ionizations in the  $V(\eta-C_5H_5)_2X$  compounds are 8.29 (Cl), 8.14 (Br), and 7.99 (I) eV. These values are notably lower and show less variation than those commonly observed in similar complexes.<sup>27</sup>

In summary, the photoelectron spectra of the halides indicate small but significant halogen p $\pi$  metal d orbital interactions, approximately constant in magnitude for all three halides; the cyclopentadienyl p $\pi$ -halogen p $\pi$  interactions are insignificant except for the chloride, and the compounds may be classified as class C;<sup>17</sup> i.e., the mainly halogen orbitals ionize at a lower energy than the mainly cyclopentadienyl orbitals.

**Bis(cyclopentadienyl)metal Aryls.** A molecular orbital diagram may be constructed by considering the interaction between a bent  $V(\eta-C_5H_5)_2$  unit and an aryl ring in  $C_{2v}$  symmetry. Since the symmetry properties of the aryl  $\pi$  orbitals are dependent on the conformation of the aryl ring, we must consider two alternate conformations: (1) aryl ring in the  $xz$  plane, parallel conformation; (2) aryl group in the  $yz$  plane, perpendicular conformation. In both conformations  $\sigma$  donation takes place through the  $a_1$  symmetry orbitals as in the halides. Aryl  $\pi$  interactions with the metal  $b_1$  orbital can only occur when the ring is in the perpendicular conformation. However the crystallographic work of Olthof et al.<sup>30</sup> on  $Ti(\eta-C_5H_5)_2(2,6-Me_2C_6H_3)$  demonstrates that the aryl ring was held rigidly in the  $xz$  plane, i.e., in the parallel conformation, by severe intramolecular interactions between the methyl groups and the cyclopentadienyl rings which greatly disfavored any alternative conformations. In a recent study of peralkylated dicyclopentadienylvanadium complexes<sup>25</sup> NMR studies have shown that the phenyl is locked between the cyclopentadienyl rings and free rotation is prevented. Since the steric effects are intramolecular rather than intermolecular we can assume the same conformation is adopted in the vapor phase. Though in the simplest aryl compound we have measured the steric crowding is less due to the absence of alkyl groups it seems reasonable to assume a parallel conformation for all the aryl compounds, with the consequence that we expect minimal ring-metal  $b_1$  orbital mixing. A representative MO scheme is given in Figure 4. This is similar to the one of Köhler et al. that is based on extended Hückel calculations.<sup>25</sup> Their calculation suggests that  $b_1$  is also destabilized by interaction with ring  $\sigma$  orbitals.

The photoelectron spectra of the aryls (Figure 5) resemble those of the halides in the regions B, C, and D, and these bands have a similar assignment except that aryl  $\sigma$  and  $\pi_1$  ionization bands are now included with cyclopentadienyl  $\sigma$  ionizations. Ionization energies and other data are now listed in Table II.4–8.

In the He I spectrum of the perfluoroaryl compound two bands are present at 15.1 and 16.35 eV which show a

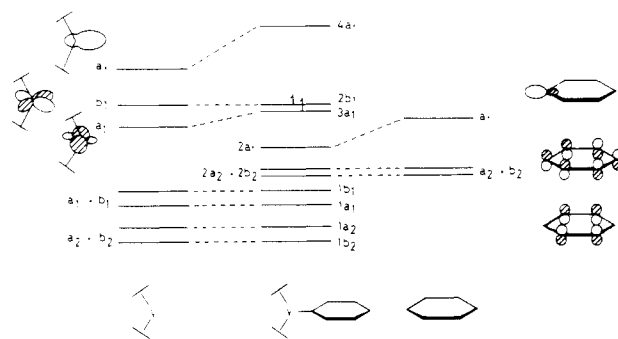


Figure 4. Qualitative energy level scheme for bis(cyclopentadienyl)vanadium aryls.

considerable intensity increase in the He II spectrum relative to the main band. These bands have no counterparts in the spectra of the other aryls and are characteristic of fluorine lone pair ionizations.<sup>31,32</sup>

The first two bands in the A' region are again identified as metal localized  $b_1 + a_1$  orbital ionizations, using He I/He II intensity comparison criteria. They are considerably closer than in the halides and as a result are only partially resolved in the He II spectra; this makes accurate estimates of their intensities difficult. However, both He II/He I intensity ratios and visual comparison of the spectra indicate little change in relative intensity, indicating similar orbital character for both bands. The separation of the first two bands for the 2,6-dimethylphenyl compound is only 0.33 eV which is consistent with the suggestion that the aryl ring adopts a parallel conformation in which no  $\pi$  interaction with the metal  $b_1$  orbital is allowed on symmetry grounds. The calculations of Köhler et al. suggest a separation of 0.2 eV.<sup>25</sup> Since the separation of the d orbital bands in the other aryl compounds varies so little from that found in the dimethylphenyl compound (it ranges from 0.28 eV for  $C_6F_5$  to 0.35 eV for *o*-tolyl), we may conclude that the extent of vanadium aryl  $\pi$  interaction must be very small, the parallel conformation being adopted in all cases.

In the 7–11-eV region four bands, A''<sub>1</sub>–A''<sub>4</sub>, are found. In Figure 6 their vertical ionization energies are plotted as a function of the aryl ligand. The first and third bands have IE that are insensitive to methyl substitution of the aryl ligand, whereas the IE of A''<sub>2</sub> and A''<sub>4</sub> decrease by 0.20–0.25 eV on each successive addition of a methyl substituent on the aryl ring. This suggests that these two bands originate from orbitals largely localized on the aryl ring, the free ligands showing a similar variation of the mean ionization energy of their two highest occupied  $\pi$  orbitals.<sup>33</sup> In addition bands A''<sub>2</sub> and A''<sub>4</sub> have He II/He I intensity ratios of  $0.6 \pm 0.1$ , compared with  $0.8 \pm 0.1$  for bands A''<sub>1</sub> and A''<sub>3</sub> (relative to the metal d ionizations taken as 1.0), demonstrating a lower metal content and thus a smaller metal bonding involvement of the former set of orbitals. The A''<sub>1</sub>, A''<sub>2</sub>, and A''<sub>3</sub> bands are therefore assigned to ionizations of the V–C  $2a_1$ , aryl ( $2a_2 + 2b_2$ ), and cyclopentadienyl ( $1a_1 + 1b_1 + 1a_2 + 1b_2$ ) orbitals, respectively, this assignment being supported by the approximately 2:4:8 He I intensity ratio, in proportion to the electron populations of the three orbital sets.

(31) Brundle, C. R.; Robin, M. B.; Kuebler, N. A.; Basch, H. *J. Am. Chem. Soc.* 1972, 94, 1466.

(32) Robin, M. B.; Kuebler, N. A.; Brundle, C. R. In "Electron Spectroscopy"; Shirley, D. A., Ed.; North-Holland Publishing Co.: Amsterdam, 1972; p 351.

(33) Heilbronner, E.; Maier, J. P. In "Electron Spectroscopy"; Brundle, C. R., Baker, A. D. Eds.; Academic Press: New York, 1977; p 245.

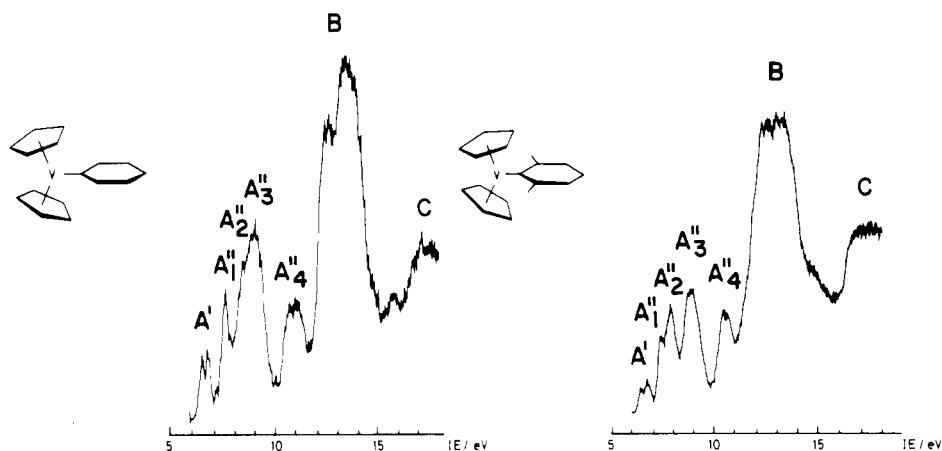


Figure 5. He I photoelectron spectra of  $V(\eta\text{-C}_5\text{H}_5)_2(\text{C}_6\text{H}_5)$  and  $V(\eta\text{-C}_5\text{H}_5)_2(2,6\text{-C}_6\text{H}_3\text{Me}_2)$ .

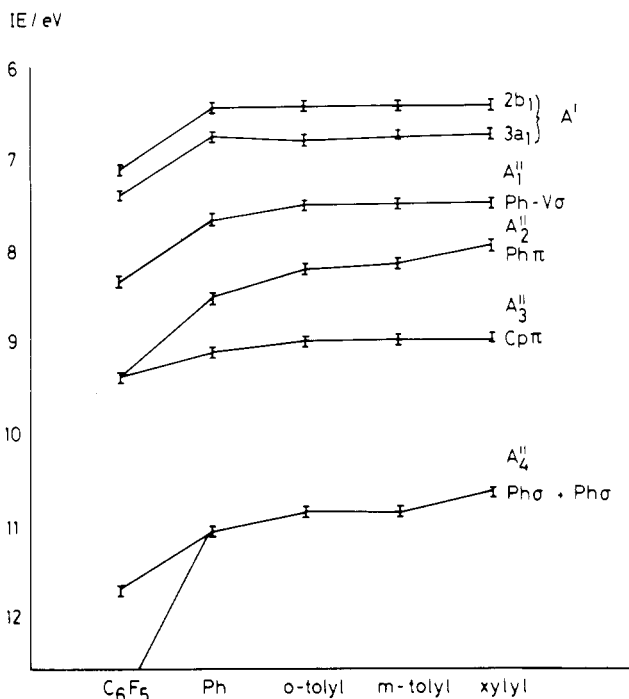


Figure 6. Vertical ionization energies of  $A'$  and  $A''$  bands of bis(cyclopentadienyl) aryls plotted as a function of aryl ligand.

To assign the  $A''_4$  band, we note that in addition to a shift of 0.6 eV to higher IE in the perfluoro derivative relative to the phenyl derivative, the intensity of this band is markedly diminished compared with the non-fluorinated

aryls. The He II/He I intensity ratios and substituent effects discussed above establish the  $A''_4$  band as being derived from aryl ring localized orbitals. The characteristically greater shift to higher IE exhibited by aryl  $\sigma$  orbitals (1.3–2.0 eV) compared with that of  $\pi$  orbitals (0.4–0.8 eV) on perfluorination of the aromatic ring<sup>31</sup> suggests that in the non-fluorinated aryls the  $A''_4$  band is composite involving ionization of the highest occupied ring  $\pi$  orbitals ( $a_1 + b_2$ ) and the lowest energy  $\pi$  orbital ( $b_2$ ). On perfluorination the former are shifted under the main band B, while the latter remains resolved on the low-energy side of this band. The He I intensity values give an approximately 3:1 ratio for the  $A''_4$  band before and after perfluorination, which argues in favor of the additional ionization of two rather than one  $\sigma$  level for the non-fluorinated aryls.

Unlike alkylation of the aryl group which to a first approximation only affects the IE of the aryl orbitals, the effect of perfluorination of the ring is seen to be transmitted throughout the entire molecule, the metal d and cyclopentadienyl  $\pi$  orbitals showing IE increases  $\sim 0.6$  and  $\sim 0.25$  eV, respectively, although the  $a_1 - b_1$  metal orbital splitting remains practically constant in accordance with minimal V-aryl  $\pi$  interactions. It is also notable that for all the aryls the aryl  $4b_2 + 2a_2$   $\pi$  ionizations occur at an IE 0.7–0.8 eV lower than in the free ligands but this may be accounted for by the more electropositive nature of the metal center, compared with the hydrogen atom.

The spectrum of the *m*-tolyl compound shows evidence of partial decomposition to vanadocene; the second band at 6.78 eV is anomalously intense and would coincide with the vanadocene d band (6.75 eV).<sup>34</sup> It has been noted that

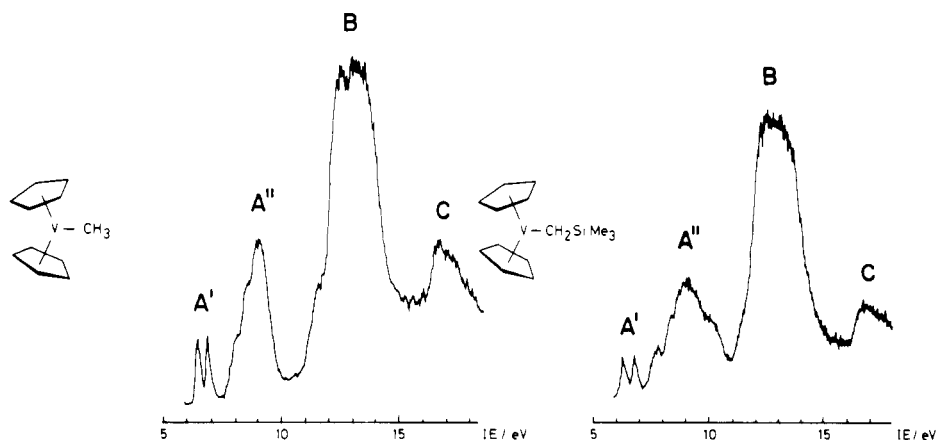


Figure 7. He I photoelectron spectra of  $V(\eta\text{-C}_5\text{H}_5)_2\text{Me}$  and  $V(\eta\text{-C}_5\text{H}_5)_2\text{SiMe}_3$ .

these compounds have a tendency to be thermally labile in solution.<sup>25,35</sup>

Discussion of the V-C  $\sigma$  orbital IE is deferred until comparison can be made with the values obtained for the alkyls.

**Biscyclopentadienylvanadium(III) Alkyls.** Representative spectra are presented in Figure 7 and the IE and other relevant data listed in Table II.9–11. They broadly resemble those of the halides, and analogous assignments may be made in the A', B, C and D spectral regions. However substantial differences are observable in the A'' region. In the spectrum of the (trimethylsilyl)methyl compound, a shoulder is present at  $\sim 10.3$  eV on the high IE side of the characteristic cyclopentadienyl ionization band centered at  $\sim 9$  eV, the former being absent in the other alkyls. From earlier work,<sup>36,37</sup> we may assign this band to C-Si bond ionization.

In all three alkyls there is a small band A''<sub>1</sub> on the low-energy side of the main cyclopentadienyl  $\pi$  band that shows an intensity decrease relative to the latter, indicating an orbital of high C 2p/2s content. It is assigned to ionization of the V-C  $a_1$   $\sigma$ -bonding orbital. In the neopentyl compound alone there is a very broad shoulder at 9.5–11.5 eV on the large central band B. It is assigned to ionization of C-C  $\sigma$  orbitals of the neopentyl group.<sup>36–38</sup>

That the separation of the first two bands is larger in the alkyl compounds than in the aryls suggests that some  $\pi$  interaction probably of a hyperconjugative nature is operative, namely, interaction between the metal  $b_1$  orbital and, for example, the appropriate combination of C-H orbitals of the methyl group. The following support may be found for  $\pi$  interactions of this nature: (a) He II/He I intensity ratio and band half-widths for the methyl and (trimethylsilyl)methyl compound indicate that the HOMO,  $b_1$ , orbital has a greater bonding involvement than the other occupied d orbital,  $a_1$ ; (b) recent <sup>1</sup>H NMR work<sup>25</sup> has shown large contact shifts ( $\sim 800$  ppm upfield) for the methyl group in VCP<sub>2</sub>Me, indicating delocalization of unpaired electron density onto the methyl protons from the vanadium atom; similar results have also been obtained for V( $\eta$ -C<sub>5</sub>Me<sub>4</sub>Et)<sub>2</sub>Me;<sup>25</sup> (c) the occurrence of hyperconjugation between alkyl groups and suitable metal orbitals is supported by the magnitude of  $J_{H-D}$  on the carbon substituents<sup>39</sup> in Mn(CO)<sub>5</sub>R and by the  $e - b_2$  orbital splitting exhibited in the PE spectra of Mn(CO)<sub>5</sub>Me and Re(CO)<sub>5</sub>Me.<sup>34</sup>

In the pe spectrum of the neopentyl compound the second d band at 6.72 eV is more than twice as intense as

the first d orbital band, in contrast to the expected 1:1 ratio. Again partial decomposition to vanadocene is likely to be the cause of this anomaly.

**Ionization Energies of Vanadium-Carbon Bonds in the Alkyls and Aryls.** The IE of the non-fluorinated aryl-vanadium orbital at  $\sim 7.6$  eV are lower than any previously reported metal-carbon bond IE, the usual range being 8–10 eV for alkyls.<sup>27</sup> The IE for the aryls are lower than that of the methyl compound, 8.14 eV, although not quite so low as that of the neopentyl compound, 7.43 eV. This is an unexpected result since sp<sup>2</sup>-hybridized carbon is more electronegative than sp<sup>3</sup>-hybridized carbon, and, in addition the bis(cyclopentadienyl)vanadium(III) aryls are thermally more stable than the corresponding alkyls. Thermal stability increases on perfluorination of the aryl ring and on ortho substitution, as demonstrated by the following decomposition temperatures for V( $\eta$ -C<sub>5</sub>H<sub>5</sub>)<sub>2</sub>X: X = Me, 138 °C; Ph, 158 °C; *o*-tolyl, 204 °C; 2,6-xylyl, 246 °C; *m*-tolyl, 135 °C; C<sub>6</sub>F<sub>5</sub>, 208 °C. The V-C bond IE however show very little variation upon methyl substitution of the aryl ring. The greater stability of the aryl compounds and the "ortho" effect must therefore be attributed to kinetic rather than thermodynamic effects, in line with previous studies.<sup>37</sup>

The vanadium-carbon  $\sigma$  bond IE in the alkyls are also lower than is usually observed. This may be related to the electropositive nature of the vanadium atom and is agreement with the trend of decreasing metal-carbon  $\sigma$  bond energies on moving from right to left across the transition series. The lower M-C  $\sigma$  bond IE observed for the neopentyl compound compared with the (trimethylsilyl)methyl compound is also in line with previous observations.<sup>37</sup>

## Conclusions

From the photoelectron spectra of the V( $\eta$ -C<sub>5</sub>H<sub>5</sub>)<sub>2</sub>X complexes, it is clear that subtle differences exist in metal-ligand bonding interactions for different types of ligand, X. These are found to be principally characterized by the separation of the d orbital bands.  $\pi$ -Bonding interactions are found to decrease in the order halides > alkyls > aryls, although even for the halides V-L bonding is relatively weak. Inductive effects are also seen to affect the IE of the metal d and ring  $\pi$  orbitals, as demonstrated for example by the trend of metal  $a_1$  orbital IE X = Cl  $\approx$  Br  $\approx$  C<sub>6</sub>F<sub>5</sub> > I > alkyl > aryl. Vanadium-aryl  $\sigma$  bond IE are found to be surprisingly low ( $\sim 7.6$  eV), and this together with their negligible dependence on ortho substitution of the aryl ring, indicates that their thermal stability is controlled by kinetic rather than thermodynamic factors.

**Acknowledgment.** We thank the S.R.C. for financial support.

**Registry No.** V( $\eta$ -C<sub>5</sub>H<sub>5</sub>)<sub>2</sub>Cl, 12701-79-0; V( $\eta$ -C<sub>5</sub>H<sub>5</sub>)<sub>2</sub>Br, 64815-29-8; V( $\eta$ -C<sub>5</sub>H<sub>5</sub>)<sub>2</sub>I, 53291-02-4; V( $\eta$ -C<sub>5</sub>H<sub>5</sub>)<sub>2</sub>C<sub>6</sub>H<sub>5</sub>, 12212-56-5; V( $\eta$ -C<sub>5</sub>H<sub>5</sub>)<sub>2</sub>(2-C<sub>6</sub>H<sub>4</sub>Me), 64439-04-9; V( $\eta$ -C<sub>5</sub>H<sub>5</sub>)<sub>2</sub>(3-C<sub>6</sub>H<sub>4</sub>Me), 64406-44-6; V( $\eta$ -C<sub>5</sub>H<sub>5</sub>)<sub>2</sub>(2,6-C<sub>6</sub>H<sub>3</sub>Me<sub>2</sub>), 64406-45-7; V( $\eta$ -C<sub>5</sub>H<sub>5</sub>)<sub>2</sub>(C<sub>6</sub>F<sub>5</sub>), 71498-26-5; V( $\eta$ -C<sub>5</sub>H<sub>5</sub>)<sub>2</sub>Me, 54111-39-6; V( $\eta$ -C<sub>5</sub>H<sub>5</sub>)<sub>2</sub>CH<sub>2</sub>SiMe<sub>3</sub>, 57603-38-0; V( $\eta$ -C<sub>5</sub>H<sub>5</sub>)<sub>2</sub>CH<sub>2</sub>CMe<sub>3</sub>, 59424-04-3.

(34) Evans, S.; Green, M. L. H.; Jewitt, B.; King, G. H.; Orchard, A. F. *J. Chem. Soc., Faraday Trans. 2* 1974, 70, 356.

(35) Boekel, C. P.; Jelsma, A.; Teuben, J. K.; de Liefde Meijer, H. J. *J. Organomet. Chem.* 1977, 136, 211.

(36) Green, J. C.; Jackson, S. E.; Evans, S. *J. Chem. Soc. Faraday Trans. 2* 1973, 69, 191.

(37) Lappert, M. F.; Pedley, J. B.; Sharp, G. *J. Organomet. Chem.* 1974, 66, 271.

(38) Evans, S.; Green, J. C.; Joachim, P. J.; Orchard, A. F.; Turner, D. W.; Maier, J. P. *J. Chem. Soc., Faraday Trans. 2* 1972, 68, 905.

(39) Duncan, J. D.; Green, J. C.; Green, M. L. H.; McLauchlan, K. A. *Discuss. Faraday Soc.* 1969, 47, 178.



# Photoelectron Study of Electron-Rich Iron(I) Cyclopentadienyl Arene Complexes and of the Related Iron(II) Cyclopentadienyl Cyclohexadienyl Complexes

Jennifer C. Green,\* M. Ruth Kelly, Martin P. Payne, and Elaine A. Seddon

*Inorganic Chemistry Laboratory, South Parks Road, Oxford OX1 3QR, England*

Didier Astruc, Jean-René Hamon, and Pascal Michaud

*Laboratoire de Chimie des Organometalliques, Université de Rennes, 35042 Rennes Cedex, France*

Received September 21, 1982

The He I and He II photoelectron spectra of  $\text{Fe}(\eta\text{-C}_5\text{H}_5)(\eta\text{-C}_6\text{Me}_6)$ ,  $\text{Fe}(\eta\text{-C}_5\text{H}_5)(\eta\text{-C}_6\text{Et}_6)$ ,  $\text{Fe}(\eta\text{-C}_5\text{H}_5)(\eta\text{-C}_6\text{H}_3(\text{CMe}_3)_3)$ , and  $\text{Fe}(\eta\text{-C}_5\text{Me}_5)(\eta\text{-C}_6\text{Me}_6)$  have been obtained and been shown to resemble that of the isoelectronic cobaltocene.  $\text{Fe}(\eta\text{-C}_5\text{Me}_5)(\eta\text{-C}_6\text{Me}_6)$  has one of the lowest recorded molecular ionization potentials of 4.21 eV. Comparison of the molecular photoelectron spectra with the optical spectra of the related cations shows that the two sets of assignments can only be made consistent by a substantial origin shift. Ligand field parameters are presented for  $\text{Fe}(\eta\text{-C}_5\text{H}_5)(\eta\text{-C}_6\text{Me}_6)$  and  $\text{Fe}(\eta\text{-C}_5\text{Me}_5)(\eta\text{-C}_6\text{Me}_6)$ . The He I and He II photoelectron spectra of some related complexes,  $\text{Fe}(\eta\text{-C}_5\text{H}_5)(\eta^5\text{-C}_6\text{H}_7)$ ,  $\text{Fe}(\eta\text{-C}_5\text{H}_5)(\eta^5\text{-C}_6\text{Me}_6\text{H})$ ,  $\text{Fe}(\eta\text{-C}_5\text{H}_5)(\eta^5\text{-C}_6\text{Me}_5\text{CH}_2)$  and  $\text{Fe}(\eta\text{-C}_5\text{H}_5)(\eta^5\text{-C}_6\text{Me}_5\text{NH})$ , have been obtained and assigned. These have higher first ionization energies and are characteristic of  $d^8$  species. The electron distribution in the benzyl complex is shown to account for the nucleophilic properties of this compound.

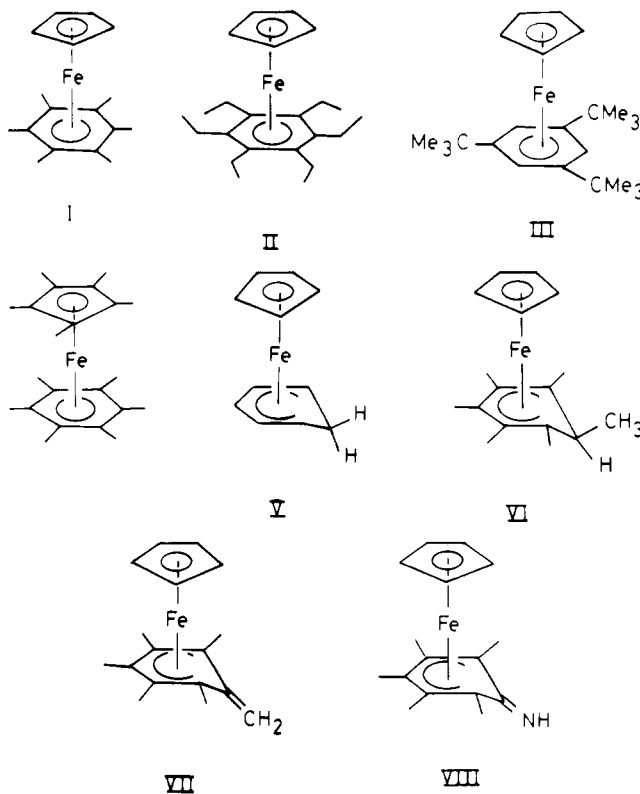
Until recently the only stable neutral 19-electron metal sandwich compounds known were cobaltocene and its derivatives.<sup>1</sup> In the last few years a series of hyperalkylated 19-electron mixed-sandwich compounds such as  $\text{Fe}(\eta\text{-C}_5\text{R}'_5)(\eta\text{-C}_6\text{R}''_6)$  where  $\text{R}' = \text{H}$  or  $\text{Me}$  and  $\text{R}'' = \text{Me}$  or  $\text{Et}$  have been prepared.<sup>2,3</sup> Unlike the parent compound the unsubstituted  $\text{Fe}(\eta\text{-C}_5\text{H}_5)(\eta\text{-C}_6\text{H}_6)$  complex, which decomposes at 20 °C,<sup>4</sup> the peralkylated benzene complexes are stable toward dimerization through the six-membered ring. The increased stability of these compounds results principally from steric protection of the aryl ring against dimerization by the bulky alkyl groups, although electronic effects also play a role.<sup>3</sup> The thermal stability of the peralkylated arene complexes renders them suitable for investigation by photoelectron (PE) spectroscopy.

Mössbauer and EPR studies<sup>3,4</sup> have established that the sandwich compounds are  $d^7$  19-electron complexes of Fe(I) with a  $^2E$  ground state. They indicate that the near degenerate HOMO  $e_1^*$  is largely metal based and has more cyclopentadienyl character than arene character. These  $d^7$  compounds, together with the corresponding  $d^8$  cations, constitute totally reversible redox systems having very negative redox potentials.<sup>3</sup>

Reaction of  $\text{Fe}(\eta\text{-C}_5\text{H}_5)(\eta\text{-C}_6\text{Me}_6)$  and  $\text{Fe}(\eta\text{-C}_5\text{Me}_5)(\eta\text{-C}_6\text{Me}_6)$  with oxygen results in abstraction of a hydrogen atom from a methyl group on the arene ring and formation of a  $\eta^5$  ring with an exocyclic  $\text{CH}_2$  group, for example,  $\text{Fe}(\eta\text{-C}_5\text{H}_5)(\eta\text{-C}_6\text{Me}_6)$  gives  $\text{Fe}(\eta\text{-C}_5\text{H}_5)(\eta^5\text{-C}_6\text{Me}_5\text{CH}_2)$ .<sup>5-7</sup> This exocyclic double bond is readily hydrogenated; for example,  $\text{Fe}(\eta\text{-C}_5\text{H}_5)(\eta^5\text{-C}_6\text{Me}_5\text{CH}_2)$  gives  $\text{Fe}(\eta\text{-C}_5\text{H}_5)(\eta^5\text{-C}_6\text{Me}_5\text{H})$  through the intermediacy of the Fe(I) semi-hydrogenated complex.<sup>8</sup> Also the benzyl complex acts as a nucleophile in an extensive series of substitution reactions.

The chemical reactivity of these compounds is thus sufficiently novel to merit further investigation of their electronic structure.

We report below the photoelectron spectra of the  $d^7$  complexes  $\text{Fe}(\eta\text{-C}_5\text{H}_5)(\eta\text{-C}_6\text{Me}_6)$ , I,  $\text{Fe}(\eta\text{-C}_5\text{H}_5)(\eta\text{-C}_6\text{Et}_6)$ , II,  $\text{Fe}(\eta\text{-C}_5\text{H}_5)(\eta\text{-C}_6\text{H}_3(\text{CMe}_3)_3)$ , III, and  $\text{Fe}(\eta\text{-C}_5\text{Me}_5)(\eta\text{-C}_6\text{Me}_6)$ , IV, and the  $d^8$  complexes  $\text{Fe}(\eta\text{-C}_5\text{H}_5)(\eta^5\text{-C}_6\text{H}_7)$ , V,  $\text{Fe}(\eta\text{-C}_5\text{H}_5)(\eta^5\text{-C}_6\text{Me}_6\text{H})$ , VI,  $\text{Fe}(\eta\text{-C}_5\text{H}_5)(\eta^5\text{-C}_6\text{Me}_5\text{CH}_2)$ , VII, and  $\text{Fe}(\eta\text{-C}_5\text{H}_5)(\eta^5\text{-C}_6\text{Me}_5\text{NH})$ , VIII.



(1) (a) Page, J. A.; Wilkinson, G. *J. Am. Chem. Soc.* 1952, 74, 7149. (b) Herlich, G. E.; Becker, H. *J. Angew. Chem., Int. Ed. Engl.* 1975, 14, 184 and references cited therein. (c) Hart, W. P.; Macomber, D. W.; Rausch, M. D. *J. Am. Chem. Soc.* 1980, 102, 1196.

(2) Astruc, D.; Hamon, J.-R.; Althoff, G.; Román, E.; Batail, P.; Michaud, P.; Mariot, J.-P.; Varret, F.; Cozak, D. *J. Am. Chem. Soc.* 1979, 101, 5445.

(3) Hamon, J.-R.; Astruc, D.; Michaud, P. *J. Am. Chem. Soc.* 1981, 103, 758.

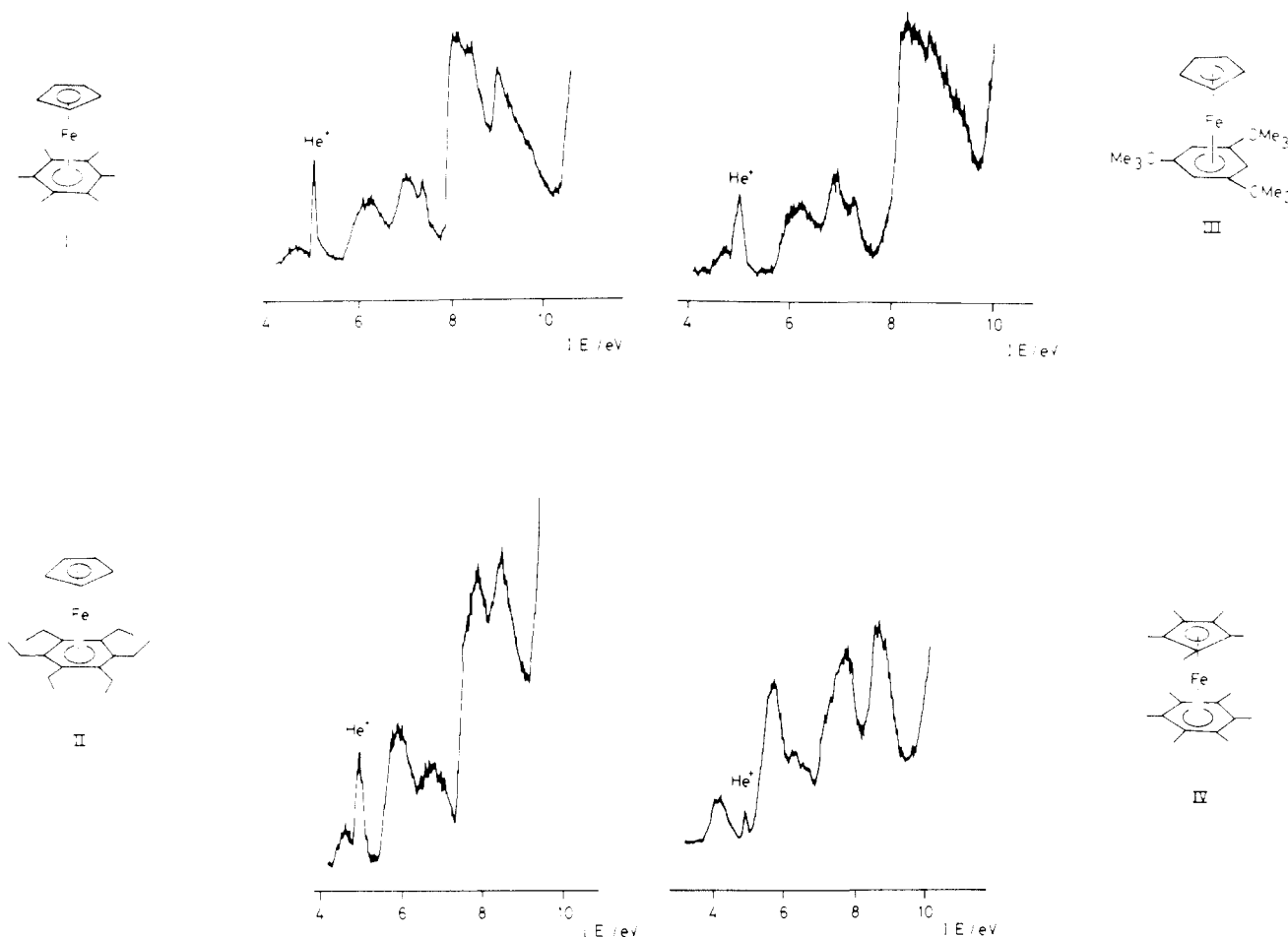
(4) Rajasekharan, M. V.; Giezyński, S.; Ammeter, J. H.; Ostwald, N.; Hamon, J.-R.; Astruc, D. *J. Am. Chem. Soc.*, in press.

(5) Astruc, D.; Román, E.; Hamon, J.-R.; Batail, P. *J. Am. Chem. Soc.* 1979, 101, 2240.

(6) Hamon, J.-R.; Astruc, D.; Román, E.; Batail, P.; Mayerle, J. J. *J. Am. Chem. Soc.* 1981, 103, 2431.

(7) Astruc, D.; Hamon, J.-R.; Román, E.; Michaud, P. *J. Am. Chem. Soc.* 1981, 103, 7502.

(8) Michaud, P.; Hamon, J.-R.; Astruc, D., submitted for publication.



**Figure 1.** He I spectra of  $\text{Fe}(\eta\text{-C}_5\text{H}_5)(\eta\text{-C}_6\text{Me}_6)$ , I,  $\text{Fe}(\eta\text{-C}_5\text{H}_5)(\eta\text{-C}_6\text{Et}_6)$ , II,  $\text{Fe}(\eta\text{-C}_5\text{H}_5)(\eta\text{-C}_6\text{H}_3(\text{CMe}_3)_3)$ , III, and  $\text{Fe}(\eta\text{-C}_5\text{Me}_5)(\eta\text{-C}_6\text{Me}_6)$ , IV.

### Experimental Section

The compounds were prepared according to the literature methods.<sup>2-8</sup>

The PE spectra were obtained by using a Perkin-Elmer PS 16/18 instrument, fitted with an Helectros lamp capable of producing both He I and He II radiation.

The samples were introduced into the spectrometer by use of a glovebag. On initial warming of the sandwich compounds I, II, and IV, the spectrum of an impurity was obtained that we assume arose as a result of partial oxidation of the sample on introduction to the spectrometer. After a time a different spectrum appeared, which remained stable for several hours, exhibited a very low ionization energy (IE) band and resembled the PE spectrum of cobaltocene. In the case of  $\text{Fe}(\eta\text{-C}_5\text{H}_5)(\eta\text{-C}_6\text{Me}_6)$  and  $\text{Fe}(\eta\text{-C}_5\text{H}_5)(\eta\text{-C}_6\text{Et}_6)$ , but not in the case of  $\text{Fe}(\eta\text{-C}_5\text{Me}_5)(\eta\text{-C}_6\text{Me}_6)$ , the subsequent spectra may retain traces of impurity in the regions ca. 7.0 and 8.0 eV so in these cases only the low ionization energy features ca. 4.5 and 6.3 eV can be rigorously assigned to these compounds, though the intensity patterns indicate that the other features are valid. The spectrum of  $\text{Fe}(\eta\text{-C}_5\text{H}_5)(\eta^5\text{-C}_6\text{Me}_5\text{CH}_2)$ , the known oxidation product of  $\text{Fe}(\eta\text{-C}_5\text{H}_5)(\eta\text{-C}_6\text{Me}_6)$ , was the same as the spectrum of the impurity found in the case of  $\text{Fe}(\eta\text{-C}_5\text{H}_5)(\eta\text{-C}_6\text{Me}_6)$ . Consideration of substituent effects on band positions also makes assignment of the impurities in the other two cases to their respective oxidation products reasonable. The spectrum of III was obtained impurity free over a range of 40 °C.

The He I pe spectrum of  $\text{Fe}(\eta\text{-C}_5\text{H}_5)(\eta^5\text{-C}_6\text{Me}_5\text{NH})$  was of low intensity at 124 °C, but the compound proved unstable under conditions of measurement at higher temperatures. It was therefore not possible to obtain a He II spectrum.

All spectra were calibrated with reference to Xe, N<sub>2</sub>, and the He self-ionization band. The vertical ionization energies are deemed accurate to  $\pm 0.05$  eV.

### Results

Ionization energies obtained and conditions of measurement are given in Table I. Representative spectra are presented in Figures 1 and 6.

### Discussion

**d<sup>7</sup> Complexes.** Mössbauer and EPR studies<sup>3,4</sup> suggest a <sup>2</sup>E ground state for these molecules arising from the d electron configuration  $e_2^4 a_1^2 e_1^*1$ . Ionization from this configuration leads to seven ion states, details of which are given in Table II; thus assignment of the spectra is complex.

Perhaps the most striking feature of the PE spectra of the iron(I) cyclopentadienyl arene compounds is that they show very low first ionization energies. For example the first band of  $\text{Fe}(\eta\text{-C}_5\text{Me}_5)(\eta\text{-C}_6\text{Me}_6)$  has a vertical IE of 4.21 eV and a band onset of 3.95 eV. These values are comparable with those of the heavier alkali metals (K, 4.339 eV; Rb, 4.176 eV; Cs, 3.893 eV). These low-energy bands may be assigned to the <sup>1</sup>A<sub>1</sub> ground state ( $e_2^4 a_1^2$ ) formed by removal of an electron from the  $e_1^*$  antibonding orbital.

In the low ionization energy region the spectrum of IV resembles that of cobaltocene<sup>9</sup> (see Figures 1 and 2). A comparison of He I and He II intensities show that the first four bands (4.21, 5.74, 6.32, 6.64 eV) are d ionizations bands, the first band showing the largest intensity increase with photon energy as is generally found for  $e_1^*$  ioniza-

(9) Evans, S.; Green, M. L. H.; Jewitt, B.; King, G. H.; Orchard, A. F. *J. Chem. Soc., Faraday Trans. 2* 1974, 70, 356.

Table I. Ionization Energies (eV) and Measurement Conditions for Fe( $\eta$ -C<sub>5</sub>H<sub>5</sub>)( $\eta$ -C<sub>6</sub>Me<sub>6</sub>) (I), Fe( $\eta$ -C<sub>5</sub>H<sub>5</sub>)( $\eta$ -C<sub>6</sub>Et<sub>6</sub>) (II), Fe( $\eta$ -C<sub>5</sub>H<sub>5</sub>)( $\eta$ -C<sub>6</sub>H<sub>3</sub>(CMe<sub>3</sub>)<sub>3</sub>) (III), Fe( $\eta$ -C<sub>5</sub>Me<sub>5</sub>)( $\eta$ -C<sub>6</sub>Me<sub>6</sub>) (IV), Fe( $\eta$ -C<sub>5</sub>H<sub>5</sub>)( $\eta$ <sup>5</sup>-C<sub>6</sub>H<sub>7</sub>) (V), Fe( $\eta$ -C<sub>5</sub>H<sub>5</sub>)( $\eta$ <sup>5</sup>-C<sub>6</sub>Me<sub>5</sub>H) (VI), Fe( $\eta$ -C<sub>5</sub>H<sub>5</sub>)( $\eta$ <sup>5</sup>-C<sub>6</sub>Me<sub>5</sub>CH<sub>2</sub>) (VII), and Fe( $\eta$ -C<sub>5</sub>H<sub>5</sub>)( $\eta$ <sup>5</sup>-C<sub>6</sub>Me<sub>5</sub>NH) (VIII)

I (93 °C, 1000 c/s)	III (80 °C, 400 c/s)	assignt
4.68	4.74	<sup>1</sup> A <sub>1</sub>
6.19	6.20	<sup>3</sup> E <sub>1</sub>
6.92	6.87	<sup>3</sup> E <sub>2</sub> + <sup>3</sup> E <sub>1</sub> + <sup>1</sup> E <sub>1</sub>
7.18	7.22	<sup>1</sup> E <sub>2</sub>
7.89	8.24	e <sub>1</sub> (Cp) + <sup>1</sup> E <sub>1</sub>
8.06	8.68	+e <sub>1</sub> (arene)
8.79		
10.6	10.2	ring alkyl
12.7	13	ring a <sub>1</sub> + $\sigma$

II (100 °C, 1500 c/s)	IV (150 °C, 3000 c/s)	assignt
4.54	4.21	<sup>1</sup> A <sub>1</sub>
6.09	5.74	<sup>3</sup> E <sub>1</sub> + <sup>3</sup> E <sub>2</sub>
6.92	6.32	<sup>1</sup> E <sub>1</sub> + <sup>3</sup> E <sub>1</sub>
	6.64	<sup>1</sup> E <sub>2</sub>
7.77	(7.20)	e <sub>1</sub> (Cp)
8.02	7.71	e <sub>1</sub> (arene)
8.70	8.58	ring alkyl
10.3	10.2	ring a <sub>1</sub> and $\sigma$
12.1	13	

V (65 °C, 2000 c/s)	assignt	VI (82 °C, 2000 c/s)	assignt
6.65 (a)	d	6.27 (a)	d
6.98 (b)	d		d
7.15 (c)	d	6.64 (b)	d
7.97 (d)	$\pi_3$	7.29 (c)	$\pi_3$
9.07 (e)	e <sub>1</sub> (Cp)	8.27 (d)	$\pi_2$
9.30 (f)	$\pi_2$	8.8 (e)	e <sub>1</sub> (Cp)
11.12 (g)	$\pi_1$	10.05 (f)	$\pi_1$ + ring Me
11.52 (h)	ring $\sigma$	10.5 (g)	
12.2 (i)		12.8 (h)	
13.6 (j)			
16.5 (h)			

VII (106 °C, 3000 c/s)	assignt	VIII (124 °C, 500 c/s)	assignt
6.22 (a)	d	6.65 (a)	d
6.95 (b)	d + $\pi_4$	7.71 (b)	d
		7.79 (c)	$\pi_4$
8.79 (c)	$\pi_3$ + $\pi_2$ + e <sub>1</sub> (Cp)	8.63 (d)	$\pi_3$ + $\pi_2$ + e <sub>1</sub> (Cp)
9.12 (d)		9.33 (e)	
10.74 (e)	$\pi_1$ + ring Me	11.26 (f)	$\pi_1$ + ring Me
13.1 (f)		13.2 (g)	

tions.<sup>10</sup> As with cobaltocene it is likely that further d ionizations lie under the subsequent ligand bands (7.71, 8.58 eV). These two bands are primarily due to the e<sub>1</sub> ring ionizations; comparison with IE of other sandwich compounds<sup>11</sup> suggests that the lower energy band (7.71 eV) is mainly cyclopentadienyl in character and the higher energy band (8.58 eV) is mainly arene in character. A shoulder on the low IE edge of the first ligand band may well be due to a d ionization band.

There are various criteria available to help in a more detailed assignment of the PE bands. As the open-shell nature of these compounds leads to a complex pattern of d ionizations, ligand field predictions as to the relative energy of the ion states should prove useful as has been found in analogous cases.<sup>10</sup> Also predictions as to

Table II. Ligand Field Energies and Interaction Matrices for States of the d<sup>6</sup> Cations Accessible by Photoionization from the d<sup>7</sup> Molecules Together with Their Anticipated Relative Band Intensities

ion configuratn	ion state	intensity	first-order ligand field energy
a <sub>1</sub> <sup>1</sup> e <sub>2</sub> <sup>4</sup> e <sub>1</sub> <sup>1</sup>	<sup>3</sup> E <sub>1</sub>	3k <sub>a1</sub> /2	15A - 13B + 12C + 2 $\Delta_2$ + $\Delta_1$
	<sup>1</sup> E <sub>1</sub>	k <sub>a1</sub> /2	15A - 11B + 14C + 2 $\Delta_2$ + $\Delta_1$
a <sub>1</sub> <sup>2</sup> e <sub>2</sub> <sup>3</sup> e <sub>1</sub> <sup>1</sup>	<sup>3</sup> E <sub>1</sub>	3/2	15A - 29B + 12C + 3 $\Delta_2$ + $\Delta_1$
	<sup>1</sup> E <sub>1</sub>	1/2	15A - 17B + 14C + 3 $\Delta_2$ + $\Delta_1$
	<sup>3</sup> E <sub>2</sub>	3/2	15A - 29B + 12C + 3 $\Delta_2$ + $\Delta_1$
	<sup>1</sup> E <sub>2</sub>	1/2	15A - 29B + 14C + 3 $\Delta_2$ + $\Delta_1$
a <sub>1</sub> <sup>2</sup> e <sub>2</sub> <sup>4</sup>	<sup>1</sup> A <sub>1</sub>	k <sub>e1</sub>	15A - 20B + 15C + 2 $\Delta_2$

Configuration Interaction Matrices for <sup>3</sup>E<sub>1</sub> and <sup>1</sup>E<sub>1</sub> States

<sup>3</sup> E <sub>1</sub>	a <sub>1</sub> <sup>2</sup> e <sub>2</sub> <sup>3</sup> e <sub>1</sub> <sup>1</sup>	a <sub>1</sub> <sup>1</sup> e <sub>2</sub> <sup>4</sup> e <sub>1</sub> <sup>1</sup>
a <sub>1</sub> <sup>2</sup> e <sub>2</sub> <sup>3</sup> e <sub>1</sub> <sup>1</sup>	-29B + 12C + 3 $\Delta_2$ + $\Delta_1$	-2(6B) <sup>1/2</sup>
a <sub>1</sub> <sup>1</sup> e <sub>2</sub> <sup>4</sup> e <sub>1</sub> <sup>1</sup>	-2(6B) <sup>1/2</sup>	-13B + 12C + 2 $\Delta_2$ + $\Delta_1$
<sup>1</sup> E <sub>1</sub>	a <sub>1</sub> <sup>2</sup> e <sub>2</sub> <sup>3</sup> e <sub>1</sub> <sup>1</sup>	a <sub>1</sub> <sup>1</sup> e <sub>2</sub> <sup>4</sup> e <sub>1</sub> <sup>1</sup>
a <sub>1</sub> <sup>2</sup> e <sub>2</sub> <sup>3</sup> e <sub>1</sub> <sup>1</sup>	-17B + 14C + 3 $\Delta_2$ + $\Delta_1$	4(6B) <sup>1/2</sup>
a <sub>1</sub> <sup>1</sup> e <sub>2</sub> <sup>4</sup> e <sub>1</sub> <sup>1</sup>	4(6B) <sup>1/2</sup>	-11B + 14C + 2 $\Delta_2$ + $\Delta_1$

relative intensities of the pe bands associated with these states have been found to be generally valid.<sup>10</sup> Expressions for the energies and intensities of accessible ion states are given in Table II. As the two <sup>3</sup>E<sub>1</sub> and the two <sup>1</sup>E<sub>1</sub> ion states are close in energy, significant configuration interaction is likely, and the matrices determining the extent of this are also given in Table II.

**Comparison with Electronic Spectra of Related Cations.** Comparable information on the ordering and separation of ion states can be obtained from the electronic absorption spectrum of the related cation. These have been investigated for the d<sup>6</sup> cations of many iron cyclopentadienyl arene systems, for the cobaltocenium cation, and also for the neutral d<sup>6</sup> molecules ferrocene and ruthenocene. A review of the absorption spectra of d<sup>6</sup> metallocenes has been given by Warren.<sup>12</sup> Ferrocene has been studied most extensively, and there now seems general agreement as to the origin of most of the absorption bands. The other d<sup>6</sup> complexes show similar spectra and have analogous assignments. The results obtained on various d<sup>6</sup> systems are given in Table III in electronvolt in order to facilitate comparison with the pe results, together with the suggested assignments.

When a PE spectrum of a neutral molecule and the electronic absorption spectrum of its cation are compared, various considerations must be borne in mind. First, the photoionization process primarily leads to ion states which correspond to vacancies in the occupied orbitals of the molecule; states in which an electron has been promoted to an unoccupied orbital of the molecule, so-called shake-up processes, are much less probable, yet they are likely to be accessible by absorption spectroscopy. Secondly, the selection rules of absorption spectroscopy may restrict the accessible states in this type of experiment; for example, in the d<sup>6</sup> cations singlet-triplet transitions are "forbidden", whereas in the PE spectrum the bands corresponding to the low-lying triplet states are expected to

(10) Cauletti, C.; Green, J. C.; Kelly, M. R.; Powell, P.; van Tilborg, J.; Robbins, J.; Smart, J. *J. Electron Spectrosc.* 1980, 19, 327.

(11) Green, J. C. *Struct. Bonding (Berlin)* 1981, 43, 37.

(12) Warren, K. D. *Struct. Bonding (Berlin)* 1976, 27, 45.

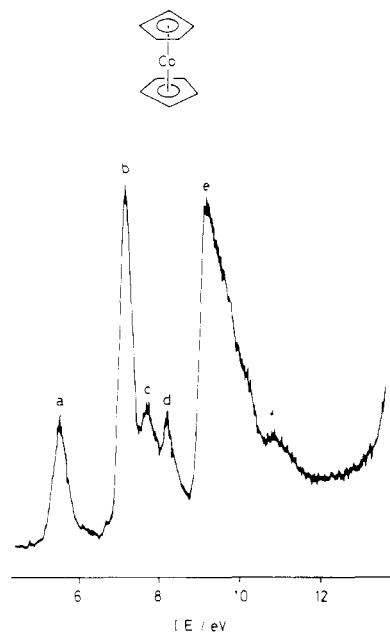


Figure 2. He I spectrum of  $\text{Co}(\eta\text{-C}_5\text{H}_5)_2$ .

be more intense than the singlet bands. Indeed, it is this sort of consideration that suggests that the absorption spectrum should be of considerable assistance in the assignment of the PE spectrum.

There must be a certain latitude in achieving a numerical fit between a PE spectrum and an absorption spectrum. Transitions in both tend to be identified by band maxima that are determined by the Franck-Condon envelopes for the two processes. As the initial states are different for the two experiments, these envelopes are not likely to correspond. Also some positions of the absorption bands are solvent dependent,<sup>3</sup> and this will further complicate any attempt to correlate them. Nevertheless the absorption spectra should give some guide to the limits of energy above the ground state of certain excited states.

Before we proceed to consideration of the iron sandwich compounds, it is informative to look in some detail at the isoelectronic cobaltocene that has been studied in some detail. The absorption spectrum of the cobaltocenium cation<sup>13</sup> shows a singlet-triplet transition at 2.68 eV and a series of three bands assigned to singlet-singlet d-d transitions at 3.00, 3.26, and 4.12 eV. These are followed by charge-transfer bands, the first of which has a maximum at 4.69 eV. Bands b-d in the PE spectrum of cobaltocene lie 1.62, 2.07, and 2.45 eV above the ground state.<sup>10</sup> If they are referred to the onset of the first PE band, ca. 0.25 eV should be added to all these values. Their intensity pattern and ligand field considerations have led to band b being assigned to  ${}^3E_1$  and  ${}^3E_2$  ion states and bands c and d to  ${}^1E_1$  and  ${}^1E_2$  ion states. (The other  ${}^3E_1$  state is probably coincident with the lowest  ${}^1E_1$  state.) Yet the most reasonable numerical coincidence is between band d of the PE spectrum and the low intensity triplet band of the absorption spectrum. A further anomaly is that from the PE spectral separation between the first band a and the first ligand  $e_1$  ionization band e of 3.1 eV, where we can be confident about both assignments, we would predict the onset of charge-transfer bands in the absorption spectrum to be around 3.1 eV. Yet charge-transfer bands are claimed to commence at 4.69 eV, and, to reconcile these two sets of data, it might seem necessary to reassign the first three

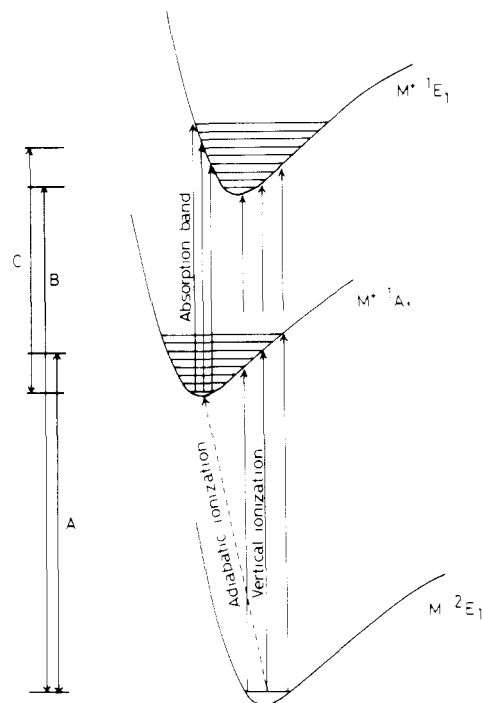


Figure 3. Schematic potential energy curves for the  $d^7$  ground-state sandwich molecule  $M$ , the ground state of the  $d^6$  cation  $M^+$ , and the lowest  ${}^1E_1$  excited state of  $M^+$ . Both the allowed absorption transitions and the PE processes are indicated by vertical arrows. The level scheme on the left indicates how the difference between the first vertical ionization energy  $A$  and the vertical ionization energy to the  ${}^1E_1$  ion state  $B$  can be significantly less than the maximum of the  ${}^1A_1 - {}^1E_1$  absorption band,  $C$ .

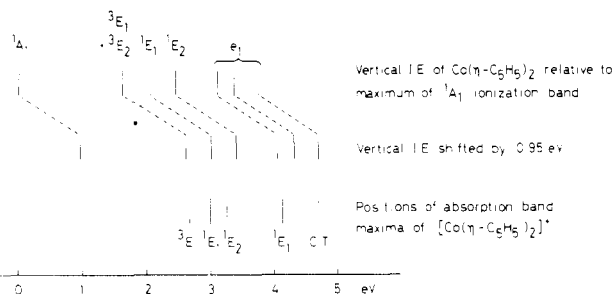


Figure 4. Diagram showing how a shift in origin of 0.95 eV results in close agreement between the maxima of the pe bands of  $\text{Co}(\eta\text{-C}_5\text{H}_5)_2$  and the absorption spectrum of  $[\text{Co}(\eta\text{-C}_5\text{H}_5)_2]^+$ .

spin-allowed bands to charge-transfer processes. This, however, does not appear to be a reasonable course of action.

An alternative method of rationalizing the data is to assume that the first pe band of cobaltocene does not show the adiabatic ionization energy. This may result if the molecular configuration is so different from that of the ground-state ion, that, on ionization, the molecular ion is only formed in vibrationally excited states. This occurs, for example, on photoionization of  $\text{Xe}_2$ ,<sup>14</sup> where there is a 0.6-eV shift between the adiabatic IE and the onset of the Franck-Condon distribution. Metal-carbon distances for the two species have been determined and are found to be 2.119 Å for  $\text{Co}(\eta\text{-C}_5\text{H}_5)_2$  and 2.029 Å for  $[\text{Co}(\eta\text{-C}_5\text{H}_5)(\eta\text{-C}_5\text{H}_4\text{COOH})]^+$ .<sup>15</sup> It is also the case that the excited states of the cation where an electron has been promoted to the  $e_{1g}^*$  orbital are likely to have longer

(13) Sohn, Y. S.; Hendrickson, D. N.; Gray, H. B. *J. Am. Chem. Soc.* 1974, 96, 3603.

(14) Dehmer, P. M.; Dehmer, J. L. *J. Chem. Phys.* 1978, 68, 3462.

(15) Haaland, A. *Acc. Chem. Res.* 1979, 12, 418.

Table III. Electronic Absorption Spectra for d<sup>6</sup> Sandwich Compounds (eV)

compd	<sup>1</sup> A <sub>1</sub> - <sup>3</sup> E <sub>1</sub>	<sup>1</sup> E <sub>1</sub>	<sup>1</sup> E <sub>2</sub>	<sup>1</sup> E <sub>1</sub>	CT		
Fe(η-C <sub>5</sub> H <sub>5</sub> ) <sub>2</sub>	2.33	2.69	2.96	3.80	4.65	5.14	6.17
[Co(η-C <sub>5</sub> H <sub>5</sub> ) <sub>2</sub> ] <sup>+</sup>	2.68	3.00	3.26	4.12	4.69		
[Fe(η-C <sub>5</sub> H <sub>5</sub> )(η-C <sub>6</sub> Me <sub>6</sub> )] <sup>+</sup>		2.70	3.06	3.81	4.66	5.05	
[Fe(η-C <sub>5</sub> Me <sub>5</sub> )(η-C <sub>6</sub> Me <sub>6</sub> )] <sup>+</sup>		2.70	3.03	3.79	4.37	4.77	

Photoelectron Band Maxima Relative to First Band Maximum (eV)

compd	<sup>3</sup> E	<sup>1</sup> E <sub>1</sub>	<sup>1</sup> E <sub>2</sub>	e <sub>1</sub>		
[Co(η-C <sub>5</sub> H <sub>5</sub> ) <sub>2</sub> ] <sup>+</sup>	1.62	2.07	2.45	3.10	3.38	3.75
[Fe(η-C <sub>5</sub> H <sub>5</sub> )(η-C <sub>6</sub> Me <sub>6</sub> )] <sup>+</sup>	1.46	2.18	2.46	3.21	3.5	4.1
[Fe(η-C <sub>5</sub> Me <sub>5</sub> )(η-C <sub>6</sub> Me <sub>6</sub> )] <sup>+</sup>	1.53	2.11	2.43	2.99	3.5	4.37

metal-ring distances than the ground state, so that the 0-0 transitions may not be observed optically. In Figure 3 we represent these points schematically showing possible potential energy surfaces for the ground state of the molecule M, the ground state of the molecular ion M<sup>+</sup>, and the lowest <sup>1</sup>E<sub>1</sub> state of the molecular ion.

In Figure 4 we demonstrate diagrammatically that a shift of 0.95 eV results in good agreement between the maxima of the two categories of bands. It is likely therefore that the adiabatic first ionization potential of Co(η-C<sub>5</sub>H<sub>5</sub>)<sub>2</sub> is significantly lower than 5.3 eV, which represents the onset of the first pe band.

If the band profiles are treated semiclassically, we are able to obtain a quantitative estimate of the full width at half maximum (fwhm) of both the first pe band and the d-d absorption bands of the cation. All potential surfaces are assumed to be parabolic, and the 0.95-eV energy discrepancy is therefore assumed to be half due to the difference between the adiabatic and vertical IE and half due to the difference between the 0-0 and the most probable transition of the absorption spectrum. The symmetric ring-metal stretching frequency is assumed to be 300 cm<sup>-1</sup> in all states. The fwhm, 2u, is given by the expression<sup>16</sup>

$$u = [2\hbar\omega\Delta E \coth(\hbar\omega/2kT)]^{1/2}$$

leading to a predicted fwhm of 0.47 eV. This is in reasonable agreement with the experimental value of 0.4 eV.

In a similar manner the difference in metal-ring distance between the neutral cobaltocene and the cobaltocenium cation of 0.17 Å is predicted.

It should be noted that Jahn-Teller distortions of the neutral molecule (and presumably the E ion states) are fully dynamic at room temperature; otherwise the distortions involved would also be expected to contribute to the energy discrepancy.

A similar problem arises in fitting the absorption spectra of the iron(II) cyclopentadienyl arene cations to the PE spectra of their respective parent molecules. As can be seen from Figures 1 and 2, there is a strong resemblance between the PE spectra of the d<sup>7</sup> iron(I) sandwich compounds II and IV and that of cobaltocene: we therefore propose a similar assignment (see Table I). The optical spectra of the iron sandwich cations<sup>3,16</sup> resemble those of ferrocene and the cobaltocenium cation; however, no singlet-triplet transition has as yet been detected, the lowest energy bands being assigned to the first <sup>1</sup>A<sub>1</sub> - <sup>1</sup>E<sub>1</sub> transition. To fit the two sets of spectral maxima, a shift of 0.6 eV is needed, for example, Fe(η-C<sub>5</sub>Me<sub>5</sub>)(η-C<sub>6</sub>Me<sub>6</sub>). A startling implication of this is that the adiabatic ionization

Table IV. Ligand Field Parameters (eV) of d<sup>6</sup> Sandwich Molecules (Assuming C = 4B)

compd	Δ <sub>1</sub>	Δ <sub>2</sub>	B
Fe(η-C <sub>5</sub> H <sub>5</sub> ) <sub>2</sub>	2.71	0.88	0.048
[Co(η-C <sub>5</sub> H <sub>5</sub> ) <sub>2</sub> ] <sup>+</sup>	2.88	0.8	0.04
[Fe(η-C <sub>5</sub> H <sub>5</sub> )(η-C <sub>6</sub> Me <sub>6</sub> )] <sup>+</sup>	2.71	0.95	0.047
[Fe(η-C <sub>5</sub> Me <sub>5</sub> )(η-C <sub>6</sub> Me <sub>6</sub> )] <sup>+</sup>	2.6	0.9	0.046
From PE Spectra			
[Co(η-C <sub>5</sub> H <sub>5</sub> ) <sub>2</sub> ] <sup>+</sup>	1.92	1.0	0.06
[Fe(η-C <sub>5</sub> Me <sub>5</sub> )(η-C <sub>6</sub> Me <sub>6</sub> )] <sup>+</sup>	1.83	1.1	0.06
[Fe(η-C <sub>5</sub> H <sub>5</sub> )(η-C <sub>6</sub> Me <sub>6</sub> )] <sup>+</sup>	1.71	1.3	0.05

energy of this molecule may well lie below even 3.95 eV though a lower limit of 3.6 eV may be set.

We predict that a singlet-triplet transition will occur at 2.12 eV (17.2 × 10<sup>3</sup> cm<sup>-1</sup>).

The spectra of I and III differ slightly (see Figure 1). They also contain a very low ionization energy band assignable to the <sup>1</sup>A<sub>1g</sub> ground state, but the subsequent d bands show a different intensity pattern. It seems likely in these cases that the two lowest triplet states are more separated and a suggested assignment is given in Table I.

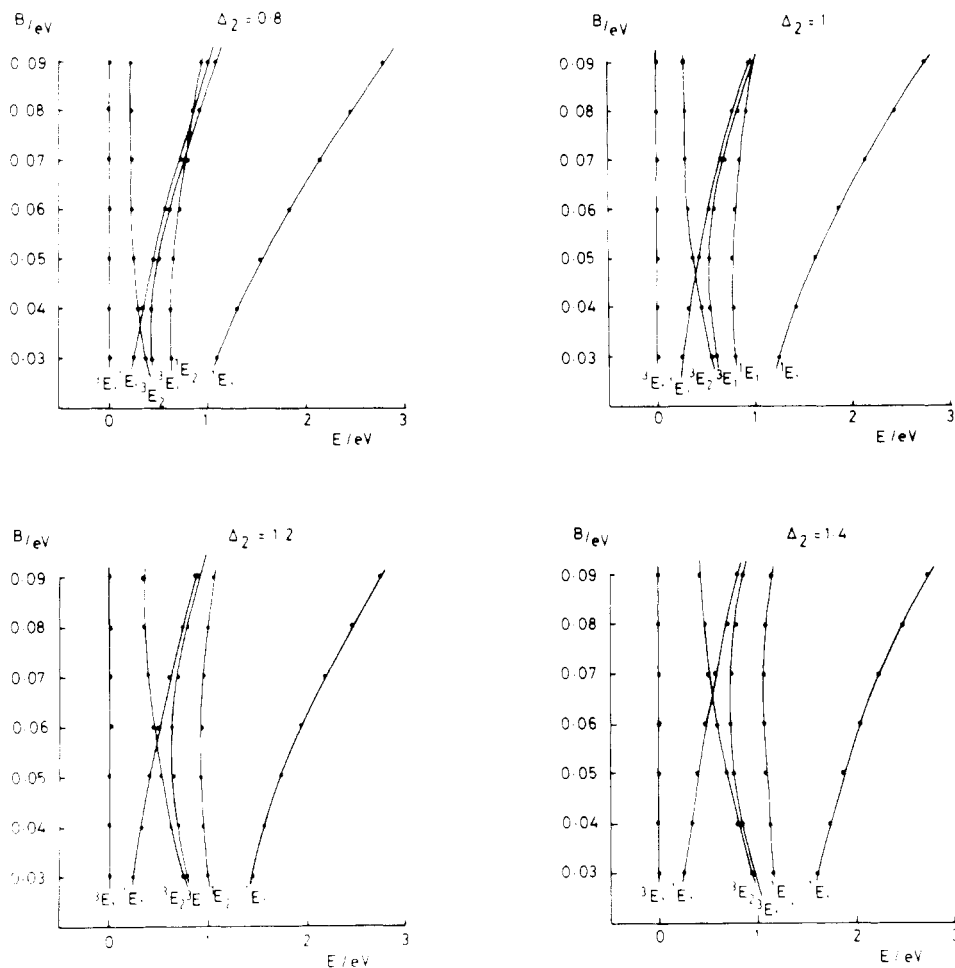
**Ligand Field Treatments.** The above considerations demonstrate that ligand field treatments of relative separation of bands are likely to be inadequate when states arising from configurations differing in the population of the e<sub>1</sub>\* set of orbitals are concerned. However, it is legitimate to use ligand field arguments to back up assignments in the very restricted case of the states arising from the e<sub>2</sub><sup>3</sup>a<sub>1</sub><sup>2</sup>e<sub>1</sub>\*<sup>1</sup> and e<sub>2</sub><sup>4</sup>a<sub>1</sub><sup>1</sup>e<sub>1</sub>\*<sup>1</sup> configurations, where for both the initial states and the final states it may reasonably be assumed that there is very little change in bond length.

We have carried out ligand field calculations (including configuration interaction) for a range of Δ<sub>2</sub> values from 0.7 to 1.7 and B values from 0.03 to 0.09 (assuming C = 4B) to investigate possible splitting patterns for the 2 × <sup>3</sup>E<sub>1g</sub>, <sup>3</sup>E<sub>2g</sub>, 2 × <sup>1</sup>E<sub>1g</sub>, and <sup>1</sup>E<sub>2g</sub> ion states. The expressions used are given in Table II, and some examples of calculated energies are shown graphically in Figure 5. The splitting of the lower <sup>3</sup>E<sub>1g</sub> and the <sup>1</sup>E<sub>2g</sub> states is relatively insensitive to B and largely depends on Δ<sub>2</sub>, increasing with the latter. It is also the case that smaller values of Δ<sub>2</sub> lead to a closer approach of the <sup>3</sup>E<sub>1g</sub> and <sup>3</sup>E<sub>2g</sub> ion states. We therefore expect the appearance of the "cobaltocene" like spectrum to be correlated with a smaller separation of the first triplet band and the highest observable d band if our assignments are correct. (The higher <sup>1</sup>E<sub>1g</sub> state is expected in all cases to lie under the ligand π bands, and intensity considerations bear this out.) That this is the case can be seen by inspection of the data of Tables I and II.

Ligand field parameters which give a reasonable fit to the PE spectrum of Co(η-C<sub>5</sub>H<sub>5</sub>)<sub>2</sub>, Fe(η-C<sub>5</sub>H<sub>5</sub>)(η-C<sub>6</sub>Me<sub>6</sub>), and

(16) Ballhausen, C. J. "Molecular Electronic Structures of Transition Metal Complexes"; McGraw Hill: London, 1979; p 127.

(17) Morrison, W. H.; Ho, E. Y.; Hendrickson, D. N. *Inorg. Chem.* 1975, 14, 500.



**Figure 5.** Results of some ligand field calculations on the  $d^7$  ion states  ${}^3E_1$ ,  ${}^3E_1$ ,  ${}^1E_1$ ,  ${}^1E_1$ ,  ${}^3E_2$ , and  ${}^1E_2$ .

$F(\eta^5-C_5H_5)(\eta^2-C_6Me_6)$  are given in Table IV. It can be seen that the values for  $\Delta_1$  differ substantially from those deduced from the optical spectra, but this is just a consequence of the lack of direct matching between the two sets of spectra. The discrepancy between the two values deduced for  $\Delta_1$ , is similar to the shift necessary to correlate the two spectra. As the ligand field parameters inferred appear so technique sensitive, we do not feel justified in using them to draw comparative bonding conclusions.

**Reactivity Implications.** The very negative redox potentials of these  $d^7$  molecules may be accounted for by their extremely low first ionization potentials. Comparison of the trends in first ionization energies and half-wave reduction potentials (relative to the standard calomel electrode) are given. Whereas the first ionization energies

compd	IV	II	I	III
first IE, eV	4.21	4.34	4.68	4.72
$F_{1/2}$ , V (aqueous LiOH (0.1 N))	-1.87	-1.66	-1.79	
$E_{1/2}$ , V (DMF)	1.75	-1.67	-1.55	-1.37

vary in the expected manner with the inductive effect of the ring substituents, the half-wave potentials in aqueous LiOH solution are of a different order, suggesting that solvation effects may well contribute to variations in the latter. We therefore also recorded the  $E_{1/2}$  values in DMF where solvation effects should be smaller. In this solvent the  $E_{1/2}$  values correlate (though not in a linear manner)

with the first IE, showing the latter to be the dominant factor in determining the trend in this case.

**$d^6$  Complexes.** In these compounds V–VIII the six-membered ring is bound to the metal through only five carbon atoms.<sup>5</sup> This is the commonly established mode of bonding for cyclohexadienyl ligands<sup>18</sup> and has also been shown to be the case for VII by an X-ray study.<sup>6</sup> In VII, the ring carbon attached to the methylene unit is clearly uncoordinated, the folding dihedral angle of the pentamethyl benzyl ligand being  $32.6^\circ$ , which is less than the range commonly found for coordinated cyclohexadienyl ligands ( $39$ – $50^\circ$ ).<sup>19</sup> The exocyclic  $CH_2$  group is twisted by  $11^\circ$  due to the steric demand of the ortho-methyl groups. The molecular symmetry in the compounds is low but may reasonably be approximated as  $C_s$ . As a consequence, there are no formal degeneracies in the MO structure. We expect a marked splitting of the  $\pi_2$  and  $\pi_3$  levels of the cyclohexadienyl system and also possibly splitting of the  $d_{xy}$  and  $d_{x^2-y^2}$  (previously  $e_2$ ) orbitals and the  $e_1(\pi)$  levels of the cyclopentadienyl ring. A MO scheme is given in Figure 8.

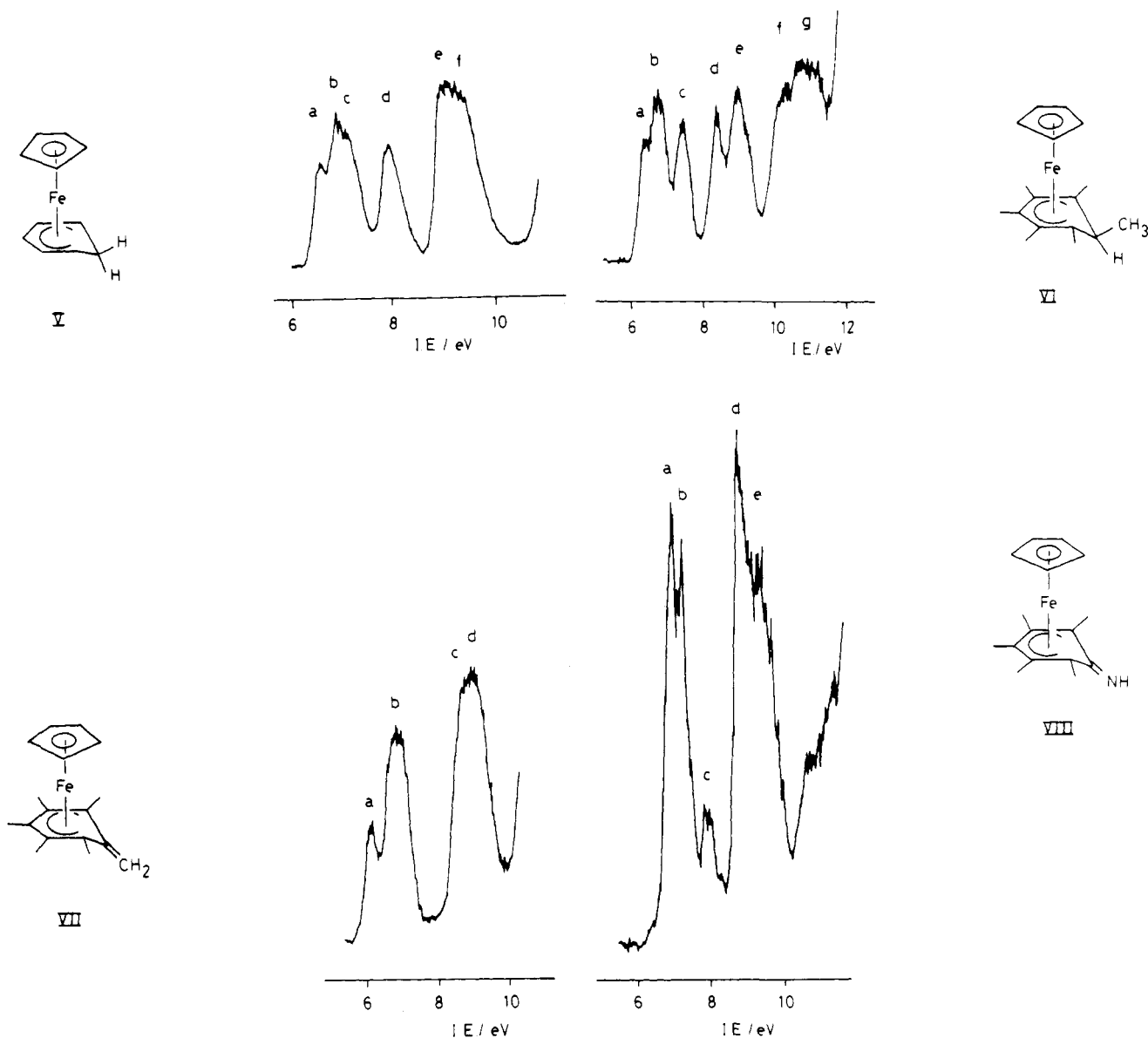
The PE spectrum of  $Mn(\eta^5-C_6H_7)(CO)_3$  serves as a guide to the expected splitting of the hexadienyl  $\pi$  levels. Ionization energies are found to be 8.59 ( $\pi_3$ ), 10.27 ( $\pi_2$ ) and probably 11.7 ( $\pi_1$ ).<sup>20</sup>

The spectrum of  $Fe(\eta^5-C_5H_5)(\eta^5-C_6H_7)$  (He I spectrum shown in Figure 6) shows several bands (a–h) in the low-energy region. Intensity variations with photon energy

(19) Hoffman, R.; Hoffman, P. *J. Am. Chem. Soc.* 1976, 98, 598.

(20) Whitesides, T. H.; Lichtenberger, D. L.; Budnik, R. A. *Inorg. Chem.* 1975, 14, 68.

(18) Churchill, M. R.; Scholer, F. R. *Inorg. Chem.* 1969, 8, 1950.



**Figure 6.** He I and He II spectra of  $\text{Fe}(\eta\text{-C}_5\text{H}_5)(\eta^5\text{-C}_6\text{H}_7)$ , V,  $\text{Fe}(\eta\text{-C}_5\text{H}_5)(\eta^5\text{-C}_6\text{Me}_6\text{H})$ , VI,  $\text{Fe}(\eta\text{-C}_5\text{H}_5)(\eta^5\text{-C}_6\text{Me}_5\text{CH}_2)$ , VII, and  $\text{Fe}(\eta\text{-C}_5\text{H}_5)(\eta^5\text{-C}_6\text{Me}_5\text{NH})$ , VIII.

point to bands a–c being largely metal d in character, whereas the remainder, d–h, show primarily ligand character. If we assign band d to the  $\pi_3$  ionization, the IE difference from the comparable band in the spectrum of  $\text{Mn}(\eta^5\text{-C}_6\text{H}_7)(\text{CO})_3$  is 0.64 eV. A similar shift for  $\pi_2$  places it in the e,f band system, which must also comprise the cyclopentadienyl  $e_1(\pi)$  ionizations. Considerable mixing between the  $\pi_2$  orbital and the cyclopentadienyl upper orbitals is therefore likely. Further ionization bands at 11.12 and 11.52 eV may be associated with ionization from the  $\pi_1$  orbital and the upper  $\sigma$  orbitals of the hexadienyl ring.

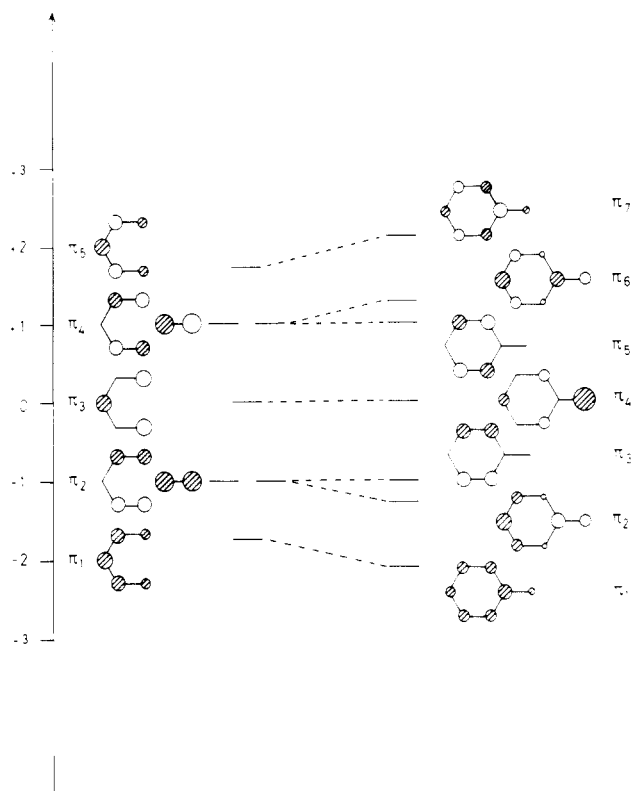
The d-band shows three components as expected, indicating that the perturbation of the hexadienyl ring is sufficient to lift the degeneracies of the metal  $e_2$  orbitals; however, it is not possible to distinguish the component ionizations ( $2 \times a' + a''$ ).

The spectrum of  $\text{Fe}(\eta\text{-C}_5\text{H}_5)(\eta^5\text{-C}_6\text{Me}_6\text{H})$  (VI) may be assigned by analogy. Substitution by the six methyl groups would be expected to have most effect on the  $\pi$ -ionizations of the hexadienyl ligand.<sup>11</sup> The PE spectrum of VI (see Figure 6) shows a d band, a and b, followed by five ligand bands, c–g. If c is a  $\pi_3$  ionization as is likely, its shift on permethylation is 0.68 eV. A comparable shift for  $\pi_2$

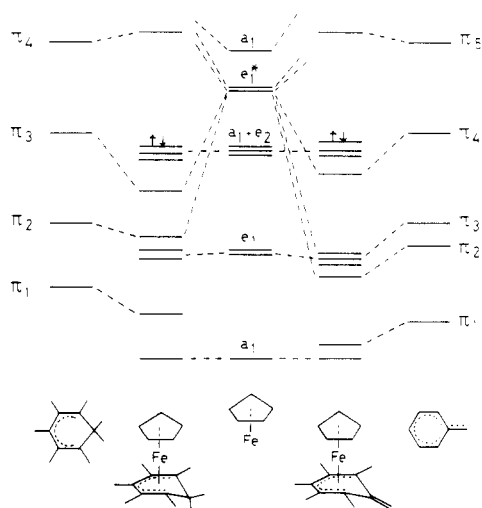
renders assignment to b and d probable, suggesting the cyclopentadienyl  $e_1(\pi)$  ionizations may be attributed to band e, as their IE should be less susceptible to methylation of the other ring. Bands f and g at 10.05 and 10.5 eV can be correlated with  $\pi_1$  and upper  $\sigma$  orbitals as before, though ionization of the ring methyl groups may well occur in this region.<sup>11</sup>

The compounds  $\text{Fe}(\eta\text{-C}_5\text{H}_5)(\eta^5\text{-C}_6\text{Me}_5\text{CH}_2)$ , VII, and  $\text{Fe}(\eta\text{-C}_5\text{H}_5)(\eta^5\text{-C}_6\text{Me}_5\text{NH})$ , VIII, have exocyclic double bonds, thus leading to an additional  $\pi$  ionization band. The additional  $\pi$  orbital is expected to perturb the  $\pi$  levels of the hexadienyl ring. We may gain a good impression of the probable extent and nature of this perturbation by correlating the Hückel MO of a pentadienyl fragment and a simple olefin with those of the benzyl radical.<sup>21</sup> This is illustrated diagrammatically in Figure 7. The geometrical deformations of the benzyl group in the complex suggest that the MO structure of the ligand is best represented by an intermediate situation where the external double bond is conjugated with the ring system but not quite to the extent as occurs in the benzyl radical.

(21) Coulson, C. A.; Streitwieser, A., Jr. "Dictionary of Electron Calculations"; Pergamon Press: Oxford, 1965.



**Figure 7.** Correlation between the Hückel MO energies of the pentadienyl radical and ethylene and those of the benzyl radical.<sup>21</sup>



**Figure 8.** Schematic MO diagram for  $\text{Fe}(\eta\text{-C}_5\text{H}_5)(\eta^5\text{-C}_6\text{Me}_6\text{H})$  and  $\text{Fe}(\eta\text{-C}_5\text{H}_5)(\eta^5\text{-C}_6\text{Me}_6\text{CH}_2)$ .

The PE spectra of VII and VIII are shown in Figure 6. Intensity analysis of the spectrum of VII suggests that band a is a d ionization and band b comprises the two remaining d bands together with ionization from the upper  $\pi$  ligand level  $\pi_4$ . Band d with shoulder c is relatively more intense than the corresponding band in the spectra of V and VI and consists of the cyclopentadienyl  $e_1$  ionization together with the  $\pi_3$  and the  $\pi_2$  band. Band e is assigned to  $\pi_1$  and the ring methyl groups.

Similar assignments may be made for VIII; see Table I. Both d and  $\pi$  bands are shifted to higher IE. This may be attributed to the withdrawing effect of the more elec-

tronegative nitrogen atom exocyclic to the six-membered ring.

It is interesting to look at the ionization energy shifts between VI and VII, consequent upon replacing the  $\text{sp}^3$  H and  $\text{CH}_3$  with  $\text{CH}_2$ . The ionization energy of the d electrons is rather similar in the two complexes, suggesting that any repulsive interaction with the external double bond has been averted by the distortion of the ligand. Perhaps the most notable difference is that the IE of the highest  $\pi$  level is less for VII than VI and is comparable to those of the d electrons. Examination of the schematic MO in Figure 7 suggests that for the pentamethylbenzyl ligand the principal metal ligand bonding interactions will be with  $\pi_2$  and  $\pi_3$  rather than  $\pi_4$ , even though the latter is the HOMO of the ligand. The upper occupied  $\pi$  orbital has very little electron density on the five binding carbons compared to that of the pentadienyl fragment. This will reduce overlap with the metal d orbitals and consequently result in weaker binding. This is a likely explanation for the reduction in IE of this level. It is noteworthy that  $\pi_4$  of the benzyl radical shows a high degree of localization on the methylene carbon: that this also occurs in the complexed benzyl ligand is demonstrated by its tendency to act as nucleophile through this carbon. Also, to judge from the IE there would not be much preference for electrophilic attack on the metal rather than the ligand. Thus the low IE of the top ligand level is consistent with the nucleophilic behavior of the molecule.

The  $a''$  symmetry orbital  $\pi_2$  in VI is unperturbed to a first approximation by introduction of the external double bond and correlates with  $\pi_3$  of VII. We therefore could anticipate rather similar IE for this orbital in the two complexes. If our assignment of band d in the spectrum of VI to  $\pi_2$  is correct it seems that this orbital is slightly stabilized in VII (ca. 0.5-eV change in IE). It should be remembered that the  $\pi$  system in VII has fewer alkyl substituents than that of VI. The general shift of the center of gravity of this complex band system is consistent with this and the introduction of the extra  $\pi$  level in VII at lower binding energies. The  $\pi_1$  ionization band also occurs at higher energy in VII than in VI.

### Conclusions

1. The  $d^7$  iron cyclopentadienyl arene complexes have extremely low ionization energies consistent with their reducing ability. That of  $\text{Fe}(\eta\text{-C}_5\text{Me}_5)(\eta\text{-C}_6\text{Me}_6)$  is the lowest molecular ionization energy yet reported.
2. The assignment of the photoelectron bands of the  $d^7$  complexes and those of cobaltocene may only be reconciled with the optical spectra of their cations by assuming either that the adiabatic transition is not observed for the first band in the former cases or that 0-0 transitions are not observed in the latter cases or both.
3. The interpretation of the photoelectron spectra of the  $d^6$  complexes suggests a high electron density on the methylene carbon of  $\text{Fe}(\eta\text{-C}_5\text{H}_5)(\eta^5\text{-C}_6\text{Me}_6\text{CH}_2)$  consistent with its reactivity as a nucleophile.

**Acknowledgment.** We thank the S.R.C. and the C. N.R.S. for financial support. Also we thank Dr. A. Cox for helpful discussions.

**Registry No.** I, 54688-69-6; II, 71713-62-7; III, 83528-73-8; IV, 83782-94-9; V, 39529-31-2; VI, 80183-08-0; VII, 70414-93-6; VIII, 82879-26-3.



# Hydrogenation of Trimetallic Clusters of the Iron Triad Containing Bridging Carbyne Ligands. Reductive Cleavage of a Triply Bridging Carbyne

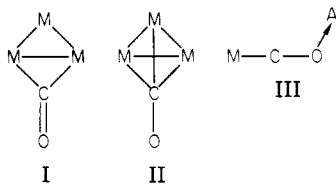
Jerome B. Keister,\* Martin W. Payne, and Michael J. Muscatella

Department of Chemistry, The State University of New York at Buffalo, Buffalo, New York 14214, and the Corporate Research Laboratories, Exxon Research and Engineering Company, Linden, New Jersey 07036

Received September 3, 1982

The clusters  $\text{HM}_3(\mu\text{-COMe})(\text{CO})_{10}$  (1) (a, M = Fe; b, M = Ru; c, M = Os), prepared by methylation of the corresponding  $\text{HM}_3(\mu\text{-CO})(\text{CO})_{10}$  monoanion, react with hydrogen to give  $\text{H}_3\text{M}_3(\mu_3\text{-COMe})(\text{CO})_9$  (2). This process may be reversed under carbon monoxide. For these and other related carbyne-containing clusters the relative stabilities of  $\text{HM}_3(\mu\text{-CX})(\text{CO})_{10-n}\text{L}_n$  and  $\text{H}_3\text{M}_3(\mu_3\text{-CX})(\text{CO})_{9-n}\text{L}_n$  are found to depend upon (i) the metal, (ii) the carbyne substituent X, and (iii) the ligands L. Thus, although 2a is unstable under ambient conditions, reverting nearly quantitatively to 1a, the substituted derivative  $\text{H}_3\text{Fe}_3(\mu_3\text{-COMe})(\text{CO})_7(\text{SbPh}_3)_2$  (5a) can be isolated in fair yield by hydrogenation of 1a in the presence of triphenylantimony. Similarly, although  $\text{HRu}_3(\mu\text{-CN}(\text{Me})\text{CH}_2\text{Ph})(\text{CO})_{10}$  (4) does not react with hydrogen to give a stable product, in the presence of 4 equiv of triphenylantimony  $\text{H}_3\text{Ru}_3(\mu_3\text{-CN}(\text{Me})\text{CH}_2\text{Ph})(\text{CO})_6(\text{SbPh}_3)_3$  (6) can be prepared in good yield. These observations are rationalized in terms of the relative importance of  $\text{M}_3\text{-CX}$  and  $\text{C-X}$   $\pi$ -bonding interactions and the relative metal-carbonyl and metal-hydrogen bond strengths. Under more severe conditions reductive cleavage of the carbyne ligand as  $\text{CH}_3\text{X}$  can be achieved. At 130 °C and 3.5 MPa of 1:1 carbon monoxide-hydrogen, 2b decomposes to dimethyl ether and  $\text{Ru}_3(\text{CO})_{12}$ . This process represents overall reduction of a carbonyl ligand by molecular hydrogen and is made possible by the activation of this carbonyl by methylation. The trends observed for cluster hydrogenation may have implications for potential Lewis acid activation of cluster-bound carbonyl ligands.

Catalytic reduction of metal-coordinated carbon monoxide by hydrogen is presently the object of intensive research because of the importance of carbon monoxide-hydrogen gas mixtures as basic petrochemical feedstocks. Two of the strategies that have been suggested for activation of carbon monoxide toward reduction are (1) reduction of the C-O bond order through formation of  $\eta^1\text{-}\mu$ - or  $\eta^1\text{-}\mu_3$ -bridging carbonyls (schematic I or II, respectively) and (2) reduction of the C-O bond order by coordination of a Lewis acid to the oxygen of a metal-bound carbonyl ligand (III) in order to activate the carbonyl carbon toward



nucleophilic attack by hydride.<sup>1,2</sup> We have sought to exploit both strategies by examining the reduction behavior of metal cluster-bound carbonyl ligands that are simultaneously O-complexed to a Lewis acid. A number of complexes having this feature have been reported.<sup>3-12</sup> Of

particular interest to us were two systems based upon trimetallic clusters, Lewis acid adducts of the  $\text{HFe}_3(\mu\text{-CO})(\text{CO})_{10}$  and  $\text{Co}_3(\mu_3\text{-CO})(\text{CO})_9$  monoanions.

Complexes of the  $\text{HFe}_3(\mu\text{-CO})(\text{CO})_{10}$  anion with Lewis acids  $\text{HNET}_3^+$ ,  $\text{BF}_3$ , and  $\text{Na}^+$  have been characterized by infrared and <sup>13</sup>C NMR spectroscopy by Todd and Wilkinson, who concluded that for each adduct the Lewis acid is coordinated to the oxygen of the bridging carbonyl.<sup>4</sup> Later Shriver and co-workers showed that the carbonyl oxygen of this anion is sufficiently nucleophilic to be methylated with methyl fluorosulfonate to give  $\text{HFe}_3(\mu\text{-COMe})(\text{CO})_{10}$ ; further work by the same group showed that protonation of the anion initially produces highly unstable  $\text{HFe}_3(\mu\text{-COH})(\text{CO})_{10}$ .<sup>8</sup>

The  $\text{Co}_3(\mu_3\text{-CO})(\text{CO})_9$  anion<sup>9</sup> also displays high nucleophilicity for the triply bridging carbonyl.<sup>5,10</sup> The O-methylated derivative  $\text{Co}_3(\mu_3\text{-COMe})(\text{CO})_9$  has been prepared.<sup>11</sup> Recently the syntheses and structures of adducts with  $\text{UCp}_3^5$  and  $\text{TiClCp}_2^6$  have been described. Protonation of this anion gives  $\text{Co}_3(\mu_3\text{-COH})(\text{CO})_9$ .<sup>12</sup>

We set out to examine the hydrogenation behavior of Lewis acid complexes of the type described above. However, due to the expected difficulty in maintaining the  $\text{M-C-O} \rightarrow \text{A}$  structure in solution, we have begun our work by studying the reactions of the O-methylated complexes  $\text{HFe}_3(\mu\text{-COMe})(\text{CO})_{10}$  and  $\text{Co}_3(\mu_3\text{-COMe})(\text{CO})_9$ , believing that these species would give more tractable products because of their high stability to heat and to air, high solubility, and relatively inert O-Me bond. Recognizing

\* Address correspondence at the State University of New York at Buffalo.

(1) (a) R. Eisenberg and D. E. Henderiksen, *Adv. Catal.*, **28**, 79-172 (1979) and references therein; (b) E. L. Muetterties and J. Stein, *Chem. Rev.*, **79**, 479 (1979).

(2) (a) A. Wong, M. Harris, and J. D. Atwood, *J. Am. Chem. Soc.*, **102**, 4259 (1980); (b) C. Van der Wande, J. A. Van Doorn, and C. Masters, *ibid.*, **101**, 1633 (1979); (c) L. I. Shoer and J. Schwartz, *ibid.*, **99**, 5831 (1977); (d) G. C. Demitras and E. L. Muetterties, *ibid.*, **99**, 2796 (1977).

(3) (a) S. Onaka and N. Furnich, *J. Organomet. Chem.*, **173**, 77 (1979); (b) J. S. Kristoff, and D. F. Shriver, *Inorg. Chem.*, **13**, 499 (1974); (c) A. Alich, N. J. Nelson, D. Strobe, and D. F. Shriver, *ibid.*, **11**, 2976 (1972); (d) N. J. Nelson, N. E. Kime, and D. F. Shriver, *J. Am. Chem. Soc.*, **91**, 5173 (1969).

(4) J. R. Wilkinson, and L. J. Todd, *J. Organomet. Chem.*, **118**, 199 (1976).

(5) B. Stutte and G. Schmid, *J. Organomet. Chem.*, **155**, 203 (1978).

(6) G. Schmid, V. Batzel, and B. Stutte, *J. Organomet. Chem.*, **113**, 67 (1976).

(7) (a) D. F. Shriver, D. Lehman, and D. Strobe, *J. Am. Chem. Soc.*, **97**, 1594 (1975); (b) H. A. Hodali and D. F. Shriver, *Inorg. Chem.*, **18**, 1236 (1979).

(8) H. A. Hodali, D. F. Shriver, and C. A. Ammlung, *J. Am. Chem. Soc.*, **100**, 5239 (1978).

(9) (a) S. A. Fieldhouse, B. H. Freeland, C. D. M. Mann, and R. J. O'Brien, *J. Chem. Soc., Chem. Commun.*, 181 (1970); (b) G. Fachinetti, *ibid.*, 396 (1979).

(10) C. D. M. Mann, A. J. Cleland, S. A. Fieldhouse, B. H. Freeland, and R. J. O'Brien, *J. Organomet. Chem.*, **24**, C61 (1970).

(11) D. Seyferth, J. E. Hallgren, and P. L. K. Hung, *J. Organomet. Chem.*, **50**, 265 (1973).

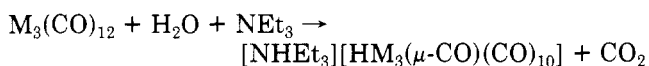
(12) (a) G. Fachinetti, *J. Chem. Soc., Chem. Commun.*, 396 (1979); (b) G. Fachinetti, S. Pucci, P. F. Zanazzi, and U. Methong, *Angew. Chem.*, **91**, 657 (1979); *Angew. Chem., Int. Ed. Engl.*, **18**, 619 (1979); (c) H.-N. Adams, G. Fachinetti, and J. Strahle, *ibid.*, **20**, 125 (1981).

the greater stabilities of clusters of the second- and third-row metals, we also have examined the hydrogenation reactions of the analogous  $\text{HM}_3(\mu\text{-COMe})(\text{CO})_{10}$  clusters for  $\text{M} = \text{Ru}$  and  $\text{Os}$ . To the extent that these complexes can be considered as acid-base adducts between cluster-bound carbonyls and the strongly acidic methyl cation, their reactivity should represent the tendencies of adducts of weaker Lewis acids.

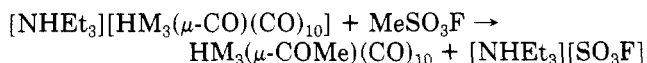
We describe here the hydrogenation of  $\text{HM}_3(\mu\text{-COMe})(\text{CO})_{10}$ ,  $\text{M} = \text{Fe}$ ,  $\text{Ru}$ , and  $\text{Os}$ , to give the corresponding  $\text{H}_3\text{M}_3(\mu_3\text{-COMe})(\text{CO})_9$ , the first functionalized methylidyne clusters of the iron triad, and the further reaction of  $\text{H}_3\text{Ru}_3(\mu_3\text{-COMe})(\text{CO})_9$  with carbon monoxide to give dimethyl ether and  $\text{Ru}_3(\text{CO})_{12}$ .<sup>13</sup> This chemistry demonstrates the facile interconversion of the  $\mu$ - and the  $\mu_3\text{-CO-A}$  ligands. The nature of the  $\mu\text{-CX}$  ( $\text{X} = \text{O}^-$ ,  $\text{OR}$ , and  $\text{NR}_2$ ) ligand and its effect in the reactivities of these clusters are also discussed.

## Results

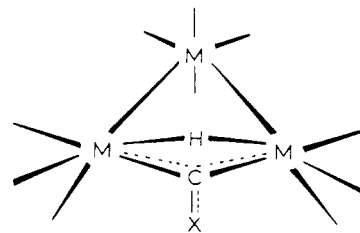
**Syntheses of  $\text{HM}_3(\mu\text{-COMe})(\text{CO})_{10}$  (1b, M = Ru; 1c, M = Os).** The O-methylated carbonyl cluster  $\text{HFe}_3(\mu\text{-COMe})(\text{CO})_{10}$  (1a) was prepared by Shriver and co-workers by reaction of  $[\text{NEt}_4][\text{HFe}_3(\mu\text{-CO})(\text{CO})_{10}]$  with methyl fluorosulfonate.<sup>7a</sup> Because of the higher stabilities of ruthenium and osmium clusters, we considered it more desirable to study hydrogenation reactions of  $\text{HM}_3(\mu\text{-COMe})(\text{CO})_{10}$  (1b, M = Ru; 1c, M = Os), which had not been reported at the time we began this work. At that time  $[\text{NMe}_4][\text{HOs}(\mu\text{-CO})(\text{CO})_{10}]$  had been prepared by reduction of  $\text{Os}_3(\text{CO})_{12}$  with potassium hydroxide in methanol,<sup>14</sup> but the ruthenium anion was poorly characterized, having been prepared by Knight and Mays through reduction of  $\text{Ru}_3(\text{CO})_{12}$  with the  $\text{Mn}(\text{CO})_5$  anion.<sup>15</sup> Thus, we wanted to develop a convenient and general synthesis for these trimetallic anions from the corresponding  $\text{M}_3(\text{CO})_{12}$ , which could be coupled with a methylation step to give the desired clusters. Using a modification of the synthesis of  $[\text{NH}_4][\text{HFe}_3(\mu\text{-CO})(\text{CO})_{10}]$ ,<sup>16</sup> we were able to prepare  $[\text{NH}_4][\text{HM}_3(\mu\text{-CO})(\text{CO})_{10}]$  in essentially quantitative yield by reacting  $\text{M}_3(\text{CO})_{12}$  with triethylamine and water in tetrahydrofuran at 60 °C:



This preparation is particularly convenient for the subsequent methylation because the only nonvolatile components of the product solution are the metal species. Thus, the synthesis of  $\text{HM}_3(\mu\text{-COMe})(\text{CO})_{10}$  can be carried out in one pot without isolation of the air-sensitive  $\text{HM}_3(\mu\text{-CO})(\text{CO})_{10}$  monoanions:



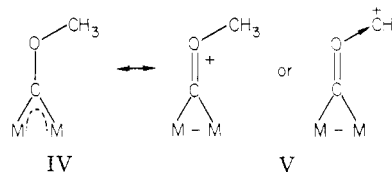
Shortly after we prepared these clusters, Lewis, Johnson, and co-workers<sup>17</sup> and Ford and co-workers<sup>18</sup> independently reported syntheses of the  $\text{HRu}_3(\mu\text{-CO})(\text{CO})_{10}$  monoanion, and reports also appeared describing syntheses similar to



**Figure 1.** Structure of  $\text{HM}_3(\mu\text{-CX})(\text{CO})_{10}$  (1a,  $\text{M} = \text{Fe}$ ,  $\text{X} = \text{OMe}$ ; 1b,  $\text{M} = \text{Ru}$ ,  $\text{X} = \text{OMe}$ ; 1c,  $\text{M} = \text{Os}$ ,  $\text{X} = \text{OMe}$ ; 3,  $\text{M} = \text{Ru}$ ,  $\text{X} = \text{NHCH}_2\text{Ph}$ ; 4,  $\text{M} = \text{Ru}$ ,  $\text{X} = \text{N}(\text{Me})\text{CH}_2\text{Ph}$ ).

ours for 1b<sup>19</sup> and 1c.<sup>20</sup> Details of the characterizations of these compounds have been reported. X-ray diffraction studies of 1b<sup>19,21</sup> have confirmed that the structure is very similar to that found for 1a<sup>7a</sup> (Figure 1).

The bonding within the  $\mu\text{-COMe}$  ligand can be described as arising primarily from two contributing resonance structures, IV and V. Structure IV represents the COMe



ligand as a bridging carbyne, while structure V expresses the multiple character of the C-OMe bond. In the most general case of a bridging carbonyl complexed to a Lewis acid, the relative importance of structure IV increases as the acid strength increases. The  $\mu\text{-COMe}$  ligand is revealed by infrared and <sup>13</sup>C NMR spectroscopy and by the crystal structures of 1a and 1b to be best described as a bridging carbyne. The stretching frequency attributed to the C-OMe bond is ca. 250  $\text{cm}^{-1}$  lower than the bridging carbonyl stretch of the anionic precursor (1a,<sup>7b</sup> 1452, 1b,<sup>19</sup> 1415, and 1c, 1456  $\text{cm}^{-1}$  vs.  $[\text{NR}_4][\text{HM}_3(\mu\text{-CO})(\text{CO})_{10}]$ ,  $\text{M} = \text{Fe}$ ,<sup>4</sup> 1718,  $\text{Ru}$ ,<sup>17</sup> 1691, and  $\text{Os}$ ,<sup>14</sup> 1667  $\text{cm}^{-1}$ ) and is consistent with a C-OMe bond order between 1 and 2. The <sup>13</sup>C NMR signal for the bridging carbon of 1 is shifted far downfield from the chemical shift of the bridging carbonyl of the corresponding  $\text{HM}_3(\mu\text{-CO})(\text{CO})_{10}$  anion (1a, 356.5,<sup>7b</sup> 1b, 366.5,<sup>19</sup> and 1c, 352.2<sup>20</sup> ppm vs.  $[\text{NR}_4][\text{HM}_3(\mu\text{-CO})(\text{CO})_{10}]$ ,  $\text{M} = \text{Fe}$ , 285.7,<sup>4</sup>  $\text{Ru}$ , 286.2,<sup>17</sup> 281.8<sup>18</sup> ppm) to a value similar to those found for mononuclear metal carbenes and carbynes.<sup>22</sup> Furthermore, the C-OMe bond length of 1.30 Å<sup>7a,19,21</sup> is intermediate between the values expected for single (1.40-Å) and double (1.20-Å) C-O bonds. The planar nature of the  $\text{M}_2(\mu\text{-COC})$  group and the restricted rotation about the  $\mu\text{-CO}$  bond (13.5 kcal for  $\text{Os}$ ,<sup>20</sup> ca. 10 kcal for  $\text{Ru}$ <sup>19</sup>) indicate that some multiple-bond character remains.

(Alkylamino)- and (dialkylamino)carbyne derivatives can also be prepared. The cluster  $\text{HRu}_3(\mu\text{-CNMe}_2)(\text{CO})_{10}$  has been prepared by reaction of  $\text{Ru}_3(\text{CO})_{12}$  with  $\text{Sn}(\text{CH}_2\text{NMe}_2)_2\text{Me}_3$ .<sup>23</sup> The osmium analogues  $\text{HOs}_3(\mu\text{-CNHR})(\text{CO})_{10}$  have been prepared by reaction of  $\text{H}_2\text{Os}_3(\text{CO})_{10}$  with isocyanides  $\text{CNR}$  ( $\text{R} = \text{CH}_2\text{Ph}$ ,  $\text{Me}$ ,  $\text{CMe}_3$ ); methylation of these compounds at nitrogen gives the corresponding  $\text{HOs}_3(\mu\text{-CN}(\text{Me})\text{R})(\text{CO})_{10}$ .<sup>24</sup> The clusters

(13) A preliminary report of this work has appeared: J. B. Keister, *J. Chem. Soc., Chem. Commun.*, 214 (1978).

(14) C. R. Eady, J. J. Guy, B. F. G. Johnson, J. Lewis, M. C. Malatesta, and G. M. Sheldrick, *J. Chem. Soc., Dalton Trans.*, 1358 (1978).

(15) J. Knight and M. J. Mays, *J. Chem. Soc., Dalton Trans.*, 1022 (1972).

(16) W. McFarlane and G. Wilkinson, *Inorg. Synth.*, 8, 178 (1966).

(17) B. F. G. Johnson, J. Lewis, P. R. Raithby, and G. Suss, *J. Chem. Soc., Dalton Trans.*, 1356 (1979).

(18) C. Ungerman, V. Laudis, S. A. Moya, H. Cohen, H. Walker, R. G. Pearson, R. G. Rinker, and P. C. Ford, *J. Am. Chem. Soc.*, 101, 5922 (1979).

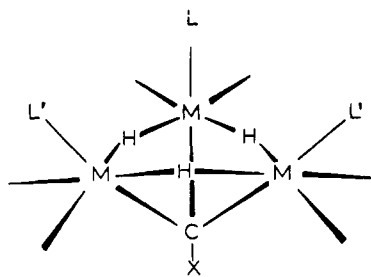
(19) B. F. G. Johnson, J. Lewis, A. G. Orpen, P. R. Raithby, and G. Suss, *J. Organomet. Chem.*, 173, 187 (1979).

(20) P. D. Gavens and M. J. Mays, *J. Organomet. Chem.*, 162, 389 (1978).

(21) G. B. Ansell and J. B. Keister, unpublished results.

(22) E.g. 331.0 ppm for the carbyne carbon of  $\text{Os}(\text{C}_6\text{H}_4\text{CH}_3)(\text{CO})_2(\text{PPh}_3)_2^+$ : W. R. Roper, J. M. Waters, L. J. Wright, and F. Van Meurs, *J. Organomet. Chem.*, 201, C27 (1980).

(23) M. R. Churchill, B. G. DeBoer, F. J. Rotella, E. W. Abel, and R. J. Rowley, *J. Am. Chem. Soc.*, 97, 7158 (1975).



**Figure 2.** Structure of  $H_3M_3(\mu_3-CX)(CO)_{9-n}L_n$  (**2a**,  $M = Fe$ ,  $X = OMe$ ,  $L = L' = CO$ ; **2b**,  $M = Ru$ ,  $X = OMe$ ,  $L = L' = CO$ ; **2c**,  $M = Os$ ,  $X = OMe$ ,  $L = L' = CO$ ; **5a**,  $M = Fe$ ,  $X = OMe$ ,  $L = CO$ ,  $L' = SbPh_3$ ; **6**,  $M = Ru$ ,  $X = N(Me)CH_2Ph$ ,  $L = L' = SbPh_3$ ).

$HOs_3(\mu-CNMeR)(CO)_{10}$  ( $R = Me, CH_2Ph$ ) have also been prepared from  $Os_3(CO)_{12}$  with trimethyl- or benzyldimethylamine at high temperatures.<sup>25</sup> Iron analogues have been prepared by several methods,<sup>26</sup> but a general synthesis from  $HF_3(\mu-CO)(CO)_{11}^-$  and isocyanides CNR, followed by methylation, has recently appeared.<sup>27</sup>

Using the method of Howell and Mathur,<sup>27</sup> we have prepared  $HRu_3(\mu-CNHCH_2Ph)(CO)_{10}$  (**3**) and  $HRu_3(\mu-CN(Me)CH_2Ph)(CO)_{10}$  (**4**). Direct reaction of  $[NH_4Et_3][HRu_3(\mu-CO)(CO)_{10}]$  with benzyl isocyanide in dichloromethane gives **3** in up to 77% yield. The N-methylated derivative **4** is obtained in 90% yield from **3** by reaction with sodium methoxide and methyl iodide in methanol. Characterizations of **3** and **4** are straightforward. The mass spectrum of each displays the molecular ion and usual fragmentation pattern. The infrared and  $^1H$  NMR spectra of **3** and **4** are very similar to those of their osmium analogues.<sup>24,25</sup> The substantial double-bond character for the  $\mu-C-N$  bond results in restricted rotation and the methylene protons for each compound are diastereotopic, giving rise to an AB pattern in the  $^1H$  NMR spectrum. For **3** the  $^1H$  NMR spectrum consists of signals at  $\tau$  1.4 (br, 1  $H_A$ ), 2.67 (m, 5 H), 5.02 (dd, 1  $H_B$ ), 5.15 (dd, 1  $H_C$ ), and 24.70 (d, 1  $H_D$ ) with  $J_{AB} = 1.5$  Hz,  $J_{AC} = 3.4$  Hz,  $J_{BC} = 14.7$  Hz, and  $J_{AD} = 1.4$  Hz; these signals are respectively assigned to the NH proton, the protons on the phenyl ring, the two diastereotopic methylene protons, and the bridging hydride ligand. The spectrum of **4** is as expected for the N-methylated analogue:  $\tau$  2.7 (m, 5 H), 4.61 (d, 1  $H_A$ ), 4.96 (d, 1  $H_B$ ), 6.43 (s, 3 H), and 24.74 (s, 1 H) with  $J_{AB} = 14.7$  Hz, assigned respectively to the phenyl protons, the two diastereotopic methylene protons, the methyl group, and the hydride ligand.

**Cluster Hydrogenation.** With the methylated clusters in hand we examined their reactions with hydrogen. When hydrogen is bubbled through a solution of **1b** in refluxing hexane, the infrared absorptions due to the starting material gradually diminish and are replaced with bands at 2106 (vw), 2078 (s), 2075 (s), 2036 (vs), 2028 (m), 2018 (s), 2014 (m), and 2000 (w)  $cm^{-1}$ . After 2 h a single, orange, crystalline product, characterized as  $H_3Ru_3(\mu_3-COMe)(CO)_9$  (**2b**), is isolated in 90% yield after recrystallization from methanol.

The methylidyne cluster **2b** (Figure 2) is proposed to be isostructural with  $H_3Ru_3(\mu_3-CX)(CO)_9$  ( $X = Me$ ,<sup>28</sup>

$CH_2CMe_3$ ,<sup>29</sup> and  $Cl$ <sup>30</sup>) for which the structures have been established by X-ray crystallography. The  $^1H$  NMR spectrum of **2b** consists of two singlets of equal intensities at  $\tau$  6.23 and 27.53, which are assigned to the methyl protons and three equivalent bridging hydrides, respectively. The electron-impact mass spectrum displays the molecular ion ( $m/e$  608 ( $^{104}Ru_3$ )), followed by ions resulting from stepwise loss of nine carbonyls and the COMe unit;  $Ru_3C^+$  ions are also observed. The compound is mildly air-sensitive, particularly in solution, decomposing to a dark red, sparingly soluble material that has not been characterized.

Similarly, **1c** reacts with hydrogen at 1 atm and 120 °C in decane to give  $H_3Os_3(\mu_3-COMe)(CO)_9$  (**2c**) in 75% yield after 1 h. The infrared spectrum of this product in cyclohexane solution consists of only terminal carbonyl absorptions: 2107 (w), 2077 (s), 2074 (s), 2022 (vs), 2013 (m), 2008 (m), and 1995 (w)  $cm^{-1}$ . The  $^1H$  NMR spectrum in deuteriochloroform consists of two singlets of equal intensities at  $\tau$  6.20 and 28.58.<sup>31</sup> As for **2b**, the electron-impact mass spectrum displays the molecular ion ( $m/e$  900 ( $^{192}Os_3$ )) and ions resulting from sequential loss of nine carbonyls and the COMe moiety, down to the bare  $Os_3^+$  ion; intense, doubly charged trinuclear ions are also observed.

Additional evidence for the proposed structure is obtained from the proton-decoupled  $^{13}C$  NMR spectrum of **2c**. In deuteriochloroform (0.2 M chromium(III) acetylacetonate) this consists of resonances at 69.3 (1 C), 166.4 (3 C), 167.0 (6 C), and 205.2 (1 C) ppm downfield from  $Me_4Si$ . These signals are assigned to the methyl carbon, three equivalent axial carbonyls, the six equivalent radical carbonyls, and the methylidyne carbon,<sup>34</sup> respectively. The  $^{13}C$  resonances for the carbonyls of  $H_3Ru_3(\mu_3-CMe)(CO)_9$  have been reported to occur at 190.1 (6 C) and 189.3 (3C) ppm; the methylidyne carbon resonance was not observed.<sup>39</sup>

While the iron analogue **1a** does react with hydrogen (1 atm) at 60 °C to give a new species, as evidenced by infrared spectroscopy, this product is unstable under ambient conditions, reverting nearly quantitatively to the starting cluster. The instability of the new species seems to be related to both temperature and hydrogen pressure, and factors affecting its stability are currently under investigation. Strictly on the basis of the similarity of the

(28) G. M. Sheldrick and J. P. Yesinowski, *J. Chem. Soc., Dalton Trans.*, 873 (1975).

(29) M. Castiglioni, G. Gervasio, and E. Sappa, *Inorg. Chim. Acta*, **49**, 217 (1981).

(30) N. J. Zhu, C. Lecomte, P. Coppens, and J. B. Keister, *Acta Crystallogr., Sect. B*, **B38**, 1286 (1982).

(31)  $^1H$  NMR spectrum of  $H_3Os_3(\mu_3-CMe)(CO)_9$ , isostructural with the ruthenium analogue,<sup>32</sup> consists of equally intense singlets at  $\tau$  5.55 and 28.58.<sup>33</sup>

(32) J. P. Yesinowski and D. Bailey, *J. Organomet. Chem.*, **65**, C27 (1974).

(33) (a) A. J. Deeming and M. Underhill, *J. Chem. Soc., Chem. Commun.*, 227 (1973); (b) A. J. Deeming and M. Underhill, *J. Organomet. Chem.*, **42**, C60 (1972).

(34) Previously, the only reports of chemical shifts for methylidyne carbons bridging three metal atoms were 118.4 ppm for  $H_3Os_3(\mu_3-CH)(CO)_9$ <sup>35</sup> and 255–310 ppm for  $Co_3(\mu_3-CR)(CO)_9$ .<sup>36</sup> More recently values of 303.2 ppm for  $[Rh_3(\mu_3-CH)(CO)_2Cp_3]^+$ <sup>37</sup> and 295.8 ppm for  $Mo_3O(\mu_3-CCH_3)(OAc)_6(H_2O)_3$ <sup>38</sup> have been reported.

(35) (a) R. B. Calvert and J. R. Shapley, *J. Am. Chem. Soc.*, **99**, 5225 (1977); (b) *ibid.*, **100**, 6544 (1978).

(36) D. Seyferth, C. S. Eschbach, and M. O. Nestle, *J. Organomet. Chem.*, **97**, C11 (1975).

(37) W. A. Hermann, J. Plank, D. Riedel, M. L. Ziegler, K. Weidenhammer, E. Guggolz, and B. Balbach, *J. Am. Chem. Soc.*, **103**, 63 (1981).

(38) A. Bino, F. A. Cotton, and Z. Dori, *J. Am. Chem. Soc.*, **103**, 243 (1981).

(39) A. J. Canty, B. F. G. Johnson, J. Lewis, and J. R. Norton, *J. Chem. Soc., Chem. Commun.*, 1331 (1972).

(24) (a) R. D. Adams and N. M. Golembeski, *J. Am. Chem. Soc.*, **101**, 2579 (1979). (b) J. B. Keister, Ph.D. thesis, University of Illinois (1978).

(25) (a) C. Choo Yin and A. J. Deeming, *J. Organomet. Chem.*, **133**, 123 (1977).

(26) (a) J. Altman and N. Welman, *J. Organomet. Chem.*, **165**, 353 (1979); (b) R. Greatrex, N. N. Greenwood, I. Rhee, M. Ryang, and S. Tsutsumi, *J. Chem. Soc., Chem. Commun.*, 1193 (1970); (c) I. Rhee, M. Ryang, and S. Tsutsumi, *ibid.*, 455 (1968).

(27) J. A. S. Howell and P. Mathur, *J. Chem. Soc., Dalton Trans.*, 43 (1982).

new bands in the infrared spectrum of the product solution to the spectra of **2b** and **2c**, the unstable iron product is proposed to be  $\text{H}_3\text{Fe}_3(\mu_3\text{-COMe})(\text{CO})_9$  (**2a**). From subtraction of the absorptions due to **1a** (2096 (m), 2049 (s), 2038 (vs), 2018 (s), 2008 (sh), 1992 (m), 1980 (m)  $\text{cm}^{-1}$ ) the infrared spectrum of **2a** displays terminal carbonyl absorptions at 2060 (s), 2023 (s), and 2004 (m)  $\text{cm}^{-1}$ ; other bands may be masked by those of **1a**. Very recently a stable iron methylidyne cluster  $\text{H}_3\text{Fe}_3(\mu_3\text{-CMe})(\text{CO})_9$  has been isolated and characterized by X-ray crystallography.<sup>40</sup>

The stability of the hydrogenated cluster product can be increased by substituting group 5 donor ligands for carbonyls. Hydrogenation of **1a** at 1 atm and 60–70 °C in the presence of 3 equiv of triphenylantimony gives a dark brown, crystalline product, characterized as  $\text{H}_3\text{Fe}_3(\mu_3\text{-COMe})(\text{CO})_7(\text{SbPh}_3)_2$  (**5a**; Figure 2), in 22% yield after chromatography. The infrared spectrum of this compound displays only terminal carbonyl stretches; the  $^1\text{H}$  NMR spectrum in deuteriochloroform consists of resonances at  $\tau$  2.83 (m, 30 H), 5.49 (s, 3 H), 31.15 (t, 1 H), and 32.02 (d, 2 H,  $J$  5.3 Hz), assigned respectively to the aryl protons of the  $\text{SbPh}_3$  ligands, the methyl group, the hydride bridging the  $(\text{Ph}_3\text{Sb})(\text{OC})_3\text{FeFe}(\text{CO})_3(\text{SbPh}_3)$  vector, and the two hydrides bridging to the  $\text{Fe}(\text{CO})_3$  moiety. Both spectra of **5a** are very similar to those of  $\text{H}_3\text{Ru}_3(\mu_3\text{-COMe})(\text{CO})_7(\text{SbPh}_3)_2$  (**5b**), which can be prepared by direct substitution on **2b**.

The NMR spectra in the hydride region for the substituted products  $\text{H}_3\text{M}_3(\mu_3\text{-CX})(\text{CO})_{9-n}\text{L}_n$  are particularly useful for characterization. The monosubstituted derivatives display a triplet (1 H) close to the chemical shift of the unsubstituted parent cluster and a doublet (2 H) about 0.5 ppm to lower field with a coupling constant of 3–5 Hz; the disubstituted derivatives display a triplet (1 H) about 0.5 ppm downfield from a doublet (2 H,  $J$  = ca. 3 Hz), both of which are downfield from the signals due to the monosubstituted derivative; the trisubstituted clusters display a singlet hydride resonance, which is slightly downfield from the lowest field hydride resonance of the disubstituted derivative. Thus, the  $^1\text{H}$  NMR spectra of  $\text{H}_3\text{Ru}_3(\mu_3\text{-COMe})(\text{CO})_{9-n}(\text{SbPh}_3)_n$  in deuteriochloroform are as follows:  $n = 3$ ,  $\tau$  25.78 (s, 3 H);  $n = 2$ , 26.15 (t, 1 H), 26.74 (d, 2 H,  $J$  = 3.4 Hz);  $n = 1$ , 26.91 (d, 2 H), 27.58 (t, 1 H,  $J$  = 3.4 Hz);  $n = 0$ , 27.50 (s, 3 H). Resonances due to hydrides bridging to metal atoms substituted with a group 5 ligand are shifted downfield relative to hydrides bridging to unsubstituted metal atoms. The spectra of the mono- and disubstituted derivatives are consistent with either axial coordination of the group 5 donor ligand, which would make two of the hydrides chemically equivalent, or with radial coordination and fluxional exchange of the group 5 ligand between the two radial sites on the metal atom. The isoelectronic  $\text{Co}_3(\mu_3\text{-CMe})(\text{CO})_8(\text{P}(\text{Me})_3)_3$  was shown to have radially coordinated phosphite ligands.<sup>41</sup> However, very recently  $\text{H}_3\text{Os}_3(\mu_3\text{-CMe})(\text{CO})_8(\text{PPh}_3\text{Et})$  was shown by  $^{13}\text{C}$  NMR spectroscopy to have an axially coordinated phosphine ligand;<sup>42</sup> the similarity between the  $^1\text{H}$  NMR spectra of this compound and  $\text{H}_3\text{Ru}_3(\mu_3\text{-COMe})(\text{CO})_8\text{L}$  implies that the group 5 donor ligands in all these complexes are axially coordinated as well.

Although **4** does not react with hydrogen to form the analogous  $\text{H}_3\text{Ru}_3(\mu_3\text{-CN}(\text{Me})\text{CH}_2\text{Ph})(\text{CO})_9$  up to the temperature of decomposition, in the presence of 4 equiv of

triphenylantimony and at 60–70 °C for 8 h under 1 atm of hydrogen red-orange  $\text{H}_3\text{Ru}_3(\mu_3\text{-CN}(\text{Me})\text{CH}_2\text{Ph})(\text{CO})_6(\text{SbPh}_3)_3$  **6** can be isolated after recrystallization from methanol in good yield. This product is isostructural (Figure 2) with  $\text{H}_3\text{Ru}_3(\mu_3\text{-CX})(\text{CO})_6\text{L}_3$  (X = Cl, Ph, OMe; L =  $\text{AsPh}_3$ ,  $\text{SbPh}_3$ ) that can be prepared by direct reaction of the corresponding  $\text{H}_3\text{Ru}_3(\mu_3\text{-CX})(\text{CO})_9$  with L,<sup>43</sup> and its infrared spectrum is very similar to those of the latter molecules. The  $^1\text{H}$  NMR spectrum of **6** consists of a singlet hydride resonance at  $\tau$  25.58 (3 H) and signals due to the carbyne ligand at  $\tau$  5.25 (s, 2 H) and 6.82 (s, 3 H), in addition to resonances due to phenyl protons.

**Reductive Elimination of Dimethyl Ether.** The objective of our study was the ultimate reduction of a cluster-bound carbonyl ligand. Conversion of  $\text{HM}_3(\mu\text{-COMe})(\text{CO})_{10}$  to  $\text{H}_3\text{M}_3(\mu_3\text{-COMe})(\text{CO})_9$  results in a small reduction in the C–OCH<sub>3</sub> bond order, as shown by the lowering of the C–OCH<sub>3</sub> stretching frequency from ca. 1450 to 1170  $\text{cm}^{-1}$ . Perhaps more importantly the reaction also introduces into the cluster the two hydrogen atoms needed to complete the reduction of the bridging CO unit. Under more severe conditions reductive elimination of dimethyl ether can be induced. When **2b** was heated in toluene at 130 °C under carbon monoxide and hydrogen (1:1, 3.5 MPa) for 23 h, mass spectroscopic analysis of the portion of the gas phase that could be trapped out by venting the autoclave slowly through a U trap at –196 °C showed a significant quantity of dimethyl ether. The predominant metal-containing product was  $\text{Ru}_3(\text{CO})_{12}$  (89% isolated yield). However, traces of  $\text{Ru}(\text{CO})_5$  collected in the trap along with the volatile products. A more careful analysis of the gases was performed after the reaction was repeated by using paraffin oil as solvent; mass spectrometric analysis of the condensable gases showed traces of 1,2-dimethoxyethane and methyl formate, in addition to a considerable amount (ca. 10% yield) of dimethyl ether. Quantitative analysis was not attempted under these conditions because of the difficulty of recovering dimethyl ether quantitatively at this pressure. Hydrogen is required in this reaction because of the equilibrium between **1b** and **2b**.

Hydrogenation of (methylidyne)tricobalt clusters has been investigated under photolytic conditions by Geoffroy and Epstein.<sup>44</sup> Photolysis of  $\text{Co}_3(\mu_3\text{-CH})(\text{CO})_9$  under a carbon monoxide–hydrogen atmosphere yielded methane and  $\text{Co}_2(\text{CO})_8$ . We had independently observed that  $\text{Co}_3(\mu_3\text{-CCO}_2\text{CH}_3)(\text{CO})_9$  reacted with hydrogen (1 atm) in refluxing toluene to give methyl acetate and metallic cobalt, but we observed no new cluster products or intermediates by infrared spectroscopy. Geoffroy and Epstein have proposed homolytic cleavage of Co–Co bonds upon photolysis as a possible mechanism leading to activation of hydrogen, although photolysis also leads to carbon monoxide dissociation. Our experiments were performed at temperatures sufficiently high for either carbon monoxide dissociation or metal–metal bond cleavage to be occurring. In considering the origin of the trace of 1,2-dimethoxyethane observed in thermolysis of **2b**, it is interesting to note that thermolysis of  $\text{Co}_3(\mu_3\text{-CC}_6\text{H}_5)(\text{CO})_9$  in the absence of hydrogen has been reported to give small amounts of diphenylacetylene.<sup>45</sup> Very recently Fachinetti has reported that reaction of  $\text{Co}_3(\mu_3\text{-COMe})(\text{CO})_9$  with carbon monoxide and hydrogen yields  $\text{MeOCH}_2\text{CH}_2\text{OH}$  (60%),  $\text{Me}_2\text{O}$  (10%), and  $\text{MeOCH}_2\text{CH}_2\text{CHO}$  (10%).<sup>46</sup>

(40) K. S. Wong, and T. P. Fehlner, *J. Am. Chem. Soc.*, **103**, 966 (1981).

(41) P. A. Dawson, B. H. Robinson, and J. Simpson, *J. Chem. Soc., Dalton Trans.*, 1762 (1979).

(42) S. C. Brown and J. Evans, *J. Chem. Soc., Dalton Trans.*, 1049 (1982).

(43) Zuraidah Abdul Raman and J. B. Keister, unpublished results.

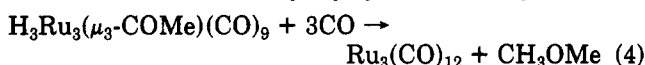
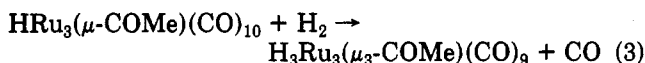
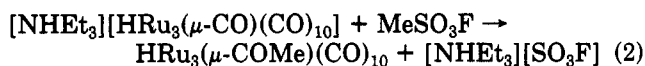
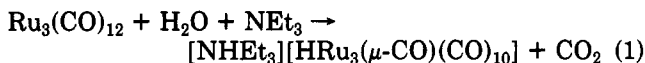
(44) G. L. Geoffroy, and R. A. Epstein, *Inorg. Chem.*, **16**, 2795 (1977).

(45) I. U. Khand, G. R. Knox, P. L. Pauson, and W. E. Watts, *J. Organomet. Chem.*, **73**, 383 (1974).

## Discussion

Our original objective was to determine the reactivity of O-alkylated carbonyl ligands toward reducing agents, primarily molecular hydrogen. The reaction sequence (Scheme I) for conversion of carbon monoxide on  $\text{Ru}_3(\text{C}-\text{O})_{12}$  to dimethyl ether (eq 1-4) effects the reduction of a carbonyl ligand by hydrogen under mild conditions due to the activation of the carbonyl by "coordination" of the strongly acidic methyl cation. This type of activation is, of course, impractical for catalytic reduction of carbon monoxide since the "acid" stoichiometrically reacts with the reduced carbonyl product. However, activation might also be achieved by using an acid that could be recovered economically. Therefore, it may be useful to consider the role of the methyl group in facilitating carbonyl reduction.

## Scheme I



Methylation of the bridging carbonyl of the  $\text{HM}_3(\mu\text{-CO})(\text{CO})_{10}$  anion, as previously discussed, effectively reduces the C-O bond order from ca. 2 to 1.5. In comparing the C-O stretching frequencies and  $^{13}\text{C}$  chemical shifts for the bridging carbonyl of the  $\text{HFe}_3(\mu\text{-CO})(\text{CO})_{10}$  anion in the presence of Lewis acids, Wilkinson and Todd noted that, as the acid strength increased, the C-O stretching frequency lowered and the  $^{13}\text{C}$  resonance shifted downfield.<sup>4</sup> Thus, the values for the  $\mu\text{-CO}$  stretching frequency and  $\mu\text{-}^{13}\text{C}$  NMR signal for the anion with noncoordinating cations ( $\text{NEt}_4^+$ , 1709  $\text{cm}^{-1}$ ;  $(\text{Ph}_3\text{P})_2\text{N}^+$ , 285.7 ppm) are shifted with the hydrogen-bonding triethylammonium cation (1639  $\text{cm}^{-1}$ , 301.3 ppm), and in the presence of boron trifluoride the  $^{13}\text{C}$  chemical shift (355.1 ppm) is nearly as far downfield as for  $\text{HFe}_3(\mu\text{-COMe})(\text{CO})_{10}$  (356.5 ppm).<sup>7</sup> Shriver<sup>47</sup> has attributed the trend of decreasing C-O stretching frequency with increasing acid strength to decreasing C-O bond order because of increasing delocalization of electrons from metal d orbitals to the carbonyl  $\pi^*$  orbital.

The first step in the reduction of the activated carbonyl is oxidative addition of molecular hydrogen to give  $\text{H}_3\text{M}_3(\mu_3\text{-COMe})(\text{CO})_9$  (2), a reaction which, in addition to introducing the two remaining hydrogen atoms needed to complete reduction of the COMe ligand, also reduces the C-OMe bond order still further.<sup>48</sup> Although several examples of additions of molecular hydrogen by clusters are known,<sup>49</sup> neither mechanistic nor systematic studies of cluster hydrogenations have been reported. In this work we have established three factors which influence hydrogenation of  $\text{HM}_3(\mu\text{-CX})(\text{CO})_{10-n}\text{L}_n$ : (i) the identity of the metal, (ii) the nature of the CX moiety, and (iii) the nature of the other ligands on the cluster.

Only limited data are available at this time concerning the influence of the metal upon cluster hydrogenation. In our series, 1a does hydrogenate to 2a, but 2a is unstable at ambient temperatures and reverts to 1a; on the other

hand, elevated temperatures are required to carbonylate 2b and 2c back to 1b and 1c. In this case it would appear that the relative stability of  $\text{H}_3\text{M}_3(\mu_3\text{-COMe})(\text{CO})_9$ , rather than the reactivity of  $\text{HM}_3(\mu_3\text{-COMe})(\text{CO})_{10}$ , is responsible for this difference. For different carbyne groups CX coordinated to the same metal framework, the trend of increasing ease of hydrogenation is  $\text{X} = \text{O}^- < \text{NR}_2 < \text{OR}$ . On the other hand, for  $\text{X} = \text{Cl}, \text{Br}, \text{H}, \text{Ph}, \text{alkyl}, \text{and } \text{CO}_2\text{R}$ , the analogues  $\text{HM}_3(\mu\text{-CX})(\text{CO})_{10}$  cannot be prepared by carbonylation of the known  $\text{H}_3\text{M}_3(\mu_3\text{-CX})(\text{CO})_9$ .<sup>50</sup> Here again, the relative stabilities of  $\text{HM}_3(\mu\text{-CX})(\text{CO})_{10}$  and  $\text{H}_3\text{M}_3(\mu_3\text{-CX})(\text{CO})_9$  may be responsible. Demethylation of  $\text{H}_3\text{Ru}_3(\mu_3\text{-COMe})(\text{CO})_9$  by reaction with amines even at room temperature does not give the expected  $\text{H}_3\text{Ru}_3(\mu_3\text{-CO})(\text{CO})_9^-$  but only  $\text{HRu}_3(\mu\text{-CO})(\text{CO})_{10}^-$  and  $\text{H}_3\text{Ru}_4(\text{CO})_{12}^-$ . Replacing carbonyl ligands with group 5 ligands stabilizes the hydrogenated product. Thus, both 5a and 6 are stable under ambient conditions, even though neither of the parent carbonyls can be isolated.

Upon hydrogenation of  $\text{HM}_3(\mu\text{-CX})(\text{CO})_{10-n}\text{L}_n$  to  $\text{H}_3\text{M}_3(\mu_3\text{-CX})(\text{CO})_{9-n}\text{L}_n$  the changes in bonding are (a) replacement of one carbonyl ligand with two hydride ligands, (b) an increase in the degree of metal-to-CX bonding upon conversion from a  $\mu\text{-}$  to  $\mu_3\text{-}$ carbyne, and (c) a decrease in the C-X bond order. The trends observed undoubtedly are the cumulative result of all of these factors. The relative metal-hydride bond energies may account substantially for the influence of the metal and ligands L. Metal-hydride bond strengths increase in the order  $\text{Fe} < \text{Ru} < \text{Os}$ ,<sup>49</sup> and, thus, the relative stabilities of the  $\text{H}_3\text{M}_3(\mu_3\text{-CX})(\text{CO})_{9-n}\text{L}_n$  clusters might be expected to follow the same order. There is also evidence that metal-hydride bond strengths are increased by replacement of carbonyl ligands with ligands having lower ionization potentials.<sup>51</sup> However, it is difficult to account for the effect of the carbyne ligand in terms of relative metal-hydride bond strengths.

A major factor influencing the relative stabilities of  $\text{HM}_3(\mu\text{-CX})(\text{CO})_{10-n}\text{L}_n$  and  $\text{H}_3\text{M}_3(\mu_3\text{-CX})(\text{CO})_{9-n}\text{L}_n$  may be the relative importance of M-CX and C-X  $\pi$  bonding. The  $\mu\text{-C-X}$  bond order is expected to decrease as X changes from  $\text{O}^-$  to  $\text{NR}_2$  to OMe as the electronegativity of X increases. Indeed, there is substantial support for this in the C-X stretching frequencies,<sup>17,19,20</sup> C-X bond lengths,<sup>17,19,23</sup> and free energies of activation for rotation about the C-X bond.<sup>19,20</sup> Since conversion from a  $\mu\text{-}$  to  $\mu_3\text{-}$ carbyne increases the metal-to-carbyne bonding at the expense of C-X  $\pi$  bonding, substituents X that favor a strong C-X  $\pi$  bond (such as  $\text{O}^-$  and  $\text{NR}_2$ ) might understandably make hydrogenation more difficult than substituents that do not. Since O coordination of Lewis acids to the  $\mu\text{-CO}$  ligand lowers the C-O bond order for  $\text{HM}_3(\mu\text{-CO})(\text{CO})_{10}^-$ , the Lewis acid also should facilitate cluster hydrogenation. In this light, it is interesting that at low temperature, protonation at the  $\text{HFe}_3(\mu\text{-CO})(\text{CO})_{10}$  monoanion forms  $\text{HFe}_3(\mu\text{-COH})(\text{CO})_{10}$ , which, on the basis of the extremely low-field  $^{13}\text{C}$  NMR signal for the  $\mu\text{-}$ carbon (359 ppm), is very similar in structure to 1a.<sup>8</sup> Similar results are observed for the  $\text{HRu}_3(\mu\text{-CO})(\text{CO})_{10}$  monoanion.<sup>52</sup> However, hydrogenation of  $\text{HM}_3(\mu\text{-COH})(\text{CO})_{10}$  to  $\text{H}_3\text{M}_3(\mu_3\text{-COH})(\text{CO})_9$  has not been possible because of the

(49) (a) A. P. Humphries and H. D. Kaesz, *Prog. Inorg. Chem.*, **25**, 145 (1979); (b) B. F. G. Johnson and J. Lewis, *Adv. Inorg. Chem. Radiochem.*, **24**, 225 (1981).

(50) J. B. Keister and T. L. Horling, *Inorg. Chem.*, **19**, 2304 (1980).

(51) (a) R. G. Pearson and C. T. Kresge, *Inorg. Chem.*, **20**, 1878 (1981);

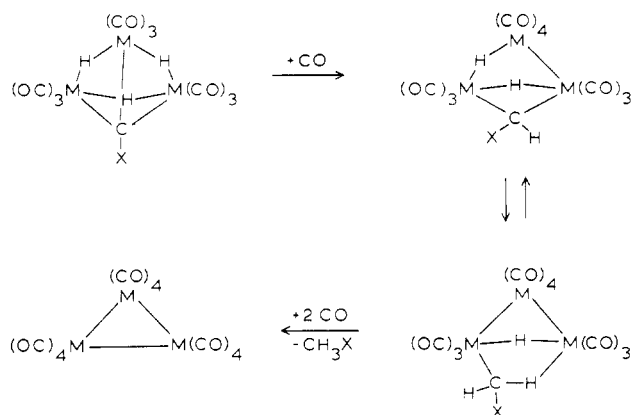
(b) M. J. Mays, R. N. F. Simpson, and F. P. Stefanini, *J. Chem. Soc. A*, **3000** (1976).

(52) J. B. Keister, *J. Organomet. Chem.*, **190**, C36 (1980).

(46) G. Fachinetti, R. Lazzaroni, and S. Pucci, *Angew. Chem., Int. Ed. Engl.*, **20**, 1063 (1981).

(47) R. E. Stimson and D. F. Shriver, *Inorg. Chem.*, **19**, 1141 (1980).

(48) This may be demonstrated by comparison of the C-OMe stretching frequencies for 1c (1460  $\text{cm}^{-1}$ ) and 2c (1195, 1140  $\text{cm}^{-1}$ ).



**Figure 3.** Proposed mechanism for elimination of  $\text{CH}_3\text{X}$  ( $\text{X} = \text{OMe}, \text{H}, \text{CO}_2\text{Me}$ ) from  $\text{H}_3\text{M}_3(\mu_3\text{-CX})(\text{CO})_9$ .

very rapid rearrangement of these species to the corresponding  $\text{H}_2\text{M}_3(\text{CO})_{11}$  at temperatures above ca.  $-40^\circ\text{C}$ . Thus, effective acid cocatalysts for carbon monoxide reduction via the chemistry described here must be strong acids ( $\text{BF}_3$ ,  $\text{H}^+$ ,  $\text{CH}_3^+$ ) to facilitate hydrogenation to  $\text{H}_3\text{M}_3(\mu_3\text{-CO-A})(\text{CO})_9$  but must not react with the product irreversibly and must not provide alternative decomposition pathways. Recently, the isoelectronic  $\text{Co}_3(\mu_3\text{-COH})(\text{CO})_9$  has been isolated and characterized by X-ray crystallography.<sup>12c</sup>

The final step of reduction of the COMe ligand (eq 4) is reductive elimination of three M-C  $\sigma$  bonds and three M-H-M bonds to give dimethyl ether and either  $\text{M}_3(\text{CO})_{12}$  or  $\text{M}(\text{CO})_5$ . We favor the mechanism shown in Figure 3, on the basis of the reverse sequence found by Calvert and Shapley<sup>35</sup> for conversion of  $\text{HOs}_3(\text{CH}_3)(\text{CO})_{10}$  to  $\text{H}_3\text{Os}_3(\mu_3\text{-CH})(\text{CO})_9$ , that is, sequential C-H bond formation without metal-metal bond cleavage. Since, under the conditions used for cleavage of dimethyl ether from **2b**,  $\text{Ru}_3(\text{CO})_{12}$  and  $\text{Ru}(\text{CO})_5$  are in equilibrium,<sup>53</sup> no conclusion can be reached at this time about the importance of metal-metal bond cleavage in this instance. Mechanistic studies of both hydrogenation and reductive cleavage steps and quantitative evaluations of the influence of the metal, carbyne ligand, and other ligands upon these processes are in progress.

### Experimental Section

**Chemicals.**  $\text{Ru}_3(\text{CO})_{12}$  was prepared according to literature procedures.<sup>54</sup>  $\text{Os}_3(\text{CO})_{12}$  was purchased from Strem Chemical. Methyl fluorosulfonate was purchased from Chemical Dynamics Corp. and ethyl fluorosulfonate from Aldrich.  $\text{HFe}_3(\mu\text{-COMe})(\text{CO})_{10}$  was prepared by the procedure of Shriver.<sup>7</sup>

**Characterizations.** The  $^1\text{H}$  NMR spectra were recorded on Varian CFT-80, EM-360, EM-390, or XL-100 spectrometers.  $^{13}\text{C}$  NMR spectra were recorded on Varian CFT-80 or XL-100 spectrometers with 0.02 M chromium(III) acetylacetonate as a relaxation agent. Mass spectra were obtained by Allen Claus at the University of Illinois Mass Spectrometry Laboratory on a Varian CH-5 instrument at 70 eV and a solid probe temperature of 25–150  $^\circ\text{C}$ . Infrared spectra were generally run on cyclohexane solutions by using a Perkin-Elmer 467 or Beckman 4250 spectrophotometer and were calibrated with the 2138.5- $\text{cm}^{-1}$  absorption of cyclohexane or with polystyrene. Analyses were performed by Galbraith Laboratories.

**$\text{HRu}_3(\mu\text{-COMe})(\text{CO})_{10}$  (1b).** **Warning!** Due to the extreme toxicity of methyl and ethyl fluorosulfonate, all operations involving these compounds should be carried out in an efficient

hood. Excess reagent may be destroyed with a slurry of potassium carbonate in methanol.

To a solution of  $\text{Ru}_3(\text{CO})_{12}$  (502 mg, 0.79 mmol) in tetrahydrofuran (100 mL) in a 500-mL, three-necked, round-bottomed flask, equipped with reflux condenser, nitrogen gas inlet, pressure-equalizing dropping funnel, Vigreux column topped with stopcock to a vacuum trap, and magnetic stir bar was added nitrogen-saturated water (50 mL) and nitrogen-saturated triethylamine (15 mL). The resulting solution was heated at  $60^\circ\text{C}$  with stirring for 2 h. Then the solvent was removed by vacuum transfer until only water and a brick red precipitate remained. The water was removed with a pipet, keeping the flask under a blanket of nitrogen, and the precipitate was dried under vacuum. Then a solution of methyl fluorosulfonate (300  $\mu\text{L}$ , 3.7 mmol) in dry dichloromethane (50 mL) was added from the dropping funnel, and the dark red solution was stirred overnight under nitrogen. After the reaction was complete, the solvent was vacuum transferred to a liquid nitrogen-cooled trap and the excess methyl fluorosulfonate in the trap was destroyed with a slurry of potassium carbonate in methanol. Methanol (50 mL) was added to the reaction flask, as well, and the resulting orange solution stirred for 2 h. Then the methanol was removed on a rotary evaporator, and the solid residue was purified by preparative thin-layer chromatography on silica gel eluting with cyclohexane. The product  $\text{HRu}_3(\mu\text{-COMe})(\text{CO})_{10}$  was isolated by extraction of the highest  $R_f$  band with dichloromethane and was recrystallized from methanol to give yellow crystals: 342 mg (70%); mass spectrum,  $m/e$  627 ( $^{101}\text{Ru}_3$ );  $^1\text{H}$  NMR ( $\text{CDCl}_3$ )  $\tau$  5.44 (s, 3 H), 24.85 (s, 1 H); IR ( $\text{C}_6\text{H}_{12}$ ) 2104 (w), 2064 (vs), 2054 (s), 2030 (vs), 2018 (m), 2004 (m), 1990 (w), 1968 (w)  $\text{cm}^{-1}$ . Anal. Calcd for  $\text{C}_{12}\text{H}_4\text{O}_{11}\text{Ru}_3$ : C, 22.95; H, 0.65; Ru, 48.35. Found: C, 22.95; H, 0.71; Ru, 48.49.

The ethyl derivative was prepared in the same manner by using ethyl fluorosulfonate:  $^1\text{H}$  NMR ( $\text{CDCl}_3$ )  $\tau$  5.33 (q, 2 H,  $J$  6.9 Hz), 8.31 (t, 3 H), 24.80 (s, 1 H); IR ( $\text{C}_6\text{H}_{12}$ ) 2103 (w), 2064 (vs), 2054 (s), 2030 (vs), 2018 (m), 2006 (sh), 2002 (m), 1996 (w), 1986 (vw)  $\text{cm}^{-1}$ .

**$\text{HOs}_3(\mu\text{-COMe})(\text{CO})_{10}$  (1c).** **Warning!** Due to the extreme toxicity of methyl and ethyl fluorosulfonate, all operations involving these compounds should be carried out in an efficient hood. Excess reagent can be destroyed with a potassium carbonate slurry in methanol.

A solution of  $\text{Os}_3(\text{CO})_{12}$  (200 mg, 0.2 mmol), deoxygenated water (10 mL), and deoxygenated triethylamine (9 mL) in air-free tetrahydrofuran (40 mL) was heated with stirring at  $60^\circ\text{C}$  for 2 h in a three-necked, 100-mL, round-bottomed flask equipped with nitrogen gas inlet, magnetic stirring bar, pressure-equalizing dropping funnel, and reflux condenser. After the solution was cooled to room temperature, tetraethylammonium bromide (150 mg, 0.7 mmol) was added and the tetrahydrofuran and triethylamine were removed by vacuum transfer. The water was then removed with a pipet, and the red precipitate remaining was washed with air-free water (10 mL) and dried under vacuum.

Next a solution of methyl fluorosulfonate (50  $\mu\text{L}$ , 0.62 mmol) in dry dichloromethane (50 mL) was added, and the resulting red solution was stirred under nitrogen for 2 h. At this point the solution was bright yellow. Excess methyl fluorosulfonate was destroyed by stirring with methanol (20 mL) for 2 h. Then the solvent was evaporated, and the residue was purified by preparative thin-layer chromatography on silica gel, eluting with cyclohexane. The product was isolated by extraction with dichloromethane of the second, yellow band, trailing a trace of purple  $\text{H}_2\text{Os}_3(\text{CO})_{10}$ : yield 159 mg (81%); the sample could be recrystallized from methanol; mass spectrum,  $m/e$  900 ( $^{192}\text{Os}_3$ );  $^1\text{H}$  NMR ( $\text{CDCl}_3$ )  $\tau$  5.41 (s, 3 H), 26.39 (s, 1 H); IR ( $\text{C}_6\text{H}_{12}$ ) 2109 (w), 2064 (s), 2067 (m), 2025 (s), 2012 (m), 1998 (m), 1982 (sh, vw)  $\text{cm}^{-1}$ . Anal. Calcd for  $\text{C}_{12}\text{H}_4\text{O}_{11}\text{Os}_3$ : C, 16.10; H, 0.45. Found: C, 16.16; H, 0.41.

The ethyl derivative was prepared in the same manner by using ethyl fluorosulfonate:  $^1\text{H}$  NMR ( $\text{CDCl}_3$ )  $\tau$  5.36 (q, 2 H,  $J$  = 7.2 Hz), 8.38 (t, 3 H), and 26.31 (s, 1 H); IR ( $\text{C}_6\text{H}_{12}$ ) 2105 (m), 2062 (s), 2055 (s), 2022 (s), 2007 (s), 1994 (s), 1989 (sh), 1977 (m)  $\text{cm}^{-1}$ .

**$\text{HRu}_3(\mu\text{-CNHCH}_2\text{Ph})(\text{CO})_{10}$  (3).** A solution of  $\text{Ru}_3(\text{CO})_{12}$  (99 mg, 0.15 mmol), triethylamine (5 mL), and water (5 mL) in THF (25 mL) was heated at 60–70  $^\circ\text{C}$  under nitrogen for 1 h. The solvent was removed under vacuum to give  $[\text{NHET}_3][\text{HRu}_3(\text{CO})_{11}]$ .

(53) (a) J. S. Bradley, *J. Am. Chem. Soc.*, **101**, 7419 (1979); (b) R. B. King, Jr., and K. Tanaka, *J. Mol. Catal.*, **10**, 75 (1981); (c) R. Whyman, *J. Organomet. Chem.*, **56**, 339 (1973).

(54) A. Mantovani and S. Cenini, *Inorg. Synth.*, **16**, 47 (1975).

This residue was dissolved in dichloromethane and benzyl isocyanide (25  $\mu$ L) was added to the stirred solution. After about 15 min the initially bright red solution had turned orange. Then the solvent was removed under vacuum, and the residue was purified by preparative thin-layer chromatography on silica, eluting with cyclohexane. The second yellow band was extracted with dichloromethane to give the product, after evaporation of solvent, as a bright yellow solid: 84 mg (77%); IR ( $C_6H_{12}$ ) 2098 (w), 2060 (vs), 2050 (s), 2025 (s), 2012 (s), 2002 (m), 1998 (s), 1986 (w)  $cm^{-1}$ ;  $^1H$  NMR ( $CDCl_3$ ) 1.4  $\tau$  (br, 1  $H_A$ ), 2.67 (br, 5 H), 5.02 (dd, 1  $H_B$ ), 5.15 (dd, 1  $H_C$ ), 24.70 (d, 1  $H_D$ ),  $J_{AB} = 1.5$ ,  $J_{AC} = 3.4$ ,  $J_{BC} = 14.7$ , and  $J_{AD} = 1.4$  Hz; mass spectrum,  $m/e$  702 ( $^{101}Ru_3$ ).

**$H_3Ru_3(\mu-CN(Me)CH_2Ph)(CO)_{10}$  (4).** 3 (84 mg, 0.12 mmol) was dissolved in methanol (25 mL) containing excess sodium methoxide under nitrogen. The solution immediately became dark orange. Then methyl iodide (200  $\mu$ L, 3.2 mmol) was added with stirring. After 45 min. the solution was bright yellow. Next saturated aqueous ammonium chloride was added, and the solution was extracted with dichloromethane until no yellow color remained. The organic layer was evaporated to dryness with a rotary evaporator, and the residue was redissolved in dichloromethane and dried over magnesium sulfate. Chromatography of this material on silica eluting with 10% dichloromethane in cyclohexane gave one yellow band, which was extracted with dichloromethane to give the product (76 mg, 90%): IR ( $C_6H_{12}$ ) 2096 (m), 2058 (s), 2047 (s), 2024 (s), 2010 (s), 2002 (m), 1995 (s), 1985 (m)  $cm^{-1}$ ;  $^1H$  NMR ( $CDCl_3$ )  $\tau$  2.7 (m, 5 H), 4.61 (d, 1  $H_A$ ), 4.96 (d, 1  $H_B$ ), 6.43 (s, 3 H), 24.74 (s, 1 H),  $J_{AB} = 14.7$ ; mass spectrum,  $m/e$  716 ( $^{101}Ru_3$ ).

**$H_3Ru_3(\mu_3-COMe)(CO)_9$  (2b).** A solution of 1b (209 mg, 0.13 mmol) in hexane (100 mL) was heated at reflux with hydrogen bubbling through the solution for 2 h. The solvent was removed under vacuum, and the red-orange residue was recrystallized from methanol under nitrogen to give bright orange crystals of  $H_3Ru_3(\mu_3-COMe)(CO)_9$ . The mother liquor was evaporated to dryness, and the residue was purified by preparative thin-layer chromatography on silica gel, eluting with cyclohexane to give additional product by extraction of the second band with dichloromethane: yield 186 mg (93%); mass spectrum,  $m/e$  601 ( $^{101}Ru_3$ );  $^1H$  NMR ( $CDCl_3$ )  $\tau$  6.23 (s, 3 H), 27.53 (s, 3 H); IR ( $C_6H_{12}$ ) 2106 (vw), 2076 (s), 2075 (s), 2036 (vs), 2028 (m), 2018 (sh), 2014 (m), 2000 (vw)  $cm^{-1}$ . Anal. Calcd for  $C_{11}H_6O_{10}Ru_3$ : C, 21.95; H, 1.01; Ru, 50.43. Found: C, 22.19; H, 1.11; Ru, 50.26.

**$H_3Os_3(\mu_3-COMe)(CO)_9$  (2c).** A solution of 1c (65 mg, 0.07 mmol) in decane (50 mL) was heated at 120  $^{\circ}C$  in a 100-mL, three-necked, round-bottomed flask, equipped with reflux condenser, stir bar, and gas inlet tube, for 1 h with hydrogen bubbling through the solution. The solvent was removed under vacuum, and the residue was purified by preparative thin-layer chromatography on silica gel, eluting with cyclohexane. The major product  $H_3Os_3(\mu_3-COMe)(CO)_9$  was isolated by extraction of the third, yellow band with dichloromethane. The compound was recrystallized from methanol: yield 44 mg (79%); mass spectrum,  $m/e$  874 ( $^{192}Os_3$ );  $^1H$  NMR ( $CDCl_3$ )  $\tau$  6.20 (s, 3 H), 28.53 (s, 3 H). IR ( $C_6H_{12}$ ) 2107 (vw), 2077 (s), 2074 (s), 2022 (vs), 2013 (m), 2008 (m), 1995 (vw)  $cm^{-1}$ . Anal. Calcd for  $C_{11}H_6O_{10}Os_3$ : C, 15.20; H, 0.70. Found: C, 15.08; H, 0.67.

**$H_3Fe_3(\mu_3-COMe)(CO)_7(SbPh_3)_2$  (5a).** A hexane solution of 1a (890 mg, 1.81 mmol) and triphenylantimony (2.292 g, 6.50 mmol) was heated at 60–70  $^{\circ}C$  for 2.5 h with hydrogen gas bubbling through the stirred solution. Then the solution was

evaporated to dryness and the product mixture was separated by preparative thin-layer chromatography on silica eluting with 10% dichloromethane in cyclohexane. The product was isolated by extraction of the brown band that trailed a dark purple band: yield 451 mg (22%); IR ( $C_6H_{12}$ ) 2066 (m), 2058 (m), 2018 (sh), 2008 (s), 1998 (sh), 1972 (m), 1904 (m)  $cm^{-1}$ ;  $^1H$  NMR ( $CDCl_3$ )  $\tau$  2.83 (m, 30 H), 5.49 (s, 3 H), 31.15 (t, 1 H), 32.02 (d, 2 H,  $J = 5.3$  Hz).

**$H_3Ru_3(\mu_3-CN(Me)CH_2Ph)(CO)_8(SbPh_3)_3$  (6).** A hexane solution of 4 (76 mg, 0.11 mmol) and triphenylantimony (150 mg, 0.43 mmol) was heated at 60–70  $^{\circ}C$  for 8 h with hydrogen gas bubbling through the solution. When the IR spectrum of the solution showed that complete conversion to the product had occurred, the solution was evaporated to dryness and the residue was recrystallized from dichloromethane–methanol to give red-orange crystals (112 mg, 63%). The product decomposed during chromatography but appeared to be air-stable: IR ( $C_6H_{12}$ ) 2061 (vw), 2034 (vs), 2014 (s), 2007 (s), 1993 (w), 1965 (s), 1947 (vw), 1877 (vw)  $cm^{-1}$ ;  $^1H$  NMR ( $CDCl_3$ )  $\tau$  2.8 (m, 50 H), 6.80 (s, 2 H), 5.23 (s, 3 H), 25.56 (s, 3 H). Anal. Calcd for  $C_{69}H_{58}NO_8Ru_3Sb_3$ : C, 49.75; H, 3.51. Found: C, 48.93; H, 3.91.

**Reductive Cleavage of Dimethyl Ether from 2b.** A solution of 2b (200 mg) in toluene (10 mL) was placed in the glass liner of a 75-mL Parr autoclave. The autoclave was pressurized to 500 psig with 1:1 carbon monoxide–hydrogen and was heated at 130  $^{\circ}C$  for 23 h. Then the autoclave was cooled, and the gases were vented slowly through a U-that trap was filled with glass beads and cooled with liquid nitrogen. When all the gas had been vented, the U-trap was closed off and removed. The noncondensable gases were pumped out of the U-trap, and analysis by mass spectrometry was performed on the condensable gases. Results showed a significant quantity of dimethyl ether. The toluene solution remaining in the autoclave was filtered to remove precipitated  $Ru_3(CO)_{12}$  (identified by infrared spectroscopy), and the filtrate was evaporated to dryness. Additional  $Ru_3(CO)_{12}$  was obtained by preparative thin-layer chromatography, on silica gel with cyclohexane. Total yield of  $Ru_3(CO)_{12}$  was 188 mg (89%). Some  $Ru_3(CO)_{12}$  and  $Ru(CO)_5$  were noted in the U-trap.

The experiment was repeated by using paraffin oil as solvent to allow for more careful analysis of the condensable gases. In these cases, in addition to dimethyl ether, traces of methyl formate and 1,2-dimethoxyethane were identified in the vapor by mass spectroscopy. The yield of dimethyl ether was estimated as 10%.

**Acknowledgment.** We gratefully acknowledge the donors of the Petroleum Research Fund, administered by the American Chemical Society, and the Joint Awards Council/University Awards Committee of the Research Foundation of the State University of New York for support of this work. Early stages of the project were conducted at and supported by Exxon Research and Engineering Co.

**Registry No.** 1a, 55992-19-3; 1b, 71737-42-3; 1b (ethyl derivative), 84027-61-2; 1c, 69048-01-7; 1c (ethyl derivative), 69047-99-0; 2a, 71562-46-4; 2b, 71562-47-5; 2c, 71562-48-6; 3, 84027-57-6; 4, 84027-58-7; 5a, 84027-59-8; 6, 84027-60-1;  $Ru_3(CO)_{12}$ , 15243-33-1;  $MeSO_3F$ , 421-20-5;  $Os_3(CO)_{12}$ , 15696-40-9;  $[NHEt_2][HRu_3(CO)_{11}]$ , 12693-45-7; ethyl fluorosulfonate, 371-69-7; benzyl isocyanide, 10340-91-7; methyl iodide, 74-88-4; dimethyl ether, 115-10-6.

# Nucleophilic Addition of *N,N*-Dimethylaniline to the (Cyclobutadiene)nitrosyldicarbonyliron Cation: A Kinetic and Structural Study<sup>†</sup>

Joseph C. Calabrese and Steven D. Ittel\*

Central Research and Development Department, E. I. du Pont de Nemours and Company, Wilmington, Delaware 19898

Hyung Soo Choi, Steven G. Davis, and Dwight A. Sweigart\*

Department of Chemistry, Brown University, Providence, Rhode Island 02912

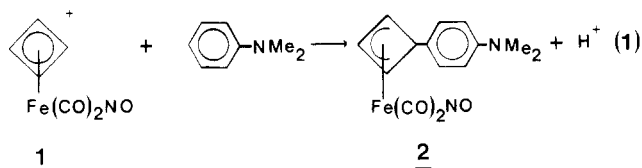
Received September 3, 1982

The electrophilic aromatic substitution reaction between *N,N*-dimethylaniline and the cyclobutadiene ring in [(C<sub>4</sub>H<sub>4</sub>)Fe(CO)<sub>2</sub>NO]PF<sub>6</sub> yields the η<sup>3</sup>-cyclobutenyl complex [(Me<sub>2</sub>NC<sub>6</sub>H<sub>4</sub>C<sub>4</sub>H<sub>4</sub>)Fe(CO)<sub>2</sub>NO] (2). Spectroscopic studies suggest that substitution occurs exclusively at the carbon para to the NMe<sub>2</sub> group and that the product has exo stereochemistry. A kinetic study in acetonitrile showed the reaction to be second order overall with the following activation parameters: Δ*H*<sup>‡</sup> = 11.2 ± 1.5 kcal; Δ*S*<sup>‡</sup> = -31 ± 5 cal deg<sup>-1</sup> mol<sup>-1</sup>. A mechanism is suggested that involves initial π-complex formation followed by rate-determining conversion to a σ complex. A single-crystal X-ray analysis of 2 at -100 °C showed that it crystallizes in the monoclinic space group *P*2<sub>1</sub>/*c* with *a* = 16.690 (2) Å, *b* = 6.310 (1) Å, *c* = 26.716 (3) Å, β = 96.46 (1)°, *Z* = 8, *R* = 0.036, and *R*<sub>w</sub> = 0.044. The structure confirms the exo attack of the *N,N*-dimethylaniline para carbon on the coordinated cyclobutadiene. The bond distances and angles in the cyclobutenyl group are similar to previously reported structures. The dihedral angle between the enyl plane (C<sub>7</sub>, C<sub>4</sub>, C<sub>5</sub>) and the nonbonded plane (C<sub>5</sub>, C<sub>6</sub>, C<sub>7</sub>) is 26.5° (Figure 1).

## Introduction

Cyclic π-hydrocarbons can be made electrophilic by coordination to transition metals. Subsequent nucleophilic attack on the activated π-hydrocarbon is a reaction of increasing utility in catalytic and stoichiometric transformations. The most significant synthetic uses involve the direct addition of a carbanion nucleophile to the coordinated ring, thus forming a new carbon-carbon bond.<sup>1</sup> However, with very electrophilic systems, activated aromatic molecules can function as the nucleophile. Thus *N,N*-dimethylaniline and pyrrole undergo<sup>2</sup> electrophilic aromatic substitution with the cyclohexadienyl ring in [(C<sub>6</sub>H<sub>7</sub>)Fe(CO)<sub>3</sub>]<sup>+</sup> and the tropylium ring in [(C<sub>7</sub>H<sub>7</sub>)Cr(CO)<sub>3</sub>]<sup>+</sup>.

Several years ago we reported<sup>3</sup> that *N,N*-dimethylaniline reacts with the cyclobutadiene ring in [(C<sub>4</sub>H<sub>4</sub>)Fe(CO)<sub>2</sub>NO]<sup>+</sup> according to reaction 1. In this paper we present the



synthesis and X-ray structure of 2 and a kinetic study of reaction 1. The substitution in reaction 1 occurs quantitatively, with exclusive electrophilic attack at the carbon para to the dimethylamino group. The dimethylanilino substituent in the cyclobutenyl ring in 2 is positioned exo to the metal.

This report appears to be only the fourth full X-ray structure of a transition-metal cyclobutenyl complex.<sup>4-6</sup>

## Experimental Section

**General Remarks.** Nitromethane and acetonitrile were dried and fractionally distilled under nitrogen prior to use. *N,N*-dimethylaniline was distilled from KOH pellets. [(C<sub>4</sub>H<sub>4</sub>)Fe(CO)<sub>2</sub>NO]PF<sub>6</sub> was prepared according to a published procedure.<sup>7</sup>

Infrared spectra were recorded on a Perkin-Elmer 680 spectrophotometer and <sup>1</sup>H NMR spectra at 250 MHz on a Bruker WM 250 spectrometer.

**Synthesis of (Me<sub>2</sub>NC<sub>6</sub>H<sub>4</sub>C<sub>4</sub>H<sub>4</sub>)Fe(CO)<sub>2</sub>(NO) (2).** *N,N*-Dimethylaniline (0.15 g, 1.24 mmol) was added to [(C<sub>4</sub>H<sub>4</sub>)Fe(CO)<sub>2</sub>NO]PF<sub>6</sub> (0.30 g, 0.88 mmol) in 10 mL of nitromethane under nitrogen. The reaction mixture was covered with aluminum foil and left for 2.5 h at room temperature. An IR spectrum then showed that the reaction had gone to completion. The solution then was placed on top of an acidic alumina column and eluted with diethyl ether to give a red solution. This solution was washed with water and evaporated. The resulting red solid was dissolved in pentane and slowly cooled to -10 °C to give 0.22 g (79%) of well-formed, deep red crystals: mp 99-100 °C dec; IR (cyclohexane) ν(CO) 2037, 1989 cm<sup>-1</sup>, ν(NO) 1755 cm<sup>-1</sup>; NMR (CDCl<sub>3</sub>) δ 2.94 (6 H, CH<sub>3</sub>), 3.77 (d, *J* = 5 Hz, 1 H, endo H), 5.20 (s, 2 H, enyl H), 5.40 (d, *J* = 5 Hz, 1 H, enyl H), 6.70 and 7.18 (d, *J* = 9 Hz, 4 H, phenyl). Anal. Calcd for C<sub>14</sub>H<sub>14</sub>N<sub>2</sub>O<sub>3</sub>Fe: C, 53.53; H, 4.49; N, 8.92. Found: C, 53.39; H, 4.48; N, 8.92.

**Kinetic Studies.** Reaction 1 was followed in nitromethane and acetonitrile solvents under nitrogen. Pseudo-first-order conditions were used with *N,N*-dimethylaniline in excess (0.05-1.0 M) over the [(C<sub>4</sub>H<sub>4</sub>)Fe(CO)<sub>2</sub>NO]PF<sub>6</sub> concentration, which was (1-5) × 10<sup>-3</sup> M. The pseudo-first-order rate constant, *k*<sub>obsd</sub>, was determined at least twice at each of seven or more nucleophile concentrations. For the nucleophile at 1.0 M, a Durrum stop-

(1) Alper, H., Ed. "Transition Metal Organometallics in Organic Synthesis"; Academic Press: New York, 1976; Vol. I; 1978, Vol. II. Becker, E. G.; Tsutsui, M., Eds. "Organometallic Reactions and Syntheses"; Plenum Press: New York, 1977. Birch, A. J. *Acc. Chem. Res.* 1980, 13, 463.

(2) John, G. R.; Mansfield, C. A.; Kane-Maguire, L. A. P. *J. Chem. Soc., Dalton Trans.* 1977, 574. John, G. R.; Kane-Maguire, L. A. P. *Ibid.* 1979, 1196. Atton, J. G.; Hassan, L. A.; Kane-Maguire, L. A. P. *Inorg. Chim. Acta* 1980, 41, 245.

(3) Davis, S.; Gelfand, L.; Summers, R.; Sweigart, D. A., Abstracts of Second International Symposium on the Mechanism of Reactions in Solution, Canterbury, U.K., 1979, p P55.

(4) Oberhansli, W.; Dahl, L. F. *Inorg. Chem.* 1965, 4, 150.

(5) Dahl, L. F.; Oberhansli, W. E. *Inorg. Chem.* 1965, 4, 629.

(6) Potenza, J.; Johnson, R.; Mastropaolo, D.; Efraty, A. *J. Organomet. Chem.* 1974, 64, C13. Potenza, J. A.; Johnson, R.; Williams, D.; Toby, B. H.; Lalancette, R. A.; Efraty, A. *Acta Crystallogr., Sect. B* 1981, B37, 442.

(7) Efraty, A.; Bystrek, R.; Geaman, J. A.; Sandhu, S. S.; Huang, M. H. A.; Herber, R. H. *Inorg. Chem.* 1971, 13, 1269. Efraty, A.; Sandhu, S. S.; Bystrek, R.; Denney, D. Z. *Ibid.* 1977, 16, 2522.

<sup>†</sup> Contribution No. 3096.



Table I. Summary of X-ray Diffraction Data

complex formula	$(Me_2NC_6H_4C_4H_4)Fe(CO)_2(NO)$ $FeO_3N_2C_{14}H_{14}$
fw	314.127
$a$ , Å	16.690 (2)
$b$ , Å	6.310 (1)
$c$ , Å	26.716 (3)
$\beta$ , deg	96.46 (1)
$V$ , Å <sup>3</sup>	2795.70
$\rho$ (calcd), g cm <sup>-3</sup>	1.4924
space group	$P2_1/c-C_{2h}^5$ (No: 14)
cryst dimens, mm	$0.25 \times 0.22 \times 0.38$
temp, °C	-100
radiant	Mo $K\alpha$ 0.710 69 Å from a graphite monochromator
$\mu$ , cm <sup>-1</sup>	10.835
$2\theta$ limits, deg	4-55
observns	7137
unique data	4773
$F_o^2 > 3\sigma(F_o^2)$	
final no. of variables	473
$R$	3.61
$R_w$	4.37

ped-flow apparatus was used (470 nm). For other concentrations, a Gilford Model 250 spectrophotometer, thermostated at 25 °C, was used. Rate constants also were determined by following the disappearance of the reactant IR  $\nu_{CO}$  and  $\nu_{NO}$  bands and the appearance of the product IR bands. All three techniques gave consistent results. Plots of  $k_{obsd}$  vs. nucleophile concentration were linear with zero intercepts. In acetonitrile solvent the activation parameters for reaction 1 were determined by measuring  $k_{obsd}$  at four temperatures in the range 25-47 °C with the nucleophile concentration fixed at 0.05 M. The second-order rate constants,  $k_{obsd}/(0.05)$ , were used to make a standard Eyring plot.

**X-ray Data Collection, Structure Solution, and Refinement.** Crystals of  $(Me_2NC_6H_4C_4H_4)Fe(CO)_2(NO)$  suitable for

diffraction studies were obtained by slow cooling of a pentane solution to -10 °C. The selected crystal of approximate dimensions  $0.25 \times 0.22 \times 0.38$  mm was mounted in a glass capillary under nitrogen. Data were collected on a Syntex P3 diffractometer at -100 °C. The crystal was shown to be suitable by  $\omega$  scans having a peak width at half-height of 0.25°. Cell parameters refined on 50 computer-centered reflections chosen from diverse regions of reciprocal space are presented in Table I together with other crystallographic data.

Intensity data were collected by using the  $\omega$ -scan technique (scan range 1.0° at 4.0-10.0° min<sup>-1</sup>); total background time equals scan time. Four standard reflections checked every 200 reflections deviated less than 0.1%. Absorption corrections were not made.

The structure was solved by the Patterson heavy-atom method and the positions of the remaining non-hydrogen atoms were obtained by the usual refinement techniques. In the full-matrix least-squares refinements, the function minimized was  $\sum w(|F_o| - |F_c|)^2$ , where  $|F_o|$  and  $|F_c|$  are the observed and calculated structure amplitudes and  $w = 1/\sigma^2(F_o)$  and  $\sigma(F) = [\sigma(I)^2 + 0.003(I^2)]^{1/2}$ . The hydrogen atoms were found in a difference Fourier map. All non-hydrogen atoms were refined with anisotropic thermal parameters, and hydrogen atoms were refined isotropically. Least square refinement converged to values of  $R = 0.036$  and  $R_w = 0.044$ . Several peaks of  $0.36 \text{ e } \text{Å}^{-3}$  were located on the midpoints of the aromatic bonds in the final difference Fourier map.

The final positional parameters of the refined atoms appear in Table II. Selected bond distances and angles are presented in Table III.

## Results and Discussion

**Synthesis and Kinetic Study.** The activated aromatic nucleophile  $N,N$ -dimethylaniline readily attacks the cyclobutadiene ring in 1. The reaction is very clean with only a single product being formed. The IR  $\nu_{CO}$  and  $\nu_{NO}$  bands shift to lower frequencies in 2 as expected. The <sup>1</sup>H NMR spectrum strongly suggests that the substitution occurs

Table II. Fractional Coordinates ( $\times 10^4$ ) for  $(Me_2NC_6H_4C_4H_4)Fe(CO)_2NO$ 

atom	molecule 1			molecule 2		
	$x$	$y$	$z$	$x$	$y$	$z$
Fe(1)	1088.2 (2)	477.0 (6)	6099.2 (1)	3900.7 (2)	-2986.2 (6)	11337.4 (1)
O(1)	-186 (1)	2227 (4)	5358 (1)	5209 (1)	-779 (4)	11972 (1)
O(2)	2406 (1)	2771 (3)	5686 (1)	2577 (1)	-737 (3)	11756 (1)
O(3)	1182 (1)	-3700 (3)	5738 (1)	3861 (1)	-7051 (4)	11776 (1)
N(1)	1130 (1)	-2059 (4)	5940 (1)	3889 (1)	-5462 (4)	11547 (1)
N(2)	1465 (1)	23 (4)	9192 (1)	3474 (2)	-5332 (4)	8274 (1)
C(1)	292 (2)	1623 (5)	5656 (1)	4711 (2)	-1597 (5)	11722 (1)
C(2)	1891 (2)	1899 (4)	5842 (1)	3093 (2)	-1557 (4)	11595 (1)
C(4)	1045 (2)	2458 (4)	6718 (1)	3883 (2)	-1259 (5)	10676 (1)
C(5)	1664 (2)	933 (4)	6826 (1)	3284 (2)	-2846 (5)	10615 (1)
C(6)	1064 (1)	-610 (4)	7041 (1)	3888 (2)	-4438 (4)	10422 (1)
C(7)	450 (2)	865 (4)	6735 (1)	4496 (2)	-2806 (4)	10675 (1)
C(8)	1105 (1)	-500 (4)	7610 (1)	3815 (1)	-4633 (4)	9854 (1)
C(9)	725 (2)	1061 (4)	7862 (1)	4131 (2)	-3157 (4)	9538 (1)
C(10)	826 (2)	1224 (5)	8383 (1)	4016 (2)	-3366 (4)	9019 (1)
C(11)	1333 (1)	-192 (4)	8677 (1)	3579 (2)	-5076 (4)	8790 (1)
C(12)	1699 (2)	-1814 (4)	8422 (1)	3257 (2)	-6552 (5)	9107 (1)
C(13)	1580 (2)	-1936 (4)	7900 (1)	3384 (2)	-6309 (5)	9626 (1)
C(14)	2008 (2)	-1396 (6)	9491 (1)	2962 (2)	-7005 (6)	8046 (1)
C(15)	1110 (2)	1737 (6)	9444 (1)	3839 (2)	-3893 (6)	7949 (1)
H(4)	976 (20)	3931 (57)	6663 (12)	3901 (18)	254 (51)	10695 (11)
H(5)	2253 (21)	988 (54)	6904 (12)	2698 (18)	-2816 (45)	10556 (10)
H(6)	1057 (18)	-2087 (51)	6935 (11)	3886 (17)	-5793 (46)	10573 (10)
H(7)	-123 (18)	966 (45)	6718 (10)	5076 (19)	-2785 (51)	10700 (11)
H(9)	364 (18)	2101 (48)	7669 (10)	4459 (16)	-1907 (45)	9679 (10)
H(10)	568 (20)	2418 (53)	8525 (12)	4217 (18)	-2346 (47)	8809 (10)
H(12)	2025 (19)	-2916 (52)	8609 (11)	2960 (19)	-7776 (51)	8980 (11)
H(13)	1869 (17)	-3090 (46)	7747 (10)	3173 (20)	-7314 (52)	9817 (11)
H(14A)	1859 (24)	-2851 (69)	9446 (14)	2408 (23)	-6916 (58)	8124 (13)
H(14B)	2051 (25)	-1069 (69)	9840 (16)	3135 (22)	-8383 (63)	8150 (13)
H(14C)	2574 (24)	-1217 (63)	9403 (14)	2950 (20)	-6994 (55)	7687 (13)
H(15A)	545 (25)	1677 (64)	9382 (14)	4391 (23)	-3681 (60)	8071 (13)
H(15B)	1245 (20)	1625 (56)	9788 (13)	3579 (27)	-2597 (73)	7892 (16)
H(15C)	1278 (23)	3165 (69)	9302 (14)	3831 (23)	-4499 (63)	7608 (15)

Table III. Selected<sup>a</sup> Bond Distances (Å) and Angles (deg) for (Me<sub>2</sub>NC<sub>6</sub>H<sub>4</sub>C<sub>4</sub>H<sub>4</sub>)Fe(CO)<sub>2</sub>NO

	molecule 1	molecule 2		molecule 1	molecule 2
Bond Distances					
Fe-N(1)	1.659 (2)	1.660 (2)	C(1)-O(1)	1.127 (3)	1.131 (3)
Fe-C(1)	1.828 (3)	1.827 (3)	C(2)-O(2)	1.138 (3)	1.132 (3)
Fe-C(2)	1.811 (3)	1.819 (3)	C(4)-C(5)	1.418 (4)	1.412 (4)
Fe-C(4)	2.081 (2)	2.074 (3)	C(4)-C(7)	1.417 (4)	1.413 (4)
Fe-C(5)	2.088 (3)	2.084 (3)	C(5)-C(6)	1.552 (3)	1.552 (4)
Fe-C(7)	2.119 (3)	2.127 (3)	C(6)-C(7)	1.549 (3)	1.547 (4)
N(1)-O(3)	1.174 (3)	1.179 (3)	C(6)-C(8)	1.515 (3)	1.512 (3)
Bond Angles					
N(1)-Fe-C(1)	105.3 (1)	107.4 (1)	Fe-N(1)-O(3)	167.2 (2)	168.0 (2)
N(1)-Fe-C(2)	109.0 (1)	107.6 (1)	Fe-C(1)-O(1)	175.2 (3)	177.8 (3)
N(1)-Fe-C(4)	142.2 (1)	141.4 (1)	Fe-C(2)-O(2)	178.7 (4)	177.5 (3)
N(1)-Fe-C(5)	110.1 (1)	109.2 (1)	Fe-C(4)-C(5)	70.4 (1)	70.5 (2)
N(1)-Fe-C(7)	110.9 (1)	110.8 (1)	Fe-C(4)-C(7)	71.8 (1)	72.4 (2)
C(1)-Fe-C(2)	94.2 (1)	94.7 (1)	Fe-C(5)-C(4)	69.8 (1)	69.8 (1)
C(1)-Fe-C(4)	100.9 (1)	99.5 (1)	Fe-C(5)-C(6)	90.5 (1)	90.5 (2)
C(1)-Fe-C(5)	140.7 (1)	139.2 (1)	Fe-C(7)-C(4)	68.8 (1)	68.3 (1)
C(1)-Fe-C(7)	94.6 (1)	93.2 (1)	Fe-C(7)-C(6)	89.4 (1)	89.1 (2)
C(2)-Fe-C(4)	95.6 (1)	97.0 (1)	C(5)-C(4)-C(7)	90.5 (2)	90.8 (2)
C(2)-Fe-C(5)	90.1 (1)	91.1 (1)	C(4)-C(5)-C(6)	90.9 (2)	91.1 (2)
C(2)-Fe-C(7)	135.0 (1)	136.3 (1)	C(5)-C(6)-C(7)	81.0 (2)	80.9 (2)
C(4)-Fe-C(5)	39.8 (1)	39.7 (1)	C(5)-C(6)-C(8)	112.6 (2)	113.9 (2)
C(4)-Fe-C(7)	39.4 (1)	39.3 (1)	C(7)-C(6)-C(8)	116.9 (2)	117.9 (2)
C(5)-Fe-C(7)	57.2 (1)	57.0 (1)	C(4)-C(7)-C(6)	91.1 (2)	91.2 (2)

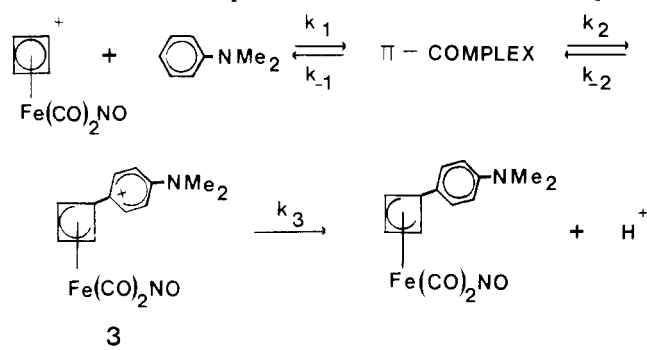
<sup>a</sup> Additional distances and angles have been deposited in the microfilm edition.

exclusively para, and this is confirmed by X-ray diffraction studies (see below). The lack of any substitution ortho to the NMe<sub>2</sub> group may be due to steric constraints.

The kinetic data for reaction 1 gave a good fit to the equation  $k_{\text{obsd}} = k[\text{N,N-dimethylaniline}]$  with the following results at 25 °C: (CH<sub>3</sub>NO<sub>2</sub>),  $k = 0.014 \pm 0.002 \text{ M}^{-1} \text{ s}^{-1}$ ; (CH<sub>3</sub>CN),  $k = 0.0045 \pm 0.0006 \text{ M}^{-1} \text{ s}^{-1}$ . In acetonitrile the activation parameters for  $k$  are  $\Delta H^\ddagger = 11.2 \pm 1.5 \text{ kcal}$  and  $\Delta S^\ddagger = -31 \pm 5 \text{ cal deg}^{-1} \text{ mol}^{-1}$ .

There are many mechanistic possibilities for reaction 1. Initial attack of the amino nitrogen at the metal or coordinated CO followed by migration to the ring seems unlikely because the product 2 has exo stereochemistry and neither visible nor IR spectroscopy gave any evidence of reaction intermediates.

The usual mechanism postulated for electrophilic aromatic substitution reactions is shown below for reaction 1. The initial  $\pi$  complex converts to a Wheland  $\sigma$  complex,



3, and proton loss gives the product. Presumably the proton loss can be assisted by excess nucleophile or the solvent. Since we found the rate law to be strictly first order in nucleophile, it seems likely that proton loss is rapid. A recent report by Kane-Maguire<sup>2</sup> suggests, however, that dimethylaniline addition to [(C<sub>7</sub>H<sub>7</sub>)Cr(CO)<sub>3</sub>]<sup>+</sup> may involve slow proton loss, which gives rise to a term in the rate law that is second order in nucleophile. We tried to test this possibility by following reaction 1 in the presence of a nonnucleophilic proton acceptor. The

base-selected 2,6-lutidine reacted with complex 1. Proton sponge rapidly reacted also, most likely by electrophilic aromatic substitution. The formation of a  $\pi$  complex prior to the Wheland intermediate is well-known<sup>8</sup> to occur in some electrophilic aromatic substitutions and occasionally can be rate determining. Formation of  $\pi$  complexes has recently been shown<sup>9</sup> to be rapid compared to substitution in the reaction of methoxy benzenes with [(C<sub>6</sub>H<sub>7</sub>)Fe(CO)<sub>3</sub>]<sup>+</sup>. We are investigating the reaction of complex 1 with a variety of aromatic nucleophiles so that the mechanistic features such as the importance of  $\pi$  complexes can be better understood.

If the formation of the  $\sigma$  intermediate 3 is rate determining, our results are given by eq 2,

$$k_{\text{obsd}} = (k_1 k_2 / k_{-1}) [\text{nucleophile}] \quad (2)$$

which also includes the assumption that the preequilibrium formation of the  $\pi$  complex does not saturate to a significant degree. This is supported by the failure to observe any evidence for reaction intermediates. The activation parameters calculated in acetonitrile are clearly consistent with eq 2. In particular the quite negative  $\Delta S^\ddagger$  is reasonable for the composite constant  $k_1 k_2 / k_{-1}$  and would be equal to  $\Delta S^\circ + \Delta S_2^\ddagger$  where  $\Delta S^\circ$  refers to the  $\pi$ -complex equilibrium constant and  $\Delta S_2^\ddagger$  to the  $\pi \rightarrow \sigma$  conversion.

There is evidence suggesting that the mechanism of reaction 1 is not simply rate-determining formation of the  $\sigma$  complex from separated reactants. Studies<sup>10-13</sup> of phosphine, phosphite, and nitrogen donor nucleophile additions to the rings in [(C<sub>4</sub>H<sub>4</sub>)Fe(CO)<sub>2</sub>NO]<sup>+</sup> and [(C<sub>6</sub>H<sub>7</sub>)Fe(CO)<sub>3</sub>]<sup>+</sup> consistently show the latter complex to be about a factor of seven less electrophilic than the former. These reactions can not involve the type of  $\pi$ -com-

(8) Olah, G. A. *Acc. Chem. Res.* 1971, 4, 240.

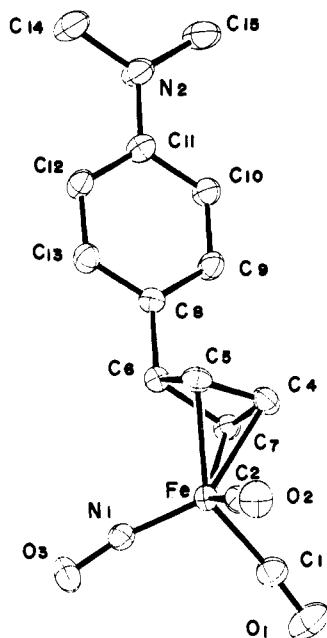
(9) John, G. R.; Kane-Maguire, L. A. P. *J. Chem. Soc., Dalton Trans.*, in press.

(10) John, G. R.; Kane-Maguire, L. A. P. *J. Chem. Soc., Dalton Trans.* 1979, 873.

(11) Choi, H. S.; Sweigart, D. A. *Organometallics* 1982, 1, 60.

(12) Choi, H. S.; Chung, Y. K.; Sweigart, D. A., unpublished results.

(13) Kane-Maguire, L. A. P., personal communication.



**Figure 1.** Perspective view and atom labeling scheme of  $(Me_2NC_6H_4C_4H_4)Fe(CO)_2(NO)$  with thermal ellipsoids drawn at the 50% level. Hydrogen atoms have been omitted for clarity.

plex formation discussed here and probably follow a single bimolecular mechanism. In sharp contrast to this behavior, the reaction of dimethylaniline with  $[(C_4H_4)Fe(CO)_2NO]^+$  and  $[(C_6H_7)Fe(CO)_3]^+$  occurs at nearly the same rate and with similar activation parameters in acetonitrile. With the assumption that eq 2 hold for both electrophiles, the unexpectedly small reactivity difference with dimethylaniline may merely reflect a smaller  $\pi$ -complex equilibrium constant ( $K = k_1/k_{-1}$ ) for complex 1.

At least two additional mechanisms for reactions such as (1) remains as possibilities. Initial attack on the coordinated ring by the amino nitrogen in dimethylaniline, followed by conversion to a Wheland  $\sigma$  complex cannot be ruled out although at this time there is no evidence for a nitrogen-bonded intermediate. A significant concentration of such an intermediate would be readily detectable by its effect on the IR  $\nu_{CO}$  and  $\nu_{NO}$  bands. A mechanism involving rate-determining electron transfer from the nucleophile to the electrophile, followed by collapse of the resulting radicals to products has yet to be suggested for nucleophilic additions to coordinated  $\pi$ -hydrocarbons but is known<sup>14</sup> to occur with some Grignard additions to carbonyl groups. Studies of the reactions of complexes like 1 with other

activated aromatic nucleophiles are planned and should help to elucidate the mechanistic pathways followed in these interesting electrophilic substitutions.

**Description of the Structure of  $(4-Me_2NC_6H_4C_4H_4)Fe(CO)_2(NO)$  (2).** The structure of 2 consists of two molecules in the asymmetric unit. The discrete molecules are well separated having no strong intermolecular contacts. The bond distances and angles compiled in Table III indicate the remarkable similarity between the two independent molecules. Figure 1 presents a perspective view of one molecule and gives the atom-labeling scheme.

The observed structure confirms the *exo* attack of the *N,N*-dimethylaniline para carbon on the coordinated cyclobutadiene inferred from spectroscopic results.

The inner coordination sphere is a distorted square pyramid if the  $\eta^3$ -cyclobutenyl group is considered to occupy two coordination sites. The linear nitrosyl group ( $\angle Fe-N-O = 167.6(2)^\circ$ ) occupies the apical site and the central carbon of the  $\eta^3$ -enyl group is below the basal plane. The complex can be considered to be an 18-electron  $Fe(0)$  complex with  $NO^+$  and  $enyl^-$  groups.

The bond distances and angles in the cyclobutenyl group are very similar to those reported in previous cyclobutenyl structures.<sup>4,5</sup> At  $26.5^\circ$  the dihedral angle between the enyl plane ( $C_7, C_4, C_5$ ) and the nonbonded plane ( $C_5, C_6, C_7$ ) is also very similar to previous reports ( $25^\circ, 22^\circ, 27^\circ$ , and  $24^\circ$ ).<sup>4,6</sup> These values differ significantly from that observed in a 2-4- $\eta$ -1-oxo-cyclobutenyl system ( $11^\circ$ ),<sup>6</sup> but this variation can be attributed to constraints imposed by the  $sp^2$  hybridization of the carbonyl carbon atom. There is a statistically significant difference in the chemically equivalent  $Fe-C_5$  and  $Fe-C_7$  distances with  $Fe-C_5$  being shorter. This variation is also reflected in the carbonyl  $Fe-C$  distances with  $Fe-C$  trans to  $C_5$  being the longer of the two. We attribute this variation to the packing forces and orientation of the phenyl ring, whose plane more closely parallels the  $C_6-C_7$  bond.

**Acknowledgment.** We wish to thank Mr. L. Lardear for skilled technical assistance. Discussions with Dr. L. A. P. Kane-Maguire are gratefully acknowledged. This work was supported by a grant from the National Science Foundation (No. CHE-8023964).

**Registry No.**  $[(C_6H_4)Fe(CO)_2NO]PF_6$ , 43175-640;  $(Me_2NC_6H_4C_4H_4)Fe(CO)_2(NO)$ , 84050-91-9; *N,N*-dimethylaniline, 121-69-7.

**Supplementary Material Available:** Tables of observed and calculated structure factors, anisotropic thermal parameters, hydrogen isotopic thermal parameters, interatomic distances, and intramolecular angles (25 pages). Ordering information is given on any current masthead page.

(14) Ashby, E. C.; Bowers, J. R. *J. Am. Chem. Soc.* 1981, 103, 2242.

# $\alpha$ -Trimethylsilyl Boronic Esters. Pinacol Lithio(trimethylsilyl)methaneboronate, Homologation of Boronic Esters with [Chloro(trimethylsilyl)methyl]lithium, and Comparisons with Some Phosphorus and Sulfur Analogues

Donald S. Matteson\* and Debesh Majumdar

Department of Chemistry, Washington State University, Pullman, Washington 99164

Received August 24, 1982

Pinacol (trimethylsilyl)methaneboronate has been prepared from (trimethylsilyl)methylmagnesium chloride and has been lithiated with lithium 2,2,6,6-tetramethylpiperidide. Pinacol lithio(trimethylsilyl)methaneboronate with alkyl halides efficiently yields pinacol 1-(trimethylsilyl)alkane-1-boronates and with aldehydes or ketones eliminates silicon exclusively to form pinacol 1-alkene-1-boronates, with mostly *Z* isomers resulting from the aldehydes. The latter behavior contrasts with a boron-substituted Wittig reagent, [(1,3,2-dioxaborin-2-yl)methylene]phosphorane, which eliminates boron first and phosphorus second, converting benzophenone to tetraphenylallene and benzaldehyde to 1,3-diphenylallene. The lithio(trimethylsilyl)methaneboronate does eliminate boron first in its condensation with carboxylic esters, which yields (trimethylsilyl)methyl ketones. Attempted lithiation of  $\alpha$ -trimethylsilyl boronic esters beyond the first member of the series failed.  $\alpha$ -Trimethylsilyl boronic esters were also synthesized efficiently by homologation of boronic esters with [chloro(trimethylsilyl)methyl]lithium. Attempted analogous homologations with [halo(phenylthio)methyl]lithium were unsuccessful.

$\alpha$ -Trimethylsilyl boronic esters constitute a new class in the series of  $\alpha$ -substituted boronic esters we have been investigating.<sup>1-4</sup> In view of the  $\alpha$  lithiations of alkane-1,1-diboronic esters<sup>3</sup> and  $\alpha$ -(phenylthio)alkaneboronic esters,<sup>4</sup> as well as the numerous reported  $\alpha$  lithiations of silyl compounds,<sup>5,6</sup> we anticipated the lithiation of  $\alpha$ -(trimethylsilyl)alkaneboronic esters. This hope has been realized only in the case of pinacol (trimethylsilyl)methaneboronate (1), the lithio derivative 2 of which has shown useful reactivity toward alkyl halides, aldehydes, ketones, and esters. An alternative to the synthesis of  $\alpha$ -(trimethylsilyl)alkaneboronic esters by reaction of 2 with alkyl halides is the homologation of boronic esters with [(trimethylsilyl)chloromethyl]lithium, the first homologation of boronic esters to be successfully developed. This has precedent in the analogous homologations of trialkylboranes.<sup>7</sup> However, equally precedented homologa-

Table I. Pinacol  $\alpha$ -(Trimethylsilyl)alkaneboronates,  $RCH(SiMe_3)BO_2C_2Me_4$  (3), from Alkylation of Pinacol Lithio(trimethylsilyl)methaneboronate (2) with Alkyl Halides (R-X)

R of R-X and 3	X	bp of 3, °C (torr)	% yield
CH <sub>3</sub> (CH <sub>2</sub> ) <sub>3</sub>	I	47-50 (0.05)	74
CH <sub>3</sub> (CH <sub>2</sub> ) <sub>4</sub>	Br	58-62 (0.05)	85
CH <sub>3</sub> (CH <sub>2</sub> ) <sub>5</sub>	Br	68-71 (0.05)	79
C <sub>6</sub> H <sub>5</sub> CH <sub>2</sub>	Br	90-94 (0.15)	83
C <sub>6</sub> H <sub>5</sub> CH <sub>2</sub> CH <sub>2</sub>	I	96-101 (0.07)	79
C <sub>6</sub> H <sub>5</sub> OCH <sub>2</sub> CH <sub>2</sub>	Br	106-111 (0.07)	81
CH <sub>3</sub> C(O <sub>2</sub> C <sub>2</sub> H <sub>5</sub> )(CH <sub>2</sub> ) <sub>3</sub>	Cl	104-108 (0.07)	53

Table II. Pinacol Alkeneboronates,  $RR'C=CHBO_2C_2Me_4$  (4), from Reaction of Pinacol Lithio(trimethylsilyl)methaneboronate (2) with Carbonyl Compounds (RCOR')

R	R'	bp of 4, °C (torr)	% yield
CH <sub>3</sub> (CH <sub>2</sub> ) <sub>5</sub>	H	75-79 (0.15)	73
CH <sub>3</sub> (CH <sub>2</sub> ) <sub>3</sub>	CH <sub>3</sub> (CH <sub>2</sub> ) <sub>3</sub>	72-76 (0.1)	74
C <sub>6</sub> H <sub>5</sub>	H	80-84 (0.2)	84
C <sub>6</sub> H <sub>5</sub>	C <sub>6</sub> H <sub>5</sub>	135-139 (0.2)	85
-(CH <sub>2</sub> ) <sub>5</sub> -		58-62 (0.1)	87

tions with PhSCHXLi<sup>8</sup> have proved inapplicable to boronic esters.

## Results

**Lithiated Pinacol (Trimethylsilyl)methaneboronate (2).** The Grignard reagent from (chloromethyl)trimethylsilane<sup>9</sup> reacted with trimethyl borate followed by aqueous workup to yield crude (trimethylsilyl)methaneboronic acid, which was esterified with pinacol to form pinacol (trimethylsilyl)methaneboronate (1) (systematic name 2-[(trimethylsilyl)methyl]-4,4,5,5-tetramethyl-1,3,2-dioxaborolane).

(8) (a) Yamamoto, S.; Shiono, M.; Mukaiyama, T. *Chem. Lett.* 1973, 961-962. (b) Hughes, R. J.; Pelter, A.; Smith, K. *J. Chem. Soc., Chem. Commun.* 1974, 863. (c) Mendoza, A.; Matteson, D. S. *J. Organomet. Chem.* 1978, 156, 149-157.

(9) (a) Whitmore, F. C.; Sommer, L. H. *J. Am. Chem. Soc.* 1946, 68, 481-484. (b) Peterson, D. *J. Org. Chem.* 1968, 33, 780-784.

(1) Preliminary communications: (a) Matteson, D. S.; Majumdar, D. *J. Chem. Soc., Chem. Commun.* 1980, 39-40. (b) Matteson, D. S.; Majumdar, D. *J. Organomet. Chem.* 1980, 184, C41-C43.

(2) (a) Matteson, D. S.; Mah, R. W. H. *J. Am. Chem. Soc.* 1963, 85, 2599-2603. (b) Review: Matteson, D. S. *Acc. Chem. Res.* 1970, 3, 186-193. (c) Review: Matteson, D. S. *Synthesis* 1975, 147-158. (d) Review: "Gmelin Handbuch der Anorganischen Chemie", 8th ed.; New Supplement Series; Niedenzu, K., Buschbeck, K.-C., Eds.; Springer-Verlag: Berlin, 1977; Vol. 48, Part 16, pp 37-72.

(3) (a) Matteson, D. S.; Moody, R. J. *Organometallics* 1982, 1, 20-28. (b) *J. Am. Chem. Soc.* 1977, 99, 3196-3197.

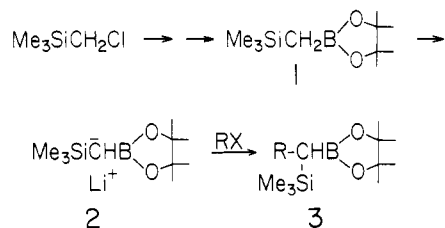
(4) (a) Matteson, D. S.; Arne, K. H. *Organometallics* 1982, 1, 280-288. (b) *J. Am. Chem. Soc.* 1978, 100, 1325-1326.

(5) Burford, C.; Cooke, F.; Ehlinger, E.; Magnus, P. *J. Am. Chem. Soc.* 1977, 99, 4536-4537.

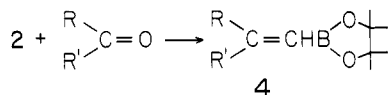
(6) Some examples: (a) Carey, F. A.; Court, A. S. *J. Org. Chem.* 1972, 37, 939-943, 1926-1929. (b) Jones, P. F.; Lappert, M. F. *J. Chem. Soc., Chem. Commun.* 1972, 526. (c) Seebach, D.; Gröbel, B.-T.; Beek, A. K.; Braun, M.; Geiss, K.-H. *Angew. Chem., Int. Ed. Engl.* 1972, 11, 443-444. (d) Seebach, D.; Kolb, M.; Gröbel, B.-T. *Tetrahedron Lett.* 1974, 3171-3174. (e) Gröbel, B.-T.; Bürstinghaus, R.; Seebach, D. *Synthesis* 1976, 121-123. (f) Taguchi, H.; Shimoi, K.; Yamamoto, H.; Nozaki, H. *Bull. Chem. Soc. Jpn.* 1974, 47, 2529-2531. (g) Sachdev, K.; Sachdev, H. S. *Tetrahedron Lett.* 1976, 4223-4226. (h) Reich, H. J.; Shah, S. K. *J. Org. Chem.* 1977, 42, 1773-1776. (i) Ayalon-Chass, D.; Ehlinger, E.; Magnus, P. *J. Chem. Soc., Chem. Commun.* 1977, 772-773. (j) Cooke, F.; Magnus, P. *Ibid.* 1977, 513.

(7) (a) Rosario, O.; Oliva, A.; Larson, G. L. *J. Organomet. Chem.* 1978, 146, C8-C10. (b) Larson, G. L.; Arguelles, R.; Rosario, O.; Sandoval, S. *Ibid.* 1980, 198, 15-23.

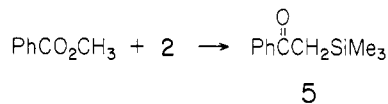
Lithiation of 1 was accomplished under conditions similar to those reported for lithiation of bis(propanediol) methanediborate,<sup>3</sup> with lithium tetramethylpiperidide (LiTMP) as base, tetramethylethylenediamine (TMEDA) as activator, and tetrahydrofuran (THF) as solvent. Treatment of the resulting solution of pinacol lithio(trimethylsilyl)methaneboronate (2) with various alkyl halides gave good yields of the corresponding pinacol 1-(trimethylsilyl)alkane-1-boronates (3), summarized in Table I. In exploratory experiments, the use of lithium diisopropylamide (LDA) in place of LiTMP lowered the yields of 3 by 10–15%. No test of the necessity of the TMEDA was made.



Reaction of pinacol lithio(trimethylsilyl)methaneboronate (2) with aldehydes or ketones yielded pinacol alkeneboronates 4 as summarized in Table II. The distilled products 4 showed no trimethylsilyl peaks near  $\delta$  0 in the proton NMR spectra, indicating that silicon is eliminated exclusively, presumably as the volatile bis(trimethylsilyl) ether. From the characteristic vinylic proton patterns in the NMR spectra, which had been well established previously,<sup>10</sup> it was found that the alkeneboronates 4 derived from aldehydes consisted of a mixture of about 70% *Z* and 30% *E* isomers.



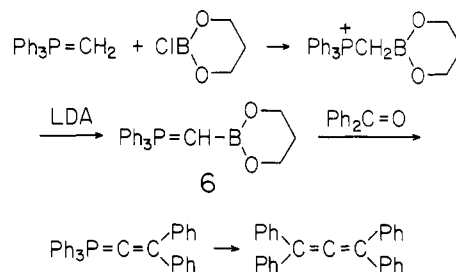
In contrast to the exclusive elimination of silicon in the reactions with aldehydes and ketones, reaction of 2 with methyl benzoate resulted in boron elimination as the major pathway, yielding  $\alpha$ -(trimethylsilyl)acetophenone (5). Similar results were obtained with methyl cyclohexanecarboxylate, which yielded mostly (trimethylsilyl)methyl cyclohexyl ketone. However, the presence of bis(pinacol) diborate,  $\text{Me}_4\text{C}_2\text{O}_2\text{BOBO}_2\text{C}_2\text{Me}_4$ , interfered with the purification of these (trimethylsilyl)methyl ketones by distillation.



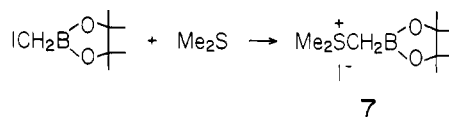
Several attempts were made to deprotonate  $\alpha$ -(trimethylsilyl)alkaneboronic esters other than 1, all of them totally unsuccessful. For example, treatment of pinacol 1-(trimethylsilyl)hexane-1-boronate with LiTMP and TMEDA at various temperatures, followed by addition of 1-bromopentane, led only to recovery of unchanged starting boronic ester. Similarly negative results were obtained with 1,3-propanediol cyclohexyl(trimethylsilyl)methaneboronate. 1,3-Propanediol (trimethylsilyl)methaneboronate was prepared and tested as an alternative to 1 but was recovered unchanged when subjected to conditions that led to lithiation and alkylation of 1.

**A Boron-Substituted Wittig Reagent.** The chemistry of the lithio(trimethylsilyl)methaneboronic ester 2 just

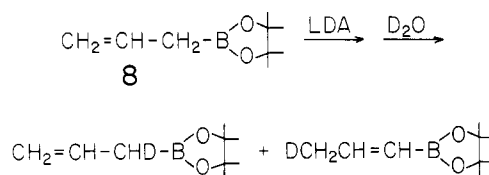
described has much in common with that of Wittig reagents. We have also prepared a boron-substituted Wittig reagent (6) by treatment of methylenetriphenylphosphorane with 1,3-propanediol-boron chloride followed by LDA. Reaction in situ with benzophenone gave tetraphenylallene, or with benzaldehyde gave 1,3-diphenylallene, in 40–60% yields. Heptanal with 6 failed to yield any allenic product.



**Other Attempted Lithiations.** A sulfonium-substituted boronic ester, dimethyl[(4,4,5,5-tetramethyl-1,3,2-dioxaborol-2-yl)methyl]sulfonium iodide (7), was prepared. An attempt to lithiate 7 and condense it with benzaldehyde failed to yield any unsaturated product, and it appeared that the acidic and less hindered *S*-methyl groups were attacked preferentially.



Pinacol allylboronate 8 was readily lithiated by LiTMP and TMEDA, as shown by proton NMR analysis of the recovered 8 and its 1-propeneboronate isomer after treatment with  $\text{D}_2\text{O}$ , which attacked mainly the  $\alpha$ -position. Methyl iodide also appeared to attack lithiated 8 mainly at the  $\alpha$ -position, but butyl iodide and trimethylsilyl chloride attacked mainly at the  $\gamma$ -position. Gross mixtures were obtained in all cases, and it did not appear that lithiated 8 could function as a useful synthetic reagent.



**Homologation of Boronic Esters.** Reactions of alkyl halides with boron-substituted carbanions work well only if the alkyl group is primary. In order to make  $\alpha$ -substituted boronic esters that were inaccessible by the alkylation route, we undertook a search for homologations of boronic esters analogous to the well-known homologations of trialkylboranes. For example, trialkylboranes,  $\text{R}_3\text{B}$ , are homologated by [bis(phenylthio)methyl]lithium,  $(\text{PhS})_2\text{CHLi}$ , to form  $\alpha$ -phenylthio boranes  $\text{R}_2\text{BCH}(\text{SPh})\text{R}$ .<sup>8</sup> However, numerous attempts to homologate boronic esters,  $\text{RB}(\text{OR}')_2$ , with  $\text{PhSCHXLi}$ , where X was  $\text{SPh}$ ,  $\text{SMe}_2^+$ ,  $\text{NMe}_3^+$ , or  $\text{Cl}$ , all failed. 1,2-Bis(phenylthio)ethene,  $\text{PhSCH}=\text{CHSPh}$ , was the characteristic by-product, in addition to unchanged  $\text{RB}(\text{OR}')_2$ . Two typical examples of the many attempts are described in the Experimental Section. Mediocre successes have been reported elsewhere when the postulated tetracoordinate borate intermediate was assembled in reverse order, starting with  $\text{PhSCHXB}(\text{OR}')_2$  and  $\text{RMgX}$  or  $\text{RLi}$ .<sup>4a,11</sup> In the best of these, X was Br and R was Ph, but the reaction

(10) Matteson, D. S.; Jesthi, P. K. *J. Organomet. Chem.* 1976, 110, 25–37.

(11) Mendoza, A.; Matteson, D. S. *J. Org. Chem.* 1979, 44, 1352–1354.

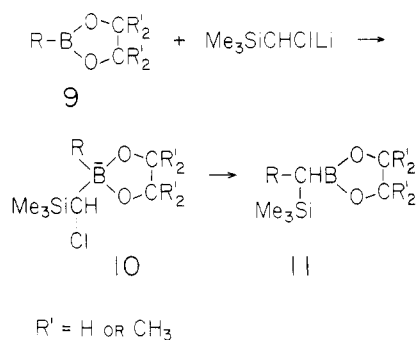
Table III. Homologation of Cyclic Boronic Esters,  $RBO_2(CR'_2)_2$  (9), with [Chloro(trimethylsilyl)methyl]lithium,  $Me_3SiCHClLi$ , To Form  $\alpha$ -Trimethylsilyl Boronic Esters,  $RCH(SiMe_3)BO_2(CR'_2)_2$  (11)

R	R'	bp of 11, °C (torr)	%
1-butyl	H	80-84 (4)	86
1-butyl	CH <sub>3</sub>	48-51 (0.07)	80
2-butyl	H	86-90 (5)	85
1-octyl	H	80-85 (0.15)	83
allyl	CH <sub>3</sub>	90-94 (4)	78
1-propenyl <sup>a</sup>	CH <sub>3</sub>	86-90 (3.5)	74
cyclopentyl	H	96-99 (4)	80
cyclohexyl	H	72-75 (1)	81
phenyl	H, CH <sub>3</sub> <sup>b</sup>	85-89 (0.1)	76
benzyl	H	80-85 (0.1)	77
C <sub>6</sub> H <sub>5</sub> SCH <sub>2</sub>	H	108-110 (0.05)	80

<sup>a</sup> *Z, E* mixture. <sup>b</sup> The ethylene glycol ester was homologated, and the product was transesterified with pinacol to yield 11, R = Ph, R' = CH<sub>3</sub>.

failed when R was *n*-butyl,<sup>4a</sup> even though simpler  $\alpha$ -halo boronic esters have long been known to undergo replacement of halide by alkyl on treatment with Grignard reagents.<sup>2a</sup>

In sharp contrast to all of the difficulties with the sulfur-substituted series, [chloro(trimethylsilyl)methyl]lithium<sup>5,12</sup> was found to homologate cyclic boronic esters 9 very efficiently to the corresponding  $\alpha$ -trimethylsilyl boronic esters 11, presumably by way of the usual type of tetra-coordinate borate intermediate 10. Results are summarized in Table III.

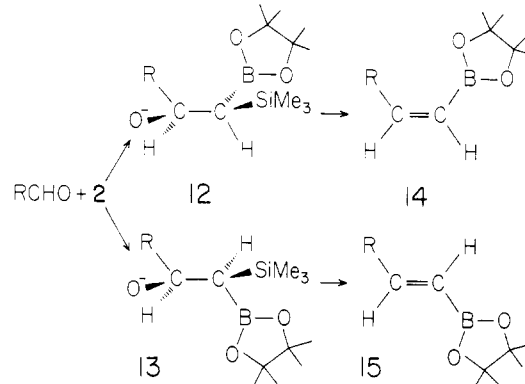


### Discussion

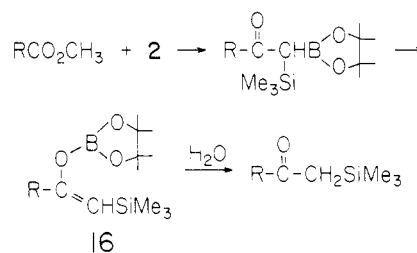
**Silicon Elimination.** We had not expected the elimination of silicon in preference to boron in the reactions of pinacol lithio(trimethylsilyl)methaneboronate (2) with aldehydes and ketones. Usually, boron-carbon bonds are more easily cleaved than silicon-carbon bonds, perhaps because boron coordinates more easily with bases that typically catalyze such cleavages. Our experience with Wittig-like boronic ester reagents indicated them to be much more efficient in condensations with ketones than the corresponding trimethylsilyl reagents,<sup>11</sup> though the efficiency of the boron reagents may lie in lesser steric hindrance to the initial carbon-carbon bond formation or in lower basicity toward enolizable ketones and may have nothing to do with the subsequent elimination step.

The predominance of the *Z* isomer 14 in the mixture of 1-alkene-1-boronic esters formed from 2 and aldehydes was also unanticipated and may be contrasted with the high predominance of the *E* isomer 15 from reactions of aldehydes with lithiomethanediboronic esters.<sup>3,10</sup> However, in the latter case, the choice between the two boron atoms

is not made until the elimination step itself, and the result is reasonable on steric grounds. In contrast, the initial attack of the silyl reagent 2 on the aldehyde to form the postulated intermediates 12 and 13 probably fixes the ultimate geometry of the products 14 and 15. Since deprotonation of  $\beta$ -hydroxy silanes normally results in stereospecific syn elimination,<sup>13</sup> that pathway is illustrated. However, the preference for formation of intermediate 12 over 13 is not readily explained.



The preferential elimination of boron in the reaction of 2 with carboxylic esters was what we expected and is postulated to proceed by way of boron enolate 16.  $\alpha$ -Silyl ketones isomerize readily to silyl enolates only on heating above 100 °C,<sup>14</sup> and in view of our previous failure to observe any evidence for stability of postulated  $\alpha$ -boryl ketone intermediates,<sup>3</sup> it appears likely that the 1,3 shift of boron from the  $\alpha$ -carbon to the carbonyl oxygen is many orders of magnitude faster than the analogous shift of silicon. The vacant and acidic p orbital of the boron atom makes this 1,3 shift Woodward-Hoffmann allowed, but the much less acidic d orbital of the silicon leaves the 1,3 shift with partially forbidden character, though it is intramolecular, as shown by the retention of configuration at silicon.<sup>14</sup>



### Boron Elimination in Preference to Phosphorus.

The formation of tetraphenylallene or 1,3-diphenylallene from the boron substituted Wittig reagent 6 and benzophenone or benzaldehyde, respectively, provides clear evidence that boron is eliminated in preference to phosphorus. If the phosphorus were eliminated first, the product would be an alkeneboronic ester. An attempt to deprotonate an alkeneboronic ester has failed,<sup>3a</sup> and even the deboronation of alkene-1,1-diboronic esters, which should be easier than deprotonation, appears not to occur.<sup>15</sup>

(13) Hudrlik, P. F.; Peterson, D. *J. Am. Chem. Soc.* 1975, 97, 1464-1468.

(14) Brook, A. G.; MacRae, D. M.; Limburg, W. W. *J. Am. Chem. Soc.* 1967, 89, 5493-5495.

(15) Moody, R. J.; Matteson, D. S. *J. Organomet. Chem.* 1978, 152, 265-270. When first observed, the replacement of a boronic ester group by alkyl was thought to involve a boron-substituted vinylic carbanion, but subsequent investigation conclusively ruled out such a mechanism. Negative evidence lost in the refereeing process included the fact that the supposed anion could not be trapped by butyl iodide: Moody, R. J., Ph.D. Thesis, WSU, 1977.

(12) We thank Professor George Rubottom of the University of Idaho for a timely reminder of the availability of this reagent.

Initial boron elimination, on the other hand, would yield a phosphonium salt which could be deprotonated to a vinylidenephosphorane that would lead to the allene.

In view of the apparent limitation of this synthesis to symmetrical aryllallenes, no further work has been undertaken.

**Homologation of Boronic Esters.** The failure of attempted homologations of boronic esters with PhSCHXLi and the formation of 1,2-bis(phenylthio)ethene instead suggests that the boron of boronic esters, in sharp contrast to that of trialkylboranes, is not acidic enough to bind the stabilized anions of the class PhSCHX<sup>-</sup> irreversibly. Loss of X<sup>-</sup> leaves the relatively stable carbene PhSCH, which could dimerize if it accumulated in high enough concentration, but which can probably faster attack the more abundant PhSCHX<sup>-</sup> or even its boronic ester complex directly to form the "carbene dimer".

In contrast to the sulfur-substituted carbanions, [chloro(trimethylsilyl)methyl]lithium is a very strong base and probably cannot dissociate from the boronic ester once it is bound. Silylcarbenes are generated only with difficulty<sup>16</sup> and would be unlikely to form directly or indirectly. Thus, the only reaction pathway available to the postulated [chloro(trimethylsilyl)methyl]borate intermediate **10** is the observed rearrangement to  $\alpha$ -trimethylsilyl boronic ester **11**, a reaction type which has ample precedent.<sup>2</sup>

We have reported the efficient analogous homologation of boronic esters with (dichloromethyl)lithium elsewhere.<sup>17,18</sup>

**Synthetic Potential.** Pinacol (trimethylsilyl)methaneboronate (**1**) is easier to make than diboronic esters<sup>3</sup> or triboronic esters.<sup>2c,d</sup> alternative reagents suitable for conversion of carbonyl compounds to the homologous alkene-1-boronic esters. One rather prosaic use of alkene-1-boronic esters is as precursors to aldehydes,<sup>19</sup> though the pinacol esters produced in the present work require longer oxidation times than the ethylene glycol esters described previously, and the direct use of [chloro(trimethylsilyl)methyl]lithium to accomplish the same net homologation<sup>5</sup> would normally be chosen, with a few possible exceptions.<sup>19</sup> The alkeneboronic esters are ultimately of more interest for their potential utility as starting materials for chiral synthesis.<sup>18</sup> The predominantly *Z* geometry of the alkene-1-boronic esters derived from **2** and aldehydes is of particular interest in that regard. The possibility of increasing the *Z/E* ratio by varying the relative bulk of the silyl and boronic ester groups remains to be explored.

$\alpha$ -Silylated boranes produced by homologation of trialkylboranes are readily oxidized to  $\alpha$ -hydroxy silanes by hydrogen peroxide,<sup>7</sup> and  $\alpha$ -trimethylsilyl boronic esters are expected to behave similarly, as has been demonstrated for one example.<sup>20</sup>

Our failure to deprotonate  $\alpha$ -(trimethylsilyl)alkaneboronic esters other than the silylmethaneboronic ester **1** is a considerable limitation on the synthetic utility of these compounds. The much greater flexibility of  $\alpha$ -chloro boronic esters as synthetic intermediates has turned our major efforts in that direction. However, some additional useful properties of trimethylsilyl boronic esters are explored in the following paper.<sup>20</sup>

Our brief investigation of the synthesis of (trimethylsilyl)methyl ketones is insufficient to define how useful this route might become. Published routes to the two examples we made lack convenience or efficiency,<sup>21,22</sup> and with the assumption that the purification problems we encountered could be overcome with modest effort (careful redistillation or chromatography), our route offers considerable advantage.

## Experimental Section

**General Data.** Reactions involving carbanions were carried out under argon. Tetrahydrofuran (THF) was freshly distilled from sodium benzophenone ketyl. Amines were distilled from calcium hydride and stored over molecular sieves. Butyllithium was titrated against 2-propanol to the 1,10-phenanthroline endpoint. (Chloromethyl)trimethylsilane was purchased from Petrarch, Inc. Proton NMR spectra were taken at 60 MHz with a Varian EM-360 instrument and are referred to the trimethylsilyl group of trimethylsilyl compounds or to internal tetramethylsilane for other compounds. (The trimethylsilyl peak was verified to be at  $\delta$  0.0 compared to internal tetramethylsilane in three cases: pinacol  $\alpha$ -(trimethylsilyl)benzylboronate, ethylene glycol cyclohexyl(trimethylsilyl)methaneboronate, and ethylene glycol cyclopentyl(trimethylsilyl)methaneboronate.) Elemental analyses were by Galbraith Laboratories, Knoxville, TN.

**Pinacol (Trimethylsilyl)methaneboronate (1).** The Grignard reagent was prepared from (chloromethyl)trimethylsilane in ether on a 0.1-mol scale as described in the literature.<sup>9</sup> The Grignard solution was transferred under argon to an addition funnel, and 13 mL of trimethyl borate in 25 mL of ether was placed in a separate addition funnel, both attached to a flask equipped with a mechanical Teflon paddle stirrer and containing 50 mL of ether. The flask was cooled in a  $-78$  °C bath, and the contents were stirred vigorously during the simultaneous dropwise addition of the Grignard and trimethyl borate solutions.<sup>23</sup> The mixture was stirred 2–3 h at  $-78$  °C and allowed to warm to 25 °C overnight and then treated with 100 mL of ice-cold 2 M hydrochloric acid. The product was extracted with 3  $\times$  100 mL of 5:1 ether/dichloromethane, the solution was concentrated, and the solid residue was recrystallized from water to yield 65–75% (trimethylsilyl)methaneboronic acid, which was not characterized but treated with an equivalent amount of pinacol hydrate in hexane overnight. Separation and distillation yielded the pinacol ester **1**: bp 70–72 °C (12 torr); 60-MHz NMR (CCl<sub>4</sub>)  $\delta$  0.0 (s, 11, CH<sub>2</sub>SiCH<sub>3</sub>), 1.25 (s, 12, CCH<sub>3</sub>). Anal. Calcd for C<sub>10</sub>H<sub>23</sub>BO<sub>2</sub>Si: C, 56.08; H, 10.82; B, 5.05; Si, 13.11. Found: C, 55.83; H, 10.87; B, 4.91; Si, 13.30.

**Pinacol Lithio(trimethylsilyl)methaneboronate (2) Solutions.** Lithium tetramethylpiperidide was made from 10 mmol of 2,2,6,6-tetramethylpiperidine in 15 mL of THF by addition of 10 mmol of 2 M butyllithium in hexane with stirring at 0 °C. A solution of 10 mmol (2.14 g) of pinacol (trimethylsilyl)methaneboronate (**1**) in 10 mL of THF was added by syringe, followed by addition of 10 mmol of 1,2-bis(dimethylamino)ethane (TMEDA). The solution was stirred 2–3 h at 0 °C before use.

**Reaction of Pinacol Lithio(trimethylsilyl)methaneboronate (2) Solutions with Alkyl Halides.** A 10-mmol sample of the alkyl halide was added by syringe to the solution of **2** described in the preceding paragraph, and the mixture was allowed to warm to 25 °C overnight. A 50-mL sample of 5:1 ether/dichloromethane was added, and the solution was washed with saturated sodium chloride and dried over magnesium sulfate. Distillation yielded the corresponding pinacol  $\alpha$ -trimethylsilyl boronates **3**. Yields and boiling points are summarized in Table I and proton NMR and analytical data in Table IV.

**Reaction of Pinacol Lithio(trimethylsilyl)methaneboronate (2) Solutions with Aldehydes and Ketones.** The solution of **2** prepared as described above was cooled to  $-78$  °C, and the aldehyde or ketone (10 mmol) was added by syringe. The

(16) Seyferth, D.; Hanson, E. M. *J. Am. Chem. Soc.* **1968**, *90*, 2438–2440.

(17) Matteson, D. S.; Majumdar, D. *J. Am. Chem. Soc.* **1980**, *102*, 7588–7590.

(18) Matteson, D. S.; Ray, R. *J. Am. Chem. Soc.* **1980**, *102*, 7590–7591.

(19) Matteson, D. S.; Moody, R. J. *J. Org. Chem.* **1980**, *45*, 1091–1095.

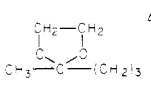
(20) Tsai, D. J. S.; Matteson, D. S. *Organometallics*, following article in this issue.

(21) Brook, A. G.; Limburg, W. W.; MacRae, D. M.; Fieldhouse, S. A. *J. Am. Chem. Soc.* **1967**, *89*, 704–706.

(22) Ruden, R. A.; Gaffney, B. L. *Synth. Commun.* **1975**, *5*, 15–19.

(23) Washburn, R. M.; Levens, E.; Albright, C. F.; Billig, F. A. "Organic Syntheses"; Wiley: New York, 1963; Coll. Vol. 4, 68–72.

Table IV. 60-MHz Proton NMR Spectra (CCl<sub>4</sub>) and Elemental Analyses for Pinacol  $\alpha$ -Trimethylsilyl Boronates, RCH(SiMe<sub>3</sub>)BO<sub>2</sub>C<sub>2</sub>Me<sub>4</sub> (3)

R	NMR, <sup>a</sup> $\delta$		calcd (found)			
	SiCHB	R	C	H	B	Si
CH <sub>3</sub> (CH <sub>2</sub> ) <sub>3</sub> <sup>b,c</sup>	0.33	0.9-1.3	62.21 (61.33 <sup>d</sup> )	11.56 (11.74)	4.00 (3.81)	10.39 (10.48)
CH <sub>3</sub> (CH <sub>2</sub> ) <sub>4</sub> <sup>b</sup>	0.33	0.9-1.3	63.37 (63.20)	11.70 (11.59)	3.80 (3.62)	9.88 (10.04)
CH <sub>3</sub> (CH <sub>2</sub> ) <sub>5</sub> <sup>b</sup>	0.33	0.9-1.3	64.41 (64.21)	11.82 (11.66)	3.62 (3.61)	9.41 (9.42)
C <sub>6</sub> H <sub>5</sub> <sup>e</sup>	1.90	7.2	66.20 (65.96)	9.38 (9.51)	3.72 (3.72)	9.68 (9.88)
C <sub>6</sub> H <sub>5</sub> CH <sub>2</sub> <sup>b</sup>	0.73	2.69 (d), 7.23	67.10 (66.71)	9.61 (9.74)	3.55 (3.39)	9.23 (9.21)
C <sub>6</sub> H <sub>5</sub> CH <sub>2</sub> CH <sub>2</sub> <sup>b</sup>	0.33	1.66, 2.59, 7.23	67.91 (68.10)	9.82 (9.83)	3.40 (3.19)	8.82 (8.99)
C <sub>6</sub> H <sub>5</sub> OCH <sub>2</sub> CH <sub>2</sub> <sup>b</sup>	0.33	1.83, 3.83, 6.8-7.2	64.66 (64.47)	9.35 (9.48)	3.23 (3.06)	8.40 (8.65)
	0.33	1.5, 3.89 (s)	59.64 (59.55)	10.30 (10.12)	3.16 (3.01)	8.20 (8.50)
CH <sub>2</sub> =CHCH <sub>2</sub> <sup>c</sup>	0.33	2.16, 5.03-5.82	61.41 (61.23)	10.70 (10.89)	4.25 (4.05)	11.05 (11.30)
CH <sub>3</sub> CH=CH <sup>c</sup>	1.50	1.66, 5.43	61.41 (61.22)	10.70 (10.65)	4.25 (4.02)	11.05 (11.24)

<sup>a</sup> All spectra showed a singlet assigned the value  $\delta$  0.00 [(CH<sub>3</sub>)<sub>3</sub>Si] and a singlet near  $\delta$  1.2 (range of 1.13-1.23) [(CH<sub>3</sub>)<sub>2</sub>C]. The SiCHB peak was characteristically broad, with fine structure partially resolved. Appropriate splittings and satisfactory integrals were observed. <sup>b</sup> Compound prepared by alkylation of 2. <sup>c</sup> Prepared by homologation of RBO<sub>2</sub>C<sub>2</sub>Me<sub>4</sub> (9). <sup>d</sup> Through oversight, no attempt was made to correct this single errant analysis. <sup>e</sup> Prepared by homologation of PhBO<sub>2</sub>C<sub>2</sub>H<sub>4</sub> and transesterification with pinacol.

Table V. 60-MHz Proton NMR Spectra (CCl<sub>4</sub>) and Elemental Analyses for Pinacol Alkene-1-boronates, RR'C=CHBO<sub>2</sub>C<sub>2</sub>Me<sub>4</sub> (4)

R	R'	NMR (CCl <sub>4</sub> ), <sup>a</sup> $\delta$			calcd (found)		
		R	R'	=CHB	C	H	B
CH <sub>3</sub> (CH <sub>2</sub> ) <sub>5</sub>	H <sup>b</sup>	0.9-1.4, 2.3	6.53	5.35 <sup>c</sup>	70.60 (70.76)	11.43 (11.67)	4.54 (4.38)
CH <sub>3</sub> (CH <sub>2</sub> ) <sub>3</sub>	CH <sub>3</sub> (CH <sub>2</sub> ) <sub>3</sub>	0.9-1.4, 2.3		5.10	72.18 (72.20)	11.74 (11.80)	4.06 (3.92)
C <sub>6</sub> H <sub>5</sub>	H <sup>b</sup>	7.2-7.7	(7.5)	5.56 <sup>d</sup>	73.07 (72.91)	8.32 (8.51)	4.70 (4.46)
C <sub>6</sub> H <sub>5</sub>	C <sub>6</sub> H <sub>5</sub>	7.4	7.4	6.03	78.45 (78.30)	7.57 (7.64)	3.53 (3.29)
-(CH <sub>2</sub> ) <sub>5</sub> -		1.63, 2.4		5.03	71.81 (72.01)	9.90 (9.75)	4.62 (4.48)

<sup>a</sup> Pinacol CCH<sub>3</sub> characteristically at  $\delta$  1.23, range of 1.13-1.26. Multiplicities and integrals of all peaks are consistent with assigned structures. <sup>b</sup> About two-thirds *Z* isomer. <sup>c</sup> For *Z* isomer,  $J = 13$  Hz. *E* isomer,  $\delta$  5.40 ( $J = 20$  Hz). <sup>d</sup> *Z* isomer,  $J = 14$  Hz. *E* isomer,  $\delta$  6.13 ( $J = 18$  Hz). The *E* isomer has been characterized previously.<sup>3,8</sup>

mixture was stirred 2-3 h at -78 °C and allowed to warm to 25 °C overnight. Treatment with 50 mL of cold 2 M hydrochloric acid, extraction with 5:1 ether/dichloromethane, washing with saturated sodium chloride, drying over magnesium sulfate, and distillation yielded the alkeneboronic esters 4. Yields and boiling points are summarized in Table II and 60-MHz proton NMR spectra and analytical data in Table V.

**$\alpha$ -(Trimethylsilyl)acetophenone (5).** A solution of 2 (10 mmol) at -78 °C was treated with 10 mmol of methyl benzoate, stirred 3 h at -78 °C, and allowed to warm to 25 °C overnight. A 50-mL sample of 10% potassium dihydrogen phosphate solution was added to 0 °C. After extraction with 5:1 ether/dichloromethane, washing with saturated sodium chloride, and drying over magnesium sulfate, the product 5 was distilled: bp 52-58 °C (0.25 torr) [lit.<sup>21</sup> bp 104 °C (3 torr)]; 1.1 g, 49% corrected for the presence of 14% bis(pinacol) diborate as indicated by the NMR peak at  $\delta$  1.2; NMR (CCl<sub>4</sub>)  $\delta$  0.0 (s, 9, SiCH<sub>3</sub>), 2.82 (s, 2, SiCH<sub>2</sub>CO), 7.6-8.0 (m, 5, C<sub>6</sub>H<sub>5</sub>).

**Cyclohexyl (Trimethylsilyl)methyl Ketone.** The procedure described for the preparation of 5 in the preceding paragraph was followed, substituting methyl cyclohexanecarboxylate for methyl benzoate. Cyclohexyl (trimethylsilyl)methyl ketone, bp 59-63 °C (0.25 torr), containing 10% bis(pinacol) diborate by NMR analysis was obtained in 67% contained yield: NMR (CCl<sub>4</sub>)  $\delta$  0.0 (s, 9, SiCH<sub>3</sub>), 1.50 (m, 10, CH<sub>2</sub>), 2.00 (m, 1, CHCO), 2.06 (s, 2, SiCH<sub>2</sub>CO) (Lit.<sup>22</sup>  $\delta$  2.02 (SiCH<sub>2</sub>CO)).

**1,3-Propanediol (Trimethylsilyl)methaneboronate.** (Trimethylsilyl)methaneboronic acid and 1,3-propanediol in hexane were refluxed with a Dean-Stark trap to remove the water, and the product was distilled: bp 63-65 °C (45 torr); NMR (CCl<sub>4</sub>)  $\delta$  0.0 (s, 11, CH<sub>2</sub>SiCH<sub>3</sub>), 1.93 (m, 2, CH<sub>2</sub>), 4.03 (t, 4, CH<sub>2</sub>O).

**Attempted Deprotonation of Other  $\alpha$ -Trimethylsilyl Boronic Esters.** The deprotonation procedure successfully used to convert 1 to 2 was tested with 1,3-propanediol (trimethylsilyl)methaneboronate, 1,3-propanediol (trimethylsilyl)cyclohexylmethaneboronate, and pinacol 1-(trimethylsilyl)hexane-1-

boronate, followed by addition of 1-iodobutane or 1-bromopentane. In all three cases, 80-85% of the unchanged starting boronic ester was recovered. The attempted deprotonations were all repeated at 25 °C, again with no evidence of reaction. Lithium diethylamide or diisopropylamide failed to deprotonate pinacol 1-(trimethylsilyl)hexane-1-boronate, and *sec*-butyllithium or *tert*-butyllithium led to 50% loss of the boronic ester but no evidence of alkylation.

**Boronic Esters 9.** Boronic acids were prepared by a variant of the standard procedure,<sup>23</sup> as described in some detail for 1. Esterification with pinacol was carried out as in the preparation of 1. Esterification with ethylene glycol was accomplished by distilling the water azeotrope from a hexane solution and collecting the water in a Dean-Stark trap. Residual ethylene glycol was removed by treatment with anhydrous calcium chloride. The products 9 were distilled under reduced pressure. Several have been reported previously: **ethylene glycol 1-butaneboronate**, bp 60-62 °C (5 torr) (lit.<sup>24</sup> bp 122-122.5 °C); **pinacol 1-butaneboronate**;<sup>11</sup> **ethylene glycol phenylboronate**, bp 85-89 °C (5 torr) (lit.<sup>24</sup> bp 218-220 °C); **ethylene glycol benzylboronate**, bp 55 °C (0.1 torr) [lit.<sup>25</sup> bp 60 °C (0.1 torr)]; **ethylene glycol (phenylthio)methaneboronate**;<sup>4</sup> **1,3-propanediol cyclohexaneboronate**, bp 85-90 °C (5 torr) [lit.<sup>26</sup> bp 93-94 °C (6 torr)]; **ethylene glycol cyclohexaneboronate**, bp 73-76 °C (5 torr) (lit.<sup>27</sup> lacks experimental details). Anal. Calcd for C<sub>6</sub>H<sub>15</sub>BO<sub>2</sub>: C, 62.39; H, 9.82; B, 7.02. Found: C, 62.44; H, 9.75; B, 7.24. The others were not found in the literature. **Pinacol allylboronate** was distilled from a little galvinoxyl to prevent polymerization encountered otherwise: bp 50-53 °C (5 torr); NMR (CCl<sub>4</sub>)  $\delta$  1.26

(24) Laurent, J. P. C. R. *Hebd. Seances Acad. Sci.* 1962, 254, 866-868.(25) Korcek, S.; Watts, G. B.; Ingold, K. U. *J. Chem. Soc. Perkin Trans. 2* 1972, 242-248.(26) Brown, H. C.; Gupta, S. K. *J. Am. Chem. Soc.* 1970, 92, 6983-6984.(27) Tokuda, M. Chung, V. V.; Inagaki, K.; Itoh, M. *J. Chem. Soc., Chem. Commun.* 1977, 690-691.



Table VI. 60 MHz Proton NMR Spectra ( $\text{CCl}_4$ ) and Elemental Analyses for Ethylene Glycol  $\alpha$ -Trimethylsilyl Boronates,  $\text{RCH}(\text{SiMe}_3)\text{BO}_2\text{C}_2\text{H}_4$  (11, R = H)

R	NMR, <sup>a</sup> $\delta$		calcd (found)			
	SiCHB	R	C	H	B	Si
1-butyl	0.35	1.06, 1.33	56.08 (56.32)	10.82 (10.97)	5.05 (4.93)	13.11 (13.27)
2-butyl	0.4	1.0, 1.33	56.08 (55.85)	10.82 (10.52)	5.05 (4.90)	13.11 (13.00)
1-octyl	0.35	1.06, 1.33	62.21 (62.39)	11.56 (11.65)	4.00 (3.74)	10.39 (10.11)
cyclopentyl	0.5	1.66	58.41 (58.18)	10.25 (10.16)	4.78 (4.50)	12.42 (12.49)
cyclohexyl	0.3	1.5	60.00 (59.70)	10.49 (10.32)	4.50 (4.32)	11.69 (11.90)
benzyl	0.73	2.69, 7.23	62.91 (63.04)	8.53 (8.73)	4.36 (4.12)	11.32 (11.04)
$\text{C}_6\text{H}_5\text{SCH}_2$ -	0.83	2.82, 7.30	55.71 (55.54)	7.55 (7.54)	3.86 (3.65)	10.02 (9.81)

<sup>a</sup> All spectra showed a singlet assigned the value  $\delta$  0.00 [ $(\text{CH}_3)_3\text{Si}$ ] and a singlet near  $\delta$  4.2 (range of 4.06–4.26). The SiCHB peaks were broad. Appropriate splittings and satisfactory integrals were observed.

(s, 12,  $\text{CCH}_3$ ), 1.73 (d, 2,  $\text{CH}_2\text{B}$ ), 5.06–5.93 (m, 3,  $\text{CH}=\text{CH}_2$ ). Anal. Calcd for  $\text{C}_9\text{H}_{17}\text{BO}_2$ : C, 64.33; H, 10.20; B, 6.43. Found: C, 64.09; H, 10.45; B, 6.22. **Pinacol 1-propene-1-boronate** was made by transesterification of the known butyl ester<sup>28</sup> with pinacol: bp 46–47 °C (4 torr); NMR ( $\text{CDCl}_3$ ) shows splittings similar to those previously described for the *E* and *Z* boronic acids and ethylene glycol esters,<sup>10</sup> *E/Z* ratio about 2,  $\delta$  1.28 ( $\text{CCH}_3$ ), 1.85 (*E*  $\text{CHCH}_3$ ), 1.97 (*Z*  $\text{CHCH}_3$ ), 5.4 (*Z*  $\text{BCH}=\text{}$ ), 5.5 (*E*  $\text{BCH}=\text{}$ ), 6.6 ( $=\text{CHCH}_3$ ). Anal. Calcd: see preceding isomer. Found: C, 64.51; H, 9.91; B, 6.57. **Ethylene glycol 2-butaneboronate**: bp 38 °C (10–12 torr); NMR ( $\text{CCl}_4$ )  $\delta$  1.03 (m, 6,  $\text{CH}_3$ ), 1.50 (m, 3,  $\text{CHCH}_2$ ), 4.29 (s, 4,  $\text{OCH}_2$ ). Anal. Calcd for  $\text{C}_8\text{H}_{13}\text{BO}_2$ : C, 56.31; H, 10.24; B, 8.45. Found: C, 56.15; H, 10.21; B, 8.47. **Ethylene glycol cyclopentaneboronate**: bp 57–58 °C (5 torr); NMR ( $\text{CCl}_4$ )  $\delta$  1.93 (m, 11,  $\text{CH}(\text{CH}_2)_4$ ), 4.26 (s, 4,  $\text{OCH}_2$ ). Anal. Calcd for  $\text{C}_7\text{H}_{13}\text{BO}_2$ : C, 60.06; H, 9.36; B, 7.72. Found: C, 60.28; H, 9.57; B, 7.68. **Ethylene glycol 1-octaneboronate**: bp 68–72 °C (0.8 torr); NMR ( $\text{CCl}_4$ )  $\delta$  0.89 (t, 3,  $\text{CH}_3$ ), 1.29 (m, 14,  $\text{CH}_2$ ), 4.23 (s, 4,  $\text{OCH}_2$ ). Anal. Calcd for  $\text{C}_{16}\text{H}_{21}\text{BO}_2$ : C, 65.25; H, 11.50; B, 5.87. Found: C, 65.58; H, 11.61; B, 5.90.

**Homologation of Boronic Esters 9 to  $\alpha$ -Trimethylsilyl Boronic Esters 11.** A solution of 2.25 g (18.4 mmol) of (chloromethyl)trimethylsilane in 24 mL of THF was stirred at –78 °C during the dropwise addition of 20.3 mmol of *sec*-butyllithium by syringe. A 20-mmol sample of 1,2-bis(dimethylamino)ethane (TMEDA) was added, and the mixture was stirred 45 min at –78 °C and then allowed to warm to –55 °C.<sup>5</sup> A solution of 14 mmol of the boronic ester 9 in 5 mL of tetrahydrofuran was added by syringe, and the mixture was stirred 10 min at –55 °C (except that when ethylene glycol (phenylthio)methaneboronate was used, better results were obtained when the mixture was cooled to –78 °C immediately after addition of the boronic ester). The mixture was cooled to –78 °C immediately after addition of the boronic ester. The mixture was cooled to –78 °C, and the cooling bath was allowed to warm slowly to 25 °C overnight. A 50-mL sample of ice-cold 2 M hydrochloric acid was added, and the product was extracted with 3  $\times$  60 mL of 5:1 ether/dichloromethane. The organic phase was concentrated under reduced pressure. Ethylene glycol esters were treated with 14 mmol of ethylene glycol and 200 mL of hexane or benzene and refluxed with a Dean–Stark trap to remove water. (Partial hydrolysis of these esters during aqueous workup was observed. Pinacol esters proved stable to water and needed no analogous treatment). Excess ethylene glycol was removed by drying over calcium chloride. The solution was concentrated, and the product (11) was distilled under vacuum. Yields and boiling points are summarized in Table III and 60-MHz proton NMR spectra and elemental analyses in Table IV for pinacol esters and in Table VI for ethylene glycol esters. In addition to the tabulated compounds, 1,3-propanediol (trimethylsilyl)cyclohexylmethaneboronate was similarly prepared, bp 80–85 °C (0.25 torr); 82%; NMR consistent with assigned structure, analysis not obtained.

**[(1,3,2-Dioxaborin-2-yl)methylene]phosphorane 6 in the Synthesis of Aryllallenes.** A suspension of 1.57 g (5 mmol) of methyltriphenylphosphonium bromide in 25 mL of THF was treated with 5 mmol of butyllithium at 25 °C, stirred 30 min, and cooled to –78 °C. A solution of 2-chloro-1,3,2-dioxaborinane<sup>29</sup> in

5 mL of THF was added in one portion, yielding an immediate precipitate. After being stirred 10 min at –78 °C and warmed to 0 °C, the mixture was treated with 5 mmol of lithium diisopropylamide in 10 mL of THF and stirred 1 h at 0 °C to form 6. Either 10 mmol of benzophenone or benzaldehyde in 5 mL of THF was added, and the mixture was stirred 30 min at 0 °C and then refluxed 4–5 h. A 50-mL of cold 10 M phosphoric acid was added, and the product was extracted with 2  $\times$  50 mL of 5:1 ether/dichloromethane. The solution was concentrated, and the product was isolated by chromatography on a silica gel plate with hexane. Tetraphenylallene was recrystallized from ethanol: 0.82 g (47%); mp 162–164 °C (lit.<sup>30</sup> mp 164–165 °C). 1,3-Diphenylallene was obtained in 48% yield: mp 48–50 °C (lit.<sup>31</sup> mp 49–51 °C and 53.5–55.5 °C); NMR ( $\text{CDCl}_3$ )  $\delta$  6.53 (s, 1,  $\text{CH}=\text{}$ ), 7.5 (m, 5,  $\text{C}_6\text{H}_5$ ).

**Deprotonation of Pinacol Allylboronate.** Pinacol allylboronate (5 mmol) was added to lithium tetramethylpiperidide (5 mmol) stirred in 10 mL of THF at –78 °C. TMEDA (5 mmol) was added and the mixture was stirred 2 h at –78 °C, warmed to –45 °C and stirred 10 min, and then cooled to –78 °C. Excess deuterium oxide was added, and the solution was allowed to warm to room temperature and worked up with aqueous acid in the usual manner. The product recovered had essentially the same 60-MHz proton NMR spectrum as pinacol allylboronate, except that the integral of the doublet at  $\delta$  1.73 (CDHB) was diminished to 1 H, and small impurity bands attributed to the isomeric 1-propene-1-boronic ester were present. Mixtures resulted from treatment with chlorotrimethylsilane, 1-iodobutane, or iodomethane in place of deuterium oxide. From the NMR spectra, it appeared that  $\gamma$  attack predominated with the first two of these electrophiles and  $\alpha$  attack with the third.

**[(4,4,5,5-Tetramethyl-1,3,2-dioxaborol-2-yl)methyl]dimethylsulfonium Iodide (7).** A solution of 1.34 g (5 mmol) of pinacol iodomethaneboronate in 8 mL of dichloromethane was added to 0.37 mL (5 mmol) of dimethyl sulfide in 5 mL of dichloromethane at 0 °C and kept 2 h at 0 °C. Addition of 50 mL of cold ether precipitated the product (7), which was collected and washed with ether and dried under vacuum: 1.65 g (94%); mp 180–183 °C; NMR ( $\text{CDCl}_3$ )  $\delta$  1.33 (s, 12,  $\text{CCH}_3$ ), 2.17 (s, 2,  $\text{SCH}_2\text{B}$ ), 3.50 (s, 6,  $\text{S}(\text{CH}_3)_2$ ). Anal. Calcd for  $\text{C}_9\text{H}_{20}\text{BIO}_2\text{S}$ : C, 32.75; H, 6.11; B, 3.28; I, 38.45; S, 9.72. Found: C, 32.58; H, 5.98; B, 3.19; I, 38.66; S, 9.52. Treatment of 7 with an equivalent amount of lithium diisopropylamide in ether at 0 °C followed by benzaldehyde overnight at 25 °C, then dissolving the product in water, and precipitating with sodium hexafluorophosphate yielded a solid. This material showed no evidence of vinylic protons near  $\delta$  6 in the NMR.

**Attempted Homologation of Dibutyl 1-Butaneboronate with [Bis(phenylthio)methyl]lithium.** Bis(phenylthio)methane was lithiated with butyllithium in THF at 0 °C, cooled to –78 °C, and treated with an equivalent amount of dibutyl 1-butaneboronate. After warming to room temperature and the usual aqueous workup, distillation yielded unchanged dibutyl butaneboronate and bis(phenylthio)methane. Repetition with

(29) Finch, A.; Lockhart, J. C.; Pearn, J. *J. Org. Chem.* 1961, 26, 3250–3253.

(30) Vorlander, D.; Siebert, C. *Chem. Ber.* 1906, 39, 1024–1035.

(31) (a) Jacobs, T. L.; Dankner, D. *J. Org. Chem.* 1957, 22, 1424–1427. (b) Staab, H. A.; Kurmeier, H. A. *Chem. Ber.* 1968, 101, 2697–2708.

addition of mercuric chloride, lead(II) chloride, cuprous iodide, or methyl fluorosulfonate after the boronic ester yielded the same result.

**Attempted Homologation of Ethylene Glycol Benzeneboronate with (Dimethylsulfonium)(phenylthio)methylide.** Addition of 5 mmol of butyllithium to a suspension of [(phenylthio)methyl]dimethylsulfonium bromide in 40 mL of ether at  $-40^{\circ}\text{C}$  and stirring 2 h at  $-40^{\circ}\text{C}$  yielded a clear solution, to which 5 mmol of ethylene glycol phenylboronate was added. A white precipitate resulted immediately. After another hour at  $-40^{\circ}\text{C}$  and overnight at up to  $25^{\circ}\text{C}$ , the solution was concentrated and distilled. The proton NMR spectrum indicated that the product was a mixture of ethylene glycol benzeneboronate (characteristic phenyl multiplet, clearly not a phenyl-C compound) and 1,2-bis(phenylthio)ethene.

**Acknowledgment.** We thank the National Science Foundation for support, Grants CHE 77-11283 and CHE-8025229.

**Registry No.** 1, 74213-42-6; 2, 83947-62-0; 3 (R =  $\text{CH}_3(\text{CH}_2)_3$ ), 83947-46-0; 3 (R =  $\text{CH}_3(\text{CH}_2)_4$ ), 74213-44-8; 3 (R =  $\text{CH}_3(\text{CH}_2)_5$ ), 83947-47-1; 3 (R =  $\text{C}_6\text{H}_5\text{CH}_2$ ), 74213-45-9; 3 (R =  $\text{C}_6\text{H}_5\text{CH}_2\text{CH}_2$ ), 74213-46-0; 3 (R =  $\text{C}_6\text{H}_5\text{OCH}_2\text{CH}_2$ ), 83947-48-2; 3 (R =  $\text{CH}_3\text{C}(\text{O}_2\text{C}_2\text{H}_4)(\text{CH}_2)_3$ ), 83947-49-3; 3 (R =  $\text{CH}_2=\text{CHCH}_2$ ), 72823-99-5;

(*E*)-3 (R =  $\text{CH}_3\text{CH}=\text{CH}$ ), 83947-51-7; (*Z*)-3 (R =  $\text{CH}_3\text{CH}=\text{CH}$ ), 83947-53-9; 3 (R =  $\text{C}_6\text{H}_5$ ), 83947-57-3; (*Z*)-4 (R =  $\text{CH}_3(\text{CH}_2)_6$ , R' = H), 74213-47-1; (*E*)-4 (R =  $\text{CH}_3(\text{CH}_2)_5$ , R' = H), 83947-55-1; 4 (R = R' =  $\text{CH}_3(\text{CH}_2)_3$ ), 74213-50-6; (*Z*)-4 (R =  $\text{C}_6\text{H}_5$ , R' = H), 74213-48-2; (*E*)-4 (R =  $\text{C}_6\text{H}_5$ , R' = H), 83947-56-2; 4 (R = R' =  $\text{C}_6\text{H}_5$ ), 83947-50-6; 4 (R = R' =  $(\text{CH}_2)_5$ ), 74213-49-3; 5, 13735-78-9; 6, 83947-64-2; 7, 83947-65-3; 9 (R = 1-butyl, R' = H), 10173-39-4; 9 (R = 1-butyl, R' =  $\text{CH}_3$ ), 69190-62-1; 9 (R = 2-butyl, R' = H), 72824-01-2; 9 (R = 1-octyl, R' = H), 83947-60-8; 9 (R = allyl, R' =  $\text{CH}_3$ ), 72824-04-5; (*E*)-9 (R = 1-propenyl, R' =  $\text{CH}_3$ ), 83947-58-4; (*Z*)-9 (R = 1-propenyl, R' =  $\text{CH}_3$ ), 83947-59-5; 9 (R = cyclopentyl, R' = H), 72824-02-3; 9 (R = cyclohexyl, R' = H), 66217-60-5; 9 (R = phenyl, R' = H), 4406-72-8; 9 (R = benzyl, R' = H), 35895-82-0; 9 (R =  $\text{C}_6\text{H}_5\text{SCH}_2$ , R' = H), 72824-03-4; 11 (R = 1-butyl, R' = H), 72823-93-9; 11 (R = 2-butyl, R' = H), 72823-94-0; 11 (R = 1-octyl, R' = H), 83947-52-8; 11 (R = cyclopentyl, R' = H), 72823-95-1; 11 (R = cyclohexyl, R' = H), 72823-96-2; 11 (R = phenyl, R' = H), 83947-54-0; 11 (R = benzyl, R' = H), 72823-97-3; 11 (R =  $\text{C}_6\text{H}_5\text{SCH}_2$ , R' = H), 72823-98-4; cyclohexyl (trimethylsilyl)methyl ketone, 55629-29-3; 1,3-propanediol (trimethylsilyl)methaneboronate, 83947-63-1; 1,3-propanediol cyclohexaneboronate, 30169-75-6; 1,3-propanediol (trimethylsilyl)cyclohexylmethaneboronate, 83947-61-9; tetraphenylallene, 1674-18-6; 1,3-diphenylallene, 19753-98-1; pinacol iodomethaneboronate, 70557-99-2.

## Pinanediol [ $\alpha$ -(Trimethylsilyl)allyl]boronate and Related Boronic Esters

David J. S. Tsai and Donald S. Matteson\*

Department of Chemistry, Washington State University, Pullman, Washington 99164

Received August 24, 1982

Homologation of (+)-pinanediol phenylboronate with [chloro(trimethylsilyl)methyl]lithium yielded ( $\alpha$ S)- and ( $\alpha$ R)-[ $\alpha$ -(trimethylsilyl)benzyl]boronic esters in a 73:27 ratio, as shown by peroxidic deboronation to the known  $\alpha$ -(trimethylsilyl)benzyl alcohol. Similar homologations of pinanediol vinyl, (*Z*)-1-propenyl, and isobutyl boronates were carried out, but the diastereoisomeric ratios were not determined. Reaction of the allylic  $\alpha$ -trimethylsilyl boronic esters with aldehydes was studied. Pinanediol or pinacol 3-(trimethylsilyl)-1-propene-3-boronates yielded mainly (*Z*)-1-(trimethylsilyl)-1-alken-4-ols with aldehydes. Pinanediol (*Z*)-1-(trimethylsilyl)-2-butene-1-boronate with benzaldehyde yielded (*E*)-1-(trimethylsilyl)-3-methyl-4-phenylbut-1-en-4-ol with only 4% *Z* isomer. The stereochemical implications and utility of these reactions in synthesis are discussed. A brief investigation indicated that pinanediol  $\alpha$ -trimethylsilyl boronic esters can be desilylated to boronic esters by tetrabutylammonium fluoride in moist THF.

The homologation of boronic esters with [chloro(trimethylsilyl)methyl]lithium,<sup>1</sup> the directed chiral synthesis by way of homologation of pinanediol boronic esters with (dichloromethyl)lithium,<sup>2</sup> and the utility of allylic boronic esters<sup>3,4</sup> and boranes<sup>5</sup> in stereocontrolled synthesis suggested the possible synthetic utility of pinanediol  $\alpha$ -trimethylsilyl boronic esters. We report here a highly stereoselective assembly of four adjacent carbon atoms (two

chiral, two olefinic) in the reaction of pinanediol (*Z*)-[ $\alpha$ -(trimethylsilyl)crotyl]boronate with benzaldehyde. The synthetic applicability of this reaction is deferred by the low diastereoselectivity (73:27) observed in the homologation of a pinanediol bromide ester with [chloro(trimethylsilyl)methyl]lithium. An apparently general and potentially useful reaction of  $\alpha$ -trimethylsilyl boronic esters is the mild and efficient protodesilylation in the presence of fluoride ion, which provides the final step in the first efficient route from boronic esters,  $\text{RB}(\text{OR}')_2$ , to their simple homologues,  $\text{RCH}_2\text{B}(\text{OR}')_2$ .

### Results

**Homologations.** The reaction with [chloro(trimethylsilyl)methyl]lithium<sup>1</sup> has proved readily applicable to the conversion of (+)-pinanediol boronic esters 1 to the homologous diastereoisomeric (+)-pinanediol boronic esters 2 and 3. One unsatisfactory result was encountered.

(1) Matteson, D. S.; Majumdar, D. *Organometallics*, preceding article in this issue.

(2) Matteson, D. S.; Ray, R. *J. Am. Chem. Soc.* 1980, 102, 7590-7591.

(3) (a) Hoffmann, R. W.; Zeiss, H. J. *J. Org. Chem.* 1981, 46, 1309-1314 and references cited therein. (b) Hoffmann, R. W.; Kemper, B. *Tetrahedron Lett.* 1980, 4883-4886. (c) Hoffmann, R. W.; Weidmann, U. *J. Organomet. Chem.* 1980, 195, 137-146.

(4) Matteson, D. S.; Tsai, D. J. S. *Tetrahedron Lett.* 1981, 22, 2751-2752.

(5) Yamamoto, Y.; Yatagai, H.; Maruyama, K. *J. Am. Chem. Soc.* 1981, 103, 3229-3231.

addition of mercuric chloride, lead(II) chloride, cuprous iodide, or methyl fluorosulfonate after the boronic ester yielded the same result.

**Attempted Homologation of Ethylene Glycol Benzeneboronate with (Dimethylsulfonium)(phenylthio)methylide.** Addition of 5 mmol of butyllithium to a suspension of [(phenylthio)methyl]dimethylsulfonium bromide in 40 mL of ether at  $-40^{\circ}\text{C}$  and stirring 2 h at  $-40^{\circ}\text{C}$  yielded a clear solution, to which 5 mmol of ethylene glycol phenylboronate was added. A white precipitate resulted immediately. After another hour at  $-40^{\circ}\text{C}$  and overnight at up to  $25^{\circ}\text{C}$ , the solution was concentrated and distilled. The proton NMR spectrum indicated that the product was a mixture of ethylene glycol benzeneboronate (characteristic phenyl multiplet, clearly not a phenyl-C compound) and 1,2-bis(phenylthio)ethene.

**Acknowledgment.** We thank the National Science Foundation for support, Grants CHE 77-11283 and CHE-8025229.

**Registry No.** 1, 74213-42-6; 2, 83947-62-0; 3 (R =  $\text{CH}_3(\text{CH}_2)_3$ ), 83947-46-0; 3 (R =  $\text{CH}_3(\text{CH}_2)_4$ ), 74213-44-8; 3 (R =  $\text{CH}_3(\text{CH}_2)_5$ ), 83947-47-1; 3 (R =  $\text{C}_6\text{H}_5\text{CH}_2$ ), 74213-45-9; 3 (R =  $\text{C}_6\text{H}_5\text{CH}_2\text{CH}_2$ ), 74213-46-0; 3 (R =  $\text{C}_6\text{H}_5\text{OCH}_2\text{CH}_2$ ), 83947-48-2; 3 (R =  $\text{CH}_3\text{C}(\text{O}_2\text{C}_2\text{H}_4)(\text{CH}_2)_3$ ), 83947-49-3; 3 (R =  $\text{CH}_2=\text{CHCH}_2$ ), 72823-99-5;

(*E*)-3 (R =  $\text{CH}_3\text{CH}=\text{CH}$ ), 83947-51-7; (*Z*)-3 (R =  $\text{CH}_3\text{CH}=\text{CH}$ ), 83947-53-9; 3 (R =  $\text{C}_6\text{H}_5$ ), 83947-57-3; (*Z*)-4 (R =  $\text{CH}_3(\text{CH}_2)_6$ , R' = H), 74213-47-1; (*E*)-4 (R =  $\text{CH}_3(\text{CH}_2)_5$ , R' = H), 83947-55-1; 4 (R = R' =  $\text{CH}_3(\text{CH}_2)_3$ ), 74213-50-6; (*Z*)-4 (R =  $\text{C}_6\text{H}_5$ , R' = H), 74213-48-2; (*E*)-4 (R =  $\text{C}_6\text{H}_5$ , R' = H), 83947-56-2; 4 (R = R' =  $\text{C}_6\text{H}_5$ ), 83947-50-6; 4 (R = R' =  $(\text{CH}_2)_5$ ), 74213-49-3; 5, 13735-78-9; 6, 83947-64-2; 7, 83947-65-3; 9 (R = 1-butyl, R' = H), 10173-39-4; 9 (R = 1-butyl, R' =  $\text{CH}_3$ ), 69190-62-1; 9 (R = 2-butyl, R' = H), 72824-01-2; 9 (R = 1-octyl, R' = H), 83947-60-8; 9 (R = allyl, R' =  $\text{CH}_3$ ), 72824-04-5; (*E*)-9 (R = 1-propenyl, R' =  $\text{CH}_3$ ), 83947-58-4; (*Z*)-9 (R = 1-propenyl, R' =  $\text{CH}_3$ ), 83947-59-5; 9 (R = cyclopentyl, R' = H), 72824-02-3; 9 (R = cyclohexyl, R' = H), 66217-60-5; 9 (R = phenyl, R' = H), 4406-72-8; 9 (R = benzyl, R' = H), 35895-82-0; 9 (R =  $\text{C}_6\text{H}_5\text{SCH}_2$ , R' = H), 72824-03-4; 11 (R = 1-butyl, R' = H), 72823-93-9; 11 (R = 2-butyl, R' = H), 72823-94-0; 11 (R = 1-octyl, R' = H), 83947-52-8; 11 (R = cyclopentyl, R' = H), 72823-95-1; 11 (R = cyclohexyl, R' = H), 72823-96-2; 11 (R = phenyl, R' = H), 83947-54-0; 11 (R = benzyl, R' = H), 72823-97-3; 11 (R =  $\text{C}_6\text{H}_5\text{SCH}_2$ , R' = H), 72823-98-4; cyclohexyl (trimethylsilyl)methyl ketone, 55629-29-3; 1,3-propanediol (trimethylsilyl)methaneboronate, 83947-63-1; 1,3-propanediol cyclohexaneboronate, 30169-75-6; 1,3-propanediol (trimethylsilyl)cyclohexylmethaneboronate, 83947-61-9; tetraphenylallene, 1674-18-6; 1,3-diphenylallene, 19753-98-1; pinacol iodomethaneboronate, 70557-99-2.

## Pinanediol [ $\alpha$ -(Trimethylsilyl)allyl]boronate and Related Boronic Esters

David J. S. Tsai and Donald S. Matteson\*

Department of Chemistry, Washington State University, Pullman, Washington 99164

Received August 24, 1982

Homologation of (+)-pinanediol phenylboronate with [chloro(trimethylsilyl)methyl]lithium yielded ( $\alpha$ S)- and ( $\alpha$ R)-[ $\alpha$ -(trimethylsilyl)benzyl]boronic esters in a 73:27 ratio, as shown by peroxidic deboronation to the known  $\alpha$ -(trimethylsilyl)benzyl alcohol. Similar homologations of pinanediol vinyl, (*Z*)-1-propenyl, and isobutyl boronates were carried out, but the diastereoisomeric ratios were not determined. Reaction of the allylic  $\alpha$ -trimethylsilyl boronic esters with aldehydes was studied. Pinanediol or pinacol 3-(trimethylsilyl)-1-propene-3-boronates yielded mainly (*Z*)-1-(trimethylsilyl)-1-alken-4-ols with aldehydes. Pinanediol (*Z*)-1-(trimethylsilyl)-2-butene-1-boronate with benzaldehyde yielded (*E*)-1-(trimethylsilyl)-3-methyl-4-phenylbut-1-en-4-ol with only 4% *Z* isomer. The stereochemical implications and utility of these reactions in synthesis are discussed. A brief investigation indicated that pinanediol  $\alpha$ -trimethylsilyl boronic esters can be desilylated to boronic esters by tetrabutylammonium fluoride in moist THF.

The homologation of boronic esters with [chloro(trimethylsilyl)methyl]lithium,<sup>1</sup> the directed chiral synthesis by way of homologation of pinanediol boronic esters with (dichloromethyl)lithium,<sup>2</sup> and the utility of allylic boronic esters<sup>3,4</sup> and boranes<sup>5</sup> in stereocontrolled synthesis suggested the possible synthetic utility of pinanediol  $\alpha$ -trimethylsilyl boronic esters. We report here a highly stereoselective assembly of four adjacent carbon atoms (two

chiral, two olefinic) in the reaction of pinanediol (*Z*)-[ $\alpha$ -(trimethylsilyl)crotyl]boronate with benzaldehyde. The synthetic applicability of this reaction is deferred by the low diastereoselectivity (73:27) observed in the homologation of a pinanediol bromide ester with [chloro(trimethylsilyl)methyl]lithium. An apparently general and potentially useful reaction of  $\alpha$ -trimethylsilyl boronic esters is the mild and efficient protodesilylation in the presence of fluoride ion, which provides the final step in the first efficient route from boronic esters,  $\text{RB}(\text{OR}')_2$ , to their simple homologues,  $\text{RCH}_2\text{B}(\text{OR}')_2$ .

### Results

**Homologations.** The reaction with [chloro(trimethylsilyl)methyl]lithium<sup>1</sup> has proved readily applicable to the conversion of (+)-pinanediol boronic esters 1 to the homologous diastereoisomeric (+)-pinanediol boronic esters 2 and 3. One unsatisfactory result was encountered.

(1) Matteson, D. S.; Majumdar, D. *Organometallics*, preceding article in this issue.

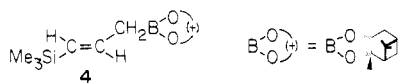
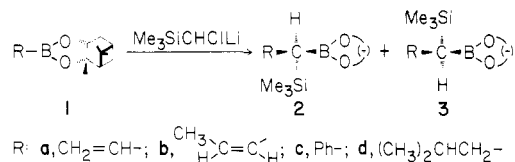
(2) Matteson, D. S.; Ray, R. *J. Am. Chem. Soc.* 1980, 102, 7590-7591.

(3) (a) Hoffmann, R. W.; Zeiss, H. J. *J. Org. Chem.* 1981, 46, 1309-1314 and references cited therein. (b) Hoffmann, R. W.; Kemper, B. *Tetrahedron Lett.* 1980, 4883-4886. (c) Hoffmann, R. W.; Weidmann, U. *J. Organomet. Chem.* 1980, 195, 137-146.

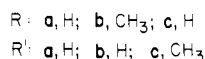
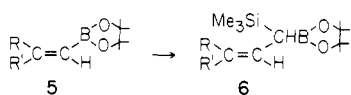
(4) Matteson, D. S.; Tsai, D. J. S. *Tetrahedron Lett.* 1981, 22, 2751-2752.

(5) Yamamoto, Y.; Yatagai, H.; Maruyama, K. *J. Am. Chem. Soc.* 1981, 103, 3229-3231.

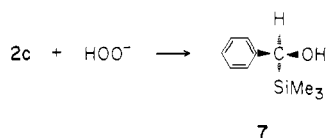
(+)-Pinanediol vinylboronate (or etheneboronate<sup>6</sup>) (1a) yielded a mixture of the normal homologation products, (+)-pinanediol (3*R*)- and (3*S*)-3-(trimethylsilyl)-1-propene-3-boronate (2a and 3a), together with the product of allylic migration of boron, (+)-pinanediol 1-(trimethylsilyl)-1-propene-3-boronate (4), in a 60:40 ratio.



The two regioisomeric classes of product were readily distinguishable by their proton NMR spectra and were separable by liquid chromatography (HPLC) (though the diastereoisomers 2a and 3a were not separable from each other). No evidence for any similar rearrangement could be seen in either the homologation of (+)-pinanediol (*Z*)-1-propene-1-boronate (1b) to the (*Z*)-1-(trimethylsilyl)-2-butene-1-boronates (2b/3b) or that of pinacol vinylboronate (5a) to pinacol 3-(trimethylsilyl)-1-propene-3-boronate (6a).



In order to determine the diastereoselectivity of a typical homologation, the (+)-pinanediol ( $\alpha$ *R*)- and ( $\alpha$ *S*)-[ $\alpha$ -(trimethylsilyl)benzyl]boronate (2c/3c) mixture was oxidized with alkaline hydrogen peroxide. The predominant product was (*S*)-(-)- $\alpha$ -(trimethylsilyl)benzyl alcohol (7), for which the optical rotation and absolute configuration are well established.<sup>7</sup> The observed enantiomeric excess (ee) was 42.5%. Corrected for the use of (+)-pinanediol of ee 92%, the theoretical ee of 7 is 46%, which corresponds to a 2c/3c diastereoisomer ratio of 73:27. Retention of configuration is well established in the oxidation of alkylboranes by hydrogen peroxide,<sup>8</sup> and therefore the (*S*)-7 is derived from ( $\alpha$ *R*)-2c, which correspond in configuration and differ in nomenclature.



**Aldehydes with [ $\alpha$ -(Trimethylsilyl)allyl]boronic Esters.** Pinacol 3-(trimethylsilyl)-1-propene-3-boronate (6a) was tested with benzaldehyde,  $\alpha$ -naphthaldehyde, and heptanal. The reactions of 6a were considerably slower than those of its  $\gamma$ -isomer, pinacol 1-(trimethylsilyl)-1-propene-3-boronate,<sup>4</sup> but good yields of mixtures of (*Z*)- and (*E*)-1-(trimethylsilyl)-1-alken-4-ols (8 and 9) were obtained, with no evidence of byproducts, after the usual borate ester cleavage<sup>3</sup> with triethanolamine. The isomers

(6) Systematic name: (1*S*,2*S*,6*R*,8*S*)-2,9,9-trimethyl-4-vinyl-3,5-dioxo-4-boratricyclo[6,1,1,0<sup>2,6</sup>]decane.

(7) Mosher, H.; Biernbaum, M. S. *J. Org. Chem.* 1971, 36, 3168-3177.

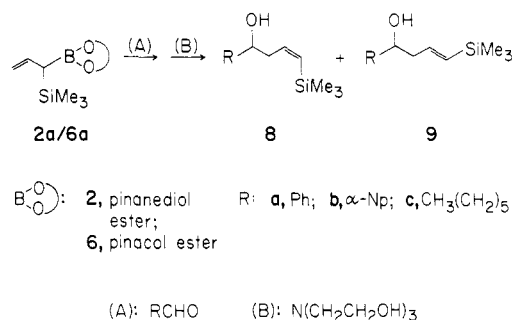
(8) Kabalka, G. W.; Newton, R. J., Jr.; Jacobus, J. *J. Org. Chem.* 1978, 43, 1567-1569.

Table I. Ratios of (*Z*) and (*E*)-1-(Trimethylsilyl)-1-alken-4-ols from [ $\alpha$ -(Trimethylsilyl)allyl]boronic Esters and Aldehydes

boronic ester	aldehyde	products	yield, %	isomer ratio, <i>Z/E</i>
6a	PhCHO	8a + 9a	89	88:12
2a <sup>a</sup>	PhCHO	8a + 9a	91	78:22
6a	$\alpha$ -NpCHO	8b + 9b	63	84:16
6a	CH <sub>3</sub> (CH <sub>2</sub> ) <sub>5</sub> CHO	8c + 9c	80	67:33
6b <sup>b</sup>	PhCHO	10 + 11	c	10:90
6c <sup>b</sup>	PhCHO	12 + 13	c	87:13
2b <sup>a</sup>	PhCHO	10 + 11	c	4:96

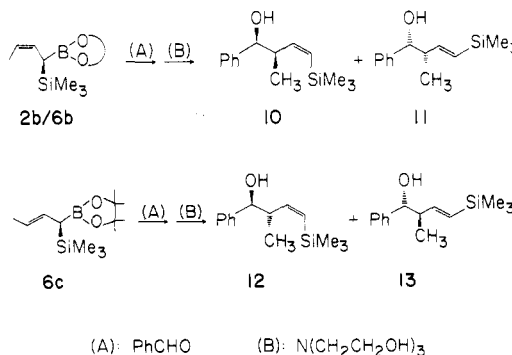
<sup>a</sup> Predominant isomer. The diastereoisomer 3 was also present. <sup>b</sup> Reaction carried out on a mixture of 6b and 6c. <sup>c</sup> Not determined.

8 and 9 were readily distinguished by their vinylic proton patterns in the 200-MHz NMR spectra. The *Z/E* ratios observed are summarized in Table I. The *Z* isomers 8 were the major products.



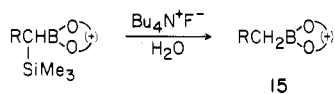
(+)-Pinanediol 3-(trimethylsilyl)-1-propene-3-boronate (2a/3a) reacted more slowly than the pinacol ester 6a with benzaldehyde. Pyridine has been used to catalyze analogous borane reactions<sup>5</sup> and proved effective in this case.

A mixture of pinacol (*Z*)- and (*E*)-1-(trimethylsilyl)-2-butene-1-boronate (6b and 6c; ratio ~2:1) was tested with benzaldehyde and pyridine. Not surprisingly, all four possible stereoisomers (10-13) were obtained. In contrast to all of the other observations, the erythro isomers 10 and 11, which were presumably formed mainly if not entirely from the (*Z*)-buteneboronic ester 6b, showed a high proportion of *E* isomer (Table I). Similar reaction of (+)-pinanediol (*Z*)-1-(trimethylsilyl)-2-butene-1-boronate (2b/3b) yielded only 10 and 11 in a *Z/E* ratio of 4:96. The products from 6b/6c were, of course, racemic, and those from 2b contained lesser amounts of their enantiomers derived from diastereoisomer 3b but for clarity of interpretation are represented here as the enantiomers theoretically expected<sup>3</sup> from the presumed predominant *R* isomer of the  $\alpha$ -trimethylsilyl boronic ester 2b (see Discussion).

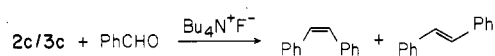


**Desilylation with Fluoride.** Tetrabutylammonium fluoride in refluxing tetrahydrofuran (THF) containing a

small amount of water has been found to protodesilylate three examples of pinanediol  $\alpha$ -trimethylsilyl boronates (**2c/3c**; **2d/3d**; **14**) to the unsubstituted boronic esters **15** with high efficiency (72–95%). Attempts to capture the possible carbanionic intermediate with butyl bromide were unsuccessful, but the reaction of the [ $\alpha$ -(trimethylsilyl)-benzyl]boronic ester (**2c/3c**) with fluoride and benzaldehyde in the presence of molecular sieves yielded stilbene, *Z/E* ratio 70:30. The analogous use of tetraalkylammonium fluorides in the presence of molecular sieves to cleave silyl enol ethers under anhydrous conditions has been reported by Kuwajima and co-workers.<sup>9</sup>

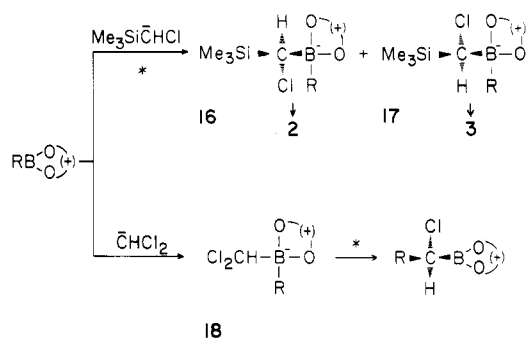


**2c, d/3c, d**; **14** (R=H)



### Discussion

**Homologations.** The contrast between the high diastereoselectivities observed in homologations with (dichloromethyl)lithium<sup>2</sup> and the ratio of merely 3 for **2c/3c** from phenylboronic ester **1c** with [chloro(trimethylsilyl)methyl]lithium can be rationalized by the fact that these differing diastereoselections occur at two different steps of the mechanistically parallel reactions. For the silicon compounds, selection must occur in the first step, formation of the diastereoisomeric tetracoordinate borates **16** and **17**. Alkyl migration must then displace the chlorine stereospecifically with inversion.<sup>10</sup> In contrast, the analogous intermediate **18** contains only a prochiral dichloromethyl group, and selection occurs when one of the two chlorines is displaced by the migrating alkyl group. There is no precise theoretical basis for predicting the stereochemical results observed, but it is hardly surprising that they are different.<sup>11</sup> We have not examined any R group other than phenyl in the silicon series **16** and **17** because the stereoselectivity might be inconvenient to prove in the absence of literature data on optical purities of the  $\alpha$ -trimethylsilyl alcohols.

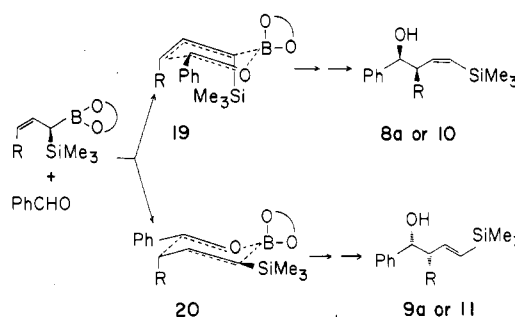


\* Diastereoselective step

Although the low diastereoselectivity limits the immediate utility of these  $\alpha$ -trimethylsilyl boronic esters in chiral synthesis, the fact that  $\alpha$ -chloro boronic esters can be made with high stereoselectivity may provide future routes to these or sterically similar compounds, and the stereoselectivity observed in the allylic replacement of boron by aldehydes is therefore of potential applicability to chiral synthesis.

The degradation of (+)-pinanediol 3-(trimethylsilyl)-1-propene-3-boronate (**2a/3a**) by way of allylic boron migration to form **4** evidently occurred during the preparation, inasmuch as **2a** and **3a** proved perfectly stable on subsequent handling. It is likely that base catalysis was involved. None of these reactions were run more than once or twice, and no great significance can be attributed to the particular rearrangement observed, other than a warning that similar rearrangement might occur with any allylboronic ester, perhaps especially in case of an error in the reaction conditions.

**Aldehydes with [ $\alpha$ -(Trimethylsilyl)allyl]boronic Esters.** The reaction is presumed to proceed by way of the usual six-membered cyclic transition state,<sup>3</sup> which fixes the relative stereochemistry of most of the substituents with a high degree of control. The one position that is not controlled almost stereospecifically is that of the  $\alpha$ -trimethylsilyl group. For example, transition states **19** and **20** both yield erythro<sup>12</sup> products. Only boat form rings could convert (*Z*)-allylboronic esters to threo<sup>12</sup> products, and this pathway was not observed. However, the relative energies of **19** and **20** are closely matched. If the terminal substituent R is hydrogen, then the trimethylsilyl substituent is less hindered in the axial position, favoring transition state **19** and consequently the *Z* product **8a**. If R is methyl, then the trimethylsilyl substituent is forced to the equatorial position, favoring transition state **20** and consequently the *E* product **11**. These opposite geometries require opposite pairs of chirality at the carbon atoms being joined. Thus, for purposes of chiral synthesis, the *Z* and *E* products would have to be separated before proceeding further, even if the *Z/E* relationship is irrelevant (as for example, if the olefin is to be oxidized to an aldehyde), in order to avoid mixing opposite chiralities. The degree of stereocontrol achieved in the synthesis of **11** (96%) is therefore noteworthy and potentially useful.



Our stereochemical assignments for the four isomeric 1-(trimethylsilyl)-3-methyl-4-phenylbut-1-en-4-ols (**10–13**) agree with those reported previously by Yamamoto, Yatagai, and Maruyama.<sup>5</sup> Starting from an (*E*)-[ $\alpha$ -(trimethylsilyl)crotyl]borane, their products were mainly the threo isomers **12** and **13**, and they detected but did not distinguish the erythro isomers **10** and **11**. We have assigned the *Z* and *E* geometries on the basis of the sub-

(12) Named according to the convention used in the antibiotic series, which is opposite that of the sugar series unless the methyl substituent is regarded as part of the fundamental carbon chain.

(9) Kuwajima, I.; Nakamura, E.; Shimizu, M. *J. Am. Chem. Soc.* **1982**, *104*, 1025–1030.

(10) Midland, M. M.; Zolopa, A. R.; Halterman, R. L. *J. Am. Chem. Soc.* **1979**, *101*, 248–249. Although this study utilized trialkylboranes rather than boronic esters, the nature of the nucleophilic displacement at the chiral center is the same. Evidence that the stereoselectivity of such migrations is high in the boronic ester series is provided by ref. 2.

(11) In this argument we assume that the carbanions attack the boron atom of pinanediol boronates almost exclusively from the less hindered side, and that different chiralities at the boron atom are not involved. Evidence regarding this point will be published later.

stantially larger trans proton coupling constant compared to the cis in the 200-MHz NMR spectra.

**Desilylation with Fluoride.** The desilylation of  $\alpha$ -trimethylsilyl boronic esters provides an interesting demonstration of the selectivity of fluoride for silicon and also furnishes an efficient route for the homologation of  $\text{RBO}_2\text{C}_{10}\text{H}_{16}$  to  $\text{RCH}_2\text{BO}_2\text{C}_{10}\text{H}_{16}$ , which could be useful in an extended chiral synthesis scheme where two chiral centers are separated by a methylene group. However, it appears to be inapplicable to allylic boronic esters. NMR evidence indicated that the desilylation product from **2a/3a** was a mixture of allyl- and 1-propenylboronic esters.

The condensation of the [ $\alpha$ -(trimethylsilyl)benzyl]boronic ester **2c/3c** with benzaldehyde provides evidence for an  $\alpha$ -borylbenzyl anion intermediate, which should have properties similar to the boryllallyl anion obtained by the deprotonation of an allylboronic ester.<sup>1</sup> The lack of any stereoselectivity in the condensation discouraged us from further investigation, as did the failure to alkylate with butyl bromide. Whether unactivated  $\alpha$ -trimethylsilyl boronic esters could be desilylated and condensed with carbonyl compounds rather than merely protodesilylated, or whether any carbonyl compounds other than benzaldehyde could be used, has not been investigated.

### Experimental Section

**General Data.** Reactions were run under argon. Tetrahydrofuran (THF) was distilled from sodium benzophenone ketyl. The *sec*-butyllithium was routinely titrated with isopropyl alcohol with 1,10-phenanthroline as indicator. <sup>1</sup>H NMR spectra were recorded at 60 MHz with a Varian EM-360 instrument and at 200 MHz with a Nicolet Technology Corp. NT-200 instrument. For compounds containing a trimethylsilyl group, spectra were run by setting the chemical shift of the trimethylsilyl peak at zero.<sup>1</sup> For others, spectra were referred to internal tetramethylsilane. <sup>13</sup>C NMR spectra were recorded at 22.62 MHz with a Bruker WH 90 instrument. Optical rotations were measured by using a Jasco DIP-181 digital polarimeter. Analytical thin-layer chromatography was performed on premade Merck glass-backed silica gel 60F-254 plates. Preparative thin-layer purification was done on Merck silica gel 60 PF-254 plates. Column chromatography was done on Baker 60-200 mesh silica gel. High-pressure liquid chromatography (HPLC) was done with a Waters Prep LC/System 500A using Prep Pak-500/Silica cartridges. Elemental analyses were performed by Galbraith Laboratories, Knoxville, TN.

**(+)-Pinanediol Etheneboronate (1a).** (+)- $\alpha$ -Pinanediol and dibutyl etheneboronate<sup>13</sup> (43.39 g, 235.8 mmol) were stirred in 250 mL of ether overnight. Concentration followed by distillation in the presence of galvinoxyl free radical (inhibitor) gave (+)-pinanediol etheneboronate (44.93 g, 92%): bp 61 °C (0.7 torr); 60-MHz <sup>1</sup>H NMR ( $\text{CDCl}_3$ )  $\delta$  0.70–2.50 (m, 15), 4.32 (d of d's,  $J$  = 8.8 and 2 Hz, CHO), 6.10 (br, 3,  $\text{CH}=\text{CH}_2$ ). Anal. Calcd for  $\text{C}_{12}\text{H}_{28}\text{BO}_2$ : C, 69.94; H, 9.29; B, 5.25. Found: C, 69.63; H, 9.30; B, 5.35.

**(+)-Pinanediol (Z)- and (E)-1-Propene-1-boronates.** The same procedure used for the preparation of **1a** gave (+)-pinanediol (Z)- and (E)-1-propene-1-boronates (96%), bp 70–80 °C (0.6 torr). Anal. Calcd for  $\text{C}_{13}\text{H}_{21}\text{BO}_2$ : C, 70.94; H, 9.62; B, 4.91. Found: C, 70.84; H, 9.75; B, 5.01.

The separation of *E* and *Z* isomers was done by HPLC ( $\text{CH}_2\text{Cl}_2/\text{hexane}$  = 3:7): 200-MHz <sup>1</sup>H NMR ( $\text{CDCl}_3$ ) (+)-pinanediol (Z)-1-propene-1-boronate (**1b**) (less polar, >99% pure)  $\delta$  0.70–2.50 (m, 15), 1.95 (d, 3,  $J$  = 6.0 Hz,  $\text{CH}_3$ ), 4.32 (d of d's,  $J$  = 13.9 and 6.0 Hz  $\text{HC}=\text{CB}$ ); (+)-pinanediol (E)-1-propene-1-boronate (more polar, >95% pure)  $\delta$  0.07–2.50 (m, 15), 1.83 (d, 3,  $J$  = 6.0 Hz,  $\text{CH}_3$ ), 4.26 (d of d's, 1,  $J$  = 8.7 and 2.0 Hz, CHO), 5.48 (d of q's,  $J$  = 19.0 Hz,  $\text{C}=\text{CHB}$ ), 6.61 (d of q's,  $J$  = 19.0 and 6.5 Hz,  $\text{HC}=\text{CB}$ ).

**(+)-Pinanediol 1-Propene-2-boronate.** (+)- $\alpha$ -Pinanediol and 1-propene-2-boronic acid<sup>13</sup> yielded (+)-pinanediol 1-propene-2-

boronate (77%): bp 67 °C (0.2 torr); 200-MHz <sup>1</sup>H NMR ( $\text{CDCl}_3$ )  $\delta$  0.07–2.50 (m, 15), 1.78 (s, 3,  $\text{C}=\text{CCH}_3$ ), 4.26 (d of d's, 1,  $J$  = 8.7 and 2.0 Hz, CHO), 5.58 (s, 1, br, (H)HC=C(B)CH<sub>3</sub>), 5.69 (s, 1, br, (H)HC=C(B)CH<sub>3</sub>). Anal. Calcd for  $\text{C}_{13}\text{H}_{21}\text{BO}_2$ : C, 70.94; H, 9.62; B, 4.91. Found: C, 70.95; H, 9.90; B, 5.12.

**(+)-Pinanediol 2-Methylpropaneboronate (1d).** (+)- $\alpha$ -Pinanediol and 2-methylpropaneboronic acid in ether yielded **17b** (78%): bp 75–77 °C (0.5 torr); 60-MHz <sup>1</sup>H NMR ( $\text{CDCl}_3$ )  $\delta$  0.60–2.70 (m, 24), 4.26 (d of d's, 1,  $J$  = 8.7 and 2.0 Hz, CHO). Anal. Calcd for  $\text{C}_{14}\text{H}_{25}\text{BO}_2$ : C, 71.20; H, 10.67; B, 4.58. Found: C, 71.26; H, 10.61; B, 4.41.

**(+)-Pinanediol (Trimethylsilyl)methaneboronate (14).** (+)- $\alpha$ -Pinanediol and (trimethylsilyl)methaneboronic acid<sup>1</sup> gave **14** (80%): bp 78–82 °C (0.7 torr); 60-MHz <sup>1</sup>H NMR ( $\text{CDCl}_3$ )  $\delta$  0.00 (s, 9,  $\text{SiCH}_3$ ), 0.75–2.50 (m, 17), 4.20 (d of d's, 1,  $J$  = 8 and 2 Hz, CHO). Anal. Calcd for  $\text{C}_{14}\text{H}_{27}\text{BO}_2\text{Si}$ : C, 63.15; H, 10.22; B, 4.06; Si, 10.55. Found: C, 63.03; H, 10.30; B, 3.82; Si, 10.30.

**Pinacol 3-(Trimethylsilyl)-1-propene-3-boronate (6a).** A solution of [(trimethylsilyl)chloromethyl]lithium was prepared on a 51.3-mmol scale as described in the preceding paper<sup>1</sup> and pinacol etheneboronate<sup>1</sup> (7.57 g, 49.2 mmol) was added in 5 mL of THF at –55 °C. Usual workup and distillation produced **6a** (6.36 g, 54%): bp 52–55 °C (0.7 torr); 60-MHz <sup>1</sup>H NMR ( $\text{CDCl}_3$ )  $\delta$  0.00 (s, 9,  $\text{SiCH}_3$ ), 1.06 (s, 12,  $\text{CCH}_3$ ), 1.45 (d,  $J$  = 10 Hz, 1, CH), 4.5–4.9 (m, 2,  $\text{C}=\text{CH}_2$ ), 5.50–6.15 (m, 1,  $\text{SiHC}=\text{C}$ ). Anal. Calcd for  $\text{C}_{12}\text{H}_{25}\text{BO}_2\text{Si}$ : C, 60.00; H, 10.49; B, 4.50; Si, 11.69. Found: C, 59.74; H, 10.25; B, 4.56; Si, 11.46.

**Pinanediol 3-(Trimethylsilyl)-1-propene-3-boronate (2a/3a).** A solution of [(trimethylsilyl)chloromethyl]lithium (70.88 mmol) was prepared according to the general procedure described previously, and pinanediol etheneboronate (13.65 g, 66.23 mmol) was added in 5 mL of THF at –78 °C. After overnight stirring and the usual workup, distillation yielded a 3:2 mixture of **2a/3a** and (E)-1-(trimethylsilyl)-1-propene-3-boronate<sup>4</sup> (8.77 g, 45%), bp 96–100 °C (0.5 torr). Purification of **11b** was achieved with HPLC using 3:7 dichloromethane/hexane: 200-MHz <sup>1</sup>H NMR ( $\text{CDCl}_3$ )  $\delta$  0.12 (s, 9,  $\text{SiCH}_3$ ), 0.90 (s, 3,  $\text{CCH}_3$ ), 1.22 (d,  $J$  = 10.7 Hz, 1), 1.34 (s, 3,  $\text{CCH}_3$ ), 1.43 (s, 3,  $\text{CCH}_3$ ), 1.62 (d,  $J$  = 10.8 Hz, 1,  $\text{CHSi}$ ), 1.72–1.90 (m, 2), 2.11 (t, 5.5 Hz, 1), 2.20–2.40 (m, 2), 4.32 (d of d's,  $J$  = 8.8 and 1.7–2.0 Hz, 1, CHOB), 4.84 (d of d's,  $J$  = 16.1 and 2.3 Hz, 1, C(H)C=CH(H)), 4.86 (d of d's,  $J$  = 11.1 and 2.6 Hz, C(H)C=CH(H)), 5.94 (d of t's,  $J$  = 16.1, 11.1, and 10.8 Hz, 1,  $\text{SiHC}=\text{C}$ ). Anal. Calcd for  $\text{C}_{16}\text{H}_{29}\text{BO}_2\text{Si}$ : C, 65.75; H, 10.0; B, 3.70; Si, 9.61. Found: C, 65.76; H, 10.16; B, 3.58; Si, 9.71.

**(+)-Pinanediol (Z)-1-(Trimethylsilyl)-2-butene-1-boronate (2b/3b).** A solution of [(trimethylsilyl)chloromethyl]lithium (8.84 mmol) was prepared according to the general procedure and the (+)-pinanediol (Z)-1-propene-1-boronate (8.23 mmol) in 5 mL of THF was added to the solution in one portion at –78 °C. After overnight stirring and the usual workup, distillation yielded **2b/3b** (1.60 g, 64%): bp 105–107 °C (0.55 torr); 200-MHz <sup>1</sup>H NMR ( $\text{CDCl}_3$ )  $\delta$  0.03 (s, 9,  $\text{SiCH}_3$ ), 0.08–2.40 (m, 16), 1.50 (d of d's,  $J$  = 6.7 and 1.6 Hz, 3,  $\text{CH}_3$ ), 4.23 (d of d's,  $J$  = 8.8 and 2.0 Hz, 1, CHO), 5.30 (d of q's,  $J$  = 10.7 and 6.6 Hz, 1,  $\text{CH}_3\text{HC}=\text{C}$ ), 5.51 (t of q's,  $J$  = 10.7 and 1.7 Hz, 1,  $\text{CH}_3\text{C}=\text{CH}$ ).

**Pinanediol [1-(Trimethylsilyl)benzyl]boronate (2c/3c).** At –55 °C, pinanediol benzeneboronate (10.78 g, 42.1 mmol) in 20 mL of THF was added to a stirred solution of [(trimethylsilyl)chloromethyl]lithium (53.8 mmol) prepared according to the general procedure described previously. After overnight stirring and usual workup, distillation yielded **2c/3c** (12.72 g, 88%): bp 150–154 °C (1.5 torr); 60-MHz <sup>1</sup>H NMR ( $\text{CDCl}_3$ )  $\delta$  0.00 (s, 9,  $\text{SiCH}_3$ ), 0.70–2.80 (m, 16), 4.25 (d of d's,  $J$  = 8 and 2 Hz, 1, CHO), 6.95–7.20 (m, 5,  $\text{C}_6\text{H}_5$ ). Anal. Calcd for  $\text{C}_{20}\text{H}_{31}\text{BO}_2\text{Si}$ : C, 70.17; H, 9.13; B, 3.16; Si, 8.20. Found: C, 70.40; H, 9.34; B, 2.80; Si, 8.39.

**Pinanediol 1-(Trimethylsilyl)-3-methylbutane-1-boronate (2d/3d).** At –78 °C, pinanediol 2-methylpropane-1-boronate (**1d**) (4.75 g, 20.11 mmol) in 5 mL of THF was added to the [(trimethylsilyl)chloromethyl]lithium solution (20 mL). After overnight stirring and usual workup, distillation yielded **2d/3d** (3.90 g, 60%): bp 100–105 °C (0.55 torr); 60-MHz <sup>1</sup>H NMR ( $\text{CDCl}_3$ )  $\delta$  0.00 (s, 9,  $\text{SiCH}_3$ ), 0.70–2.50 (m, 25), 4.19 (d of d's,  $J$  = 8 and 2 Hz, 1, CHO). Anal. Calcd for  $\text{C}_{13}\text{H}_{25}\text{BO}_2\text{Si}$ : C, 67.07; H, 10.94; B, 3.35; Si, 8.71. Found: C, 67.22; H, 11.10; B, 2.90; Si, 8.49.

**1-(Trimethylsilyl)-4-hydroxy-4-phenyl-1-butene (8a/9a) from Pinacol 3-(Trimethylsilyl)-1-propene-3-boronate (6a).** The reaction was done as described in the preceding paragraph. A solution of benzaldehyde (0.55 g, 5.2 mmol) in 10 mL of ether was refluxed with pinacol boronate **6a** (1.23 g, 5.13 mmol) for 36 h. Triethanolamine (5.3 mmol) was added to the mixture, and the milky mixture was stirred for 2 h. After filtration the filtrate was concentrated, and distillation gave 1.0 g (89%) of a 88:12 mixture of **8a(Z)** and **9a(E)**: bp 68 °C (0.08 torr); 200-MHz <sup>1</sup>H NMR (CDCl<sub>3</sub>) δ 0.11 (s, 9, SiCH<sub>3</sub>), 2.00 (br, OH), 2.50–2.70 (m, 2, CH<sub>2</sub>), 4.73 (m, 1, CHO), 5.70 (d of t's, *J* = 14.1 and 1.2 Hz, 1, SiHC=C), 6.32 (overlapped d of t's (5 peaks), *J* = 14.1 and 7.1 Hz, 1, C=CHC). Anal. Calcd for C<sub>13</sub>H<sub>20</sub>OSi: C, 70.85; H, 9.15; Si, 12.74. Found: C, 70.87; H, 9.23; Si, 12.54.

The isomer ratio was determined from the 200-MHz <sup>1</sup>H NMR spectra of the reaction mixture: *Z/E* = 88:12, from the area ratio of δ 6.32 (d of t's, *J* = 14.1 and 7.1 Hz)/δ 6.02 (d of t's, *J* = 18.5 and 6.2 Hz).

**1-(Trimethylsilyl)-4-hydroxy-4-phenyl-1-butene (8a/9a) from Pinanediol 3-(Trimethylsilyl)-1-propene-3-boronate (2a/3a).** A solution of pinanediol boronate **1a** (1.24 g, 4.2 mmol) and pyridine<sup>5</sup> (0.65 mL, 8.1 mmol) in 2 mL of ether was treated with benzaldehyde (0.88 mL, 8 mmol) and stirred for 5 min at room temperature. The ether was removed by distillation as above mixture was slowly warmed up to 120 °C (oil bath) and stirred for 14 h (reaction complete by TLC). Ether (10 mL) and triethanolamine (0.79 g, 5.3 mmol) were added to the reaction mixture and stirred for 2 h. After filtration the filtrate was concentrated and purified by preparative TLC. Bulb-to-bulb distillation gave 0.84 g, (91%) of a 78:22 mixture of **13(Z)** and **13(E)**.

The isomer ratio was determined from the 200-MHz <sup>1</sup>H NMR spectra of the reaction mixture: *Z/E* = 78:22, from the area ratio of δ 6.32/δ 6.02.

**1-(Trimethylsilyl)-4-hydroxy-4-naphthyl-1-butene (8b/9b).** A solution of 1-naphthaldehyde (0.37 g, 2.37 mmol) and pinacol boronate **6a** (0.63 g, 2.6 mmol) in 10 mL of ether was refluxed overnight. The ether was found to have escaped the next morning. Ether (25 mL) and triethanolamine (3 mmol) were added to the reaction mixture, and the mixture was stirred for 2 h. After filtration the filtrate was concentrated and purified by preparative TLC. Bulb-to-bulb distillation gave 0.40 g (63%) of a 84:16 mixture of **8b(Z)** and **9b(E)**: 200-MHz <sup>1</sup>H NMR (CDCl<sub>3</sub>) δ 0.20 (s, 9, SiCH<sub>3</sub>), 2.62 (br, 1, OH), 2.65–3.0 (m, 2, CH<sub>2</sub>), 5.52 (m, 1, CHO), 5.79 (d of t's, *J* = 13.9 and 0.9 Hz, C=CHSi), (overlapped d of t's (5 peaks), *J* = 13.9 and 7.2 Hz, 1, HC=CSi). Anal. Calcd for C<sub>17</sub>H<sub>22</sub>O<sub>2</sub>Si: C, 75.50; H, 8.20; Si, 10.39. Found: C, 75.60; H, 8.33; Si, 10.56.

The isomer ratio was determined from the 200-MHz <sup>1</sup>H NMR spectra of the mixture; *Z/E* = 84:16, from the area ratio of δ 6.51 (d of t's, *J* = 13.9 and 7.2 Hz)/δ 6.19 (d of t's, *J* = 18.5 and 6.4 Hz).

**1-(Trimethylsilyl)-4-hydroxy-1-decene (8c/9c).** A solution of pinacol boronate **6a** (0.393 g, 1.64 mmol) and heptaldehyde (1.90 mmol) in 25 mL of ether was refluxed for 17 h, and the reaction was not complete (by TLC). The above mixture was slowly warmed up to 130 °C (oil bath) and stirred overnight. Ether (20 mL) and triethanolamine (2 mmol) were added to the reaction mixture, and the milky suspension was stirred for 2 h. After usual workup and purification by preparative TLC, bulb-to-bulb distillation gave 0.30 g (80%) of 67:33 mixture of **8c(Z)** and **9c(E)**: 200-MHz <sup>1</sup>H NMR (CDCl<sub>3</sub>) δ 0.10 (s, 9, SiCH<sub>3</sub>), 0.88 (t, 3, CCH<sub>3</sub>), 1.20–1.50 (m, 10), 1.65–1.80 (br, 1, OH), 2.1–2.45 (m, 2, CH<sub>2</sub>C=C), 3.55–3.75 (m, 1, CHO), 5.66 (d of t's, *J* = 14.1 and 1.3 Hz, C=CHSi), 6.32 (overlapped d of t's (5 peaks), *J* = 14.1 and 7.2 Hz, HC=CSi). Anal. Calcd for C<sub>15</sub>H<sub>22</sub>O<sub>2</sub>Si: C, 68.35; H, 12.35; Si, 12.29. Found: C, 68.48; H, 12.42; Si, 12.05.

The isomer ratio was determined from the 200-MHz <sup>1</sup>H NMR spectra of the reaction mixture *Z/E* = 67:33, being obtained from the area ratio of δ 6.32 (d of t's, *J* = 14.1 and 7.2 Hz)/δ 6.02 (d of t's, *J* = 19.4 and 5.9 Hz).

**1-(Trimethylsilyl)-4-hydroxy-4-phenyl-3-methyl-1-butenes (10–13) from Pinacol (Z)- and (E)-3-(Trimethylsilyl)-1-butene-3-boronate (6b and 6c).** A solution of pinacol boronates **6b(Z)** and **6c(E)** (1 mmol) and benzaldehyde (2 mmol) in 2 mL of ether was heated up to 125 °C (oil bath) and stirred overnight.

The next morning triethanolamine (2 mmol) and ether 10 mL were added to the reaction mixture and stirred for 2 h. After filtration the filtrate was concentrated and purified by preparative TLC. 200-MHz <sup>1</sup>H NMR (CDCl<sub>3</sub>) showed a mixture of four isomers.

The isomer ratio was determined from the 200-MHz <sup>1</sup>H NMR spectra of the mixture: 11(erythro, *E*)/10(erythro, *Z*)/12(threo, *Z*)/13(threo, *E*) = 62:7:27:4, being obtained from the peak height ratio of δ 4.53 (d, *J* = 5.6 Hz)/δ 4.50 (d, 5.6 Hz)/δ 4.25 (d, 8.4 Hz)/δ 4.32 (d, 8.4 Hz).

**erythro-(E)-1-(Trimethylsilyl)-4-hydroxy-4-phenyl-3-methyl-1-butenes (10 and 11) from Pinanediol (Z)-3-(Trimethylsilyl)-1-butene-3-boronate (2b).** The reaction was done according to the general procedure. A solution of pinanediol boronate **2b** (0.26 mmol) and pyridine (42 μL) in 2 mL of ether was treated with benzaldehyde (60 μL) and stirred for 1 h. The above mixture was heated up to 120 °C (oil bath) and stirred overnight. The next morning triethanolamine (1 mmol) and ether (10 mL) were added to the above reaction mixture, and the mixture was stirred for 15 h. After usual workup and purification by preparative TLC, bulb-to-bulb distillation gave enough of the desired product for a 200-MHz <sup>1</sup>H NMR spectrum: 200-MHz <sup>1</sup>H NMR (CDCl<sub>3</sub>) 11(erythro, *E*) δ 0.00 (s, 9, SiCH<sub>3</sub>), 0.99 (d, *J* = 6.8 Hz, 3, CCH<sub>3</sub>), 1.96 (br, 1, OH), 2.56 (m, 1, CHC=C), 4.60 (d, *J* = 5.5 Hz, CHO), 5.65 (d, *J* = 18.8 Hz, 1, C=CHSi), 5.93 (d of d's, *J* = 18.8 and 6.5 Hz, 1, HC=CSi).

The isomer ratio was determined from the 200-MHz <sup>1</sup>H NMR spectra of the mixture: 11(erythro, *E*)/10(erythro, *Z*) = 96:4, being obtained from the peak height ratio of δ 4.60 (d, *J* = 5.5 Hz)/δ 4.57 (d, *J* = 5.5 Hz).

**(+)-Pinanediol Benzylboronate (5, R = Ph).** (+)-Pinanediol [α-(trimethylsilyl)benzyl]boronate (**2c/3c**; 0.36 g, 1.05 mmol) and 1 tetrabutylammonium fluoride in THF (<5% water; Aldrich Chemical Co.) (1 mmol) were stirred in 10 mL of THF at -78 °C and allowed to warm to room temperature. The reaction was complete at room temperature (by TLC), and the above mixture was passed through a short column of silica gel (60–200 mesh, 10 cm). The solution was concentrated and purified by preparative TLC. Bulb-to-bulb distillation gave 0.233 g (82%) of (+)-pinanediol benzylboronate, which has been reported previously.<sup>14</sup>

**(+)-Pinanediol Methaneboronate (15, R = CH<sub>3</sub>).** A solution of (+)-pinanediol (trimethylsilyl)methaneboronate (**14**; 1.11 mol) and tetrabutylammonium fluoride (1.20 mmol) in 10 mL of THF was refluxed for 4 h. After workup and purification by preparative TLC, bulb-to-bulb distillation gave 0.155 g (72%) of (+)-pinanediol methaneboronate, which has been reported previously.<sup>2</sup>

**(+)-Pinanediol 3-Methylbutaneboronate (15, R = (CH<sub>3</sub>)<sub>2</sub>CHCH<sub>2</sub>).** A solution of (+)-pinanediol 1-(trimethylsilyl)-3-methylbutaneboronate (0.33 g, 1.03 mmol) and tetrabutylammonium fluoride 1.1 mmol) in 10 mL of THF was refluxed for 2 hr. After workup and purification by preparative TLC, bulb-to-bulb distillation gave 0.237 g (95%) of (+)-pinanediol 3-methylbutaneboronate: 60-MHz <sup>1</sup>H NMR (CDCl<sub>3</sub>) δ 0.70–2.8 (m, 26), 4.38 (d of d's, *J* = 8.8 and 2.0 Hz, 1, CHO). Anal. Calcd for C<sub>15</sub>H<sub>29</sub>BO<sub>2</sub>: C, 72.01; H, 10.88; B, 4.32. Found: C, 71.99; H, 10.65; B, 4.22.

**Stilbenes.** A solution of 1 M tetrabutylammonium fluoride in THF (5% water, Aldrich Chemical Co.) was dried over molecular sieves overnight, and 1.4 mL of this solution was added to 1.1 mmol of (+)-pinanediol [α-(trimethylsilyl)benzyl]boronate (**2c/3c**), 1.3 mL (10-fold excess) of benzaldehyde, 0.8 g of 4-Å molecular sieves, and 10 mL of THF. After being stirred 2 h at 20–25 °C, the solution was filtered through a short column of silica gel and concentrated and the residue purified by preparative TLC. The yield of stilbenes was 0.162 g (76%) shown to be a 70:30 *Z/E* mixture by the proton NMR spectrum.

**(S)-(-)-Phenyl(trimethylsilyl)carbinol (7).** Hydrogen peroxide (30%, 4 mL) was added to a stirred solution of 92% ee (+)-pinanediol [1-(trimethylsilyl)benzyl]boronate (**2c/3c**; 2.85 g, 8.32 mmol), sodium hydroxide (15 mmol), THF (10 mL), and water (15 mL) at 0 °C, and the reaction mixture was warmed up to room temperature for 10 min, saturated with concentrated

(14) Matteson, D. S.; Sadhu, K. M.; Lienhard, G. E. *J. Am. Chem. Soc.* 1981, 103, 5241–5242.

sodium chloride solution (20 mL), and extracted with ether (50 mL  $\times$  3). The organic layer was filtered and dried over anhydrous magnesium sulfate. Distillation gave 1.38 g (92%) of phenyl-(trimethylsilyl)carbinol (7):<sup>7</sup> 60-MHz <sup>1</sup>H NMR (CDCl<sub>3</sub>)  $\delta$  0.00 (s, 9, SiCH<sub>3</sub>), 1.85 (s, 1, OH), 4.42 (s, 1, CH), 7.15 (s, 5, C<sub>6</sub>H<sub>5</sub>); [ $\alpha$ ]<sup>24</sup><sub>D</sub> -48.40° (c 1.78, toluene); [ $\alpha$ ]<sup>21</sup><sub>D</sub> -39.56° (neat) [Lit.<sup>7</sup> [ $\alpha$ ]<sup>25</sup><sub>D</sub> 93.0°

(neat)].

**Acknowledgment.** We thank the National Science Foundation for support, Grant CHE-8025229. We thank the Boeing Corp. for a gift in support of purchase of the 200-MHz NMR spectrometer.

## Stepwise Displacement of the Tertiary Phosphine Ligand in Square-Planar [PdR<sub>2</sub>L<sub>2</sub>]-Type Complexes by Organolithium Reagents with Stereochemical Retention Affording Organopalladate Complexes

Hiroshi Nakazawa, Fumiyuki Ozawa, and Akio Yamamoto\*

Research Laboratory of Resources Utilization, Tokyo Institute of Technology,  
Nagatsuta, Midori-ku, Yokohama 227, Japan

Received August 24, 1982

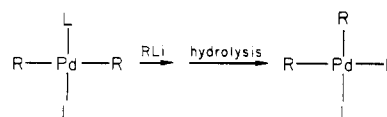
Reactions of *trans*- and *cis*-[PdR<sub>2</sub>L<sub>2</sub>] (R = Me, Et, Ph; L = tertiary phosphine) with R'Li (R' = Me, Ph) in ether or THF solution lead to stepwise displacement of L by R' with stereochemical retention to afford alkylpalladate complexes Li[PdR<sub>2</sub>R'L] and Li<sub>2</sub>[PdR<sub>2</sub>R'<sub>2</sub>], as established by means of <sup>1</sup>H, <sup>31</sup>P, and <sup>13</sup>C NMR spectroscopy. The displacement of PEt<sub>3</sub> in *trans*-[PdPh<sub>2</sub>(PEt<sub>3</sub>)<sub>2</sub>] by MeLi is a slow process, and the rate is independent of the MeLi concentration with indication of a dissociative mechanism generating a three-coordinate, T-shaped intermediate, whereas the reaction of PdR<sub>2</sub>L<sub>2</sub> (R = Me, Et) with MeLi is much faster. Displacement of PEt<sub>2</sub>Ph in Li[PdMe<sub>3</sub>(PEt<sub>2</sub>Ph)] by MeLi is a slow process and first order in concentrations of the complex and MeLi and independent of L. An associative mechanism involving a five-coordinate intermediate is proposed for the second displacement to account for the stereochemical retention. Factors influencing the <sup>1</sup>H and <sup>13</sup>C NMR chemical shifts of the neutral and palladate complexes are discussed.

### Introduction

In contrast to the well-known anionic transition-metal complexes having  $\pi$ -acceptor ligands such as CO, examples of more electron-rich anionic organotransition-metal complexes are still limited<sup>1</sup> except for the conspicuously well-utilized alkylcuprate complexes<sup>2a</sup> and recently developed alkali-metal-transition-metal  $\pi$  complexes.<sup>2b</sup> For palladium, which ranks among the most frequently employed transition metals for organic synthesis,<sup>1,3</sup> the chemistry of organopalladate complexes has been very poorly exploited.<sup>4</sup> In some cases, where palladium compounds are used in combination with alkylating or arylating agents such as alkyl- (aryl-) lithium or magnesium compounds, particularly when the alkylating agent is used in excess to the palladium complexes, the possibility of

formation of alkylpalladate complexes is considered not at all negligible, although generally neutral or cationic organopalladium complexes have been postulated in most cases.<sup>3,5</sup>

In the course of our studies on the preparation of dialkylpalladium complexes having two tertiary phosphine ligands,<sup>6,7</sup> we have observed that *trans*-[PdR<sub>2</sub>L<sub>2</sub>] (R = alkyl group; L = monodentate tertiary phosphine) can be prepared by the reaction of bis(acetylacetonato)palladium with an alkylaluminum in the presence of L, whereas *cis*-[PdR<sub>2</sub>L<sub>2</sub>] can be synthesized by treating bis(tertiary phosphine)palladium dihalides with an excess of an alkylolithium followed by hydrolysis of the unreacted alkylolithium. Examination of the cause of this puzzling effect of the nature of the alkylating agent on the configuration of the final product led us to the finding that the isomerization of *trans*-[PdR<sub>2</sub>L<sub>2</sub>] to the *cis* isomer was promoted by addition of alkylolithium to the system.



In order to account for the *trans* to *cis* isomerization, we

(1) For example: Heck, R. F. "Organotransition Metal Chemistry"; Academic Press: New York, 1974. Collman, J. P.; Hegedus, L. S. "Principles and Application of Organotransition Metal Chemistry"; University Science Book: Mill Valley, CA 1980. Tsuji, J. "Organic Synthesis by Means of Transition Metal Complexes"; Springer-Verlag: Berlin, 1975. Kochi, J. K. "Organometallic Mechanisms and Catalysis"; Academic Press: New York, 1978.

(2) (a) Posner, G. H. "An Introduction to Synthesis Using Organocopper Reagents"; Wiley-Interscience: New York, 1980. (b) Jonas, K. *Adv. Organomet. Chem.* 1981, 19, 97.

(3) Hartley, F. R. "The Chemistry of Platinum and Palladium"; Applied Science Publishers Ltd: London, 1973. Maitlis, P. M. "The Organic Chemistry of Palladium"; Academic Press: New York, 1971. Tsuji, J. "Organic Syntheses with Palladium Compounds"; Springer-Verlag: Berlin, 1980.

(4) Uson, R.; Fornies, J.; Espinet, P.; Martinez, F.; Tomas, M. *J. Chem. Soc., Dalton Trans.* 1981, 463. Uson, R.; Fornies, J.; Martinez, F.; Tomas, M. *Ibid.* 1980, 888.

(5) Loar, M. K.; Stille, J. K. *J. Am. Chem. Soc.* 1981, 103, 4174. Moravskiy, A.; Stille, J. K. *Ibid.* 1981, 103, 4182. Gillie, A.; Stille, J. K. *Ibid.* 1980, 102, 4933. Milstein, D.; Stille, J. K. *Ibid.* 1979, 101, 4981.

(6) Ito, T.; Tsuchiya, H.; Yamamoto, A. *Bull. Chem. Soc. Jpn.* 1977, 50, 1319.

(7) Ozawa, F.; Ito, T.; Nakamura, Y.; Yamamoto, A. *Bull. Chem. Soc. Jpn.* 1981, 54, 1868.



## Stepwise displacement of the tertiary phosphine ligand in square-planar [PdR<sub>2</sub>L<sub>2</sub>]-type complexes by organolithium reagents with stereochemical retention affording organopalladate complexes

Hiroshi Nakazawa, Fumiyuki Ozawa, and Akio Yamamoto

*Organometallics*, **1983**, 2 (2), 241-250 • DOI: 10.1021/om00074a007 • Publication Date (Web): 01 May 2002

Downloaded from <http://pubs.acs.org> on April 24, 2009

### More About This Article

---

The permalink <http://dx.doi.org/10.1021/om00074a007> provides access to:

- Links to articles and content related to this article
- Copyright permission to reproduce figures and/or text from this article



ACS Publications  
High quality. High impact.

sodium chloride solution (20 mL), and extracted with ether (50 mL  $\times$  3). The organic layer was filtered and dried over anhydrous magnesium sulfate. Distillation gave 1.38 g (92%) of phenyl-(trimethylsilyl)carbinol (7):<sup>7</sup> 60-MHz <sup>1</sup>H NMR (CDCl<sub>3</sub>)  $\delta$  0.00 (s, 9, SiCH<sub>3</sub>), 1.85 (s, 1, OH), 4.42 (s, 1, CH), 7.15 (s, 5, C<sub>6</sub>H<sub>5</sub>); [ $\alpha$ ]<sub>D</sub><sup>20</sup> -48.40° (c 1.78, toluene); [ $\alpha$ ]<sub>D</sub><sup>21</sup> -39.56° (neat) [Lit.<sup>7</sup> [ $\alpha$ ]<sub>D</sub><sup>25</sup> 93.0°

(neat)].

**Acknowledgment.** We thank the National Science Foundation for support, Grant CHE-8025229. We thank the Boeing Corp. for a gift in support of purchase of the 200-MHz NMR spectrometer.

## Stepwise Displacement of the Tertiary Phosphine Ligand in Square-Planar [PdR<sub>2</sub>L<sub>2</sub>]-Type Complexes by Organolithium Reagents with Stereochemical Retention Affording Organopalladate Complexes

Hiroshi Nakazawa, Fumiyuki Ozawa, and Akio Yamamoto\*

Research Laboratory of Resources Utilization, Tokyo Institute of Technology,  
Nagatsuta, Midori-ku, Yokohama 227, Japan

Received August 24, 1982

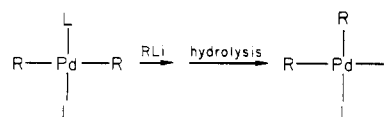
Reactions of *trans*- and *cis*-[PdR<sub>2</sub>L<sub>2</sub>] (R = Me, Et, Ph; L = tertiary phosphine) with R'Li (R' = Me, Ph) in ether or THF solution lead to stepwise displacement of L by R' with stereochemical retention to afford alkylpalladate complexes Li[PdR<sub>2</sub>R'L] and Li<sub>2</sub>[PdR<sub>2</sub>R'<sub>2</sub>], as established by means of <sup>1</sup>H, <sup>31</sup>P, and <sup>13</sup>C NMR spectroscopy. The displacement of PEt<sub>3</sub> in *trans*-[PdPh<sub>2</sub>(PEt<sub>3</sub>)<sub>2</sub>] by MeLi is a slow process, and the rate is independent of the MeLi concentration with indication of a dissociative mechanism generating a three-coordinate, T-shaped intermediate, whereas the reaction of PdR<sub>2</sub>L<sub>2</sub> (R = Me, Et) with MeLi is much faster. Displacement of PEt<sub>3</sub>Ph in Li[PdMe<sub>3</sub>(PEt<sub>3</sub>Ph)] by MeLi is a slow process and first order in concentrations of the complex and MeLi and independent of L. An associative mechanism involving a five-coordinate intermediate is proposed for the second displacement to account for the stereochemical retention. Factors influencing the <sup>1</sup>H and <sup>13</sup>C NMR chemical shifts of the neutral and palladate complexes are discussed.

### Introduction

In contrast to the well-known anionic transition-metal complexes having  $\pi$ -acceptor ligands such as CO, examples of more electron-rich anionic organotransition-metal complexes are still limited<sup>1</sup> except for the conspicuously well-utilized alkylcuprate complexes<sup>2a</sup> and recently developed alkali-metal-transition-metal  $\pi$  complexes.<sup>2b</sup> For palladium, which ranks among the most frequently employed transition metals for organic synthesis,<sup>1,3</sup> the chemistry of organopalladate complexes has been very poorly exploited.<sup>4</sup> In some cases, where palladium compounds are used in combination with alkylating or arylating agents such as alkyl- (aryl-) lithium or magnesium compounds, particularly when the alkylating agent is used in excess to the palladium complexes, the possibility of

formation of alkylpalladate complexes is considered not at all negligible, although generally neutral or cationic organopalladium complexes have been postulated in most cases.<sup>3,5</sup>

In the course of our studies on the preparation of di-alkylpalladium complexes having two tertiary phosphine ligands,<sup>6,7</sup> we have observed that *trans*-[PdR<sub>2</sub>L<sub>2</sub>] (R = alkyl group; L = monodentate tertiary phosphine) can be prepared by the reaction of bis(acetylacetonato)palladium with an alkylaluminum in the presence of L, whereas *cis*-[PdR<sub>2</sub>L<sub>2</sub>] can be synthesized by treating bis(tertiary phosphine)palladium dihalides with an excess of an alkylolithium followed by hydrolysis of the unreacted alkylolithium. Examination of the cause of this puzzling effect of the nature of the alkylating agent on the configuration of the final product led us to the finding that the isomerization of *trans*-[PdR<sub>2</sub>L<sub>2</sub>] to the *cis* isomer was promoted by addition of alkylolithium to the system.



In order to account for the *trans* to *cis* isomerization, we

(1) For example: Heck, R. F. "Organotransition Metal Chemistry"; Academic Press: New York, 1974. Collman, J. P.; Hegedus, L. S. "Principles and Application of Organotransition Metal Chemistry"; University Science Book: Mill Valley, CA 1980. Tsuji, J. "Organic Synthesis by Means of Transition Metal Complexes"; Springer-Verlag: Berlin, 1975. Kochi, J. K. "Organometallic Mechanisms and Catalysis"; Academic Press: New York, 1978.

(2) (a) Posner, G. H. "An Introduction to Synthesis Using Organocopper Reagents"; Wiley-Interscience: New York, 1980. (b) Jonas, K. *Adv. Organomet. Chem.* 1981, 19, 97.

(3) Hartley, F. R. "The Chemistry of Platinum and Palladium"; Applied Science Publishers Ltd: London, 1973. Maitlis, P. M. "The Organic Chemistry of Palladium"; Academic Press: New York, 1971. Tsuji, J. "Organic Syntheses with Palladium Compounds"; Springer-Verlag: Berlin, 1980.

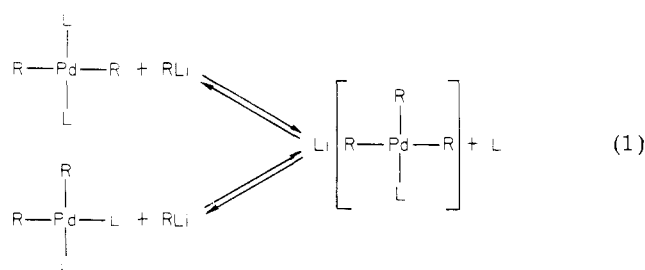
(4) Uson, R.; Fornies, J.; Espinet, P.; Martinez, F.; Tomas, M. *J. Chem. Soc., Dalton Trans.* 1981, 463. Uson, R.; Fornies, J.; Martinez, F.; Tomas, M. *Ibid.* 1980, 888.

(5) Loar, M. K.; Stille, J. K. *J. Am. Chem. Soc.* 1981, 103, 4174. Moravskiy, A.; Stille, J. K. *Ibid.* 1981, 103, 4182. Gillie, A.; Stille, J. K. *Ibid.* 1980, 102, 4933. Milstein, D.; Stille, J. K. *Ibid.* 1979, 101, 4981.

(6) Ito, T.; Tsuchiya, H.; Yamamoto, A. *Bull. Chem. Soc. Jpn.* 1977, 50, 1319.

(7) Ozawa, F.; Ito, T.; Nakamura, Y.; Yamamoto, A. *Bull. Chem. Soc. Jpn.* 1981, 54, 1868.

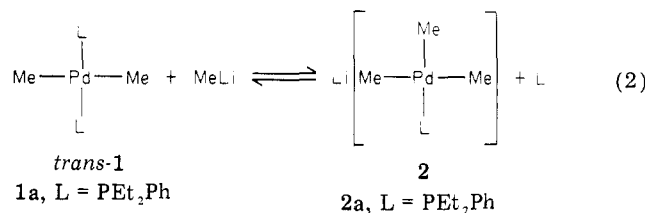
previously proposed a mechanism involving a trialkylpalladate intermediate on the basis of the observation of alkyl group scrambling in  $[\text{PdR}_2\text{L}_2]$  with the alkyllithium in a study using deuterium-labeled methyl lithium (eq 1).<sup>7</sup>



Further spectroscopic study of the system revealed in fact the formation of the trialkylpalladate species and, furthermore, its conversion to a tetraalkylpalladate complex. We now report here the results of spectroscopic studies which reveal that the conversion of the dialkyl species to the trialkylpalladate proceeds by a dissociative process, whereas the transformation of the trialkylpalladate to the tetraalkylpalladate proceeds by an associative mechanism with stereochemical retention in the square-planar geometry of Pd(II) complexes.

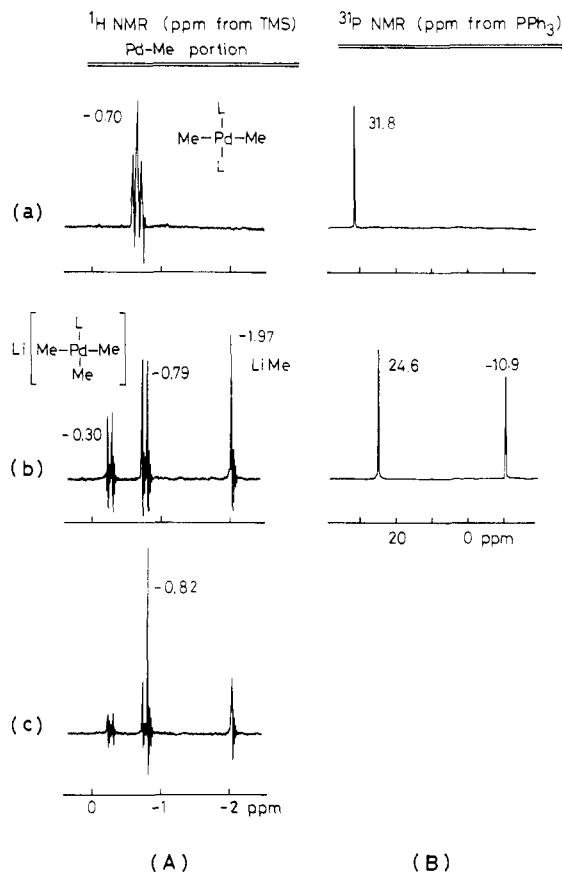
### Results

**Reaction of  $[\text{PdMe}_2\text{L}_2]$  (1) with MeLi.** On addition of 2 mol of methyl lithium per mol of *trans*- $[\text{PdMe}_2(\text{PEt}_2\text{Ph})_2]$ , *trans*-1a, in diethyl ether at room temperature, the initial triplet  $^1\text{H}$  NMR signal of the palladium-bonded methyl groups is instantly transformed to two sets of doublets in a 1:2 intensity ratio at  $-0.30$  and  $-0.79$  ppm (upfield from tetramethylsilane,  $\text{Me}_4\text{Si}$ ) as shown in Figure 1A. The other singlet at  $-1.97$  ppm in Figure 1A arises from unreacted MeLi. The doublets collapse to singlets on irradiation of the sample solution with the resonance frequency for phosphorus. On the other hand, the  $^{31}\text{P}\{^1\text{H}\}$  NMR spectrum of the same solution indicates the spectral change of the initial  $^{31}\text{P}\{^1\text{H}\}$  NMR spectrum of *trans*-1a having a single peak at 31.8 ppm (downfield from  $\text{PPh}_3$  added as an external reference) to the spectrum having a new singlet at 24.6 ppm ascribed to the coordinated phosphine ligand in the newly formed complex and another singlet at  $-10.9$  ppm (upfield from  $\text{PPh}_3$ ) arising from the  $\text{PEt}_2\text{Ph}$  ligand liberated from 1a. The spectral change suggests the rapid conversion of *trans*- $[\text{PdMe}_2\text{L}_2]$  to  $\text{Li}[\text{PdMe}_3\text{L}]$  with release of  $\text{PEt}_2\text{Ph}$  on addition of MeLi to 1a (eq 2).



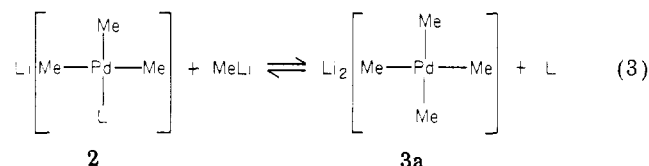
The exactly same pattern of the  $^1\text{H}$  and  $^{31}\text{P}\{^1\text{H}\}$  NMR are observed when *cis*-1a instead of *trans*-1a was used, supporting the formation of the trialkyl(tertiary phosphine)palladate 2 in the reaction starting either from *trans*-1a or *cis*-1a, in agreement with our previous proposal as expressed by eq 1. In the  $^1\text{H}$  NMR spectra, the doublet at lower field can be assigned to the methyl group trans to the phosphine ligand and the doublet at higher field with twice the intensity can be ascribed to the methyl groups cis to the phosphine ligand.

Following the instantaneous conversion of 1a to 2a, a slow reaction ensues as observed in the  $^1\text{H}$  NMR spectrum



**Figure 1.** (A)  $^1\text{H}$  NMR spectra in the Pd-Me portion (parts per million from  $\text{Me}_4\text{Si}$ , downfield positive) and (B)  $^{31}\text{P}\{^1\text{H}\}$  NMR spectra (parts per million from  $\text{PPh}_3$ , downfield positive), in  $\text{Et}_2\text{O}$  at room temperature: (a) *trans*- $[\text{PdMe}_2(\text{PEt}_2\text{Ph})_2]$ , *trans*-1a; (b) immediately after the treatment of *trans*-1a with  $\text{LiMe}$  in a 1:2 molar ratio, (c) after reaching an equilibrium for the solution of b.

by the decrease of the two sets of doublets and of the singlet at  $-1.97$  ppm and the growing of a new singlet at  $-0.82$  ppm which overlaps with one of the doublet peaks of the methyl groups Figure 1A(c). The reaction reaches an equilibrium in several hours at room temperature. Absence of coupling to phosphorus in the new species suggests the formation of a methylpalladium complex without a coordinated tertiary phosphine. The most likely candidate is  $\text{Li}_2[\text{PdMe}_4]$ , 3a, produced by the displacement of the tertiary phosphine ligand by MeLi as shown in eq 3. A related palladate complex with pentafluorophenyl groups has been recently prepared by Uson.<sup>4</sup>



To substantiate the equilibrium as expressed by eq 3, the intensity change of the peaks due to the methyl group trans to the phosphine in 2 and the free MeLi as well as the new singlet peak at  $-0.82$  ppm was plotted in Figure 2. It can be seen from Figure 2 that the intensities of the methyl group trans to L and of the free MeLi decrease with time in exactly the same manner, whereas the new peak at  $-0.82$  ppm develops quite rapidly. It was confirmed from comparison of the peak intensity data that the new species having four methyl groups was generated at the cost of one equivalent each of MeLi and 2 in support of eq 3.

Table I.  $^1\text{H}$  NMR Data of  $[\text{PdR}_2\text{L}_2]$ ,  $\text{Li}[\text{PdR}_2\text{R}'\text{L}]$ , and  $\text{Li}_2[\text{PdR}_2\text{R}'_2]$ <sup>a</sup>

complex	Pd-R	chem shift, <sup>b</sup> ppm from Me <sub>4</sub> Si	
		in Et <sub>2</sub> O	in THF
<i>trans</i> -1a, <i>trans</i> -[PdMe <sub>2</sub> (PEt <sub>2</sub> Ph) <sub>2</sub> ]	Pd-CH <sub>3</sub>	-0.70 (t, <sup>c</sup> <i>J</i> = 5.0 <sup>d</sup> )	-0.67 (t, <i>J</i> = 5.0)
<i>cis</i> -1a, <i>cis</i> -[PdMe <sub>2</sub> (PEt <sub>2</sub> Ph) <sub>2</sub> ]	Pd-CH <sub>3</sub>	+0.11 (q)	+0.08
<i>cis</i> -1b, <i>cis</i> -[PdMe <sub>2</sub> (PEt <sub>3</sub> ) <sub>2</sub> ]	Pd-CH <sub>3</sub>	-0.03 (q)	
<i>trans</i> -1c, <i>trans</i> -[PdEt <sub>2</sub> (PMe <sub>2</sub> Ph) <sub>2</sub> ]	Pd-CH <sub>2</sub> -CH <sub>3</sub>		+0.95 (t, <i>J</i> = 7.5)
	Pd-CH <sub>2</sub> -CH <sub>3</sub>		+0.41 (sex., <i>J</i> = 8.0)
[PdMe <sub>2</sub> (tmed)] <sup>e</sup>	Pd-CH <sub>3</sub>	-0.30 (s)	
2a, Li[PdMe <sub>3</sub> (PEt <sub>2</sub> Ph)]	Pd-CH <sub>3</sub> trans to L	-0.30 (d)	-0.26 (d, <i>J</i> = 5.6)
	Pd-CH <sub>3</sub> cis to L	-0.79 (d)	-0.76 (d, <i>J</i> = 6.2)
2b, Li[PdMe <sub>3</sub> (PEt <sub>3</sub> )]	Pd-CH <sub>3</sub> trans to L	-0.45 (d, <i>J</i> = 5.0)	
	Pd-CH <sub>3</sub> cis to L	-0.85 (d, <i>J</i> = 6.5)	
<i>trans</i> -2e, <i>trans</i> -Li[PdPh <sub>2</sub> Me(PEt <sub>2</sub> Ph)]	Pd-CH <sub>3</sub>		-0.18 (d)
<i>trans</i> -2d, <i>trans</i> -Li[PdPh <sub>2</sub> Me(PEt <sub>3</sub> )]	Pd-CH <sub>3</sub>		-0.27 (d, <i>J</i> = 6.1)
<i>trans</i> -2c, <i>trans</i> -Li[PdEt <sub>2</sub> Me(PMe <sub>2</sub> Ph)]	Pd-CH <sub>2</sub> -CH <sub>3</sub>		+1.09 (t, <i>J</i> = 7.5)
	Pd-CH <sub>2</sub> -CH <sub>3</sub>		+0.05 (qui., <i>J</i> = 8.2)
	Pd-CH <sub>3</sub>		-0.24 (d, <i>J</i> = 6.5)
<i>trans</i> -2f, <i>trans</i> -Li[PdPhMe <sub>2</sub> (PEt <sub>2</sub> Ph)]	Pd-CH <sub>3</sub>		-0.67 (d, <i>J</i> = 6.4)
<i>cis</i> -2f, <i>cis</i> -Li[PdPhMe <sub>2</sub> (PEt <sub>2</sub> Ph)]	Pd-CH <sub>3</sub> trans to L		-0.26 (d, <i>J</i> = 6.0)
	Pd-CH <sub>3</sub> cis to L		-0.68 (d, <i>J</i> = 6.0)
3a, Li <sub>2</sub> [PdMe <sub>4</sub> ]	Pd-CH <sub>3</sub>	-0.82 (s)	-0.79 (s)
<i>trans</i> -3d, <i>trans</i> -Li <sub>2</sub> [PdPh <sub>2</sub> Me <sub>2</sub> ]	Pd-CH <sub>3</sub>	-0.52 (s)	-0.63 (s)
<i>cis</i> -3d, <i>cis</i> -Li <sub>2</sub> [PdPh <sub>2</sub> Me <sub>2</sub> ]	Pd-CH <sub>3</sub>		-0.68 (s)
LiMe		-1.97 (s)	-2.06 (s)

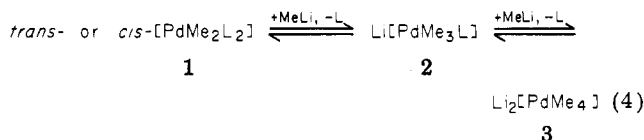
<sup>a</sup> R and R' represent alkyl and/or aryl group(s) and L stands for tertiary phosphine. <sup>b</sup> Downfield positive. <sup>c</sup> Abbreviation: s, singlet; d, doublet; t, triplet; q, quartet; qui, quintet; sex., sextet. <sup>d</sup> *J* means <sup>3</sup>*J*(H-P), values in hertz. Since the related sign has not been determined, the absolute value is presented. <sup>e</sup> tmed stands for *N,N,N',N'*-tetramethylethylenediamine.

Table II.  $^{31}\text{P}$  NMR Data of  $[\text{PdR}_2\text{L}_2]$  and  $\text{Li}[\text{PdR}_2\text{R}'\text{L}]$ <sup>a</sup>

complex	chem shifts, <sup>b</sup> ppm from PPh <sub>3</sub>	
	in Et <sub>2</sub> O	in THF
<i>trans</i> -1a, <i>trans</i> -[PdMe <sub>2</sub> (PEt <sub>2</sub> Ph) <sub>2</sub> ]	31.8	31.8
<i>cis</i> -1a, <i>cis</i> -[PdMe <sub>2</sub> (PEt <sub>2</sub> Ph) <sub>2</sub> ]	16.6	17.1
<i>trans</i> -1e, <i>trans</i> -[PdPh <sub>2</sub> (PEt <sub>2</sub> Ph) <sub>2</sub> ]		20.3
<i>trans</i> -1d, <i>trans</i> -[PdPh <sub>2</sub> (PEt <sub>3</sub> ) <sub>2</sub> ]	17.2	17.3
2a, Li[PdMe <sub>3</sub> (PEt <sub>2</sub> Ph)]	24.6	24.6
<i>trans</i> -2e, <i>trans</i> -Li[PdPh <sub>2</sub> Me(PEt <sub>2</sub> Ph)]		16.1
<i>trans</i> -2d, <i>trans</i> -Li[PdPh <sub>2</sub> Me(PEt <sub>3</sub> )]		16.2
PEt <sub>2</sub> Ph	-10.9	-10.7
PEt <sub>3</sub>	-13.8	-13.8

<sup>a</sup> R and R' represent alkyl and/or aryl group(s) and L stands for tertiary phosphine. <sup>b</sup> Down field positive.

It is thus indicated that the reaction of *trans*- or *cis*-[PdMe<sub>2</sub>L<sub>2</sub>] with MeLi is a two-step equilibrium process as summarized by eq 4.



When an appropriate amount of the phosphine is added to the equilibrium system of eq 4, an increase in the amount of 1 and a decrease in the amount of 3 are observed, the fact implying an equilibrium shift from right to left in eq 4. Because of these equilibria, attempts to isolate 2 and 3 were unsuccessful. The  $^1\text{H}$  and  $^{31}\text{P}\{^1\text{H}\}$  NMR data of the palladate complexes 2 and 3 are summarized, together with spectroscopic data of other complexes, in Table I and II.

The  $^{13}\text{C}$  NMR spectra in tetrahydrofuran (THF) solution also support the formation of trimethylpalladate 2, and tetramethylpalladate 3 (see Table III). In the system of *trans*-1a-MeLi mixed in a 1:2 ratio, two sets of doublets at 0.4 and -5.2 ppm (downfield positive from the external reference of Me<sub>4</sub>Si) were observed together with a triplet at -6.0 ppm ascribed to the methyl carbons of the starting

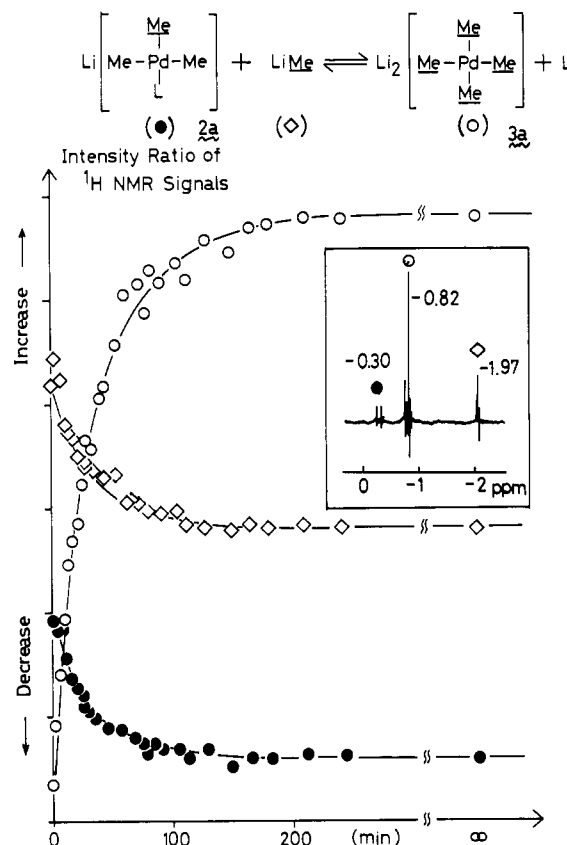


Figure 2. Time course of relative intensity of  $^1\text{H}$  NMR signals on the reaction of  $\text{Li}[\text{PdMe}_3(\text{PEt}_2\text{Ph})]$ , 2a, with  $\text{LiMe}$  in  $\text{Et}_2\text{O}$  at 21.7 °C affording  $\text{Li}_2[\text{PdMe}_4]$ , 3a: ●, the doublet at -0.30 ppm due to the methyl group trans to the phosphine ligand in 2a; ○, the singlet at -0.82 ppm due to 3a; ◇, the singlet at -1.97 ppm due to  $\text{LiMe}$ .

complex *trans*-1a and a singlet at -15.5 ppm assigned to the methyl carbon of unreacted MeLi. The doublet at 0.4 ppm can be ascribed to the methyl carbon trans to the phosphine and the doublet at -5.2 ppm to the methyl carbons cis to the phosphine of 2a. After the solution was

Table III.  $^{13}\text{C}$  NMR Data of  $[\text{PdR}_2\text{L}_2]$ ,  $\text{Li}[\text{PdR}_2\text{R}'\text{L}]$ , and  $\text{Li}_2[\text{PdR}_2\text{R}'_2]^\text{a}$ 

complex		methyl, $\text{CH}_3$	ethyl		phenyl			
			$\text{CH}_2-\text{CH}_3$	$-\text{CH}_2-\text{CH}_3$	$\text{C}_\text{b}^\text{b}$	$\text{C}_\text{o}$	$\text{C}_\text{m}$	$\text{C}_\text{p}$
<i>trans</i> - $[\text{PdMe}_2(\text{PEt}_2\text{Ph})_2]$ , <i>trans</i> -1a	R	-6.0 (t, $J = 10$ )						
	L		17.6 (t, $J = 12$ )	9.1 (s)	135.0 (t, $J = 20$ )	133.5 (t, $J = 6$ )	128.4 (t, $J = 4$ )	129.7 (s)
<i>cis</i> - $[\text{PdMe}_2(\text{PEt}_2\text{Ph})_2]$ , <i>cis</i> -1a	R	+5.5 (dd, $J =$ $110, J = 16$ )						
	L		17.7 (t, $J = 10$ )	8.8 (s)	137.4 (t, $J = 14$ )	132.7 (t, $J = 5$ )	128.5 (t, $J = 4$ )	129.4 (s)
<i>trans</i> - $[\text{PdPh}_2(\text{PEt}_3)_2]$ , <i>trans</i> -1d	R				169.2 (t, $J = 13$ )	139.5 (s)	126.9 (s)	122.1 (s)
	L		15.2 (t, $J = 13$ )	8.3 (s)				
<i>trans</i> - $[\text{PdPh}_2(\text{PEt}_2\text{Ph})_2]$ , <i>trans</i> -1e	R				167.6 (t, $J = 12$ )	139.7 (t, $J = 2$ )	126.6 (s)	122.1 (s)
	L		16.2 (t, $J = 13$ )	10.1 (d, $J = 15$ )	133.8 (t, $J = 20$ )	132.4 (t, $J = 5$ )	129.5 (s)	128.5 (s)
$\text{Li}[\text{PdMe}_3(\text{PEt}_2\text{Ph})]$ , 2a	R	+0.4 (d, $J = 123$ )		[trans to L]				
	L	-5.2 (d, $J = 10$ )		[cis to L]				
<i>trans</i> - $\text{Li}[\text{PdPh}_2\text{Me}(\text{PEt}_2\text{Ph})]$ , <i>trans</i> -2e	R	+2.9 (d, $J = 112$ )			138.1 (d, $J = 23$ )	133.0 (d, $J = 11$ )	128.0 (d, $J = 9$ )	128.5 (s)
	L		17.6 (d, $J = 17$ )	8.2 (s)	179.6 (d, $J = 13$ )	140.7 (d, $J = 2$ )	125.6 (s)	120.3 (s)
<i>trans</i> - $\text{Li}[\text{PdPh}_2\text{Me}(\text{PEt}_3)]$ , <i>trans</i> -2d	R	+2.2 (d, $J = 114$ )			138.0 (d, $J = 23$ )	132.6 (d, $J = 10$ )	128.0 (s)	127.7 (s)
	L		17.1 (d, $J = 17$ )	7.9 (s)	180.0 (d, $J = 12$ )	140.7 (d, $J = 4$ )	125.8 (s)	120.3 (s)
$\text{Li}_2[\text{PdMe}_4]$ , 3a	R	-8.3 (s)						
	R	+1.2 (s)			159.0 (s)	141.8 (s)	125.8 (s)	121.4 (s)
<i>trans</i> - $\text{Li}_2[\text{PdPh}_2\text{Me}_2]$ , <i>trans</i> -3d								
		-15.5 (s)						
$\text{LiMe}$			19.4 (d, $J = 56$ )	9.9 (d, $J = 15$ )				
$\text{PEt}_3$			20.9 (d, $J = 12$ )	10.2 (d, $J = 15$ )	139.7 (d, $J = 18$ )	312.9 (d, $J = 18$ )	129.1 (d, $J = 4$ )	128.7 (s)

<sup>a</sup> R and R' represent alkyl and/or aryl group(s) and L stands for tertiary phosphine. In THF at room temperature. Chemical shift: ppm from  $\text{Me}_4\text{Si}$  (downfield positive). Coupling constant: Hz, coupling between C and P. Since the relative sign has not been determined, the absolute value is represented. Abbreviation: s, singlet; d, doublet; t, triplet; dd, doublet of doublets. <sup>b</sup>  $\text{C}_\text{b}$ , Pd- or P-bonded carbon.

allowed to stand for several hours at room temperature, a singlet corresponding to the methyl carbons in 3a was observed at -8.3 ppm.

A comparison of the coupling constant  $^3J(\text{H-P})$  with  $^2J(\text{C-P})$  of 2a in THF is of interest. The coupling constant between the phosphorus atom in phosphine ligand and the methyl protons trans to it ( $^3J(\text{trans-H-P}) = 5.6$  Hz) is less than that between phosphorus in the phosphine ligand and the methyl protons cis to it ( $^3J(\text{cis-H-P}) = 6.2$  Hz), whereas the coupling constant between the phosphine P and the methyl carbon trans to it ( $^2J(\text{trans-C-P}) = 123$  Hz) is greater than that between P in the phosphine and the methyl carbons cis to it ( $^2J(\text{cis-C-P}) = 10$  Hz).

The reaction of  $\text{Na}_2\text{PdCl}_4$  or  $\text{Pd}(\text{OAc})_2$  suspended in  $\text{Et}_2\text{O}$  solution with MeLi led to deposition of palladium metal without affording 3. Thus the presence of the tertiary phosphine serves to stabilize the dimethyl and trimethyl complexes 1 and 2 and helps to stabilize the whole system in equilibria. In fact, it is not necessary to start from the isolated dimethylpalladium complex 1 in order to produce 2 and 3 in situ. Addition of  $\text{PEt}_2\text{Ph}$  to a heterogeneous ether solution of  $\text{Na}_2\text{PdCl}_4$  yields a yellow precipitate of  $\text{PdCl}_2(\text{PEt}_2\text{Ph})_2$ . Treatment of the system with an ether solution of MeLi at room temperature converts it into a colorless solution containing the white powder LiCl. The  $^1\text{H}$  NMR spectrum of the supernatant

solution shows the existence of *cis*-1a, *trans*-2a, and 3a.

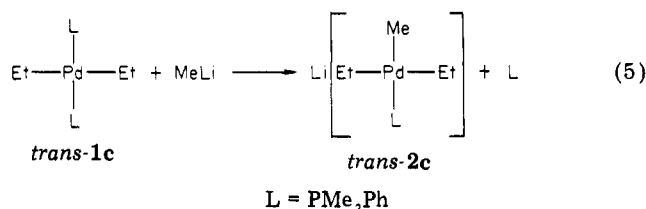
Similar displacement of the tertiary phosphine ligands in  $[\text{PdR}_2\text{L}_2]$  by the methyl group in MeLi is observed also in a dimethylpalladium complex with triethylphosphine ligands (see Table I and II). The  $\text{A}_3\text{XX}'\text{A}'_3$  pattern of the  $^1\text{H}$  NMR signal due to the Pd-bonded methyl groups in *cis*-1b disappeared with increase of the two sets of doublets in a 1:2 intensity ratio at -0.45 and -0.85 ppm, suggesting the formation of  $\text{Li}[\text{PdMe}_3(\text{PEt}_3)]$ , 2b. The former doublets are assigned to the Pd-bonded methyl groups trans to the triethylphosphine and the latter to the two methyl groups cis to the triethylphosphine. As in the  $\text{PEt}_2\text{Ph}$ -containing complex 2a, the  $^3J(\text{H-P})$  coupling constant due to the trans phosphine was slightly smaller than the coupling constant due to the cis phosphine. Following the formation of 2b, growth of the singlet at -0.82 ppm due to  $\text{Li}_2[\text{PdMe}_4]$  is observed.

**Reaction of  $[\text{PdEt}_2\text{L}_2]$  with MeLi.** The  $^1\text{H}$  NMR spectrum of *trans*- $[\text{PdEt}_2(\text{PMe}_2\text{Ph})_2]$ , *trans*-1c, in THF solution exhibits a triplet at 0.95 ppm due to the methyl and a sextet at 0.41 ppm due to the methylene in the Pd-bonded ethyl groups.

In the reaction of *trans*-1c with an equimolar amount of MeLi in THF at room temperature, a doublet  $^1\text{H}$  NMR signal at -0.24 ppm, a quintet at 0.05 ppm, and a triplet at 1.09 ppm arise at the expense of the signals due to the

starting complex *trans-1c*. The spectrum also shows the doublet signal assigned to the methyl protons of the liberated  $\text{PMe}_2\text{Ph}$  in addition to the doublet ascribed to the methyl protons of the coordinated  $\text{PMe}_2\text{Ph}$  ligand in approximately 1:1 ratio.

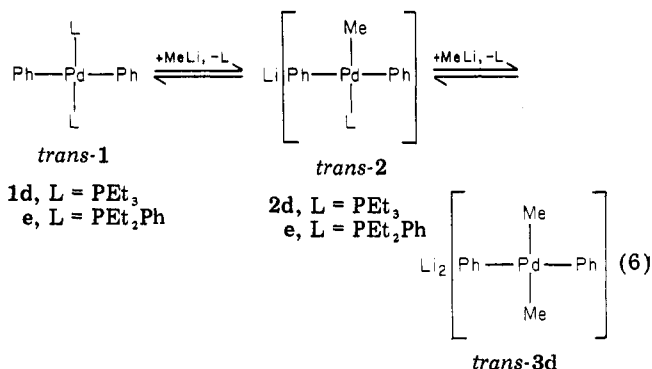
These  $^1\text{H}$  NMR data indicate the formation of  $\text{Li}[\text{PdEt}_2\text{Me}(\text{PMe}_2\text{Ph})]$ , *2c*, by the reaction of *trans-1c* with  $\text{MeLi}$ . The doublet at  $-0.24$  ppm is assigned to the methyl protons of the Pd-bonded methyl group, the quintet at  $0.05$  ppm to the methylene protons, and the triplet at  $1.09$  ppm to the methyl protons of the Pd-bonded ethyl groups. If the palladate complex *2c* has a *cis* configuration, two ethyl groups directly bonded to palladium would be magnetically different. The  $^1\text{H}$  NMR spectrum, however, shows the existence of only one kind of the ethyl groups, indicating that the complex *2c* produced in the reaction of *trans-1c* with  $\text{MeLi}$  has a *trans* configuration.



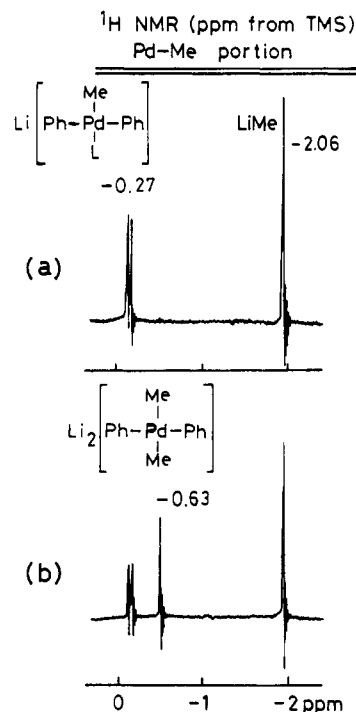
The result shows that the tertiary phosphine *trans* to the other phosphine ligand has been displaced by the methyl group from  $\text{MeLi}$  with *retention* of the stereochemistry. Study of the reaction of the dimethylpalladium complexes with ethyllithium was not feasible because of the instability of ethyllithium in THF.

Allowing the reaction mixture of *trans-1c* with methyllithium to stand for a longer period of several hours caused further reaction as reflected by the development of a complicated NMR spectrum that suggests the occurrence of isomerization of *trans-2c* to *cis-Li[PdMe}\_2\text{EtL}*, *trans-Li[PdMe}\_2\text{EtL}*,  $\text{Li}[\text{PdMe}_3\text{L}]$ , and other species accompanied by the evolution of ethane. Because of the decomposition of the resulting complexes and of the complexity of the spectrum, no further study was attempted.

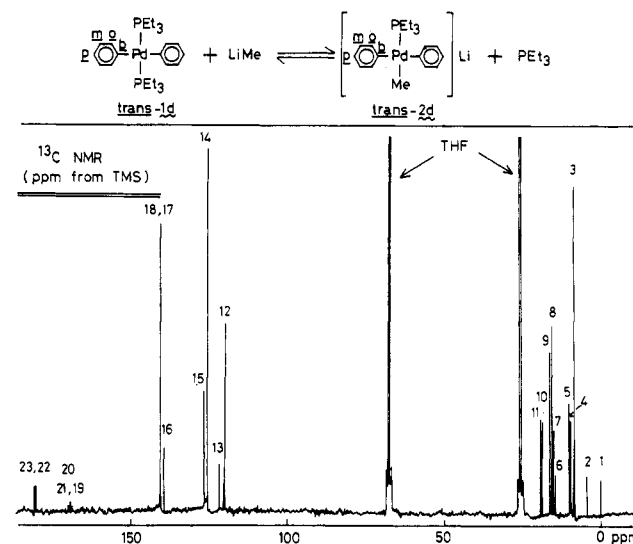
**Reaction of  $[\text{PdPh}_2\text{L}_2]$  with  $\text{MeLi}$ .** For obtaining information regarding the stereochemistry of the ligand displacement reaction of  $[\text{PdR}_2\text{L}_2]$  by alkylolithium, the reaction of *trans*- $[\text{PdPh}_2(\text{PEt}_3)_2]$ , *trans-1d*, with  $\text{MeLi}$  was examined. The result can be expressed by eq 6, representing the stereospecific stepwise displacement of the tertiary phosphine ligand by the methyl group in  $\text{MeLi}$  with retention of the original configuration in *1d*.



The  $^1\text{H}$  NMR spectrum of the THF solution of *trans*- $[\text{PdPh}_2(\text{PEt}_3)_2]$ , *trans-1d*, after its treatment with an equimolar amount of  $\text{MeLi}$  shows a slow conversion of *trans-1d* to *trans-2d* as indicated by development of a doublet at  $-0.27$  ppm arising from the methyl group in addition to the singlet peak at  $-2.06$  ppm due to the re-



**Figure 3.**  $^1\text{H}$  NMR spectra in the Pd-Me portion (parts per million from  $\text{Me}_4\text{Si}$ ) in THF at room temperature: 3 h (a) and 9 days (b) after the treatment of *trans*- $[\text{PdPh}_2(\text{PEt}_3)_2]$ , *trans-1d*, with  $\text{MeLi}$  in 1:1 (a) and 1:2 (b) molar ratios at room temperature.



**Figure 4.**  $^{13}\text{C}$  NMR spectrum (parts per million from  $\text{Me}_4\text{Si}$ , downfield positive) in THF at room temperature 1 h after *trans*- $[\text{PdPh}_2(\text{PEt}_3)_2]$  was mixed with  $\text{MeLi}$  in a 1:1 molar ratio.

maining  $\text{MeLi}$ . When *trans-1d* was mixed with more than an equimolar amount of  $\text{MeLi}$ , a further spectral change was observed: a singlet developed at  $-0.63$  ppm at the expense of the doublet at  $-0.27$  ppm and of the singlet at  $-2.06$  ppm (Figure 3), suggesting the occurrence of the stepwise reactions represented by eq 6.

In order to determine the configurations of *trans-2d* and *trans-3d*, the  $^{13}\text{C}\{^1\text{H}\}$  NMR spectrum of *trans-1d* in THF after it was mixed with an equimolar amount of  $\text{MeLi}$  in THF was observed after 1 day (Figure 4). The spectrum of the reaction mixture is considerably complicated but can be accounted for in terms of a mixture of *trans-1d*, *trans-2d*, and liberated  $\text{PEt}_3$  by comparison with the  $^{13}\text{C}\{^1\text{H}\}$  NMR spectra of *trans-1d* and free  $\text{PEt}_3$ . Each peak in Figure 4 is numbered from the high field to the lower

field except for the strong peaks centered at 26.3 and 68.1 ppm due to THF. The two doublets [4, 5] and [10, 11] are due to the methyl and methylene carbons coupled to phosphorus in free  $\text{PEt}_3$  released from **1d** on reaction with MeLi. Each counterpart of the doublet [4, 5] splits to a quartet and each counterpart of the doublet [10, 11] splits to a triplet in the nondecoupled spectrum, supporting the assignment of the signals to the methyl and methylene groups in free  $\text{PEt}_3$ , respectively. The  $^{13}\text{C}\{^1\text{H}\}$  NMR signals of the starting complex *trans*-**1d** are observed as follows. The signal [3] is due to the methyl carbons in the  $\text{PEt}_3$  ligands. The signals [6, 7, 8] are triplets arising from the methylene carbons in the coordinated  $\text{PEt}_3$  split by virtual coupling to two mutually *trans*-situated phosphorus nuclei. The peak [8] overlaps with a part of the doublet [8, 9] due to *trans*-**2d**. The peaks [13], [15], [16], and [19, 20, 21] are assigned to the phenyl carbons bonded to Pd in the starting complex *trans*-**1d**. They are respectively assigned in the order to the  $C_p$  (para),  $C_m$  (meta),  $C_o$  (ortho), and  $C_b$  (Pd-bonded) carbons of the phenyl groups. The triplet [19, 20, 21] indicates the *trans* configuration of the starting complex **1d**. The rest of the signals can be assigned to *trans*-**2d** existing as the sole anionic species. The peaks [1, 2] are the doublet due to the methyl carbon in the methyl group bonded to Pd in *trans*-**2d** coupled to the phosphorus in the  $\text{PEt}_3$  ligand. The singlet [3] is due to the methyl carbons in the coordinated  $\text{PEt}_3$  ligand in *trans*-**2d** overlapped with the signal of methyl carbons in the coordinated  $\text{PEt}_3$  in *trans*-**1d**. The doublet [8, 9] is due to the methylene carbons in the coordinated  $\text{PEt}_3$  in *trans*-**2d** partly overlapped with the triplet of the coordinated  $\text{PEt}_3$  in *trans*-**1d**. Signals [12], [14], [17, 18], and [22, 23] in the lower field arise from the phenyl carbons in the palladate complex *trans*-**2d**. They are assigned in turn to the  $C'_p$ ,  $C'_m$ ,  $C'_o$ , and  $C'_b$  (Pd-bonded) carbons in the phenyl groups in *trans*-**2d**. If the palladate complex should have phenyl groups situated in mutually *cis* positions, the phenyl groups would be magnetically nonequivalent. The presence of only one kind of the phenyl groups strongly suggests the *trans* isomer existing as the sole diphenylmonomethylpalladate species. The splitting to doublets of the carbon signals [1, 2], [8, 9], [17, 18], and [22, 23] by coupling to the phosphorus in the coordinated mono tertiary phosphine ligand supports the formulation of the palladate complex as *trans*-**2d** shown in eq 6 and Figure 4.

The  $^{31}\text{P}$  NMR spectrum of the THF solution of *trans*-**1d** after its treatment with an equimolar amount of MeLi also supports the formation of *trans*-**2d**. A singlet at 16.2 ppm appears together with a singlet at -13.8 ppm due to free  $\text{PEt}_3$  liberated from *trans*-**1d** at the expense of a singlet at 17.3 ppm due to the starting complex *trans*-**1d** (see Table II).

The  $^1\text{H}$  NMR spectrum of the THF solution containing *trans*-**1d** mixed with more than an equimolar amount of MeLi shows a singlet at -0.63 ppm in addition to the doublet at -0.27 ppm arising from the methyl protons of the Pd-bonded methyl group in *trans*-**2d** and a singlet at -2.06 ppm due to free MeLi. The  $^{13}\text{C}$  NMR spectrum of the same solution exhibits a singlet at 1.2 ppm arising from Pd-bonded methyl groups and singlets at 121.4, 125.8, 141.8, and 159.0 ppm due, in turn, to the  $C''_p$ ,  $C''_m$ ,  $C''_o$ , and  $C''_b$  carbons in the phenyl groups bonded to palladium, together with signals due to *trans*-**2d**, free  $\text{PEt}_3$ , and MeLi. The  $^1\text{H}$  and  $^{13}\text{C}$  NMR spectra suggest the formation of the dianionic palladate  $\text{Li}_2[\text{PdPh}_2\text{Me}_2]$ , **3d**. Since **3d** is formed from *trans*-**2d**, it probably has a *trans* configuration. The *trans* geometry of  $\text{Li}_2[\text{PdPh}_2\text{Me}_2]$  (**3d**) is further supported

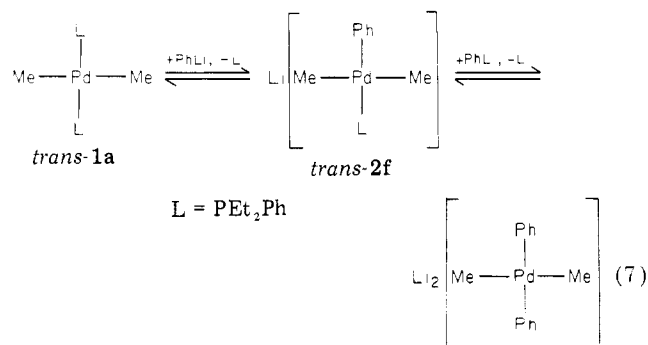
by the appearance of a singlet at -0.63 ppm in  $^1\text{H}$  NMR spectrum when *trans*- $[\text{PdMe}_2(\text{PEt}_2\text{Ph})_2]$  is treated with LiPh in THF solution (vide infra).

A completely analogous spectroscopic pattern is observed when  $\text{PEt}_2\text{Ph}$ -coordinated complex *trans*- $[\text{PdPh}_2(\text{PEt}_2\text{Ph})_2]$ , *trans*-**1e**, is treated with MeLi. The spectroscopic change is consistent with the slow formation of *trans*- $\text{Li}[\text{PdPh}_2\text{Me}(\text{PEt}_2\text{Ph})]$ , *trans*-**2e**, followed by its slow conversion into *trans*- $\text{Li}_2[\text{PdPh}_2\text{Me}_2]$ , *trans*-**3d**.

Thus the stepwise displacement of the tertiary phosphine ligands in *trans*-**1** by the methyl groups of MeLi with retention of the *trans* geometry has been confirmed.

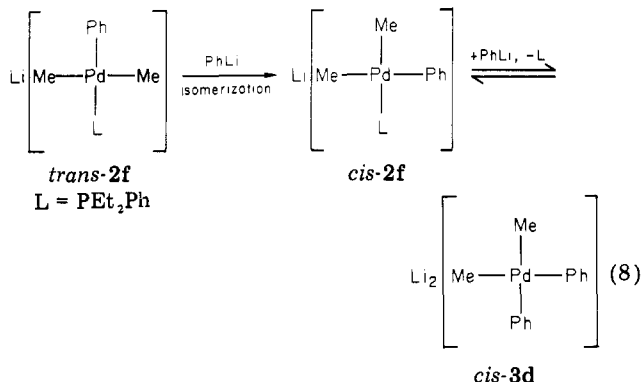
Hydrolysis of the equilibrium system containing *trans*- $\text{Li}[\text{PdPh}_2\text{MeL}]$  and *trans*- $\text{Li}_2[\text{PdPh}_2\text{Me}_2]$  reveals the formation of only *trans*- $[\text{PdPh}_2\text{L}_2]$ . The formation of the *trans*-diphenyl complex by hydrolysis is in contrast to the formation of the *cis*-dimethyl complex when the solution containing  $\text{Li}[\text{PdMe}_3\text{L}]$  and  $\text{Li}_2[\text{PdMe}_4]$  was hydrolyzed. The  $[\text{PdPh}_2\text{L}_2]$ -type complex seems to have a strong inclination to take the *trans* geometry.

**Reaction of *trans*- and *cis*- $[\text{PdMe}_2(\text{PEt}_2\text{Ph})_2]$  (**1a**) with PhLi.** For an examination of the stereospecific displacement reaction in the square-planar palladium complexes, the reaction of  $[\text{PdMe}_2\text{L}_2]$  with PhLi was studied. The reaction of *trans*-**1a** with an equimolar amount of PhLi in THF gives instantly a doublet at -0.67 ppm in the  $^1\text{H}$  NMR spectrum, suggesting the formation of *trans*- $\text{Li}[\text{PdPhMe}_2(\text{PEt}_2\text{Ph})]$ , *trans*-**2f**. The  $^1\text{H}$  NMR spectrum changes further when the reaction mixture is left standing for a few minutes at room temperature with the growth of a singlet at -0.63 ppm. The chemical shift of the singlet is identical with that of *trans*- $\text{Li}_2[\text{PdPh}_2\text{Me}_2]$ , *trans*-**3d**, previously obtained by the reaction of *trans*- $[\text{PdPh}_2(\text{PEt}_2\text{Ph})_2]$ , *trans*-**1e**, with MeLi. Thus the displacement of the tertiary phosphine ligand in *trans*-**1** by LiPh proceeds by stereochemical retention in two steps as expressed by eq 7.

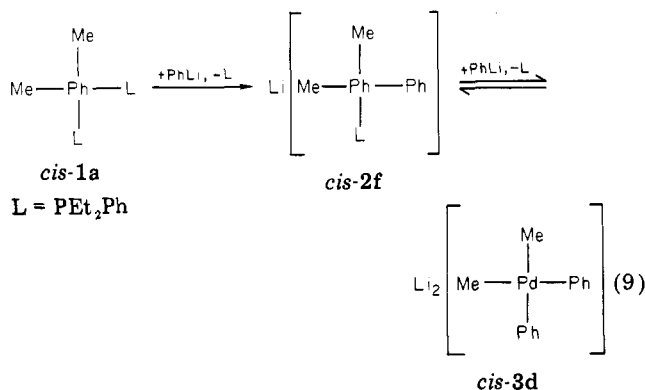


When the reaction system is left standing for several days, the other types of reactions take place as observed by appearance of a set of two doublets at -0.26 and -0.68 ppm with an equal intensity. The two doublets are due to *cis*- $\text{Li}[\text{PdPhMe}_2(\text{PEt}_2\text{Ph})]$ , *cis*-**2f**, formed by isomerization of *trans*-**2f** (vide infra). The  $^1\text{H}$  NMR of the reaction system shows the formation of still another species as a singlet at -0.68 ppm, which is tentatively assigned to *cis*- $\text{Li}_2[\text{PdMe}_2\text{Ph}_2]$ , *cis*-**3d**, because the same resonance is observed on treatment of *cis*- $[\text{PdMe}_2\text{L}_2]$  with PhLi (vide infra). The reactions may be expressed as shown in eq 8.

A similar experiment to eq 7 also was carried out by using *cis*- $[\text{PdMe}_2\text{L}_2]$  instead of *trans*- $[\text{PdMe}_2\text{L}_2]$  with PhLi in THF solution. When *cis*- $[\text{PdMe}_2(\text{PEt}_2\text{Ph})_2]$  was mixed with an equimolar amount of PhLi in THF, an  $^1\text{H}$  NMR spectrum showing two sets of doublets of equal intensity at -0.26 and -0.68 ppm was obtained. The spectral pattern



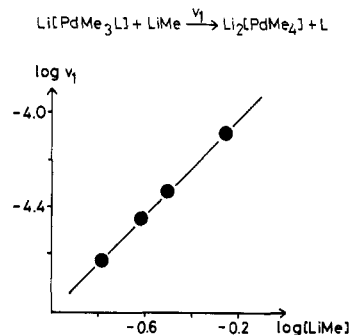
and the chemical shifts agree well with those of the species formed by spontaneous isomerization of *trans*-2f and suggest the formation of *cis*-2f.



By referring to the assignment of the chemical shift of the methyl groups in  $\text{Li}[\text{PdMe}_3(\text{PEt}_2\text{Ph})]$ , where the methyl signal at the lower field was assigned to the methyl group trans to L and the higher ones to the methyl groups cis to L, we ascribe the doublet at  $-0.26$  ppm to the methyl group trans to L while the other doublet at  $-0.68$  ppm to the methyl group cis to L. When the solution was allowed to stand for a few days, further complication of the  $^1\text{H}$  NMR spectrum ensued with growth of a signal due to MeLi, the fact indicating the displacement of the Pd-bonded methyl group(s) by PhLi with the release of MeLi. The growing of a singlet at  $-0.68$  ppm suggests the formation of *cis*- $\text{Li}_2[\text{PdPh}_2\text{Me}_2]$ , *cis*-3d.

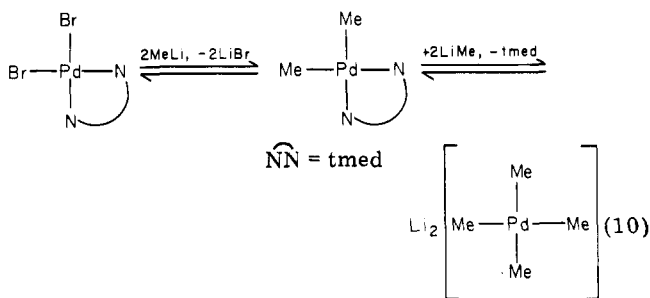
Comparison of the reaction of *trans*- $[\text{PdPh}_2\text{L}_2]$  with MeLi expressed by eq 6 with that of *trans*- and *cis*- $[\text{PdMe}_2\text{L}_2]$  with PhLi represented by eq 7 and 8 shows the trend that *trans*-2d having two phenyl ligands in mutually trans positions is more reluctant to isomerize. The higher reactivity of *trans*-2f toward isomerization may be due to the greater trans effect of the methyl group than that of the phenyl group.

**Reaction of  $[\text{PdBr}_2(\text{tmed})]$  with MeLi.** Treatment of  $[\text{PdBr}_2(\text{tmed})]$  ( $\text{tmed} = N,N,N',N'$ -tetramethylethylenediamine) with MeLi in a 1:5 molar ratio with  $\text{Et}_2\text{O}$  at  $0^\circ\text{C}$  gives a colorless homogenous solution. The  $^1\text{H}$  NMR spectrum of the solution exhibits two singlets at  $-0.82$  and  $-0.30$  ppm in a Pd-bonded methyl region in addition to a singlet at  $-1.97$  ppm due to free MeLi. The signal at  $-0.82$  ppm can be readily assigned to the methyl protons of  $\text{Li}_2[\text{PdMe}_4]$  (vide supra). Four signals that are ascribed to tmed are observed at 2.32, 2.39, 2.41, and 2.48 ppm. The first two singlets are identified with signals due to free tmed. The  $^1\text{H}$  NMR data indicate the formation of  $[\text{PdMe}_2(\text{tmed})]$  by the displacement of Br in  $[\text{PdBr}_2(\text{tmed})]$  by the methyl groups. The signal at  $-0.30$  ppm is assigned to the Pd-bonded methyl protons, and the two signals at 2.41 and 2.48 ppm are assigned to the methyl



**Figure 5.** A plot of  $\log v_1$  vs.  $\log [\text{MeLi}]$  in the reaction of  $\text{Li}[\text{PdMe}_3(\text{PEt}_2\text{Ph})]$  with MeLi in  $\text{Et}_2\text{O}$  at  $21.7^\circ\text{C}$ , where  $v_1$  is the formation rate of  $\text{Li}_2[\text{PdMe}_4]$ .

and methylene protons of the coordinated tmed, respectively. It is a general trend that signals due to tmed move to low field on coordination.  $\text{Li}_2[\text{PdMe}_4]$  is considered to be formed by the displacement of tmed in  $[\text{PdMe}_2(\text{tmed})]$  by the methyl groups as follows.



Thus a tetramethylpalladate complex can be prepared not only from the displacement reaction of tertiary phosphine in  $[\text{PdMe}_2\text{L}_2]$  by the methyl groups but also from the reaction of  $[\text{PdBr}_2(\text{tmed})]$  with MeLi.

**Kinetic Study of the Palladate Formation Reactions.** After characterization of the palladate complexes, we examined the kinetics of the reactions of organopalladium complexes to find the considerable difference in reaction rates of the stepwise reactions depending on the nature of the starting diorganopalladium complexes. The difference in rates enabled us to study each reaction step under appropriate conditions. It was found that the second step in eq 4, namely, the reaction of trimethylpalladate to tetramethylpalladate, proceeds at a rate amenable to a kinetic study by means of  $^1\text{H}$  NMR spectroscopy, whereas the first step involving the displacement of L by the methyl group to give 2 is completed within the time it takes to mix 1 with MeLi.

The initial rate of formation of 3a from 2a was observed by following the  $^1\text{H}$  NMR spectral change of the methyl resonances at  $21.7^\circ\text{C}$ . Analysis of the later stage of the reaction is hindered by occurrence of a reverse reaction from 3a to 2a. The results are summarized in Table IV which shows that the rate of reaction,  $v_1$ , increases with the increase in the MeLi concentration and also with the increase in the concentration of 2a. As shown in Figure 5, the plot of  $\log v_1$  against  $\log [\text{LiMe}]$  gives a straight line with the slope of unity. A similar plot of  $\log v_1$  against  $\log [2\text{a}]$  gives also a straight line with the slope of unity. On the other hand, the comparison of runs 3, 8, and 9 reveals that the addition of  $\text{PEt}_2\text{Ph}$  to the system scarcely affects the reaction rate. Thus, the rate equation may be expressed as shown in eq 11.

$$v_1 = -\frac{d[2]}{dt} = \frac{d[3]}{dt} = k_1[2][\text{MeLi}] \quad (11)$$



Table IV. Kinetic Data for the Reaction  $\text{Li}[\text{PdMe}_3\text{L}] + \text{MeLi} \xrightarrow{\nu_1} \text{Li}_2[\text{PdMe}_4] + \text{L}$  (Where  $\text{L} = \text{PEt}_2\text{Ph}$ ) in  $\text{Et}_2\text{O}$  at  $21.7^\circ\text{C}$ 

run	$\text{Li}[\text{PdMe}_3\text{L}]$ , $\text{mol L}^{-1}$	$\text{MeLi}$ , $\text{mol L}^{-1}$	$\text{L}$ , $\text{mol L}^{-1}$	$10^5 \nu_1^a$ , $\text{mol L}^{-1} \text{s}^{-1}$	$10^4 k_1^b$ , $\text{mol}^{-1} \text{L s}^{-1}$
1	0.18	0.56	0	8.1	8.1
2	0.18	0.31	0	4.7	8.3
3	0.18	0.24	0	3.5	8.1
4	0.18	0.17	0	2.4	7.9
5	0.11	0.18	0	1.6	8.4
6	0.16	0.18	0	2.3	8.1
7	0.21	0.18	0	3.0	8.0
8	0.18	0.24	0.54	3.5	8.0
9	0.17	0.24	1.07	3.3	7.5
					av $8.0 \pm 0.5$

<sup>a</sup> Formation rate of  $\text{Li}_2[\text{PdMe}_4]$ . <sup>b</sup> Second-order rate constant.

Table V. Kinetic Data for the Reaction  $\text{trans-}[\text{PdPh}_2\text{L}_2] + \text{MeLi} \xrightarrow{\nu_2} \text{Li}[\text{PdPh}_2\text{MeL}] + \text{L}$  (Where  $\text{L} = \text{PEt}_3$ ) in THF at  $21.7^\circ\text{C}$ 

run	$\text{trans-}[\text{PdPh}_2\text{L}_2]$ , $\text{mol L}^{-1}$	$\text{MeLi}$ , $\text{mol L}^{-1}$	$\text{L}$ , $\text{mol L}^{-1}$	$10^5 \nu_2^a$ , $\text{mol L}^{-1} \text{s}^{-1}$	$10^4 k_1^b$ , $\text{s}^{-1}$
1	0.18	0.27	0	1.9	1.1
2	0.18	0.46	0	2.1	1.2
3	0.18	0.69	0	2.0	1.1
4	0.12	0.69	0	1.4	1.2
5	0.24	0.69	0	2.7	1.1
6	0.18	0.69	0.18	1.9	1.1
7	0.18	0.69	0.90	2.1	1.2
					av $1.1 \pm 0.1$

<sup>a</sup> Formation rate of  $\text{Li}[\text{PdPh}_2\text{MeL}]$ . <sup>b</sup> First-order rate constant.

In contrast to the very rapid transformation of *trans*- $[\text{PdMe}_2(\text{PEt}_2\text{Ph})_2]$ , **1a**, on reaction with  $\text{MeLi}$  to form the trialkylpalladate complex **2a**, the reaction of *trans*- $[\text{PdPh}_2(\text{PEt}_3)_2]$  **1d** with  $\text{MeLi}$  to afford *trans*-**2d** is a slow process proceeding at a rate convenient to observe by means of  $^1\text{H}$  NMR spectroscopy. The rates of formation of *trans*-**2d** in THF are summarized in Table V. It can be seen that the variation of  $\text{MeLi}$  concentration does not affect the reaction rate  $\nu_2$ , while the rate increases with increase in the concentration of **1d**. The addition of  $\text{PEt}_3$  to the system does not affect the reaction rate. Thus, the rate equation may be expressed as shown in eq 12.

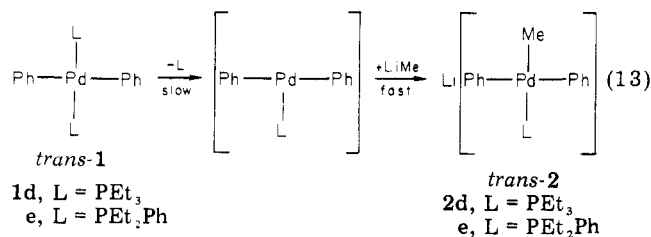
$$\nu_2 = d[\mathbf{2d}]/dt = k_2[\mathbf{1d}] \quad (12)$$

The results suggest that the reaction of formation of **2d** proceeds through a dissociative pathway involving the partial dissociation of the  $\text{PEt}_3$  ligand from **1d** followed by rapid reaction with  $\text{MeLi}$ .<sup>8</sup>

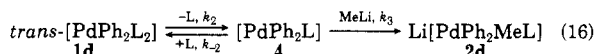
### Discussion

As revealed unequivocally by NMR spectroscopy, the displacement of the tertiary phosphine ligands in  $[\text{PdR}_2\text{L}_2]$ -type complexes by the alkyl group in  $\text{RLi}$  proceeds in two steps to afford triorganopalladate **2** and tetraorganopalladate **3** with retention of the original configuration. Although there have been detailed studies on the mechanism of ligand displacement reactions in  $[\text{PdX}_2\text{L}_2]$  ( $\text{X} = \text{halogen}$ ),<sup>9</sup> precedents for studies on the

ligand displacement reaction of the organopalladium complexes are extremely limited. It is noteworthy that the tertiary phosphine ligand displacement in *trans*- $[\text{PdPh}_2\text{L}_2]$  by the methyl groups of  $\text{MeLi}$  is a slow process proceeding by a dissociative mechanism, whereas the second displacement reaction proceeds by an associative mechanism, both with stereochemical retention of the geometry of the initial diorganopalladium complexes. The kinetic studies by Stille<sup>5</sup> and ourselves<sup>7</sup> demonstrated previously that the thermolysis of *cis*- $[\text{PdMe}_2\text{L}_2]$  proceeded by a dissociative mechanism through the intermediacy of the "T-shaped" *cis* isomer  $[\text{PdMe}_2\text{L}]$  and there was a kinetic barrier between the T-shaped "cis" and "trans"  $[\text{PdR}_2\text{L}]$  isomers. The formation of the T-shaped intermediate has been postulated in thermolysis of the dialkylplatinum<sup>10</sup> and trialkylgold<sup>11</sup> complexes and supported by molecular orbital calculations.<sup>11,12</sup> In one example, a T-shaped molecular structure has been established by X-ray crystallography for a three-coordinate cationic rhodium complex.<sup>13</sup> The results of the present study add another example supporting the intermediacy of a T-shaped species.



(8) Assumption of ligand dissociation as the rate-determining process and of the steady-state approximation for the concentration of the three-coordinate intermediate **4** in the following scheme leads to the kinetic equation eq 17.



$$\frac{d[\mathbf{2d}]}{dt} = \frac{k_2 k_3 [\text{MeLi}][\mathbf{1d}]}{k_{-2}[\text{L}] + k_3[\text{MeLi}]} \quad (17)$$

If  $k_3[\text{MeLi}]$  is much greater than  $k_{-2}[\text{L}]$ , eq 17 can be approximated by eq 12.

(9) Anderson, G. K.; Cross, R. J. *Chem. Soc. Rev.* **1980**, *9*, 185.

(10) McCarthy, T. J.; Nuzzo, R. G.; Whitesides, G. M. *J. Am. Chem. Soc.* **1981**, *103*, 1676 and references cited therein. Komiya, S.; Morimoto, Y.; Yamamoto, A.; Yamamoto, T. *Organometallics* **1982**, *1*, 1528.

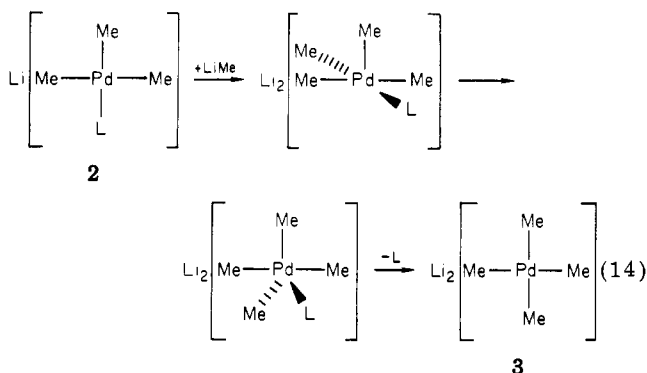
(11) Komiya, S.; Albright, T. A.; Hoffmann, R.; Kochi, J. K. *J. Am. Chem. Soc.* **1977**, *99*, 8440.

(12) Tatsumi, K.; Hoffmann, R.; Yamamoto, A.; Stille, J. K. *Bull. Chem. Soc. Jpn.* **1981**, *54*, 1857.

(13) Yared, Y. W.; Miles, S. L.; Bau, R.; Reed, C. A. *J. Am. Chem. Soc.* **1977**, *99*, 7076.

The dissociative mechanism through the T-shaped intermediate postulated for the reaction from *trans*-[PdPh<sub>2</sub>L<sub>2</sub>] to *trans*-Li[PdPh<sub>2</sub>MeL] may be applied also to the reaction from *trans*-[PdMe<sub>2</sub>L<sub>2</sub>] to Li[PdMe<sub>3</sub>L].<sup>14</sup>

The ligand displacement reaction of *trans*- or *cis*-[PdMe<sub>2</sub>L<sub>2</sub>] by MeLi was revealed to be a rapid process, followed by a slow bimolecular displacement independent of the added phosphine concentration and dependent on the MeLi concentration. To account for the associative pathway, assumption of the mechanism involving the following five-coordinate intermediate(s) is reasonable and compatible with stereochemical retention in ligand placement of Li[PdMe<sub>3</sub>L] by MeLi.



The overall reactions of conversion of [PdR<sub>2</sub>L<sub>2</sub>] to Li<sub>2</sub>[PdR<sub>4</sub>] may be regarded as a nucleophilic ligand displacement by carbanionic alkyl or aryl groups making the palladate complex more electron rich. We can estimate indirectly to what extent the neutral [PdEt<sub>2</sub>L<sub>2</sub>] becomes electron rich in its reaction with MeLi to produce *trans*-[PdEt<sub>2</sub>MeL] by observing the change in the chemical shift difference, Δ, between the CH<sub>2</sub> and CH<sub>3</sub> protons in the Pd-bonded ethyl groups (eq 5). It is known that there is a linear relationship between the chemical shift difference Δ and the electronegativity χ of the element attached to an ethyl group as shown in eq 15.<sup>15,16</sup>

$$\chi = 0.62\Delta + 2.07 \quad (15)$$

The electronegativity values calculated by using the above equation and the observed chemical shift difference of the methyl and methylene protons in the ethyl groups in *trans*-[PdEt<sub>2</sub>(PMe<sub>2</sub>Ph)<sub>2</sub>] and *trans*-Li[PdEt<sub>2</sub>Me(PMe<sub>2</sub>Ph)] were 1.74 and 1.43, respectively.<sup>17</sup> Thus a considerable decrease in the electronegativity of the entity bound to the ethyl groups is indicated. This result explains reasonably well that the nucleophilic attack by the methyl group on the palladium complex is slower in the second step starting from Li[PdR<sub>3</sub>L] than in the first step where the neutral diorganopalladium is attacked.

We have here three groups of methylpalladium complexes of neutral, monoanionic, and dianionic types with and without the tertiary phosphine ligand and phenyl

(14) Although a five-coordinate intermediate Li[PdMe<sub>3</sub>L<sub>2</sub>] was proposed in our previous paper for the conversion of [PdR<sub>2</sub>L<sub>2</sub>] to Li[PdR<sub>3</sub>L] during the *trans*-*cis* isomerization of [PdMe<sub>2</sub>L<sub>2</sub>] promoted by MeLi,<sup>7</sup> the present study makes the associative mechanism unlikely, although the displacement of R in Li[PdR<sub>3</sub>L] by L to convert it into [PdR<sub>2</sub>L<sub>2</sub>] may well proceed by an associative mechanism.

(15) Ham, N. S.; Mole, T. In "Progress in Nuclear Magnetic Resonance Spectroscopy"; Emsley, J. W., Feeney, F., Sutcliffe, L. H., Ed.; Pergamon Press: New York, 1969; Vol. 4, p 101.

(16) Narashimhan, P. T.; Rogers, M. T. *J. Chem. Soc., Dalton Trans.* 1960, 5983.

(17) Because the both complexes have the ethyl groups in mutually *trans* positions, the *trans* influence of the ethyl groups may be cancelled and may not affect the following reasoning.

<sup>1</sup>H NMR Chemical Shifts (Pd-Me portion)

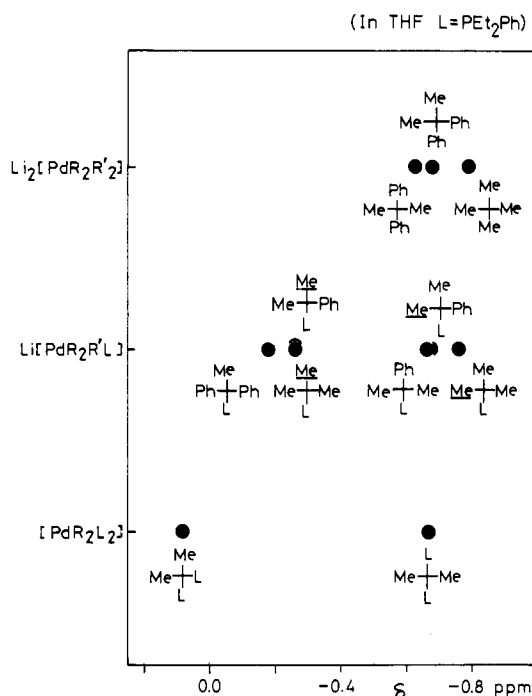


Figure 6. <sup>13</sup>C NMR chemical shifts of the methyl portion for a series of Li<sub>n</sub>[PdMe<sub>2</sub>R<sub>n</sub>(PEt<sub>2</sub>Ph)<sub>2-n</sub>] in THF at room temperature, where R stands for the methyl or phenyl group.

groups. As Figure 6 shows, the <sup>1</sup>H chemical shift of the methyl group is observed in THF in approximately the same region, independent of the charge on the complex and dependent on the nature of the ligand *trans* to the methyl group. For example, the methyl group resonating in the region of -0.6 to -0.8 ppm has a methyl or phenyl group *trans* to the methyl group referred to, irrespective of the charge on the complex. On the other hand, the resonance of the methyl group *trans* to the phosphine is observed at the lower field of -0.18 to -0.26 ppm for the triorganopalladate complexes and +0.08 ppm for neutral dimethylpalladium complex. The methyl proton resonances of other [PdMe<sub>2</sub>L<sub>2</sub>]-type complexes having a tertiary phosphine ligand other than PEt<sub>2</sub>Ph and of *trans*-Li[PdEt<sub>2</sub>Me(PMe<sub>2</sub>Ph)] (not shown in Figure 6) are also observed in a similar region.

The implication of this trend is the importance of the ligand *trans* to the methyl group rather than the charge on the complex in determining the chemical shift of the methyl group. The tertiary phosphine appears to have a higher ability to deshield the methyl group *trans* to the phosphine than the methyl or phenyl group.

It is known that the <sup>13</sup>C chemical shifts of the carbon directly bonded to platinum in the methyl- and phenyl-platinum complexes are correlated with each other, and the shielding is determined by σ interaction in the Pt-C bond.<sup>18</sup> Inspection of the <sup>13</sup>C chemical shifts of the phenyl carbons in *trans*-[PdPh<sub>2</sub>L<sub>2</sub>], *trans*-Li[PdPh<sub>2</sub>MeL], and *trans*-Li<sub>2</sub>[PdPh<sub>2</sub>Me<sub>2</sub>] reveals that the chemical shifts of the C<sub>o</sub>, C<sub>m</sub>, and C<sub>p</sub> carbons are relatively invariant, while that of the quaternary carbon bonded to Pd(C<sub>q</sub>) shows a conspicuously irregular variation as shown in Table III, suggesting the dominant contribution of σ interaction in the phenyl-palladium bond. The <sup>13</sup>C chemical shift of the quaternary carbon observed at 167.6 ppm in *trans*-[PdPh<sub>2</sub>(PEt<sub>2</sub>Ph)<sub>2</sub>] (1e) moves downfield to 179.6 ppm in

(18) Clark, H. C.; Ward, J. E. *J. Am. Chem. Soc.* 1974, 96, 1741.

*trans*-Li[PdPh<sub>2</sub>Me(PET<sub>2</sub>Ph)] (**2e**) by displacement of the tertiary phosphine ligand by the methyl group despite of the anionic nature of **2e**, whereas the further displacement of PET<sub>2</sub>Ph by the methyl group caused the upfield shift to 159.0 ppm. The PET<sub>3</sub>-coordinated complex *trans*-**1d** shows similar behavior in the stepwise displacement of PET<sub>3</sub> by the methyl group. Displacement of the PET<sub>2</sub>Ph ligand in *trans*-[PdMe<sub>2</sub>(PET<sub>2</sub>Ph)<sub>2</sub>] by the methyl group shows a similar trend but in a less marked manner. The first displacement of PET<sub>2</sub>Ph by the methyl group causes the slight deshielding of the *trans*-methyl carbon from -6.0 to -5.2 ppm, followed by an upfield shift to -8.3 ppm on the second displacement of a PET<sub>2</sub>Ph ligand in *trans*-Li[PdMe<sub>3</sub>(PET<sub>2</sub>Ph)] by the methyl group, giving Li<sub>2</sub>[PdMe<sub>4</sub>]. Since the <sup>13</sup>C chemical shift is expected to reflect the electron density of the carbon atom in question, it would be anticipated that the <sup>13</sup>C chemical shift of the Pd-bonded carbon moves upfield when the negative charge on palladium is increased, if the electronic factor alone should play the dominant role in determining the shielding at the Pd-bonded carbon. The observed anomaly in the <sup>13</sup>C chemical shift of the carbon bonded to palladium on displacement of the tertiary phosphine ligand in [PdR<sub>2</sub>L<sub>2</sub>] by the methyl group may be related to steric influence. However, we refrain from discussing this question further because of the limited NMR data on organopalladium complexes.

### Experimental Section

All measurements were carried out under an atmosphere of nitrogen or argon or in vacuo. Solvents were dried in the usual manner, distilled, and stored under a nitrogen atmosphere.

<sup>1</sup>H, <sup>13</sup>C, and <sup>31</sup>P NMR spectra were measured on JEOL PS-100 and FX-100 spectrometers at room temperature and at 21.7 °C in kinetic studies. <sup>1</sup>H and <sup>13</sup>C NMR signals are referred to Me<sub>4</sub>Si and <sup>31</sup>P NMR signals to PPh<sub>3</sub>. Elemental analyses were carried out by Mr. T. Saito of our laboratory using Yanagimoto CHN autocorder type MT-2. Methylolithium purchased from Alfa Products (low halide) was used after several recrystallizations. Phenyllithium was prepared prior to use from PhBr and Li wire by the literature method. The concentration was determined by acid/base titration after hydrolysis. *trans*-[PdMe<sub>2</sub>(PET<sub>2</sub>Ph)<sub>2</sub>] (*trans*-**1a**), *cis*-[PdMe<sub>2</sub>(PET<sub>2</sub>Ph)<sub>2</sub>] (*cis*-**1a**), *cis*-[PdMe<sub>2</sub>(PET<sub>3</sub>)<sub>2</sub>] (*cis*-**1b**), and *trans*-[PdEt<sub>2</sub>(PMe<sub>2</sub>Ph)<sub>2</sub>] (*trans*-**1c**) were prepared according to the method described previously.<sup>7</sup> *trans*-[PdPh<sub>2</sub>(PET<sub>3</sub>)<sub>2</sub>] (*trans*-**1d**) was synthesized by the published procedure.<sup>19</sup>

**Preparation of *trans*-[PdPh<sub>2</sub>(PET<sub>2</sub>Ph)<sub>2</sub>] (*trans*-**1e**).** To the heterogeneous mixture of [PdCl<sub>2</sub>(PET<sub>2</sub>Ph)<sub>2</sub>] (1.32 g, 2.59 mmol) and Et<sub>2</sub>O (36 mL) cooled to -75 °C was added carefully an ether solution of LiPh (1.04 g, 5.18 mmol). The reaction mixture was stirred for 40 min at -75 °C to give a white precipitate, which was filtered, washed with 20 mL of cold Et<sub>2</sub>O, and recrystallized

from 40 mL of acetone to yield pure crystals of *trans*-**1e** (0.62 g, 41%). Characterization of this complex was carried out by means of IR and <sup>1</sup>H, <sup>13</sup>C, and <sup>31</sup>P NMR spectroscopy and elemental analysis. Anal. Calcd for C<sub>32</sub>H<sub>40</sub>P<sub>2</sub>Pd: C, 64.8; H, 6.8. Found: C, 64.7; H, 6.9.

**Characterization of *trans*-[PdPh<sub>2</sub>L<sub>2</sub>] (L = PET<sub>3</sub> (*trans*-**1d**), PET<sub>2</sub>Ph (*trans*-**1e**)).** In <sup>13</sup>C NMR spectra, the signals due to the quaternary carbons of coordinated phenyl groups were observed as a triplet at 169.2 (<sup>2</sup>J(C-P) = 13 Hz) and 167.6 ppm (<sup>2</sup>J(C-P) = 12 Hz) for *trans*-**1d** and *trans*-**1e**, respectively (see Table III).

In the <sup>1</sup>H NMR spectrum of *trans*-**1e** in CD<sub>2</sub>Cl<sub>2</sub>, the signal assigned to the methyl groups in PET<sub>2</sub>Ph ligands showed a quintet pattern characteristic of complexes having ethyl-substituted phosphines in mutually *trans* positions at +0.90 ppm (<sup>4</sup>J(H-P) = 7.5 Hz), while the superposition of the methyl and methylene signals of the ethyl groups in the phosphine ligands for *trans*-**1d** prevented the measurement of the coupling constants. The <sup>13</sup>C and <sup>1</sup>H NMR data described above are typical for complexes having mutually *trans* phosphine groups.

**Preparation of [PdBr<sub>2</sub>(tmed)].** Addition of *N,N,N',N'*-tetramethylethylenediamine (tmed) (1.0 mL, 6.77 mmol) to an aqueous solution containing PdCl<sub>2</sub> (1.0 g, 5.64 mmol) and KBr (5.37 g, 45 mmol) generated a yellowish orange precipitate of [PdBr<sub>2</sub>(tmed)], which was filtered, washed with water and acetone, and dried in vacuo (yield 1.97 g, 91%). Anal. Calcd for C<sub>6</sub>H<sub>16</sub>Br<sub>2</sub>N<sub>2</sub>Pd: C, 18.8; H, 4.2; N, 7.3; Br, 41.8. Found: C, 18.9; H, 4.4; N, 7.4; Br, 41.1.

**Reaction of *trans*-[PdR<sub>2</sub>L<sub>2</sub>] with MeLi or PhLi.** To an Et<sub>2</sub>O or THF solution of accurately weighed [PdR<sub>2</sub>L<sub>2</sub>] was added a calculated amount of Et<sub>2</sub>O or THF solution of MeLi or PhLi at -75 °C. The resulting homogeneous solution was transferred to NMR sample tubes under a nitrogen atmosphere. The tubes, chilled in liquid nitrogen, were sealed under vacuum, and <sup>1</sup>H, <sup>13</sup>C, and <sup>31</sup>P NMR measurements were carried out at room temperature to observe the spectroscopic change of the solution.

**Kinetic Studies of Palladate Formation Reactions.** To a Schlenk tube containing a weighed amount of [PdR<sub>2</sub>L<sub>2</sub>] complex was added a calculated amount of Et<sub>2</sub>O or THF solution of MeLi at -75 °C. The resulting homogeneous solution was transferred to NMR sample tubes under a nitrogen atmosphere. The sealed tube was placed in a thermostated NMR probe (±1.0 °C). The amounts of palladate complexes were determined by measuring the intensities of Pd-Me signals at suitable time intervals at 21.7 °C.

**Acknowledgment.** We are grateful to Mr. Y. Nakamura for NMR measurements. This work was supported by a Grant-in Aid for scientific research, No. 57750738, from the Ministry of Education, Japan.

**Registry No.** *trans*-**1a**, 77831-30-2; *cis*-**1a**, 77881-04-0; *cis*-**1b**, 65732-09-4; *trans*-**1c**, 75108-70-2; *trans*-**1d**, 83947-32-4; *trans*-**1e**, 83947-33-5; **2a**, 83947-24-4; **2b**, 83947-25-5; *trans*-**2c**, 83947-28-8; *trans*-**2d**, 83947-27-7; *trans*-**2e**, 83947-26-6; *trans*-**2f**, 83947-29-9; *cis*-**2f**, 83997-78-8; **3a**, 83947-30-2; *trans*-**3d**, 83947-31-3; *cis*-**3d**, 83997-79-9; PdCl<sub>2</sub>(PET<sub>2</sub>Ph)<sub>2</sub>, 29484-77-3; PhLi, 591-51-5; PdBr<sub>2</sub>(tmed), 83947-34-6; PdCl<sub>2</sub>, 7647-10-1; KBr, 7758-02-3; MeLi, 917-54-4.

(19) Calvin, G.; Coates, G. E. *J. Chem. Soc.* 1960, 2008.

## Synthesis, NMR studies, and catalytic activity of cationic and neutral olefin complexes of platinum(II) containing the $\eta^3$ -allyl ligand

Hideo Kurosawa, and Naonori Asada

*Organometallics*, 1983, 2 (2), 251-257 • DOI: 10.1021/om00074a008 • Publication Date (Web): 01 May 2002

Downloaded from <http://pubs.acs.org> on April 24, 2009

### More About This Article

---

The permalink <http://dx.doi.org/10.1021/om00074a008> provides access to:

- Links to articles and content related to this article
- Copyright permission to reproduce figures and/or text from this article



ACS Publications  
High quality. High impact.

# Synthesis, NMR Studies, and Catalytic Activity of Cationic and Neutral Olefin Complexes of Platinum(II) Containing the $\eta^3$ -Allyl Ligand

Hideo Kurosawa\* and Naonori Asada

Department of Petroleum Chemistry, Faculty of Engineering, Osaka University,  
Yamadaoka, Suita, Osaka 565, Japan

Received June 16, 1982

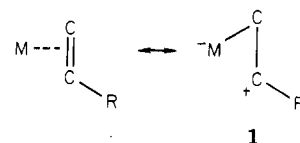
Cationic Pt<sup>II</sup> complexes containing terminal olefin ligands [Pt( $\eta^3$ -CH<sub>2</sub>CMeCH<sub>2</sub>)(PPh<sub>3</sub>)(CH<sub>2</sub>=CHR)]ClO<sub>4</sub> (2, R = CH<sub>2</sub>Ph, Et, Me) were prepared. Formation of the neutral analogues of 2, i.e., Pt( $\eta^3$ -CH<sub>2</sub>CMeCH<sub>2</sub>)Cl(CH<sub>2</sub>=CHR) (3, R = CH<sub>2</sub>Ph, Et, Me, C<sub>6</sub>H<sub>4</sub>Y-*p*; Y = NMe<sub>2</sub>, OMe, Me, H, Cl, NO<sub>2</sub>), from [Pt( $\eta^3$ -CH<sub>2</sub>CMeCH<sub>2</sub>)Cl]<sub>2</sub> and the olefin in solution was confirmed by <sup>1</sup>H and <sup>13</sup>C NMR spectra. Comparison of the <sup>13</sup>C NMR data and the stability trends in 2 and 3 indicated a much greater electrophilic activation of the olefin in 2 than in 3. All complexes of type 2 showed high catalytic activity in the double-bond migration of olefins under mild conditions, with catalysts recovered from the reaction mixture having been confirmed to almost completely retain the  $\eta^3$ -methallyl and the PPh<sub>3</sub> ligands. Deuterium-labeling experiments employing CH<sub>2</sub>=CDCH<sub>3</sub> suggested a key intermediate to be a Pt-H species. In contrast, complexes of type 3 were totally inactive in catalyzing the same transformations. A possible relevance of the different nature of the metal-olefin bond in 2 and 3 to the different catalytic activity was discussed.

## Introduction

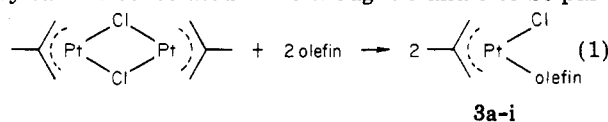
Activity of some transition-metal catalysts in transformations of olefinic substrates is remarkably enhanced by the use of cationic complexes or cocatalysts that are capable of producing cationic olefin complexes.<sup>1-6</sup> The central role of these complexes in catalysis appears to be the electrophilic activation of the coordinated olefin. More characteristic of the cationic olefin complex would be the formation of incipient carbonium ions (1) that has recently been proposed<sup>5-7</sup> to play a vital role in double-bond migration, oligomerization, and polymerization of olefins catalyzed by [Pd(MeCN)<sub>4</sub>]<sup>2+</sup>.

Evidence supporting the significance of the electrophilic activation of olefins or the bonding mode 1 in the olefin complexes of Pd<sup>II</sup> and Pt<sup>II</sup> was presented by X-ray crystallographic,<sup>8</sup> stability,<sup>9,10</sup> and <sup>13</sup>C NMR<sup>11</sup> studies of square-planar,<sup>12</sup> substituted styrene complexes of these metals. In the earlier studies, there was some discrepancy between the <sup>13</sup>C NMR and stability trends of the Pt<sup>II</sup> complexes,<sup>11</sup> but our recent study<sup>10</sup> on the <sup>13</sup>C NMR spectra and stabilities of [Pt( $\eta^3$ -CH<sub>2</sub>CMeCH<sub>2</sub>)(PPh<sub>3</sub>)(ole-

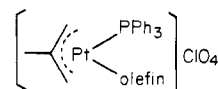
fin)]<sup>+</sup> (2, olefin = CH<sub>2</sub>=CHC<sub>6</sub>H<sub>4</sub>Y-*p*) consistently supported the electrophilic nature of Pt<sup>II</sup> toward the coordinated olefin. Very few reports, however, paid attention to a comparison of both bonding modes and catalytic activities between neutral and cationic olefin complexes possessing closely related structures.



We have now found that a series of the neutral analogues of 2, namely, 3, can be formed readily in solution (eq 1) and fully characterized by NMR spectroscopy, although they cannot be isolated. We thought 2 and 3 to be par-



- 3a, olefin = CH<sub>2</sub>=CHCH<sub>2</sub>Ph  
 b, olefin = CH<sub>2</sub>=CHCH<sub>2</sub>CH<sub>3</sub>  
 c, olefin = CH<sub>2</sub>=CHCH<sub>3</sub>  
 d, olefin = CH<sub>2</sub>=CHC<sub>6</sub>H<sub>4</sub>NMe<sub>2</sub>-*p*  
 e, olefin = CH<sub>2</sub>=CHC<sub>6</sub>H<sub>4</sub>OMe-*p*  
 f, olefin = CH<sub>2</sub>=CHC<sub>6</sub>H<sub>4</sub>Me-*p*  
 g, olefin = CH<sub>2</sub>=CHC<sub>6</sub>H<sub>5</sub>  
 h, olefin = CH<sub>2</sub>=CHC<sub>6</sub>H<sub>4</sub>Cl-*p*  
 i, olefin = CH<sub>2</sub>=CHC<sub>6</sub>H<sub>4</sub>NO<sub>2</sub>-*p*



- 2a, olefin = CH<sub>2</sub>=CHCH<sub>2</sub>Ph  
 b, olefin = CH<sub>2</sub>=CHCH<sub>2</sub>CH<sub>3</sub>  
 c, olefin = CH<sub>2</sub>=CHCH<sub>3</sub>

ticularly suited for a comparative <sup>13</sup>C NMR study, because both contain the same trans group with regard to the olefin ligand. We describe here the remarkably different <sup>13</sup>C NMR and stability trends of 3, compared with those of 2. We further describe the far greater catalytic activity of 2 than 3 in the double-bond migration of olefins and the possible relevance of this difference to the difference in the nature of the olefin-Pt<sup>II</sup> bond.

- (1) Bogdanovic, B. *Adv. Organomet. Chem.* 1979, 17, 105.  
 (2) Pardy, R. B. A.; Tkatchenko, I. *J. Chem. Soc. Chem. Commun.* 1981, 49.  
 (3) Ishimura, Y.; Maruya, K.; Nakamura, Y.; Mizoroki, T.; Ozaki, A. *Chem. Lett.* 1981, 657.  
 (4) de Renzi, A.; Panunzi, A.; Vitagliano, A.; Paiaro, G. *J. Chem. Soc., Chem. Commun.* 1976, 47.  
 (5) Sen, A.; Lai, T. W. *J. Am. Chem. Soc.* 1981, 103, 4627.  
 (6) Sen, A.; Lai, T. W. *Organometallics* 1982, 1, 415.  
 (7) Sen, A.; Lai, T. W. *Inorg. Chem.* 1981, 20, 4036.  
 (8) Nyburg, S. C.; Simpson, K.; Wong-Ng, W. *J. Chem. Soc. Dalton Trans.* 1976, 1865.  
 (9) Ban, E.; Hughes, R. P.; Powell, J. J. *Organomet. Chem.* 1974, 69, 455.  
 (10) Kurosawa, H.; Asada, N. *J. Organomet. Chem.* 1981, 217, 259.  
 (11) Cooper, D. G.; Powell, J. *Inorg. Chem.* 1976, 15, 1959.  
 (12) The nature of the olefin-metal bond in the 18-electron complex<sup>13</sup> [Pd( $\eta^3$ -C<sub>3</sub>H<sub>5</sub>)(PR<sub>3</sub>)(CH<sub>2</sub>=CHC<sub>6</sub>H<sub>4</sub>Y-*p*)]<sup>+</sup> is somewhat different from that in the square-planar complexes.<sup>14-16</sup>  
 (13) Kurosawa, H.; Majima, T.; Asada, N. *J. Am. Chem. Soc.* 1980, 102, 6996.  
 (14) Harley, F. R. *J. Organomet. Chem.* 1981, 216, 277.  
 (15) Albright, T. A.; Hoffmann, R.; Thibeault, J. C.; Thorn, D. L. *J. Am. Chem. Soc.* 1979, 101, 3801.  
 (16) Miki, K.; Shiotani, O.; Kai, Y.; Kasai, N.; Kanatani, H.; Kurosawa, H. *Organometallics*, in press.

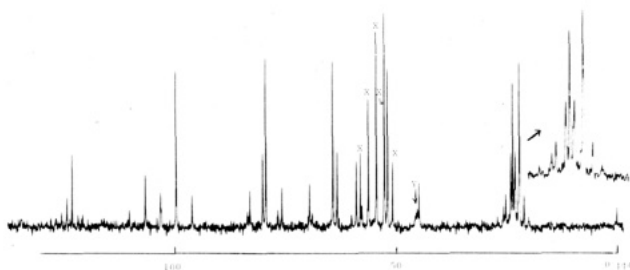


Figure 1.  $^{13}\text{C}$  NMR spectrum of **3c** in  $\text{CD}_2\text{Cl}_2$  at  $-10^\circ\text{C}$ . X denotes the solvent peaks and Y the peaks due to **4**.

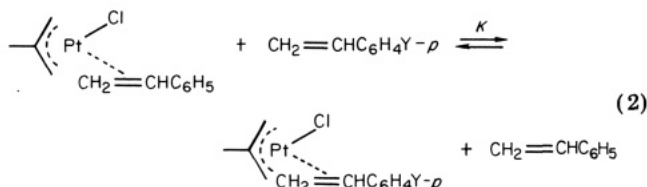
### Experimental Section

**Instruments.**  $^1\text{H}$  and  $^{13}\text{C}$  NMR spectra were obtained on JEOL PS-100 and JEOL FX-60 spectrometers, respectively, both with tetramethylsilane as internal standard. Mass spectra were obtained on a Hitachi RMU-6E spectrometer. GLC analyses were carried out on Hitachi 163 (FID) and 164 (TCD) chromatographs.

**Materials.** *p*-Nitro and *p*-(dimethylamino)styrene were prepared by the reported methods.<sup>17</sup> 2-Deuteriopropene was prepared from 2-propenylmagnesium bromide and  $\text{D}_2\text{O}$  ( $\geq 99\%$ ) in  $\text{Et}_2\text{O}$ . The mass spectrum indicated  $\geq 99\%$  deuterium content, and the  $^1\text{H}$  NMR spectrum ( $\text{CDCl}_3$ ) exhibited only the methyl and the methylene proton signals with the peak ratio 3/2. The other olefins were purchased from Tokyo Kasei Co. Ltd., and used without further purifications. The complexes  $[\text{Pt}(\text{CH}_2\text{CRCH}_2)\text{Cl}]_n$  ( $\text{R} = \text{H}, \text{Me}$ ) were prepared by the reported methods.<sup>18</sup>

**Cationic Olefin Complexes.** **2a** was prepared in a manner similar to that for the styrene complexes described before.<sup>10</sup> The method of preparation of **2b,c** employing gaseous olefins was similar to that of the carbonyl complex  $[\text{Pt}(\eta^3\text{-CH}_2\text{CMeCH}_2)(\text{PPh}_3)(\text{CO})]\text{PF}_6$  described before.<sup>10</sup> All manipulations were carried out at below  $5^\circ\text{C}$ . **2a**: mp  $138\text{--}140^\circ\text{C}$  dec. Anal. Calcd for  $\text{C}_{31}\text{H}_{32}\text{O}_4\text{PClPt}$ : C, 51.00; H, 4.42. Found: C, 50.72; H, 4.54. **2b**: mp  $116\text{--}119^\circ\text{C}$  dec. Anal. Calcd for  $\text{C}_{26}\text{H}_{30}\text{O}_4\text{PClPt}$ : C, 46.75; H, 4.53. Found: C, 46.52; H, 4.52. **2c**: mp  $100\text{--}102^\circ\text{C}$  dec. Anal. Calcd for  $\text{C}_{26}\text{H}_{28}\text{O}_4\text{PClPt-C}_6\text{H}_5$ : C, 50.50; H, 4.64. Found: C, 50.86; H, 4.68 (benzene from crystallization confirmed by  $^1\text{H}$  NMR spectrum).

**Neutral Olefin Complexes.** Compounds **3a-i** were formed by adding to  $[\text{Pt}(\eta^3\text{-CH}_2\text{CMeCH}_2)\text{Cl}]_2$  (4, 0.1–0.6 mol/L) in  $\text{CD}_2\text{Cl}_2$  or  $\text{CDCl}_3$  an equimolar or 2–3-fold excess of the olefin, and the solution was examined by  $^{13}\text{C}$  and  $^1\text{H}$  NMR spectra at  $-10^\circ\text{C}$ . Typical spectra are shown in Figures 1 and 2.  $^1\text{H}$  NMR spectra were somewhat complex owing to the presence of two stereoisomers in comparable concentrations, unlike the isomer ratio in **2**,<sup>10</sup> and thus not all of the proton resonances could be assigned unambiguously. However, the  $^{13}\text{C}$  spectra were much more straightforward to confirm the formation of **3** unambiguously. Attempts to isolate **3** either by removing the solvent under vacuum or by allowing  $\text{CH}_2\text{Cl}_2$ -*n*-hexane solutions to stand in the refrigerator resulted in almost quantitative precipitation of **4**. The equilibrium constant of eq 2 was determined in  $\text{CDCl}_3$  at  $-10^\circ\text{C}$  by means of  $^1\text{H}$  and  $^{13}\text{C}$  NMR spectroscopy. The procedure of



determining  $K$  was essentially the same as that employed before for **2**<sup>10</sup> except that sufficiently excess amounts of styrenes were used to compel eq 1 to proceed almost completely. However, since the ratio of the two stereoisomers in each of **3d-i** is not constant (e.g., major/minor = 1.3 for  $\text{Y} = \text{NMe}_2$ , 1.4 for  $\text{Y} = \text{H}$ , and 2.5

for  $\text{Y} = \text{NO}_2$ ) and since some resonances of the minor isomers could not be separated well from those of the major isomers, the  $K$  values were calculated from the combined concentrations of the two isomers in each styrene complex. The  $K$  values thus obtained are  $3.5 \pm 0.5$  ( $\text{Y} = \text{NMe}_2$ ),  $1.5 \pm 0.3$  ( $\text{Y} = \text{Me}$ ), and  $0.25 \pm 0.05$  ( $\text{Y} = \text{NO}_2$ ).

$^1\text{H}$  and  $^{13}\text{C}$  NMR spectral data of **2** and **3** are shown in Tables I and II.

**Double-Bond Migration of Olefins.** In a typical catalysis reaction, to a  $\text{CH}_2\text{Cl}_2$  solution of 1-butene (0.5–1.0 mol/L) was added **2b** (0.005–0.015 mol/L) and the solution kept at  $25^\circ\text{C}$ . The progress of the reaction was followed by GLC (Sebacconitrile, 3 mm  $\times$  10 m,  $40^\circ\text{C}$ ). The percent yield of 2-butenes ( $Z/E = 1/3$ ) increased almost linearly with time up to ca. 60% conversion. The slopes of these time-conversion plots were almost linearly dependent on the initial concentrations of **2b**. GLC analysis (PEG-1000, 3 mm  $\times$  2 m,  $70^\circ\text{C}$ ) of the isomerization of allylbenzene showed that  $\beta$ -methylstyrene produced has predominantly the *E* configuration. Experiments to recover the catalyst were carried out by allowing carbon monoxide to pass through the catalysis solution ( $[\mathbf{2b}]_{\text{initial}} = 0.015$  mol/L,  $[\text{1-butene}]_{\text{initial}} = 0.5$  mol/L, 24 h, 80% conversion) for 5 min, followed by evaporation of the solvent under vacuum. The residual solids had an IR band at  $2120\text{ cm}^{-1}$  ( $\nu_{\text{CO}}$ ). The solids were dissolved in  $\text{CD}_2\text{Cl}_2$  completely, and this solution was examined by  $^1\text{H}$  NMR spectroscopy to show, within the  $^1\text{H}$  NMR detection limit, the presence of only  $[\text{Pt}(\eta^3\text{-CH}_2\text{CMeCH}_2)(\text{PPh}_3)(\text{CO})]\text{ClO}_4$ , the absorptions of which agreed with those of the  $\text{PF}_6$  salt.<sup>10</sup> Particularly informative was the relative peak ratio of the phenyl region protons and the 2-methylallyl ligand protons (calcd, 2.14/1; found, 2.20/1).

Deuterium scrambling experiments employing  $[\text{Pt}(\eta^3\text{-CH}_2\text{CMeCH}_2)(\text{PPh}_3)(\text{CH}_2=\text{CDCH}_3)]\text{ClO}_4$  (**2c-d**) were performed by quenching with  $\text{PPh}_3$  a  $\text{CDCl}_3$  solution (0.2 mol/L) of **2c-d** after it was allowed to stand at room temperature for 24 h. After this solution was examined by  $^1\text{H}$  NMR spectroscopy, gaseous products were collected in a gas sampler for mass spectroscopy through trap-to-trap techniques under vacuum. A  $\text{CDCl}_3$  solution of  $\text{CH}_2=\text{CDCH}_3$  (0.35 mol/L) in the presence of **2c-d** (0.02 mol/L) was examined similarly except that no quenching by  $\text{PPh}_3$  was necessary. Mass spectral analysis of propene recovered from a  $\text{CH}_2\text{Cl}_2$  solution (0.1 mol/L) containing  $\text{CH}_3\text{OD}$  (5 mol/L) (2 days) was carried out in a similar way to show less than 5% deuterium incorporation. Similarly, after a  $\text{CH}_2\text{Cl}_2$  solution of **2a** (0.05 mol/L) containing  $\text{CH}_3\text{OD}$  (2 mol/L) was allowed to stand for 4 days (ca. 85% conversion),  $\beta$ -methylstyrene was liberated from the complex by adding  $\text{PPh}_3$  and separated by preparative GLC. Mass spectral analysis indicated the presence of only a trace amount of the monodeuterated product.

**$\eta^3$ -Allyl Olefin Complexes  $[\text{Pt}(\eta^3\text{-CH}_2\text{CHCH}_2)(\text{PPh}_3)(\text{olefin})]\text{ClO}_4$  (**5**).** **5a** (olefin =  $\text{CH}_2=\text{CMe}_2$ ) was prepared in a manner similar to that for **2** described above; mp  $135\text{--}138^\circ\text{C}$  dec. Anal. Calcd for  $\text{C}_{25}\text{H}_{28}\text{O}_4\text{PClPt}$ : C, 45.91; H, 4.31. Found: C, 45.65; H, 4.35.  $^1\text{H}$  NMR ( $\text{CD}_2\text{Cl}_2$ ) at  $-20^\circ\text{C}$ : olefin portion,  $\delta$  2.02 (d,  $J_{\text{P}} = 1$ ,  $J_{\text{Pt}} = 42$  Hz) and 2.42 (d,  $J_{\text{P}} = 1.5$ ,  $J_{\text{Pt}} = 40$  Hz) (Me), 3.13 (d,  $J_{\text{P}} = 1.5$  Hz) and 3.20 (d,  $J_{\text{P}} = 2.3$  Hz) ( $=\text{CH}_2$ ; satellites due to  $^{195}\text{Pt}$  not identified); allyl portion (for proton numbering, see Table I),  $\delta$  2.75 (d,  $J_{\text{H}} = 11.3$ ,  $J_{\text{Pt}} = 58$  Hz) ( $\text{H}^4$ ), 3.47 (dd,  $J_{\text{H}} = 8.0$ ,  $J_{\text{P}} = 4.5$  Hz) ( $\text{H}^7$ ), 3.83 (br s) ( $\text{H}^5$ ), 4.78 (br m) ( $\text{H}^6$ ); the central proton multiplet overlapped with  $\text{CH}_2\text{Cl}_2$  peak contained in commercial  $\text{CD}_2\text{Cl}_2$  samples. Allowing the  $\text{CD}_2\text{Cl}_2$  solution of **5a** to stand at room temperature for 24 h resulted in the appearance of the resonances due to **2c** with the ratio **2c/5a** being approximately 85/15. **5b** (olefin =  $\text{CH}_2=\text{CHMe}$ ) was prepared similarly; mp  $143\text{--}148^\circ\text{C}$  dec. Anal. Calcd for  $\text{C}_{24}\text{H}_{26}\text{O}_4\text{PClPt}$ : C, 45.04; H, 4.10. Found: C, 44.85; H, 4.10.  $^1\text{H}$  NMR ( $\text{CD}_2\text{Cl}_2$ ): olefin portion,  $\delta$  1.56 (d,  $J_{\text{H}} = 6.0$ ,  $J_{\text{Pt}} = 38$  Hz) and 1.93 (d,  $J_{\text{H}} = 6.0$ ,  $J_{\text{Pt}} = 39$  Hz) (Me), 3.52 (dd,  $J_{\text{H}} = 9.0$ ,  $J_{\text{P}} = 3$  Hz) and 4.05 (dd,  $J_{\text{H}} = 13.5$ ,  $J_{\text{P}} = 5$ ,  $J_{\text{Pt}} = 59$  Hz) ( $=\text{CH}_2$ ), 5.8 (m) ( $\text{CH}=\text{}$ ); allyl portion, 2.89 (d,  $J_{\text{H}} = 11.3$ ,  $J_{\text{Pt}} = 59$  Hz) ( $\text{H}^4$ ), 3.90 (br m) ( $\text{H}^5$ ), 5.0–5.4 (br m) ( $\text{H}^6$  and the central proton); the peak of  $\text{H}^7$  overlapped with that of the olefin proton at  $\delta$  3.52.

### Results and Discussion

**Preparation and NMR Studies of the Olefin Complexes.** The cationic complexes **2a-c** can be isolated as

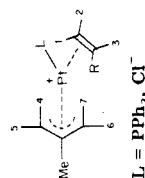
(17) Strassburg, R. W.; Gregg, R. A.; Walling, C. J. *Am. Chem. Soc.* 1947, 69, 2141.

(18) (a) Mabbott, D. J.; Mann, B. E.; Maitlis, P. M. *J. Chem. Soc., Dalton Trans.* 1977, 294. (b) Lukas, J. *Inorg. Synth.* 1974, 15, 79.

Table I.  $^1\text{H}$  NMR Data<sup>a</sup> of Complexes 2 and 3

complex	olefin			allyl					
	H <sup>1</sup>	H <sup>2</sup>	H <sup>3</sup>	R	H <sup>4</sup>	H <sup>5</sup>	H <sup>6</sup>	H <sup>7</sup>	Me
2a	4.06 ( $J_{\text{H}^3} = 14.2$ , $J_{\text{P}} = 6.0$ )	b	5.98	b	2.79 ( $J_{\text{Pt}} = 59$ )	3.65	5.19	b	1.92 ( $J_{\text{Pt}} = 66$ ) [1.89 ( $J_{\text{Pt}} = 68$ )]
2b	3.89 ( $J_{\text{H}^3} = 13.0$ , $J_{\text{P}} = 5.5$ , $J_{\text{Pt}} = 56$ )	3.50 ( $J_{\text{H}^3} = 8.5$ , $J_{\text{P}} = 3$ )	5.85	0.86 ( $J_{\text{H}} = 8.0$ , $\text{CH}_3$ ) [0.95 ( $\text{CH}_3$ )], 1.5- 1.9 ( $\text{CH}_2$ )	2.88 ( $J_{\text{Pt}} = 57$ )	c	5.17 [5.05]	3.48 ( $J_{\text{P}} = 8.0$ )	1.96 ( $J_{\text{Pt}} = 65$ ) [1.93 ( $J_{\text{Pt}} = 66$ )]
2c	3.99 ( $J_{\text{H}^3} = 13.5$ , $J_{\text{P}} = 5.5$ , $J_{\text{Pt}} = 58$ )	d	5.89	1.60 ( $J_{\text{H}^3} = 6.0$ , $J_{\text{Pt}} = 37$ ) [1.91 ( $J_{\text{H}^3} = 6.0$ , $J_{\text{Pt}} = 39$ )]	2.92 ( $J_{\text{Pt}} = 58$ )	d	5.19	d	1.96 ( $J_{\text{Pt}} = 67$ ) [1.93]
3a	4.63 ( $J_{\text{H}^3} = 14.0$ )	4.41 ( $J_{\text{H}^3} = 8.0$ )	5.76	3.0-3.7 ( $\text{CH}_2$ )	2.60 ( $J_{\text{Pt}} = 35$ )	4.27	e	2.03	1.47 ( $J_{\text{Pt}} = 84$ ) [1.85 ( $J_{\text{Pt}} = 80$ )]
3c	4.64 ( $J_{\text{H}^3} = 14.5$ )	f	g	1.82 ( $J_{\text{H}^3} = 6.0$ )	2.69 ( $J_{\text{Pt}} = 37$ )	f	3.66 ( $J_{\text{Pt}} = 21$ ) [3.43 ( $J_{\text{Pt}} = 22$ )]	2.11 [2.47]	2.01 ( $J_{\text{Pt}} = 83$ ) [2.05 ( $J_{\text{Pt}} = 80$ )]
3g	5.12 ( $J_{\text{H}^3} = 14.5$ , $J_{\text{Pt}} = 57$ ) [5.50 ( $J_{\text{H}^3} = 14.0$ )]	4.29 ( $J_{\text{H}^3} = 9.0$ , $J_{\text{Pt}} = 61$ ) [4.46 ( $J_{\text{H}^3} = 9.0$ )]	6.50 ( $J_{\text{Pt}} = 55$ ) [6.49 ( $J_{\text{Pt}} = 60$ )]		2.76 ( $J_{\text{Pt}} = 36$ ) [2.58]	h [4.16]	3.69 ( $J_{\text{Pt}} = 21$ )	2.01 ( $J_{\text{Pt}} = 72$ ) [2.47]	1.82 ( $J_{\text{Pt}} = 83$ ) [1.47 ( $J_{\text{Pt}} = 80$ )]

<sup>a</sup> In  $\text{CD}_2\text{Cl}_2$  (2a-c) or  $\text{CDCl}_3$  (3a,c,g) at  $-10^\circ\text{C}$ . Chemical shifts in ppm; coupling constants in Hz. The resonances due to the minor isomers well resolved are shown in square brackets. Proton numbering is

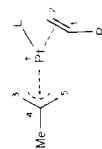


<sup>b</sup> Overlapping in the range 3.0-3.6 ppm. <sup>c</sup> Approximately at 3.5 ppm. <sup>d</sup> Overlapping in the range 3.4-3.6 ppm. <sup>e</sup> Approximately at 3.45 ppm. <sup>f</sup> Overlapping in the range 4.2-4.5 ppm. <sup>g</sup> Overlapping with free propene at 5.85 ppm. <sup>h</sup> Approximately at 4.35 ppm.

Table II.  $^{13}\text{C}$  NMR Data<sup>a</sup> of Complexes 2 and 3

complex	C <sup>1</sup>	C <sup>2</sup>	R	C <sup>3</sup>	C <sup>4</sup>	C <sup>5</sup>	Me
2a	92.4 (83.0)	71.8 (100.1)	40.6 (26.9, CH <sub>2</sub> )	66.5 (153.8) [67.6]	b	74.1 <sup>c</sup>	23.2 (35.4)
2b	95.1 (79.4) [96.0 (76.3)]	71.3 (102.5)	15.0 (36.6, CH <sub>3</sub> ) [15.5 (39.1, CH <sub>3</sub> )], 28.4 (24.4, CH <sub>2</sub> ) [27.7 (CH <sub>2</sub> )]	66.2 (158.7) [67.4 (150.2)]	b	74.4 <sup>d</sup>	23.2 (36.0)
2c	89.5 (75.5) [87.0]	73.2 (104.9) [72.6]	21.3 (30.2) [20.7]	65.9 (159.0) [67.1]	b	74.4 <sup>e</sup>	23.4 (35.7)
3a	100.1 (135.5) [105.3]	77.4 (101.3) [76.8]	41.2 (31.7, CH <sub>3</sub> ) [41.8 (CH <sub>3</sub> )]	65.4 (155.0) [65.1]	123.5 (70.7) [124.3]	51.2 (211.2) [51.5]	22.4 (46.4) [23.3 (46.4)]
3b	105.1 (120.8) [112.2 (113.5)]	78.0 (104.4)	14.4 (37.8, CH <sub>3</sub> ) [14.8 (43.9, CH <sub>3</sub> )], 29.1 (29.9, CH <sub>2</sub> ) [30.1 (29.3, CH <sub>2</sub> )]	64.7 (157.5) [63.7]	122.6 (71.5) [123.7 (74.4)]	51.1 (211.8) [51.6]	23.5 (46.4) [23.8]
3c	99.3 (106.2) [106.2 (108.7)]	79.1 (108.6) [79.8 (102.5)]	21.9 (32.9) [22.9]	63.9 (158.7) [63.0 (168.5)]	122.6 (71.4) [123.8 (75.7)]	51.6 (212.4) [52.3 (222.8)]	23.4 (47.6) [23.8 (48.8)]
3d	100.7 (76.3)	66.8 (115.4) [67.5 (114.8)]		61.8 (161.8) [58.9 (195.3)]	120.5 (71.4)	51.9 (218.5) [55.4 (246.6)]	22.4 (47.0)
3e	97.5 (84.9) [108.4 (86.6)]	68.6 (114.2) [70.1 (108.6)]		63.4 (156.3) [60.4 (189.2)]	122.2 (69.5) [123.8]	53.4 (208.7) [56.3 (237.4)]	22.9 (48.2) [23.2]
3f	96.9 (87.9) [107.3 (91.0)]	69.0 (115.4) [70.9 (105.0)]		63.9 (153.6) [60.9 (189.3)]	122.6 (69.5) [124.1]	53.9 (203.7) [56.7 (229.4)]	22.9 (47.6)
3g	96.2 (89.7) [106.3 (95.2)]	69.3 (116.0) [71.4 (106.3)]		64.6 (151.4) [61.5 (185.6)]	123.1 (69.0) [124.6 (77.0)]	54.3 (201.4) [57.1 (230.7)]	22.9 (47.6)
3h	94.4 (91.5) [103.6 (93.2)]	69.1 (116.6) [71.2 (106.2)]		65.0 (150.1) [62.3 (181.9)]	123.5 (67.7) [124.9 (74.4)]	54.3 (199.0) [56.7 (224.0)]	22.9 (47.6) [23.2]
3i	91.3 (94.1) [97.8 (101.3)]	68.4 (121.4) [70.8 (107.4)]		67.1 (141.6) [65.3 (163.6)]	124.8 (64.9)	55.4 (188.0) [56.8 (206.9)]	23.0 (47.0)

<sup>a</sup> In CD<sub>2</sub>Cl<sub>2</sub> at -10 °C. Chemical shifts in ppm, and  $J_{\text{PI}}$  (in parentheses) in Hz. The resonances due to the minor isomers well resolved are shown in square brackets. Carbon numbering is



L = PPh<sub>3</sub> or Cl<sup>-</sup>

<sup>b</sup> Obscured by the phenyl carbon resonances. <sup>c</sup>  $J_{\text{P}} = 22.0$ . <sup>d</sup>  $J_{\text{P}} = 23.2$ . <sup>e</sup>  $J_{\text{P}} = 24.0$ .



Table III. Correlation ( $X = a\sigma^+ + b$ ) between  $^{13}\text{C}$  NMR Data of the Styrene Complexes and Hammett  $\sigma^+$  Constants<sup>a</sup>

X <sup>b</sup>	3d-i			2 (olefin = $\text{CH}_2=\text{CHC}_6\text{H}_4\text{Y-p}$ ) <sup>c</sup>		
	a, ppm or Hz	b, ppm or Hz	r	a, ppm or Hz	b, ppm or Hz	r
$\delta_{\text{C}^1}(\text{maj})$	-3.47	95.0	0.965	-6.04	89.6	0.994
$\delta_{\text{C}^1}(\text{min})$	-6.98	104.4	0.946	-9.51	94.9	0.992
$\delta_{\text{C}^2}(\text{maj})$	0.74	68.8	0.713	2.72	66.5	0.987
$\delta_{\text{C}^2}(\text{min})$	1.43	70.8	0.862	3.31	67.3	0.981
$J_{\text{PtC}^1}(\text{maj})$	7.09	89.7	0.991	16.58	61.9	0.988
$J_{\text{PtC}^1}(\text{min})$	9.26	93.8	0.980			
$J_{\text{PtC}^2}(\text{maj})$	2.06	117.2	0.715	-10.54	105.6	0.979
$J_{\text{PtC}^2}(\text{min})$	-3.18	107.0	0.791			

<sup>a</sup> By linear regression analyses. <sup>b</sup> maj refers to the major isomer series and min to the minor isomer series. <sup>c</sup> Ref 10.

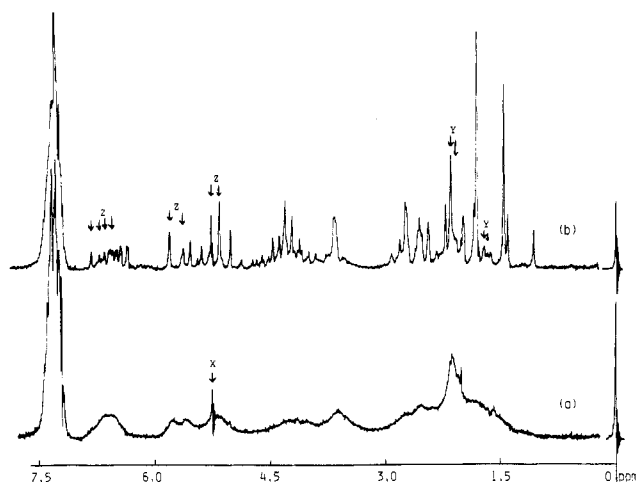


Figure 2.  $^1\text{H}$  NMR spectrum of **3g** in  $\text{CDCl}_3$  at (a)  $23^\circ\text{C}$  and (b)  $-10^\circ\text{C}$ . X denotes solvent impurity, Y the peaks due to **4**, and Z the peaks due to styrene.

crystalline solids by a method which is essentially similar to that used for the corresponding styrene complexes **2** (olefin =  $\text{CH}_2=\text{CHC}_6\text{H}_4\text{Y-p}$ ).<sup>10</sup> Also,  $^1\text{H}$  and  $^{13}\text{C}$  NMR spectral features of **2a-c** are similar to those of the styrene complexes. Namely, two isomers were detected in the spectra, which presumably correspond to a diastereomeric pair (see ref 10). Two rotational isomers are possible in each diastereomer. However, one rotamer may possibly predominate or almost exclude the other, because the  $^1\text{H}$  NMR spectra of **2a-c** were almost temperature independent down to  $-90^\circ\text{C}$ . The presence of an excess of free olefins did not affect the NMR spectral aspects of each complex of type **2**.

The  $^1\text{H}$  and  $^{13}\text{C}$  NMR spectra of a solution containing  $[\text{Pt}(\eta^3\text{-CH}_2\text{CMeCH}_2)\text{Cl}]_2$  (**4**) and more than the equivalent amount of free olefins showed features essentially similar to those for **2** described above except that the resonances at room temperature were somewhat broader (see Figure 2). Presumably the exchange between the coordinated and the free olefins is more rapid in **3** than in **2**. Moreover, the formation of **3** according to eq 1 is reversible,<sup>19</sup> and, indeed, attempts to isolate **3** from the reaction mixture resulted in almost quantitative recovery of **4** (see Experimental Section).

Comparison of the  $^{13}\text{C}$  NMR data of **2** and **3** is of particular relevance in gaining insight into the nature of the olefin-Pt bond.<sup>11</sup> The sensitivity of the chemical shifts and the  $^{195}\text{Pt}$  coupling constants of the olefinic carbon resonances to the para substituent of a series of the styrene

complexes is compared in Table III. It is clear that the change of both  $\delta$  and  $J_{\text{Pt-C}}$  values in **2** (olefin =  $\text{CH}_2=\text{CHC}_6\text{H}_4\text{Y-p}$ ) as a function of the Hammett  $\sigma^+$  constant of the para substituent is greater and more regular than the change of these values in **3d-i**. The particularly poor correlation of the data of the  $\text{C}^2$  resonances in the latter with  $\sigma^+$  is noteworthy. These observations, together with the signs of the slopes shown in Table III, all are consistent<sup>11</sup> with the degree of the contribution of **1** ( $\text{M} = \text{Pt}$ ,  $\text{R} = \text{C}_6\text{H}_4\text{Y-p}$ ) to the overall bonding being greater in **2** than in **3**.

The relative magnitude of the  $J_{\text{Pt-C}}$  values of the two olefin carbons in the allylbenzene, 1-butene, and propene complexes (Table II) is of further comment. In **2a-c**,  $J_{\text{Pt-C}^2}$  is considerably greater than  $J_{\text{Pt-C}^1}$ , while the reversed trend is seen with **3a,b**. Two  $J_{\text{Pt-C}}$  values in **3c** are almost the same. These results are again consistent with the greater contribution of **1** ( $\text{M} = \text{Pt}$ ,  $\text{R} = \text{CH}_2\text{C}_6\text{H}_5$ ,  $\text{CH}_2\text{CH}_3$ ,  $\text{CH}_3$ ) in **2** than in **3**.

The relative stability of **3d,f,g,i** was roughly evaluated by  $^1\text{H}$  and  $^{13}\text{C}$  NMR spectra from equilibrium **2**. We could not separate the equilibrium constants ( $K$ ) for the two stereoisomeric series (see Experimental Section). Therefore, a Hammett equation, i.e.,  $\log K = \rho\sigma$ , derived from the overall  $K$  values does not correspond to, in a rigorous sense, the relationship within a series of the complexes possessing closely related structures. Nevertheless, such an apparent equation would not deviate too much from the respective, real equations in view of the relatively narrow range of the isomer ratio in each of **3d-i**. The apparent  $\rho$  value for **3** thus estimated at  $-10^\circ\text{C}$  ( $-0.73$ ,  $r = 0.990$ ) is considerably less negative than that for **2** (olefin =  $\text{CH}_2=\text{CHC}_6\text{H}_4\text{Y-p}$ ;  $\rho = -1.45$ ,  $r = 0.997$ ) determined in  $\text{CDCl}_3$  at the same temperature. This is again in accord with the less electrophilic nature of the  $\text{Pt}(\eta^3\text{-CH}_2\text{CMeCH}_2)\text{Cl}$  than the  $[\text{Pt}(\eta^3\text{-CH}_2\text{CMeCH}_2)(\text{PPh}_3)]^+$  moiety toward the coordinated olefin.

**Catalytic Double-Bond Migration with the Cationic Olefin Complexes.** All the cationic complexes **2** were found to catalyze the double-bond migration of allylbenzene and 1-butene under mild conditions. These two olefins isomerized at comparable rates with the initial rate equal to  $k[2]^{20}$  ( $k = 1.5\text{--}2.0\text{ h}^{-1}$  at  $25^\circ\text{C}$  in  $\text{CH}_2\text{Cl}_2$ ), although the isomerization of allylbenzene exhibited slight induction periods. In marked contrast to **2**, the cationic complex  $[\text{Pt}(\eta^3\text{-CH}_2\text{CMeCH}_2)(\text{PPh}_3)_2]\text{ClO}_4$  (**6**)<sup>21</sup> and the neutral one  $\text{Pt}(\eta^3\text{-CH}_2\text{CMeCH}_2)\text{Cl}(\text{PPh}_3)$  (**7**)<sup>22</sup> were totally inactive in the double-bond migration under the similar

(19) The equilibrium concentration of **3a** at  $[\text{Pt}]_{\text{total}} = [\text{allylbenzene}]_{\text{total}} = 0.2\text{ mol/L}$  in  $\text{CD}_2\text{Cl}_2$  at  $-10^\circ\text{C}$  was ca. 90% of the total platinum species. Similarly, ca. 80% of **4** was converted to **3g** (Figure 2) from  $0.4\text{ mol/L}$  of **4** and styrene.

(20) The olefin exchange in **2** is fast compared to the rate of the olefin isomerization, and thus at the mole ratio of  $[\text{olefin}]/[2]$  employed the identical complex is assumed to be formed at the initial stage of the isomerization whichever **2** is used as the catalyst.

(21) Clark, H. C.; Kurosawa, H. *Inorg. Chem.* **1973**, *12*, 357.

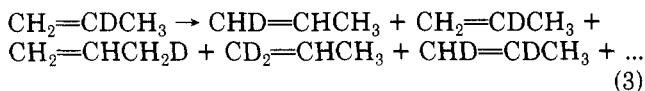
(22) Mann, B. E.; Shaw, B. L.; Shaw, G. *J. Chem. Soc. A* **1971**, 3536.

conditions. We have no  $^1\text{H}$  NMR spectral evidence to indicate complex formation between **6** or **7** and the olefins. Somewhat surprisingly, **3**, or actually **4**, was also inactive in the double-bond migration. Thus, the olefin coordination is a requisite, but not necessarily an adequate factor to the catalytic activity. Instead, treatment of **3** with an equimolar quantity of  $\text{AgClO}_4$  to create the cationic center in the presence of an excess of allylbenzene led to the very facile double-bond migration.

Notably, more than 95% of the catalyst recovered from the catalysis mixture (80% completion: initial condition,  $[\mathbf{2b}] = 0.015$  mol/L,  $[\text{1-butene}] = 0.5$  mol/L) retained the  $\eta^3$ -methylallyl framework. This was confirmed by quenching the reaction mixture by adding CO, followed by  $^1\text{H}$  NMR characterization of the metallic residue as  $[\text{Pt}(\eta^3\text{-CH}_2\text{CMeCH}_2)(\text{PPh}_3)(\text{CO})]\text{ClO}_4$ .

Allowing a  $\text{CH}_2\text{Cl}_2$  solution of **2a** or **2b** to stand at room temperature for long periods also gave a mixture of complexes containing allylbenzene and  $\beta$ -methylstyrene or isomeric butenes, respectively. This was confirmed by GLC analyses of the solution after being quenched by adding benzonitrile, and, notably again, the complex was recovered as the known complex  $[\text{Pt}(\eta^3\text{-CH}_2\text{CMeCH}_2)(\text{PPh}_3)(\text{C}_6\text{H}_5\text{CN})]\text{ClO}_4$ <sup>10</sup> almost quantitatively.

In order to gain insight into an active species, we have examined stoichiometric and catalytic deuterium scrambling of  $[\text{Pt}(\eta^3\text{-CH}_2\text{CMeCH}_2)(\text{PPh}_3)(\text{CH}_2=\text{CDCH}_3)]\text{ClO}_4$  (**2c-d**) and  $\text{CH}_2=\text{CDCH}_3$ , respectively.  $^1\text{H}$  NMR and mass spectral analyses of the propene recovered after a  $\text{CDCl}_3$  solution of **2c-d** was allowed to stand at room temperature for 20 h<sup>23</sup> revealed that intermolecular deuterium scrambling had occurred in a statistical fashion (eq 3); the ratio



of the  $^1\text{H}$  NMR peak areas corresponding to the methyl, methylene, and methine protons of propene was nearly 3/2/1, and the relative amounts of the multiple-deuterium-containing propenes ( $d_4/d_3/d_2/d_1/d_0$ ) were 1/8/18/37/36 that can be compared to the statistical calculation value of 0.1/5.4/20.1/40.2/33.5. Similarly, the deuterium distribution pattern in the propene recovered after  $\text{C}_6\text{H}_5\text{CH}=\text{CDCH}_3$  (0.35 mol/L) was allowed to contact **2c-d** (6 mol %) was found to be 1/7/18/40/34. No appreciable loss of the total deuterium content was apparent during the isomerization.

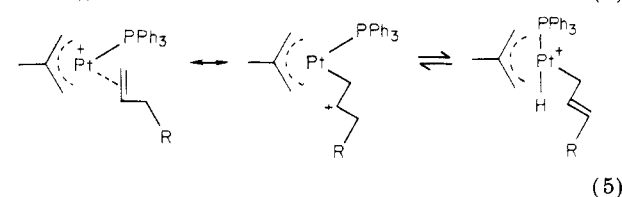
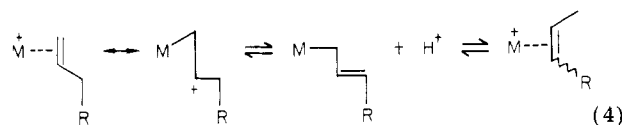
The occurrence of eq 3 suggests that a platinum-hydrido species is present as a chain-carrying catalyst in both the stoichiometric and the catalytic transformations.<sup>24</sup> The addition-elimination sequence involving metal hydrides and the free olefins is well recognized to accompany the 1,2 shift of hydrogen (or deuterium).<sup>25</sup> The alternative mechanisms involving the  $\eta^3$ -allyl hydrido intermediate<sup>26</sup> and the deprotonation-protolysis sequence (eq 4)<sup>7</sup> are incompatible with the 1,2 shift of deuterium shown above.

(23) That no appreciable decomposition products were present was confirmed by the  $^1\text{H}$  NMR spectra. GLC analyses of gaseous products after being quenched by  $\text{PPh}_3$  revealed the presence of only propene except for a very small amount of isobutene.

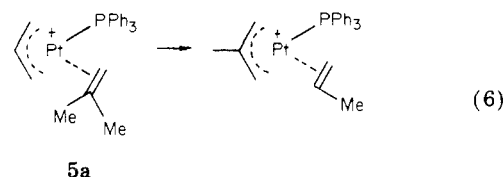
(24) (a) The rate of stoichiometric isomerization was very slow, possibly because an extremely low concentration of the free olefins is liberated under the reaction conditions. (b) Although the solutions remained clear and no bulk metal was precipitated during the isomerization, a possibility that unperceived colloidal metal catalyzed the isomerization cannot be excluded at the moment.

(25) Clark, H. C.; Kurosawa, H. *Inorg. Chem.* **1973**, *12*, 1566, and references therein.

(26) Tulip, T. H.; Ibers, J. A. *J. Am. Chem. Soc.*, **1979**, *101*, 4201, and references therein.



Finally, the way to the Pt-H intermediate is a matter of great speculation. No Pt-H intermediates nor precursors to Pt-H other than **2c** could be detected by  $^1\text{H}$  NMR spectra during both the catalytic and the stoichiometric deuterium scrambling of  $\text{CH}_2=\text{CDCH}_3$ . Modification of eq 4 to include the formation of the Pt-H bond, instead of the liberation of the proton, (e.g., eq 5), is not an unreasonable postulate in view of the greater contribution of the form **1** in **2** than in **3** and the greater activity of the former than the latter. The similar facile formation of the Pd-H bond as a result of the electrophilic activation of the olefin has been suggested, without firm evidence, during the formation of the ( $\eta^3$ -allyl)palladium(II) complexes from olefins and  $\text{Pd}(\text{OOCF}_3)_2$ .<sup>28</sup> It is feasible that the allylic C-H bond activation, as in eq 5, is also involved in the facile allyl-olefin ligand exchange shown in eq 6,<sup>29</sup> although eq 6 does not necessarily require the intermediate formation of the Pt-H bond. For a possibility of intramolecular C-H bond activation assisted by coexisting ligands without M-H bond formation, see ref 30.



Other routes to the Pt-H intermediate include the allyl olefin insertion, as in the  $\text{Ni}(\eta^3\text{-allyl})(\text{X})$  (olefin) catalysts,<sup>1</sup> and the Wacker-type attack by a trace of water at the olefin ligand.<sup>31</sup> Both processes would give alkylplatinum intermediates that would lead, via  $\beta$  elimination, to the Pt-H bond and some byproducts. In fact, however, no such byproducts could be detected<sup>32</sup> during the catalyses except for isobutene, the formation of which is consistent with eq 5. Further work is in progress to clarify more

(27) Allowing a  $\text{CH}_2\text{Cl}_2$  solution of **2a** or **2c** to stand in the presence of MeOD ( $[\text{MeOD}]/[\mathbf{2}] \geq 40$ ) for more than 2 days resulted in no significant deuterium incorporation into  $\beta$ -methylstyrene or propene.

(28) (a) Trost, B. M. *Acc. Chem. Res.* **1980**, *13*, 385. (b) Trost, B. M.; Metzner, P. J. *J. Am. Chem. Soc.* **1980**, *102*, 3572.

(29) Though eq 6 may well be reversible (cf. ref 23), the equilibrium concentration of **5a** seems extremely low so that the initial deuterium content in **2c-d** was almost retained in the propene ligand under the scrambling experimental conditions. In contrast, there was observed fast deuterium shift from the olefin to the  $\eta^3$ -allyl ligand in **5b** containing  $\text{CD}_2=\text{CDCH}_3$  or  $\text{CH}_2=\text{CDCH}_3$ .

(30) Tulip, T. H.; Thorn, D. L. *J. Am. Chem. Soc.* **1981**, *103*, 2448.

(31) The stoichiometric isomerization in  $\text{CH}_2\text{Cl}_2$  that either gets saturated with  $\text{H}_2\text{O}$  or contains 5 vol % MeOH was somewhat slower than in dry  $\text{CH}_2\text{Cl}_2$ .

(32) We cannot exclude the possibility that extremely low concentrations of the byproducts provide the real catalyst of sufficiently high activity. Also, a reviewer suggested that ortho metalation involving  $\text{PPh}_3$  is consistent with all the isomerization data. We presume this possibility to be less likely because (1) keeping a solution containing  $[\text{Pt}(\eta^3\text{-CH}_2\text{CMeCH}_2)(\text{P}(\text{C}_6\text{D}_5)_3)(\text{olefin})]\text{ClO}_4$  and an excess of the olefin under the isomerization conditions did not cause the  $^1\text{H}$  NMR peaks due to the phosphine phenyls to appear and (2) the catalyst containing no  $\text{PPh}_3$  ( $+ \text{AgClO}_4$ ) was as active as **2**.

detailed mechanisms of the double-bond migration catalyzed by the cationic complexes.

**Acknowledgment.** Valuable discussions with Prof. N. Kasai and Dr. K. Miki are gratefully acknowledged. This work was partly supported by a Grant-in-Aid for Scientific Research from the Ministry of Education, Japan (No. 57550539).

**Registry No.** 2a, 83947-72-2; 2b, 83947-74-4; 2c, 83947-76-6;

3a, 83947-77-7; 3b, 83947-78-8; 3c, 83947-79-9; 3d, 83947-80-2; 3e, 83947-81-3; 3f, 83947-82-4; 3g, 83947-83-5; 3h, 83947-84-6; 3i, 83947-85-7; 4, 35770-44-6; 5a, 83947-87-9; 5b, 83947-89-1; CH<sub>2</sub>=CDCH<sub>3</sub>, 1184-59-4; CH<sub>2</sub>=CHCH<sub>2</sub>Ph, 300-57-2; CH<sub>2</sub>=CHCH<sub>2</sub>CH<sub>3</sub>, 106-98-9; CH<sub>2</sub>=CHCH<sub>3</sub>, 115-07-1; CH<sub>2</sub>=CHC<sub>6</sub>H<sub>4</sub>NMe<sub>2</sub>-*p*, 2039-80-7; CH<sub>2</sub>=CHC<sub>6</sub>H<sub>4</sub>OMe-*p*, 637-69-4; CH<sub>2</sub>=CHC<sub>6</sub>H<sub>4</sub>Me-*p*, 622-97-9; CH<sub>2</sub>=CHC<sub>6</sub>H<sub>5</sub>, 100-42-5; CH<sub>2</sub>=CHC<sub>6</sub>H<sub>4</sub>Cl-*p*, 1073-67-2; CH<sub>2</sub>=CHC<sub>6</sub>H<sub>4</sub>NO<sub>2</sub>-*p*, 100-13-0; 2-propenyl bromide, 106-95-6; (*Z*)-2-butene, 590-18-1; (*E*)-2-butene, 624-64-6; (*E*)- $\beta$ -methylstyrene, 873-66-5; (*Z*)- $\beta$ -methylstyrene, 766-90-5.

## Bis(dimethylmethylenephosphoranyl)dihydroborato(1-) Complexes of Manganese(II) and Cobalt(II): Stable, Homoleptic Tetraalkyls of Paramagnetic Transition-Metal Centers

Gerhard Müller, Dietmar Neugebauer, Walter Geike, Frank H. Köhler, Jürgen Pebler,<sup>†</sup> and Hubert Schmidbaur\*

Anorganisch-chemisches Institut, Technische Universität München, D 8046 Garching, West Germany

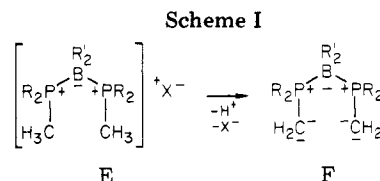
Received August 11, 1982

Treatment of tetrahydrofuran solutions of lithium bis(dimethylmethylenephosphoranyl)dihydroborate (Li<sup>+</sup>L<sup>-</sup>), prepared from bis(trimethylphosphane)dihydroboron(III) bromide and 2 mol equiv of *tert*-butyllithium, with anhydrous MnBr<sub>2</sub> or CoCl<sub>2</sub> in the molar ratio 2:1 at -20 °C results in the formation of binary metal ylide complexes MnL<sub>2</sub> and CoL<sub>2</sub>, respectively. The magnetic moments, measured in solution at 300 K for both CoL<sub>2</sub> and MnL<sub>2</sub> and in the solid state between 4.2 K and 300 K for CoL<sub>2</sub>, correspond to a normal high-spin configuration of strongly paramagnetic d<sup>5</sup> and d<sup>7</sup> metal ions in a tetrahedral environment. The Curie-Weiss law is obeyed throughout this temperature range. This structure also follows from IR measurements. These spectra show close similarities for MnL<sub>2</sub> and CoL<sub>2</sub> and with the spectra of the corresponding Zn(II), Cd(II), and Hg(II) complexes. There are pronounced discrepancies, however, especially in the low wavenumber region, with the spectra of the complexes of diamagnetic d<sup>8</sup> analogues NiL<sub>2</sub>, PdL<sub>2</sub>, and PtL<sub>2</sub> for which the square-planar coordination of the metal centers has been proven by X-ray crystallography. Paramagnetic <sup>1</sup>H NMR spectra, obtained in benzene solution, reveal the two ligands to be equivalent. X-ray precession photographs show crystals of both complexes to be isomorphous (space group P2<sub>1</sub>/c; Z = 4; MnL<sub>2</sub>, a = 8.386 (3) Å, b = 11.286 (5) Å, c = 23.880 (10) Å,  $\beta$  = 94.87 (3)°; CoL<sub>2</sub>, a = 8.38 (1) Å, b = 11.24 (1) Å, c = 23.61 (2) Å,  $\beta$  = 94.8 (1)°). A complete single-crystal X-ray diffraction study of the manganese complex establishes the proposed structure. The manganese atom is almost perfectly tetrahedrally surrounded by four carbon atoms, with angles averaging at 109.53°. They form a spirobicyclic structure of two six-membered rings in a chair conformation joined by the manganese atom. The homologous boron-alkylated ligand L<sup>-</sup> is prepared by conversion of bis(trimethylphosphane)dihydroboron(III) bromide into its lithium derivative. LiL<sup>-</sup> is reacted further with the bis(trimethylphosphane) adduct of NiCl<sub>2</sub> to form the diamagnetic yellow organonickel(II) species NiL<sub>2</sub> whose composition and structure have been determined by analytical and spectroscopic means. Its general properties resemble those of its BH<sub>2</sub> congener NiL<sub>2</sub>.

### Introduction

In recent years ylides of phosphorus and sulfur have been recognized as novel powerful ligand systems to transition metals.<sup>1-5</sup> They are now known to stabilize uncommon coordination numbers and oxidation states, to form extremely stable metal-to-carbon bonds with metals from virtually all parts of the Periodic Table, and to afford organometallic compounds of potential use in various areas of application.<sup>6-8</sup>

Whereas the field of monofunctional ylides, characterized by one carbanionic function adjacent to an onium center like phosphorus, has already been explored to some depth, recent emphasis focused on the chemistry of polyfunctional ylides ("polyylides", "multiple ylides") carrying



two or more carbanionic functions. Thus ylides of types A-D could be shown to be effective ligand systems even

- (1) Schmidbaur, H. *Acc. Chem. Res.* 1975, 8, 62.
- (2) Schmidbaur, H. *Pure Appl. Chem.* 1978, 50, 19; 1980, 52, 1057.
- (3) Schmidbaur, H. *ACS Symp. Ser.* 1981, No. 171, 87-92.
- (4) Schmidbaur, H. In "Transition Metal Chemistry: Current Problems"; Müller, A., Diemann E. Eds.; Verlag Chemie: Weinheim, Germany 1981; pp 107-124.
- (5) Schmidbaur, H. *Inorg. Synth.* 1978, 18, 136.

<sup>†</sup>Fachbereich Chemie, Universität Marburg.

## Bis[boranatobis(dimethylphosphoniumylidenemethylide)] complexes of manganese(II) and cobalt(II): stable, homoleptic tetraalkyls of paramagnetic transition-metal centers

Gerhard Mueller, Dietmar Neugebauer, Walter Geike,  
Frank H. Koehler, Juergen Pebler, and Hubert Schmidbaur

*Organometallics*, 1983, 2 (2), 257-263 • DOI: 10.1021/om00074a009 • Publication Date (Web): 01 May 2002

Downloaded from <http://pubs.acs.org> on April 24, 2009

### More About This Article

---

The permalink <http://dx.doi.org/10.1021/om00074a009> provides access to:

- Links to articles and content related to this article
- Copyright permission to reproduce figures and/or text from this article



ACS Publications  
High quality. High impact.

detailed mechanisms of the double-bond migration catalyzed by the cationic complexes.

**Acknowledgment.** Valuable discussions with Prof. N. Kasai and Dr. K. Miki are gratefully acknowledged. This work was partly supported by a Grant-in-Aid for Scientific Research from the Ministry of Education, Japan (No. 57550539).

**Registry No.** 2a, 83947-72-2; 2b, 83947-74-4; 2c, 83947-76-6;

3a, 83947-77-7; 3b, 83947-78-8; 3c, 83947-79-9; 3d, 83947-80-2; 3e, 83947-81-3; 3f, 83947-82-4; 3g, 83947-83-5; 3h, 83947-84-6; 3i, 83947-85-7; 4, 35770-44-6; 5a, 83947-87-9; 5b, 83947-89-1; CH<sub>2</sub>=CDCH<sub>3</sub>, 1184-59-4; CH<sub>2</sub>=CHCH<sub>2</sub>Ph, 300-57-2; CH<sub>2</sub>=CHCH<sub>2</sub>CH<sub>3</sub>, 106-98-9; CH<sub>2</sub>=CHCH<sub>3</sub>, 115-07-1; CH<sub>2</sub>=CHC<sub>6</sub>H<sub>4</sub>NMe<sub>2</sub>-*p*, 2039-80-7; CH<sub>2</sub>=CHC<sub>6</sub>H<sub>4</sub>OMe-*p*, 637-69-4; CH<sub>2</sub>=CHC<sub>6</sub>H<sub>4</sub>Me-*p*, 622-97-9; CH<sub>2</sub>=CHC<sub>6</sub>H<sub>5</sub>, 100-42-5; CH<sub>2</sub>=CHC<sub>6</sub>H<sub>4</sub>Cl-*p*, 1073-67-2; CH<sub>2</sub>=CHC<sub>6</sub>H<sub>4</sub>NO<sub>2</sub>-*p*, 100-13-0; 2-propenyl bromide, 106-95-6; (*Z*)-2-butene, 590-18-1; (*E*)-2-butene, 624-64-6; (*E*)- $\beta$ -methylstyrene, 873-66-5; (*Z*)- $\beta$ -methylstyrene, 766-90-5.

## Bis(dimethylmethylenephosphoranyl)dihydroborato(1-) Complexes of Manganese(II) and Cobalt(II): Stable, Homoleptic Tetraalkyls of Paramagnetic Transition-Metal Centers

Gerhard Müller, Dietmar Neugebauer, Walter Geike, Frank H. Köhler, Jürgen Pebler,<sup>†</sup> and Hubert Schmidbaur\*

Anorganisch-chemisches Institut, Technische Universität München, D 8046 Garching, West Germany

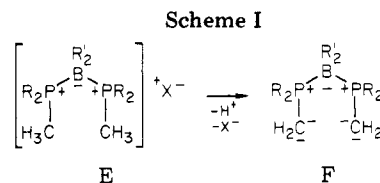
Received August 11, 1982

Treatment of tetrahydrofuran solutions of lithium bis(dimethylmethylenephosphoranyl)dihydroborate (Li<sup>+</sup>L<sup>-</sup>), prepared from bis(trimethylphosphane)dihydroboron(III) bromide and 2 mol equiv of *tert*-butyllithium, with anhydrous MnBr<sub>2</sub> or CoCl<sub>2</sub> in the molar ratio 2:1 at -20 °C results in the formation of binary metal ylide complexes MnL<sub>2</sub> and CoL<sub>2</sub>, respectively. The magnetic moments, measured in solution at 300 K for both CoL<sub>2</sub> and MnL<sub>2</sub> and in the solid state between 4.2 K and 300 K for CoL<sub>2</sub>, correspond to a normal high-spin configuration of strongly paramagnetic d<sup>5</sup> and d<sup>7</sup> metal ions in a tetrahedral environment. The Curie-Weiss law is obeyed throughout this temperature range. This structure also follows from IR measurements. These spectra show close similarities for MnL<sub>2</sub> and CoL<sub>2</sub> and with the spectra of the corresponding Zn(II), Cd(II), and Hg(II) complexes. There are pronounced discrepancies, however, especially in the low wavenumber region, with the spectra of the complexes of diamagnetic d<sup>8</sup> analogues NiL<sub>2</sub>, PdL<sub>2</sub>, and PtL<sub>2</sub> for which the square-planar coordination of the metal centers has been proven by X-ray crystallography. Paramagnetic <sup>1</sup>H NMR spectra, obtained in benzene solution, reveal the two ligands to be equivalent. X-ray precession photographs show crystals of both complexes to be isomorphous (space group P2<sub>1</sub>/c; Z = 4; MnL<sub>2</sub>, a = 8.386 (3) Å, b = 11.286 (5) Å, c = 23.880 (10) Å,  $\beta$  = 94.87 (3)°; CoL<sub>2</sub>, a = 8.38 (1) Å, b = 11.24 (1) Å, c = 23.61 (2) Å,  $\beta$  = 94.8 (1)°). A complete single-crystal X-ray diffraction study of the manganese complex establishes the proposed structure. The manganese atom is almost perfectly tetrahedrally surrounded by four carbon atoms, with angles averaging at 109.53°. They form a spirobicyclic structure of two six-membered rings in a chair conformation joined by the manganese atom. The homologous boron-alkylated ligand L<sup>-</sup> is prepared by conversion of bis(trimethylphosphane)dihydroboron(III) bromide into its lithium derivative. LiL<sup>-</sup> is reacted further with the bis(trimethylphosphane) adduct of NiCl<sub>2</sub> to form the diamagnetic yellow organonickel(II) species NiL<sub>2</sub> whose composition and structure have been determined by analytical and spectroscopic means. Its general properties resemble those of its BH<sub>2</sub> congener NiL<sub>2</sub>.

### Introduction

In recent years ylides of phosphorus and sulfur have been recognized as novel powerful ligand systems to transition metals.<sup>1-5</sup> They are now known to stabilize uncommon coordination numbers and oxidation states, to form extremely stable metal-to-carbon bonds with metals from virtually all parts of the Periodic Table, and to afford organometallic compounds of potential use in various areas of application.<sup>6-8</sup>

Whereas the field of monofunctional ylides, characterized by one carbanionic function adjacent to an onium center like phosphorus, has already been explored to some depth, recent emphasis focused on the chemistry of polyfunctional ylides ("polyylides", "multiple ylides") carrying



two or more carbanionic functions. Thus ylides of types A-D could be shown to be effective ligand systems even

- (1) Schmidbaur, H. *Acc. Chem. Res.* 1975, 8, 62.
- (2) Schmidbaur, H. *Pure Appl. Chem.* 1978, 50, 19; 1980, 52, 1057.
- (3) Schmidbaur, H. *ACS Symp. Ser.* 1981, No. 171, 87-92.
- (4) Schmidbaur, H. In "Transition Metal Chemistry: Current Problems"; Müller, A., Diemann E. Eds.; Verlag Chemie: Weinheim, Germany 1981; pp 107-124.
- (5) Schmidbaur, H. *Inorg. Synth.* 1978, 18, 136.

<sup>†</sup>Fachbereich Chemie, Universität Marburg.

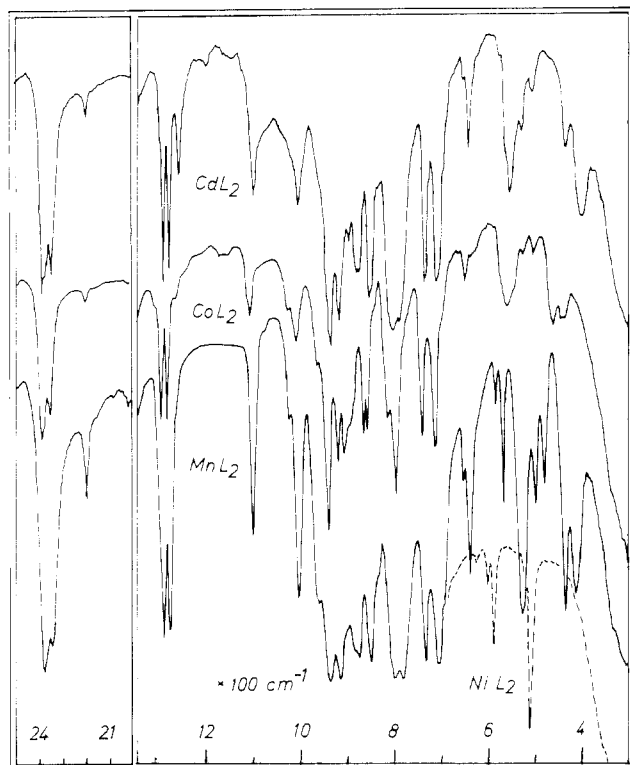
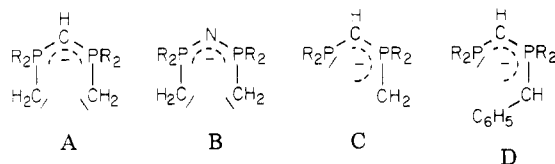


Figure 1. IR spectra for  $MnL_2$  (3),  $CoL_2$  (4), and related complexes.

to inherently weak acceptor centers like the alkaline or alkaline-earth metals.<sup>9-15</sup>



A similar scope is lately also becoming apparent for the corresponding derivatives of *phosphane-boranes* and *dihydrobis(phosphane)boron(1+)* precursors.<sup>16-23</sup> Especially

(6) Manzer, L. E. *Inorg. Chem.* **1978**, *15*, 2567. Gray, R. A.; Andersen, L. R. *Ibid.* **1977**, *16*, 3187.

(7) Keim, W.; Kowalott, F. H.; Goddard, R.; Krüger, C. *Angew. Chem.* **1978**, *90*, 493; *Angew. Chem., Int. Ed. Engl.* **1978**, *17*, 466.

(8) Schmidbaur, H.; Mandl, J. R.; Wohlleben-Hammer, A.; Fügner, A. *Z. Naturforsch., B: Anorg. Chem., Org. Chem.* **1978**, *33B*, 1325.

(9) Schmidbaur, H.; Deschler, U.; Zimmer-Gasser, B.; Milewski-Mahrla, B. *Chem. Ber.* **1981**, *114*, 608.

(10) Schmidbaur, H.; Costa, Th.; Milewski-Mahrla, B. *Chem. Ber.* **1981**, *114*, 1428.

(11) Schmidbaur, H.; Deschler, U.; Zimmer-Gasser, B.; Neugebauer, D.; Schubert, U. *Chem. Ber.* **1980**, *113*, 902.

(12) Schmidbaur, H.; Füller, H.-J. *Chem. Ber.* **1977**, *110*, 3528.

(13) Schmidbaur, H.; Gasser, O.; Krüger, C.; Sekutowski, J. C. *Chem. Ber.* **1977**, *110*, 3517.

(14) Schmidbaur, H.; Deschler, U.; Milewski-Mahrla, B. *Angew. Chem.* **1981**, *63*, 598; *Angew. Chem., Int. Ed. Engl.* **1981**, *20*, 586.

(15) Schmidbaur, H.; Mörtl, A.; Zimmer-Gasser, B. *Chem. Ber.* **1981**, *114*, 3161.

(16) Schmidbaur, H. *J. Organomet. Chem.* **1980**, *200*, 287.

(17) Schmidbaur, H.; Müller, G. *Monatsh. Chem.* **1980**, *111*, 1233.

(18) Schmidbaur, H.; Müller, G.; Dash, K. C.; Milewski-Mahrla, B. *Chem. Ber.* **1981**, *114*, 441.

(19) Müller, G.; Schubert, U.; Orama, O.; Schmidbaur, H. *Chem. Ber.* **1979**, *112*, 3302.

(20) Schmidbaur, H.; Müller, G.; Schubert, U.; Orama, O. *Angew. Chem.* **1978**, *90*, 126; *Angew. Chem. Int. Ed. Engl.* **1978**, *17*, 126.

(21) Schmidbaur, H.; Füller, H.-J.; Müller, G.; Frank, A. *Chem. Ber.* **1979**, *112*, 1448.

Table I. Magnetic Susceptibility Data and Effective Magnetic Moments for 3 and 4

	$MnL_2^a$ (3)	$CoL_2^a$ (4)	$CoL_2^b$ (4)
$10^4 \chi_{mol}$ , $emu\ mol^{-1}$	142.21884	71.97454	68.09659 <sup>c</sup>
$C$ , $emu\ K\ mol^{-1}$			2.09 (5) <sup>d</sup>
$\theta$ , K			-1.5 (9) <sup>d</sup>
$\mu_{eff}$ , $\mu_B$	5.84 <sup>e</sup>	4.16 <sup>e</sup>	4.1 (1) <sup>f</sup>
no. of unpaired electrons	5		3
calcd spin-only values	5.92		3.87

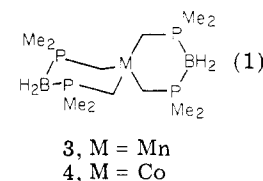
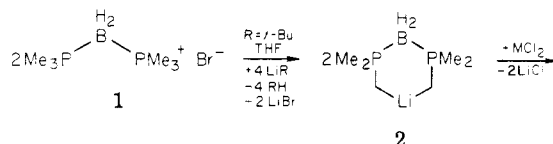
<sup>a</sup> In toluene solution at 300 K. <sup>b</sup> Solid state. <sup>c</sup> At 300 K. <sup>d</sup> From Figure 2 by least-squares fit. <sup>e</sup>  $\mu_{eff} = (8\chi_{mol}/300)^{1/2}$ . <sup>f</sup>  $\mu_{eff} = (8C)^{1/2}$ .

the latter could be functionalized to give bis ylidic species (Scheme I) and integrated successfully into compounds again with elements from most parts of the Periodic Table.<sup>16-21</sup>

We report here for the first time on novel paramagnetic manganese(II) and cobalt(II) compounds containing the (dimethylmethylenephosphoranyl)dihydroborate anion  $L^-$  ( $F, R = Me, R' = H$ ) as the sole ligand. A compound of the corresponding B-alkylated system  $L^-$  ( $F, R = R' = Me$ ) with nickel(II) is also included. Preliminary data on the cobalt(II) compound have already been mentioned in a review article.<sup>16</sup>

## Results

**Preparation and Characterization of  $MnL_2$  and  $CoL_2$ .** Treatment of a tetrahydrofuran solution of lithium bis(dimethylmethylenephosphoranyl)dihydroborate (2,  $Li^+L^-$ ), prepared from dihydrobis(trimethylphosphane)-boron(1+) bromide (1) and 2 molar equiv of *tert*-butyllithium,<sup>17</sup> with the anhydrous metal halides  $MnBr_2 \cdot 2THF$  or  $CoCl_2$  in a molar ratio of 2:1 at  $-20^\circ C$  results in reaction mixtures from which the title compounds  $MnL_2$  (3) and  $CoL_2$  (4) can be isolated in greater than 70% yield. Whereas 3 is only slightly yellow, crystals and solutions of 4 are deep blue.



Both complexes are exceedingly sensitive to air and moisture. Especially when solutions of 4 are handled, utmost care must be taken to guarantee the purity of the inert-gas atmosphere and the solvents. 3 and 4 are thermally fairly stable. 3 melts at  $91^\circ C$  without decomposition, and 4 slowly decomposes above  $80^\circ C$ . Upon rapid heating of 4, a melting point of  $94^\circ C$  may be observed. The proposed constitution is supported by elemental analysis and mass spectrometric results. The appearance of the molecular ion with  $m/e$  385 (for  $C_{12}H_{36}^{11}B_2CoP_4$ )

(22) Schmidbaur, H.; Weiss, E.; Zimmer-Gasser, B. *Angew. Chem.* **1979**, *91*, 848; *Angew. Chem. Int. Ed. Engl.* **1979**, *18*, 782.

(23) Schmidbaur, H.; Weiss, E. *Angew. Chem.* **1981**, *93*, 300; *Angew. Chem., Int. Ed. Engl.* **1981**, *20*, 283.

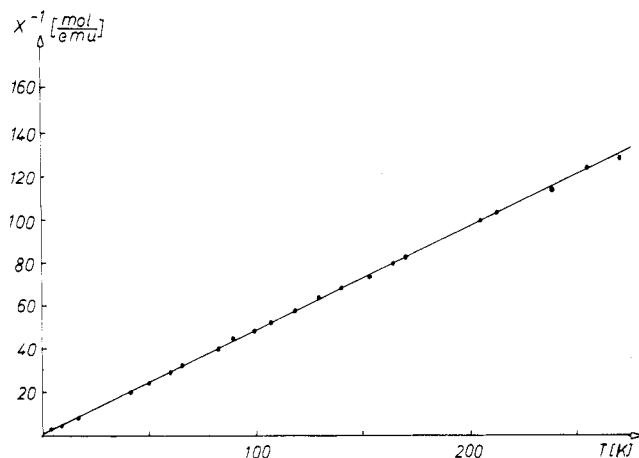


Figure 2. Reciprocal molar susceptibility  $1/\chi$  for  $CoL_2$  (4) as a function of temperature.

as the base peak in the EI mass spectrum of 4 (40 °C) confirms the monomeric molecular mass. Other prominent ions result from loss of methyl groups or one of the ligands ( $m/e$  355, 222, 207, 177, 163). In 3 the molecular ion  $m/e$  381 is of 16% intensity.

In the infrared spectra of Nujol mulls of 3 and 4 very close mutual similarities between the spectra of 3 and 4 and between the spectra of 3 and 4 and the spectra of the corresponding  $ZnL_2$ ,  $CdL_2$ , and  $HgL_2$  complexes<sup>17</sup> are immediately obvious and suggest not only a pronounced structural analogy but also a similar population of conformations (Figure 1). There are distinct differences, however, especially in the low wavenumber region, from the spectra of the  $NiL_2$ ,  $PdL_2$ , and  $PtL_2$  complexes,<sup>19,20</sup> which are known to have a square-planar arrangement of ligand atoms around the central atom, as elucidated by X-ray crystallography and from the observed diamagnetism.<sup>19,20</sup> A tetrahedral configuration is thus indicated from the vibrational data.

This result is also borne out by magnetic susceptibility measurements for  $MnL_2$  and  $CoL_2$  in solution at 300 K and for solid  $CoL_2$  in the range from 4.2 to 300 K. The results are summarized in Table I and Figure 2. As illustrated in Figure 2, the Curie-Weiss law is obeyed throughout this temperature range. An effective magnetic moment,  $\mu_{eff} = 4.1$  (1)  $\mu_B$ , for 4 is derived from the data, in satisfactory agreement with the spin-only value for three unpaired electrons ( $\mu_{eff} = 3.87 \mu_B$ ) of an  $^4A_2$  term of Co(II) in a pseudotetrahedral environment ( $e^4t_2^3$ ). This value is only slightly different from the effective magnetic moment measured in toluene solution at 300 K. For  $MnL_2$  (3)  $\mu_{eff} = 5.84 \mu_B$  comes close to the theoretical value of  $5.92 \mu_B$  for five unpaired electrons ( $e^2t_2^3$ ), the deviation being probably due to small amounts of diamagnetic impurities and experimental errors.

$CoL_2$  (4) shows no ESR spectrum in toluene solution at room temperature or in a toluene glass matrix as obtained on quenching the solution to liquid-nitrogen temperature (77 K). Very surprisingly, however, very well-resolved  $^1H$  NMR spectra can be obtained for both compounds. As shown in Figure 3 for  $CoL_2$ , three different types of hydrogen atoms are easily distinguished. The resonances of the methylene hydrogens, which are closest to the paramagnetic metal center, are shifted by about 259 ppm (!) to a lower field. The  $CH_3$  resonance appears at  $-17.5$  ppm, accompanied by the quadrupole-broadened  $BH_2$  signal at the highest field ( $-11.4$  ppm, at 287.5 K). The spectrum is temperature dependent, with decreasing shifts at higher temperature. Again, the Curie law is obeyed. Due to the

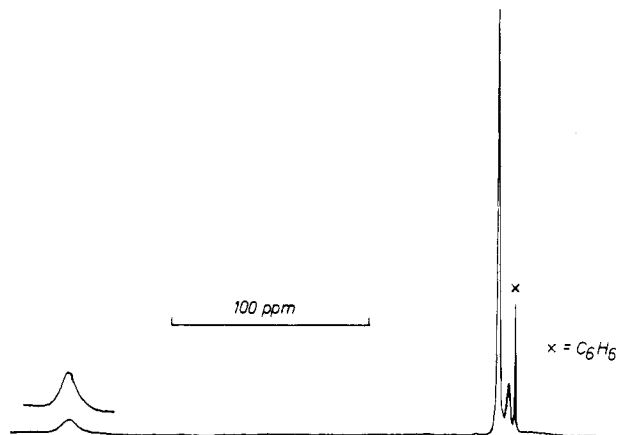


Figure 3.  $^1H$  NMR spectrum for  $CoL_2$  (4) in benzene- $d_6$  at 320 K.

Table II. Observed and Corrected (Isotropic) Paramagnetic  $^1H$  NMR Shifts for  $MnL_2$  (3) and  $CoL_2$  (4) and Values for the Corresponding Reference Compound  $CdL_2$ <sup>a</sup>

	$MnL_2$ (3) ( $T =$ 288 K)	$CoL_2$ (4) ( $T =$ 287.5 K)	$CoL_2$ (4) ( $T =$ 320 K)	$CdL_2$ <sup>b</sup> ( $T =$ 300 K)
$\delta(CH_3)_{obsd}$	-24.1	-17.47	-15.89	+1.3
$\delta(CH_2)_{obsd}$	<sup>c</sup>	-258.87	-232.57	+0.05
$\delta(BH_2)_{obsd}$	-13.4	-11.37	-10.62	<sup>c</sup>
$\delta(CH_3)_{corr}$	-22.8	-16.17	-14.59	
$\delta(CH_2)_{corr}$		-258.82	-232.52	

<sup>a</sup> All spectra in  $C_6D_6$ ,  $\delta$  converted to  $Me_4Si$ . Values in ppm. See Experimental Section for sign convention and correction formula used. <sup>b</sup> From ref 17. <sup>c</sup> Too broad to be observed.

Table III. Crystal Data for 3 and 4

	4	
formula	$C_{12}H_{36}B_2MnP_4$	$C_{12}H_{36}B_2CoP_4$
$M_r$	380.9	384.9
space group	$P2_1/c$	$P2_1/c$
$a$ , Å	8.386 (3)	8.38 (1)
$b$ , Å	11.286 (5)	11.24 (1)
$c$ , Å	23.880 (10)	23.61 (2)
$\beta$ , deg	94.87 (3)	94.8 (1)
$V$ , Å <sup>3</sup>	2251.9	2216.1
$Z$	4	4
$d_{calcd}$ , g/cm <sup>3</sup>	1.12	1.15

paramagnetic broadening of the signals no spin-spin couplings to  $^{11}B$  or  $^{31}P$  are observed. For  $MnL_2$  (3) essentially the same pattern is observed. The line widths are considerably larger, however, not allowing the detection of the  $CH_2$  hydrogens. Paramagnetic  $^1H$  NMR shifts for 3 and 4 are given in Table II, and the corrected (isotropic) shifts are included in Table II as well, the correction being done by using the diamagnetic shifts for  $CdL_2$ .<sup>17</sup> (See Experimental Section for the correction formula applied).

**X-ray Crystallographic Studies and Description of the Structure of  $MnL_2$  (3).** On slow concentration of pentane solutions at low temperatures, single crystals of 3 and 4 could be obtained that proved to be suitable for X-ray crystallography. Crystals of 4 tended to be twinned, however, if growth occurred from very concentrated solutions. Preliminary precession photographs showed crystals of both compounds to be isomorphous with almost identical cell constants (Table III). The cell of 4 has a slightly smaller volume despite the higher molecular weight. A complete X-ray diffraction study was undertaken for  $MnL_2$  (3) which established the proposed structure. Table IV

Table IV. Positional<sup>a</sup> and Thermal Parameters and Their Estimated Standard Deviations for 3

atom	<i>x/a</i>	<i>y/b</i>	<i>z/c</i>	atom	<i>x/a</i>	<i>y/b</i>	<i>z/c</i>
Mn	0.67606 (24)	0.11757 (21)	0.11397 (8)	H31	0.946	0.220	0.176
P1	0.8267 (4)	-0.1402 (3)	0.1609 (1)	H32	0.812	0.330	0.159
P2	0.5747 (4)	0.0027 (4)	0.2322 (1)	H41	0.468	0.276	0.056
P3	0.9712 (4)	0.2926 (3)	0.0838 (1)	H42	0.455	0.145	0.021
P4	0.6647 (4)	0.2616 (3)	-0.0072 (1)	H112	0.904	-0.340	0.187
C1	0.771 (1)	-0.062 (1)	0.097 (1)	H113	0.998	-0.294	0.130
C2	0.494 (1)	0.080 (1)	0.174 (1)	H122	0.992	0.014	0.209
B12	0.663 (1)	-0.149 (1)	0.212 (1)	H123	1.102	-0.065	0.166
C21	0.713 (1)	0.102 (1)	0.271 (1)	H212	0.656	0.182	0.285
C22	0.435 (1)	-0.028 (1)	0.284 (1)	H213	0.811	0.130	0.251
C11	0.890 (1)	-0.293 (1)	0.150 (1)	H222	0.356	0.045	0.291
C12	1.010 (1)	-0.070 (1)	0.191 (1)	H223	0.489	-0.050	0.325
C3	0.865 (1)	0.248 (1)	0.140 (1)	H312	1.209	0.183	0.060
C4	0.541 (1)	0.209 (1)	0.041 (1)	H313	1.043	0.131	0.022
B34	0.837 (2)	0.360 (1)	0.022 (1)	H322	1.164	0.388	0.144
C31	1.084 (1)	0.165 (1)	0.063 (1)	H323	1.077	0.483	0.095
C32	1.128 (1)	0.399 (1)	0.101 (1)	H412	0.739	0.051	-0.026
C41	0.739 (1)	0.133 (1)	-0.043 (1)	H413	0.856	0.144	-0.061
C42	0.560 (1)	0.347 (1)	-0.064 (1)	H422	0.478	0.293	-0.087
H211	0.750	0.048	0.310	H423	0.646	0.375	-0.092
H121	1.044	-0.124	0.224	H111	0.797	-0.327	0.123
H311	1.071	0.095	0.095	H221	0.362	-0.099	0.270
H321	1.237	0.403	0.081	H421	0.505	0.422	-0.049
H411	0.647	0.146	-0.077	HB1	0.716	-0.201	0.256
H11	0.874	-0.060	0.071	HB2	0.554	-0.215	0.193
H12	0.686	-0.117	0.070	HB3	0.926	0.385	-0.012
H21	0.397	0.030	0.154	HB4	0.788	0.452	0.041
H22	0.443	0.159	0.188				

atom	<i>B</i> <sub>11</sub>	<i>B</i> <sub>22</sub>	<i>B</i> <sub>33</sub>	<i>B</i> <sub>12</sub>	<i>B</i> <sub>13</sub>	<i>B</i> <sub>23</sub>
Mn	2.4 (1)	4.6 (1)	3.1 (1)	-0.0 (1)	0.6 (1)	0.7 (1)
P1	2.3 (1)	4.4 (2)	4.6 (2)	0.2 (1)	0.3 (1)	0.4 (1)
P2	2.4 (1)	5.3 (2)	3.4 (1)	-0.7 (1)	0.6 (1)	0.2 (1)
P3	2.3 (1)	3.5 (2)	4.1 (1)	-0.8 (1)	-0.4 (1)	-0.1 (1)
P4	2.7 (1)	4.8 (2)	3.4 (1)	-0.7 (1)	-0.4 (1)	0.7 (1)
C1	1.8 (6)	6.5 (9)	3.7 (7)	-0.9 (6)	-0.2 (5)	0.4 (7)
C2	1.7 (6)	4.3 (8)	4.3 (7)	-0.0 (6)	-0.0 (5)	0.3 (6)
B12	3.4 (8)	7.3 (14)	3.9 (8)	-0.0 (9)	1.1 (7)	2.6 (9)
C21	3.0 (7)	5.8 (9)	5.3 (8)	-1.9 (7)	-0.1 (6)	-0.7 (7)
C22	3.7 (8)	8.3 (12)	5.1 (8)	-1.0 (8)	2.2 (7)	-0.2 (8)
C11	4.7 (9)	5.9 (10)	6.9 (9)	2.3 (8)	1.6 (7)	0.5 (8)
C12	2.4 (7)	9.0 (12)	5.5 (8)	0.6 (7)	0.2 (6)	-0.1 (8)
C3	3.3 (7)	6.4 (9)	2.9 (6)	0.2 (7)	0.6 (5)	-0.5 (6)
C4	1.6 (6)	5.6 (9)	4.5 (7)	0.5 (6)	-0.1 (5)	0.1 (7)
B34	3.7 (12)	2.1 (11)	6.0 (13)	-0.1 (10)	-1.0 (10)	1.2 (10)
C31	3.4 (7)	5.4 (9)	6.6 (9)	1.0 (7)	1.5 (6)	-0.2 (8)
C32	4.8 (8)	5.5 (10)	6.9 (9)	-1.6 (8)	-1.7 (7)	1.5 (8)
C41	5.6 (9)	5.9 (10)	6.3 (9)	-0.5 (8)	1.3 (7)	-0.4 (8)
C42	6.0 (10)	7.0 (11)	6.8 (9)	-1.9 (9)	-2.7 (7)	3.4 (8)

<sup>a</sup> *B* = 7.0 Å<sup>2</sup>.

contains a list of positional and thermal parameters and their estimated standard deviations. Table V collects the bond distances and angles between atoms and some molecular planes, and Figure 4 shows a plot of the molecular structure.

The manganese atom is almost perfectly tetrahedrally surrounded by four carbon atoms of the two ligands. The angles CMnC inside the chelating rings are slightly smaller, however, than between the rings. The five-membered ligands together with the manganese atom form six-membered rings in chair conformation, the metal ion thus being the link in a spirobicyclic structure. The manganese-carbon distances, averaging at 2.226 Å, lie within the range observed in similar manganese alkyls.<sup>24,25</sup> Bond distances in the ligands are identical within standard deviation with the distances found in other complexes of L<sup>-</sup>, namely, in

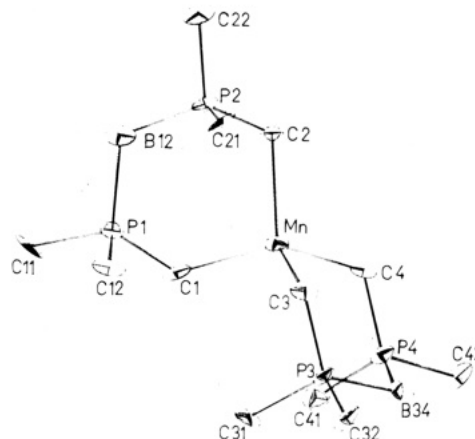


Figure 4. Molecular structure of the manganese complex 3 as determined by X-ray diffraction analysis.

(24) Schmidbaur, H.; Costa, T.; Milewski-Mahrla, B.; Köhler, F. H.; Tsay, Y.-H.; Krüger, C.; Abart, J.; Wagner, F. E., *Organometallics* 1982, 1, 1266.

(25) Andersen, R. A.; Carmona-Guzman, E.; Gibson, J. F.; Wilkinson, G. *J. Chem. Soc. Dalton Trans.* 1976, 2204.

NiL<sub>2</sub><sup>19</sup> and Me<sub>2</sub>AuL.<sup>18</sup> Noteworthy are the ylidic P-C distances (1.746 Å) which are considerably longer than the P=C distance in true ylides like Me<sub>3</sub>P=CH<sub>2</sub> (1.64 Å),<sup>26</sup>



Table V. Bond Distances (Å) and Angles (deg) between Atoms and Selected Molecular Planes for 3

Bond Distances			
Mn-C1	2.222 (15)	Mn-C3	2.214 (14)
Mn-C2	2.227 (13)	Mn-C4	2.239 (13)
P1-P2	3.253 (6)	P3-P4	3.241 (5)
C1-C2	3.467 (19)	C3-C4	3.477 (18)
C1-P1	1.777 (14)	C3-P3	1.755 (14)
C2-P2	1.727 (14)	C4-P4	1.723 (13)
P1-B12	1.920 (17)	P3-B34	1.931 (20)
P2-B12	1.941 (21)	P4-B34	1.910 (20)
P1-C11	1.825 (17)	P3-C31	1.816 (16)
P1-C12	1.817 (15)	P3-C32	1.799 (16)
P2-C21	1.810 (15)	P4-C41	1.820 (17)
P2-C22	1.805 (16)	P4-C42	1.831 (17)

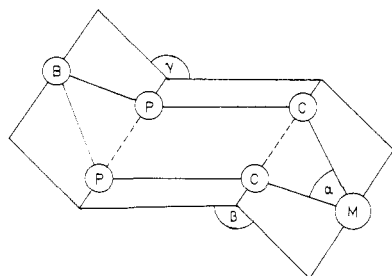
  

Bond Angles			
C1-Mn-C3	113.4 (5)	C2-Mn-C4	105.1 (5)
C1-Mn-C2	102.4 (5)	C3-Mn-C4	102.7 (5)
C2-Mn-C3	117.1 (5)	C1-Mn-C4	116.5 (5)
P1-C1-Mn	112.2 (7)	P3-C3-Mn	111.6 (7)
B12-P1-C1	114.7 (7)	B34-P3-C3	113.6 (8)
P2-B12-P1	114.8 (9)	P4-B34-P3	115.1 (10)
C2-P2-B12	112.5 (7)	C4-P4-B34	115.7 (8)
Mn-C2-P2	111.7 (7)	Mn-C4-P4	112.9 (7)
C21-P2-C22	101.2 (7)	C41-P4-C42	103.4 (7)
C11-P1-C12	102.4 (7)	C31-P3-C32	101.8 (7)

Angles between Planes			
plane Mn-C1-C2/plane C2-P2-C1-P1	132.50		
plane P2-B12-P1/plane C2-P2-C1-P1	130.45		
plane Mn-C3-C4/plane C4-P4-C3-P3	133.84		
plane P4-B34-P3/plane C4-P4-C3-P3	132.15		

Chart I



indicating the reduction in the bond order upon coordination of the ylidic function to the metal center. The P-B distances (1.926 Å) come close to the values observed in tri- and tetrameric phosphinoboranes ( $Me_2PBH_2$ )<sub>3,4</sub><sup>27,28</sup> (and in  $H_3P \cdot BH_3$ )<sup>29</sup>. A comparison with the above-mentioned Ni(II) and Au(III) complexes reveals that  $L^-$  adapts to the different coordination geometries of the metal centers ( $NiL_2$  and  $Me_2AuL$ : square planar) and to the different metal to carbon bond lengths mainly through small adjustments of the bond angles at the ring atoms. This leads, under retention of the adopted chair conformation, to considerable differences in the folding angles of the ring system and in the C...C distances ("span" of the ligand), whereas all other bond lengths and even the P...P distances undergo only minor changes (see Chart I and Table VI).

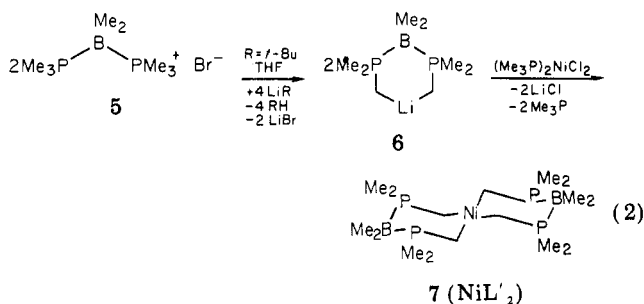
**Preparation and Characterization of  $NiL_2$ .** It has now been demonstrated in one example that *boron-alkylated* homologues of  $L^-$  are also easily prepared. Thus (dimethylboranato)bis(trimethylphosphonium) bromide (5), prepared from  $BMe_2Br$  and excess  $PMe_3$  in a sealed

Table VI. Mean Values of Angles (deg) between Molecular Planes and Mean Distances (Å) P...P and C...C (Chart I) for  $MnL_2$  (3),  $Me_2AuL$ , and  $NiL_2$ 

	$MnL_2$ (3)	$Me_2AuL^a$	$NiL_2^b$
$\alpha$	102.55	91.84	90.0
$\beta$	133.17	118.01	96.80
$\gamma$	131.30	139.87	140.9
M-C	2.226	2.167	1.995
C...C	3.472	3.112	2.822
P...P	3.247	3.158	3.120

<sup>a</sup> From ref 18. <sup>b</sup> From ref 19.

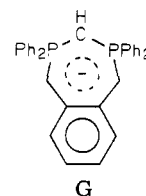
tube, could be converted into its lithium derivative 6 and then reacted with the bis(trimethylphosphane) adduct of  $NiCl_2$  to form a 62% yield of the yellow organonickel species 7 (eq 2).



The general properties of 7 resemble those of its  $BH_2$  congener  $NiL_2$ <sup>19,20</sup> derived from 1/2. Identification by analytical and spectral data is straightforward. Thus the square-planar coordination of the nickel atom again is clearly obvious from the analogies in the IR spectra of 7 and  $NiL_2$ .<sup>19</sup> The equivalence of the phosphorus, boron, methyl, and methylene carbon and hydrogen atoms in the NMR spectra prove the symmetrical bonding of two equivalent  $L^-$  to the nickel center.

## Discussion

Manganese and cobalt alkyls without additional auxiliary ligands are generally very unstable, and only a few examples are described in the literature.<sup>24,25</sup> Binary manganese(II) dialkyls show a pronounced tendency for oligomerization.<sup>25</sup> There is no precedent for a neutral peralkylated cobalt(II) compound.<sup>16</sup> In another study we recently investigated complexes of Mn(II) and Co(II) with the cyclic tris ylidic ligand G, however, which also lead to onium-stabilized metal tetraalkyls.<sup>24</sup>



Results on the bis ylidic ligand  $L^-$  supplement these findings. In all these complexes the metal ions are pseudotetrahedrally coordinated and form stable metal to carbon  $\sigma$  bonds which lead to very similar magnetic moments.<sup>24</sup> It should also be pointed out that a cobalt(II) bis(carboranate) anion,  $[(B_{10}C_2H_{10})_2]_2Co^{2-}$ , was assigned a similar tetrahedral structure with four carbon atoms as the ligating centers of two difunctional bis(carboranate) chelates.<sup>30,31</sup>

(26) Ebsworth, E. A. V.; Fraser, T. E.; Rankin, D. W. H. *Chem. Ber.* 1977, 110, 3494.

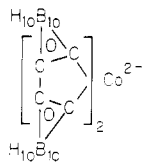
(27) Hamilton, W. C. *Acta Crystallogr.* 1955, 8, 199.

(28) Goldstein, P.; Jacobson, R. A. *J. Am. Chem. Soc.* 1962, 84, 2457.

(29) Durig, J. R.; Li, Y. S.; Carreira, L. A.; Odom, J. D. *J. Am. Chem. Soc.* 1973, 95, 2491.

(30) Owen, D. A.; Hawthorne, M. F. *J. Am. Chem. Soc.* 1970, 92, 3194.

(31) Owen, D. A.; Hawthorne, M. F. *J. Am. Chem. Soc.* 1971, 93, 873.



A magnetic moment of 4.1  $\mu_B$  was determined for the tetraethylammonium salt, in excellent agreement with the result for 4.

As in previous examples<sup>16-21</sup> the findings on the paramagnetic  $MnL_2$  and  $CoL_2$  complexes show that the exceptional properties of  $L^-$  as a ligand to both main-group and transition metals originate from the strong  $\sigma$ -donating capabilities of the two ylidic centers associated with only very limited means for delocalization of electron density into the framework of the ligand ("back-bonding"). These poor acceptor properties of  $L^-$  appear to be the most significant feature. They are obviously compensated for, however, by the strong polarizing (inductive) effect of the onium centers.

### Experimental Section

**Materials and Physical Measurements.** All reactions and purifications were routinely performed under a prepurified dinitrogen atmosphere. Tetrahydrofuran and diethyl ether were dried over and distilled twice from sodium wire. Pentane was dried over calcium hydride. Bis(trimethylphosphane)dihydroboron(III) bromide was prepared as described elsewhere.<sup>17,32</sup>  $MnBr_2 \cdot 2THF$  was obtained by Soxhlet extraction of the commercially available anhydrous metal dibromide with dry THF. Anhydrous  $CoCl_2$  was prepared from the hydrate with  $SOCl_2$  and by pumping on the so obtained material for several hours at 80 °C ( $10^{-4}$  torr).  $NiCl_2 \cdot 2PMe_3$ ,<sup>33</sup>  $PMe_3$ ,<sup>34</sup> and  $BMe_2Br$ <sup>35</sup> were prepared via literature procedures.

IR spectra were run as Nujol mulls between KBr windows on a Perkin-Elmer 283 B instrument. Mass spectra were recorded on a Varian MAT 311 A. Solid-state susceptibility measurements were performed on a Princeton Applied Research magnetometer, Model 155, in the temperature range between 4.2 and 300 K. The resulting data were corrected for the diamagnetic ligand anions following the increment procedure given in ref 36. Magnetic moments in solution were determined through the method by Evans<sup>37,38</sup> on a JEOL C 60 HL NMR instrument at 300 K. Toluene was used as a solvent, and determinations were made at various concentrations between 6.9 and 14.7 mg/mL. The instrument was calibrated with  $K_3Fe(CN)_6$  solutions in 2% *t*-BuOH/ $H_2O$  in the concentration range between 6.5 and 30.2 mg/mL. Paramagnetic  $^1H$  NMR measurements (200 MHz) were performed on a Bruker CXP 200 instrument in  $C_6D_6$  solvent. Diamagnetic corrections were introduced through the shifts observed for the analogous Cd compound, according to the equation  $\delta_{para} = \delta_{obsd} + \delta_{dia}$ , with  $\delta_{para}$  and  $\delta_{obsd}$  being the corrected and observed paramagnetic shifts, respectively (negative signs refer to low field) and  $\delta_{dia}$  being the diamagnetic shift of the Cd(II) reference compound (negative signs refer to high field). Diamagnetic NMR spectra were recorded on JEOL FX 60, Bruker HX 90, and Bruker WP 200 spectrometers at 60 ( $^1H$ ), 15.08 ( $^{13}C$ ), 36.43 ( $^{31}P$ ), and 64.2 MHz ( $^{11}B$ ). Chemical shifts are reported in parts per million and coupling constants in Hz. Negative signs refer to high field. Double and triple resonance experiments confirmed the assignments. Melting points were determined in sealed capillaries by using a Büchi capillary melting point apparatus and are uncorrected.

(32) Schmidbaur, H.; Müller, G. submitted for publication in *Inorg. Synth.*

(33) Dahl, O. *Acta Chem. Scand.* **1969**, *23*, 2342.

(34) Wolfsberger, W.; Schmidbaur, H. *Synth. React. Inorg. Met-Org. Chem.* **1974**, *4*, 149.

(35) Nöth, H.; Vahrenkamp, H. *J. Organomet. Chem.* **1963**, *11*, 399.

(36) Weiss, A.; Witte, H. "Magnetochemie"; Verlag Chemie: Weinheim, Germany, 1973.

(37) Evans, D. F. *J. Chem. Soc.* **1959**, 2003.

(38) Fritz, H. P.; Schwarzshans, K.-E. *J. Organomet. Chem.* **1964**, *1*, 208.

**Preparation of Compounds. Bis[bis(dimethylmethylene phosphoranyl)borato(1-)]manganese(II),  $MnL_2$  (3).** A stirred suspension of 1.23 g (5 mmol) of 1 in 50 mL of THF was treated at -20 °C dropwise with 2 molar equiv of *tert*-butyllithium in pentane to yield a clear solution of  $Li^+L^-$  in THF. This solution was stirred for 1 h, and 0.90 g (2.5 mmol) of  $MnBr_2 \cdot 2THF$  was added. After the solution was stirred for an additional 12 h at room temperature, the solvent was removed in vacuo and the residue treated with pentane to remove LiCl by filtration through an all glass frit. Cooling to -78 °C yielded 0.75 g (79% of theory) of  $MnL_2$  as clear, slightly brown needles: mp 91 °C; mass spectrum,  $m/e$  (relative intensity) 381 (16,  $M^+$  for  $C_{12}H_{36}^{11}B_2MnP_4$ ), 355 (100), 341 (14), 166 (28); IR 2390, 2350, 2200 ( $\nu(BH_2)$ ); 1300, 1280 ( $\delta(PCH_3)$ ), 1105, 1020 ( $^{10}B$ ), 1010 ( $\delta(BH_2)$ ), 740, 710 ( $\nu(PC_2)$ )  $cm^{-1}$ . Anal. Calcd for  $C_{12}H_{36}B_2MnP_4$ : C, 37.84; H, 9.53. Found: C, 37.74; H, 9.44.

**Bis[bis(dimethylmethylene phosphoranyl)borato(1-)]cobalt(II),  $CoL_2$  (4).** Proceeding in the same way as described above, 0.69 g (72% of theory) of  $CoL_2$  was prepared from 1.23 g (5 mmol) of 1 and 0.33 g (2.5 mmol) of anhydrous  $CoCl_2$ . 4 crystallizes in deep blue needles: mp 94 °C (decomposition above 80 °C); mass spectrum,  $m/e$  (relative intensity) 385 (100,  $M^+$  for  $^{11}B$ ), 355 (4%,  $(M - 2 CH_3)^+$ ), 222 (20%,  $(M - 1 \text{ ligand})^+$ ); 207 (22%,  $(M - 1 \text{ ligand} - CH_3)^+$ ); 177 (100), 163 (31%, (ligand) $^+$ ); IR 2390, 2350, 2200 ( $\nu(BH_2)$ ), 1300, 1280 ( $\delta(PCH_3)$ ), 1105, 1025 ( $^{10}B$ ), 1010 ( $\delta(BH_2)$ ); 740, 710 ( $\nu(PC_2)$ )  $cm^{-1}$ . Anal. Calcd for  $C_{12}H_{36}B_2CoP_4$ : C, 37.45; H, 9.43. Found: C, 37.80, H, 9.70.

**Bis(trimethylphosphane)dimethylboron(III) Bromide (5).** A 3.0-g (40-mmol) sample of trimethylphosphane and 2.4 g (20 mmol) of bromodimethylborane were condensed into a heavy walled glass tube. After being sealed, the tube was kept at 60 °C for 10 days. The white product was washed with ether, recrystallized from methylene chloride/pentane and dried at room temperature ( $10^{-2}$  torr): yield 4.42 g (81% of theory); when the product is heated above 150 °C, slow decomposition sets in; IR 1330, 1310 ( $\delta(PCH_3)$ )  $cm^{-1}$ ;  $^1H$  NMR ( $CD_2Cl_2$ ,  $Me_4Si$  external)  $\delta +2.46$  ( $A_nXX'A'_n$ ,  $^2J(PH) = 12.0$  Hz, 18 H),  $+0.69$  (br t,  $^3J(PH) = 18.6$  Hz, 6 H);  $^{13}C$  NMR ( $CD_2Cl_2$ ,  $Me_4Si$ )  $\delta +8.06$  ( $AXX'$ ,  $^1J(PC) = 42.0$  Hz), 0 (br m,  $^2J(PC) = 54$  Hz);  $^{11}B$  NMR ( $CD_2Cl_2$ ,  $BF_3 \cdot OEt_2$ )  $\delta -21.7$  (t,  $^1J(PB) = 77.7$  Hz);  $^{31}P$  NMR ( $CD_2Cl_2$ , 85%  $H_3PO_4$ )  $\delta -5.0$  (q,  $^1J(PB) = 75.3$  Hz). Anal. Calcd for  $C_8H_{24}BB_2P_2$ : C, 35.20; H, 8.86. Found: C, 34.14; H, 8.82.

**Bis[bis(dimethylmethylene phosphoranyl)borato(1-)]nickel(II),  $NiL_2$  (7).** Following a procedure analogous to that described for  $MnL_2$  and  $CoL_2$ , above, 7 can be obtained in 62% yield (0.65 g) from 1.37 g (5 mmol) of 5 and 0.7 g (2.5 mmol) of  $(Me_3P)_2NiCl_2$ .  $NiL_2$  crystallizes in yellow needles which decompose without melting above 150 °C; mass spectrum,  $m/e$  (relative intensity) 440 (6,  $M^+$ ); IR 510 ( $\nu(NiC)$ );  $^1H$  NMR ( $C_6D_6$ ,  $Me_4Si$ )  $\delta -0.28$  ( $A_nXX'A'_n$ ,  $J(PH) = 16.4$  Hz, 12 H), 1.35 ( $A_nXX'A'_n$ ,  $^2J(PH) = 10.0$  Hz, 24 H);  $^{13}C$  NMR ( $C_6D_6$ ,  $Me_4Si$ )  $\delta 4.1$  ( $AXX'$ ), 13.6 ( $AXX'$ ,  $^1J(PC) = 37.1$  Hz);  $^{11}B$  NMR ( $C_6D_6$ ,  $BF_3 \cdot Et_2O$ )  $\delta -23.4$  (t,  $^1J(PB) = 86.0$  Hz);  $^{31}P$  NMR ( $C_6D_6$ , 85%  $H_3PO_4$ )  $\delta -3.37$  (q,  $^1J(PB) = 84.1$  Hz). Anal. Calcd for  $C_{16}H_{44}B_2NiP_4$ : C, 43.60; H, 10.06. Found: C, 43.42; H, 9.61.

### X-ray Data Collection and Structure Determination.

Single crystals of  $C_{12}H_{36}B_2MnP_4$  (3) and  $C_{12}H_{36}B_2CoP_4$  (4) were grown from pentane solutions at -78 °C. Precession photographs showed them to be isomorphous in the monoclinic space group  $P2_1/c$  and served for the determination of the unit-cell dimensions of 4. A suitable crystal of 3 was mounted on a four-circle diffractometer (Syntex P2<sub>1</sub>), and intensity measurements were made at  $T = 20$  °C by using graphite-monochromatized Mo  $K\alpha$  radiation ( $\lambda = 0.71069$  Å) and a scintillation counter ( $\omega$  scan mode). A total of 3520 independent reflections were measured. After Lorentz and polarization corrections 1684 structure factors with  $F_o \geq 3.92\sigma(F_o)$  remained which were used to refine the structure; absorption correction was not applied. The manganese and phosphorus atoms were located by direct methods (Mulan 74, Syntex-XTL). Subsequent difference Fourier syntheses gave the positions of the remaining atoms except the hydrogen atoms which were introduced at idealized calculated positions. Full-matrix least-squares refinement with anisotropic thermal parameters (parameters of the hydrogen atoms were held constant) minimizing the function  $\sum w(|F_o| - |F_c|)^2$ , where  $w = 1/[\sigma^2(F_o) + c|F_o|^2]$  and  $c = 0.02$ , gave final convergence with  $R = \sum(|F_o| - |F_c|) / \sum|F_o| =$

0.099 and  $R_w = [\sum w(|F_o| - |F_c|)^2 / \sum w|F_o|^2]^{1/2} = 0.087$ . A final difference map revealed no anomalies in the unit cell. Table III contains the crystal data. Table IV lists the final positional and thermal parameters. The thermal parameter expression is defined as  $\exp(-1/4(B_{11}h^2a^{*2} + B_{22}k^2b^{*2} + B_{33}l^2c^{*2} + 2B_{12}hka^{*}b^{*} + 2B_{13}hla^{*}c^{*} + 2B_{23}klb^{*}c^{*}))$ . Bond distances (angstroms) and angles (degrees) between atoms and selected planes are collected in Table V. Table VII, observed and calculated structure factors, is available as supplementary material.

**Acknowledgment.** We are greatly indebted to Dr. B. Wrackmeyer (Universität München) for measuring the  $^{11}\text{B}$

NMR spectra and Mr. J. Riede for obtaining the X-ray precession photographs. This work was generously supported by Fonds der Chemischen Industrie, Frankfurt (Main) and Deutsche Forschungsgemeinschaft.

**Registry No.** 1, 65293-66-5; 2, 77076-57-4; 3, 83649-34-7; 4, 83632-58-0; 5, 83679-73-6; 6, 83632-59-1; 7, 83632-60-4;  $\text{MnBr}_2$ , 13446-03-2;  $\text{CoCl}_2$ , 7646-79-9;  $(\text{Me}_3\text{P})_2\text{NiCl}_2$ , 19232-05-4; *tert*-butyllithium, 594-19-4; bromodimethylborane, 5158-50-9.

**Supplementary Material Available:** Table VII, a listing of observed and calculated structure factors (16 pages). Ordering information is given on any current masthead page.

## Preparation and Properties of $\text{Ge}(\text{CF}_3)_3$ Adducts of Transition-Metal Carbonyls: X-ray Structure of $(\text{CF}_3)_3\text{GeMn}(\text{CO})_5$

David J. Brauer and Reint Eujen\*

Fachbereich 9, Anorganische Chemie, Universität-Gesamthochschule-Wuppertal, 5600 Wuppertal 1, West Germany

Received August 11, 1982

Photolysis of  $(\text{CF}_3)_3\text{GeH}$  in the presence of  $\text{Mn}_2(\text{CO})_{10}$  and  $\text{Co}_2(\text{CO})_8$  leads to  $(\text{CF}_3)_3\text{GeMn}(\text{CO})_5$  (I) and  $(\text{CF}_3)_3\text{GeCo}(\text{CO})_4$  (II), respectively, in high yields. I may also be obtained from  $\text{NaMn}(\text{CO})_5$  and  $(\text{CF}_3)_3\text{GeX}$  ( $\text{X} = \text{Cl}, \text{I}$ ). IR and Raman spectra are reported. The close correspondence of the CO stretching frequencies of the  $\text{Ge}(\text{CF}_3)_3$  derivatives to those of the respective  $\text{GeCl}_3$  analogues confirms the previously established similarity between these groups. Normal coordinate analyses of the CO stretching frequencies afforded  $k_{\text{ax}}$  and  $k_{\text{eq}}$  stretching force constants of 16.90 and 17.37  $\text{N}\cdot\text{cm}^{-1}$  for I and 17.58 and 17.30  $\text{N}\cdot\text{cm}^{-1}$  for II. For I, a Graham-type treatment of these force constants attest to the  $\sigma$ -withdrawing nature of the  $\text{Ge}(\text{CF}_3)_3$  group, a conclusion supported by the  $^{55}\text{Mn}$  NMR chemical shift. Crystals of I belong to the space group  $P2_1/n$  with  $a = 14.509$  (3) Å,  $b = 12.749$  (2) Å,  $c = 8.2525$  (8) Å,  $\beta = 92.128$  (8)°,  $Z = 4$ , and  $d_{\text{calcd}} = 2.07$   $\text{g}/\text{cm}^3$ . The structure was solved and refined to a conventional  $R$  value of 0.041 by using 2083 counter-measured observed reflections. Interesting structural features include the short Ge-Mn bond (2.4132 (9) Å) and the small mean C-Ge-C bond angle (100.8 (3)°). The latter implies high Ge 4s character in the metal-metal bond, an implication consistent with the librational corrected Ge-C bonds (2.024 (4) Å) being relatively long.

### Introduction

Recently numerous (trifluoromethyl)germanium compounds have been prepared.<sup>1,2</sup> They have attracted special interest since vibrational spectroscopic<sup>3</sup> and electron diffraction<sup>4</sup> investigations have shown that the Ge-CF<sub>3</sub> bonds are markedly weaker than the Ge-CH<sub>3</sub> bonds in analogous compounds. In addition, replacement of CH<sub>3</sub> groups by CF<sub>3</sub> moieties leads to a strengthening of the remaining germanium-ligand bonds that is very similar to the effect of Cl substitution. Both X-ray<sup>5</sup> and UV<sup>6</sup> photoelectron spectroscopy have confirmed this second-order effect. In contrast to the CF<sub>3</sub> group, halides are  $\pi$  donors that might again cause differences in the substitution pattern of the  $\text{R}_3\text{Ge}$  group,  $\text{R} = \text{Cl}, \text{Br},$  and  $\text{CF}_3$ . Presumably Graham-

type  $\sigma$  and  $\pi$  donor/acceptor parameters for  $\text{R}_3\text{Ge}$  groups, which may be evaluated from  $\text{Mn}(\text{CO})_5$  derivatives, would be sensitive to such effects. In addition, structural studies on such derivatives should yield direct evidence on the metal-metal bond strength and germanium hybridization.

Thus we have sought preparative routes to  $\text{Ge}(\text{CF}_3)_3$ -substituted transition-metal compounds. We report here the synthesis and properties of  $(\text{CF}_3)_3\text{GeMn}(\text{CO})_5$  (I) and  $(\text{CF}_3)_3\text{GeCo}(\text{CO})_4$  (II) as well as the crystal and molecular structure of I.

### Experimental Section

**Materials.** The starting materials  $(\text{CF}_3)_3\text{GeI}$ ,  $(\text{CF}_3)_3\text{GeCl}$ , and  $(\text{CF}_3)_3\text{GeH}$  were prepared as described previously.<sup>1</sup> All manipulations were carried out under a nitrogen atmosphere or by utilizing a greaseless stopcock vacuum line.  $^{19}\text{F}$  NMR spectra were recorded on a Varian EM 390 spectrometer and  $^{55}\text{Mn}$  NMR spectra on a Varian FT80A spectrometer. Infrared spectra were taken on a PE 580B spectrometer employing 20-cm gas cells ( $(\text{CF}_3)_3\text{GeCo}(\text{CO})_4$ , 0.2-mm liquid cells (cyclohexane solutions), or KBr disks. Raman spectra were obtained with a Cary 82 spectrometer, utilizing  $\text{Kr}^+$  excitation at 647.1 nm (200 mW at the sample). Force constants were calculated by utilizing the program NORCOR.<sup>7</sup>

(1) Lagow, R. J.; Eujen, R.; Gerchman, L. L.; Morrison, J. A. *J. Am. Chem. Soc.* 1978, 100, 1722.

(2) Eujen, R.; Mellies, R., to be submitted for publication.

(3) Eujen, R.; Bürger, H. *Spectrochim. Acta, Part A* 1979, 35A, 541, 549, 1135.

(4) Oberhammer, H.; Eujen, R. *J. Mol. Struct.* 1979, 51, 211.

(5) Drake, J. E.; Eujen, R.; Gorzelska, K. *Inorg. Chem.* 1982, 21, 558.

(6) Drake, J. E.; Gorzelska, K.; White, G. S.; Eujen, R. *J. Electron Spectrosc. Relat. Phenom.* 1982, 26, 1.

0.099 and  $R_w = [\sum w(|F_o| - |F_c|)^2 / \sum w|F_o|^2]^{1/2} = 0.087$ . A final difference map revealed no anomalies in the unit cell. Table III contains the crystal data. Table IV lists the final positional and thermal parameters. The thermal parameter expression is defined as  $\exp(-1/4(B_{11}h^2a^{*2} + B_{22}k^2b^{*2} + B_{33}l^2c^{*2} + 2B_{12}hka^*b^* + 2B_{13}hla^*c^* + 2B_{23}klb^*c^*))$ . Bond distances (angstroms) and angles (degrees) between atoms and selected planes are collected in Table V. Table VII, observed and calculated structure factors, is available as supplementary material.

**Acknowledgment.** We are greatly indebted to Dr. B. Wrackmeyer (Universität München) for measuring the  $^{11}\text{B}$

NMR spectra and Mr. J. Riede for obtaining the X-ray precession photographs. This work was generously supported by Fonds der Chemischen Industrie, Frankfurt (Main) and Deutsche Forschungsgemeinschaft.

**Registry No.** 1, 65293-66-5; 2, 77076-57-4; 3, 83649-34-7; 4, 83632-58-0; 5, 83679-73-6; 6, 83632-59-1; 7, 83632-60-4;  $\text{MnBr}_2$ , 13446-03-2;  $\text{CoCl}_2$ , 7646-79-9;  $(\text{Me}_3\text{P})_2\text{NiCl}_2$ , 19232-05-4; *tert*-butyllithium, 594-19-4; bromodimethylborane, 5158-50-9.

**Supplementary Material Available:** Table VII, a listing of observed and calculated structure factors (16 pages). Ordering information is given on any current masthead page.

## Preparation and Properties of $\text{Ge}(\text{CF}_3)_3$ Adducts of Transition-Metal Carbonyls: X-ray Structure of $(\text{CF}_3)_3\text{GeMn}(\text{CO})_5$

David J. Brauer and Reint Eujen\*

Fachbereich 9, Anorganische Chemie, Universität-Gesamthochschule-Wuppertal, 5600 Wuppertal 1, West Germany

Received August 11, 1982

Photolysis of  $(\text{CF}_3)_3\text{GeH}$  in the presence of  $\text{Mn}_2(\text{CO})_{10}$  and  $\text{Co}_2(\text{CO})_8$  leads to  $(\text{CF}_3)_3\text{GeMn}(\text{CO})_5$  (I) and  $(\text{CF}_3)_3\text{GeCo}(\text{CO})_4$  (II), respectively, in high yields. I may also be obtained from  $\text{NaMn}(\text{CO})_5$  and  $(\text{CF}_3)_3\text{GeX}$  ( $\text{X} = \text{Cl}, \text{I}$ ). IR and Raman spectra are reported. The close correspondence of the CO stretching frequencies of the  $\text{Ge}(\text{CF}_3)_3$  derivatives to those of the respective  $\text{GeCl}_3$  analogues confirms the previously established similarity between these groups. Normal coordinate analyses of the CO stretching frequencies afforded  $k_{ax}$  and  $k_{eq}$  stretching force constants of 16.90 and 17.37  $\text{N}\cdot\text{cm}^{-1}$  for I and 17.58 and 17.30  $\text{N}\cdot\text{cm}^{-1}$  for II. For I, a Graham-type treatment of these force constants attest to the  $\sigma$ -withdrawing nature of the  $\text{Ge}(\text{CF}_3)_3$  group, a conclusion supported by the  $^{55}\text{Mn}$  NMR chemical shift. Crystals of I belong to the space group  $P2_1/n$  with  $a = 14.509$  (3) Å,  $b = 12.749$  (2) Å,  $c = 8.2525$  (8) Å,  $\beta = 92.128$  (8)°,  $Z = 4$ , and  $d_{\text{calcd}} = 2.07$   $\text{g}/\text{cm}^3$ . The structure was solved and refined to a conventional  $R$  value of 0.041 by using 2083 counter-measured observed reflections. Interesting structural features include the short Ge–Mn bond (2.4132 (9) Å) and the small mean C–Ge–C bond angle (100.8 (3)°). The latter implies high Ge 4s character in the metal–metal bond, an implication consistent with the librationaly corrected Ge–C bonds (2.024 (4) Å) being relatively long.

### Introduction

Recently numerous (trifluoromethyl)germanium compounds have been prepared.<sup>1,2</sup> They have attracted special interest since vibrational spectroscopic<sup>3</sup> and electron diffraction<sup>4</sup> investigations have shown that the Ge– $\text{CF}_3$  bonds are markedly weaker than the Ge– $\text{CH}_3$  bonds in analogous compounds. In addition, replacement of  $\text{CH}_3$  groups by  $\text{CF}_3$  moieties leads to a strengthening of the remaining germanium–ligand bonds that is very similar to the effect of Cl substitution. Both X-ray<sup>5</sup> and UV<sup>6</sup> photoelectron spectroscopy have confirmed this second-order effect. In contrast to the  $\text{CF}_3$  group, halides are  $\pi$  donors that might again cause differences in the substitution pattern of the  $\text{R}_3\text{Ge}$  group,  $\text{R} = \text{Cl}, \text{Br},$  and  $\text{CF}_3$ . Presumably Graham-

type  $\sigma$  and  $\pi$  donor/acceptor parameters for  $\text{R}_3\text{Ge}$  groups, which may be evaluated from  $\text{Mn}(\text{CO})_5$  derivatives, would be sensitive to such effects. In addition, structural studies on such derivatives should yield direct evidence on the metal–metal bond strength and germanium hybridization.

Thus we have sought preparative routes to  $\text{Ge}(\text{CF}_3)_3$ -substituted transition-metal compounds. We report here the synthesis and properties of  $(\text{CF}_3)_3\text{GeMn}(\text{CO})_5$  (I) and  $(\text{CF}_3)_3\text{GeCo}(\text{CO})_4$  (II) as well as the crystal and molecular structure of I.

### Experimental Section

**Materials.** The starting materials  $(\text{CF}_3)_3\text{GeI}$ ,  $(\text{CF}_3)_3\text{GeCl}$ , and  $(\text{CF}_3)_3\text{GeH}$  were prepared as described previously.<sup>1</sup> All manipulations were carried out under a nitrogen atmosphere or by utilizing a greaseless stopcock vacuum line.  $^{19}\text{F}$  NMR spectra were recorded on a Varian EM 390 spectrometer and  $^{55}\text{Mn}$  NMR spectra on a Varian FT80A spectrometer. Infrared spectra were taken on a PE 580B spectrometer employing 20-cm gas cells ( $(\text{CF}_3)_3\text{GeCo}(\text{CO})_4$ ), 0.2-mm liquid cells (cyclohexane solutions), or KBr disks. Raman spectra were obtained with a Cary 82 spectrometer, utilizing  $\text{Kr}^+$  excitation at 647.1 nm (200 mW at the sample). Force constants were calculated by utilizing the program NORCOR.<sup>7</sup>

(1) Lagow, R. J.; Eujen, R.; Gerchman, L. L.; Morrison, J. A. *J. Am. Chem. Soc.* 1978, 100, 1722.

(2) Eujen, R.; Mellies, R., to be submitted for publication.

(3) Eujen, R.; Bürger, H. *Spectrochim. Acta, Part A* 1979, 35A, 541, 549, 1135.

(4) Oberhammer, H.; Eujen, R. *J. Mol. Struct.* 1979, 51, 211.

(5) Drake, J. E.; Eujen, R.; Gorzelska, K. *Inorg. Chem.* 1982, 21, 558.

(6) Drake, J. E.; Gorzelska, K.; White, G. S.; Eujen, R. *J. Electron Spectrosc. Relat. Phenom.* 1982, 26, 1.

Table I. Crystal Data for  $(CF_3)_3GeMn(CO)_5$ 

Crystal Data	
cryst system	monoclinic
<i>a</i>	14.509 (3) Å
<i>b</i>	12.749 (2) Å
<i>c</i>	8.2525 (8) Å
$\beta$	92.128 (8) Å
<i>Z</i>	4
$d_{\text{calcd}}$	2.07 g/cm <sup>3</sup>
<i>t</i>	21 °C
systematic absences	$h0l, h + l = 2n + 1$
space group	$P2_1/n$
Data Collection	
radiatn	Mo $K_{\alpha}$
wavelength	0.710 69 Å
cryst shape	plate
cryst size	0.46 × 0.44 × 0.30 mm <sup>3</sup>
$\mu(\text{Mo } K_{\alpha})$	28.5 cm <sup>-1</sup>
octants measd	$hkl, \bar{h}kl$
$\theta$ limits	1.00–27.44°
scan width ( $\omega$ )	(0.80 + 0.346° tan $\theta$ )°
scan speed (2 $\theta$ )	1.25–10°/min
unique reflectns	3436

**Tris(trifluoromethyl)(pentacarbonylmanganese)germanium.** (a)  $(CF_3)_3GeMn(CO)_5$  was prepared from  $(CF_3)_3GeCl$  and  $NaMn(CO)_5$ . To a THF solution (25 mL) containing ca. 8.0 mmol of  $NaMn(CO)_5$  was added 2.0 g of  $(CF_3)_3GeCl$  (6.4 mmol) dissolved in 5 mL of THF. After being stirred for 12 h at room temperature, the solution was filtered and the solvent was removed on a vacuum line, yielding white and yellow crystals in a 0 °C trap. The residue was sublimed in vacuo at 60 °C; the united sublimed materials were recrystallized from hexane to remove  $Mn_2(CO)_{10}$  and re-sublimed at 40 °C to yield 1.5 g (49%) of nearly colorless  $(CF_3)_3GeMn(CO)_5$ , mp 114 °C.

(b)  $(CF_3)_3GeMn(CO)_5$  was prepared by irradiation of  $(CF_3)_3GeH$  and  $Mn_2(CO)_{10}$ . A 230-mg sample of  $Mn_2(CO)_{10}$  was dissolved in an excess (ca. 500 mg) of  $(CF_3)_3GeH$  and sealed under vacuum in a 6-mm tube. On irradiation with a high-pressure mercury lamp (Hanau TQ 150) ( $t \approx 40$  °C) the solution turned orange-red and finally nearly colorless. The ampule was opened to a vacuum line, the excess of  $(CF_3)_3GeH$  was removed, and the residue was sublimed to yield 490 mg (86%) of  $(CF_3)_3GeMn(CO)_5$ ; mass spectrum,  $M^+$ ,  $(M - F)^+$ ,  $(M - CF_3)^+$  etc.;  $^{19}F$  NMR  $\delta$  -51.3 upfield from internal standard  $CFCl_3$ ;  $^{55}Mn$  NMR  $\delta$  -2160 ( $W_{1/2} = 250$  Hz) in THF (internal standard  $Mn_2(CO)_{10}$   $\delta$  -2265 from external standard  $KMnO_4$ ),  $\delta$  -2210 in hexane.

**Tris(trifluoromethyl)(tetracarbonylcobalt)germanium** was prepared by irradiation of 150 mg of  $Co_2(CO)_8$  in an excess of  $(CF_3)_3GeH$ . After the solution had turned dark green, the ampule was opened to a vacuum line. The volatile materials were fractionated, yielding 280 mg of pale yellow  $(CF_3)_3GeCo(CO)_4$  (mp 55 °C;  $p_{25} = 0.7$  mbar). The mass spectrum showed the ions  $M^+$  and  $(M - n CO)^+$  ( $n = 1 - 3$ );  $^{19}F$  NMR  $\delta$  -52.2.

**Structure Determination.** Crystals used in the X-ray study were grown by slow sublimation ( $10^{-2}$  mbar, 30 °C) and sealed in thin-walled glass capillaries. The space group was derived from Weissenberg photographs. Diffractometer measurements were made with a CAD-4 instrument. Rapid  $\omega$ - $2\theta$  scans of 317 reflections and  $\omega$  scans of three strong, low-angle peaks proved the suitability of the crystal for a diffraction study. Intensity data were collected by the  $\omega$ - $2\theta$  scan technique. The small, random variations of three periodically monitored standards attested to the stability of the crystal and instrumentation during the experiment. Cell constants, which were derived from 75 Bragg angles, and data collection details are given in Table I. Structure factor amplitudes and their standard deviations were calculated from the counting statistics. No absorption correction was made,  $\psi$  scans indicating that relative absorption effects were less than  $\pm 6\%$  in  $|F_o|$ . Only reflections with  $|F_o| \geq 4 \sigma(|F_o|)$  were used to solve and refine the structure.

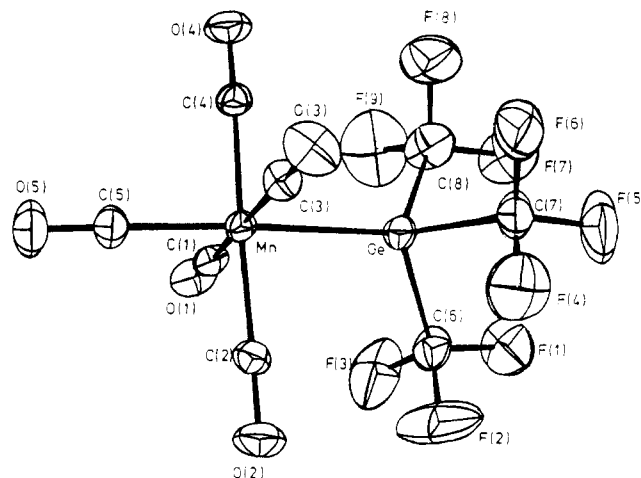


Figure 1. A perspective drawing of  $(CF_3)_3GeMn(CO)_5$  using 20% probability thermal ellipsoids.

Coordinates of the Ge and Mn atoms were derived from a sharpened Patterson function. A subsequent difference Fourier map revealed the other atoms. The structure was refined by full-matrix least-squares methods—the function  $\sum w\Delta^2$ ,  $w = 1/(\sigma^2(|F_o|) + 0.0004|F_o|^2)$  and  $\Delta = ||F_o| - |F_c||$ , being minimized. Dispersion corrected<sup>8a</sup> relativistic Hartree-Fock scattering factors<sup>8b</sup> were used for all atoms. After two weak reflections were omitted since  $|F_o| \gg |F_c|$ , the full anisotropic refinement converged (maximum  $|\zeta/\sigma| < 0.4$ ) with  $R = \sum \Delta/\sum |F_o| = 0.041$  and  $R_w = [\sum w\Delta^2/\sum w|F_o|^2]^{1/2} = 0.049$ . The corresponding discrepancy indices for all 3436 reflections are 0.089 and 0.053, respectively. The final difference Fourier densities varied between 0.50 and -0.42 e/Å<sup>3</sup> and revealed no chemically significant feature. Coordinates are given in Table II. Distances and angles are collected in Table III and IV, respectively, and the numbering scheme is defined in Figure 1.<sup>9</sup>

In order to calculate librational corrections to the Ge-C and C-F bond lengths, we did rigid body motion analyses on the thermal parameters of the  $MnGeC_3$  and three  $GeCF_3$  fragments, respectively. While the mean correction (0.026 Å) to the Ge-C bond lengths appears reasonable, that derived for the C-F bonds (0.078 Å) seems too large to be accepted uncritically. We can only conclude that the true C-F distance lies between the uncorrected (1.30 (1) Å) and corrected (1.38 (1) Å) values. Unless otherwise indicated, uncorrected bond lengths are mentioned in this paper.

**Description of the Crystal Structure.** Crystals of I consist of discrete monomeric molecules. No unusually short intermolecular contacts are present; in fact, even the shortest,  $F(5)-F(5)$  ( $-x, 1-y, 2-z$ ) = 3.00(1) Å, exceeds the van der Waals value of 2.94 Å.<sup>10</sup>

Formed from units having  $C_{3v}$  ( $Ge(CF_3)_3$ ) and  $C_{4v}$  ( $Mn(CO)_5$ ) symmetry, I can obtain at most  $C_s$  symmetry; however, the  $C(7)-Ge-Mn-C(3)$  torsion angle of 8.6 (5)° shows that the mirror plane is only approximate. Packing effects on the manganese valence angles are made manifest by statistically significant, albeit small deviations of these angles (Table IV) from  $C_{4v}$  and  $C_s$  symmetry.

Bonding between the  $(CF_3)_3Ge$  and  $Mn(CO)_5$  groups results in several unusual features. First, the Ge-Mn bond length, 2.4132 (9) Å, is the shortest reported for a  $X_3GeMn(CO)_5$  compound. It is 0.03, 0.074 (2) and 0.13 (2) Å shorter than those found for  $X = Br$ ,<sup>11</sup> H,<sup>12</sup> and  $C_6H_5$ ,<sup>13</sup> respectively. The Ge-Mn bond length,

(8) (a) Ibers, J. A.; Hamilton, W. C., Ed. "International Tables for X-ray Crystallography"; Kynoch Press: Birmingham, 1974; Vol. IV; Table 2.3.1. (b) *Ibid.*; Table 2.2B.

(9) Computer programs used were Sheldrick's SHELX-76, Roberts and Sheldrick's XANADU, Johnson's ORTEP-2, and locally written routines.

(10) Bondi, A. J. *Phys. Chem.* **1964**, *68*, 441.

(11) Gapotchenko, N. I.; Alekseev, N. V.; Antonova, A. B.; Anisimov, K. N.; Kolobova, N. E.; Ronova, I. A.; Struchkov, Yu. T. *J. Organomet. Chem.* **1970**, *23*, 525.

(12) Rankin, D. W. H.; Robertson, A. J. *Organomet. Chem.* **1975**, *85*, 225.

Table II. Positional Parameters<sup>a</sup> for (CF<sub>3</sub>)<sub>3</sub>GeMn(CO)<sub>5</sub>

atom	x	y	z	atom	x	y	z
Ge	9179 (3)	24278 (4)	78409 (6)	O(2)	117 (3)	1194 (4)	3924 (6)
Mn	18573 (5)	15936 (5)	58611 (9)	O(3)	2097 (3)	3666 (3)	4200 (5)
F(1)	-763 (4)	2154 (5)	9401 (8)	O(4)	3576 (3)	2033 (4)	7866 (6)
F(2)	-864 (4)	1834 (9)	6995 (10)	O(5)	2910 (4)	499 (4)	3340 (6)
F(3)	-281 (4)	791 (4)	8431 (13)	C(1)	1711 (3)	357 (4)	7023 (7)
F(4)	64 (5)	4007 (4)	6080 (10)	C(2)	767 (4)	1339 (4)	4666 (7)
F(5)	-10 (4)	4299 (4)	8537 (9)	C(3)	2001 (4)	2881 (5)	4828 (6)
F(6)	1224 (4)	4554 (3)	7349 (9)	C(4)	2919 (4)	1876 (4)	7127 (7)
F(7)	890 (4)	2943 (7)	11180 (6)	C(5)	2525 (5)	916 (5)	4284 (8)
F(8)	2197 (5)	3150 (6)	10142 (7)	C(6)	-298 (5)	1757 (7)	8239 (11)
F(9)	1717 (7)	1631 (7)	10660 (7)	C(7)	540 (5)	3921 (5)	7452 (11)
O(1)	1643 (3)	-401 (3)	7725 (6)	C(8)	1438 (7)	2518 (11)	10105 (10)

<sup>a</sup> ×10<sup>4</sup>, except for Mn and Ge, ×10<sup>5</sup>.

Table III. Bond Distances (Å) in (CF<sub>3</sub>)<sub>3</sub>GeMn(CO)<sub>5</sub>

Mn-Ge	2.4132 (9)	Ge-C(6)	1.999 (7)
		Ge-C(7)	2.004 (7)
		Ge-C(8)	1.992 (8)
		av 1.998 (4)	
Mn-C(1)	1.862 (6)		
Mn-C(2)	1.862 (6)		
Mn-C(3)	1.865 (6)		
Mn-C(4)	1.864 (6)	C(6)-F(1)	1.296 (8)
	av 1.863 (3) <sup>a</sup>	C(6)-F(2)	1.294 (10)
		C(6)-F(3)	1.242 (9)
Mn-C(5)	1.863 (6)	C(7)-F(4)	1.309 (9)
		C(7)-F(5)	1.313 (8)
C(1)-O(1)	1.132 (6)	C(7)-F(6)	1.283 (8)
C(2)-O(2)	1.121 (6)	C(8)-F(7)	1.328 (10)
C(3)-O(3)	1.138 (6)	C(8)-F(8)	1.364 (12)
C(4)-O(4)	1.130 (6)	C(8)-F(9)	1.280 (13)
	av 1.130 (7)	av 1.30 (1)	
C(5)-O(5)	1.111 (6)		

<sup>a</sup> Errors in these average values are the larger of  $[\Sigma(l-i)^2/n(n-1)]^{1/2}$  and  $(\Sigma\sigma^2)^{1/2}/n$ .

Table IV. Bond Angles (deg) in (CF<sub>3</sub>)<sub>3</sub>GeMn(CO)<sub>5</sub>

Ge-Mn-C(1)	86.9 (2)	C(6)-Ge-C(7)	101.3 (3)
Ge-Mn-C(2)	86.8 (2)	C(6)-Ge-C(8)	100.2 (4)
Ge-Mn-C(3)	89.8 (2)	C(7)-Ge-C(8)	100.8 (5)
Ge-Mn-C(4)	90.7 (2)	av 100.8 (3)	
	av 88.6 (10) <sup>a</sup>		
		Ge-C(6)-F(1)	116.2 (6)
		Ge-C(6)-F(2)	112.0 (6)
Ge-Mn-C(5)	176.9 (2)	Ge-C(6)-F(3)	115.6 (6)
		Ge-C(7)-F(4)	110.5 (5)
C(5)-Mn-C(1)	92.2 (3)	Ge-C(7)-F(5)	114.1 (6)
C(5)-Mn-C(2)	90.2 (3)	Ge-C(7)-F(6)	113.6 (5)
C(5)-Mn-C(3)	91.1 (2)	Ge-C(8)-F(7)	115.8 (7)
C(5)-Mn-C(4)	92.3 (2)	Ge-C(8)-F(8)	109.4 (7)
	av 91.4 (5)	Ge-C(8)-F(9)	112.8 (8)
		av 113.3 (8)	
C(1)-Mn-C(2)	90.8 (2)		
C(1)-Mn-C(4)	89.0 (2)	F(1)-C(6)-F(2)	103.0 (8)
C(2)-Mn-C(3)	91.0 (2)	F(1)-C(6)-F(3)	107.5 (8)
C(3)-Mn-C(4)	89.0 (2)	F(2)-C(6)-F(3)	100.7 (9)
	av 90.0 (6)	F(4)-C(7)-F(5)	104.2 (7)
		F(4)-C(7)-F(6)	105.9 (8)
C(1)-Mn-C(3)	176.2 (2)	F(5)-C(7)-F(6)	107.8 (6)
C(2)-Mn-C(4)	177.5 (2)	F(7)-C(8)-F(8)	104.4 (9)
	av 176.8 (7)	F(7)-C(8)-F(9)	108.1 (10)
		F(8)-C(8)-F(9)	105.6 (10)
		av 105.2 (8)	
Mn-Ge-C(6)	116.5 (2)		
Mn-Ge-C(7)	117.9 (2)		
Mn-Ge-C(8)	117.2 (3)		
	av 117.2 (4)		

<sup>a</sup> Errors as in Table III.

2.500 Å, estimated from appropriate distances in CF<sub>3</sub>Mn(CO)<sub>5</sub>,<sup>14</sup> Ge(CF<sub>3</sub>)<sub>4</sub>,<sup>4</sup> and C<sub>2</sub>F<sub>6</sub>,<sup>15</sup> also clearly exceeds that in I. Second, the

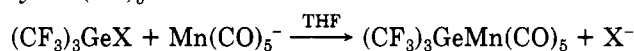
mean C-Ge-C bond angle, 100.8 (3)°, is remarkably small. While the corresponding angle was not published for (C<sub>6</sub>H<sub>5</sub>)<sub>3</sub>GeMn(CO)<sub>5</sub>,<sup>13</sup> those in (*μ*-pentalene)[(CH<sub>3</sub>)<sub>3</sub>GeRu(CO)<sub>2</sub>]<sub>2</sub>, 107 (1)°,<sup>16</sup> and (C<sub>6</sub>H<sub>5</sub>)<sub>3</sub>Ge[(*η*-C<sub>5</sub>H<sub>5</sub>)Mo(CO)<sub>2</sub>C(OC<sub>2</sub>H<sub>5</sub>)C<sub>6</sub>H<sub>5</sub>], 105 (2)°,<sup>17</sup> are not nearly as small as in I. For Mn(CO)<sub>5</sub> derivatives, the smallest previously documented, analogous angle was revealed in Cl<sub>3</sub>SnMn(CO)<sub>5</sub>, 100.7 (2)°,<sup>18</sup> the value in Br<sub>3</sub>GeMn(CO)<sub>5</sub>, 105°,<sup>11</sup> being clearly larger.

Since each CF<sub>3</sub> group assumes an approximately staggered conformation with respect to the Ge-Mn and other Ge-C bonds, closing the C-Ge-C angles increases the mutual steric crowding of fluorine atoms anti to the Mn atoms—F(1), F(5), and F(7). Thus these three intramolecular contacts (2.942 (8)–3.040 (9) Å) are distinctly smaller than those in Ge(CF<sub>3</sub>)<sub>4</sub>, 3.306 (4) Å.<sup>4</sup> Inspection of Table III reveals that the Ge-C-F bond angles involving F(1), F(5), and F(7) are the largest for each CF<sub>3</sub> group. Thus the CF<sub>3</sub> groups appear to be tilted so as to relax the above-mentioned contacts.

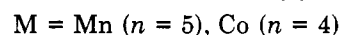
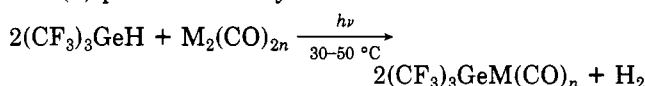
Besides the corrected Ge-C bond length (2.024 (4) Å) being significantly longer than that in Ge(CF<sub>3</sub>)<sub>4</sub> (1.989 (2) Å<sup>4</sup>), the mean C(axial)-Mn-C(equatorial) angle (91.4 (5)°) deserves mention. Previous values for this angle in Mn(CO)<sub>5</sub> derivatives range from 92.0 (6)° in Cl<sub>3</sub>SnMn(CO)<sub>5</sub><sup>18</sup> to 97.2 (8)° in HMn(CO)<sub>5</sub>.<sup>19</sup> In I, steric repulsion may be contributing to the small value of this angle since 10 intramolecular nonbonded contacts between the Ge(CF<sub>3</sub>)<sub>3</sub> and Mn(CO)<sub>5</sub> moieties are 0.03–0.11 Å shorter than the van der Waals radii sums.<sup>10</sup>

## Discussion

Trifluoromethyl-substituted germanes have been found to undergo reactions very similar to other alkyl- or halogermanes, as long as conditions are avoided (e.g., strong bases) that could lead to evolution of HCF<sub>3</sub>. The formation of metal carbonyl derivatives of (trifluoromethyl)germanes is achieved by two routes, namely, (i) halide replacement by Mn(CO)<sub>5</sub><sup>-</sup>



and (ii) photochemically



The electron-withdrawing power of the CF<sub>3</sub> groups leads to a group electronegativity of the (CF<sub>3</sub>)<sub>3</sub>Ge moiety that is comparable to that of iodine, and as a consequence, competitive attack on the halide with formation of IMn-

(15) Gallaher, K. L.; Yokozeki, A.; Bauer, S. H. *J. Phys. Chem.* 1974, 78, 2389.

(16) Howard, J. A. K.; Woodward, P. *J. Chem. Soc., Dalton Trans.* 1978, 412.

(17) Chan, L. Y. Y.; Dean, W. K.; Graham, W. A. G. *Inorg. Chem.* 1977, 16, 1067.

(18) Onaka, S. *Bull. Chem. Soc. Jpn.* 1975, 48, 319.

(19) La Placa, S. J.; Hamilton, W. C.; Ibers, J. A.; Davison, A. *Inorg. Chem.* 1969, 8, 1928.

(13) Kilborn, B. T.; Blundell, T. L.; Powell, H. M. *J. Chem. Soc., Chem. Commun.* 1965, 444.

(14) Beagley, B.; Young, G. G. *J. Mol. Struct.* 1977, 40, 295.

Table V. Infrared and Raman Spectra ( $\text{cm}^{-1}$ ) of  $(\text{CF}_3)_3\text{GeCo}(\text{CO})_4$  (II) and  $(\text{CF}_3)_3\text{GeMn}(\text{CO})_5$  (I)

Raman (melt)	$(\text{CF}_3)_3\text{GeCo}(\text{CO})_4$		$(\text{CF}_3)_3\text{GeMn}(\text{CO})_5$		assignt
	Raman (solid)	IR (gas)	Raman (solid)	IR (KBr)	
72 m					$\delta(\text{GGeC})$
105 s	110 s		115 vs		$\delta(\text{COMCO})$
202 vs, p	203 s		197 s		$\nu(\text{GeM})$
223 vw, sh	224 w		226 w		} $\rho(\text{CF}_3)$
250 w	251 } <sub>m</sub>		248 w		
	256 } <sub>m</sub>		257 w		
335 vw	332 w	334 s	328 w	325 s	$\nu_{\text{as}}(\text{GeC}_3)$
409 m, p	410 m		401 m		$\nu(\text{MCO})_{\text{eq}}$
440 vw					} $\nu(\text{MCO})/\delta(\text{MCO})$
465 vw	467 vw	467 m	444 w	444 m	
487 vw		491 m		458 s	
532 vw	528 vw		527 w		$\delta_{\text{as}}(\text{CF}_3)$
553 w, p	550 vw	557 s	642 vw	638 vs	} $\nu(\text{MCO})/\delta(\text{MCO})$
			657 w-m	660 s	
725 m, p	725 m	728 w	721 m	721 m	$\delta_{\text{s}}(\text{CF}_3)$
		1114 s	1107 w	1080 s	} $\nu_{\text{as}}(\text{CF}_3)$
1135 vw, b		1139 m-s	1126 w	1110 s	
			1148 w	1149 s	
1153 vw	1150 vw	1156 vs	1155 w		} $\nu_{\text{s}}(\text{CF}_3)$
1185 vw, p	1185 vw	1192.5 vs	1188 w	1190 s	
		2020 vw			$\nu(\text{CO})(^{13}\text{C})$
2055 w, b	2045 m-s	2058 vs <sup>a</sup>	2043 w	2040 s, b <sup>a</sup>	} $\nu(\text{CO}_{\text{eq}})$
			2065 m		
2084 w	2085 m	2075 s <sup>a</sup>	2070 sh		
			2082 s	2080 sh	} $\nu(\text{CO}_{\text{ax}})$
2131 m, p	2134 m	2128 s <sup>a</sup>	2138 m	2138 m <sup>a</sup>	

<sup>a</sup> CO frequencies in cyclohexane solution: 2011 w ( $^{13}\text{CO}_{\text{eq}}$ ), 2049 s (e), 2070.5 m ( $a_1$ ), and 2124.5 m ( $a_1$ ) for II; 2011 w ( $^{13}\text{CO}_{\text{eq}}$ ), 2037 m ( $a_1$ ), 2045 s (e), and 2130 m ( $a_1$ ) for I.

$(\text{CO})_5$  is observed for X = I, whereas no  $\text{ClMn}(\text{CO})_5$  was observed for X = Cl.

Pentacarbonylmanganese derivatives have widely been used<sup>20</sup> to estimate  $\sigma$  and  $\pi$  donor/acceptor qualities of ligands on the basis of CO stretch force constants mainly derived by the Cotton-Kraihanzel approximation.<sup>21</sup> The vibrational spectra of  $(\text{CF}_3)_3\text{GeCo}(\text{CO})_4$  and  $(\text{CF}_3)_3\text{GeMn}(\text{CO})_5$  are listed in Table V. The interactions between the  $(\text{CF}_3)_3\text{Ge}$  and  $\text{M}(\text{CO})_n$  parts of the molecule are small and, consequently, the spectra almost appear as a superposition of those of  $(\text{CF}_3)_3\text{GeI}^3$  and other  $\text{M}(\text{CO})_n$  derivatives.<sup>22,23</sup> The loss of effective  $C_{4v}$  symmetry in the solid-state spectra of I is most likely to be due to intermolecular effects because the higher symmetry is found in solution. In cyclohexane solution, the close correspondence of  $\text{M}(\text{CO})_n$  frequencies to those of the  $\text{Cl}_3\text{Ge}$  derivatives<sup>22,24</sup> thus confirms the previously found equivalence in second-order substitution effects of  $\text{CF}_3$  and  $\text{Cl}$ .<sup>3</sup> The C-O force constants listed in Table VI were calculated from the infrared  $\nu(\text{CO})$  frequencies of cyclohexane solutions including a ( $^{13}\text{CO}$ )<sub>eq</sub> absorption of the mono  $^{13}\text{C}$  substituted species (see footnote a in Table V). For the  $\text{Mn}(\text{CO})_5$  fragment, the frequency of the infrared-inactive  $b_1$  mode was taken from the Raman spectrum. According to a Graham-type interpretation<sup>25</sup> of these force constants, the  $\sigma$ -withdrawing properties of  $\text{GeCl}_3$  and  $\text{Ge}(\text{CF}_3)_3$  are much greater than those of  $\text{Ge}(\text{C}_6\text{H}_5)_3$  while these three groups have similar  $\pi$ -acceptor properties. In addition, the high-frequency  $^{55}\text{Mn}$  shift of ca. 100 ppm for I with respect

Table VI. Carbonyl Force Constants<sup>a</sup> [ $\text{N}\cdot\text{cm}^{-1}$ ] and Graham Constants

	$(\text{CF}_3)_3\text{GeMn}(\text{CO})_5$	$(\text{CF}_3)_3\text{GeCo}(\text{CO})_4$
$f_{\text{ax}}$	16.90 (16.92)	17.58 (17.58)
$f_{\text{eq}}$	17.37 (17.40)	17.30 (17.30)
$f_{\text{ax}}/f_{\text{eq}}$	0.23 (0.23)	0.24 (0.24)
$f_{\text{eq}}/f_{\text{eq}}(\text{cis})$	0.17 (0.17)	
$f_{\text{eq}}/f_{\text{eq}}(\text{trans})$	0.48 (0.45)	0.34 (0.32)
$\Delta f_1^b$	0.68 (0.70)	
$\Delta f_2^b$	0.56 (0.59)	
$\sigma$	0.44 (0.48)	
$\pi$	0.12 (0.11)	

<sup>a</sup> Calculated from frequencies of cyclohexane solutions. Values in parentheses refer to  $\text{Cl}_3\text{Ge}$  derivatives. <sup>b</sup> Referred to  $\text{CH}_3\text{Mn}(\text{CO})_5$ .<sup>25</sup>

to  $\text{Mn}_2(\text{CO})_{10}$  also indicates the relative electron-withdrawing nature of the  $\text{Ge}(\text{CF}_3)_3$  group.<sup>26</sup>

Several factors may contribute to the shortness of the Ge-Mn bond length in I. First, the Ge 4s character  $\alpha_{\text{Ge}}^2$  in this bond, as calculated from the bond angle C-Ge-C( $\theta$ ) by the equation<sup>27</sup>  $\alpha_{\text{Ge}}^2 = (1 + 2 \cos \theta)/(1 - \cos \theta) = 0.53$ , is much larger than the  $\text{sp}^3$  value 0.25. As a result, the Ge atom should be aspherical—smaller on the Mn side and larger on the  $\text{CF}_3$  side. This prediction is supported by the corrected Ge-C bond lengths in I being longer than those in  $\text{Ge}(\text{CF}_3)_4$ .<sup>4</sup> A factor contributing to this Ge rehybridization may be the low demand of the  $\text{CF}_3$  groups for Ge 4s character as revealed by CNDO calculations.<sup>28</sup> Second and probably of greater moment may be the intrinsic ability of  $\text{Mn}(\text{CO})_5$  and other  $\text{M}(\text{CO})_n$  fragments to shorten their radii toward  $\text{M}'\text{R}_3$  moieties as the elec-

(20) Graham, W. A. G. *Inorg. Chem.* **1968**, *7*, 315.

(21) Cotton, F. A.; Kraihanzel, C. S. *J. Am. Chem. Soc.* **1962**, *84*, 4432.

(22) Watters, K. L.; Brittain, J. N.; Risen, W. M., Jr., *Inorg. Chem.* **1969**, *8*, 1347.

(23) Terzis, A.; Strekas, T. C.; Spiro, T. G. *Inorg. Chem.* **1974**, *13*, 1346.

(24) Jetz, W.; Graham, W. A. G. *J. Am. Chem. Soc.* **1967**, *89*, 2773.

(25) Force constants are related to the value of  $\text{CH}_3\text{Mn}(\text{CO})_5$  as calculated by: Kaesz, H. D.; Bau, R.; Hendrickson, D.; Smith, J. M. *J. Am. Chem. Soc.* **1967**, *89*, 2844.

(26) Harris, R. K.; Mann, B. E. "NMR and the Periodic Table"; Academic Press: London, 1978; p 218, and references cited therein.

(27) Hitchcock, P. B.; Jacobson, B.; Pidcock, A. *J. Chem. Soc., Dalton Trans.* **1977**, 2043.

(28) Drake, J. E.; Gorzelska, K.; Helbing, R.; Eujen, R. *J. Electron Spectrosc. Relat. Phenom.* **1982**, *26*, 19.

tron-withdrawing power of R increases. This effect is nicely displayed by the  $(\text{CO})_5\text{Mn}-\text{CF}_3$  bond<sup>14</sup> being 0.129 (12) Å shorter than the  $(\text{CO})_5\text{Mn}-\text{CH}_3$ <sup>29</sup> linkage, a difference very similar to that between Ge-Mn in I and  $(\text{C}_6\text{H}_5)_3\text{GeMn}(\text{CO})_5$ . Noteworthy is the  $\text{Mn}-\text{CF}_3/\text{Mn}-\text{CH}_3$  shortening apparently being unassisted by  $\text{Mn}(3d\pi) \rightarrow \text{CF}_3(\pi^*)$  back-donation,<sup>20,30</sup> that is, changes in  $\sigma$  bonding

alone may well be sufficient to account for the substitution effects discussed here.

**Acknowledgment.** We wish to thank Dr. C. Krüger of the Max-Planck-Institut für Kohlenforschung, Mülheim/Ruhr, for diffractometer time.

**Registry No.** I, 83801-95-0; II, 83815-90-1.

**Supplementary Material Available:** Tables of anisotropic temperature factors and structure factor amplitudes (21 pages). Ordering information is given on any current masthead page.

(29) Seip, H. M.; Seip, R. *Acta Chem. Scand.* 1970, 24, 3431.

(30) Hall, M. B.; Fenske, R. F. *Inorg. Chem.* 1972, 11, 768.

## Phosphine-Linked Phosphazenes as Carrier Molecules for Transition-Metal Complexes<sup>1</sup>

Harry R. Allcock,\* Karen D. Lavin, Norris M. Tollefson, and Thomas L. Evans

Department of Chemistry, The Pennsylvania State University, University Park, Pennsylvania 16802

Received September 28, 1982

The phosphine-bearing poly((aryloxy)phosphazenes)  $[\text{NP}(\text{OC}_6\text{H}_4\text{PPh}_2)_x(\text{OPh})_{2-x}]_n$  (1a, where  $x \approx 0.3$ , or 1b, where  $x \approx 0.6$ ) have been investigated as high polymeric ligands for binding to transition-metal species. The cyclic trimeric phosphazenes  $[\text{NP}(\text{OPh})_2]_3$  (2),  $\text{N}_3\text{P}_3(\text{OC}_6\text{H}_4\text{PPh}_2)(\text{OPh})_5$  (3), and  $[\text{NP}(\text{OC}_6\text{H}_4\text{PPh}_2)_2]_3$  (4) were examined as model donors for comparisons with the high polymers. Species 1-4 were allowed to interact with  $\text{AuCl}$ ,  $\text{H}_2\text{Os}_3(\text{CO})_{10}$ ,  $\text{Mn}(\text{CO})_3(\eta\text{-C}_6\text{H}_5)$ ,  $\text{Fe}(\text{CO})_3(\text{PhCH}=\text{CHC}(\text{O})\text{CH}_3)$ , and  $[\text{RhCl}(\text{CO})_2]_2$ . Coordination of pendent phosphine units to all five metals occurred without interference from the skeletal nitrogen atoms. Both intra- and intermolecular complexation took place when the metal could accept two phosphine ligands. The NMR and infrared spectra of these complexes resembled those of the analogous (triphenylphosphine)metal complexes. The coordinated metals exerted a strong influence on the physical properties of the high polymers, with evidence being obtained for coordinative cross-linking. Evidence was also obtained for a facile ligand exchange process with the rhodium-bound species. The osmium-bound species  $\text{N}_3\text{P}_3(\text{OC}_6\text{H}_4\text{PPh}_2\text{Os}_3\text{H}_2(\text{CO})_{10})(\text{OPh})_5$  (6),  $[\text{NP}(\text{OC}_6\text{H}_4\text{PPh}_2\text{Os}_3\text{H}_2(\text{CO})_{10})_2]_3$ , and  $[\text{NP}(\text{OC}_6\text{H}_4\text{PPh}_2\text{Os}_3\text{H}_2(\text{CO})_{10})_{0.3}(\text{OPh})_{1.7}]_n$  (11) function as catalysts for the isomerization of 1-hexene to 2-hexene.

A strong interest exists in the use of macromolecules as "carrier" ligands for transition-metal catalyst systems.<sup>2-7</sup> A reason for this interest is the prospect that soluble macromolecules can be designed to control the activity of catalyst systems in a manner reminiscent of the active site in metalloproteins. Moreover, the possibility exists that polymers (whether insoluble or forming a swollen, cross-linked gel) may "immobilize" a catalyst moiety, thereby allowing homogeneous catalysis to occur under heterogeneous-type conditions. The possibility that sequential catalytic steps can be carried out within the domain of a polymer matrix is an added prospect.

Traditionally, polystyrene, bearing diarylalkylphosphine ligand sites, has been used as a carrier polymer, mainly because of its ready availability. However, polystyrene is not an ideal carrier molecule. It has a restricted solubility in many media (including water); it has a relatively low thermooxidative stability; and severe synthetic problems must be overcome before it can be modified structurally

to provide a range of solubilities and chain flexibilities.

The poly(organophosphazenes) constitute a new class of macromolecules with special advantages as coordination ligands for transition metals. The substitutive method of synthesis used for these polymers<sup>8-10</sup> allows a wide range of different side groups to be attached to the macromolecular skeleton. Polyphosphazenes that bear alkoxy, aryloxy, amino acid ester, steroidal, azo, and many other groups have been prepared.<sup>10</sup> Phosphazenes with metallo units linked directly to the phosphorus atoms of the skeleton are also known.<sup>11,12</sup>

We have synthesized a series of high polymeric and cyclic phosphazenes (1, 3, 4) that bear diphenylphosphine units linked to the phosphazene skeleton through aryloxy spacer groups.<sup>13,14</sup> In this paper we consider the behavior of these species as coordinative ligands for transition metals and compare them with the control compound 2, which contains only skeletal nitrogen atoms as potential coordination sites. Species 3 is a good direct model for 1. Compound 4 is an exploratory model designed to mimic

(1) Presented at the 182nd National Meeting of the American Chemical Society, New York, Aug 23-28, 1981.

(2) Collman, J. P.; Hegedus, L. S.; Cooke, M. P.; Norton, J. N.; Dolecetti, G. Marquardt, D. N. *J. Am. Chem. Soc.* 1972, 94, 1789.

(3) Pittman, C. U. In "Polymer-Supported Reactions in Organic Synthesis"; Hodge, P., Sherrington, D. C., Eds.; Wiley: New York, 1980; Chapter 5.

(4) Grubbs, R. H. *Chemtech.* 1977, 7, 512.

(5) Chauvin, Y.; Chemereuc, D.; Dawans, F. *Prog. Polym. Sci.* 1977, 5, 95.

(6) Grubbs, R. H.; Gibbons, C.; Kroll, L. C.; Bonds, W. D.; Brubaker, C. H. *J. Am. Chem. Soc.* 1973, 95, 2373.

(7) Sekiya, A.; Stille, J. K. *J. Am. Chem. Soc.* 1981, 103, 5096.

(8) Allcock, H. R.; Kugel, R. L.; Valan, K. *J. Inorg. Chem.* 1966, 5, 1709, 1716.

(9) Allcock, H. R. "Phosphorus-Nitrogen Compounds"; Academic Press: New York: 1972.

(10) Allcock, H. R. *Makromol. Chem.* 1981, Suppl. 4, 3.

(11) Allcock, H. R.; Greigger, P. P. *J. Am. Chem. Soc.* 1979, 101, 2492.

(12) Allcock, H. R.; Wagner, L. J.; Greigger, P. P.; Bernheim, M. Y. *Inorg. Chem.* 1981, 20, 716.

(13) Allcock, H. R.; Evans, T. L.; Fuller, T. J. *Inorg. Chem.* 1980, 19, 1026.

(14) Allcock, H. R.; Evans, T. L.; Fuller, T. J. *Macromolecules* 1980, 13, 1325.



tron-withdrawing power of R increases. This effect is nicely displayed by the  $(\text{CO})_5\text{Mn}-\text{CF}_3$  bond<sup>14</sup> being 0.129 (12) Å shorter than the  $(\text{CO})_5\text{Mn}-\text{CH}_3$ <sup>29</sup> linkage, a difference very similar to that between Ge-Mn in I and  $(\text{C}_6\text{H}_5)_3\text{GeMn}(\text{CO})_5$ . Noteworthy is the Mn-CF<sub>3</sub>/Mn-CH<sub>3</sub> shortening apparently being unassisted by Mn(3dπ) → CF<sub>3</sub>(π\*) back-donation,<sup>20,30</sup> that is, changes in σ bonding

alone may well be sufficient to account for the substitution effects discussed here.

**Acknowledgment.** We wish to thank Dr. C. Krüger of the Max-Planck-Institut für Kohlenforschung, Mülheim/Ruhr, for diffractometer time.

**Registry No.** I, 83801-95-0; II, 83815-90-1.

**Supplementary Material Available:** Tables of anisotropic temperature factors and structure factor amplitudes (21 pages). Ordering information is given on any current masthead page.

(29) Seip, H. M.; Seip, R. *Acta Chem. Scand.* 1970, 24, 3431.

(30) Hall, M. B.; Fenske, R. F. *Inorg. Chem.* 1972, 11, 768.

## Phosphine-Linked Phosphazenes as Carrier Molecules for Transition-Metal Complexes<sup>1</sup>

Harry R. Allcock,\* Karen D. Lavin, Norris M. Tollefson, and Thomas L. Evans

Department of Chemistry, The Pennsylvania State University, University Park, Pennsylvania 16802

Received September 28, 1982

The phosphine-bearing poly((aryloxy)phosphazenes)  $[\text{NP}(\text{OC}_6\text{H}_4\text{PPh}_2)_x(\text{OPh})_{2-x}]_n$  (1a, where  $x \approx 0.3$ , or 1b, where  $x \approx 0.6$ ) have been investigated as high polymeric ligands for binding to transition-metal species. The cyclic trimeric phosphazenes  $[\text{NP}(\text{OPh})_2]_3$  (2),  $\text{N}_3\text{P}_3(\text{OC}_6\text{H}_4\text{PPh}_2)(\text{OPh})_5$  (3), and  $[\text{NP}(\text{OC}_6\text{H}_4\text{PPh}_2)_2]_3$  (4) were examined as model donors for comparisons with the high polymers. Species 1-4 were allowed to interact with AuCl,  $\text{H}_2\text{Os}_3(\text{CO})_{10}$ ,  $\text{Mn}(\text{CO})_3(\eta\text{-C}_6\text{H}_5)$ ,  $\text{Fe}(\text{CO})_3(\text{PhCH}=\text{CHC}(\text{O})\text{CH}_3)$ , and  $[\text{RhCl}(\text{CO})_2]_2$ . Coordination of pendent phosphine units to all five metals occurred without interference from the skeletal nitrogen atoms. Both intra- and intermolecular complexation took place when the metal could accept two phosphine ligands. The NMR and infrared spectra of these complexes resembled those of the analogous (triphenylphosphine)metal complexes. The coordinated metals exerted a strong influence on the physical properties of the high polymers, with evidence being obtained for coordinative cross-linking. Evidence was also obtained for a facile ligand exchange process with the rhodium-bound species. The osmium-bound species  $\text{N}_3\text{P}_3(\text{OC}_6\text{H}_4\text{PPh}_2\text{Os}_3\text{H}_2(\text{CO})_{10})(\text{OPh})_5$  (6),  $[\text{NP}(\text{OC}_6\text{H}_4\text{PPh}_2\text{Os}_3\text{H}_2(\text{CO})_{10})_2]_3$ , and  $[\text{NP}(\text{OC}_6\text{H}_4\text{PPh}_2\text{Os}_3\text{H}_2(\text{CO})_{10})_{0.3}(\text{OPh})_{1.7}]_n$  (11) function as catalysts for the isomerization of 1-hexene to 2-hexene.

A strong interest exists in the use of macromolecules as "carrier" ligands for transition-metal catalyst systems.<sup>2-7</sup> A reason for this interest is the prospect that soluble macromolecules can be designed to control the activity of catalyst systems in a manner reminiscent of the active site in metalloproteins. Moreover, the possibility exists that polymers (whether insoluble or forming a swollen, cross-linked gel) may "immobilize" a catalyst moiety, thereby allowing homogeneous catalysis to occur under heterogeneous-type conditions. The possibility that sequential catalytic steps can be carried out within the domain of a polymer matrix is an added prospect.

Traditionally, polystyrene, bearing diarylalkylphosphine ligand sites, has been used as a carrier polymer, mainly because of its ready availability. However, polystyrene is not an ideal carrier molecule. It has a restricted solubility in many media (including water); it has a relatively low thermooxidative stability; and severe synthetic problems must be overcome before it can be modified structurally

to provide a range of solubilities and chain flexibilities.

The poly(organophosphazenes) constitute a new class of macromolecules with special advantages as coordination ligands for transition metals. The substitutive method of synthesis used for these polymers<sup>8-10</sup> allows a wide range of different side groups to be attached to the macromolecular skeleton. Polyphosphazenes that bear alkoxy, aryloxy, amino acid ester, steroidal, azo, and many other groups have been prepared.<sup>10</sup> Phosphazenes with metallo units linked directly to the phosphorus atoms of the skeleton are also known.<sup>11,12</sup>

We have synthesized a series of high polymeric and cyclic phosphazenes (1, 3, 4) that bear diphenylphosphine units linked to the phosphazene skeleton through aryloxy spacer groups.<sup>13,14</sup> In this paper we consider the behavior of these species as coordinative ligands for transition metals and compare them with the control compound 2, which contains only skeletal nitrogen atoms as potential coordination sites. Species 3 is a good direct model for 1. Compound 4 is an exploratory model designed to mimic

(1) Presented at the 182nd National Meeting of the American Chemical Society, New York, Aug 23-28, 1981.

(2) Collman, J. P.; Hegedus, L. S.; Cooke, M. P.; Norton, J. N.; Dolecki, G. Marquardt, D. N. *J. Am. Chem. Soc.* 1972, 94, 1789.

(3) Pittman, C. U. In "Polymer-Supported Reactions in Organic Synthesis"; Hodge, P., Sherrington, D. C., Eds.; Wiley: New York, 1980; Chapter 5.

(4) Grubbs, R. H. *Chemtech.* 1977, 7, 512.

(5) Chauvin, Y.; Chemereuc, D.; Dawans, F. *Prog. Polym. Sci.* 1977, 5, 95.

(6) Grubbs, R. H.; Gibbons, C.; Kroll, L. C.; Bonds, W. D.; Brubaker, C. H. *J. Am. Chem. Soc.* 1973, 95, 2373.

(7) Sekiya, A.; Stille, J. K. *J. Am. Chem. Soc.* 1981, 103, 5096.

(8) Allcock, H. R.; Kugel, R. L.; Valan, K. *J. Inorg. Chem.* 1966, 5, 1709, 1716.

(9) Allcock, H. R. "Phosphorus-Nitrogen Compounds"; Academic Press: New York: 1972.

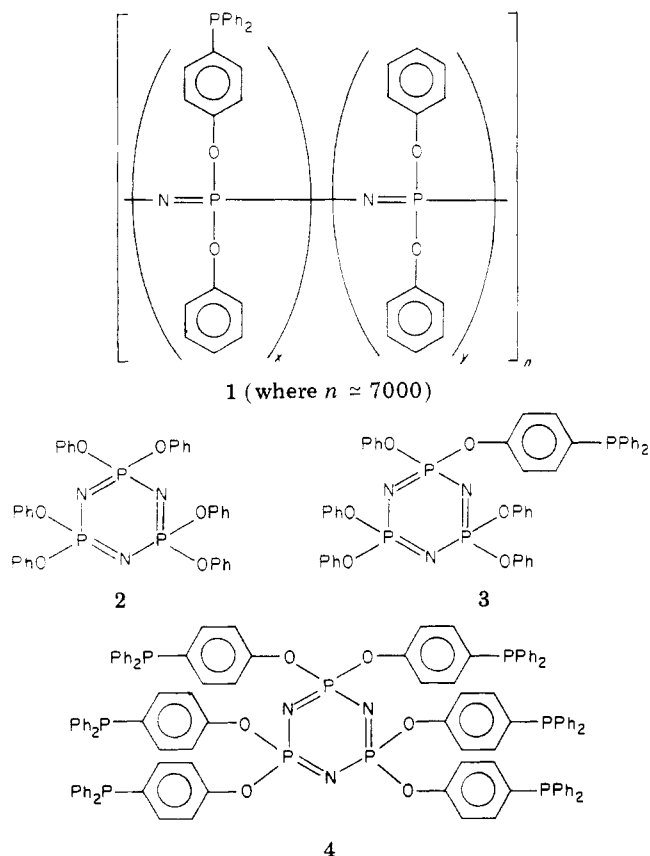
(10) Allcock, H. R. *Makromol. Chem.* 1981, Suppl. 4, 3.

(11) Allcock, H. R.; Greigger, P. P. *J. Am. Chem. Soc.* 1979, 101, 2492.

(12) Allcock, H. R.; Wagner, L. J.; Greigger, P. P.; Bernheim, M. Y. *Inorg. Chem.* 1981, 20, 716.

(13) Allcock, H. R.; Evans, T. L.; Fuller, T. J. *Inorg. Chem.* 1980, 19, 1026.

(14) Allcock, H. R.; Evans, T. L.; Fuller, T. J. *Macromolecules* 1980, 13, 1325.



the behavior of polymers with a high local or average density of phosphine units along the chain. Two high polymers were used in this work, each having different ratios of the phosphinophenoxy and phenoxy groups. In polymer 1a, approximately 15% of the side groups bore phosphine ligands, whereas, in polymer 1b, approximately 30% of the side groups were of this type.

The metallo species investigated for reactions with 1–4 included AuCl,  $\text{H}_2\text{Os}_3(\text{CO})_{10}$ ,  $\text{Mn}(\text{CO})_3(\eta\text{-C}_5\text{H}_5)$ ,  $\text{Fe}(\text{CO})_3\text{-}(\text{PhCH}=\text{CH}(\text{O})\text{CH}_3)$ , and  $[\text{RhCl}(\text{CO})_2]_2$ . Gold chloride was used because it represents an uncomplicated system free from the possibility of diphosphine coordination. Gold complexes are also of biomedical interest. The complexes  $\text{Mn}(\text{CO})_2(\text{PPh}_3)(\eta\text{-C}_5\text{H}_5)$  and  $\text{Fe}(\text{CO})_3(\text{PPh}_3)_2$  have catalytic activity. The osmium cluster  $\text{H}_2\text{Os}_3(\text{CO})_{10}$  is a well-known olefin isomerization catalyst,<sup>15,16</sup> and  $\text{RhCl}(\text{CO})(\text{PPh}_3)_2$  is an isomerization and hydroformylation catalyst.<sup>17</sup> However, these metallo units were chosen mainly for their stability and ease of characterization. Thus, the complexes studied are prototypes for less stable systems that have greater catalytic utility.

The main purpose of this investigation was to answer the following questions: (1) Do ligands such as 1, 3, or 4 coordinate to transition-metal systems in a manner reminiscent of the behavior of triphenylphosphine? (2) Is this coordination behavior complicated by the existence of competing coordination sites (nitrogen atoms) in the phosphazene skeleton? (3) Can 1 or 4 function as chelating ligands? (4) Are cyclic trimers such as 3 or 4 good models for the behavior of the high polymer? (5) Does linkage of a metal to a phosphazene ring or polymer allow catalytic activity to be retained?

## Results and Discussion

**General Principles.** First, it was found that model compound 2, which contained no phosphine ligands, showed no evidence of coordination to any of the five transition-metal systems. Moreover, the analogous high polymer  $[\text{NP}(\text{OPh})_2]_n$  appeared to be equally unreactive, although the sensitivity of detection of coordination was necessarily lower than in the small molecule model system. Thus, it can be concluded that the skeletal nitrogen atoms in these systems are inactive for coordination to the metallo systems studied in this work. This could reflect a low basicity brought about by the presence of the nearby phenoxy units, but more likely it is a consequence of extremely effective steric shielding of the skeleton by the bulky phenoxy groups. Molecular models illustrate this shielding effect very clearly, as do conformational energy calculations.<sup>18</sup>

However, strong coordination was detected when triarylphosphine side units were present in compounds 1, 3, and 4. The interactions for model compound 3 are summarized in Scheme I and those for the polymers in Scheme II. The behavior of compound 4 was more complex, and this will be discussed later.

An additional general principle is that, if the transition-metal system can accommodate two phosphine ligands, the prospect exists that the two ligands will be accepted from different carrier molecules to form a crosslink. The structure of crosslinked macromolecules can be studied only with difficulty. Thus, it was of paramount importance to deduce the mode of coordination in the small molecule model systems 3 and 4. Evidence from the small molecule model systems suggested that coordinative cross-linking could occur for all the high polymeric complexes except for those that involved AuCl. Each of the five transition-metal systems will be discussed in turn.

**Reactions of AuCl with 1, 3, and 4.** Addition of AuCl to the high polymers 1a or b in tetrahydrofuran yielded species 10a or b. These latter products were white polymers that were soluble in tetrahydrofuran. Thus, no cross-linking took place. The model compound 3 also reacted readily with AuCl in aqueous tetrahydrofuran to yield 5 (Scheme I). Complex 5 was a white solid that was soluble in tetrahydrofuran or chlorinated solvents. Similarly, cyclophosphazene 4 formed a soluble hexagold chloride complex,  $[\text{NP}(\text{OC}_6\text{H}_4\text{PPh}_2\text{AuCl})_2]_3$ , under similar conditions. In each case, essentially all the phosphine residues were coordinated to the metal. The structures of these complexes were confirmed by a combination of <sup>31</sup>P NMR and microanalytical data (Tables I and II). For example, the cyclic trimeric complexes gave <sup>31</sup>P NMR peaks at +33 ppm (gold-bound phosphine) and +8 ppm (skeletal phosphorus) and at +33 ppm and -19 ppm for the polymer analogues. The <sup>31</sup>P NMR spectrum of AuCl(PPh<sub>3</sub>) shows a peak at +33 ppm.

Although the complexation of AuCl with 1, 3, and 4 was quite straightforward, the same simplicity was not evident when CuI was used in place of AuCl. Treatment of 3 with CuI in aqueous KI solution yielded a soluble complex, but both 4 and 1 were precipitated as a cross-linked matrix under the same conditions. It is known<sup>19</sup> that the triphenylphosphine complex of CuI agglomerates to form a tetramer,  $[\text{CuI}(\text{PPh}_3)]_4$ , and presumably this is responsible for the behavior with 4 and 1.

**Reactions of  $\text{H}_2\text{Os}_3(\text{CO})_{10}$  with 1, 3, and 4.** Phosphines react with  $\text{H}_2\text{Os}_3(\text{CO})_{10}$  by addition across the os-

(15) Deeming, A. J.; Hasso, S. J. *Organomet. Chem.* 1976, 114, 313.

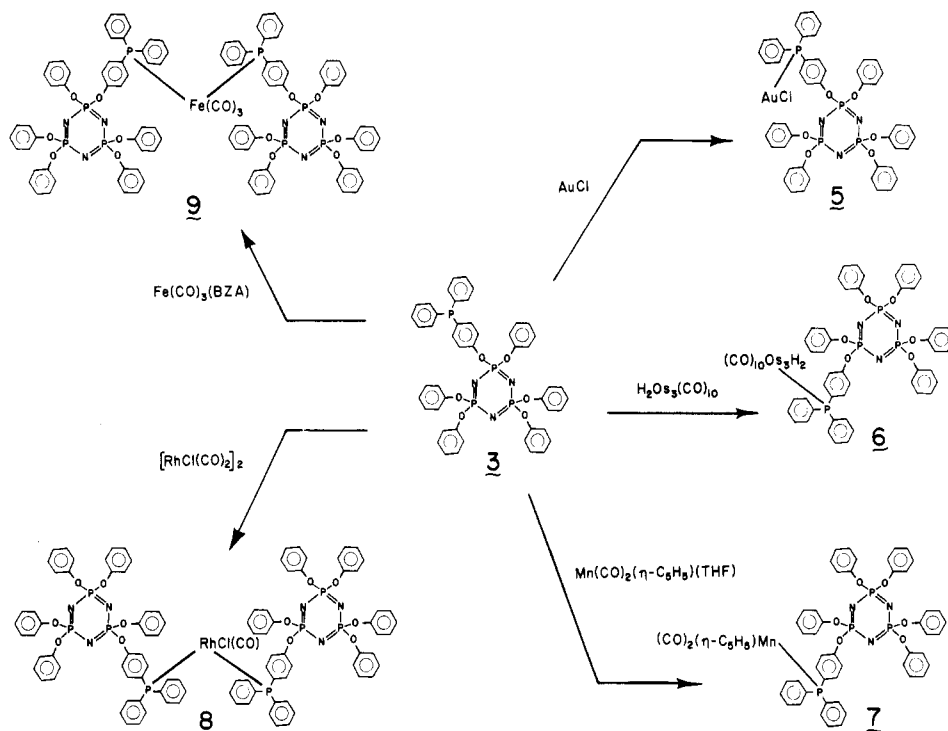
(16) Freeman, M. B.; Patrick, M. A.; Gates, B. C. *J. Catal.* 1982, 73, 82.

(17) Strohmeier, W.; Fleischmann, R.; Rehder-Stirnweiss, W. *J. Organomet. Chem.* 1973, 47, C37.

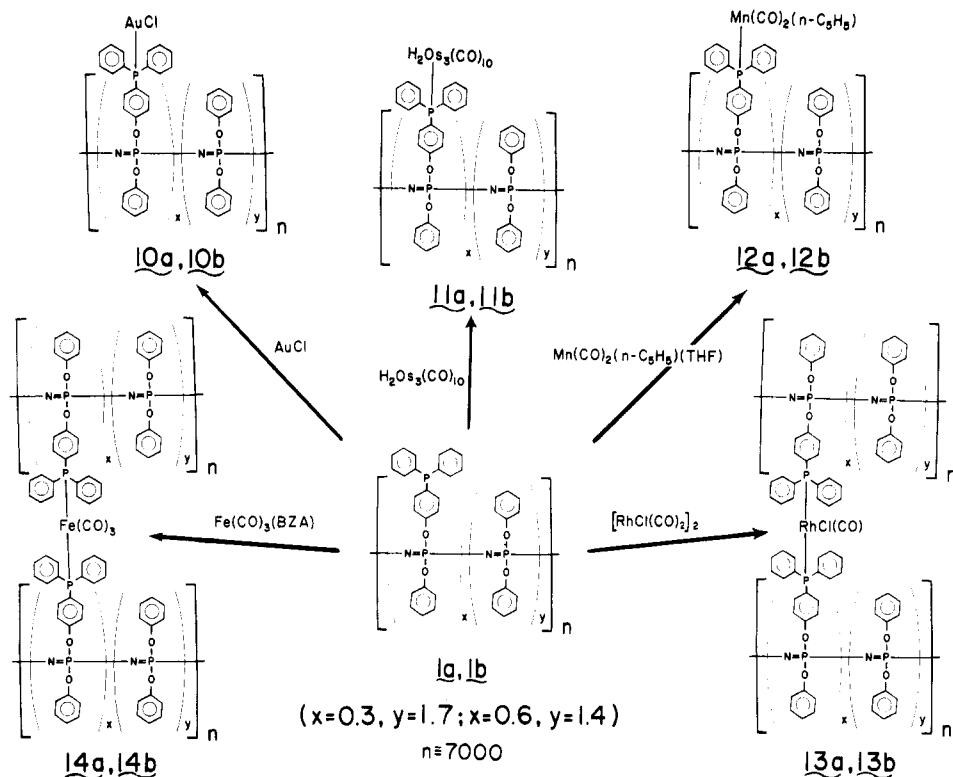
(18) Allen, R. W.; Allcock, H. R. *Macromolecules* 1976, 9, 956.

(19) Mann, F. G.; Purdie, D.; Wells, A. F. *J. Chem. Soc.* 1936, 1503; 1937, 1828.

Scheme I



Scheme II



mium-osmium double bond. Species **1**, **3**, and **4** behave in a similar manner. For example, the reaction of **3** with  $\text{H}_2\text{Os}_3(\text{CO})_{10}$  yielding the yellow, soluble complex  $\text{N}_3\text{P}_3(\text{OC}_6\text{H}_4\text{PPh}_2\text{Os}_3\text{H}_2(\text{CO})_{10})(\text{OPh})_5$  (**6**). The mode of binding between the osmium cluster and the phosphine was deduced from a combination of infrared,  $^{31}\text{P}$  NMR, and microanalytical data (Tables I and II). First, the color change from purple to yellow was indicative of coordination of the triosmium cluster to the pendent phosphine unit of **3**. The infrared spectra were essentially identical with that of  $\text{H}_2\text{Os}_3(\text{CO})_{10}\text{PPh}_3$ , with absorbances at 2110 (m),

2070 (s), 2050 (s), 2025 (s), and 1980  $\text{cm}^{-1}$ .

The  $^{31}\text{P}$  NMR spectrum of **6** showed two resonances (Table II), at  $-3$  ppm (osmium-bound phosphine) and  $+8$  ppm (skeletal phosphorus). The triphenylphosphine complex of the osmium cluster gave a similar  $^{31}\text{P}$  NMR spectrum. This is the first  $^{31}\text{P}$  NMR chemical shift reported for a phosphine-bound osmium cluster, and it is interesting that this metal cluster had a smaller influence on the  $^{31}\text{P}$  NMR chemical shift of the ligand than any of the other metals studied in this work. Colorimetric titration of **3** with increasing amounts of  $\text{H}_2\text{Os}_3(\text{CO})_{10}$  was

Table I. Microanalytical Data

compd	% C	% H	% N	% P	% others
5	calcd 51.92	3.52	3.79	11.18	
	found 51.81	3.68	3.70	11.13	
6	calcd 40.24	2.37	2.43	7.17	
	found 41.42	3.55	2.49	7.20	
7	calcd 62.62	4.17	3.98	11.76	
	found 62.67	4.30	3.99	12.01	
8	calcd 60.63	4.06	4.37	12.91	
	found 60.01	4.71	3.83	12.00	
9	calcd 62.73	4.12	4.44	13.09	
	found 62.08	4.62	4.54		
10a <sup>a,c</sup>	calcd 52.61	3.57	3.93	11.33	
	found 52.21	3.74	3.86	11.21	
10b <sup>a</sup>	calcd 50.81	3.40	3.16	10.94	
	found 50.81	3.67	3.71	10.75	
11a <sup>a</sup>	calcd 46.22	2.87	3.06	8.82	
	found 46.22	3.57	2.83	8.95	
11b <sup>a</sup>	calcd 40.23	2.33	2.05	7.12	
	found 40.23	2.62	4.28	7.09	
12a <sup>a,b</sup>	calcd 60.53	4.19			
	found 56.45	4.26			
12b <sup>a,c</sup>	calcd 63.90	4.21	3.33	11.87	
	found 60.34	4.35	3.79	11.87	
13a <sup>a,b</sup>	calcd 60.75	4.08	4.50	12.95	
	found 49.92	4.24	3.18	9.78	
13b	calcd 58.75	3.92	3.47	12.66	% Cl 2.80, % Rh 8.24
	found 55.46	4.00	4.41	12.16	2.43 7.12
14a <sup>a,b</sup>	calcd 63.76	4.29			
	found 55.83	4.56			
14b <sup>a</sup>	calcd 62.66	4.04	3.34	12.46	
	found 59.68	4.27	3.46	12.44	
[NP(OC <sub>6</sub> H <sub>4</sub> PPh <sub>2</sub> AuCl) <sub>2</sub> ] <sub>3</sub>	calcd 40.61	2.66			% Cl 6.66, % Au 37.01
	found 40.76	2.83			6.43 34.01
[NP(OC <sub>6</sub> H <sub>4</sub> PPh <sub>2</sub> Os <sub>3</sub> H <sub>2</sub> (CO) <sub>10</sub> ) <sub>2</sub> ] <sub>3</sub> <sup>d</sup>	calcd 29.16	1.39	0.61	4.03	
	found 38.70	3.38	0.54	3.60	
N <sub>3</sub> P <sub>3</sub> (OC <sub>6</sub> H <sub>4</sub> PPh <sub>2</sub> Mn(CO) <sub>2</sub> (η-C <sub>5</sub> H <sub>5</sub> ))(OC <sub>6</sub> H <sub>4</sub> PPh <sub>2</sub> ) <sub>3</sub>	calcd 69.94	4.51	2.14	14.14	
	found 69.64	4.71	2.26	13.90	
N <sub>3</sub> P <sub>3</sub> (OC <sub>6</sub> H <sub>4</sub> PPh <sub>2</sub> ) <sub>2</sub> ·Fe(CO) <sub>5</sub> (OC <sub>6</sub> H <sub>4</sub> PPh <sub>2</sub> ) <sub>4</sub>	calcd 68.77	4.34	2.17		
	found 68.70	5.35	2.30		
N <sub>3</sub> P <sub>3</sub> (OC <sub>6</sub> H <sub>4</sub> PPh <sub>2</sub> ) <sub>2</sub> ·RhCl(CO)(OC <sub>6</sub> H <sub>4</sub> PPh <sub>2</sub> ) <sub>4</sub>	calcd 66.63	4.28	2.14	14.21	
	found 66.56	4.34	2.20	13.98	
[NP(OC <sub>6</sub> H <sub>4</sub> PPh <sub>2</sub> ) <sub>2</sub> ·RhCl(CO)] <sub>3</sub>	calcd 58.04	3.66	1.83	12.16	
	found 56.89	3.88	1.72	11.89	
N <sub>3</sub> P <sub>3</sub> (OC <sub>6</sub> H <sub>4</sub> PPh <sub>2</sub> ) <sub>2</sub> ·Mn(η-C <sub>5</sub> H <sub>5</sub> )(CO)(OC <sub>6</sub> H <sub>4</sub> PPh <sub>2</sub> ) <sub>4</sub>	calcd 70.95	4.58	2.16	14.34	
	found 70.18	4.54	2.15	13.86	
[N <sub>3</sub> P <sub>3</sub> (OC <sub>6</sub> H <sub>4</sub> PPh <sub>2</sub> ) <sub>6</sub> ] <sub>2</sub> ·Mn(η-C <sub>5</sub> H <sub>5</sub> )(CO)	calcd 69.27	4.49	2.24	14.91	
	found 70.58	4.90	2.15	14.77	

<sup>a</sup> These elemental analyses were calculated based on [NP(OC<sub>6</sub>H<sub>4</sub>PPh<sub>2</sub>M)<sub>x</sub>(OPh)<sub>2-x</sub>]<sub>n</sub> (M = metal) as the repeat unit. <sup>b</sup> The % C in all these polymeric samples are low due to incomplete pyrolysis of the samples. <sup>c</sup> <sup>31</sup>P NMR showed that approximately 65% of all phosphine units in these samples were coordinated by metallo groups (see Table II). <sup>d</sup> The % C and % H in this sample are high because of solvent entrapment in the crystals. The analytical results correspond to one molecule of the osmium-phosphazene complex associated with 16 hexane molecules. (Calcd: C, 38.22; H, 3.86; N, 0.51; P, 3.37). Mass spectroscopy confirmed the inclusion of hexane molecules in the crystalline sample.

accompanied by a progressive decline in the uncoordinated phosphine peak at -7 ppm, and a growth of the coordinated form at -3 ppm. No uncoordinated phosphine groups could be detected at the end point of the titration.

Similarly, the addition of 6 equiv of H<sub>2</sub>Os<sub>3</sub>(CO)<sub>10</sub> to 4 gave [NP(OC<sub>6</sub>H<sub>4</sub>PPh<sub>2</sub>Os<sub>3</sub>H<sub>2</sub>(CO)<sub>10</sub>)<sub>2</sub>]<sub>3</sub>. Again, all the phosphine residues coordinated to the osmium cluster, as indicated by microanalytical (Table I) and <sup>31</sup>P NMR (Table II) data. The same two resonances at -3 and +8 ppm were present in a 2:1 ratio.

The behavior of the two high polymers 11a,b was more complex. Following addition of the osmium cluster, an immediate color change from purple to yellow occurred. The polymeric system retained its solubility in tetrahydrofuran at this stage (and, hence, was not coordinatively crosslinked). However, precipitation of the polymer into hexane yielded a solid polymer that did not redissolve in tetrahydrofuran. Infrared spectra provided some evidence for the presence of a decarbonylated complex of the type (phosphine)<sub>x</sub>H<sub>2</sub>Os<sub>3</sub>(CO)<sub>9</sub>, and it is speculated that

cross-links of this type are formed.

**Reactions of Mn(CO)<sub>3</sub>(η-C<sub>5</sub>H<sub>5</sub>) with 1, 3, and 4.** THF complexes derived from Mn(CO)<sub>3</sub>(η-C<sub>5</sub>H<sub>5</sub>) can be prepared by photolytic decarbonylation in tetrahydrofuran to yield Mn(CO)<sub>2</sub>(η-C<sub>5</sub>H<sub>5</sub>)·THF.<sup>20</sup> The THF ligand can then be displaced by strongly coordinating ligands such as phosphine to yield Mn(CO)<sub>2</sub>(η-C<sub>5</sub>H<sub>5</sub>)(phosphine). A color change from red to yellow accompanies phosphine binding. This color change was observed when excess Mn(CO)<sub>2</sub>(η-C<sub>5</sub>H<sub>5</sub>)·THF was brought into contact with 1, 3, or 4. The <sup>31</sup>P NMR spectra and microanalyses (Tables I and II) were consistent with the coordination of all the available phosphine groups. For example, two <sup>31</sup>P NMR resonances were detected in each case, at +92 ppm (Mn-bound phosphine) and +8 ppm (trimeric skeletal phosphorus) or -19 ppm (polymer skeletal phosphorus). The infrared spectra in the carbonyl region (1934 and 1870 cm<sup>-1</sup>) were

Table II.  $^{31}\text{P}$  NMR and Infrared Characterization Data

compd	$^{31}\text{P}$ NMR, <sup>a</sup> ppm			IR, <sup>b</sup> $\text{cm}^{-1}$
	P	PN	PM	
3	-8 (1)	8 (3)		
1	-8	-19		
4	-7 (6)	8 (3)		
5		8 (3)	33 (1)	
6		8 (3)	-3 (1)	2110 m, 2070 s, 2050 s, 2025 s, 1980 s
7		8 (3)	93 (1)	1934 s, 1870 s
8		8 (3)	29 (1, $J_{\text{Rh-P}} = 129 \text{ Hz}$ )	1979 s
9		8 (3)	83 (1)	1881 s
10a		-19	33	
10b		-19	33	
11a	-7 (5%)	-20	-3	2110 m, 2067 s, 2050 s, 2025 s, 1985 s
11b		-20	-3	2110 m, 2067 s, 2050 s, 2025 s, 1985 s
12a		-19	92	1934 s, 1870 s
12b	-7 (8%)	-20	c	2015 s, <sup>d</sup> 1934 s, 1871 s
13a		-20	28	1980 s
13b		-19	29 ( $J_{\text{Rh-P}} = 134 \text{ Hz}$ )	1985 s
14a		-20	51, 82 ( $J_{\text{Rh-P}} = 128 \text{ Hz}$ )	1990 s, 1934 s, 1886 s
14b		-20	51, 81	1998 s, 1940 s, 1880 s
[NP(OC <sub>6</sub> H <sub>4</sub> PPh <sub>2</sub> ·AuCl) <sub>2</sub> ] <sub>3</sub>		8 (3)	33 (6)	
AuCl(PPh <sub>3</sub> )			33	
H <sub>2</sub> Os <sub>3</sub> (CO) <sub>10</sub> (PPh <sub>3</sub> )			-2	2110 m, 2067 s, 2050 s, 2025 s, 1985 s
[NP(OC <sub>6</sub> H <sub>4</sub> PPh <sub>2</sub> ·H <sub>2</sub> Os <sub>3</sub> (CO) <sub>10</sub> ) <sub>2</sub> ] <sub>3</sub>		8 (3)	-3 (6)	2110 m, 2070 s, 2050 s, 2025 s, 1980 s
Mn(CO) <sub>2</sub> (η-C <sub>5</sub> H <sub>5</sub> )(PPh <sub>3</sub> )			92, 2 <sup>24,25</sup>	1937 s, 1870 s
Mn(CO)(η-C <sub>5</sub> H <sub>5</sub> )(PPh <sub>3</sub> ) <sub>2</sub>			92 <sup>24,25</sup>	1827 s
N <sub>3</sub> P <sub>3</sub> (OC <sub>6</sub> H <sub>4</sub> PPh <sub>2</sub> ) <sub>2</sub> Mn(CO) <sub>2</sub> (η-C <sub>5</sub> H <sub>5</sub> )(OC <sub>6</sub> H <sub>4</sub> PPh <sub>2</sub> ) <sub>5</sub>	-7 (5)	8 (3)	92 (1)	1932 s, 1865 s
Fe(CO) <sub>3</sub> (PPh <sub>3</sub> ) <sub>2</sub>			82	1886 s
Fe(CO) <sub>3</sub> (BZA)(PPh <sub>3</sub> )			54	1996 s, 1933 s
N <sub>3</sub> P <sub>3</sub> (OC <sub>6</sub> H <sub>4</sub> PPh <sub>2</sub> ) <sub>2</sub> ·Fe(CO) <sub>3</sub> (OC <sub>6</sub> H <sub>4</sub> PPh <sub>2</sub> ) <sub>4</sub>	-6 (4)	9 (3)	82 (2)	1970 w, 1887 sh, 1876 s
RhCl(CO)(PPh <sub>3</sub> ) <sub>2</sub>			29 ( $J_{\text{Rh-P}} = 127 \text{ Hz}$ )	1980 s
RhCl(CO) <sub>2</sub> PPh <sub>3</sub>			45 ( $J_{\text{Rh-P}} = 175 \text{ Hz}$ )	2088 s, 2002 s
N <sub>3</sub> P <sub>3</sub> (OC <sub>6</sub> H <sub>4</sub> PPh <sub>2</sub> ) <sub>2</sub> ·RhCl(CO)(OC <sub>6</sub> H <sub>4</sub> PPh <sub>2</sub> ) <sub>4</sub> <sup>e</sup>	-8 (4)	8 (3)	27 ( $J_{\text{Rh-P}} = 129 \text{ Hz}$ ) (2)	1980 s
Mn(η-C <sub>5</sub> H <sub>5</sub> )(CO) <sub>3</sub>				2025 s, 1935 s
Fe(CO) <sub>3</sub> (PhCH=CHC(O)CH <sub>3</sub> )				2069 s, 2006 s, 1987 s
H <sub>2</sub> Os <sub>3</sub> (CO) <sub>10</sub>				2112 w, 2078 s, 2065 m, 2024 s, 2011 s, 1988 m, 1973 w, 1957 w
[RhCl(CO) <sub>2</sub> ] <sub>2</sub>				2068 s, 1994 <sup>f</sup> s 2107 m, 2092 s, 2080 w, 2036 s, 2002 w <sup>g</sup>

<sup>a</sup> Resonances are reported as positive values downfield from 85% H<sub>3</sub>PO<sub>4</sub>. P = uncoordinated phosphine; PN = phosphazene phosphorus; PM = metal coordinated phosphine. Peak integrations are given in parentheses. <sup>b</sup> 2200-1700  $\text{cm}^{-1}$ . Spectra obtained as solutions of THF. <sup>c</sup> Not available. <sup>d</sup> Starting material. <sup>e</sup> At -80 °C. <sup>f</sup> In THF. <sup>g</sup> In hexane.

very similar to that of Mn(CO)<sub>2</sub>(η-C<sub>5</sub>H<sub>5</sub>)(PPh<sub>3</sub>) (1937 and 1870  $\text{cm}^{-1}$ ). The bis(phosphine) species Mn(CO)(η-C<sub>5</sub>H<sub>5</sub>)(PPh<sub>3</sub>)<sub>2</sub>, which is an alternative type of product, absorbs at 1827  $\text{cm}^{-1}$ . It should be noted that saturation of all the available phosphine sites in 1, 3, and 4 required the presence of an excess of the metal carbonyl. The interaction of 1 equiv each of Mn(CO)<sub>2</sub>(η-C<sub>5</sub>H<sub>5</sub>)·THF with 4 left some phosphine groups uncomplexed [N<sub>3</sub>P<sub>3</sub>(OC<sub>6</sub>H<sub>4</sub>PPh<sub>2</sub>)<sub>5</sub>(OC<sub>6</sub>H<sub>4</sub>PPh<sub>2</sub>)<sub>2</sub>Mn(η-C<sub>5</sub>H<sub>5</sub>)(CO)<sub>2</sub>]. The  $^{31}\text{P}$  NMR spectrum of the yellow product showed resonance at +92 ppm (Mn-bound phosphine), +8 ppm (skeletal phosphorus), and -7 ppm (uncoordinated phosphorus).

Once again, the high polymers behaved in an anomalous fashion after being isolated in the solid state. When first prepared, the complexes were soluble in tetrahydrofuran. However, after precipitation into degassed hexane, this solubility was lost. It is speculated that the close proximity of functional groups in the solid state favors reorganization

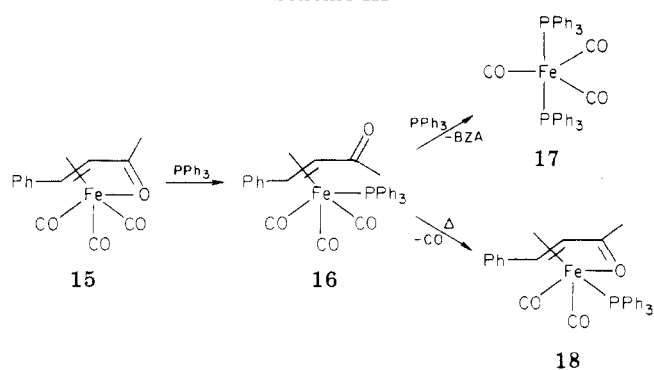
and further decarbonylation to yield a matrix cross-linked by Mn(CO)(η-C<sub>5</sub>H<sub>5</sub>)(phosphine)<sub>2</sub> units. Only one cross-link per chain (i.e., one cross-linked per ≈ 15 000 repeating units) would be sufficient to insolubilize most of the system, and this may explain why the characteristic (bis(phosphine)) infrared band at 1827  $\text{cm}^{-1}$  was not detected.

The role of 4 as a multidentate ligand for reactions with Mn(CO)<sub>2</sub>(η-C<sub>5</sub>H<sub>5</sub>)·THF is discussed in a later section.

**Reactions of Fe(CO)<sub>3</sub>(PhCH=CHC(O)CH<sub>3</sub>) with 1, 3, and 4.** Complexes between phosphines and transition metals may also be generated by displacement of the benzylideneacetone (BZA) ligand from the metal. For example, Fe(CO)<sub>3</sub>(PhCH=CHC(O)CH<sub>3</sub>) reacts with phosphines to displace either the benzylideneacetone unit or carbon monoxide.<sup>21</sup> For triphenylphosphine, the

(21) Vessieres, A.; Dixneuf, P. *Tetrahedron Lett.* 1974, 16, 1499. Reckziegel, A.; Bigorgne, M. *J. Organomet. Chem.* 1965, 3, 341.

Scheme III



pathways shown in Scheme III are possible (see Experimental Section). Presumably, these options are also available for the complexes of 1, 3, and 4.

Polymers **1a,b** reacted with  $\text{Fe}(\text{CO})_3(\text{BZA})$  to form soluble polymeric complexes. Subsequent manipulation of these complexes in concentrated solutions or in the solid state yielded cross-linked macromolecules of the type shown in 14. In **14a**, with a lower density of pendent groups, the cross-linking process yielded a swollen gel in tetrahydrofuran after concentration.  $^{31}\text{P}$  NMR spectra before insolubilization showed resonances at +82 ppm ( $\text{Fe}(\text{CO})_3(\text{phosphine})_2$  species), +54 ppm ( $\text{Fe}(\text{CO})_2(\text{BZA})(\text{phosphine})$ ), and -19 ppm (skeletal phosphorus). The first two assignments were made by comparison with the cyclic model systems (see below). The infrared spectra were also compatible with the assigned structure. Polymer **1b**, with its higher loading of phosphine residues, formed an insoluble and largely nonswellable matrix, cross-linked via  $\text{Fe}(\text{CO})_3(\text{phosphine})_2$  units.

Compound **3** reacted with  $\text{Fe}(\text{CO})_3(\text{BZA})$  with total displacement of benzylideneacetone to yield the analogue of 17, viz.,  $[\text{N}_3\text{P}_3(\text{OC}_6\text{H}_4\text{PPh}_2)(\text{OPh})_5]_2\text{Fe}(\text{CO})_3$  (**9**), a yellow solid that was soluble in THF or chlorinated organic media. An infrared spectrum of **9** contained only one carbonyl absorbance peak at  $1881(\text{s})\text{ cm}^{-1}$ , which was indicative of coordination to iron by two phosphine units. The related complex  $\text{Fe}(\text{CO})_3(\text{PPh}_3)_2$  has a similar spectrum, with an infrared absorption at  $1886(\text{s})\text{ cm}^{-1}$ . By contrast,  $\text{Fe}(\text{CO})_2(\text{BZA})(\text{PPh}_3)$  absorbs at  $1996(\text{s})$  and  $1934(\text{s})\text{ cm}^{-1}$ . Elemental microanalyses data for **9** are summarized in Table I. The  $^{31}\text{P}$  NMR spectrum of **9** consisted of two resonances, at +83 ppm (iron-bound phosphine) and +10 ppm (skeletal phosphorus).

Species **4** reacted with  $\text{Fe}(\text{CO})_3(\text{BZA})$  to yield an unusual product,  $\text{N}_3\text{P}_3(\text{OC}_6\text{H}_4\text{PPh}_2)_2\text{Fe}(\text{CO})_3(\text{OC}_6\text{H}_4\text{PPh}_2)_4$ , which will be discussed in a later section.

It should be noted that compounds analogous to **18** were also formed as byproducts in these reactions. For the cyclic model systems, these species could be separated readily from the other products by column chromatography techniques.

**Reactions of  $[\text{RhCl}(\text{CO})_2]_2$  with 1, 3, and 4.** It is well-known that  $[\text{RhCl}(\text{CO})_2]_2$  reacts readily with triphenylphosphine to yield  $\text{RhCl}(\text{CO})(\text{PPh}_3)_2$ . The high polymers **1a,b** were interacted with  $[\text{RhCl}(\text{CO})_2]_2$  in tetrahydrofuran to yield yellow-orange, insoluble polymeric complexes. The insolubility is almost certainly a consequence of crosslink formation in which CO is displaced from rhodium by two phosphine units on different polymer chains. The evidence for this was provided by the behavior of the small molecule model phosphazenes.

Treatment of **3** with  $[\text{RhCl}(\text{CO})_2]_2$  yielded **8**, an analogue of **9**. This illustrates the tendency of these systems to cross-link by the introduction of two phosphine units into

the metal coordination sphere. However, because only one cross-link site is available in **3**, the solid yellow product **8** was soluble in tetrahydrofuran or chlorinated organic solvents. Confirmation of the structure of **8** was obtained by a combination of  $^{31}\text{P}$  NMR and microanalytical data (Tables I and II). For example, two  $^{31}\text{P}$  NMR resonances were detected at +29 ppm ( $J_{\text{Rh-P}} = 129\text{ Hz}$ ) and +8 ppm (skeletal phosphorus). The infrared spectra showed one absorbance only in the carbonyl region at  $\approx 1979(\text{s})\text{ cm}^{-1}$ , which can be compared to the value of  $1980(\text{s})\text{ cm}^{-1}$  for  $\text{RhCl}(\text{CO})(\text{PPh}_3)_2$ . By contrast, mono(phosphine) complexation yielded two bands, found at  $2093(\text{s})$  and  $2009(\text{s})\text{ cm}^{-1}$  for  $\text{RhCl}(\text{CO})_2(\text{PPh}_3)$ .<sup>22</sup>

Internal bis(phosphine) complexation occurred with **4**, and this will be considered in the following section.

#### Behavior of **4** as a Mono- or Bidentate Ligand.

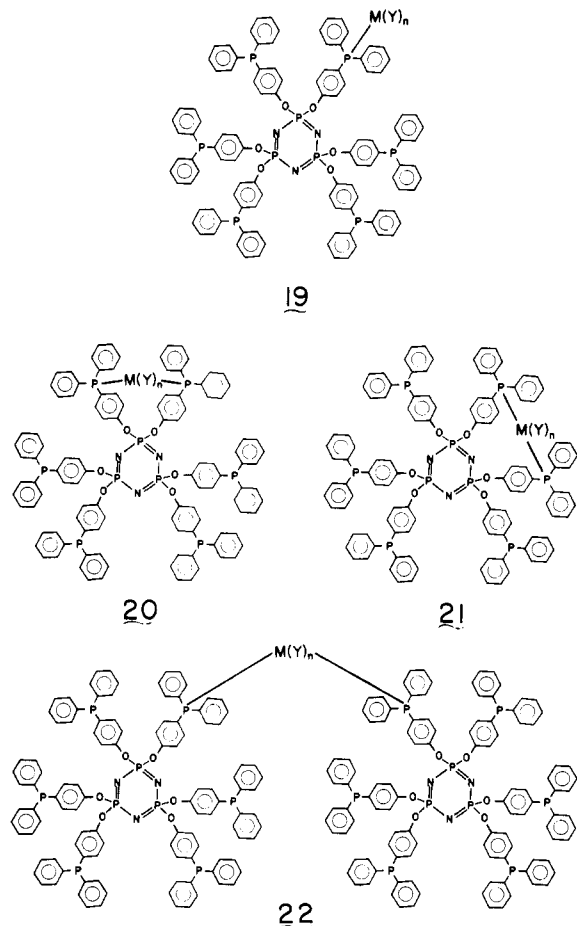
Compound **4** is, in principle, capable of forming three types of complexes with transition-metal compounds. The simplest possibility is that it can function as a monodentate ligand for six metallo units. This behavior is seen with  $\text{AuCl}$ . The second, and most complex, possibility would involve cross-linking reactions in which each phosphine unit in **4** is independently capable of coordination to a metallo unit that can itself accept two (or more) phosphine donor units. Such three-dimensional matrices would be totally insoluble and difficult to study structurally, although the degree of cross-linking would depend on the molar ratios of the reactants. Only at the stoichiometric limit of two phosphazene molecules to one metal unit would intermolecular linkage lead to a discrete, soluble product. Third, the possibility exists that, under the limiting stoichiometric conditions of one molecule of phosphazene reacting with one of organometallic reagent, each molecule of **4** could provide two phosphine units for chelation to a metallo unit. Such species would also be non-cross-linked and, therefore, soluble. As will be shown, all three types of behavior are possible when **4** reacts with  $\text{Mn}(\eta\text{-C}_5\text{H}_5)(\text{CO})_2(\text{THF})$ ,  $\text{Mn}(\eta\text{-C}_5\text{H}_5)(\text{CO})_3$ ,  $\text{Fe}(\text{CO})_3(\text{BZA})$ , or  $[\text{RhCl}(\text{CO})_2]_2$ . Hence, a study of these reactions is likely to provide an insight into the factors that effect cross-linking or chelation in the high polymers, especially those that contain a high ratio of phosphine sites per repeating unit. For simplicity, these reactions were studied under conditions in which one molecule of **4** would be expected to react with only one molecule of organometallic reagent. In fact, under different reaction conditions, three different types of structures were formed, as depicted in **19–22**. It was not possible to distinguish between **20** and **21**.

$\text{Mn}(\eta\text{-C}_5\text{H}_5)(\text{CO})_2(\text{THF})$  reacted with **4** in a two-step reaction—first with displacement of THF and formation of a derivative of type **19**,  $[\text{N}_3\text{P}_3(\text{OC}_6\text{H}_4\text{PPh}_2)_2\text{Mn}(\eta\text{-C}_5\text{H}_5)(\text{CO})_2(\text{OC}_6\text{H}_4\text{PPh}_2)_5]$ , and subsequently, following ultraviolet irradiation and decarbonylation, to form a species of type **20** or **21**,  $[\text{N}_3\text{P}_3(\text{OC}_6\text{H}_4\text{PPh}_2)_2\text{Mn}(\eta\text{-C}_5\text{H}_5)(\text{CO})(\text{OC}_6\text{H}_4\text{PPh}_2)_4]$ . This second step was monitored by  $^{31}\text{P}$  NMR and infrared spectroscopy (see Experimental Section). The identity of **20/21** was also confirmed by its molecular weight (1962, compared with a calculated value of 1945).<sup>23</sup>

Species **20/21** was also prepared by an alternative route that involved the photolysis of  $\text{Mn}(\eta\text{-C}_5\text{H}_5)(\text{CO})_3$  in the presence of **4**. Compound **19** was not detected from this reaction (except after very short irradiation times), but

(22) Rollman, L. D. *Inorg. Chim. Acta.* 1972, 6, 137.

(23) Molecular weights were determined by Galbraith Laboratories, Knoxville, Tenn., with the use of vapor-phase osmometry in benzene. The compounds  $[\text{NP}(\text{OC}_6\text{H}_4\text{Br-}p)_2]_3$  and **4** were used as standards.



compound 22 was isolated as a coproduct. This suggests the possibility of an interconversion of the intra- and intermolecularly bonded forms and that 19 and 4 react to form 22. As might be expected, the infrared spectra of 20/21 and 22 were identical, and the  $^{31}\text{P}$  NMR spectrum of 22 was similar to that of 19.<sup>24</sup> However, a solution molecular weight measurement<sup>23</sup> suggested a value of 3755. The calculated value for 22 is 3742.

The reaction of  $\text{Fe}(\text{CO})_3(\text{BZA})$  with 4 resulted in displacement of the BZA ligand and formation of a product of type 20 or 21,  $[\text{N}_3\text{P}_3(\text{OC}_6\text{H}_4\text{PPh}_2)_2\text{Fe}(\text{CO})_3(\text{OC}_6\text{H}_4\text{PPh}_2)_4]$ . The structure of this complex was confirmed by comparison of the  $^{31}\text{P}$  NMR (Table II) and infrared data of this compound with those of  $\text{Fe}(\text{CO})_3(\text{PPh}_3)_2$ . This latter model gives rise to one infrared band at  $1886\text{ cm}^{-1}$ , while the phosphazene analogue (20 or 21) shows peaks at  $1970\text{ (w)}$ ,  $1887\text{ (s)}$  (shoulder), and  $1876\text{ (s)}$   $\text{cm}^{-1}$ . This difference between the model and the phosphazene may indicate a slight distortion from the idealized geometry around iron in species 20 or 21. The measured molecular weight<sup>23</sup> was 1980, compared to a calculated value of 1937 for 20/21. No products of type 22 were detected.

$[\text{RhCl}(\text{CO})_2]_2$  also reacted with 4 to yield a species of type 20/21. The infrared absorbance at  $1980\text{ cm}^{-1}$  ( $\text{RhCO}$ ) matched the similar absorbance found in the spectrum of  $\text{RhCl}(\text{CO})(\text{PPh}_3)_2$ . Again, under the reaction conditions

(24) With  $\text{Mn}(\eta\text{-C}_5\text{H}_5)(\text{CO})_2$  or  $\text{Mn}(\eta\text{-C}_5\text{H}_5)(\text{CO})$  as the complex, species 19, 20/21, and 22 all gave  $^{31}\text{P}$  NMR resonances at +92 ppm (coordinated phosphine), +8 ppm (skeletal phosphorus), and -7 ppm (uncoordinated phosphine). The relative areas of these resonances were 1:3:5 for 19 and 2:3:4 for 20. Reported values for  $\text{Mn}(\eta\text{-C}_5\text{H}_5)(\text{CO})_2(\text{PPh}_3)$  and  $\text{Mn}(\eta\text{-C}_5\text{H}_5)(\text{CO})(\text{PPh}_3)_2$  are 92.0 and 92.2 ppm, respectively.<sup>25</sup>

(25) Ginzberg, A. G.; Federov, L. A.; Petrovski, P. V.; Fedin, E. I.; Setkira, V.; Kursanov, D. N. *J. Organomet. Chem.* 1974, 73, 77.

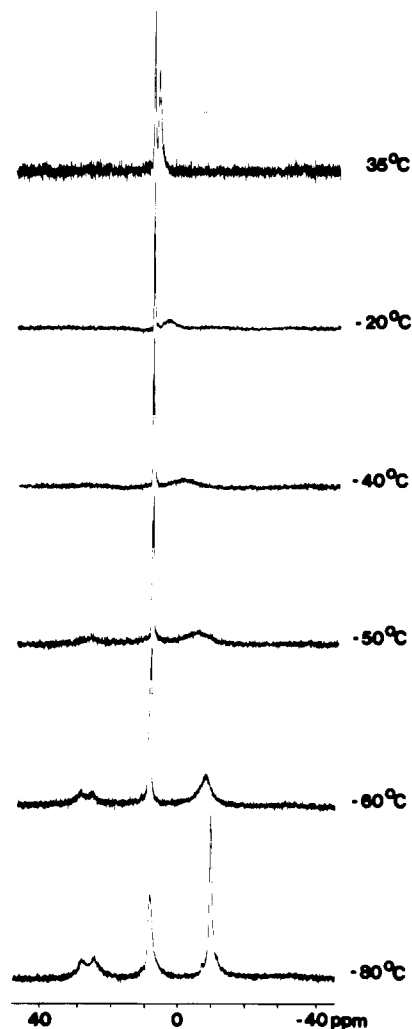


Figure 1.  $^{31}\text{P}$  NMR spectra of  $[\text{RhCl}(\text{CO})][\text{N}_3\text{P}_3(\text{OC}_6\text{H}_4\text{PPh}_2)_6]$  (27) in  $\text{CD}_2\text{Cl}_2$  at various temperatures.

employed, no products corresponding to 19 or 22 were isolated or detected.

One other consideration needs to be taken into account—the ease of intra- or intermolecular phosphine ligand exchange between species such as 20 or 21 or between either of these and transient cycloliner polymers derived from 22. This has important practical ramifications since it could explain why most of the high polymeric complexes are soluble (and, hence, non-cross-linked) when first formed but become cross-linked after concentration to form a solid polymer.

Variable-temperature  $^{31}\text{P}$  NMR analysis of the  $\text{RhCl}(\text{CO})$  complex with 4 provided strong evidence for ligand exchange and for the probable interconversion of species of types 20 and 21 at room temperature. At  $-80\text{ }^\circ\text{C}$  in  $\text{CD}_2\text{Cl}_2$ , the  $^{31}\text{P}$  NMR spectrum showed the expected doublet at +27 ppm for the rhodium-bound phosphine ( $J_{\text{Rh-P}} = 129\text{ Hz}$ ) and a singlet at -8 ppm from the uncoordinated phosphine ligands. This is consistent with a static system containing 20, 21, or both. However, when the system was warmed, these signals broadened and coalesced at  $-40\text{ }^\circ\text{C}$  and emerged as a singlet at +4 ppm ( $35\text{ }^\circ\text{C}$ ) (Figure 1). This situation is consistent with a time-averaged exchanging system that involves all forms of 20, 21, and 22. When recooled to  $-80\text{ }^\circ\text{C}$ , the signal was resolved back into the original spectrum of the static system. Rapid exchange of this type is clearly important for the development of catalytic properties. In a polymer system, it is almost certain to generate transient cross-links.

The larger the number of metallo units attached to the chain, the greater is the probability that at any instant enough cross-links will be present to insolubilize the chains.

The  $^{31}\text{P}$  NMR spectra derived from the complexes of 4 with the other organometallic species provided no evidence for rapid exchange of the phosphine ligands. The manganese derivative of type 19 was studied over the temperature range of  $-80$  to  $+110$  °C, the osmium derivative of type 19 over the range of  $-80$  to  $+100$  °C and the iron derivative of type 20/21 over the range of  $-95$  to  $+80$  °C.

**Catalytic Activity.** The osmium-bound phosphazenes  $\text{N}_3\text{P}_3(\text{OC}_6\text{H}_4\text{PPh}_2\text{Os}_3\text{H}_2(\text{CO})_{10})(\text{OPh})_5$  (6),  $[\text{NP}(\text{OC}_6\text{H}_4\text{PPh}_2\text{Os}_3\text{H}_2(\text{CO})_{10})_2]_3$ ,  $[\text{NP}(\text{OC}_6\text{H}_4\text{PPh}_2\text{Os}_3\text{H}_2(\text{CO})_{10})_{0.3}(\text{OPh})_{1.7}]_n$  (11), and  $\text{H}_2\text{Os}_3(\text{CO})_{10}\text{PPh}_3$  were compared as catalysts for the isomerization of 1-hexene to 2-hexene (see Experimental Section). The disappearance of 1-hexene and formation of 2-hexene were observed for all four catalyst systems. The activities found for 6,  $[\text{NP}(\text{OC}_6\text{H}_4\text{PPh}_2\text{Os}_3\text{H}_2(\text{CO})_{10})_2]_3$ , and  $\text{H}_2\text{Os}_3(\text{CO})_{10}\text{PPh}_3$  were similar, with 77–84% conversions to 2-hexene taking place during 300 min at 65 °C and a substrate to metal cluster ratio of 100:1. The polymer-bound catalyst was slightly less active; a 60% conversion to 2-hexene occurred under the same conditions. This slight retardation by the polymer can probably be ascribed to steric effects and reduced diffusional mobility within the polymer matrix. Similar effects have been reported when polystyrene serves as a carrier molecule.<sup>16</sup> In all four cases, the catalytic activity ceased following the formation of  $[\text{HOs}_3(1\text{-hexene})(\text{CO})_{10}(\text{phosphine})]$ . This is also in agreement with other studies.<sup>16</sup>

### Experimental Section<sup>26</sup>

**Materials.** Tetrahydrofuran (THF) was distilled under nitrogen from sodium benzophenone ketyl. Tricarbonylcyclopentadienylmanganese and nonacarbonyliron (Alfa-Ventron), dodecacarbonyltriosmium, and hydrogen tetrachloroaurate (Strem) were used as received. Dichlorotetracarbonyliron (Strem) and benzylideneacetone (Aldrich) were sublimed before use. Flosil (Applied Science) was used for column chromatography. All synthesis reactions were carried out under an atmosphere of dry nitrogen (Matheson).

**Synthesis of Phosphazenes.** The synthesis of 1, 3, and 4 were reported in earlier publications.<sup>13,14</sup> They involved the preparation of (*p*-bromophenoxy)phosphazenes, with or without phenoxy cosubstituent groups, replacement of bromo by lithio units by treatment with *n*-butyllithium, and reaction of the lithio derivatives with diphenylchlorophosphine. Some modifications to the earlier procedure were used in the present work. In the synthesis of 3, the lithiation step took place over a period of 0.5 h (instead of 1 h), and the final phosphine-coupled product was isolated by medium-pressure column chromatography with toluene used as the eluent. The authenticity of 1, 3, and 4 was confirmed by  $^{31}\text{P}$  NMR spectroscopy. For 1a or b, the degree of incorporation of phosphine units (*x*) was estimated from the  $^{31}\text{P}$  NMR peak integration of the phosphine and phosphazene nuclei. Elemental analysis at the (bromophenoxy)phosphazene stage was also used as a method for the indirect estimation of the final phosphine content.

(26)  $^{31}\text{P}$  NMR spectra were obtained in the Fourier transform mode at 40.4 MHz with a JEOL PS-100 FT, a Bruker WP-200 FT, or a Varian CFT-20 FT NMR spectrometer.  $^1\text{H}$  NMR spectra were also obtained with the Bruker WP-200 FT instrument. Infrared spectra were recorded with the use of a Perkin-Elmer Model PE 580 high-resolution spectrometer. Elemental microanalyses were obtained by Galbraith Laboratories, Knoxville, Tenn. The composition of the reaction mixtures during the catalytic experiments was established by the use of a Varian Model 3700 gas chromatography instrument with a flame ionization detector. Separation was accomplished on a column containing 20% ethylene glycol and  $\text{AgNO}_3$  on 45/60 Chromosorb supplied by Supelco, Inc. Identification of the products was accomplished by using coinjection procedures with the appropriate reference materials.

**Reactions of AuCl with 1, 3, and 4.** Gold chloride was prepared from chloroauric acid by the method of Mann, Purdie, and Wells.<sup>19</sup> Typically, a solution of AuCl (0.20 g) in water/ethanol (5–10 mL) was diluted to 50 mL with freshly distilled THF. (Residual thiodiethanol reducing agent was also present.) The appropriate amount of this solution was then added dropwise to chilled ( $-10$  to  $0$  °C) solutions of 1, 3, or 4 in THF ( $\approx 150$  mL). Typically, 0.5 g of the polymers was used. The reactant stoichiometries were adjusted to provide a slight molar excess of AuCl over that required to coordinate to the available phosphine groups in 1, 3, or 4. The solvent volume was then reduced, and water (for 3 or 4) or hexane (for 1) was added until the product precipitated. The polymers were precipitated into water to remove included, unreacted AuCl. The products were washed thoroughly with pentane and were dried in vacuo. No oxidation products were detected. Elemental microanalysis and  $^{31}\text{P}$  NMR data are summarized in Tables I and II.

**Reactions of  $\text{H}_2\text{Os}(\text{CO})_{10}$  with 1, 3, and 4.** The osmium cluster  $\text{H}_2\text{Os}_3(\text{CO})_{10}$  was prepared from  $\text{Os}_3(\text{CO})_{12}$  and hydrogen by the method described by Knox, Koepke, Andrews, and Kaesz.<sup>27</sup>  $\text{H}_2\text{Os}_3(\text{CO})_{10}$  (0.2 g) in THF (50 mL) was added to a solution of the phosphazene in  $\approx 150$  mL of THF. The exact molar ratios of the reactants were adjusted to ensure saturation of all the phosphine sites in each carrier molecule. The characteristic color change from purple to yellow occurred in each case. The products derived from 3 and 4 were purified by column chromatography and were isolated by removal of the solvents under vacuum. Compound 6, derived from 3, was a yellow oil that was soluble in THF or chlorinated organic solvents. The product from 4 was a yellow solid. The product from 1 became insoluble only after removal of the THF solvent. Characterization was by a combination of elemental microanalysis,  $^{31}\text{P}$  NMR spectroscopy, and infrared spectroscopy (see Tables I and II).

**Reactions of  $\text{Mn}(\text{CO})_3(\eta\text{-C}_5\text{H}_5)$  with 1, 3, 4, or  $\text{PPh}_3$ .** The complex  $\text{Mn}(\text{CO})_3(\eta\text{-C}_5\text{H}_5)$  (0.3 g) in THF (50 mL) was irradiated in a quartz reaction vessel for 1–2 h by means of a Black-Ray ultraviolet lamp (250 W) to yield a red solution of  $\text{Mn}(\text{CO})_2(\eta\text{-C}_5\text{H}_5)(\text{THF})$ . A solution of the phosphazene (sufficient to ensure the correct reactant stoichiometry) in THF (150 mL) was then treated with the manganese reagent. The polymeric ligands required repeated treatment with the manganese reagent. A slow color change, from red to yellow, took place during 4–15 h at 25 °C. The polymeric complexes from 1 were prepared by a 3-h vacuum photolysis of  $\text{Mn}(\text{CO})_3(\eta\text{-C}_5\text{H}_5)$ , followed by dropwise addition of this reagent to the polyphosphazene solution. The resultant solution was used for the spectroscopic analyses, and the polymer was isolated by precipitation under vacuum into degassed hexane. This material did not redissolve in THF. Similarly, removal of the solvent from the crude reaction mixture led to insolubilization of the polymer. The products derived from 3, 4, or  $\text{PPh}_3$  were isolated by removal of the solvent on a rotary evaporator, followed by chromatography with the use of hexane/methylene chloride mixtures as eluents. Characterization data are listed in Tables I and II.

Derivatives of type 19, 20/21, or 22 were prepared by the interaction of equimolar amounts of 4 and  $\text{Mn}(\text{CO})_3(\eta\text{-C}_5\text{H}_5)$ . Species 19 formed following ultraviolet irradiation; compounds 20/21 and 22 formed during irradiation over a period of 25 h. These latter two products were separated by column chromatography. Species 20/21 eluted first with methylene chloride as eluent; compound 22 was then recovered by elution with acetone.

The controlled conversion of 19 to 20/21 was accomplished in the following way: compound 19 (0.152 g, 0.077 mol) in THF (4 mL) was irradiated in a 10-mm NMR tube under nitrogen.  $^{31}\text{P}$  NMR spectra were recorded after 0, 30, 60, 105, 165, and 270 min of irradiation. After each  $^{31}\text{P}$  NMR analysis, a 0.2-mL aliquot was withdrawn by syringe for infrared analysis. In the  $^{31}\text{P}$  NMR spectra, the area of the phosphine resonance decreased from the equivalent of 5 uncoordinated phosphine units to 4. At the same time, the area of the manganese–phosphine resonance doubled. The phosphazene resonance became resolved into a distinct doublet (relative areas of 2:1) as irradiation proceeded. The infrared spectra showed a growth of a peak at  $1820\text{ cm}^{-1}$  (from

(27) Knox, S. A. R.; Koepke, J. W.; Andrews, M. A.; Kaesz, H. D. *J. Am. Chem. Soc.* 1975, 97, 3942.



20/21), and a decrease and eventual disappearance of the bands at 1932 and 1865  $\text{cm}^{-1}$ , characteristic of 19.

**Reactions of  $\text{Fe}(\text{CO})_3(\text{PhCH}=\text{CHC}(\text{O})\text{CH}_3)$  with 1, 3, 4, and Triphenylphosphine.**  $\text{Fe}(\text{CO})_3(\text{PhCH}=\text{CHC}(\text{O})\text{CH}_3)$  was prepared by the method of Evans, Johnson, and Lewis.<sup>28</sup> This compound (0.18 g, 0.63 mmol) in THF (50 mL) was added dropwise to the phosphazene in THF (150 mL) at 0–10 °C, with the reaction allowed to proceed at this temperature for several hours and at 20 °C for several days. The stoichiometry of the reactants was varied to form different products. The disappearance of  $\text{Fe}(\text{CO})_3(\text{PhCH}=\text{CHC}(\text{O})\text{CH}_3)$  was monitored by infrared spectroscopy. The cyclophosphazene products were isolated by column chromatography with elution by methylene chloride/hexane mixtures. The high polymeric products were characterized first by solution spectroscopic methods and were then precipitated into hexane or ethanol. Characterization data are listed in Tables I and II.

The analogous complexes with triphenylphosphine were prepared as follows:  $\text{Fe}(\text{CO})_3(\text{PhCH}=\text{CHC}(\text{O})\text{CH}_3)$  (0.2 g, 0.7 mmol) and triphenylphosphine (0.41 g, 1.56 mmol) in THF (50 mL) were stirred at 68 °C for 14 h. The two main products were separated by column chromatography.  $\text{Fe}(\text{CO})_3(\text{PPh}_3)_2$  was characterized by infrared and  $^{31}\text{P}$  NMR spectroscopy.  $\text{Fe}(\text{CO})_2(\text{PhCH}=\text{CHC}(\text{O})\text{CH}_3)(\text{PPh}_3)$  was identified by  $^1\text{H}$  NMR spectroscopy,<sup>29</sup>  $^{31}\text{P}$  NMR and infrared spectroscopy, and mass spectrometry. When a molar deficiency of triphenylphosphine was used, the intermediate  $\text{Fe}(\text{CO})_3(\text{PhCH}=\text{CHC}(\text{O})\text{CH}_3)(\text{PPh}_3)$  was detected by infrared spectroscopy.

**Reactions of  $[\text{RhCl}(\text{CO})_2]_2$  with 1, 3, and 4.**  $[\text{RhCl}(\text{CO})_2]_2$  (0.075 g, 0.19 mmol) in THF (50 mL) was added slowly to 1, 3, or 4 in THF (200 mL). The reactant stoichiometry depended on the type of complex to be prepared. Typically, 0.5 g of 1 was used. The products formed bright yellow solutions in THF. The species  $[\text{RhCl}(\text{CO})][\text{N}_3\text{P}_3(\text{OC}_6\text{H}_4\text{PPh}_2)(\text{OPh})_5]_2$  (similar to 22) was purified by column chromatography with methylene chloride/hexane mixtures used for elution. The product  $[\text{N}_3\text{P}_3(\text{OC}_6\text{H}_4\text{PPh}_2)_6][\text{RhCl}(\text{CO})]$  crystallized without prior chromatography.  $[\text{NP}(\text{OC}_6\text{H}_4\text{PPh}_2)_2\text{RhCl}(\text{CO})]_3$  precipitated from solution and was isolated by filtration.<sup>30</sup>

**Treatment of Metal Complexes with  $[\text{NP}(\text{OC}_6\text{H}_5)_2]_3$  (2) and  $[\text{NP}(\text{OC}_6\text{H}_5)_2]_n$ .** The procedures used for the synthesis of (phosphine)metal complexes were repeated with the use of 2 or  $[\text{NP}(\text{OC}_6\text{H}_5)_2]_n$  instead of 3. Under these conditions, no reaction was observed between these phosphazenes and  $\text{AuCl}$ ,  $\text{H}_2\text{Os}_3(\text{CO})_{10}$ ,  $\text{Mn}(\text{CO})_2(\eta\text{-C}_5\text{H}_5)(\text{THF})$ ,  $\text{Fe}(\text{CO})_3(\text{BZA})$ , or  $[\text{RhCl}(\text{CO})_2]_2$ .  $^{31}\text{P}$  NMR spectra of the crude reaction mixtures were consistent with the presence of only unchanged 2 or  $[\text{NP}(\text{OC}_6\text{H}_5)_2]_n$ . The infrared spectra of the carbonyl-containing metal complexes were identical before and after the addition of 2 or  $[\text{NP}(\text{OC}_6\text{H}_5)_2]_n$ .

**Isomerization of 1-Hexene in the Presence of  $\text{H}_2\text{Os}_3(\text{CO})_{10}(\text{PPh}_3)$ ,  $[\text{N}_3\text{P}_3(\text{OC}_6\text{H}_4\text{PPh}_2\text{Os}_3\text{H}_2(\text{CO})_{10})(\text{OPh})_5]$  (6),  $[\text{NP}(\text{OC}_6\text{H}_4\text{PPh}_2\text{Os}_3\text{H}_2(\text{CO})_{10})_2]_3$ , and  $[\text{NP}(\text{OC}_6\text{H}_4\text{PPh}_2\text{Os}_3\text{H}_2(\text{CO})_{10})_{0.3}(\text{OPh})_{1.7}]_n$  (11a).** Experiments were carried out with  $5 \times 10^{-3}\text{M}$  solutions of the catalyst (based on the concentration of metallo component) in tetrahydrofuran (25 mL) with a 100:1 molar ratio of 1-hexene to the catalyst at 65 °C in a closed system under a nitrogen atmosphere. The reaction mixture was sampled periodically, and the products were separated from the catalyst by vacuum transfer. The reaction mixtures were analyzed by gas chromatography.<sup>26</sup>

**Acknowledgment.** This work was supported by the Army Research Office. The authors acknowledge the advice and technical assistance provided by Dr. G. H. Riding, R. A. Nissan, and J. L. Desorcie.

**Registry No.** 5, 83846-05-3; 6, 83846-12-2; 7, 83861-72-7; 8, 83861-73-8; 9, 83846-06-4;  $[\text{NP}(\text{OC}_6\text{H}_4\text{PPh}_2\text{AuCl})_2]_3$ , 83846-07-5;  $[\text{NP}(\text{OC}_6\text{H}_4\text{PPh}_2\text{Os}_3\text{H}_2(\text{CO})_{10})_2]_3$ , 83983-90-8;  $\text{N}_3\text{P}_3(\text{OC}_6\text{H}_4\text{PPh}_2\text{Mn}(\text{CO})_2(\eta\text{-C}_5\text{H}_5))(\text{OC}_6\text{H}_4\text{PPh}_2)_5$ , 83846-08-6;  $\text{N}_3\text{P}_3(\text{OC}_6\text{H}_4\text{PPh}_2)_2\text{Fe}(\text{CO})_3(\text{OC}_6\text{H}_4\text{PPh}_2)_4$ , 83846-09-7;  $\text{N}_3\text{P}_3(\text{OC}_6\text{H}_4\text{PPh}_2)_2\text{RhCl}(\text{CO})(\text{OC}_6\text{H}_4\text{PPh}_2)_4$ , 83846-10-0;  $\text{N}_3\text{P}_3(\text{OC}_6\text{H}_4\text{PPh}_2)_2\text{Mn}(\eta\text{-C}_5\text{H}_5)(\text{CO})(\text{OC}_6\text{H}_4\text{PPh}_2)_4$ , 83846-11-1;  $[\text{N}_3\text{P}_3(\text{OC}_6\text{H}_4\text{PPh}_2)_6]_2\text{Mn}(\eta\text{-C}_5\text{H}_5)(\text{CO})$ , 83983-91-9;  $\text{AuCl}(\text{PPh}_3)$ , 14243-64-2;  $\text{H}_2\text{Os}_3(\text{CO})_{10}(\text{PPh}_3)$ , 56398-26-6;  $\text{Mn}(\text{CO})_2(\eta\text{-C}_5\text{H}_5)(\text{PPh}_3)$ , 12100-41-3;  $\text{Mn}(\text{CO})(\eta\text{-C}_5\text{H}_5)(\text{PPh}_3)_2$ , 12120-58-0;  $\text{Fe}(\text{CO})_3(\text{PPh}_3)_2$ , 14741-34-5;  $\text{Fe}(\text{CO})_2(\text{BZA})(\text{PPh}_3)$ , 56556-41-3;  $\text{RhCl}(\text{CO})(\text{PPh}_3)_2$ , 13938-94-8;  $\text{RhCl}(\text{CO})_2\text{PPh}_3$ , 35679-01-7; 1-hexene, 592-41-6; 2-hexene, 592-43-8.

(28) Evans, G.; Johnson, B. F. G.; Lewis, J. J. *Organomet. Chem.* **1975**, *102*, 507.

(29) The resonance position of the olefinic protons of the benzylideneacetone ligand were sensitive to changes in the iron-coordination sphere. Therefore,  $^1\text{H}$  NMR spectroscopy was an excellent method for the identification of  $\text{Fe}(\text{CO})_3(\text{PPh}_3)_2$  and  $\text{Fe}(\text{CO})_2(\text{BZA})(\text{PPh}_3)$ .

(30) Species  $[\text{NP}(\text{OC}_6\text{H}_4\text{PPh}_2)_2\text{RhCl}(\text{CO})]_3$  was formed when a large excess of  $[\text{RhCl}(\text{CO})_2]_2$  was allowed to react with 4. Its composition was deduced from microanalytical data and from its carbonyl infrared spectrum that was identical with that of  $\text{RhCl}(\text{CO})(\text{PPh}_3)_2$ . It was insoluble in all common organic media. This is strong evidence for a highly cross-linked matrix structure.

# Coupling of Diazomethane and a Carbonyl Ligand To Give a New Metallacycle: Crystal Structure of the Complex $[\text{Mn}_2(\text{CO})_4\{\mu\text{-C}(\text{O})\text{CH}_2\text{N}_2\}(\mu\text{-Ph}_2\text{PCH}_2\text{PPh}_2)_2]\cdot 2\text{CH}_2\text{Cl}_2$

George Ferguson,<sup>1a</sup> W. John Laws,<sup>1b</sup> Masood Parvez,<sup>1a</sup> and Richard J. Puddephatt\*<sup>1b</sup>

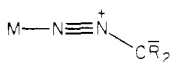
Chemistry Department, The University of Guelph, Guelph, Ontario, Canada, N1G 2W1, and Department of Chemistry, University of Western Ontario, London, Ontario, Canada, N6A 5B7

Received August 3, 1982

Reaction of diazomethane with  $[\text{Mn}_2(\text{CO})_4(\mu\text{-CO})(\mu\text{-dppm})_2]$  (I,  $\text{dppm} = \text{Ph}_2\text{PCH}_2\text{PPh}_2$ ) gives  $[\text{Mn}_2(\text{CO})_4\{\mu\text{-C}(\text{O})\text{CH}_2\text{N}_2\}(\mu\text{-dppm})_2]$  (II). The structure of II was established by our X-ray analysis. Crystals of  $(\text{II})\cdot 2(\text{CH}_2\text{Cl}_2)$  are triclinic of space group  $P\bar{1}$  with two formula units in a cell of dimensions  $a = 12.549$  (6) Å,  $b = 13.447$  (2) Å,  $c = 19.140$  (6) Å,  $\alpha = 104.34$  (2)°,  $\beta = 95.99$  (3)°, and  $\gamma = 111.11$  (2)°. The structure was solved by the heavy-atom method and refined by full-matrix least-squares calculations to a final  $R$  value of 0.087 for 4360 reflections with  $I > 3\sigma(I)$ . The diazomethane ligand has reacted to bridge asymmetrically via nitrogen the Mn atoms of the  $[\text{Mn}_2(\text{CO})_5(\text{dppm})_2]$  moiety and also to form a C-C bond with an adjacent CO ligand, yielding a planar five-membered  $\text{Mn}_2\text{C}_2\text{N}_2$  ring. The manganese stereochemistry is derived from octahedral geometry with the addition of a Mn-Mn bond. Principal bond lengths are as follows: Mn-Mn = 2.898 (2) Å; Mn-N = 1.894 and 1.967 (7) Å; Mn-P = 2.287-2.295 (2) Å; Mn-C (terminal carbonyl) = 1.764-1.809 (12) Å; Mn-C (bridging carbonyl) = 1.826 and 2.524 (8) Å; Mn-C (ring) = 2.001 (9) Å; N=N = 1.238 (9) Å. The spectroscopic data (IR and  $^1\text{H}$  and  $^{31}\text{P}$  NMR) are fully consistent with the above structure and show that the molecule is not fluxional in solution. However, the long C-C bond of the metallacycle is cleaved on thermolysis or photolysis of II, and complex I is reformed.

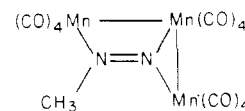
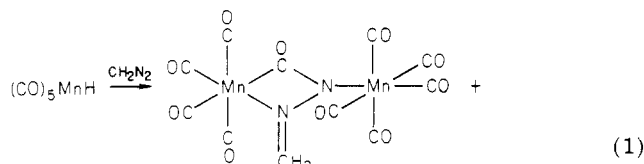
## Introduction

The reactions of diazoalkanes with transition-metal complexes have been the subject of intensive research over the past few years.<sup>2</sup> It is generally believed that diazoalkane complexes, for which several bonding modes are possible, are formed first but only rarely are such complexes isolated.<sup>2-5</sup> An example of particular relevance to the present work is the complex  $[\text{Mn}(\eta^5\text{-C}_5\text{H}_5)(\text{CO})_2\{\text{N}_2\text{C}(\text{CO}_2\text{Me})_2\}]$  in which the metal-diazoalkane bonding is of the form



with presumably carbanion character of the carbon center.<sup>2</sup> More commonly, dinitrogen is lost to give an alkylidene that may then insert into a metal-metal, metal-hydrogen, or metal-phosphorus bond or that may combine with coordinated carbon monoxide, alkyne, alkene, or other ligands to give more complex derivatives.<sup>2,5-8</sup> Catalytic cyclopropanation of alkenes may result from such reactions.<sup>9</sup>

There are few examples known in which the diazoalkane itself undergoes insertion reactions, but two relevant examples are shown in eq 1 and 2.<sup>10,11</sup>



While the reaction of diazomethane with the complex  $[\text{Mn}_2(\text{CO})_5(\mu\text{-dppm})_2]$  (I,  $\text{dppm} = \text{Ph}_2\text{PCH}_2\text{PPh}_2$ )<sup>12-16</sup> was studied, we discovered a 1:1 adduct of formula  $[\text{Mn}_2(\text{CO})_5(\text{CH}_2\text{N}_2)(\mu\text{-dppm})_2]$  (II). This complex is shown to have a unique metallacyclic unit formed by a new type of coupling of diazomethane with a carbonyl ligand, and its synthesis, structure, and properties form the basis for this article.

## Experimental Section

$^1\text{H}$  and  $^{31}\text{P}\{^1\text{H}\}$  NMR spectra were recorded by using a Varian XL 100 spectrometer at 100.1 and 40.5 MHz, respectively. Chemical shifts are quoted with respect to  $\text{Me}_4\text{Si}$  or  $(\text{MeO})_3\text{PO}$ , respectively. IR and mass spectra were recorded by using a Beckman IR 4250 and Varian MAT 311 spectrometers, respectively.

$[\text{Mn}_2(\text{CO})_5(\mu\text{-dppm})_2]$  (I) was prepared by the literature method<sup>13</sup> and purified by chromatography on Florisil eluting with  $\text{CH}_2\text{Cl}_2$ : mp 228-234 °C dec; IR  $\nu(\text{CO})$  ( $\text{cm}^{-1}$ , Nujol) 1942 (m), 1930 (s), 1860 (s), 1835 (m), 1645 (m); NMR ( $\text{CH}_2\text{Cl}_2$ )  $\delta$  3.51 ( $\text{PCH}_2\text{P}$ ),  $\delta(^{31}\text{P})$  75.9, 59.5.<sup>14</sup>

- (1) (a) University of Guelph. (b) University of Western Ontario.  
 (2) For an excellent review of early work see: Herrmann, W. A. *Angew. Chem., Int. Ed. Engl.* 1978, 17, 800; *J. Organomet. Chem.* 1975, 84, C25. Herrmann, W. A.; Kriechbaum, G.; Liegler, M. L.; Wulknitz, P. *Chem. Ber.* 1981, 114, 276.  
 (3) Schramm, K. D.; Ibers, J. A. *J. Am. Chem. Soc.* 1978, 100, 2932.  
 (4) Chisholm, M. H.; Foltling, K.; Huffman, J. C.; Ratermann, A. L. *J. Chem. Soc., Chem. Commun.* 1981, 1229.  
 (5) Messerle, L.; Curtis, M. D. *J. Am. Chem. Soc.* 1980, 102, 7789.  
 (6) Clauss, A. D.; Shapley, J. R.; Wilson, S. R. *J. Am. Chem. Soc.* 1981, 103, 7387.  
 (7) Schultz, A. J.; Williams, J. M.; Calvert, R. B.; Shapley, J. R.; Stucky, G. D. *Inorg. Chem.* 1979, 18, 319 and references therein.  
 (8) Azam, K. A.; Frew, A. A.; Lloyd, B. R.; Manojlović-Muir, Lj.; Muir, K. W.; Puddephatt, R. J. *J. Chem. Soc., Chem. Commun.*, in press.  
 (9) Nakamura, A.; Konishi, A.; Tsujitani, R.; Kudo, M.; Otsuka, S. *J. Am. Chem. Soc.* 1978, 100, 3449.  
 (10) Herrmann, W. A.; Ziegler, M. L.; Weidenhammer, K.; Biersack, H.; Mayer, K. K.; Minard, R. D. *Angew. Chem., Int. Ed. Engl.* 1976, 15, 164. Herrmann, W. A.; Ziegler, M. L.; Weidenhammer, K. *Ibid.* 1976, 15, 368.  
 (11) Gambarotta, S.; Basso-Bert, M.; Floriani, C.; Guastini, G. *J. Chem. Soc., Chem. Commun.* 1982, 374.

- (12) Commons, C. J.; Hoskins, B. F. *Aust. J. Chem.* 1975, 28, 1663.  
 (13) Colton, R.; Commons, C. J. *Aust. J. Chem.* 1975, 28, 1673.  
 (14) Caulton, K. G.; Adair, P. J. *J. Organomet. Chem.* 1976, 114, C11.  
 (15) Balch, A. L.; Benner, L. S. *J. Organomet. Chem.* 1977, 135, 339.  
 (16) Aspinall, H. C.; Deeming, A. J. *J. Chem. Soc., Chem. Commun.* 1981, 724.

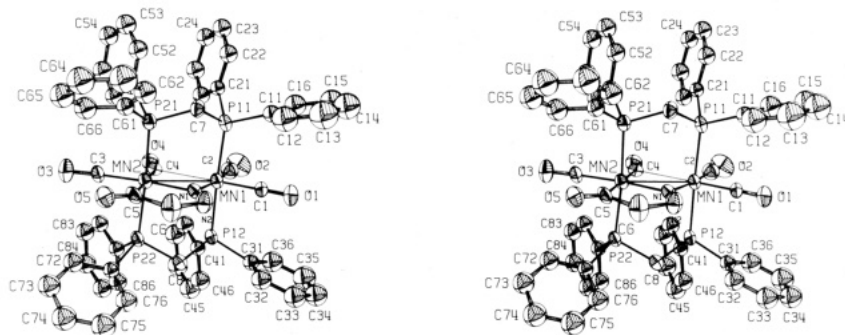


Figure 1. Stereoview of II with our numbering scheme.

$[\text{Mn}_2(\text{CO})_4(\mu\text{-C}(\text{O})\text{CH}_2\text{N}_2)(\mu\text{-dppm})_2]$  (II). This was prepared by reaction of complex I ( $2.5150 \text{ g}$ ,  $2.471 \times 10^{-3} \text{ mol}$ ) in  $\text{CH}_2\text{Cl}_2$  (100 mL) with ethereal  $\text{CH}_2\text{N}_2$  (105 mL of 0.60% solution,  $1.482 \times 10^{-2} \text{ mol}$ ). The color of the solution slowly changed from red to yellow-orange over a period of 1 day at room temperature. The mixture was purified by chromatography on Florisil (100–200 mesh). Elution with  $\text{CH}_2\text{Cl}_2$  gave complex I ( $0.2273 \text{ g}$ ,  $2.231 \times 10^{-4} \text{ mol}$ , 9.0%) and then with 20%  $\text{CH}_3\text{OH}/\text{CH}_2\text{Cl}_2$  gave complex II ( $1.9448 \text{ g}$ ,  $1.835 \times 10^{-3} \text{ mol}$ , ~74%), recovered as an orange solid, which was recrystallized from  $\text{CH}_2\text{Cl}_2/\text{pentane}$ . The initially formed solvated crystals lost  $\text{CH}_2\text{Cl}_2$  rapidly to give the product as an orange powder: mp 197.5–199.5 °C; IR  $\nu(\text{CO})$  ( $\text{cm}^{-1}$ , Nujol) 1960 (m), 1920 (s), 1858 (s), 1818 (m), 1610 (m); NMR ( $\text{CH}_2\text{Cl}_2$ )  $\delta$  2.76 (PCH<sub>2</sub>P), 4.81 (CH<sub>2</sub>N), integration 4:2,  $\delta(^{31}\text{P})$  53.7, 56.4; parent ion ( $m/e$  1060) not observed,  $m/e$  (assignment) 1018 (P – CH<sub>2</sub>N<sub>2</sub>), 962 (P – CH<sub>2</sub>N<sub>2</sub> – 2CO), 934 (P – CH<sub>2</sub>N<sub>2</sub> – 3CO), 884 (P – CH<sub>2</sub>N<sub>2</sub> – 2CO – C<sub>6</sub>H<sub>6</sub>). Anal. Calcd for  $\text{C}_{56}\text{H}_{46}\text{Mn}_2\text{N}_2\text{O}_5\text{P}_4$ : C, 63.4; H, 4.3; N, 2.6. Found: C, 63.5; H, 4.35; N, 2.6.

**Thermal and Photochemical Decomposition of II.** A solution of complex II (0.047 g) in benzene (15 mL), in a closed vessel fitted with a vacuum tap and a serum cap, was heated at 80 °C for 1 day. Analysis of the gas phase by GC showed  $\text{C}_2\text{H}_6$  as the major volatile organic product. The residue was chromatographed on Florisil to give a mixture of complex I (0.01 g) and II (0.03 g), identified by comparison with authentic samples. Heating in an open vessel gave more rapid conversion to I.

Similarly photolysis (Xe lamp, Pyrex filter) of complex II in  $\text{CH}_2\text{Cl}_2$  occurred slowly to give ethane and complex I.

**Crystallographic Studies.** Recrystallization of II from dichloromethane afforded large single crystals of what was later shown to be the bis(dichloromethane) solvate. The crystals lost solvent rapidly and were very unstable in air; for the data collection a suitable crystal was coated with several thin layers of epoxy resin within seconds of its being removed from the mother liquor.

**Crystal data:**  $\text{Mn}_2(\text{CO})_4(\text{OCCH}_2\text{N}_2)(\text{Ph}_2\text{PCH}_2\text{PPh}_2)_2 \cdot 2\text{CH}_2\text{Cl}_2$ ,  $\text{C}_{56}\text{H}_{46}\text{Mn}_2\text{N}_2\text{O}_5\text{P}_4 \cdot 2\text{CH}_2\text{Cl}_2$ ;  $M_r = 1088.8$ ; triclinic;  $a = 12.549$  (6) Å,  $b = 13.447$  (2) Å,  $c = 19.140$  (6) Å;  $\alpha = 104.34$  (2)°,  $\beta = 95.99$  (2)°,  $\gamma = 111.11$  (2)°;  $U = 2851.4$  Å<sup>3</sup>,  $Z = 2$ ;  $D_{\text{calcd}} = 1.27 \text{ g cm}^{-3}$ ,  $F(000) = 1260$ ; Mo K $\alpha$  radiation;  $\lambda = 0.71069$  Å,  $\mu(\text{Mo K}\alpha) = 8.1 \text{ cm}^{-1}$ . Space group  $P\bar{1}$  or  $P1$ ;  $P\bar{1}$  assumed and confirmed by analysis.

After preliminary photographic studies, accurate unit-cell constants and crystal orientation matrix were determined on an Enraf-Nonius Cad-4 diffractometer by a least-squares treatment of the setting angles of 25 reflections with  $\theta$  in the range 10–15°. Intensity data were collected by the  $\omega$ -2 $\theta$  scan method using monochromatized Mo K $\alpha$  radiation. The intensities of three reflections, chosen as standards, were monitored at regular intervals and decreased by 11.7% over the course of the data collection; this decay was corrected for by appropriate scaling. Intensities of 5302 reflections were measured, of which 4360 had  $I > 3\sigma(I)$  and were used in structure solution and refinement. Data were corrected for Lorentz, polarization factors, and for absorption. Maximum and minimum values of the transmission coefficients are 0.7228 and 0.5613, respectively.

The coordinates of the atoms of the  $\text{Mn}_2\text{P}_4$  fragment were deduced from a careful examination of the three-dimensional Patterson function, and the remaining non-hydrogen atoms were located from subsequent heavy-atom phased electron density maps

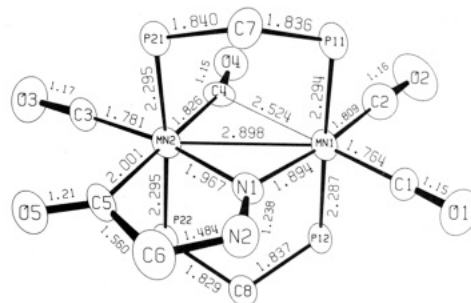


Figure 2. View of the manganese coordination with bond lengths (Å). Estimated standard deviations are as follows: Mn–Mn = 0.002 Å; Mn–P = 0.002 Å; Mn–N = 0.007 Å; Mn–C = 0.008–0.012 Å; P–C = 0.006–0.009 Å; C–O, N–N, C–C, and C–N = 0.009–0.013 Å.

which also showed the presence of two  $\text{CH}_2\text{Cl}_2$  molecules of solvation. Initial refinement<sup>17</sup> by full-matrix least-squares calculations with isotropic thermal parameters lowered  $R$  to 0.160. In subsequent refinement cycles to save computer time, the phenyl rings were constrained to be regular hexagons (with C–C = 1.395 Å) and refined isotropically; the other non-hydrogen atoms were allowed anisotropic vibration. When  $R$  was 0.10, a difference synthesis revealed electron density maxima in positions anticipated for the hydrogen atoms of 1. In subsequent refinement cycles, the hydrogen atoms were included in geometrically idealized positions (C–H = 0.95 Å) but not refined; only an overall isotropic thermal parameter was refined for hydrogen. The solvent molecules showed evidence of disorder (diffuse electron density maxima, abnormal geometry, and abnormally large thermal parameters), and their hydrogen atoms were not located. In the final rounds of calculations a weighting scheme of the form  $w = 1/[\sigma^2(F)]$  was employed. Scattering factors used in the calculations were taken from ref 18 and 19, and allowance was made for anomalous dispersion.<sup>20</sup> Refinement converged with  $R = 0.087$  and  $R_w = (\sum w\Delta^2/\sum wF_o^2)^{1/2} = 0.107$ . A final difference map showed no chemically significant maxima. Final fractional coordinates and their estimated standard deviations are in Table I, and details of molecular dimensions are in Table II. Tables of calculated hydrogen coordinates and thermal parameters and a listing of observed and calculated structure amplitudes have been deposited as supplementary material. Figure 1 is a stereoview of 1, and Figure 2 shows the main coordination geometry with principal dimensions.

## Discussion

With the aim of synthesizing complexes with the  $\text{Mn}_2$ -( $\mu\text{-CR}_2$ ) grouping, a study of reactions of diazoalkanes with Colton's complex  $[\text{Mn}_2(\text{CO})_5(\mu\text{-dppm})_2]$  (I), having an

(17) Sheldrick, G. M. SHELX, a program system for crystal structure determination, University of Cambridge, England, 1976.

(18) Cromer, D. T.; Mann, J. B. *Acta Crystallogr., Sect. A* 1968, A24, 321–323.

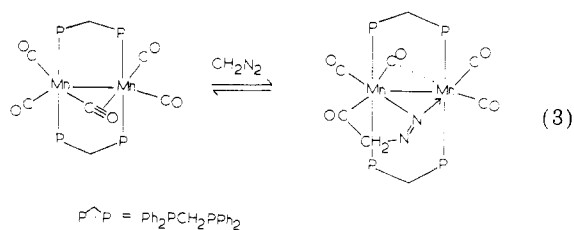
(19) Stewart, R. F.; Davidson, E. R.; Simpson, W. T. *J. Chem. Phys.* 1965, 42, 3175–3187.

(20) Cromer, D. T.; Liberman, D. *J. Chem. Phys.* 1970, 53, 1891–1898.

Table I. Final Fractional Coordinates ( $\times 10^4$ ) with Estimated Standard Deviations in Parentheses

atom	x	y	z	atom	x	y	z
Mn(1)	1444 (1)	2331 (1)	2795 (1)	C(26)	3312 (5)	4990 (4)	4405 (3)
Mn(2)	3178 (1)	2879 (1)	1908 (1)	C(31)	-281 (5)	-487 (5)	2310 (3)
P(11)	1565 (2)	4136 (2)	3122 (1)	C(32)	-1070 (5)	-847 (5)	1638 (3)
P(12)	1228 (2)	504 (2)	2451 (1)	C(33)	-2243 (5)	-1524 (5)	1568 (3)
P(21)	3360 (2)	4701 (2)	2178 (1)	C(34)	-2627 (5)	-1842 (5)	2168 (3)
P(22)	3006 (2)	1062 (2)	1496 (1)	C(35)	-1838 (5)	-1482 (5)	2839 (3)
Cl(1)	62 (10)	6575 (9)	722 (6)	C(36)	-665 (5)	-805 (5)	2910 (3)
Cl(2)	-1231 (23)	5705 (13)	1543 (9)	C(41)	2013 (5)	-53 (4)	2999 (3)
Cl(3)	0 (8)	7413 (9)	4370 (6)	C(42)	2943 (5)	647 (4)	3595 (3)
Cl(4)	1633 (13)	9109 (11)	5498 (7)	C(43)	3546 (5)	190 (4)	3983 (3)
O(1)	-1069 (7)	1554 (6)	2690 (4)	C(44)	3219 (5)	-967 (4)	3776 (3)
O(2)	1743 (7)	2389 (7)	4363 (4)	C(45)	2289 (5)	-1667 (4)	3180 (3)
O(3)	5571 (6)	3622 (6)	1644 (4)	C(46)	1686 (5)	-1210 (4)	2792 (3)
O(4)	4210 (6)	3130 (5)	3423 (4)	C(51)	4561 (5)	5796 (5)	2924 (3)
O(5)	3185 (6)	2945 (5)	358 (4)	C(52)	4585 (5)	6874 (5)	3156 (3)
N(1)	1474 (6)	2353 (5)	1812 (4)	C(53)	5483 (5)	7708 (5)	3727 (3)
N(2)	763 (7)	2127 (7)	1237 (5)	C(54)	6356 (5)	7464 (5)	4066 (3)
C(1)	-78 (9)	1867 (7)	2736 (5)	C(55)	6332 (5)	6386 (5)	3833 (3)
C(2)	1661 (9)	2383 (8)	3755 (6)	C(56)	5435 (5)	5552 (5)	3262 (3)
C(3)	4636 (8)	3345 (7)	1766 (5)	C(61)	3564 (5)	5381 (6)	1459 (4)
C(4)	3620 (7)	2989 (6)	2874 (5)	C(62)	2746 (5)	5729 (6)	1163 (4)
C(5)	2690 (8)	2754 (7)	850 (5)	C(63)	2967 (5)	6250 (6)	617 (4)
C(6)	1331 (8)	2274 (10)	607 (5)	C(64)	4004 (5)	6424 (6)	366 (4)
C(7)	2031 (7)	4836 (7)	2429 (5)	C(65)	4821 (5)	6076 (6)	661 (4)
C(8)	1585 (7)	76 (7)	1548 (5)	C(66)	4601 (5)	5555 (6)	1208 (4)
C(9)	-1403 (25)	6278 (27)	1074 (22)	C(71)	3053 (4)	483 (4)	539 (3)
C(10)	559 (32)	9179 (31)	4815 (13)	C(72)	4103 (4)	966 (4)	328 (3)
C(11)	161 (7)	4208 (6)	3192 (3)	C(73)	4207 (4)	567 (4)	-396 (3)
C(12)	-618 (7)	4092 (6)	2572 (3)	C(74)	3261 (4)	-315 (4)	-910 (3)
C(13)	-1737 (7)	4034 (6)	2627 (3)	C(75)	2211 (4)	-798 (4)	-699 (3)
C(14)	-2077 (7)	4093 (6)	3302 (3)	C(76)	2107 (4)	-399 (4)	26 (3)
C(15)	-1298 (7)	4208 (6)	3922 (3)	C(81)	4060 (5)	632 (3)	1949 (3)
C(16)	-179 (7)	4266 (6)	3867 (3)	C(82)	5090 (5)	1429 (3)	2438 (3)
C(21)	2486 (5)	5193 (4)	3981 (3)	C(83)	5895 (5)	1089 (3)	2757 (3)
C(22)	2382 (5)	6217 (4)	4205 (3)	C(84)	5671 (5)	-47 (3)	2589 (3)
C(23)	3104 (5)	7039 (4)	4853 (3)	C(85)	4641 (5)	-844 (3)	2100 (3)
C(24)	3930 (5)	6836 (4)	5277 (3)	C(86)	3836 (5)	-505 (3)	1781 (3)
C(25)	4034 (5)	5811 (4)	5054 (3)				

unusual 4-electron bridging carbonyl ligand,<sup>12,13</sup> was initiated. The reaction of excess diazomethane with I occurs slowly at room temperature and more rapidly if acid catalysis<sup>16</sup> is employed. The product is not a methylene complex however but is a new type of metallacycle (II) formed according to eq 3.



Since the structure could not be deduced from the spectroscopic data, a structure determination by X-ray methods was undertaken. The crystal structure of (II)·2(CH<sub>2</sub>Cl<sub>2</sub>) contains discrete molecules separated by normal van der Waals distances. Figure 1 is a stereoview of the structure of II, and Figure 2 shows details of the manganese environment with principal bond lengths.

The structure of II is very similar to that reported<sup>12</sup> for [Mn<sub>2</sub>(CO)<sub>5</sub>(dppm)<sub>2</sub>] (I) but with the additional unique<sup>21</sup> feature of a diazomethane ligand that bridges the Mn atoms and also forms a C-C single bond to what had been a carbonyl carbon atom in I.

The stereochemistry at each manganese may be regarded as being derived from octahedral geometry with the

addition of a Mn-Mn bond, 2.898 (2) Å. The manganese atoms and those of the carbonyl and diazomethane ligands form an equatorial plane and, as in I, the phosphine ligands occupy trans axial sites. The angle between the Mn<sub>2</sub>P<sub>4</sub> plane and that of manganese and equatorial ligands is 89.8°.

The manganese atom Mn(1) (Figure 2) forms two normal Mn-C bonds to terminal carbonyl groups (Mn(1)-C(1) = 1.76 (1) Å, Mn(1)-C(2) = 1.81 (1) Å, a Mn-N bond to the bridging diazo ligand (Mn-N = 1.894 (7) Å), and there is also a much weaker interaction to a semibridging equatorial carbonyl Mn-C(4) = 2.524 (8) Å. The resulting trans effects are marked, with Mn-C(1) (trans to Mn...C(4)) shorter than Mn-C(2) (trans to N(1)).

The equatorial environment at Mn(2) is quite different from that at Mn(1). There is one terminal carbonyl (Mn(2)-C(3) = 1.782 (10) Å), the bridging carbonyl (Mn(2)-C(4) = 1.826 (9) Å), and the bridging diazomethane (Mn(2)-N(1) = 1.967(7) Å), and the remaining carbonyl ligand has been incorporated into the five-membered MnC<sub>2</sub>N<sub>2</sub> ring (Mn(2)-C(5) = 2.001 (9) Å). The Mn-N distances are significantly different with the shorter Mn-N bond being to Mn(1), the manganese atom with only a weak interaction to the bridging carbonyl C(4). In the five-membered MnC<sub>2</sub>N<sub>2</sub> ring the N-N distance 1.238 (9) Å is consistent with it being a double bond.

In II, the bridging carbonyl group is much more asymmetric than was observed in I (compare Mn-C = 1.826 (9) and 2.524 (8) Å and Mn(2)-C-O = 159.9 (7)° with the corresponding data for I, 1.93 (3) and 2.01 (3) Å and 173 (3)°), but the observed geometry for II indicates a significant Mn(1)...C(4) interaction.

(21) "Cystalor"—The Cambridge Crystallographic Data Base at NRC Ottawa.

Table II. Principal Interatomic Distances (Å) and Angles (deg) and Some Mean Plane Data for 1

a. Bond Distances					
Mn(1)-Mn(2)	2.898 (2)	P(11)-C(7)	1.836 (9)	O(1)-C(1)	1.146 (10)
Mn(1)-P(11)	2.294 (2)	P(11)-C(11)	1.816 (8)	O(2)-C(2)	1.155 (11)
Mn(1)-P(12)	2.287 (2)	P(11)-C(21)	1.823 (6)	O(3)-C(3)	1.165 (10)
Mn(1)-N(1)	1.894 (7)	P(12)-C(8)	1.837 (8)	O(4)-C(4)	1.153 (9)
Mn(1)-C(1)	1.764 (10)	P(12)-C(31)	1.825 (6)	O(5)-C(5)	1.211 (10)
Mn(1)-C(2)	1.809 (12)	P(12)-C(41)	1.827 (6)	N(1)-N(2)	1.238 (9)
Mn(1)···C(4)	2.524 (8)	P(21)-C(7)	1.840 (8)	N(2)-C(6)	1.484 (12)
Mn(2)-P(21)	2.295 (2)	P(21)-C(51)	1.841 (6)	C(5)-C(6)	1.560 (13)
Mn(2)-P(22)	2.295 (2)	P(21)-C(61)	1.823 (7)	Cl(1)-C(9)	1.97 (3)
Mn(2)-N(1)	1.967 (7)	P(22)-C(8)	1.829 (8)	Cl(2)-C(9)	1.37 (4)
Mn(2)-C(3)	1.781 (10)	P(22)-C(71)	1.821 (6)	Cl(3)-C(10)	2.13 (3)
Mn(2)-C(4)	1.826 (9)	P(22)-C(81)	1.843 (6)	Cl(4)-C(10)	1.82 (3)
Mn(2)-C(5)	2.001 (9)				

Aromatic C-C Constrained To Be 1.395 Å

b. Bond Angles			
Mn(2)-Mn(1)-P(11)	90.8 (1)	Mn(1)-Mn(2)-P(21)	92.6 (1)
Mn(2)-Mn(1)-P(12)	90.8 (1)	Mn(1)-Mn(2)-P(22)	92.6 (1)
Mn(2)-Mn(1)-N(1)	42.3 (2)	Mn(1)-Mn(2)-N(1)	40.4 (2)
Mn(2)-Mn(1)-C(1)	141.2 (3)	Mn(1)-Mn(2)-C(3)	153.6 (3)
Mn(2)-Mn(1)-C(2)	128.7 (3)	Mn(1)-Mn(2)-C(4)	59.6 (3)
Mn(2)-Mn(1)-C(4)	38.6 (2)	Mn(1)-Mn(2)-C(5)	120.3 (3)
P(11)-Mn(1)-P(12)	177.3 (1)	P(21)-Mn(2)-P(22)	173.1 (1)
P(11)-Mn(1)-N(1)	89.7 (2)	P(21)-Mn(2)-N(1)	90.6 (2)
P(11)-Mn(1)-C(1)	88.3 (3)	P(21)-Mn(2)-C(3)	88.0 (3)
P(11)-Mn(1)-C(2)	90.7 (3)	P(21)-Mn(2)-C(4)	93.7 (2)
P(11)-Mn(1)···C(4)	91.8 (2)	P(21)-Mn(2)-C(5)	86.4 (2)
P(12)-Mn(1)-N(1)	90.0 (2)	P(22)-Mn(2)-N(1)	90.4 (2)
P(12)-Mn(1)-C(1)	89.0 (3)	P(22)-Mn(2)-C(3)	89.3 (3)
P(12)-Mn(1)-C(2)	90.1 (3)	P(22)-Mn(2)-C(4)	92.8 (2)
P(12)-Mn(1)···C(4)	90.8 (2)	P(22)-Mn(2)-C(5)	87.1 (2)
N(1)-Mn(1)-C(1)	98.8 (4)	N(1)-Mn(2)-C(3)	165.9 (3)
N(1)-Mn(1)-C(2)	171.0 (4)	N(1)-Mn(2)-C(4)	100.0 (3)
N(1)-Mn(1)···C(4)	80.9 (3)	N(1)-Mn(2)-C(5)	79.9 (3)
C(1)-Mn(1)-C(2)	90.2 (4)	C(3)-Mn(2)-C(4)	94.1 (4)
C(1)-Mn(1)···C(4)	179.7 (2)	C(3)-Mn(2)-C(5)	86.1 (4)
C(2)-Mn(1)···C(4)	90.1 (4)	C(4)-Mn(2)-C(5)	179.8 (1)
Mn(1)-P(11)-C(7)	112.6 (3)	Mn(2)-P(21)-C(7)	111.3 (3)
Mn(1)-P(11)-C(11)	112.6 (3)	Mn(2)-P(21)-C(51)	119.3 (2)
Mn(1)-P(11)-C(21)	122.6 (2)	Mn(2)-P(21)-C(61)	118.9 (2)
C(7)-P(11)-C(11)	103.8 (2)	C(7)-P(21)-C(51)	104.4 (3)
C(7)-P(11)-C(21)	102.4 (3)	C(7)-P(21)-C(61)	101.8 (3)
C(11)-P(11)-C(21)	100.7 (3)	C(51)-P(21)-C(61)	98.7 (3)
Mn(1)-P(12)-C(8)	112.5 (3)	Mn(2)-P(22)-C(8)	111.4 (3)
Mn(1)-P(12)-C(31)	113.1 (2)	Mn(2)-P(22)-C(71)	119.0 (2)
Mn(1)-P(12)-C(41)	123.3 (2)	Mn(2)-P(22)-C(81)	119.8 (2)
C(8)-P(12)-C(31)	102.6 (3)	C(8)-P(22)-C(71)	101.3 (3)
C(8)-P(12)-C(41)	101.3 (4)	C(8)-P(22)-C(81)	103.7 (3)
C(31)-P(12)-C(41)	101.4 (3)	C(71)-P(22)-C(81)	99.0 (3)
Mn(1)-N(1)-Mn(2)	97.3 (3)	Mn(2)-C(5)-O(5)	135.8 (7)
Mn(1)-N(1)-N(2)	137.7 (6)	Mn(2)-C(5)-C(6)	111.0 (6)
Mn(2)-N(1)-N(2)	125.0 (6)	O(51)-C(5)-C(6)	113.2 (8)
N(1)-N(2)-C(6)	112.5 (7)	N(2)-C(6)-C(5)	111.4 (7)
Mn(1)-C(1)-O(1)	179.1 (8)	P(11)-C(7)-P(21)	111.3 (4)
Mn(1)-C(2)-O(2)	176.8 (9)	P(12)-C(8)-P(22)	111.7 (4)
Mn(2)-C(3)-O(3)	177.2 (8)	Cl(1)-C(9)-Cl(2)	98.8 (17)
Mn(1)···C(4)-Mn(2)	81.9 (3)	Cl(3)-C(10)-Cl(4)	86.2 (14)
Mn(1)···C(4)-O(4)	118.2 (6)		
Mn(2)-C(4)-O(4)	159.9 (7)		

Phenyl C-C-C Angles Constrained To Be 120°

c. Torsion Angles			
Mn(1)P(11)-C(11)C(12)	-85.0	Mn(2)P(21)-C(51)C(52)	-171.4
Mn(1)P(11)-C(21)C(22)	-169.7	Mn(2)P(21)-C(61)C(62)	115.0
Mn(1)P(12)-C(31)C(32)	84.6	Mn(2)P(22)-C(71)C(72)	65.0
Mn(1)P(12)-C(41)C(42)	-11.6	Mn(2)P(22)-C(81)C(82)	-12.8

d. Least-Squares Planes and Deviations of Atoms from Planes (Å, ×10<sup>3</sup>)<sup>a</sup>Mn, P<sub>4</sub> Plane: 0.7313X - 0.0690Y + 0.06785Z = 3.9938

Mn(1) 29, Mn(2) 60, P(11) -22, P(12) -9, P(21) -23, P(22) -36 C(7)\* -779, C(8)\* -768

Equatorial Plane: 0.0871X + 0.9961Y + 0.0127Z = 2.4948

Mn(1) 11, Mn(2) 4, N(1) 3, N(2) -18, C(1) 18, O(1) 9, C(2) 14, O(2) 4, C(3) 21, O(3) 0, C(4) -7, O(4) -48, C(5) 11, O(5) 49, C(6) -71

Dihedral Angle between the Two Planes Is 89.8°

<sup>a</sup> An asterisk indicates that the atom was not included in the plane equation calculation.

In the  $\text{Mn}_2\text{P}_4$  fragment, the Mn–Mn distance 2.898 (2) Å is slightly shorter than that found in I (2.934 (6) Å)<sup>12</sup> and is consistent with a metal–metal bond formation. The Mn–P distances are in the range 2.287–2.295 (2) Å, mean 2.293 (2) Å; in I, the Mn–P distances ranged between 2.234 (9) and 2.311 (9) Å.

The bridging carbon atoms C(7) and C(8) of the dppm ligands lie out of the  $\text{Mn}_2\text{P}_4$  plane (0.78 and 0.77 Å) respectively on the same side as atom N(1) and remote from the bridging carbonyl C(4); an exactly similar situation was found in I.

Steric crowding causes the phenyl rings to be bent away from the equatorial coordination plane; all the Mn–P–C angles are greater than tetrahedral (111.4–123.3 (2)°), and the C–P–C angles are all less than tetrahedral (98.7–104.4 (3)°). Other dimensions of the dppm ligand are as expected, e.g., average P–C = 1.830 (8) Å.

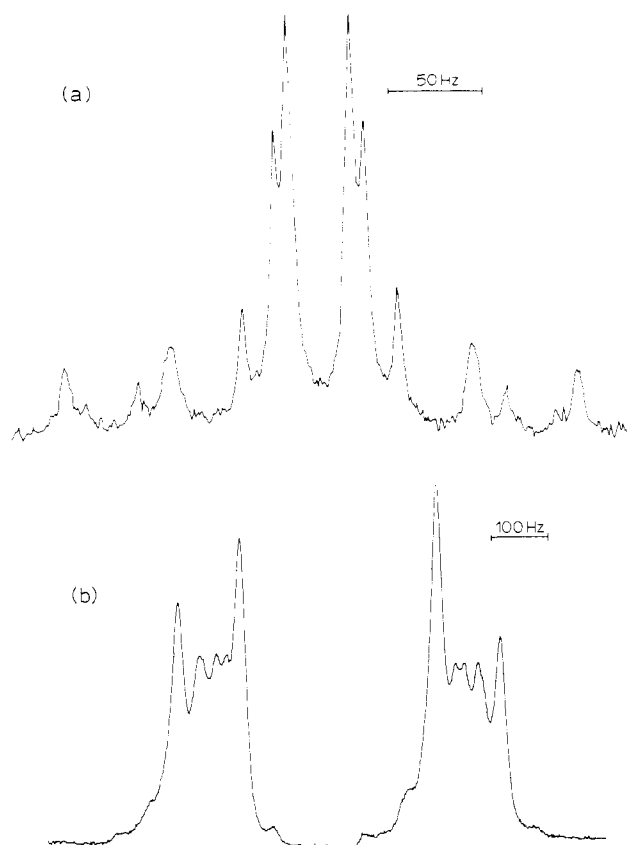
Given the molecular structure of II, it is then possible to explain the spectroscopic data and to understand the chemistry involved. The IR spectra in the carbonyl region of complexes I and II are similar in many respects (experimental). However, the band in I due to the 4-electron carbonyl at 1648  $\text{cm}^{-1}$  is missing in II, while new peaks arise at 1610 and 1818  $\text{cm}^{-1}$ . The 1610- $\text{cm}^{-1}$  peak is assigned to the C=O and N=N stretching modes of the metallocyclic ring in II while the 1818- $\text{cm}^{-1}$  peak is assigned to the semibridging carbonyl ligand. The bonding in II is most readily described as shown in eq 3, and the formal oxidation states of Mn(1) and Mn(2) are then 0 and +II, respectively. This is a classic situation for a semibridging carbonyl to be present, since the weak Mn(1)⋯C(4) interaction allows excess electron density at Mn(1) to be delocalized onto the carbonyl ligand. A low  $\nu(\text{CO})$  of 1818  $\text{cm}^{-1}$  results from this extra back-bonding.<sup>22</sup>

The  $^1\text{H}$  NMR spectrum contains resonances in the expected 2:1 ratio for  $\text{CH}_2\text{P}_2$  and  $\text{CH}_2\text{N}$  protons, the former resonance showing partially resolved coupling with  $^{31}\text{P}$  which was lost in the  $^1\text{H}\{^{31}\text{P}\}$  NMR spectrum. In principle, two resonances are expected for the  $\text{CH}_2\text{P}_2$  protons since there is no plane of symmetry containing the PCP unit, but there is presumably accidental degeneracy of the  $\text{CH}^A\text{H}^B\text{P}_2$  chemical shifts. That the molecule is not fluxional on the NMR time scale is shown by the  $^{31}\text{P}\{^1\text{H}\}$  NMR spectrum (Figure 3). At 40.5 MHz, this occurs as an  $\text{AA}^1\text{BB}^1$  multiplet as expected for structure II. The spectrum is sharp at  $-70^\circ\text{C}$  and the peaks broaden at room temperature, but no further broadening occurs up to  $+60^\circ\text{C}$ . The broadening is thus due to the presence of the quadrupolar manganese center and not to the onset of a fluxional process.<sup>14,23</sup>

The X-ray structure shows that the  $\text{CH}_2\text{-C(O)}$  bond is long for a C–C single bond [C(5)–C(6) = 1.560 (13) Å, cf. 1.516 (5) Å in  $\text{CH}_3\text{CHO}$ ]. It is therefore possible to rationalize the cleavage of this bond on heating complex II in benzene or on photolysis of complex II in dichloromethane solution. In both reactions the elements of  $\text{CH}_2\text{N}_2$  are lost, and complex I is reformed. It is not clear however whether  $\text{CH}_2\text{N}_2$  is a product of these reactions. The only organic product identified was ethane, whereas diazomethane is expected to give ethylene or methane as decomposition products.

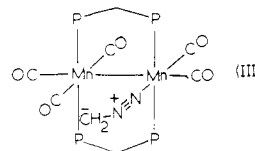
(22) Cotton, F. A.; Wilkinson, G. "Advanced Inorganic Chemistry", 4th ed.; Wiley: New York, 1980; pp 1058–1060.

(23) Preliminary results show that, in the corresponding complex derived from diazoethane, the  $^{31}\text{P}\{^1\text{H}\}$  NMR spectrum contains a singlet down to  $-90^\circ\text{C}$ , probably indicating fluxionality in this molecule. The alternative would require accidental degeneracy of all four  $^{31}\text{P}$  chemical shifts.



**Figure 3.**  $^{31}\text{P}\{^1\text{H}\}$  NMR spectra of complex II: (a) at 40.5 MHz; (b) at 162 MHz. Simulation as an  $\text{AA}^1\text{BB}^1$  multiplet gives  $\Delta\nu(\text{A,B}) = 112$  Hz at 40.5 MHz and 448 Hz at 162 MHz,  $J(\text{AB}) = 80$  Hz, and  $J(\text{AB}^1) = 32$  Hz.

The mechanism of formation of complex II could reasonably involve initial coordination of diazomethane to I as a 2-electron ligand replacing the Mn( $\pi$ -CO) bond in the usual fashion to give III. Now the carbanionic carbon<sup>2</sup>



of the diazomethane in III may act as a nucleophile in attacking a terminal carbonyl ligand and hence form the metallocyclic ring. Further studies with other diazoalkanes are in progress with the aim of clarifying the mechanisms involved.<sup>23</sup> The easy formation and cleavage of C–C bonds is perhaps the most important general feature of the chemistry of transition metallocycles, and the above reactions provide a good example of this effect.

**Acknowledgment.** Financial support from N.S.E.R.C. Canada (G.F. and R.J.P.) is gratefully acknowledged. Dr. G. H. Wood provided valuable assistance in searching CRYSTOR, the Cambridge Crystallographic Data Base at Ottawa.

**Registry No.** I, 56665-73-7; II, 83862-77-5; II·2 $\text{CH}_2\text{Cl}_2$ , 83916-58-9;  $\text{CH}_2\text{N}_2$ , 334-88-3.

**Supplementary Material Available:** Tables of hydrogen coordinates and thermal parameters and a listing of structure factor amplitudes (22 pages). Ordering information is given on any current masthead page.

# Hyperconjugation and the Structures of Metal Carbenes

M. M. Francl,<sup>1a</sup> W. J. Pietro, R. F. Hout, Jr.,<sup>1b</sup> and W. J. Hehre\*

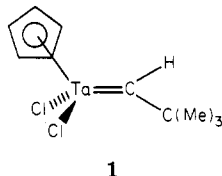
Department of Chemistry, University of California, Irvine, California 92717

Received May 25, 1982

The distorted structures of tantalum carbenes are viewed in terms of electron donation of the alkylidene CH bonding pair into a vacant orbital at the metal center, i.e., hyperconjugation. The resulting  $M\equiv C^+$  polarization suggests that electron-donating substituents will promote bridging while accepting groups will retard it. Theoretical (STO-3G level) equilibrium structures for substituted titanium carbenes provide support for the hypothesis.

## Introduction

Metal carbenes, molecules incorporating formal metal-carbon double bonds, are common structural entities in organometallic chemistry. While little is known about their thermochemical stabilities, i.e., metal-carbon  $\pi$ -bond strengths, the geometries of many metal carbenes have been determined from X-ray and neutron diffraction studies. Especially intriguing are structures of a number of alkylidene complexes. For example, the experimental geometry of the 14-electron tantalum carbene **1**<sup>2</sup> shows a

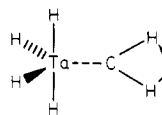


$Ta=CC$  bond angle of  $165^\circ$ , much larger than  $120^\circ$  which would be expected for a  $sp^2$ -hybridized carbon center. Related compounds in which the metal center is formally associated with 16 or fewer electrons also show comparable distortions.<sup>3</sup> The two available neutron diffraction structures<sup>3c</sup> show considerable lengthening of the alkylidene CH bond; this is consistent with the noted lowering both of CH stretching frequencies and NMR coupling constants for these compounds.<sup>3c</sup>

The structures of heteroatom-stabilized carbenes, e.g., Fischer carbenes, are generally in keeping with normal valence considerations.<sup>4</sup> Thus, the unusual structures noted for the alkylidene species may be the result of the lack of stabilizing substituents on carbon. Distorted structures are principally exhibited by electron-deficient complexes or by 18-electron complexes that are sterically crowded. Both electronic and steric factors appear to play a significant role.

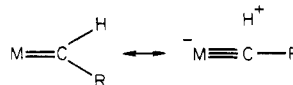
Hoffmann and co-workers have rationalized the distortions in the tantalum systems in terms of an orbital

analysis for the hypothetical molecule  $H_4Ta=CH_2$ <sup>3-</sup> formed from interaction of  $H_4Ta^{3-}$  and  $CH_2$  fragments.<sup>5</sup> These authors contend that while bending of the methylene fragment away from a symmetrical position, i.e.

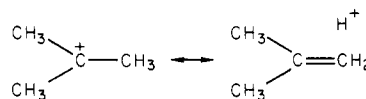


diminishes somewhat the overlap of atomic orbitals comprising the metal-carbon  $\sigma$  bond, it leaves the  $\pi$  system essentially unchanged and gives rise to the possibility of a new interaction involving another vacant pd hybrid.

An alternative and completely equivalent way in which to view the geometrical distortions in these systems is in terms of hyperconjugation, i.e.

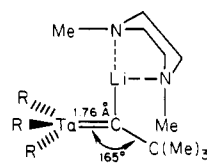


Similar structures are well known in carbocation chemistry, e.g., the *tert*-butyl cation



and account for the observed structural features in these systems, i.e., short CC bonds and lengthened CH linkages.<sup>6</sup>

Hyperconjugative resonance structures account for all the known geometrical distortions in the tantalum systems, as well as the increased acidity of the  $\alpha$ -hydrogen and its high susceptibility to abstraction. In particular, the longer than normal alkylidene CH bond, the smaller than normal MCH angle, and, most conspicuously, the large MCR bond angle are consequences of hyperconjugative resonance structures. Shortening of the MC bond relative to that for a normal  $M=C$  linkage would also be expected, by analogy with the carbocation system. Experimental structural data supports this. Note especially the exceptionally short MC bond distance in **2**, in which lithium assumes a bridging position.<sup>3f</sup> (For comparison, typical



**2**,  $R = (Me)_3CCH_2$

(5) R. J. Goddard, R. Hoffmann, and E. D. Jemmis, *J. Am. Chem. Soc.*, **102**, 7667 (1980).

(6) For a discussion, see: W. J. Hehre, *Acc. Chem. Res.*, **8**, 369 (1975).

(1) (a) Chevron fellow. (b) National Science Foundation predoctoral fellow.

(2) (a) G. D. Stucky, unpublished results, cited in: (b) C. D. Wood, W. J. McLain, and R. R. Schrock, *J. Am. Chem. Soc.*, **101**, 3210 (1979).

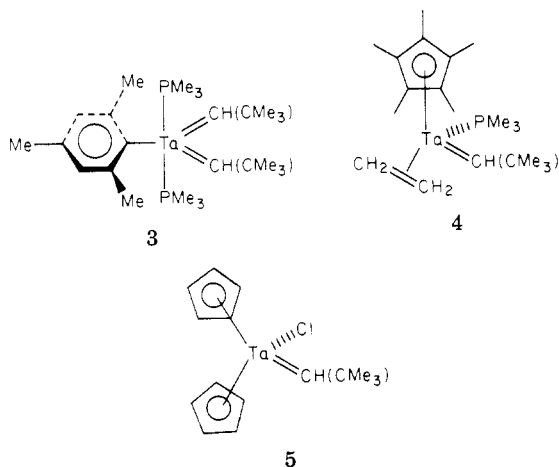
(3) (a) R. R. Schrock, L. W. Messerle, C. D. Wood, and L. J. Guggenberger, *J. Am. Chem. Soc.*, **100**, 3793 (1978); (b) M. R. Churchill and F. J. Hollander, *Inorg. Chem.*, **17**, 1957 (1978) and references therein; (c) A. J. Schultz, R. K. Brown, J. W. Williams, and R. R. Schrock, *J. Am. Chem. Soc.*, **103**, 169 (1981); (d) M. R. Churchill and W. J. Young, *Inorg. Chem.*, **18**, 1930 (1979) and references therein; (e) A. J. Schultz, J. M. Williams, R. R. Schrock, G. A. Rupprecht, and J. D. Fellmann, *J. Am. Chem. Soc.*, **101**, 1593 (1979); (f) L. J. Guggenberger and R. R. Schrock, *ibid.*, **97**, 2935 (1975); (g) M. R. Churchill and W. J. Young, *Inorg. Chem.*, **18**, 2454 (1979) and references therein; (h) P. R. Sharp, S. J. Holmes, R. R. Schrock, M. R. Churchill, and H. J. Wasserman, *J. Am. Chem. Soc.*, **103**, 965 (1981); (i) M. R. Churchill, H. J. Wasserman, H. W. Turner and R. R. Schrock, *ibid.*, **104**, 1710 (1982); (j) J. H. Wengrovius, R. R. Schrock, M. R. Churchill, and H. J. Wasserman, *ibid.*, **104**, 1739 (1982).

(4) For review see: P. J. Cardin, B. Cetinkaya, and M. F. Lappert, *Chem. Rev.*, **72**, 545 (1972).

TaC "double-bond" lengths fall in the range of 1.9–2.05 Å.<sup>3</sup> Here, hyperconjugative valence structures should be especially important due to the ability of Li to bear significant positive charge. In fact, the compound might best be described, and has been described, as a metal carbyne.

Electron-sufficient alkylidene complexes also show distortions similar to those seen in the electron-deficient compounds, although they are generally not as extreme. In these cases, hyperconjugation would not be expected to be important as it would result in an excess of 18 valence electrons associated with the metal center. Why then do coordinatively saturated systems distort from "normal" geometries? Schrock has suggested that steric effects may be responsible<sup>3c</sup> and we agree; in all cases examined thus far, the metal is congested, and the alkylidene center bears a sterically demanding substituent. Unfavorable interaction of the substituent with the ligands on the metal may be relieved by opening of the MCR angle. Although large skeletal angles are also characteristic of hyperconjugative structures (rehybridization at carbon from  $sp^2$  to  $sp$ ), the other geometrical features concomitant with hyperconjugation, e.g.,  $M=C$  bond shortening, could not easily be rationalized on steric grounds.

The subtle interplay of steric and electronic factors is clearly illustrated by the neopentylidene complexes 3–5<sup>3c,7</sup>



While both of the alkylidene moieties in 3 are distorted, one is affected to a greater extent than the other. The more severely distorted alkylidene shows a TaC bond length of 1.932 Å and a TaCC bond angle of 170°; the corresponding parameters for the other alkylidene are 1.955 Å and 154°. A neutron diffraction study on 3 would be interesting; it would be expected to show significantly elongated alkylidene CH bonds. A comparable angular distortion appears in 4 ( $\angle(\text{TaCC}) = 170^\circ$ ). However, the TaC bond length (1.946 Å) is perhaps longer than expected on the basis of the geometry of 3. Steric effects probably play some role in determining the geometry of this relatively crowded complex, although electronic factors must surely dominate; i.e., the TaC bond length in 4, with its 16 valence electrons, is nearly 0.1 Å shorter than the corresponding linkage in the 18-electron (coordinatively saturated) complex 5. Neutron diffraction studies of 4 have revealed the long alkylidene CH bonds characteristic of electronically distorted structures.<sup>3c</sup> Further examples of the effect of the degree of saturation on the geometries of tantalum carbenes are found in Table I. TaC bond lengths in the 18-electron complexes are uniformly longer

Table I. Bond Lengths (Å) and Angles (deg) for Tantalum Carbenes<sup>a</sup>

compd	elec- tron count	$r(\text{Ta}=\text{C})$	$\angle(\text{TaCC})$
$\text{TaCp}_2(\text{CH}_2)(\text{CH}_3)^b$	18	2.026	126.5
$\text{TaCp}_2(\text{CHPh})(\text{CH}_2\text{Ph})$	18	2.07	135.2
$\text{TaCp}_2(\text{CHCMe}_3)\text{Cl}$	18	2.030	150.4
$[\text{Ta}(\text{CHCMe}_3)(\text{PMe}_3)_2\text{Cl}_2]$	14	1.898	161.2
$\text{TaCp}(\text{CHPh})(\text{CH}_2\text{Ph})_2$	14	1.883	166.0

<sup>a</sup> Unless otherwise noted, references to structures may be found in ref 3. <sup>b</sup> R. R. Schrock and L. J. Guggenberger, *J. Am. Chem. Soc.*, **97**, 6578 (1975).

than those in systems in which the coordination shell about the metal is incomplete.

An interesting consequence of hyperconjugation is the  $M=C^+$  polarity of the metal-carbon double bond in the plane normal to the extant  $\pi$  system. This was originally noted by Schrock<sup>2b</sup> and, or course, is opposite to the  $M^+=C^-$  polarization of the original  $\pi$  system and suggests a reversal in substituent effects at carbon over what otherwise might be expected. We have examined this possibility by using quantitative molecular orbital theory.

### Theoretical Methods

All calculations reported herein have been performed by using the STO-3G minimal basis set, recently formulated for first- and second-row transition metals.<sup>8</sup> The GAUSSIAN 83 series of computer programs have been employed.<sup>9</sup>

The application of minimal basis sets such as STO-3G to the calculation of the structures and energies of transition-metal complexes has been much criticized in the literature, even though very few examples have actually been considered.<sup>10</sup> While some of this criticism is no doubt well founded, e.g., minimal basis sets do not fare well in the calculation of orbital energies, we believe that much of it is not and that the performance of such simple levels of theory need to be carefully and systematically explored before they are discarded. Table II presents a comparison of STO-3G equilibrium geometries for a variety of molecules containing titanium with available experimental structures as well as theoretical data obtained by using larger (double- $\zeta$ ) basis sets. The following points are worthy of comment.

Although tetramethyltitanium has as yet to be characterized experimentally, a low-temperature crystal structure for the related tetrabenzyl system has been reported.<sup>11</sup> The STO-3G TiC bond length in  $\text{TiMe}_4$  (assumed here to be of  $T_d$  symmetry) falls in the range of distances found in this latter system, which adopts a highly distorted (nontetrahedral) geometry. The calculated TiCl bond distance in titanium tetrachloride deviates by only 0.003 Å from the gas-phase experimental value.<sup>12</sup> The STO-3G

(8) First row: (a) W. J. Hehre, R. F. Stewart, and J. A. Pople, *J. Chem. Phys.*, **51**, 2657 (1969). First- and second-row transition metals: (b) W. J. Pietro and W. J. Hehre, *J. Comput. Chem.*, in press.

(9) R. F. Hout, Jr., M. M. Francl, E. S. Blurock, W. J. Pietro, D. J. DeFrees, S. K. Pollack, B. A. Levi, R. Steckler, and W. J. Hehre, Quantum Chemistry Program Exchange, Indiana University, to be submitted for publication.

(10) For a discussion see ref 8b.

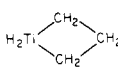

(11) (a) G. R. Davies, J. A. J. Jarvis, and B. T. Kilbourn, *J. Chem. Soc., Chem. Commun.* 1511 (1971). See also: (b) I. W. Bassi, G. Allegra, R. Scordamaglia, and G. Chioccola, *J. Am. Chem. Soc.*, **93**, 3738 (1971).

(12) J. H. Collomon, E. Hirota, K. Kuchitsu, W. J. Lafferty, A. G. Maki, and C. S. Pote, "Structure Data on Free Polyatomic Molecules", Landolt-Börnstein, New Series, Group II, Vol. 7, K. H. Hellwege and A. H. Hellwege, Eds., Springer-Verlag, Berlin, 1976.

(7) (a) M. R. Churchill and W. J. Young, *J. Chem. Soc., Chem. Commun.* 1048 (1978); (b) M. R. Churchill, F. J. Hollander, and R. R. Schrock, *J. Am. Chem. Soc.*, **100**, 647 (1978).



Table II. Comparison of STO-3G, Double- $\zeta$ , and Experimental Equilibrium Geometries for Compounds Containing Titanium<sup>a</sup>

molecule	geometrical parameter	STO-3G	double $\zeta^b$	exptl
Ti(CH <sub>3</sub> ) <sub>4</sub>	r(TiC)	2.096		2.04–2.21 <sup>c</sup>
	r(CH)	1.085		
	$\angle$ (HCH)	107.2		
TiCl <sub>4</sub>	r(TiCl)	2.167		2.170 <sup>d</sup>
	r(TiC)	1.824	1.885	
	r(TiCl)	2.196	(2.238) <sup>e</sup>	
Cl <sub>2</sub> Ti=CH <sub>2</sub>	r(CH)	1.088	1.084	
	$\angle$ (ClTiCl)	121.0	(142.0) <sup>e</sup>	
	$\angle$ (HCH)	109.4	116.5	
Cp <sub>2</sub> TiH <sub>2</sub>	r(TiC) <sup>b</sup>	2.349		2.44 <sup>f,g</sup>
	r(TiH)	1.649		
	$\angle$ (HTiH)	93.2		95.2
	tilt <sup>h</sup>	112.0		129.5
	r(TiC)	2.053	2.02 <sup>i</sup>	2.127, 2.113 <sup>j</sup>
	r(CC)	1.571	1.56	1.546, 1.579
	$\angle$ (CTiC)	76.0	75.6	75.3
	$\angle$ (CCC)	107.1	105.4	112.0
	$\angle$ (TiCC)	88.5	89.5	86.0, 85.7

<sup>a</sup> Bond lengths in Å and bond angles in deg. <sup>b</sup> Reference 13. <sup>c</sup> Range of TiC bond lengths found in Ti(CH<sub>2</sub>Ph)<sub>4</sub>.<sup>11</sup> <sup>d</sup> Reference 12. <sup>e</sup> Constrained values. <sup>f</sup> Average. <sup>g</sup> Structural parameters for Cp<sub>2</sub>TiCl<sub>2</sub>.<sup>15</sup> <sup>h</sup> Tilt angle defined as the angle between the normal to the cyclopentadienyl ring plane and the bisector of the HTiH (ClTiCl) angle. <sup>i</sup> Structural parameters for Cl<sub>2</sub>TiCH<sub>2</sub>CH<sub>2</sub>CH<sub>2</sub>.<sup>13</sup> <sup>j</sup> Structural parameters for Cp<sub>2</sub>TiCH<sub>2</sub>CH<sub>2</sub>CHPh.<sup>14</sup>

structure for dichlorotitanium carbene is in moderate accord with a theoretical structure obtained by Rappé and Goddard<sup>13</sup> using a double- $\zeta$  basis set. Note, however, that the latter was not fully optimized; TiCl bond lengths and the ClTiCl bond angle were assumed. No experimental data are available. A further comparison of STO-3G, double- $\zeta$ <sup>13</sup> and experimental<sup>14</sup> structures is available for titanacyclobutane derivatives. The minimal basis set calculations clearly reproduce all the principal features, especially a planar ring skeleton, in agreement with experimental and higher level theoretical structures. Finally the comparison between the STO-3G geometry for Cp<sub>2</sub>TiH<sub>2</sub> and the experimental crystal structure for Cp<sub>2</sub>TiCl<sub>2</sub><sup>15</sup> is again reasonable.

These comparisons and others like them<sup>8b</sup> suggest that the STO-3G basis set may provide a reasonable description of the structures of transition-metal inorganics and organometallics. In view of other work in the field,<sup>16</sup> it is also clear that higher level theoretical methods, i.e., more flexible basis sets and partial account for electron correlation, are likely to be necessary in order to accurately establish relative energetics.

## Results and Discussions

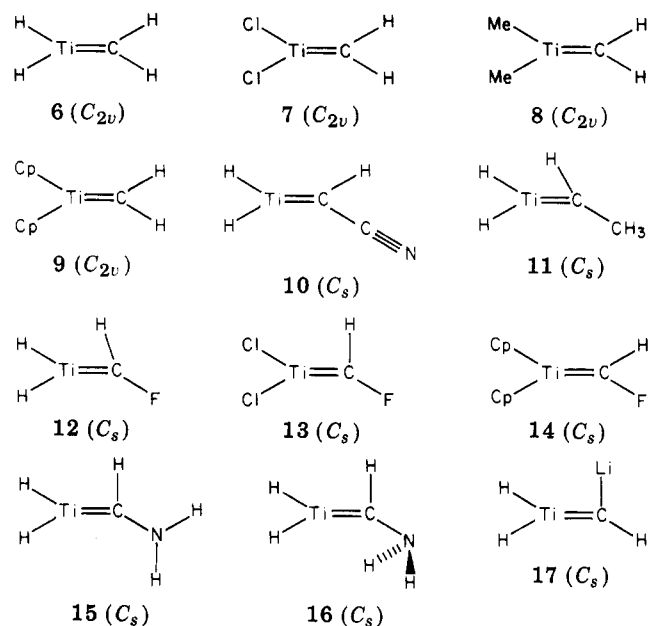
The principal features of the calculated (STO-3G) equilibrium structures for a number of metal carbenes involving titanium (6–17) are given in Table III. These

Table III. Selected Geometrical Parameters for Titanium Carbenes<sup>a</sup>

structure	geometrical parameter			
	r(Ti=C)	r(CH)	$\angle$ (TiCH)	$\angle$ (TiCX)
6	1.833	1.087	125.4	125.4
7	1.824	1.088	125.3	125.3
8	1.835	1.084	125.5	125.5
9	1.876	1.087	127.2	127.2
10	1.852	1.088	124.4	124.1
11	1.790	1.134	83.9	165.0
12	1.779	1.164	79.3	169.9
13	1.771	1.169	78.2	170.6
14	1.899	1.100	125.0	130.6
15	1.806	1.122	88.6	161.9
16	1.780	1.178	76.3	169.4
17	1.784		156.1	80.7

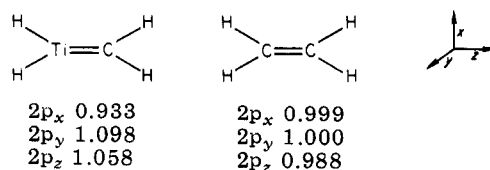
<sup>a</sup> Bond lengths in Å and bond angles in deg.

derive from complete structure optimizations carried out under a given symmetry constraint.



The calculated structures of the methylenes complexes 6–9 are all symmetrical and nonbridged. Nonsymmetrical (C<sub>s</sub> symmetry) structures were explored and found to collapse to symmetrical (C<sub>2v</sub> symmetry) forms. TiC bond lengths and TiCH bond angles in the 8-electron complexes 6–8 are in close accord with one another. The structure of the 16-electron dicyclopentadienyl adduct 9 differs but slightly; the TiC linkage is longer, and the methylenes hydrogens are bent further away from the metal center.

Calculated Mulliken orbital populations<sup>16</sup> on carbon for dihydrotitanium carbene 6, relative to those of ethylene, show the charge polarization expected from the simple hyperconjugative arguments.



In particular, while the 2p<sub>y</sub> populations support polarization of the  $\pi$  system with carbon negative, the 2p<sub>x</sub> orbital populations suggest the opposite ordering.

Substitution at carbon by cyano does not promote bridging of the alkylidene hydrogen. Structure 10 is very

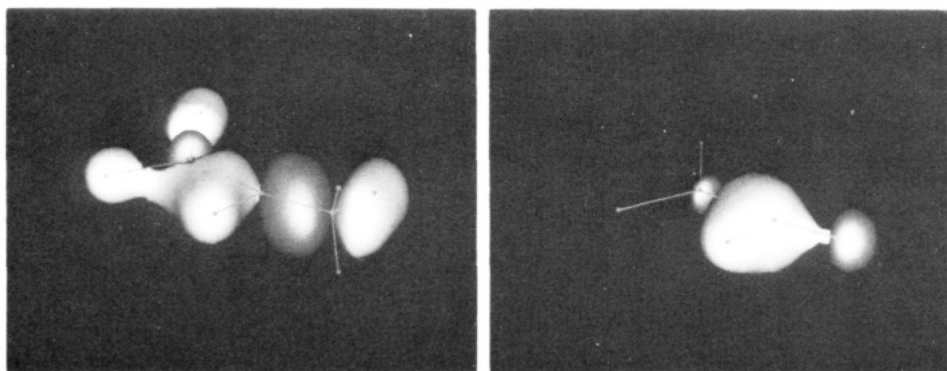
(13) A. K. Rappé and W. A. Goddard, III, *J. Am. Chem. Soc.*, **104**, 297 (1982).

(14) J. B. Lee, G. J. Gajda, W. P. Schaefer, T. R. Howard, T. Ikariya, D. A. Strauss, and R. H. Grubbs, *J. Am. Chem. Soc.*, **103**, 7358 (1981).

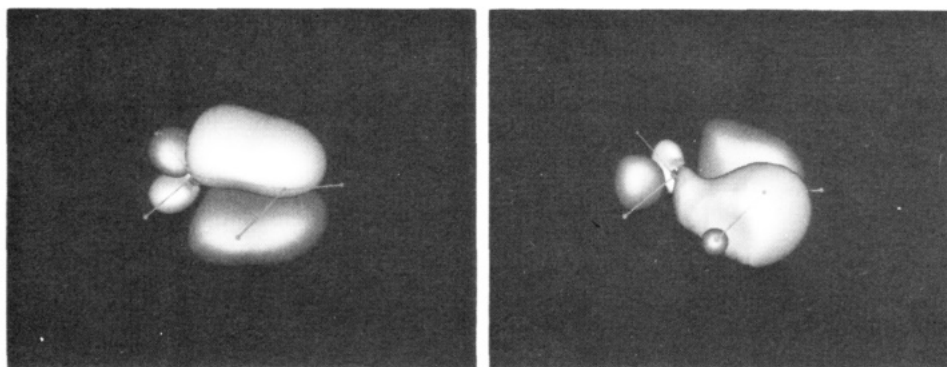
(15) V. V. Tkachev and L. O. Atomyan, *Zh. Struct. Khim.*, **13**, 287 (1972).

(16) For a recent example, see: R. M. Pitzer and H. F. Schaefer, III, *J. Am. Chem. Soc.*, **101**, 7176 (1979).

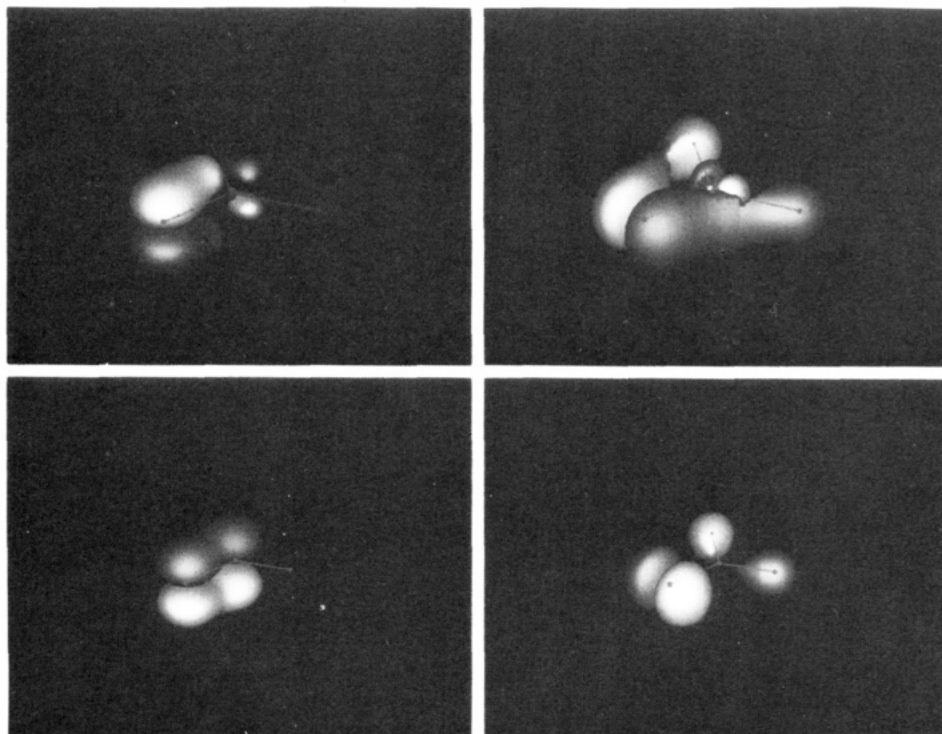
(17) R. S. Mulliken, *J. Chem. Phys.*, **23**, 1833, 1841, 2338, 2343 (1955).



**Figure 1.** Left: CH bonding orbital in  $\text{H}_2\text{Ti}=\text{CHMe}$ . Right: CH bonding orbital in  $\text{H}_2\text{Ti}=\text{CHF}$ .



**Figure 2.** Left:  $\pi$  orbital in  $\text{H}_2\text{Ti}=\text{CHLi}$ . Right: CLi bonding orbital in  $\text{H}_2\text{Ti}=\text{CHLi}$ .



**Figure 3.** Top left:  $\pi$  orbital in  $\text{H}_2\text{Ti}=\text{O}$ . Top right: n orbital in  $\text{H}_2\text{Ti}=\text{O}$ . Bottom left:  $\pi$  orbital in  $\text{H}_2\text{C}=\text{O}$ . Bottom right: n orbital in  $\text{H}_2\text{C}=\text{O}$ .

nearly "symmetrical" and displays a normal CH bond length. Significantly distorted geometries are, however, observed for all the other substituted 8-electron complexes. In particular, the 8-electron ethylidene complex 11 is severely distorted in the direction of hydrogen bridging. Here the calculations indicate an energy lowering of approximately  $6 \text{ kcal mol}^{-1}$  by comparison of the optimum

structure 11 with one artificially constrained to the geometry of the parent dihydrido complex 6. All of the fluoromethylidene complexes 12–14 also show varying degrees of distortion. Both the dihydrido complex 12 and the dichloro adduct 13 are greatly distorted; the coordinatively more saturated (16-electron) dicyclopentadienyl complex 14 exhibits only slight distortions. Taken together, these

data suggest that substitution at carbon and the electron deficiency the metal center both play a role in dictating equilibrium structure.

Orbital photographs<sup>18</sup> for the 8-electron dihydrido ethylidene and fluoromethylidene complexes **11** and **12**, respectively, clearly show the delocalization of electron density from the CH linkage onto the metal (Figure 1).

The amino derivatives **15** and **16** also show distortions to nonsymmetrical, bridged structures. Note that structure **16**, in which the amino group has been twisted perpendicular to the plane of the double bond, shows a greater tendency toward bridging than structure **15**, in which it remains in plane. This is consistent with the notion that electron donation from the nitrogen lone pair into the CH linkage, which is possible only in the perpendicular arrangement **16**, will act to stabilize hyperconjugative structures and hence promote bridging. The STO-3G calculations also show the perpendicular conformer **16** to be 5.5 kcal mol<sup>-1</sup> more stable than the corresponding planar structure **15**. In contrast, amino-substituted alkenes, e.g., vinylamine, exhibit planar or nearly planar geometries.

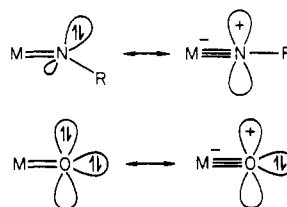
The preferential stabilization of "partial bridged" forms by methyl, fluoro, and amino substituents at the methylenidene carbon, and associated destabilization by nitrile is easily rationalized in the context of the hyperconjugative model; i.e., electron donors stabilize the M=C<sup>+</sup> valence structure and acceptors destabilize it. *The driving force for the distortion seems to be the electron deficiency of the central metal atom.* Coordinatively more saturated complexes, e.g., **14** do not exhibit extreme distortions even when the substituents at the methylenidene would stabilize a bridging structure. Distortions exhibited by both 8-electron dihydrido and dichloro complexes, e.g., **12** and **13**, are qualitatively similar.

Note the shortening of the metal-carbon linkages in the distorted structures relative to those in complexes with nonbridged geometries. The Ti=C linkages of all carbenes are, of course, significantly shorter than normal single bonds, e.g., 2.096 Å in TiMe<sub>4</sub> at the STO-3G level, 2.04–2.21 Å experimentally in Ti(CH<sub>2</sub>Ph)<sub>4</sub><sup>11</sup> (see Table II). Similar effects are found in structures of tantalum carbenes.<sup>3</sup> Also, only the distorted complexes display abnormally long alkylidene CH bonds. Again the available experimental data concur.<sup>3c</sup>

Particularly severe geometrical distortions appear in the theoretical structure of the 8-electron complex **17** in which lithium, rather than hydrogen, bridges the titanium-carbon double bond. Recall the experimentally characterized complex **2**. The extent of hyperconjugative donation from the CLi bond onto the metal is well illustrated by the orbital plots given in Figure 2. A second π-symmetry orbital delocalized over the titanium-carbon bond has formed; clearly this system is best described as incorporating a triple bond.

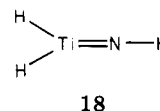
The distortion of alkylidene ligands bound to electron-deficient metal centers appears to be a general phenomena. Calculated structures for a variety of electron-deficient complexes of zirconium, vanadium, and niobium show similar effects.<sup>19</sup> Experimentally, electron deficient manganese and iron allyl complexes have been shown to exhibit distorted structures.<sup>20</sup>

Calculational studies suggest that imido and oxo complexes will also show effects of electron donation (from non-bonded lone pairs) into vacant d orbitals on the metal center, i.e.



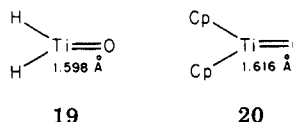
This is in keeping with the experimental observations of Schrock and others,<sup>21</sup> who have noted a monotonic decrease in bond length for the series Ta=O > Ta=N > Ta=C, as well as the observed ease of carbene substitution by imine.<sup>21a</sup> Theoretical studies by Goddard and Rappé have shown the importance of this donation in activating high-valent chromium catalysts for olefin methathesis.<sup>22</sup>

The STO-3G equilibrium geometry of the hypothetical imido complex **18** incorporates a linear nitrogen center.



While no direct comparison of TiN bond length is possible, i.e., with a "normal" double linkage, calculations show considerable lengthening of the linkage upon bending. Experimental data concur; for a series of similar Mo complexes M=N bond lengths increase with decreasing MNR angle.<sup>21b</sup>

Calculated structures for oxo complexes **19** and **20** hide any gross geometrical consequences arising from oxygen lone-pair donation into vacant orbitals on the metal center.



Note, however, a slight lengthening in the central bond length in the 16-electron complex **20** relative to that for the 8-electron system. The orbital photographs in Figure 3 clearly indicate the delocalization of the oxygen lone pair in **19** to form a new TiO π bond. Comparison with the analogous orbitals of formaldehyde shows a similar structure for the π bond but not significant electron donation from the oxygen lone pair to the carbon.

## Conclusion

The large MCR angles observed in many alkylidene complexes are consequences either of electron deficiency at the metal center or extreme steric crowding. The two effects may be distinguished by comparison of M=C bond lengths; electron donation onto the metal would result in bond shortening, steric crowding in bond lengthening. The observed geometrical distortions may clearly be rationalized in terms of hyperconjugation. In the context of this model, we have shown that in coordinately unsaturated complexes, electron-donating substituents on the alkylid-

(18) (a) R. F. Hout, Jr., W. J. Pietro, and W. J. Hehre, *J. Comput. Chem.*, in press. (b) R. F. Hout, Jr., W. J. Pietro and W. J. Hehre, "Orbital Photography: A Pictorial Approach to Structure and Reactivity", Wiley, New York, in press. (c) R. F. Hout, Jr., W. J. Pietro, and W. J. Hehre, Quantum Chemistry Program Exchange, Indiana University, to be submitted for publication.

(19) M. M. Francl and W. J. Hehre, unpublished calculations.

(20) M. Brookhart, W. Lamanna, and M. B. Humphrey, *J. Am. Chem. Soc.*, **104**, 2117 (1982).

(21) (a) G. A. Rupprecht, L. W. Messerle, J. D. Fellmann, and R. R. Schrock, *J. Am. Chem. Soc.*, **102**, 6236 (1980); S. M. Rocklage and R. R. Schrock, *ibid.*, **102**, 7808 (1980); (b) W. A. Nugent and B. L. Haymore, *Coord. Chem. Rev.*, **31**, 123 (1980).

(22) A. K. Rappé and W. A. Goddard, III, *J. Am. Chem. Soc.*, **104**, 448 (1982).

ene carbon act to stabilize distorted structures.

**Registry No.** 5, 57483-58-6; 6, 78499-81-7; 7, 79899-81-3; 8, 83876-39-5; 9, 83876-46-4; 10, 83876-40-8; 11, 83876-41-9; 12, 83876-42-0; 13, 83876-43-1; 14, 83876-47-5; 15/16, 83876-44-2; 17,

83876-45-3; TaCp<sub>2</sub>(CH<sub>2</sub>)(CH<sub>3</sub>), 57913-16-3; TaCp<sub>2</sub>(CHPh)(CH<sub>2</sub>Ph), 57483-57-5; [Ta(CHCMe<sub>3</sub>)(PMe<sub>3</sub>)Cl<sub>3</sub>]<sub>2</sub>, 70083-63-5; TaCp(CHPh)(CH<sub>2</sub>Ph)<sub>2</sub>, 83876-48-6; Ti(CH<sub>3</sub>)<sub>4</sub>, 2371-70-2; TiCl<sub>4</sub>, 7550-45-0; Cp<sub>2</sub>TiH<sub>2</sub>, 83876-49-7; H<sub>2</sub>TiCH<sub>2</sub>CH<sub>2</sub>CH<sub>2</sub>, 77934-15-7.

## Structure and Bonding in Neutral and Cationic Iron Carbonyl Phosphine Complexes. The Crystal Structures of $(\pi\text{-C}_6\text{H}_6)\text{Fe}(\text{CO})_2(\text{PPh}_3)$ , $[(\pi\text{-C}_5\text{H}_5)\text{Fe}(\text{CO})_2(\text{PPh}_3)]\text{Cl}\cdot 3\text{H}_2\text{O}$ , and $[(\pi\text{-C}_5\text{H}_5)\text{Fe}(\text{CO})(\text{Ph}_2\text{PCH}_2\text{CH}_2\text{PPh}_2)]\text{BF}_4$

Paul E. Riley and Raymond E. Davis\*

Department of Chemistry, The University of Texas at Austin, Austin, Texas 78712

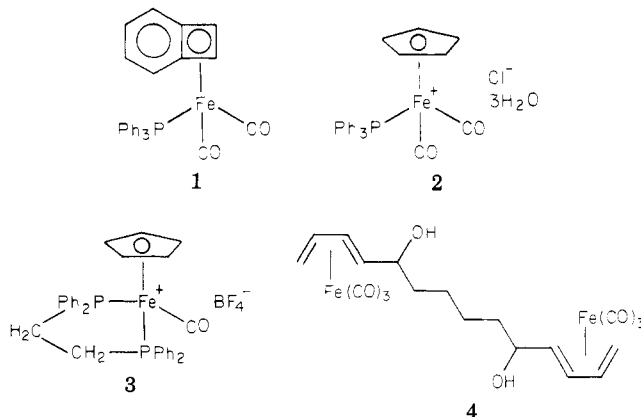
Received June 7, 1982

The structures of  $(\pi\text{-C}_6\text{H}_6)\text{Fe}(\text{CO})_2(\text{PPh}_3)$  (1),  $[(\pi\text{-C}_5\text{H}_5)\text{Fe}(\text{CO})_2(\text{PPh}_3)]\text{Cl}\cdot 3\text{H}_2\text{O}$  (2), and  $[(\pi\text{-C}_5\text{H}_5)\text{Fe}(\text{CO})(\text{Ph}_2\text{PCH}_2\text{CH}_2\text{PPh}_2)]\text{BF}_4$  (3) have been determined by single-crystal X-ray diffraction techniques with three-dimensional data gathered by counter methods. Orange prisms of 1 form in triclinic space group  $P\bar{1}$  in which four molecules of 1 are contained in a unit cell of dimensions  $a = 13.863$  (5) Å,  $b = 15.899$  (6) Å,  $c = 10.775$  (3) Å,  $\alpha = 103.49$  (3)°,  $\beta = 92.05$  (3)°, and  $\gamma = 81.18$  (3)°. Yellow plates of 2 also crystallize in space group  $P\bar{1}$  with  $Z = 2$  and  $a = 9.982$  (2) Å,  $b = 13.550$  (3) Å,  $c = 9.321$  (3) Å,  $\alpha = 101.23$  (2)°,  $\beta = 93.00$  (2)°, and  $\gamma = 93.41$  (2)°. Yellow needle-like crystals of 3 form in orthorhombic space group  $P2_12_12_1$  with  $Z = 4$  for a unit-cell defined by  $a = 15.771$  (7) Å,  $b = 17.614$  (7) Å, and  $c = 10.492$  (4) Å. Full-matrix least-squares refinements of the structures have converged with conventional  $R$  indices (on  $|F|$ ) of 0.067 for 1, 0.062 for 2, and 0.057 for 3, using the 6405, 4782, and 3619 observations with  $I_o > 2\sigma(I_o)$  for 1, 2, and 3, respectively. These three compounds are part of a series of six closely related iron carbonyl complexes for which the phosphine content and cationic charge have been systematically varied. Within this series, the changes in the Fe-C and C-O bond lengths as a function of phosphine substitution and complex charge are correlated with changes in carbonyl stretching frequencies and chemical reactivity.

### Introduction

It has been an objective of this laboratory to investigate the structural and spectroscopic consequences of the systematic substitution of phosphine ligands for carbonyl ligands in transition-metal complexes as a function of (1) degree of carbonyl replacement, (2) charge of metal complex, (3) nature of transition metal, (4) coordination geometry about the metal, and (5) donor capacity of phosphine ligand(s). Accordingly, to complement earlier work of the Ibers' group<sup>1</sup> with trigonal-bipyramidal Mn-CO complexes, we determined the structures of the two similarly coordinated, isoelectronic species  $[\text{Mn}(\text{CO})_4(\text{PPh}_3)]^-$  and  $\text{Fe}(\text{CO})_4(\text{PPh}_3)$ .<sup>2</sup> Also, in conjunction with Pettit et al.,<sup>3</sup> we reported the structures and chemical reactivities of two ( $\pi$ -allyl)cobalt compounds, an unsubstituted tricarbonyl complex and a dicarbonyl trimethylphosphite complex. Furthermore, we examined with Cowley et al.<sup>4</sup> the crystal structures of the two trigonal-bipyramidal complexes  $\text{Fe}(\text{CO})_{5-n}[\text{P}(\text{NMe}_2)_3]_n$ , where  $n = 1$  or 2, which contain the strongly electron-donating  $\text{P}(\text{NMe}_2)_3$  ligand. Additionally, the structure of  $(\text{C}_6\text{H}_6)\text{Cr}(\text{CO})_2(\text{PPh}_3)$ , which is obtained photochemically<sup>5</sup> from the parent tricarbonyl complex, was determined<sup>6</sup> for comparison to the parent complex.<sup>7</sup>

We now extend these data by presenting the crystal structures and complementary infrared spectroscopic data in the sensitive C-O stretching region for the three compounds shown which complete a small set of neutral and cationic, unsubstituted and substituted Fe-carbonyl complexes. The corresponding structural and spectroscopic data for two other members of this set, viz., 4 and 5, were published by us earlier,<sup>8,9</sup> and our interpretation of the structural aspects of these five iron complexes (1-5) and of those of the parent cationic  $\text{Fe}(\text{CO})_3$  complex<sup>10</sup> 6 is presented.



(1) Frenz, B. A.; Enemark, J. H.; Ibers, J. A. *Inorg. Chem.* 1969, 8, 1288 and references therein. Frenz, B. A.; Ibers, J. A. *Ibid.* 1972, 11, 1109.

(2) Riley, P. E.; Davis, R. E. *Inorg. Chem.* 1980, 19, 159.

(3) Cann, K.; Riley, P. E.; Davis, R. E.; Pettit, R. *Inorg. Chem.* 1978, 17, 1421.

(4) Cowley, A. H.; Davis, R. E.; Lattman, M.; McKee, M.; Remadna, K. J. *Am. Chem. Soc.* 1979, 101, 5090. Cowley, A. H.; Davis, R. E.; Remadna, K. *Inorg. Chem.* 1981, 20, 2146.

(5) Prepared in this manner by K. Cann and R. Pettit.

(6) Yep, J.; Davis, R. E., unpublished results.

(7) Rees, B.; Coppens, P. *Acta Crystallogr. Sect B* 1973, B29, 2515.

(8) Riley, P. E.; Davis, R. E. *Acta Crystallogr., Sect B* 1978, B34, 3760.

(9) Davis, R. E.; Riley, P. E. *Inorg. Chem.* 1980, 19, 674.

(10) Gress, M. E.; Jacobson, R. A. *Inorg. Chem.* 1973, 12, 1746. Davison, A.; Green, M. L. H.; Wilkinson, G. *J. Chem. Soc.* 1961, 3172.

ene carbon act to stabilize distorted structures.

**Registry No.** 5, 57483-58-6; 6, 78499-81-7; 7, 79899-81-3; 8, 83876-39-5; 9, 83876-46-4; 10, 83876-40-8; 11, 83876-41-9; 12, 83876-42-0; 13, 83876-43-1; 14, 83876-47-5; 15/16, 83876-44-2; 17,

83876-45-3; TaCp<sub>2</sub>(CH<sub>2</sub>)(CH<sub>3</sub>), 57913-16-3; TaCp<sub>2</sub>(CHPh)(CH<sub>2</sub>Ph), 57483-57-5; [Ta(CHCMe<sub>3</sub>)(PMe<sub>3</sub>)Cl<sub>3</sub>]<sub>2</sub>, 70083-63-5; TaCp(CHPh)(CH<sub>2</sub>Ph)<sub>2</sub>, 83876-48-6; Ti(CH<sub>3</sub>)<sub>4</sub>, 2371-70-2; TiCl<sub>4</sub>, 7550-45-0; Cp<sub>2</sub>TiH<sub>2</sub>, 83876-49-7; H<sub>2</sub>TiCH<sub>2</sub>CH<sub>2</sub>CH<sub>2</sub>, 77934-15-7.

## Structure and Bonding in Neutral and Cationic Iron Carbonyl Phosphine Complexes. The Crystal Structures of $(\pi\text{-C}_6\text{H}_6)\text{Fe}(\text{CO})_2(\text{PPh}_3)$ , $[(\pi\text{-C}_5\text{H}_5)\text{Fe}(\text{CO})_2(\text{PPh}_3)]\text{Cl}\cdot 3\text{H}_2\text{O}$ , and $[(\pi\text{-C}_5\text{H}_5)\text{Fe}(\text{CO})(\text{Ph}_2\text{PCH}_2\text{CH}_2\text{PPh}_2)]\text{BF}_4$

Paul E. Riley and Raymond E. Davis\*

Department of Chemistry, The University of Texas at Austin, Austin, Texas 78712

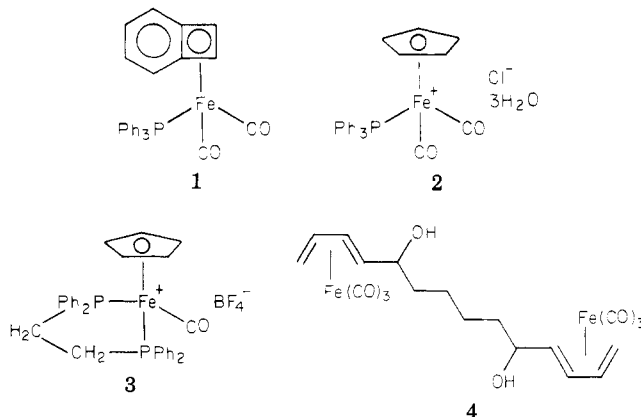
Received June 7, 1982

The structures of  $(\pi\text{-C}_6\text{H}_6)\text{Fe}(\text{CO})_2(\text{PPh}_3)$  (1),  $[(\pi\text{-C}_5\text{H}_5)\text{Fe}(\text{CO})_2(\text{PPh}_3)]\text{Cl}\cdot 3\text{H}_2\text{O}$  (2), and  $[(\pi\text{-C}_5\text{H}_5)\text{Fe}(\text{CO})(\text{Ph}_2\text{PCH}_2\text{CH}_2\text{PPh}_2)]\text{BF}_4$  (3) have been determined by single-crystal X-ray diffraction techniques with three-dimensional data gathered by counter methods. Orange prisms of 1 form in triclinic space group  $P\bar{1}$  in which four molecules of 1 are contained in a unit cell of dimensions  $a = 13.863$  (5) Å,  $b = 15.899$  (6) Å,  $c = 10.775$  (3) Å,  $\alpha = 103.49$  (3)°,  $\beta = 92.05$  (3)°, and  $\gamma = 81.18$  (3)°. Yellow plates of 2 also crystallize in space group  $P\bar{1}$  with  $Z = 2$  and  $a = 9.982$  (2) Å,  $b = 13.550$  (3) Å,  $c = 9.321$  (3) Å,  $\alpha = 101.23$  (2)°,  $\beta = 93.00$  (2)°, and  $\gamma = 93.41$  (2)°. Yellow needle-like crystals of 3 form in orthorhombic space group  $P2_12_12_1$  with  $Z = 4$  for a unit-cell defined by  $a = 15.771$  (7) Å,  $b = 17.614$  (7) Å, and  $c = 10.492$  (4) Å. Full-matrix least-squares refinements of the structures have converged with conventional  $R$  indices (on  $|F|$ ) of 0.067 for 1, 0.062 for 2, and 0.057 for 3, using the 6405, 4782, and 3619 observations with  $I_o > 2\sigma(I_o)$  for 1, 2, and 3, respectively. These three compounds are part of a series of six closely related iron carbonyl complexes for which the phosphine content and cationic charge have been systematically varied. Within this series, the changes in the Fe-C and C-O bond lengths as a function of phosphine substitution and complex charge are correlated with changes in carbonyl stretching frequencies and chemical reactivity.

### Introduction

It has been an objective of this laboratory to investigate the structural and spectroscopic consequences of the systematic substitution of phosphine ligands for carbonyl ligands in transition-metal complexes as a function of (1) degree of carbonyl replacement, (2) charge of metal complex, (3) nature of transition metal, (4) coordination geometry about the metal, and (5) donor capacity of phosphine ligand(s). Accordingly, to complement earlier work of the Ibers' group<sup>1</sup> with trigonal-bipyramidal Mn-CO complexes, we determined the structures of the two similarly coordinated, isoelectronic species  $[\text{Mn}(\text{CO})_4(\text{PPh}_3)]^-$  and  $\text{Fe}(\text{CO})_4(\text{PPh}_3)$ .<sup>2</sup> Also, in conjunction with Pettit et al.,<sup>3</sup> we reported the structures and chemical reactivities of two ( $\pi$ -allyl)cobalt compounds, an unsubstituted tricarbonyl complex and a dicarbonyl trimethylphosphite complex. Furthermore, we examined with Cowley et al.<sup>4</sup> the crystal structures of the two trigonal-bipyramidal complexes  $\text{Fe}(\text{CO})_{5-n}[\text{P}(\text{NMe}_2)_3]_n$ , where  $n = 1$  or 2, which contain the strongly electron-donating  $\text{P}(\text{NMe}_2)_3$  ligand. Additionally, the structure of  $(\text{C}_6\text{H}_6)\text{Cr}(\text{CO})_2(\text{PPh}_3)$ , which is obtained photochemically<sup>5</sup> from the parent tricarbonyl complex, was determined<sup>6</sup> for comparison to the parent complex.<sup>7</sup>

We now extend these data by presenting the crystal structures and complementary infrared spectroscopic data in the sensitive C-O stretching region for the three compounds shown which complete a small set of neutral and cationic, unsubstituted and substituted Fe-carbonyl complexes. The corresponding structural and spectroscopic data for two other members of this set, viz., 4 and 5, were published by us earlier,<sup>8,9</sup> and our interpretation of the structural aspects of these five iron complexes (1-5) and of those of the parent cationic  $\text{Fe}(\text{CO})_3$  complex<sup>10</sup> 6 is presented.



(1) Frenz, B. A.; Enemark, J. H.; Ibers, J. A. *Inorg. Chem.* 1969, 8, 1288 and references therein. Frenz, B. A.; Ibers, J. A. *Ibid.* 1972, 11, 1109.

(2) Riley, P. E.; Davis, R. E. *Inorg. Chem.* 1980, 19, 159.

(3) Cann, K.; Riley, P. E.; Davis, R. E.; Pettit, R. *Inorg. Chem.* 1978, 17, 1421.

(4) Cowley, A. H.; Davis, R. E.; Lattman, M.; McKee, M.; Remadna, K. J. *Am. Chem. Soc.* 1979, 101, 5090. Cowley, A. H.; Davis, R. E.; Remadna, K. *Inorg. Chem.* 1981, 20, 2146.

(5) Prepared in this manner by K. Cann and R. Pettit.

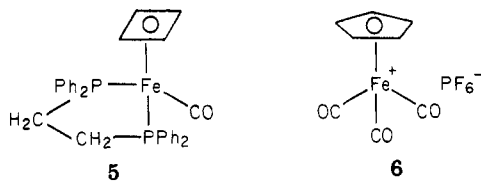
(6) Yep, J.; Davis, R. E., unpublished results.

(7) Rees, B.; Coppens, P. *Acta Crystallogr. Sect B* 1973, B29, 2515.

(8) Riley, P. E.; Davis, R. E. *Acta Crystallogr., Sect B* 1978, B34, 3760.

(9) Davis, R. E.; Riley, P. E. *Inorg. Chem.* 1980, 19, 674.

(10) Gress, M. E.; Jacobson, R. A. *Inorg. Chem.* 1973, 12, 1746. Davison, A.; Green, M. L. H.; Wilkinson, G. *J. Chem. Soc.* 1961, 3172.



### Experimental Section

Well-formed orange prisms of 1 and yellow needle-like crystals of 3 were supplied by Professor R. Pettit. Excellent large yellow plates of the trihydrate of 2 were obtained by evaporation of an aqueous solution at room temperature. A crystal of each compound was glued to a glass fiber, attached to a goniometer head, and placed on a Syntex P2<sub>1</sub> diffractometer for preliminary examination and subsequent data collection. It was necessary to cleave one of the trihydrate crystals of 2. Data for 1 were obtained under ambient conditions, while data for 2 and 3 were gathered in an atmosphere of dry N<sub>2</sub> supplied by an inert-atmosphere delivery system. In addition, the data crystal for 3 was maintained at -35 °C during all experiments, but since that of trihydrate 2 was found to fracture at this temperature, it was kept at room temperature (~20 °C) during the X-ray diffraction work. Preliminary examination of each crystal with the diffractometer indicated triclinic symmetry<sup>11</sup> for the crystals of 1 and 2 and the orthorhombic symmetry and systematic reflection absences of space group P2<sub>1</sub>2<sub>1</sub>2<sub>1</sub> for crystal 3. Crystal data and intensity data collection details for the data crystals of 1-3 are summarized in Table I. Processing of the intensity data obtained for each crystal, with  $\rho$  values given in Table I, was performed as previously delineated.<sup>12</sup>

**Solution and Refinement of the Structures.** The structures were solved by standard heavy-atom procedures and refined by full-matrix least-squares methods<sup>13</sup> using for each data set only those symmetry-independent reflections with intensities  $I_o$  for which  $I_o/\sigma(I) > 2$ . The function minimized in refinement is  $\sum w(|F_o| - |F_c|)^2$ , where the weight  $w$  is  $\sigma(|F_o|)^{-2}$ , the reciprocal square of the standard deviation of each observation  $|F_o|$ . Neutral atom scattering factors for Fe, Cl, P, F, O, C, B,<sup>14</sup> and H<sup>15</sup> were used in these calculations, with those of Fe, Cl, and P corrected for the anomalous scattering<sup>14</sup> of MoK $\alpha$  radiation.

**( $\pi$ -bzcb)Fe(CO)<sub>2</sub>(PPh<sub>3</sub>) (1).** Since satisfactory refinement of this structure was attained in centrosymmetric space group  $P\bar{1}$ , refinement in the alternative noncentrosymmetric space group  $P1$  was not necessary. The model ultimately used in refinement treated phenyl groups as rigid groups,<sup>16</sup> nongroup non-hydrogen atoms as anisotropic thermal ellipsoids, and nongroup hydrogen atoms as isotropic atoms. At convergence,<sup>17</sup>  $R = \sum(|F_o| - |F_c|) / \sum|F_o| = 0.067$ ,  $R_w = [\sum w(|F_o| - |F_c|)^2 / \sum w|F_o|^2]^{1/2} = 0.043$ , and a standard deviation of an observation of unit weight =  $[\sum w(|F_o| - |F_c|)^2 / (m - s)]^{1/2} = 2.74$  for  $m = 6405$  observations and  $s = 404$  variables. Near the conclusion of refinement, comparison of  $|F_o|$  vs.  $|F_c|$  for low-angle reflections suggested the need for a small correction for secondary extinction. Hence, a parameter<sup>18</sup> (3.79

$(5) \times 10^{-7} e^{-2}$ ) to account for this was included in the final cycles of refinement.

In the last cycle of refinement all shifts in non-hydrogen atom parameters were less than 0.35 of a corresponding estimated standard deviation (esd), while no shift of a hydrogen atom parameter<sup>19</sup> exceeded 0.22 of its esd.

**[( $\pi$ -C<sub>5</sub>H<sub>5</sub>)Fe(CO)<sub>2</sub>(PPh<sub>3</sub>)]Cl·3H<sub>2</sub>O (2).** As above, refinement in space group  $P\bar{1}$  was satisfactory, and hence refinement in space group  $P1$  was not required. Convergence was attained for a model similar to that employed for 1 (i.e., phenyl groups were treated as rigid groups, nongroup non-hydrogen atoms as anisotropic thermal ellipsoids, and nongroup hydrogen atoms<sup>20</sup> as isotropic atoms) with  $R$ ,  $R_w$ , and an estimated standard deviation of an observation of unit weight of 0.062, 0.076, and 4.18, respectively, for 4782 observations and 194 variables. Since comparison of the values of  $|F_o|$  and  $|F_c|$  for low-angle data indicated secondary extinction, a correction<sup>18</sup>  $(3.0(5) \times 10^{-6} e^{-2})$  for this effect was included in the final cycles of refinement.

In the last cycle of refinement, shifts in nongroup non-hydrogen and hydrogen atomic parameters did not exceed, respectively, 0.6 and 0.7 of a corresponding esd, while those of the group atoms were not in excess of 0.5 of an appropriate esd. The largest residual peaks on a final difference density map had heights of 0.3-0.4 e  $\text{\AA}^{-3}$  which were attributable to thermal anisotropy of phenyl ring atoms.

**[( $\pi$ -C<sub>5</sub>H<sub>5</sub>)Fe(CO)(dppe)]BF<sub>4</sub> (3).** Full-matrix least-squares refinement of a model structure, which is essentially as described for 1 and 2, converged with  $R$  and  $R_w$  indices of 0.061 and 0.069, respectively. Through this stage of refinement, corrections for the imaginary component ( $\Delta f''$ ) of anomalous scattering had not been applied to the atomic scattering factors. However, to learn whether the proper enantiomorph for the data crystal had been selected during structure solution, these corrections were now made to the Fe and P scattering curves and refinement was continued to convergence. This led to  $R$  and  $R_w$  indices of 0.067 and 0.073, respectively. However, reversal of the signs<sup>21</sup> of these corrections ( $-(\Delta f'')$ ), followed by refinement of the structure beginning with the atomic parameters obtained prior to the incorporation of these effects, converged with  $R = 0.057$  and  $R_w = 0.061$ . Since these residuals are significantly lower than those for the refinement of the initially selected model, this second model is taken as the correct enantiomorph for the crystal used in the work. The standard deviation of an observation of unit weight for this model is 2.93 for 3619 observations and 238 variables. At the conclusion of refinement, comparison of  $|F_o|$  vs.  $|F_c|$  showed no evidence of secondary extinction.

In the final cycle of refinement all shifts in nongroup non-hydrogen atom parameters were less than 0.05 of a corresponding esd, and all shifts in nongroup hydrogen atom parameters and group parameters were less than 0.69 and 0.24 of a corresponding esd, respectively. The largest peaks on a final difference Fourier map ranged from 0.4 to 1.1 e  $\text{\AA}^{-3}$  and were close to Fe or phenyl carbon positions.

Positional parameters for nongroup non-hydrogen atoms of 1, 2, and 3, with corresponding esd's as derived from the (appropriate) least-squares inverse matrix, are given in Tables II, III, and IV.<sup>22</sup> Anisotropic thermal parameters, group atom crystallographic coordinates and isotropic thermal parameters, nongroup hydrogen atom parameters, and structure factor amplitudes are available.<sup>23</sup>

### Discussion of the Crystal Structures of 1-3

The structures of 1 and 3 consist of discrete molecules or ions with no unusual intermolecular contacts. The

(11) The triclinic symmetry of the data crystals of 1 and 2 was corroborated by the computer program RCELL, a reduced cell algorithm: Collins, R. C.; The University of Texas at Austin, 1977.

(12) Riley, P. E.; Davis, R. E. *Acta Crystallogr., Sect B* 1976, B32, 381.

(13) A listing of principal computer programs used in these studies is given in ref 12.

(14) "International Tables for X-Ray Crystallography"; Kynoch Press: Birmingham, England, 1974; Vol. IV.

(15) Stewart, R. F.; Davidson, E. R.; Simpson, W. T. *J. Chem. Phys.* 1965, 42, 3175.

(16) Phenyl rings, except where indicated otherwise, were constrained as follows: C-C = 1.392 Å, C-H = 1.00 Å, C-C-C = 120°; each hydrogen atom was assigned an isotropic thermal parameters 1.0 Å<sup>2</sup> greater than that of the refined value of the carbon atom to which it is bonded.

(17) Due to the large number of variables for 1, this structure was refined by a blocked-matrix procedure, in which the two crystallographically independent molecules were refined alternately, but the heavy atoms were refined each cycle. In the final refinement cycles, parameters were blocked as follows: (final cycle - 2)—in both molecules, Fe, P, carbonyls, rigid phenyls; (final cycle - 1)—in both molecules, Fe, P, benzocyclobutadiene ligand (bzcb) including H atoms; (final cycle)—in molecule B, Fe, P, bzcb including H atoms.

(18) Zachariasen, W. H. *Acta Crystallogr. Sect A* 1968, A24, 212.

(19) The isotropic thermal parameters for all group hydrogen atoms were maintained at 6.0 Å<sup>2</sup> throughout refinement.

(20) The hydrogen atoms of the water molecules were not located.

(21) It may be demonstrated algebraically that this is computationally equivalent to refining the structure with the signs of all fractional coordinates reversed.

(22) The atomic and group coordinates presented in Table IV for the structure of 3 are those of the enantiomorph yielding the lower  $R$  indices.

(23) Supplementary material.

Table I. Crystallographic Summary

	$(\pi\text{-bzcb})\text{Fe}(\text{CO})_2(\text{PPh}_3)$ (1)	$[(\pi\text{-C}_5\text{H}_5)\text{Fe}(\text{CO})_2\text{-}(\text{PPh}_3)]\text{Cl}\cdot 3\text{H}_2\text{O}$ (2)	$[(\pi\text{-C}_5\text{H}_5)\text{Fe}(\text{CO})(\text{dppe})]\text{BF}_4$ (3)
<i>a</i> , Å	13.863 (5) <sup>a</sup>	9.982 (2) <sup>b</sup>	15.771 (7) <sup>c</sup>
<i>b</i> , Å	15.899 (6)	13.550 (3)	17.614 (7)
<i>c</i> , Å	10.775 (3)	9.321 (3)	10.492 (4)
$\alpha$ , deg	103.49 (3)	101.23 (2)	90
$\beta$ , deg	92.05 (3)	93.00 (2)	90
$\gamma$ , deg	81.18 (3)	93.41 (2)	90
<i>V</i> , Å <sup>3</sup>	2282 (5)	1238 (2)	2914 (3)
<i>d</i> <sub>calcd</sub> , g cm <sup>-3</sup>	1.387	1.418	1.445 <sup>c</sup>
empirical formula	C <sub>28</sub> H <sub>21</sub> FeO <sub>2</sub> P	C <sub>25</sub> H <sub>26</sub> ClFeO <sub>5</sub> P	C <sub>32</sub> H <sub>29</sub> BF <sub>4</sub> FeOP <sub>2</sub>
<i>fw</i>	476.30	528.76	634.21
cryst system	triclinic	triclinic	orthorhombic
systematic absences			<i>h</i> 00, <i>h</i> = 2 <i>n</i> + 1, 0 <i>k</i> 0, <i>k</i> = 2 <i>n</i> + 1, 00 <i>l</i> , <i>l</i> = 2 <i>n</i> + 1
space group	<i>P</i> 1 (No. 1) or $\bar{P}1$ (No. 2) <sup>d</sup>	<i>P</i> 1 (No. 1) or $\bar{P}1$ (No. 2) <sup>d</sup>	<i>P</i> 2 <sub>1</sub> 2 <sub>1</sub> 2 <sub>1</sub> (No. 19)
<i>z</i>	4	2	4
<i>F</i> (000), electrons	984	548	1304
Data Collection <sup>e</sup>			
radiation (Mo K $\alpha$ ), Å	0.710 69		
mode	$\omega$ scan		
scan range	symmetrically over 1.0° about K $\alpha_{1,2}$ maximum		
bkgd	offset 1.0° and -1.0° from K $\alpha_{1,2}$ maximum		
scan rate, deg min <sup>-1</sup>	variable, 3.0-10.0	variable, 2.0-5.0	variable, 1.0-4.0
check reflctns	4 remeasured after every 96 reflections; analyses <sup>f</sup> of these data indicated only random fluctuation in intensity for all 3 data sets. Hence, decay corrections were not required.		
2 $\theta$ range, deg	4.0-50.0	4.0-55.0	4.0-57.0
total reflctns measd	9985	5669	4127
<i>p</i> factor	0.00	0.02	0.02
absorption coeff, cm <sup>-1</sup>	7.77	8.36	6.95
$\mu$ (Mo K $\alpha$ ) <sup>g</sup>			

<sup>a</sup> Unit cell parameters were obtained by least-squares refinement of the setting angles of 65  $2\theta_{\alpha_1}$  and  $\theta_{\alpha_2}$  reflections for  $77 < 2\theta < 111^\circ$  with Cu K $\alpha$  radiation ( $\lambda(K_{\alpha_1}) = 1.540 50$  Å,  $\lambda(K_{\alpha_2}) = 1.544 33$  Å) at a takeoff angle of  $1.0^\circ$  and a gathering slit width of  $0.05^\circ$ . <sup>b</sup> Unit cell parameters were obtained by least-squares refinement of the setting angles of 60 reflections with  $18 < 2\theta < 20^\circ$  (Mo K $\alpha$ ). <sup>c</sup> Unit cell parameters were obtained by least-squares refinement of the setting angles, measured at room temperature, of 30 reflections with  $15 < 2\theta < 18^\circ$  (Mo K $\alpha$ ). <sup>d</sup> Shown by successful least-squares refinement to be *P*1 (see text). <sup>e</sup> Syntex P2<sub>1</sub> automated diffractometer equipped with a graphite monochromator and, for the data set obtained for 3, a Syntex LT-1 inert-gas delivery system. <sup>f</sup> Henslee, W. H.; Davis, R. E. *Acta Crystallogr., Sect. B* 1975, B31, 1511. <sup>g</sup> All data sets were corrected for absorption (see ref 12).

Table II. Fractional Coordinates for Non-Hydrogen Atoms of 1<sup>a</sup>

atom	<i>x</i>	<i>y</i>	<i>z</i>	atom	<i>x</i>	<i>y</i>	<i>z</i>
AFe	0.13188 (5)	0.04351 (4)	0.35933 (6)	BFe	0.21095 (5)	0.53523 (4)	0.41347 (6)
AP	0.22663 (9)	0.02996 (8)	0.19167 (12)	BP	0.31936 (9)	0.51785 (8)	0.25777 (11)
AO(1)	-0.0118 (3)	-0.0586 (2)	0.2229 (4)	BO(1)	0.0904 (3)	0.4024 (2)	0.2956 (4)
AO(2)	0.2470 (3)	-0.0862 (2)	0.4792 (4)	BO(2)	0.3396 (3)	0.4407 (2)	0.5698 (3)
AC(1)	0.0473 (4)	-0.0196 (3)	0.2760 (5)	BC(1)	0.1404 (4)	0.4537 (4)	0.3397 (5)
AC(2)	0.2027 (4)	-0.0359 (3)	0.4301 (5)	BC(2)	0.2898 (4)	0.4768 (3)	0.5052 (5)
AC(3)	0.1228 (4)	0.1386 (3)	0.5366 (5)	BC(3)	0.1611 (3)	0.6727 (3)	0.4256 (4)
AC(4)	0.1883 (4)	0.1449 (4)	0.6418 (5)	BC(4)	0.1522 (5)	0.7195 (3)	0.3273 (5)
AC(5)	0.2602 (4)	0.1939 (4)	0.6412 (7)	BC(5)	0.0671 (6)	0.7204 (4)	0.2614 (6)
AC(6)	0.2722 (5)	0.2371 (4)	0.5439 (7)	BC(6)	-0.0090 (5)	0.6774 (4)	0.2863 (6)
AC(7)	0.2115 (5)	0.2321 (3)	0.4420 (7)	BC(7)	-0.0042 (4)	0.6332 (4)	0.3804 (6)
AC(8)	0.1346 (4)	0.1813 (3)	0.4357 (4)	BC(8)	0.0828 (4)	0.6312 (3)	0.4530 (4)
AC(9)	0.0435 (4)	0.1589 (3)	0.3794 (5)	BC(9)	0.1340 (4)	0.6111 (4)	0.5625 (4)
AC(10)	0.0306 (4)	0.1177 (4)	0.4830 (5)	BC(10)	0.2148 (4)	0.6523 (3)	0.5346 (5)

Group Parameters for Rigid Phenyl Rings<sup>b</sup>

group	<i>x</i> <sub>0</sub>	<i>y</i> <sub>0</sub>	<i>z</i> <sub>0</sub>	$\phi$	$\theta$	$\rho$
APH1	0.3595 (2)	0.0212 (2)	0.2196 (3)	1.593 (2)	2.958 (2)	-1.886 (2)
APH2	0.2080 (2)	0.1224 (2)	0.1146 (3)	-2.938 (2)	-2.710 (2)	-0.038 (2)
APH3	0.2108 (2)	-0.0628 (2)	0.0571 (3)	-0.239 (3)	-2.330 (2)	-1.843 (3)
BPH1	0.4215 (2)	0.4286 (2)	0.2523 (3)	0.816 (2)	-3.061 (2)	2.952 (2)
BPH2	0.2744 (2)	0.4921 (2)	0.0920 (2)	-1.617 (5)	-1.925 (2)	-1.331 (5)
BPH3	0.3831 (2)	0.6122 (2)	0.2623 (3)	2.713 (2)	3.051 (2)	-1.313 (2)

<sup>a</sup> See Figure 1 for identity of the atoms; the two independent molecules are denoted by the prefix A or B on the atom or group identifier. Numbers in parentheses are estimated standard deviations in the units of the least significant digits for the corresponding parameter. <sup>b</sup> See Figure 1 for identity of the groups. For a description of these group parameters, see: Eisenberg, R.; Ibers, J. A. *Inorg. Chem.* 1965, 4, 773. Angular coordinates are in radians. The internal coordinate system of a phenyl ring is defined elsewhere: Riley, P. E.; Davis, R. E. *Acta Crystallogr., Sect. B*, 1975, B31, 2928.

Table III. Fractional Coordinates for Non-Hydrogen Atoms of 2<sup>a</sup>

atom	x	y	z	atom	x	y	z
Fe	0.27332 (5)	0.18661 (4)	0.21184 (6)	C(1)	0.3729 (6)	0.0532 (3)	0.1785 (6)
P	0.16777 (9)	0.30728 (6)	0.12738 (10)	C(2)	0.2571 (7)	0.0401 (3)	0.2527 (6)
Cl	0.6129 (1)	0.1586 (1)	0.4981 (2)	C(3)	0.1465 (5)	0.0555 (3)	0.1624 (5)
O(1)	0.5261 (3)	0.3091 (3)	0.2485 (4)	C(4)	0.1928 (5)	0.0764 (3)	0.0326 (5)
O(2)	0.1966 (4)	0.2571 (3)	0.5097 (3)	C(5)	0.3326 (5)	0.0756 (3)	0.0419 (5)
O(3)	0.9203 (4)	0.1253 (3)	0.4679 (5)	C(6)	0.4268 (4)	0.2616 (3)	0.2350 (5)
O(4)	0.1016 (3)	0.0763 (3)	0.6853 (4)	C(7)	0.2254 (4)	0.2316 (3)	0.3922 (4)
O(5)	0.3816 (4)	0.0696 (3)	0.6610 (4)				

Group Parameters for Rigid Phenyl Rings<sup>b</sup>

group	x <sub>0</sub>	y <sub>0</sub>	z <sub>0</sub>	φ	θ	ρ
Ph(1)	-0.0022 (2)	0.2661 (2)	0.0526 (3)	-1.392 (2)	-2.869 (1)	1.162 (2)
Ph(2)	0.2553 (2)	0.3592 (2)	-0.0120 (2)	2.344 (2)	-2.365 (2)	0.558 (2)
Ph(3)	0.1459 (3)	0.4210 (2)	0.2638 (3)	-3.050 (2)	2.503 (2)	-0.369 (2)

<sup>a</sup> See Figure 2 for identity of the atoms. Numbers in parentheses are estimated standard deviations in the units of the least significant digits for the corresponding parameters. <sup>b</sup> See Figure 2 for identity of the groups and caption of Table II for descriptions of the groups.

Table IV. Fractional Coordinates for Non-Hydrogen Atoms of 3<sup>a</sup>

atom	x	y	z	atom	x	y	z
Fe	-0.14232 (5)	-0.19200 (4)	0.06541 (7)	C(6)	-0.1716 (4)	-0.0287 (3)	-0.0799 (7)
P(1)	-0.22960 (9)	-0.11586 (8)	-0.03828 (13)	C(7)	-0.0964 (4)	-0.0163 (3)	0.0051 (7)
P(2)	-0.04190 (9)	-0.10757 (8)	0.02674 (14)	C(8)	-0.1597 (3)	-0.1431 (3)	0.2075 (5)
O	-0.1712 (3)	-0.1126 (3)	0.3017 (4)	B	-0.1100 (5)	-0.3349 (5)	-0.4725 (8)
C(1)	-0.1415 (5)	-0.2875 (3)	-0.0548 (5)	F(1)	-0.0816 (5)	-0.2723 (4)	-0.5379 (8)
C(2)	-0.2114 (4)	-0.2911 (3)	0.0276 (6)	F(2)	-0.1214 (5)	-0.3162 (5)	-0.3532 (4)
C(3)	-0.1805 (4)	-0.2933 (4)	0.1525 (7)	F(3)	-0.0508 (3)	-0.3895 (3)	-0.4868 (6)
C(4)	-0.0910 (4)	-0.2887 (3)	0.1498 (6)	F(4)	-0.1819 (4)	-0.3495 (5)	-0.5263 (7)
C(5)	-0.0671 (5)	-0.2863 (3)	0.0210 (7)				

Group Parameters for Rigid Phenyl Rings<sup>b</sup>

group	x <sub>0</sub>	y <sub>0</sub>	z <sub>0</sub>	φ	θ	ρ
Ph(1)	-0.3245 (2)	-0.0890 (2)	0.0507 (3)	-1.323 (2)	2.654 (2)	0.644 (3)
Ph(2)	-0.2727 (2)	-0.1428 (2)	-0.1944 (3)	-2.116 (6)	-1.981 (2)	-1.016 (5)
Ph(3)	0.0287 (2)	-0.1168 (2)	-0.1113 (3)	1.667 (4)	-2.219 (2)	-2.440 (4)
Ph(4)	0.0340 (2)	-0.0908 (2)	0.1545 (4)	1.367 (3)	2.365 (4)	-2.942 (4)

<sup>a</sup> See Figure 3 for identity of the atoms. Numbers in parentheses are estimated standard deviations in the units of the least significant digits for the corresponding parameters. <sup>b</sup> See Figure 3 for identity of the groups and the caption of Table II for descriptions of the groups.

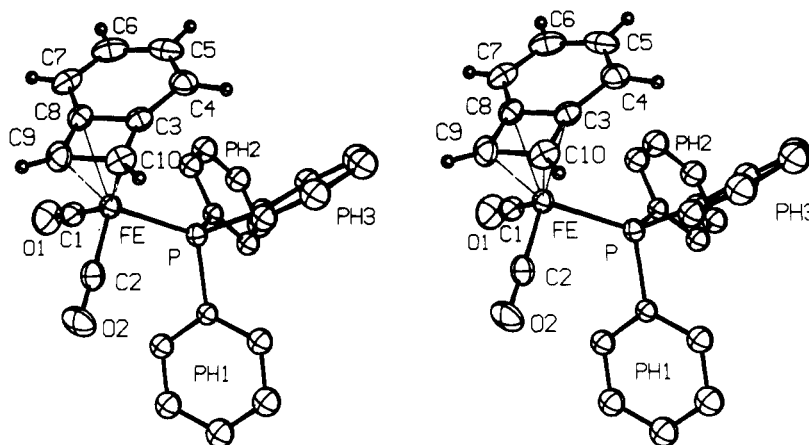


Figure 1. A stereoscopic view of the  $(\pi\text{-bzcb})\text{Fe}(\text{CO})_2(\text{PPh}_3)$  (1) molecule illustrating the atom numbering scheme used herein. Non-hydrogen atoms are shown as ellipsoids of 30% probability, and hydrogen atoms as spheres of radius 0.5 Å. Rigid-group hydrogen atoms have been omitted.

structure of 2, however, displays an extensive network of strong hydrogen bonds between the Cl<sup>-</sup> ions and the water molecules (Cl<sup>-</sup>...O = 3.14 and 3.15 Å, O...O = 2.82 and 2.85 Å). Thus, water molecules O(3) and O(4) describe a parallelogram about the inversion center at (0, 0, 1/2) which is connected on opposite O(3)...O(4) edges to Cl<sup>-</sup> ions and O(5) molecules to form another four-atom segment (O(3),

O(4), O(5), Cl<sup>-</sup>), inclined toward the first one, about the inversion center at (1/2, 0, 1/2). This in turn is linked to another pair of O(3) and O(4) molecules to create undulating ribbons of atoms that are approximately parallel to the *a* axis. The cations reside within the channels formed by these ribbons.

Figures 1, 2, and 3 provide stereoscopic view of the metal



Table V. Bond Lengths (Å) and Bond Angles (deg) for 1<sup>a</sup>

	molecule A	molecule B
Bond Lengths		
Fe-P	2.219 (1)	2.230 (1)
Fe-C(1)	1.744 (5)	1.763 (5)
Fe-C(2)	1.775 (6)	1.751 (5)
Fe-C(3)	2.133 (5)	2.162 (5)
Fe-C(8)	2.156 (5)	2.140 (5)
Fe-C(9)	2.013 (6)	1.997 (6)
Fe-C(10)	2.006 (6)	2.013 (5)
P-C(11)*	1.842 (3)	1.835 (3)
P-C(21)*	1.830 (3)	1.842 (3)
P-C(31)*	1.842 (3)	1.842 (3)
C(1)-O(1)	1.155 (7)	1.156 (7)
C(2)-O(2)	1.148 (7)	1.148 (7)
C(3)-C(4)	1.418 (8)	1.420 (7)
C(3)-C(8)	1.434 (7)	1.425 (7)
C(3)-C(10)	1.434 (8)	1.440 (7)
C(4)-C(5)	1.355 (9)	1.352 (10)
C(5)-C(6)	1.406 (10)	1.405 (10)
C(6)-C(7)	1.352 (10)	1.356 (10)
C(7)-C(8)	1.422 (8)	1.410 (8)
C(8)-C(9)	1.437 (8)	1.429 (7)
C(9)-C(10)	1.446 (8)	1.453 (8)
Bond Angles		
C(1)-Fe-C(2)	99.5 (3)	99.9 (3)
C(1)-Fe-P	95.4 (2)	98.9 (2)
C(2)-Fe-P	98.3 (2)	94.5 (2)
Fe-C(1)-O(1)	177.1 (5)	176.5 (5)
Fe-C(2)-O(2)	177.9 (5)	177.2 (5)
Fe-P-C(11)*	116.4 (1)	115.5 (1)
Fe-P-C(21)*	115.5 (1)	117.3 (1)
Fe-P-C(31)*	114.8 (1)	115.6 (1)
C(11)*-P-C(21)*	104.0 (2)	101.2 (1)
C(11)*-P-C(31)*	102.2 (2)	102.1 (1)
C(21)*-P-C(31)*	102.1 (1)	102.9 (1)
C(10)-C(3)-C(8)	89.6 (4)	90.7 (4)
C(10)-C(3)-C(4)	148.5 (5)	147.9 (5)
C(8)-C(3)-C(4)	120.8 (5)	120.7 (5)
C(3)-C(4)-C(5)	116.2 (6)	116.2 (6)
C(4)-C(5)-C(6)	123.8 (6)	122.9 (6)
C(5)-C(6)-C(7)	121.6 (6)	122.7 (6)
C(6)-C(7)-C(8)	117.8 (6)	116.5 (6)
C(7)-C(8)-C(3)	119.8 (5)	120.8 (5)
C(7)-C(8)-C(9)	148.3 (5)	148.4 (5)
C(3)-C(8)-C(9)	90.9 (4)	90.4 (4)
C(8)-C(9)-C(10)	89.0 (4)	90.1 (4)
C(9)-C(10)-C(3)	90.5 (4)	88.8 (4)

<sup>a</sup> Numbers in parentheses are the estimated standard deviations in the least significant digits. See Figure 1 for identity of the atoms. Atoms marked with asterisks are rigid-group atoms.

complexes of 1, 2, and 3, respectively, and indicate the atom numbering scheme used in this paper. Selected bond lengths and bond angles for each structure are given in Tables V, VI, and VII.

**Structural Consequences of Successive Phosphine Substitution.**<sup>24</sup> Of particular interest in this work are the changes in the Fe-C and C-O bond lengths as the phosphine content and the charge of the metal complexes are systematically altered. These changes and the values of the CO stretching frequencies are given in Table VIII, along with the corresponding data for some of the other Fe complexes mentioned in the Introduction. These data, as assembled in Table VIII, demonstrate the smooth changes in these structural parameters for a series of closely related complexes. It should be noted that the bond lengths derived from these studies were obtained from data

Table VI. Bond Lengths (Å) and Bond Angles (deg) for 2<sup>a</sup>

Bond Lengths			
Fe-P	2.242 (1)	P-C(21)*	1.830 (3)
Fe-C(1)	2.093 (5)	P-C(31)*	1.829 (3)
Fe-C(2)	2.092 (4)	C(1)-C(2)	1.398 (8)
Fe-C(3)	2.080 (4)	C(2)-C(3)	1.404 (8)
Fe-C(4)	2.101 (4)	C(3)-C(4)	1.391 (7)
Fe-C(5)	2.097 (5)	C(4)-C(5)	1.396 (7)
Fe-C(6)	1.767 (4)	C(5)-C(1)	1.409 (7)
Fe-C(7)	1.775 (4)	C(6)-O(1)	1.138 (5)
P-C(11)*	1.814 (2)	C(7)-O(2)	1.140 (5)
Bond Angles			
P-Fe-C(6)	90.7 (1)	C(21)*-P-C(31)*	101.8 (1)
P-Fe-C(7)	91.5 (1)	Fe-C(6)-O(1)	179.2 (4)
C(6)-Fe-C(7)	94.9 (2)	Fe-C(7)-O(2)	177.2 (4)
Fe-P-C(11)*	112.9 (1)	C(5)-C(1)-C(2)	107.7 (5)
Fe-P-C(21)*	114.5 (1)	C(1)-C(2)-C(3)	107.5 (5)
Fe-P-C(31)*	115.4 (1)	C(2)-C(3)-C(4)	108.7 (5)
C(11)*-P-C(21)*	107.5 (1)	C(3)-C(4)-C(5)	107.8 (4)
C(11)*-P-C(31)*	103.5 (1)	C(4)-C(5)-C(1)	108.2 (4)

<sup>a</sup> Numbers in parentheses are the estimated standard deviations in the least significant digits. See Figure 2 for identity of the atoms. Atoms marked with asterisks are rigid-group atoms.

Table VII. Bond Lengths (Å) and Bond Angles (deg) for 3<sup>a</sup>

Bond Lengths			
Fe-P(1)	2.209 (2)	P(2)-C(41)*	1.822 (4)
Fe-P(2)	2.211 (2)	C(1)-C(2)	1.404 (10)
Fe-C(1)	2.103 (6)	C(2)-C(3)	1.400 (10)
Fe-C(2)	2.096 (6)	C(3)-C(4)	1.414 (10)
Fe-C(3)	2.093 (6)	C(4)-C(5)	1.404 (10)
Fe-C(4)	2.083 (6)	C(5)-C(1)	1.417 (10)
Fe-C(5)	2.094 (6)	C(6)-C(7)	1.501 (9)
Fe-C(8)	1.744 (5)	C(8)-O	1.139 (7)
P(1)-C(6)	1.840 (6)	B-F(1)	1.374 (11)
P(1)-C(11)*	1.827 (4)	B-F(2)	1.307 (9)
P(1)-C(21)*	1.836 (3)	B-F(3)	1.349 (10)
P(2)-C(7)	1.837 (6)	B-F(4)	1.293 (10)
P(2)-C(31)*	1.834 (4)		
Bond Angles			
P(1)-Fe-P(2)	87.0 (1)	C(5)-C(1)-C(2)	107.8 (6)
P(1)-Fe-C(8)	91.3 (2)	C(1)-C(2)-C(3)	107.7 (6)
P(2)-Fe-C(8)	86.4 (2)	C(2)-C(3)-C(4)	109.1 (6)
Fe-P(1)-C(6)	108.3 (2)	C(3)-C(4)-C(5)	106.8 (6)
Fe-P(1)-C(11)*	114.6 (1)	C(4)-C(5)-C(1)	108.5 (6)
Fe-P(1)-C(21)*	120.9 (1)	P(1)-C(6)-C(7)	111.9 (4)
C(6)-P(1)-C(11)*	108.2 (2)	P(2)-C(7)-C(6)	108.4 (4)
C(6)-P(1)-C(21)*	100.8 (3)	Fe-C(8)-O	178.6 (5)
C(11)*-P(1)-C(21)*	102.7 (2)	F(1)-B-F(2)	108.8 (7)
Fe-P(2)-C(7)	106.0 (2)	F(1)-B-F(3)	106.9 (7)
Fe-P(2)-C(31)*	121.3 (1)	F(1)-B-F(4)	103.1 (7)
Fe-P(2)-C(41)*	116.4 (1)	F(2)-B-F(3)	112.5 (7)
C(7)-P(2)-C(31)*	105.3 (2)	F(2)-B-F(4)	110.3 (7)
C(7)-P(2)-C(41)*	104.9 (2)	F(3)-B-F(4)	114.6 (7)
C(31)*-P(2)-C(41)*	101.4 (2)		

<sup>a</sup> Numbers in parentheses are the estimated standard deviations in the least significant digits. See Figure 3 for identity of the atoms. Atoms marked with asterisks are rigid-group atoms.

sets which were collected at low temperature (see Table I)<sup>25</sup> and at resolutions of 0.74 to 0.84 Å. Hence, these bond lengths represent a set of structural parameters which were determined carefully, with cognizance of the limitations of the experiment and of the consequences of comparing

(24) Examination of the bonding between the cyclobutadiene moiety and the Fe atom of 1 was presented in ref. 9.

(25) Data for 1, which were obtained prior to the inception of this project, were gathered at room temperature (~20 °C), while data for 2 were also obtained at room temperature because the crystals fractured at the temperature of our cold stream (-35 °C).

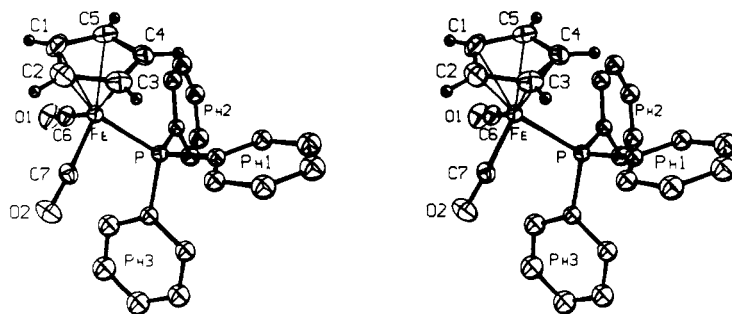


Figure 2. A stereoscopic view of the  $[(\pi\text{-C}_5\text{H}_5)\text{Fe}(\text{CO})_2(\text{PPh}_3)]^+$  ion of 2 illustrating the atom numbering scheme used herein. Atoms are drawn as ellipsoids of 30% probability. Hydrogen atoms were treated as in Figure 1.

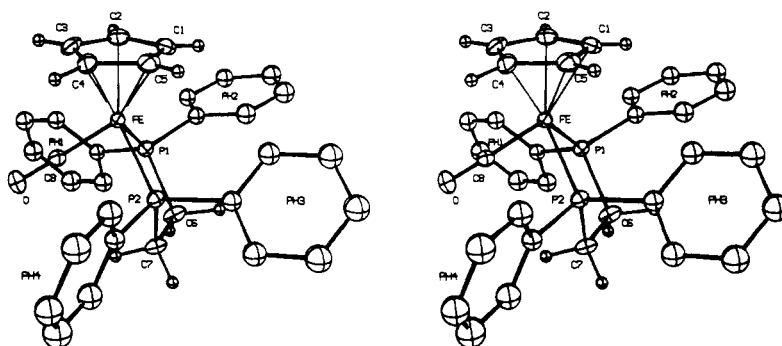


Figure 3. A stereoscopic view of the  $[(\pi\text{-C}_5\text{H}_5)\text{Fe}(\text{CO})(\text{dppe})]^+$  ion of 3 indicating the atom numbering scheme used herein. The same criteria used to produce Figure 1 were used here.

Table VIII. Mean Bond Lengths (Å) and Carbonyl Stretching Frequencies ( $\text{cm}^{-1}$ ) of Some (Phosphine)iron Carbonyl Complexes<sup>a</sup>

	4	1	5
Fe-C	1.788 (7)	1.758 (18)	1.742 (3)
C-O	1.139 (3)	1.151 (4)	1.165 (4)
$\nu(\text{CO})$	1975, 1990, 2030 (diethyl ether)	1920, 1970 (cyclohexane)	1880 (cyclohexane)
	6	2	3
Fe-C	1.816 (15)	1.771 (4)	1.744 (5)
C-O	1.112 (1)	1.139 (1)	1.139 (7)
$\nu(\text{CO})$	2068, 2120 (Nujol)	2025, 2070 (Nujol)	1980 (Nujol)

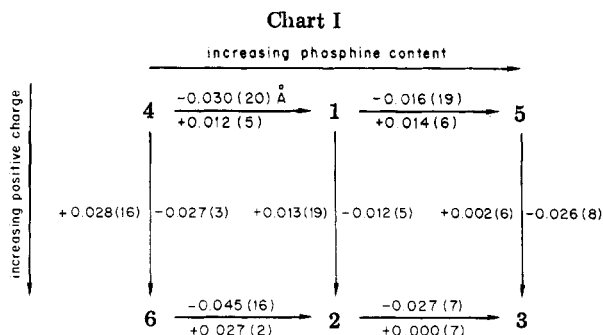
<sup>a</sup> A mean bond length  $\bar{l}$  was calculated from the expression  $\bar{l} = \sum l_i / n$  and its standard deviation  $\sigma(\bar{l})$  from  $\sigma(\bar{l}) = [\sum (l_i - \bar{l})^2 / (n - 1)]^{1/2}$ .

imprecisely determined distances.

In accordance with the Dewar description of synergic bonding,<sup>26</sup> the observed changes in the Fe-C and C-O bond lengths are consistent with the changes in the CO stretching frequencies as the complex charge and/or number of electron-donating phosphine ligands are varied. Although similar results<sup>27</sup> have been previously documented, this work allows an examination of a self-consistent series of isoelectronic complexes in which the metal

(26) Dewar, M. J. S. *Bull. Soc. Chim. Fr.* 1951, 18, C71. Chatt, J.; Duncanson, L. A. *J. Chem. Soc.* 1953, 2939.

(27) See, for example: English, R. B.; De V. Steyn, M. M. *Acta Crystallogr. Sect B* 1979, B35, 954. Reisner, G. M.; Bernal, I.; Brunner, H.; Muschiol, M. *Inorg. Chem.* 1978, 17, 783. Woodard, S. S.; Jacobson, R. A.; Angelici, R. J. *J. Organomet. Chem.* 1976, 117, C75.



center remains unchanged as the ligands and the charge are adjusted. As shown in Chart I, the changes in the Fe-C

(above or left of arrows) and C–O (below or right of arrows) bond lengths are relatively small between adjacent complexes but are substantial, consistent, and significant overall. Thus, as one passes from 4 through 1 to 5 and from 6 through 2 to 3, the Fe–C bonds decrease by 0.046 (8) and 0.072 (16) Å, while the C–O bonds increase by 0.026 (5) and 0.027 (7) Å, respectively. Consistent with the similarity of the resulting elongated C–O bonds are the changes in the CO stretching frequencies, which show a decrease of  $\sim 100\text{ cm}^{-1}$  between 4 and 5 and between 6 and 3, as the phosphorus to iron ratio is increased from 0 to 2. Furthermore, approximately the same change in carbonyl stretching frequency is noted when the phosphorus to iron ratio is maintained while the charge of the complex is raised from 0 to +1. From these data, then, it appears that substitution of two electron-donating phosphorus ligands for two electron-withdrawing carbonyl ligands tends to offset the influence of one positive charge on the metal-to-carbonyl backbonding. That is, although the Fe–C distances in 4 and 3 are substantially different, the C–O distances are the same, which suggests a similar degree of electron transfer via Fe $\rightarrow$ CO back-bonding. This suggestion is supported by the similarity of the CO stretching frequencies for these two complexes (see Table VIII).

Finally, the utility of such structural data is not restricted to correlating changes between bond lengths and carbonyl stretching frequencies. As reported by Pettit et al.,<sup>28</sup> small changes in structural and spectroscopic pa-

rameters are generally indicative of appreciable changes in chemical reactivity. Hence, in the series of positively charged complexes 6, 2, and 3, it was noted by these workers that the substitution of the diphosphine ligand Ph<sub>2</sub>PCH<sub>2</sub>CH<sub>2</sub>PPh<sub>2</sub> for two CO groups so stabilizes the positive charge on the resulting complex that, unlike the unsubstituted parent complex 6 and the monosubstituted intermediate 2, disubstituted 3 is virtually inert in basic solution. This, of course, is in agreement with the structural and spectroscopic results which indicate that appreciable electron density has been transferred from the electron-rich phosphorus atoms through the metal to the remaining CO ligand. Consequently, the carbonyl carbon atom of 3 is less positively charged than those of 2 and 6 and thus is less susceptible to nucleophilic attack.

**Acknowledgment.** This work was supported by the Robert A. Welch Foundation (Grant No. F-233). We are indebted to the late Professor Rowland Pettit and several members of his research group for providing samples of the compounds studied in this work.

**Registry No.** 1, 57408-20-5; 2, 83682-13-7; 3, 35004-56-9.

**Supplementary Material Available:** Listings of anisotropic thermal parameters, rigid-group parameters, and observed and calculated structure factor amplitudes for the structures of 1, 2, and 3 (85 pages). Ordering information is given on any current masthead page.

(28) Grice, N.; Kao, S. C.; Pettit, R. *J. Am. Chem. Soc.* **1979**, *101*, 1627.

## Synthesis and Characterization of [RuCo<sub>3</sub>(CO)<sub>12</sub>]<sup>-</sup> Clusters. Effective Catalyst Precursors for the Homologation of Methanol

Masanobu Hidai,\* Masami Orisaku, Makoto Ue, Yukio Koyasu, Teruyuki Kodama, and Yasuzo Uchida

Department of Industrial Chemistry, Faculty of Engineering, University of Tokyo, Hongo, Bunkyo-ku, Tokyo 113, Japan

Received August 3, 1982

The reaction of RuCl<sub>3</sub>·3H<sub>2</sub>O with 4 molar equiv of Na[Co(CO)<sub>4</sub>] gives a mixed cluster, Na[RuCo<sub>3</sub>(CO)<sub>12</sub>], in high yield. The cluster easily undergoes a cation exchange to afford [Et<sub>4</sub>N]<sup>+</sup>, [Ph<sub>4</sub>P]<sup>+</sup>, and [(Ph<sub>3</sub>P)<sub>2</sub>N]<sup>+</sup> salts, while treatment of the cluster with phosphoric acid produces [HRuCo<sub>3</sub>(CO)<sub>12</sub>] in moderate yield. The molecular structure of [(Ph<sub>3</sub>P)<sub>2</sub>N][RuCo<sub>3</sub>(CO)<sub>12</sub>] has been determined by X-ray crystallographic analysis. The four metals are located at the corners of a tetrahedron. Three carbonyl groups are terminally bound to Ru with an average Ru–C distance of 1.91 Å and two to each Co with an average Co–C distance of 1.70 Å. The other three carbonyl groups bridge each two cobalts with an average Co–C distance of 1.96 Å. These mixed clusters are very effective as catalyst precursors for the homologation of methanol under relatively mild conditions (180–210 °C, CO/H<sub>2</sub> ratio = 1/2, initial pressure 120 kg/cm<sup>2</sup> at ambient temperature). The yield and the selectivity of ethanol are greatly affected both by the concentration of methyl iodide as a promoter and by the reaction temperature. The selectivity of total ethanol was 64% at ca. 25% conversion of methanol with the iodide/cluster molar ratio of ca. 9 at 180 °C, while the selectivity was below 5% in the case of [Co<sub>2</sub>(CO)<sub>8</sub>] under similar conditions.

### Introduction

Transition-metal clusters are currently under intensive investigation because of their potential catalytic applications both as models for understanding the catalytic metal surface and as catalysts in their own right. Numerous reviews<sup>1</sup> have appeared on various aspects of the chemistry

of transition metal clusters. Mixed-transition-metal clusters are, in particular, expected to find important applications in homogeneous catalysis since a suitable combination of different metals in mixed-metal clusters may permit more efficient interactions with substrates than mononuclear metal complexes or homometallic clusters. Up to now, only a few mixed-metal clusters have been examined as homogeneous catalyst precursors.<sup>2</sup>

(1) (a) Chini, P.; Longoni, G.; Alvano, V. G. *Adv. Organomet. Chem.* **1976**, *14*, 285–344. (b) Humphries, A. P.; Kaesz, H. D. *Prog. Inorg. Chem.* **1979**, *25*, 145–222. (c) Wade, K. *Adv. Inorg. Chem. Radiochem.* **1976**, *18*, 1–66. (d) Muetterties, E. L.; Stein, J. *Chem. Rev.* **1979**, *79*, 479–490. (e) Ozin, G. A. *Catal. Rev.* **1977**, *16*, 191–289. (f) Gladfelter, W. L.; Geoffroy, G. L. *Adv. Organomet. Chem.* **1980**, *18*, 207–273. (g) Johnson, B. F. G., Ed. "Transition Metal Clusters"; Wiley-Interscience: New York, 1980.

(2) (a) Labroue, D.; Poilblanc, R. *J. Mol. Catal.* **1977**, *2*, 329–333. (b) Catton, G. A.; Jones, G. F. C.; Mays, M. J.; Howell, J. A. S. *Inorg. Chim. Acta* **1976**, *20*, L41. (c) Ford, P. C.; Rinker, R. G.; Ungermann, C.; Laine, R. M.; Landis, V.; Moya, S. A. *J. Am. Chem. Soc.* **1978**, *100*, 4595–4597.

(above or left of arrows) and C–O (below or right of arrows) bond lengths are relatively small between adjacent complexes but are substantial, consistent, and significant overall. Thus, as one passes from 4 through 1 to 5 and from 6 through 2 to 3, the Fe–C bonds decrease by 0.046 (8) and 0.072 (16) Å, while the C–O bonds increase by 0.026 (5) and 0.027 (7) Å, respectively. Consistent with the similarity of the resulting elongated C–O bonds are the changes in the CO stretching frequencies, which show a decrease of  $\sim 100\text{ cm}^{-1}$  between 4 and 5 and between 6 and 3, as the phosphorus to iron ratio is increased from 0 to 2. Furthermore, approximately the same change in carbonyl stretching frequency is noted when the phosphorus to iron ratio is maintained while the charge of the complex is raised from 0 to +1. From these data, then, it appears that substitution of two electron-donating phosphorus ligands for two electron-withdrawing carbonyl ligands tends to offset the influence of one positive charge on the metal-to-carbonyl backbonding. That is, although the Fe–C distances in 4 and 3 are substantially different, the C–O distances are the same, which suggests a similar degree of electron transfer via Fe $\rightarrow$ CO back-bonding. This suggestion is supported by the similarity of the CO stretching frequencies for these two complexes (see Table VIII).

Finally, the utility of such structural data is not restricted to correlating changes between bond lengths and carbonyl stretching frequencies. As reported by Pettit et al.,<sup>28</sup> small changes in structural and spectroscopic pa-

rameters are generally indicative of appreciable changes in chemical reactivity. Hence, in the series of positively charged complexes 6, 2, and 3, it was noted by these workers that the substitution of the diphosphine ligand Ph<sub>2</sub>PCH<sub>2</sub>CH<sub>2</sub>PPh<sub>2</sub> for two CO groups so stabilizes the positive charge on the resulting complex that, unlike the unsubstituted parent complex 6 and the monosubstituted intermediate 2, disubstituted 3 is virtually inert in basic solution. This, of course, is in agreement with the structural and spectroscopic results which indicate that appreciable electron density has been transferred from the electron-rich phosphorus atoms through the metal to the remaining CO ligand. Consequently, the carbonyl carbon atom of 3 is less positively charged than those of 2 and 6 and thus is less susceptible to nucleophilic attack.

**Acknowledgment.** This work was supported by the Robert A. Welch Foundation (Grant No. F-233). We are indebted to the late Professor Rowland Pettit and several members of his research group for providing samples of the compounds studied in this work.

**Registry No.** 1, 57408-20-5; 2, 83682-13-7; 3, 35004-56-9.

**Supplementary Material Available:** Listings of anisotropic thermal parameters, rigid-group parameters, and observed and calculated structure factor amplitudes for the structures of 1, 2, and 3 (85 pages). Ordering information is given on any current masthead page.

(28) Grice, N.; Kao, S. C.; Pettit, R. *J. Am. Chem. Soc.* **1979**, *101*, 1627.

## Synthesis and Characterization of [RuCo<sub>3</sub>(CO)<sub>12</sub>]<sup>-</sup> Clusters. Effective Catalyst Precursors for the Homologation of Methanol

Masanobu Hidai,\* Masami Orisaku, Makoto Ue, Yukio Koyasu, Teruyuki Kodama, and Yasuzo Uchida

Department of Industrial Chemistry, Faculty of Engineering, University of Tokyo, Hongo, Bunkyo-ku, Tokyo 113, Japan

Received August 3, 1982

The reaction of RuCl<sub>3</sub>·3H<sub>2</sub>O with 4 molar equiv of Na[Co(CO)<sub>4</sub>] gives a mixed cluster, Na[RuCo<sub>3</sub>(CO)<sub>12</sub>], in high yield. The cluster easily undergoes a cation exchange to afford [Et<sub>4</sub>N]<sup>+</sup>, [Ph<sub>4</sub>P]<sup>+</sup>, and [(Ph<sub>3</sub>P)<sub>2</sub>N]<sup>+</sup> salts, while treatment of the cluster with phosphoric acid produces [HRuCo<sub>3</sub>(CO)<sub>12</sub>] in moderate yield. The molecular structure of [(Ph<sub>3</sub>P)<sub>2</sub>N][RuCo<sub>3</sub>(CO)<sub>12</sub>] has been determined by X-ray crystallographic analysis. The four metals are located at the corners of a tetrahedron. Three carbonyl groups are terminally bound to Ru with an average Ru–C distance of 1.91 Å and two to each Co with an average Co–C distance of 1.70 Å. The other three carbonyl groups bridge each two cobalts with an average Co–C distance of 1.96 Å. These mixed clusters are very effective as catalyst precursors for the homologation of methanol under relatively mild conditions (180–210 °C, CO/H<sub>2</sub> ratio = 1/2, initial pressure 120 kg/cm<sup>2</sup> at ambient temperature). The yield and the selectivity of ethanol are greatly affected both by the concentration of methyl iodide as a promoter and by the reaction temperature. The selectivity of total ethanol was 64% at ca. 25% conversion of methanol with the iodide/cluster molar ratio of ca. 9 at 180 °C, while the selectivity was below 5% in the case of [Co<sub>2</sub>(CO)<sub>8</sub>] under similar conditions.

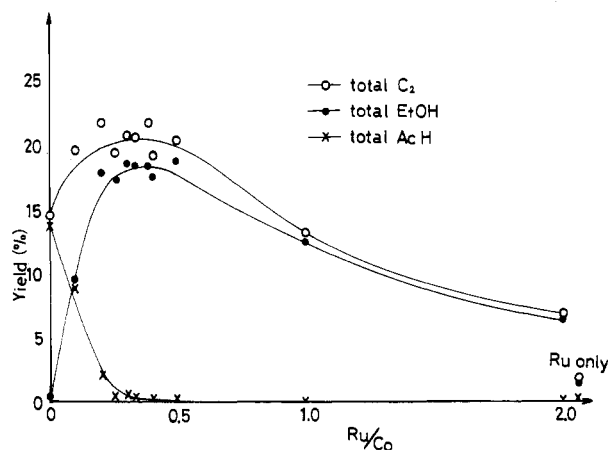
### Introduction

Transition-metal clusters are currently under intensive investigation because of their potential catalytic applications both as models for understanding the catalytic metal surface and as catalysts in their own right. Numerous reviews<sup>1</sup> have appeared on various aspects of the chemistry

of transition metal clusters. Mixed-transition-metal clusters are, in particular, expected to find important applications in homogeneous catalysis since a suitable combination of different metals in mixed-metal clusters may permit more efficient interactions with substrates than mononuclear metal complexes or homometallic clusters. Up to now, only a few mixed-metal clusters have been examined as homogeneous catalyst precursors.<sup>2</sup>

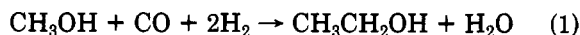
(1) (a) Chini, P.; Longoni, G.; Alvano, V. G. *Adv. Organomet. Chem.* **1976**, *14*, 285–344. (b) Humphries, A. P.; Kaesz, H. D. *Prog. Inorg. Chem.* **1979**, *25*, 145–222. (c) Wade, K. *Adv. Inorg. Chem. Radiochem.* **1976**, *18*, 1–66. (d) Muetterties, E. L.; Stein, J. *Chem. Rev.* **1979**, *79*, 479–490. (e) Ozin, G. A. *Catal. Rev.* **1977**, *16*, 191–289. (f) Gladfelter, W. L.; Geoffroy, G. L. *Adv. Organomet. Chem.* **1980**, *18*, 207–273. (g) Johnson, B. F. G., Ed. "Transition Metal Clusters"; Wiley-Interscience: New York, 1980.

(2) (a) Labroue, D.; Poilblanc, R. *J. Mol. Catal.* **1977**, *2*, 329–333. (b) Catton, G. A.; Jones, G. F. C.; Mays, M. J.; Howell, J. A. S. *Inorg. Chim. Acta* **1976**, *20*, L41. (c) Ford, P. C.; Rinker, R. G.; Ungermann, C.; Laine, R. M.; Landis, V.; Moya, S. A. *J. Am. Chem. Soc.* **1978**, *100*, 4595–4597.



**Figure 1.** Effect of Ru/Co ratio in the methanol homologation catalyzed by the  $\text{Co}_2(\text{CO})_8\text{-RuCl}_3\cdot 3\text{H}_2\text{O}$  system. Yield (%) of total  $\text{C}_2 = \text{AcH (mol)} + \text{DMA (mol)} + \text{EtOH (mol)} + \text{MeOEt (mol)} + 2 \times \text{Et}_2\text{O (mol)} + \text{AcOME (mol)}/\text{MeOH added (mol)} \times 100$  (DMA = dimethyl acetal of acetaldehyde). Yield (%) of total EtOH =  $\text{EtOH (mol)} + \text{MeOEt (mol)} + 2 \times \text{Et}_2\text{O (mol)}/\text{MeOH added (mol)} \times 100$ . Yield (%) of total AcH =  $\text{AcH (mol)} + \text{DMA (mol)}/\text{MeOH added (mol)} \times 100$ . Conditions: 180 °C, 2.5 h,  $\text{CO}$ , 40 kg/cm<sup>2</sup>;  $\text{H}_2$ , 80 kg/cm<sup>2</sup> (initial pressure at room temperature); MeOH, 500 mmol;  $\text{CH}_3\text{I}$ , 5 mmol;  $\text{Co}_2(\text{CO})_8$ , 0.2 mmol. Ru only means that 1.6 mmol of  $\text{RuCl}_3\cdot 3\text{H}_2\text{O}$  was used as the catalyst.

The synthesis of ethanol from methanol and synthesis gas is generally called methanol homologation (eq 1). This



type of reaction, catalyzed by cobalt carbonyl, was first reported by Wietzel et al.<sup>3</sup> in 1941. Later, Berty et al.<sup>4</sup> introduced iodide promoters, which led to a noticeable increase in the reaction rate. In recent years, the selectivity of ethanol has gradually been improved by employment of continuous operation instead of a batch unit,<sup>5</sup> phosphine-modified cobalt catalysts,<sup>6</sup> or special solvents.<sup>7</sup> Furthermore, recent reports<sup>8</sup> have shown that the selectivity of ethanol is remarkably improved by addition of a small amount of ruthenium iodide (Ru/Co ratio = 1/14)<sup>8a</sup> or  $[\text{Ru}_3(\text{CO})_{12}]$  (Ru/Co ratio = 1/9)<sup>8b</sup> to cobalt carbonyl.

Stimulated by these findings, we have found that ruthenium-cobalt mixed clusters containing the  $[\text{RuCo}_3(\text{C}-\text{O})_{12}]^-$  moiety prepared from ruthenium chloride and  $\text{Na}[\text{Co}(\text{CO})_4]$  show a remarkable catalytic activity for the homologation of methanol. This was briefly reported in a previous paper.<sup>9</sup> We describe here full details of synthesis and characterization of  $\text{M}[\text{RuCo}_3(\text{CO})_{12}]$  clusters ( $\text{M} = \text{H, Na, [Et}_4\text{N], [Ph}_4\text{P], or [(Ph}_3\text{P)}_2\text{N}]$ ) that are very effective as catalyst precursors for the homologation of

**Table I.** Infrared Spectra of  $\text{M}[\text{RuCo}_3(\text{CO})_{12}]$

cluster	$\nu(\text{CO}), \text{cm}^{-1}$ (above, KBr disk; below, in acetone)
$\text{Na}[\text{RuCo}_3(\text{CO})_{12}] \cdot \text{THF}$	2015 vs, 1970 vs, 1775 s 2026 vs, 1996 vs, 1967 s, 1885 w, 1813 s
$[\text{Et}_4\text{N}][\text{RuCo}_3(\text{CO})_{12}]$	1990 vs, 1950 vs, 1800 s 2025 vs, 1996 vs, 1967 s, 1887 m, 1813 s
$[\text{Ph}_4\text{P}][\text{RuCo}_3(\text{CO})_{12}]$	2000 vs, 1970 vs, 1800 s 2022 vs, 1996 vs, 1966 s, 1886 s, 1813 s
$[(\text{Ph}_3\text{P})_2\text{N}][\text{RuCo}_3(\text{CO})_{12}]$	1997 vs, 1965 vs, 1813 s, 1810 s 2024 vs, 1996 vs, 1967 s, 1887 m, 1813 s
$[\text{HRuCo}_3(\text{CO})_{12}]^a$	2050 vs, 2020 vs, 1880 s 2070 vs, 2062 vs, 2030 s, 1884 s <sup>b</sup>

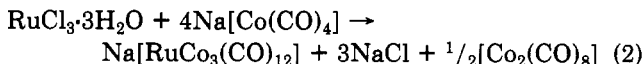
<sup>a</sup>  $\nu(\text{M-H})$  1121  $\text{cm}^{-1}$  (KBr disk). <sup>b</sup> In cyclohexane.

methanol. Recently, a patent<sup>10</sup> has appeared that also claims the similar effectiveness of the ruthenium-cobalt mixed clusters.

## Results and Discussion

**The Homologation of Methanol Catalyzed by a Mixture of  $[\text{Co}_2(\text{CO})_8]$  and  $\text{RuCl}_3\cdot 3\text{H}_2\text{O}$ .** Ruthenium compounds have recently been employed as cocatalysts of cobalt carbonyl to improve the selectivity of ethanol as described above. The influence of the Ru/Co molar ratio on the yields of products has been investigated in this study where various amounts of  $\text{RuCl}_3\cdot 3\text{H}_2\text{O}$  were added to a constant amount of cobalt carbonyl. The results are given in Figure 1. When only cobalt carbonyl was used as the catalyst, the yield of total ethanol was rather lower than those in the published literature<sup>4-7</sup> and the main  $\text{C}_2$  products were acetaldehyde and its dimethyl acetal. This is because the reaction conditions employed here were relatively mild. Although the yield of total acetaldehyde sharply decreased with increasing the Ru/Co ratio, the yields of total ethanol and total  $\text{C}_2$  compounds reached a maximum at the Ru/Co ratio of ca. 1/3. The mixture recovered after the reaction with the Ru/Co ratio in this region was homogeneous, and the color was light yellow. Further increase of the Ru/Co ratio gradually decreased the yields of total ethanol and total  $\text{C}_2$  compounds, and the color of the reaction mixture changed to dark red. The yield of dimethyl ether (ca. 30%) did not change much on varying the Ru/Co ratio. These results may suggest the formation of some cobalt-ruthenium mixed clusters such as a  $\text{RuCo}_3$  cluster that are effective for the methanol homologation. This has led us to preparation of well-defined cobalt-ruthenium mixed clusters.

**Preparation and Characterization of  $[\text{RuCo}_3(\text{C}-\text{O})_{12}]^-$  Clusters.** When a methanol solution of  $\text{RuCl}_3\cdot 3\text{H}_2\text{O}$  was treated with 4 molar equivalents of  $\text{Na}[\text{Co}(\text{CO})_4]$  in THF, the color of the mixture immediately turned dark blue and finally dark red. After the mixture was worked up, a reddish brown complex  $\text{Na}[\text{RuCo}_3(\text{CO})_{12}]$  was obtained in 54% yield. The total reaction may be described by eq 2 since cobalt carbonyl was isolated from the reaction



mixture. This mixed cluster is soluble in water, and the sodium cation is easily exchanged with bulky cations such

(3) Wietzel, G. German Patent 489764, 1941 (assigned to BASF).

(4) Berty, I.; Markó, L.; Kello, D. *Chem. Tech. Leipzig* 1956, 8, 260-266.

(5) Koerner, G. S.; Slinkland, W. E. *Ind. Eng. Chem. Prod. Res. Dev.* 1978, 17, 231-236.

(6) (a) Slauch, L. H. German Patent 2625627, 1976 (assigned to Shell).

(b) Pretzer, W. R.; Kobylinski, T. P. *Ann. N.Y. Acad. Sci.* 1980, 333, 58-66. (c) Sugi, Y.; Bando, K.; Yakami, Y. *Chem. Lett.* 1981, 63-64.

(7) Gane, B. R.; Stewart, D. G. Japan Kokai 54-73708, 54-125605 (assigned to British Pet.).

(8) (a) Butter, D.; Haute, T. U. S. Patent 3285948, 1966 (assigned to Commercial Solvent). (b) Mizoroki, M.; Matsumoto, T.; Ozaki, A. *Bull. Chem. Soc. Jpn.* 1979, 52, 479-482. (c) Pretzer, W. R.; Kobylinski, T. P.; Bozik, J. E. U. S. Patent 4133966, 1979 (assigned to Gulf Research and Development Co.).

(9) (a) Hidai, M.; Orisaku, M.; Ue, M.; Uchida, Y.; Yasufuku, K.; Yamazaki, H. *Chem. Lett.* 1981, 143-146. (b) Hidai, M.; Orisaku, M.; Ue, M.; Uchida, Y.; Yasufuku, K.; Yamazaki, H. "Proceedings of the 27th Symposium on Organometallic Chemistry"; Tokyo, Japan, 1980, 181-183.

(10) Doyle, G. Japan Kokai 56-90027, 1981 (assigned to Exxon Res.).

Table II. Selected Bond Distances (Å) and Angles (deg) of  $[(\text{Ph}_3\text{P})_2\text{N}][\text{RuCo}_3(\text{CO})_{12}]$ 

Bond Distances							
Ru-Co1	2.621 (3)	Co1-Co2	2.532 (3)	Co3-C5	1.971 (20)	C8-O8 (1)	1.27 (4)
Ru-Co2	2.630 (3)	Co1-Co3	2.525 (4)	Co3-C6	1.964 (18)	C8-O8 (2)	1.25 (4)
Ru-Co3	2.637 (3)	Co2-Co3	2.528 (3)	Co1-C7	1.718 (27)	C9-O9	1.16 (2)
Ru-C1	1.924 (20)	C1-O1	1.10 (3)	Co1-C8	1.704 (27)	C10-O10 (1)	1.26 (4)
Ru-C2	1.931 (18)	C2-O2	1.13 (2)	Co2-C9	1.709 (18)	C10-O10 (2)	1.22 (4)
Ru-C3	1.883 (20)	C3-O3	1.12 (3)	Co2-C10	1.748 (28)	C11-O11	1.19 (3)
Co1-C4	1.937 (21)	C4-O4	1.17 (3)	Co3-C11	1.663 (24)	C12-O12 (1)	1.28 (4)
Co1-C5	1.958 (23)	C5-O5	1.17 (3)	Co3-C12	1.668 (27)	C12-O12 (2)	1.35 (4)
Co2-C4	1.947 (22)	C6-O6	1.17 (2)	P1-N	1.581 (14)	P2-N	1.557 (14)
Co2-C6	1.972 (21)	C7-O7	1.18 (3)				
Bond Angles							
Co1-Ru-Co2	57.68 (8)	Co1-Ru-C1	100.5 (6)	Ru-Co2-C9	79.5 (7)	Ru-Co3-C12	164.9 (10)
Co1-Ru-Co3	57.40 (9)	Co1-Ru-C2	153.4 (6)	Co2-Co1-C7	127.6 (7)	Co1-Co3-C11	140.1 (8)
Co2-Ru-Co3	57.36 (8)	Co1-Ru-C3	100.4 (7)	Co3-Co1-C7	131.7 (7)	Co2-Co3-C11	137.5 (8)
Ru-Co1-Co2	61.34 (9)	Co2-Ru-C1	153.2 (6)	Co2-Co1-C8	118.1 (10)	Co1-Co3-C12	105.7 (10)
Ru-Co1-Co3	61.62 (9)	Co2-Ru-C2	100.2 (6)	Co3-Co1-C8	113.6 (10)	Co2-Co3-C12	106.9 (10)
Ru-Co2-Co1	60.98 (9)	Co2-Ru-C3	101.0 (7)	Co1-Co2-C9	125.5 (7)	Co1-C4-Co2	81.4 (9)
Ru-Co2-Co3	61.46 (9)	Co3-Ru-C1	98.8 (6)	Co3-Co2-C9	131.2 (7)	Co1-C5-Co3	80.0 (8)
Ru-Co3-Co1	60.98 (9)	Co3-Ru-C2	99.3 (6)	Co1-Co2-C10	119.5 (9)	Co2-C6-Co3	79.9 (7)
Ru-Co3-Co2	61.18 (9)	Co3-Ru-C3	154.3 (7)	Co3-Co2-C10	114.6 (9)		
Ru-Co1-C7	81.0 (7)	Ru-Co2-C10	175.6 (9)	Ru-C-O	178.3 (15) av	P1-N-P2	145.4 (9)
Ru-Co1-C8	175.0 (10)	Ru-Co3-C11	94.4 (8)				
Co-C-O (bridging)		139.8 (10) av		Co-C-O (axial)		156.8 (48) av	
Co-C-O (equatorial)		172.8 (24) av					

Table III. Comparison of Bond Lengths (Å) and Angles (deg) for  $\text{MCo}_3\text{L}_{12}$  Clusters (M = Co, Fe, or Ru; L = CO or  $\text{P}(\text{OCH}_3)_3$ )

bond type and angle	$[\text{Co}_4(\text{CO})_{12}]^a$ mean <sup>c</sup>	$[\text{HFeCo}_3(\text{CO})_9\text{P}(\text{OCH}_3)_3]^-$ mean <sup>c</sup>	$[(\text{Ph}_3\text{P})_2\text{N}]-$ $[\text{RuCo}_3(\text{CO})_{12}]$ mean <sup>c</sup>
Co-Co (in basal plane)	2.483 (28)	2.448 (12)	2.528 (5)
C(terminal)-M(apical) -C(terminal)	101.7 (2.3)	96 (2)	97.3 (2.5)
M(apical)-Co-C(equatorial)	92.8 (9.8)	81 (3)	85.0 (13.4)

<sup>a</sup> Reference 14. <sup>b</sup> Reference 13a. <sup>c</sup> The estimated error given is calculated from the formula  $[\sum_{i=0}^n (x_i - \bar{x})^2 / n - 1]^{1/2}$ .

as tetraethylammonium, tetraphenylphosphonium, and bis(triphenylphosphine) nitrogen ions. Treatment of an aqueous solution of  $\text{Na}[\text{RuCo}_3(\text{CO})_{12}]$  with phosphoric acid gives the hydrido cluster  $[\text{HRuCo}_3(\text{CO})_{12}]$  in moderate yield. This hydrido cluster was previously prepared by Mays and his co-workers<sup>11</sup> by the reaction of  $[\text{Ru}_3(\text{CO})_{12}]$  with cobalt carbonyl in acetone followed by acidification with hydrochloric acid, but the yield was only 7%. The infrared spectra of these clusters showed  $\nu(\text{CO})$  stretching absorptions characteristic of terminal and bridging carbonyl ligands, as shown in Table I, which are essentially similar to those of the iron-cobalt cluster analogues.<sup>12</sup>

The molecular structure of  $[(\text{Ph}_3\text{P})_2\text{N}][\text{RuCo}_3(\text{CO})_{12}]$  (1) has been determined by X-ray crystallographic analysis. Stereoviews of the complex 1, showing the atom-numbering scheme, are shown in Figure 2, while the selected bond distances and angles are given in Table II. The molecule consists of a cation and an anion. The four metal atoms in the anion form a tetrahedron with the apical Ru atom bonded to three terminal carbonyl ligands. Each Co atom is further bonded to two terminal and two bridging carbonyl ligands. The three carbonyl ligands on the Ru atom are in a staggered conformation with respect to the Ru-Co edges as in  $[\text{HFeCo}_3(\text{CO})_9\{\text{P}(\text{OCH}_3)_3\}_3]^-$  (2) and  $[\text{Co}_4(\text{C}-\text{O})_{12}]$ <sup>14</sup> (3) that also have a tetrahedral metal framework.

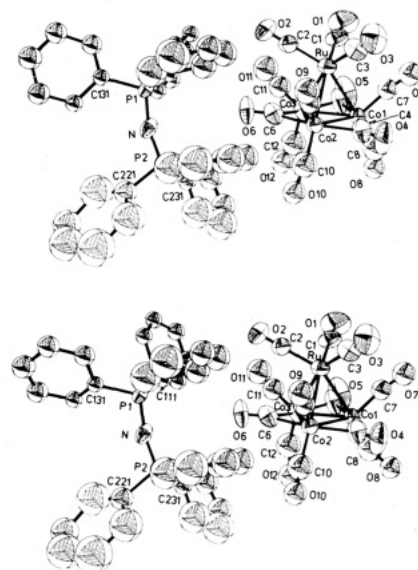


Figure 2. ORTEP plots of the two molecules of  $[(\text{Ph}_3\text{P})_2\text{N}][\text{RuCo}_3(\text{CO})_{12}]$  as viewed down from the same direction, showing some disorders of carbonyl and phenyl groups.

A comparison of bond distances and angles for these three clusters (Table III) reveals that the Co-Co bond distances in the basal plane for the compound 1 are longer than those for the compounds 2 and 3. This may arise from the occupation of the bulky Ru atom at the apical site instead of the relatively small Co or Fe atom. The equatorial carbonyl groups on the basal Co atoms of compound 1 are slightly bent toward the terminal carbonyl groups on the apical Ru atom. Thus, the angle C(terminal)-Ru-C(ter-

(11) Mays, M. J.; Simpson, R. N. F. *J. Chem. Soc. A* 1968, 1444-1447.

(12) Chini, P.; Colli, L.; Peraldo, M. *Gazz. Chim. Ital.* 1960, 90, 1005-1020.

(13) (a) Huie, B. T.; Knobler, C. B.; Kesz, H. D. *J. Am. Chem. Soc.* 1978, 100, 3059-3071. (b) Teller, R. G.; Wilson, R. D.; McMullan, R. K.; Koetzle, T. F.; Bau, R. *J. Am. Chem. Soc.* 1978, 100, 3071-3077.

(14) Carre, F. H.; Cotton, F. A.; Frenz, B. A. *Inorg. Chem.* 1976, 15, 380-387.

Table IV. Homologation of Methanol Catalyzed by Homometallic or Mixed Clusters<sup>a</sup>

catalyst <sup>b</sup>	yield, <sup>c</sup> %							selectivity, <sup>d</sup> %	
	AcH	DMA	EtOH	AcOMe	Me <sub>2</sub> O	MeOEt	Et <sub>2</sub> O	total EtOH	total C <sub>2</sub>
$[\text{Co}_2(\text{CO})_8]$	3.9	25.2	0.7	2.5	22.2	0	0	1.3	26.2
$[\text{Co}_4(\text{CO})_{12}]$	4.0	29.1	0.6	2.8	23.1	trace	trace	1.0	26.3
$\text{Na}[\text{RuCo}_3(\text{CO})_{12}]$	1.3	6.4	13.6	4.3	19.9	trace	trace	29.9	42.2
$[\text{Et}_4\text{N}][\text{RuCo}_3(\text{CO})_{12}]$	0.9	4.5	16.7	3.2	20.2	8.8	1.1	40.1	47.3
$[\text{Ph}_4\text{P}][\text{RuCo}_3(\text{CO})_{12}]$	1.1	0.3	18.7	4.2	16.3	7.6	1.2	48.0	54.7
$[(\text{Ph}_2\text{P})_2\text{N}][\text{RuCo}_3(\text{CO})_{12}]$	0.6	3.2	16.4	3.9	26.1	11.0	1.4	37.2	43.0
$[\text{HRuCo}_3(\text{CO})_{12}]$	1.6	1.0	14.5	3.4	23.4	9.1	1.1	37.3	44.0
$[\text{Et}_4\text{N}][\text{Ru}_3\text{Co}(\text{CO})_{13}]$	trace	trace	11.4	2.7	14.0	9.5	1.0	44.4	47.9
$[\text{Ru}_3(\text{CO})_{12}]^e$	0	trace	2.8	0.7	31.2	1.9	0	10.3	11.3
$[\text{Et}_4\text{N}][\text{FeCo}_3(\text{CO})_{12}]$	4.3	32.9	0.5	2.9	19.4	0	0	0.8	28.7
$[\text{Et}_4\text{N}][\text{Fe}_3\text{Co}(\text{CO})_{13}]$	2.3	15.9	0.7	3.1	6.5	0	0	2.5	34.6
$[\text{Fe}_3(\text{CO})_{12}]^f$	0.2	9.5	0.2	0.8	26.4	0	0	0.5	10.7
$[\text{RhCo}_3(\text{CO})_{12}]$	6.0	26.5	0.8	8.5	16.5	trace	0	1.4	34.1
$[\text{Rh}_2\text{Co}_2(\text{CO})_{12}]$	5.1	15.4	1.0	16.6	32.3	0.5	0	1.8	27.9
$[\text{Rh}_4(\text{CO})_{12}]^g$	0.1	1.9	0.5	9.2	26.9	0	0	1.3	15.1

<sup>a</sup> Conditions:  $\text{CH}_3\text{OH}$ , 500 mmol;  $\text{CH}_3\text{I}$ , 5 mmol;  $\text{CO}$ , 40 kg/cm<sup>2</sup>;  $\text{H}_2$ , 80 kg/cm<sup>2</sup> (initial pressure at room temperature); 180 °C; 2.5 h. <sup>b</sup> Co, 0.4 mmol. <sup>c</sup> Yield (%) = MeOH consumed for formation of a product/MeOH added  $\times$  100. The conversion of methanol was almost the same as the sum of each percent yield. <sup>d</sup> The selectivity was calculated on the basis of the methanol consumed. <sup>e</sup> Ru, 0.4 mmol. <sup>f</sup> Fe, 0.4 mmol. <sup>g</sup> Rh, 0.4 mmol.

minal) is 97.3° (av) that is smaller than the comparable C–Co–C (101.7°) in compound 3 as shown in Table III.

Three terminal carbonyl groups (C8–O8, C10–O10, and C12–O12) bonded to the Co atoms and two phenyl groups attached to the same P1 atom in the cation showed some disorder. Thus, all oxygen atoms in the above carbonyl groups appeared as two peaks in the crystallographic analysis. On the other hand, one of the phenyl groups showed rotatory disorder with respect to the P–C axis with the dihedral angle of 53.4°. The other phenyl group appeared as two different planes in which no carbon atoms occupy the same positions. Nonbonding distances far shorter than the sum of van der Waals radii of H and O atoms (2.6 Å) were found when all possible combinations of the above disorders were taken into consideration. This indicates that some of them cannot be allowed.

**The Homologation of Methanol Catalyzed by  $[\text{RuCo}_3(\text{CO})_{12}]^-$  Clusters.** The catalytic activities of  $[\text{RuCo}_3(\text{CO})_{12}]^-$  clusters for the methanol homologation have been investigated as well as those of other tetranuclear mixed clusters containing cobalt. As shown in Table IV, the mixed clusters  $\text{M}[\text{RuCo}_3(\text{CO})_{12}]$  (M = H, Na,  $[\text{Et}_4\text{N}]$ ,  $[\text{Ph}_4\text{P}]$ , or  $[(\text{Ph}_3\text{P})_2\text{N}]$ ) were very effective for the formation of ethanol from methanol and synthesis gas. The yield of ethanol depended upon the nature of the cation employed. The similar, but more dramatic, dependence upon the cation was previously observed in the synthesis of ethylene glycol from synthesis gas with ionic rhodium carbonyl clusters where bulky cations such as cesium and bis(triphenylphosphine)nitrogen ions gave the best results.<sup>15</sup> The other ruthenium–cobalt mixed cluster  $[\text{Et}_4\text{N}][\text{Ru}_3\text{Co}(\text{CO})_{13}]$ , which was originally prepared by Geoffroy et. al.,<sup>16</sup> gave ethanol in a lower yield under the same conditions, although the selectivity of total ethanol was as good as that with  $[\text{RuCo}_3(\text{CO})_{12}]^-$  clusters. On the other hand, use of the iron analogues such as  $[\text{Et}_4\text{N}][\text{FeCo}_3(\text{CO})_{12}]$ <sup>12</sup> and  $[\text{Et}_4\text{N}][\text{Fe}_3\text{Co}(\text{CO})_{13}]$ <sup>16</sup> and the rhodium–cobalt mixed clusters such as  $[\text{RhCo}_3(\text{CO})_{12}]$ <sup>17</sup> and  $[\text{Rh}_2\text{Co}_2(\text{CO})_{12}]$ <sup>17</sup> did not greatly change the distribution of the products compared with that in the case of cobalt

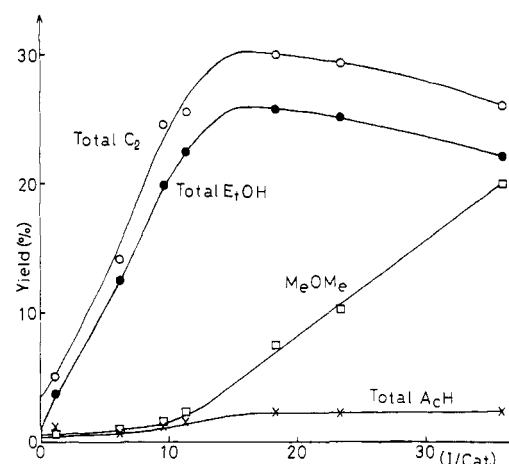


Figure 3. Influence of  $\text{CH}_3\text{I}/[\text{Et}_4\text{N}][\text{RuCo}_3(\text{CO})_{12}]$  molar ratio on the methanol homologation. Conditions:  $\text{MeOH}$ , 500 mmol;  $[\text{Et}_4\text{N}][\text{RuCo}_3(\text{CO})_{12}]$ , 0.13 mmol;  $\text{CO}$ , 40 kg/cm<sup>2</sup>;  $\text{H}_2$  80 kg/cm<sup>2</sup> (initial pressure at room temperature); 180 °C; 2.5 h.

carbonyl, although the yield of methyl acetate was slightly increased with the latter two rhodium–cobalt clusters.

A systematic investigation of the methanol homologation with  $[\text{Et}_4\text{N}][\text{RuCo}_3(\text{CO})_{12}]$  has been undertaken to determine the parameters most influencing conversion and selectivity. The results of varying the molar ratio of methyl iodide as a promoter to the cluster are shown in Figure 3. As the molar ratio was increased, the yield of total ethanol increased first linearly and then levelled off beyond ca. 20, while the yield of dimethyl ether increased first gradually and later rapidly. Thus, it is obvious that methyl iodide promoted the reaction, but much of the methanol was consumed in formation of dimethyl ether at the high molar ratios, an acid-catalyzed dehydration process not involving carbonylation, which resulted in decreasing the selectivity of total ethanol. The optimal range of the molar ratio was 6–12 (I/Co ratio = 2–4), where the selectivity of total ethanol was improved up to 60–64%. These values are quite different from the optimal range of I/Co ratio in the methanol homologation catalyzed by the  $\text{Co}(\text{acac})_2$ –(*p*-tolyl-O)<sub>3</sub>P system, i.e.,  $0 < \text{I/Co} < 1$ .<sup>6b</sup>

Effect of the reaction temperature on the product distribution is shown in Figure 4, where the molar ratio of methyl iodide to the cluster was fixed at 12. Lower temperatures favored formation of acetaldehyde, while higher

(15) (a) Cawse, J. N. U. S. Patent 4013700, 1977 (assigned to UCC).

(b) Kaplan, L. U. S. Patent 4190598, 1980 (assigned to UCC).

(16) Steinhardt, P. C.; Gladfelter, W. L.; Harley, A. D.; Fox, J. R.; Geoffroy, G. L. *Inorg. Chem.* 1980, 19, 332–339.

(17) Martinengo, S.; Chini, P.; Alvano, V. G.; Carati, F.; Salvatori, T. *J. Organomet. Chem.* 1973, 59, 379–394.

Table V. Time Dependence of Yield and Selectivity<sup>a</sup>

time, <sup>b</sup> h	yield, %							selectivity, %	
	AcH	DMA	EtOH	AcOMe	Me <sub>2</sub> O	MeOEt	Et <sub>2</sub> O	total EtOH	total AcH
0	0.28	8.7	1.5	1.0	0.7	2.0	0.08	18	22.4
0.5	0.47	4.1	6.5	1.6	0.9	5.5	0.35	50	9.5
1.5	0.72	3.6	12.6	2.5	2.5	7.4	0.90	57	6.4
2.5	0.50	3.0	18.9	3.1	3.1	8.7	1.27	63	3.9

<sup>a</sup> Conditions: CH<sub>3</sub>OH, 500 mmol; [Et<sub>4</sub>N][RuCo<sub>3</sub>(CO)<sub>12</sub>], 0.13 mmol; CH<sub>3</sub>I, 1.6 mmol; CO, 40 kg/cm<sup>2</sup>; H<sub>2</sub>, 80 kg/cm<sup>2</sup> (initial pressure at room temperature); 190 °C. <sup>b</sup> Time after the reaction mixture was heated up to 190 °C within 30 min.

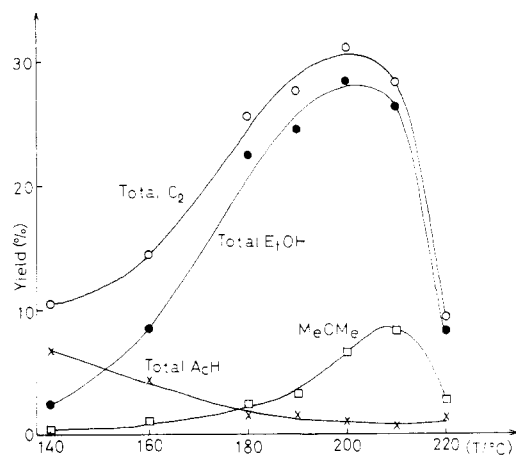


Figure 4. Effect of reaction temperature. Conditions: MeOH, 500 mmol; [Et<sub>4</sub>N][RuCo<sub>3</sub>(CO)<sub>12</sub>], 0.13 mmol; CH<sub>3</sub>I, 1.6 mmol; CO, 40 kg/cm<sup>2</sup>; H<sub>2</sub>, 80 kg/cm<sup>2</sup> (initial pressure at room temperature); 2.5 h.

temperatures led to ethanol synthesis. At 220 °C, formation of all the products was suddenly suppressed, suggesting decomposition of catalyst. The best selectivity of total ethanol (64%) was achieved at 190 °C.

Time dependence of yield and selectivity at 190 °C is shown in Table V. The selectivity of total acetaldehyde was relatively high in the early stages of the reaction, indicating that acetaldehyde is first formed and then hydrogenated to ethanol.

From the recovered solution after catalysis, [Et<sub>4</sub>N]-[Ru(CO)<sub>3</sub>I<sub>3</sub>] was isolated in moderate yield. The compound did not show catalytic activity for formation of ethanol under the above reaction conditions, but a combination of the compound and CoI<sub>2</sub>·4H<sub>2</sub>O, with the Ru/Co ratio of 1/3, did possess catalytic activity similar to that of the [RuCo<sub>3</sub>(CO)<sub>12</sub>]<sup>-</sup> clusters. It seems plausible that ruthenium-cobalt mixed-carbonyl clusters containing iodide ions are formed under the reaction conditions, but we must await further investigation to elucidate the reaction pathways.

### Experimental Section

All solvents and methyl iodide were purified by conventional methods and distilled under a nitrogen atmosphere. The compounds [Co<sub>2</sub>(CO)<sub>8</sub>], RuCl<sub>3</sub>·3H<sub>2</sub>O, RhCl<sub>3</sub>·3H<sub>2</sub>O, and [Et<sub>4</sub>N]Cl were obtained commercially and used without further purification, while the compounds Na[Co(CO)<sub>4</sub>],<sup>18</sup> [Ph<sub>4</sub>P]Br,<sup>19</sup> and [(Ph<sub>3</sub>P)<sub>2</sub>N]Cl<sup>20</sup> were prepared by published methods. Homometallic clusters and mixed-metal clusters such as [Co<sub>4</sub>(CO)<sub>12</sub>],<sup>21</sup> [RhCo<sub>3</sub>(CO)<sub>12</sub>],<sup>17</sup> [Rh<sub>2</sub>Co<sub>2</sub>(CO)<sub>12</sub>],<sup>17</sup> [Rh<sub>4</sub>(CO)<sub>12</sub>],<sup>22</sup> [Fe<sub>3</sub>(CO)<sub>12</sub>],<sup>23</sup> [Ru<sub>3</sub>(CO)<sub>12</sub>],<sup>24</sup>

[Et<sub>4</sub>N][Ru<sub>3</sub>Co(CO)<sub>13</sub>],<sup>16</sup> [Et<sub>4</sub>N][FeCo<sub>3</sub>(CO)<sub>12</sub>],<sup>12</sup> and [Et<sub>4</sub>N]-[Fe<sub>3</sub>Co(CO)<sub>13</sub>]<sup>16</sup> also were prepared according to literature procedures.

**Preparation of Na[RuCo<sub>3</sub>(CO)<sub>12</sub>]-THF.** A solution of Na[Co(CO)<sub>4</sub>] in THF (0.2 mol/L, 100 mL) was added to a red solution of RuCl<sub>3</sub>·3H<sub>2</sub>O (1.31 g, 5.01 mmol) in methanol (30 mL). The color of the solution immediately turned dark blue. The mixture was stirred at room temperature for 10–40 h until the color of the solution was dark red. The solvent was evaporated in vacuo, and the residue was extracted with THF (200 mL). After the extracts had been evaporated in vacuo, the resulting residue was washed with hexane several times and dissolved in water (300 mL). The hexane solution was concentrated and kept at -10 °C to precipitate [Co<sub>2</sub>(CO)<sub>8</sub>] (0.43 g, 1.25 mmol). On the other hand, a dark red solid was obtained by evaporating the aqueous solution to dryness. The solid was recrystallized from THF (55 mL)/hexane (100 mL) to give the title compound as swordlike black crystals. The color of the crystals turned brick red after being dried in vacuo for several hours; yield 1.723 g, 53.6%. Anal. Calcd for (C<sub>16</sub>H<sub>3</sub>O<sub>13</sub>NaRuCo<sub>3</sub>): C, 27.10; Co, 24.94; Ru, 14.25. Found: C, 26.95; Co, 25.09; Ru, 14.09.

**Preparation of [HRuCo<sub>3</sub>(CO)<sub>12</sub>].** An aqueous solution of H<sub>3</sub>PO<sub>4</sub> (350 mL) was added dropwise to a solution of Na[RuCo<sub>3</sub>(CO)<sub>12</sub>] (1.06 g, 1.66 mmol) in water (100 mL) to precipitate a bright brown solid. The solid was extracted with CH<sub>2</sub>Cl<sub>2</sub> (110 mL) twice, and the dark red extracts were dried over Na<sub>2</sub>SO<sub>4</sub>. The solution was concentrated under reduced pressure until a small amount of crystals appeared and was then allowed to stand at -11 °C for 1 day and at -78 °C for 1 day. The title compound was obtained as black crystals, which were washed with hexane and dried in vacuo; yield 0.31 g, 30%. Anal. Calcd for (C<sub>12</sub>H<sub>12</sub>O<sub>12</sub>RuCo<sub>3</sub>): C, 23.4; H, 0.16. Found: C, 23.61; H, 0.05.

**Preparation of [Et<sub>4</sub>N][RuCo<sub>3</sub>(CO)<sub>12</sub>].** A solution of [Et<sub>4</sub>N]Cl (0.756 g, 4.56 mmol) in water (20 mL) was added to a solution of Na[RuCo<sub>3</sub>(CO)<sub>12</sub>] (1.48 g, 2.33 mmol) in water (40 mL) to give immediately a dark brown precipitate. The precipitate was filtered, washed with water several times, dried in vacuo, and recrystallized from THF/hexane (55 mL/60 mL) to give the title compound as brown crystals; yield 1.07 g, 61.8%. Anal. Calcd for (C<sub>20</sub>H<sub>20</sub>O<sub>12</sub>NRuCo<sub>3</sub>): C, 32.28; H, 2.71; N, 1.88; Co, 23.76; Ru, 13.58. Found: C, 32.08; H, 2.77; N, 1.87; Co, 23.53; Ru, 13.82.

**Preparation of [Ph<sub>4</sub>P][RuCo<sub>3</sub>(CO)<sub>12</sub>].** A solution of [Ph<sub>4</sub>P]Br (0.384 g, 0.917 mmol) in CH<sub>2</sub>Cl<sub>2</sub> (5 mL) was added to a solution of Na[RuCo<sub>3</sub>(CO)<sub>12</sub>] (0.367 g, 0.576 mmol) in THF (15 mL), and the mixture then was stirred at room temperature for 20 h. After the solvent had been evaporated, the residue was extracted with THF (20 mL) to separate NaBr formed. The extracts were concentrated under a reduced pressure to ca. 2 mL, and then hexane was added slowly to give green crystals (31 mg) after several days. Anal. Found: C, 52.45; H, 2.61. IR: ν(CO) 2040(m), 1970(vs), 1922(m), 1775(s), 1730(s), and 1695(s) cm<sup>-1</sup>. After the crystals were filtered, the solution was again taken to dryness and the residue was recrystallized from THF/hexane (3 mL/18 mL) to give the title compound as dark red crystals; yield 0.229 g, 41.7%. Anal. Calcd for (C<sub>36</sub>H<sub>20</sub>O<sub>12</sub>PRuCo<sub>3</sub>): C, 45.36; H, 2.12. Found: C, 45.21; H, 1.96.

**Preparation of [(Ph<sub>3</sub>P)<sub>2</sub>N][RuCo<sub>3</sub>(CO)<sub>12</sub>].** A solution of [(Ph<sub>3</sub>P)<sub>2</sub>N]Cl (0.512 g, 0.893 mmol) in CH<sub>2</sub>Cl<sub>2</sub> (5 mL) was added to a solution of Na[RuCo<sub>3</sub>(CO)<sub>12</sub>] (0.362 g, 0.569 mmol) in THF (15 mL). The mixture was stirred at room temperature for 21

(18) McClellan, W. R. *J. Am. Chem. Soc.* **1961**, *83*, 1598–1600.

(19) Horner, L.; Mummethy, G.; Moser, H.; Beck, P. *Chem. Ber.* **1966**, *99*, 2782–2788.

(20) Ruff, J. K.; Schlientz, W. *J. Inorg. Synth.* **1974**, *15*, 84–90.

(21) Chini, P.; Aivano, V.; Martinengo, S. *J. Organomet. Chem.* **1969**, *16*, 471–477.

(22) Chini, P.; Martinengo, S. *Inorg. Chim. Acta* **1969**, *3*, 315–318.

(23) McFarlane, W.; Wilkinson, G. *Inorg. Synth.* **1966**, *8*, 181–183.

(24) Bruce, M. I.; Stone, F. G. A. *J. Chem. Soc. A* **1967**, 1238–1241.



Table VI. Crystallographic Data of  $[(\text{Ph}_3\text{P})_2\text{N}][\text{RuCo}_3(\text{CO})_{12}]$ 

cryst symmetry	monoclinic
space group	$P2_1/n$
$a$ , Å	32.364 (10)
$b$ , Å	10.939 (3)
$c$ , Å	13.908 (4)
$\beta$ , deg	100.17 (1)
$V$ , Å <sup>3</sup>	4847.3 (26)
$Z$	4
density, g/cm <sup>3</sup> (calcd)	1.58
abs coeff $\mu$ , cm <sup>-1</sup>	14.76

h and was then taken to dryness in vacuo. After the residue was extracted with THF (20 mL) to remove NaCl formed, the extracts were concentrated under reduced pressure to ca. 5 mL, and hexane (20 mL) was slowly added to this solution to form dark brown crystals (0.551 g) after several days. The crystals were recrystallized from THF/hexane (2 mL/20 mL) to give a mixture of greenish brown and white crystals (0.159 g). The compounds were not identified. The infrared spectrum of the greenish brown compound showed  $\nu(\text{CO})$  stretching absorptions at 2040 (m), 1975 (s), 1945 (vs), 1780 (s), 1750 (s), and 1710 (s) cm<sup>-1</sup>. After the mixture of crystals was filtered, the solution was again taken to dryness, and the residue was recrystallized from THF/hexane (2 mL/20 mL) to afford the title compound as dark red crystals: yield 0.159 g, 24.2%. Anal. Calcd for  $(\text{C}_{24}\text{H}_{10}\text{N}_2\text{O}_3\text{PRuCo}_3)$ : C, 50.02; H, 2.63; N, 1.22; P, 5.37. Found: C, 50.26; H, 2.43; N, 1.24; P, 5.83.

**The Homologation of Methanol Catalyzed by Mixed-Transition-Metal Clusters Containing Cobalt.** A 200-mL

stainless-steel autoclave lined with titanium was used as a reactor. In a typical run,  $[\text{Et}_4\text{N}][\text{RuCo}_3(\text{CO})_{12}]$  (0.13 mmol), methanol (20 mL, 500 mmol), methyl iodide (5 mmol) as a promoter, and benzene (10 mmol) as an internal standard were charged into the reactor under a nitrogen atmosphere. The reactor then was pressurized to 120 kg/cm<sup>2</sup> with  $\text{CO}/\text{H}_2$  (1/2) at room temperature, and heated to 180 °C within 30 min. The reaction was allowed to proceed at that temperature for 2.5 h, and then the autoclave was cooled to room temperature. A gas sample was taken, and the yellow reaction solution immediately was analyzed. Analysis of the off-gas was carried out by using gas chromatography with a 2-m column of Porapak Q (100 °C, 20 mL/min of He). Liquid products were analyzed by gas chromatography equipped with a flame ionization detector using a 3-m column of PEG 20M (70 °C, 30 mL/min of N<sub>2</sub>).

**Isolation of  $[\text{Et}_4\text{N}][\text{Ru}(\text{CO})_3\text{I}_3]$  from the Reaction Solution.** The yellow reaction solution recovered at the end of the above experiment was concentrated to ca. 3 mL to give a yellow precipitate. After being washed with water, the solid was dissolved in methanol (2 mL) at 40 °C. The yellow solution was gradually cooled to -11 °C to give the title compound as yellow crystals: yield 55 mg, 57% on the basis of the ruthenium initially added. Anal. Calcd for  $(\text{C}_{11}\text{H}_{20}\text{NO}_3\text{RuI}_3)$ : C, 18.98; N, 2.90; I, 54.70; Ru, 14.51. Found: C, 18.77; H, 2.99; N, 2.04; I, 54.43; Ru, 14.40.

The above water extracts were concentrated in vacuo to give a dark green solid (34 mg). The compound was found to contain cobalt (ca. 11%) and iodine by atomic absorption spectrochemical analysis and Beilstein test, respectively.

**Crystallographic Study.** Crystals of  $[(\text{Ph}_3\text{P})_2\text{N}][\text{RuCo}_3(\text{CO})_{12}]$  were prepared as described above, among which a dark

Table VII. Positional<sup>a</sup> and Isotropic Thermal<sup>b</sup> Parameters for  $[(\text{Ph}_3\text{P})_2\text{N}][\text{RuCo}_3(\text{CO})_{12}]$ 

atom	$x$	$y$	$z$	$U_{\text{iso}}$	atom	$x$	$y$	$z$	$U_{\text{iso}}$
Ru	4376.9 (4)	2605.6 (14)	-2969.8 (9)	6.0 <sup>c</sup>	C121	3890 (5)	6212 (15)	749 (11)	5.5 (4)
Co1	3803.8 (7)	1329.7 (24)	-4111.0 (14)	6.1 <sup>c</sup>	C122 (1)	3737 (10)	6165 (31)	-189 (23)	5.4 (8)
Co2	3801.4 (7)	1333.6 (23)	-2291.2 (14)	5.3 <sup>c</sup>	C123 (1)	3832 (12)	7055 (38)	-921 (28)	7.7 (11)
Co3	3576.3 (7)	3218.1 (24)	-3300.0 (14)	6.9 <sup>c</sup>	C124 (1)	4160 (10)	7838 (32)	-651 (24)	5.9 (9)
P1	3826.4 (12)	5201.2 (34)	1741.0 (26)	4.0 <sup>c</sup>	C125 (1)	4354 (9)	7939 (29)	-299 (21)	5.1 (7)
P2	3107.6 (11)	3435.5 (40)	1450.6 (27)	4.1 <sup>c</sup>	C126 (1)	4280 (9)	7144 (29)	1010 (21)	4.9 (7)
N	3371 (4)	4634 (12)	1511 (10)	7.0 <sup>c</sup>	C122 (2)	3452 (12)	6664 (36)	254 (26)	6.5 (10)
C1	4568 (6)	3652 (19)	-3914 (13)	7.9 <sup>c</sup>	C123 (2)	3453 (10)	7387 (33)	-599 (24)	6.1 (8)
O1	4693 (6)	4216 (18)	-4453 (13)	15.7 <sup>c</sup>	C124 (2)	3833 (12)	7550 (41)	-884 (29)	8.3 (11)
C2	4572 (5)	3645 (18)	-1860 (13)	7.0 <sup>c</sup>	C125 (2)	4189 (13)	7068 (40)	-485 (29)	8.0 (12)
O2	4691 (5)	4247 (16)	-1212 (11)	8.7 <sup>c</sup>	C126 (2)	4185 (12)	6368 (36)	445 (26)	7.1 (10)
C3	4827 (6)	1488 (19)	-2796 (13)	9.3 <sup>c</sup>	C131	3886 (4)	6122 (13)	2836 (10)	4.3 (3)
O3	5096 (6)	832 (17)	-2698 (13)	14.3 <sup>c</sup>	C132 (1)	3601 (9)	5965 (28)	3535 (21)	4.9 (7)
C4	3910 (7)	22 (22)	-3160 (13)	9.2 <sup>c</sup>	C133 (1)	3657 (11)	6622 (34)	4384 (25)	6.5 (9)
O4	4012 (6)	-1005 (14)	-3128 (10)	13.5 <sup>c</sup>	C134	3979 (6)	7522 (20)	4530 (14)	8.0 (5)
C5	3693 (6)	2976 (22)	-4640 (14)	11.4 <sup>c</sup>	C135 (1)	4262 (11)	7687 (36)	3871 (26)	7.0 (10)
O5	3675 (6)	3522 (17)	-5362 (9)	18.6 <sup>c</sup>	C136 (1)	4195 (10)	6954 (32)	3008 (23)	5.7 (8)
C6	3670 (6)	2991 (19)	-1878 (13)	8.9 <sup>c</sup>	C132 (2)	3570 (9)	6765 (27)	2990 (20)	4.5 (7)
O6	3662 (5)	3530 (13)	-1154 (8)	10.2 <sup>c</sup>	C133 (2)	3603 (11)	7470 (36)	3866 (26)	6.9 (9)
C7	4222 (6)	1060 (19)	-4690 (14)	7.8 (6)	C135 (2)	4332 (11)	6931 (36)	4279 (26)	7.1 (10)
O7	4478 (5)	780 (15)	-5150 (11)	10.4 (5)	C136 (2)	4297 (11)	6190 (33)	3468 (24)	6.3 (9)
C8	3403 (9)	607 (28)	-4855 (20)	12.6 (9)	C211	3403 (4)	2074 (12)	1598 (9)	3.6 (3)
O8 (1)	3215 (9)	-212 (28)	-5411 (21)	9.4 (9)	C212	3531 (10)	1578 (30)	2521 (22)	14.1 (11)
O8 (2)	3039 (10)	615 (32)	-5331 (23)	11.0 (10)	C213	3820 (11)	515 (34)	2557 (25)	16.6 (13)
C9	4228 (6)	1068 (19)	-1400 (14)	7.4 (5)	C214	3925 (8)	-16 (25)	1824 (18)	11.1 (8)
O9	4485 (5)	762 (15)	-756 (11)	10.2 (5)	C215	3775 (8)	409 (23)	921 (17)	10.1 (7)
C10	3397 (8)	592 (25)	-1841 (18)	11.1 (8)	C216	3504 (7)	1440 (22)	807 (16)	9.4 (7)
O10 (1)	3215 (9)	-135 (27)	-1351 (20)	8.8 (8)	C221	2774 (6)	3442 (19)	2345 (14)	7.9 (6)
O10 (2)	3037 (8)	415 (26)	-1726 (19)	8.2 (8)	C222	2655 (11)	4240 (34)	2809 (25)	17.3 (13)
C11	3670 (7)	4713 (22)	-3229 (16)	9.5 (7)	C223	2308 (8)	4055 (26)	3548 (19)	12.0 (9)
O11	3763 (6)	5770 (18)	-3195 (13)	13.1 (6)	C224	2268 (11)	3225 (35)	3891 (26)	17.5 (14)
C12	3053 (8)	3209 (26)	-3544 (19)	12.0 (9)	C225	2494 (12)	1958 (37)	3727 (27)	19.8 (15)
O12 (1)	2668 (9)	3540 (29)	-3714 (21)	9.9 (9)	C226	2765 (10)	2067 (33)	2892 (24)	16.0 (12)
O12 (2)	2678 (10)	2647 (31)	-3656 (22)	10.7 (10)	C231	2768 (5)	3325 (15)	278 (11)	5.3 (4)
C111	4248 (4)	4125 (13)	1891 (10)	4.3 (3)	C232	2757 (6)	4212 (20)	-388 (15)	7.9 (6)
C112	4398 (9)	3706 (28)	2808 (21)	13.3 (10)	C233	2481 (7)	4124 (23)	-1338 (17)	9.9 (7)
C113	4753 (10)	2853 (33)	2912 (24)	16.0 (13)	C234	2247 (8)	3143 (24)	-1494 (18)	10.9 (8)
C114	4898 (7)	2377 (22)	2150 (16)	9.0 (6)	C235	2236 (11)	2232 (36)	-912 (26)	17.9 (14)
C115	4720 (7)	2806 (23)	1232 (17)	9.9 (7)	C236	2486 (11)	2412 (36)	127 (25)	17.0 (13)
C116	4396 (7)	3673 (23)	1108 (17)	10.0 (7)					

<sup>a</sup> Positional parameters have been multiplied by a factor of 10<sup>4</sup>. <sup>b</sup> Isotropic thermal parameters (Å<sup>2</sup>) have been multiplied by a factor of 10<sup>2</sup>. <sup>c</sup>  $U_{\text{eq}} = 1/3 \sum_j U_{ij} a_i^* a_j^* a_i a_j$ .

red prism-shaped crystal of  $0.24 \times 0.26 \times 0.51$  mm was selected and sealed in a Pyrex glass capillary under argon atmosphere for X-ray data collection.

**Crystallographic Data.** Preliminary photographic data obtained by a Weissenberg camera indicated monoclinic symmetry and space group  $P2_1/n$ . The lattice parameters of the crystal were determined by a least-squares fit to the setting angles for 20 hand-centered reflections with  $9.0^\circ < \theta < 16.0^\circ$ , which were measured on an automatic Rigaku four-circle diffractometer using LiF-monochromated  $\text{Mo K}\alpha$  radiation ( $\lambda = 0.71069 \text{ \AA}$ ). The crystal data were given in Table VI. The intensity data were measured by the  $2\theta$ - $\omega$  scan mode with a scan rate of  $2^\circ/\text{min}$  and a scan range of  $1.0 + 0.45 \tan \theta$ . Background counts were measured for 10 s at the both ends of the scan range. Four standard reflections were monitored every 50 reflections to check any unfavorable effects, but no significant change of intensities was observed throughout the data collection. The intensities of 14651 unique reflections were measured out of  $2\theta = 60.0^\circ$ . A total of 6402 reflections with  $F_o > 2\sigma(F_o)$  were used for the subsequent structure determination and refinement where Lorenz, polarization, and analytical absorption corrections were made.

**Determination and Refinement of the Structure.**<sup>25</sup> The crystal structure was solved by conventional Patterson synthesis to locate the ruthenium atom. Fourier syntheses were then carried out to locate the remaining atoms except the hydrogen atoms. The positional parameters were refined by the block-diagonal least-squares technique. The atomic scattering factors were taken

(25) The UNICS program for the M-200H computers was employed at Tokyo University Computer Centre; Sakurai's RSLC-3 lattice constant program, Ueda's PAMI Patterson program, Iwasaki's ANSFR-2 Fourier synthesis program, Ashida's HBLS-4 block-diagonal least-squares program, modified Johnson's ORTEP thermal ellipsoid plot program, and diagonal least-squares program in the X-ray system's program made by Stewart et al.

from ref 26. Anomalous dispersion corrections were applied to the form factors for Ru, Co, and P. In the final refinements, the  $R$  and  $R_w$  values were 0.133 and 0.126, respectively, and the weighing scheme was  $w = 1/(A + |F_o| + B|F_o|^2)$  where  $A = 19.30$  and  $B = 0.004975$  were chosen so as to maintain  $w(|F_o| - |F_c|)^2$  essentially constant over all ranges of  $|F_o|$  and  $(\sin \theta)/\lambda$ . The standard deviation of an observation of unit weight defined as  $[\sum(|F_o| - |F_c|)^2/(m - n)]^{1/2}$  was 3.46, where the number of reflections ( $m$ ) was 6402 and the number of refined parameters ( $n$ ) was 413. Three terminal carbonyl groups on the Co atoms (C8-O8, C10-O10, and C12-O12) and two phenyl groups bonded to P1 showed some disorder, occupying two each positions with ca. 50% probability. The positional parameters obtained from the last cycle of refinement are listed in Table VII with the associated standard deviations estimated from the inverse matrix.

**Registry No.**  $\text{Na}[\text{RuCo}_3(\text{CO})_{12}]$ , 77932-75-3;  $\text{HRuCo}_3(\text{CO})_{12}$ , 24013-40-9;  $[\text{Et}_4\text{N}][\text{RuCo}_3(\text{CO})_{12}]$ , 78081-30-8;  $[\text{Ph}_4\text{P}][\text{RuCo}_3(\text{CO})_{12}]$ , 83721-24-8;  $[(\text{Ph}_3\text{P})_2\text{N}][\text{RuCo}_3(\text{CO})_{12}]$ , 83731-24-2;  $\text{Na}[\text{Co}(\text{CO})_4]$ , 14878-28-5;  $\text{RuCl}_3 \cdot 3\text{H}_2\text{O}$ , 13815-94-6;  $\text{H}_3\text{PO}_4$ , 7664-38-2;  $\text{MeOH}$ , 67-56-1;  $\text{MeI}$ , 74-88-4;  $\text{CO}$ , 630-08-0;  $[\text{Et}_4\text{N}][\text{Ru}(\text{CO})_3\text{I}_3]$ , 83721-25-9;  $\text{Co}_2(\text{CO})_8$ , 10210-68-1;  $\text{Co}_4(\text{CO})_{12}$ , 17786-31-1;  $[\text{Et}_4\text{N}][\text{Ru}_3\text{Co}(\text{CO})_{13}]$ , 77905-85-2;  $\text{Ru}_3(\text{CO})_{12}$ , 15243-33-1;  $[\text{Et}_4\text{N}][\text{FeCo}_3(\text{CO})_{12}]$ , 53509-36-7;  $[\text{Et}_4\text{N}][\text{Fe}_3\text{Co}(\text{CO})_{13}]$ , 83721-26-0;  $\text{Fe}_3(\text{CO})_{12}$ , 17685-52-8;  $\text{RhCo}_3(\text{CO})_{12}$ , 50696-79-2;  $\text{Rh}_2\text{Co}_2(\text{CO})_{12}$ , 50696-78-1;  $\text{Rh}_4(\text{CO})_{12}$ , 19584-30-6.

**Supplementary Material Available:** A listing of the thermal parameters and the observed and calculated structure amplitudes used in the refinement (19 pages). Ordering information is given on any current masthead page.

(26) (a) Cromer, D. T.; Waber, J. T. "International Tables for X-Ray Crystallography"; Kynoch Press: Birmingham, England, 1974; Vol. IV, Table 2.2a. (b) Cromer, D. T.; Liberman, D. *Ibid.*, Table 2.3.1.

## Synthesis and X-ray Crystal Structure of Tetraphenyldiarsetene

Gerard Sennyey,<sup>1a</sup> François Mathey,<sup>\*1a</sup> Jean Fischer,<sup>1b</sup> and André Mitschler<sup>1b</sup>

Laboratoire CNRS-SNPE, BP 28, 94320 Thiais, France, and Laboratoire de Cristallographie, ERA 08, Institut Le Bel, Université Louis Pasteur, 67070 Strasbourg Cedex, France

Received July 22, 1982

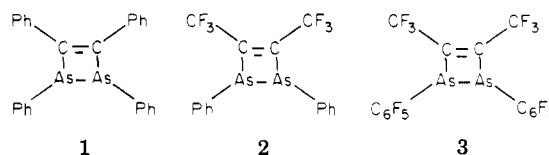
The reaction of tolan with  $(\text{PhAs})_6$  at  $160^\circ\text{C}$  yields mainly tetraphenyl-1,2-diarsetene and penta-phenyl-1,2,3-triarsetene. The diarsene  $\text{C}_{26}\text{H}_{20}\text{As}_2$  crystallizes in the triclinic system, space group  $P\bar{1}$ , with  $Z = 4$  and unit cell dimensions of  $a = 13.526$  (5)  $\text{\AA}$ ,  $b = 14.004$  (5)  $\text{\AA}$ ,  $c = 12.200$  (4)  $\text{\AA}$ ,  $\alpha = 103.76$  (2)°,  $\beta = 91.98$  (2)°,  $\gamma = 79.60$  (2)°, and  $V = 2207 \text{ \AA}^3$ . The ring is nonplanar and very strained with a very long As-As bond (2.471  $\text{\AA}$ ). The arsenic lone pairs are trans, excluding any cyclic delocalization. The reaction of the diarsene with  $\text{Fe}_3(\text{CO})_{12}$  at  $90^\circ\text{C}$  leads to the insertion of a  $\text{Fe}_2(\text{CO})_6$  unit into the As-As bond.

Whereas numerous studies have been devoted to the 1,2-diphosphetene ring,<sup>2</sup> practically nothing is known about the analogous 1,2-diarsetene ring.<sup>3</sup> In view of its potential interest in coordination chemistry, we have decided to perform a preliminary study of the still unknown 1,2,3,4-tetraphenyl-1,2-diarsetene (1).

(1) (a) Laboratoire CNRS-SNPE. (b) Laboratoire de Cristallographie. (2) (a) W. Mahler, *J. Am. Chem. Soc.*, **86**, 2306 (1964); (b) A. Ecker and U. Schmidt, *Chem. Ber.*, **106**, 1453 (1973); (c) A. H. Cowley and K. E. Hill, *Inorg. Chem.*, **12**, 1446 (1973); (d) A. H. Cowley, M. J. S. Dewar, D. W. Goodman, and M. C. Padolina, *J. Am. Chem. Soc.*, **96**, 3666 (1974); (e) T. C. Wallace, R. West, and A. H. Cowley, *Inorg. Chem.*, **13**, 182 (1974); (f) R. Appel and V. Barth, *Tetrahedron Lett.*, **21**, 1923 (1980); (g) C. Charrier, J. Guilhem, and F. Mathey, *J. Org. Chem.*, **46**, 3 (1981).

### Results and Discussion

**Synthesis.** In a work devoted to the <sup>75</sup>As NQR study of 2 and 3,<sup>3</sup> it was briefly stated that these compounds were obtained by reacting the appropriate cyclopolysarsine with hexafluorobutylene. Hence, in order to obtain 1, we chose



(3) T. J. Bastow, and P. S. Elmes, *Aust. J. Chem.*, **27**, 413 (1974).

red prism-shaped crystal of  $0.24 \times 0.26 \times 0.51$  mm was selected and sealed in a Pyrex glass capillary under argon atmosphere for X-ray data collection.

**Crystallographic Data.** Preliminary photographic data obtained by a Weissenberg camera indicated monoclinic symmetry and space group  $P2_1/n$ . The lattice parameters of the crystal were determined by a least-squares fit to the setting angles for 20 hand-centered reflections with  $9.0^\circ < \theta < 16.0^\circ$ , which were measured on an automatic Rigaku four-circle diffractometer using LiF-monochromated  $\text{Mo K}\alpha$  radiation ( $\lambda = 0.71069 \text{ \AA}$ ). The crystal data were given in Table VI. The intensity data were measured by the  $2\theta$ - $\omega$  scan mode with a scan rate of  $2^\circ/\text{min}$  and a scan range of  $1.0 + 0.45 \tan \theta$ . Background counts were measured for 10 s at the both ends of the scan range. Four standard reflections were monitored every 50 reflections to check any unfavorable effects, but no significant change of intensities was observed throughout the data collection. The intensities of 14651 unique reflections were measured out of  $2\theta = 60.0^\circ$ . A total of 6402 reflections with  $F_o > 2\sigma(F_o)$  were used for the subsequent structure determination and refinement where Lorenz, polarization, and analytical absorption corrections were made.

**Determination and Refinement of the Structure.**<sup>25</sup> The crystal structure was solved by conventional Patterson synthesis to locate the ruthenium atom. Fourier syntheses were then carried out to locate the remaining atoms except the hydrogen atoms. The positional parameters were refined by the block-diagonal least-squares technique. The atomic scattering factors were taken

(25) The UNICS program for the M-200H computers was employed at Tokyo University Computer Centre; Sakurai's RSLC-3 lattice constant program, Ueda's PAMI Patterson program, Iwasaki's ANSFR-2 Fourier synthesis program, Ashida's HBLS-4 block-diagonal least-squares program, modified Johnson's ORTEP thermal ellipsoid plot program, and diagonal least-squares program in the X-ray system's program made by Stewart et al.

from ref 26. Anomalous dispersion corrections were applied to the form factors for Ru, Co, and P. In the final refinements, the  $R$  and  $R_w$  values were 0.133 and 0.126, respectively, and the weighing scheme was  $w = 1/(A + |F_o| + B|F_o|^2)$  where  $A = 19.30$  and  $B = 0.004975$  were chosen so as to maintain  $w(|F_o| - |F_c|)^2$  essentially constant over all ranges of  $|F_o|$  and  $(\sin \theta)/\lambda$ . The standard deviation of an observation of unit weight defined as  $[\sum(|F_o| - |F_c|)^2/(m - n)]^{1/2}$  was 3.46, where the number of reflections ( $m$ ) was 6402 and the number of refined parameters ( $n$ ) was 413. Three terminal carbonyl groups on the Co atoms (C8-O8, C10-O10, and C12-O12) and two phenyl groups bonded to P1 showed some disorder, occupying two each positions with ca. 50% probability. The positional parameters obtained from the last cycle of refinement are listed in Table VII with the associated standard deviations estimated from the inverse matrix.

**Registry No.**  $\text{Na}[\text{RuCo}_3(\text{CO})_{12}]$ , 77932-75-3;  $\text{HRuCo}_3(\text{CO})_{12}$ , 24013-40-9;  $[\text{Et}_4\text{N}][\text{RuCo}_3(\text{CO})_{12}]$ , 78081-30-8;  $[\text{Ph}_4\text{P}][\text{RuCo}_3(\text{CO})_{12}]$ , 83721-24-8;  $[(\text{Ph}_3\text{P})_2\text{N}][\text{RuCo}_3(\text{CO})_{12}]$ , 83731-24-2;  $\text{Na}[\text{Co}(\text{CO})_4]$ , 14878-28-5;  $\text{RuCl}_3 \cdot 3\text{H}_2\text{O}$ , 13815-94-6;  $\text{H}_3\text{PO}_4$ , 7664-38-2;  $\text{MeOH}$ , 67-56-1;  $\text{MeI}$ , 74-88-4;  $\text{CO}$ , 630-08-0;  $[\text{Et}_4\text{N}][\text{Ru}(\text{CO})_3\text{I}_3]$ , 83721-25-9;  $\text{Co}_2(\text{CO})_8$ , 10210-68-1;  $\text{Co}_4(\text{CO})_{12}$ , 17786-31-1;  $[\text{Et}_4\text{N}][\text{Ru}_3\text{Co}(\text{CO})_{13}]$ , 77905-85-2;  $\text{Ru}_3(\text{CO})_{12}$ , 15243-33-1;  $[\text{Et}_4\text{N}][\text{FeCo}_3(\text{CO})_{12}]$ , 53509-36-7;  $[\text{Et}_4\text{N}][\text{Fe}_3\text{Co}(\text{CO})_{13}]$ , 83721-26-0;  $\text{Fe}_3(\text{CO})_{12}$ , 17685-52-8;  $\text{RhCo}_3(\text{CO})_{12}$ , 50696-79-2;  $\text{Rh}_2\text{Co}_2(\text{CO})_{12}$ , 50696-78-1;  $\text{Rh}_4(\text{CO})_{12}$ , 19584-30-6.

**Supplementary Material Available:** A listing of the thermal parameters and the observed and calculated structure amplitudes used in the refinement (19 pages). Ordering information is given on any current masthead page.

(26) (a) Cromer, D. T.; Waber, J. T. "International Tables for X-Ray Crystallography"; Kynoch Press: Birmingham, England, 1974; Vol. IV, Table 2.2a. (b) Cromer, D. T.; Liberman, D. *Ibid.*, Table 2.3.1.

## Synthesis and X-ray Crystal Structure of Tetraphenyldiarsetene

Gerard Sennyey,<sup>1a</sup> François Mathey,<sup>\*1a</sup> Jean Fischer,<sup>1b</sup> and André Mitschler<sup>1b</sup>

Laboratoire CNRS-SNPE, BP 28, 94320 Thiais, France, and Laboratoire de Cristallographie, ERA 08, Institut Le Bel, Université Louis Pasteur, 67070 Strasbourg Cedex, France

Received July 22, 1982

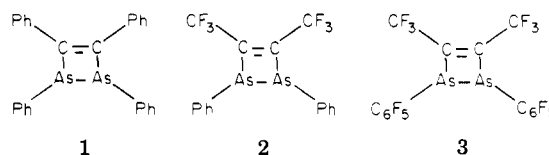
The reaction of tolan with  $(\text{PhAs})_6$  at  $160^\circ\text{C}$  yields mainly tetraphenyl-1,2-diarsetene and penta-phenyl-1,2,3-triarsetene. The diarsene  $\text{C}_{26}\text{H}_{20}\text{As}_2$  crystallizes in the triclinic system, space group  $P\bar{1}$ , with  $Z = 4$  and unit cell dimensions of  $a = 13.526(5) \text{ \AA}$ ,  $b = 14.004(5) \text{ \AA}$ ,  $c = 12.200(4) \text{ \AA}$ ,  $\alpha = 103.76(2)^\circ$ ,  $\beta = 91.98(2)^\circ$ ,  $\gamma = 79.60(2)^\circ$ , and  $V = 2207 \text{ \AA}^3$ . The ring is nonplanar and very strained with a very long As-As bond (2.471  $\text{ \AA}$ ). The arsenic lone pairs are trans, excluding any cyclic delocalization. The reaction of the diarsene with  $\text{Fe}_3(\text{CO})_{12}$  at  $90^\circ\text{C}$  leads to the insertion of a  $\text{Fe}_2(\text{CO})_6$  unit into the As-As bond.

Whereas numerous studies have been devoted to the 1,2-diphosphetene ring,<sup>2</sup> practically nothing is known about the analogous 1,2-diarsetene ring.<sup>3</sup> In view of its potential interest in coordination chemistry, we have decided to perform a preliminary study of the still unknown 1,2,3,4-tetraphenyl-1,2-diarsetene (1).

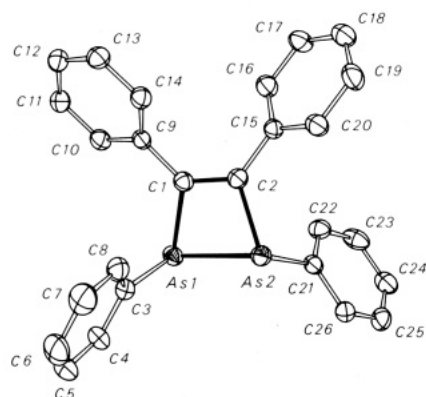
(1) (a) Laboratoire CNRS-SNPE. (b) Laboratoire de Cristallographie. (2) (a) W. Mahler, *J. Am. Chem. Soc.*, **86**, 2306 (1964); (b) A. Ecker and U. Schmidt, *Chem. Ber.*, **106**, 1453 (1973); (c) A. H. Cowley and K. E. Hill, *Inorg. Chem.*, **12**, 1446 (1973); (d) A. H. Cowley, M. J. S. Dewar, D. W. Goodman, and M. C. Padolina, *J. Am. Chem. Soc.*, **96**, 3666 (1974); (e) T. C. Wallace, R. West, and A. H. Cowley, *Inorg. Chem.*, **13**, 182 (1974); (f) R. Appel and V. Barth, *Tetrahedron Lett.*, **21**, 1923 (1980); (g) C. Charrier, J. Guilhem, and F. Mathey, *J. Org. Chem.*, **46**, 3 (1981).

### Results and Discussion

**Synthesis.** In a work devoted to the <sup>75</sup>As NQR study of 2 and 3,<sup>3</sup> it was briefly stated that these compounds were obtained by reacting the appropriate cyclopolysarsine with hexafluorobutylene. Hence, in order to obtain 1, we chose

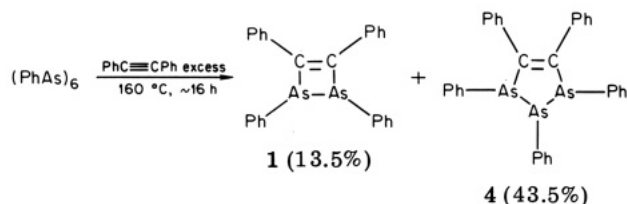


(3) T. J. Bastow, and P. S. Elmes, *Aust. J. Chem.*, **27**, 413 (1974).

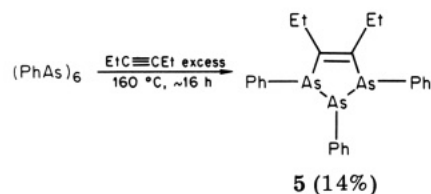


**Figure 1.** ORTEP plot of molecule A with the labeling scheme used. Thermal ellipsoids are scaled to enclose 30% of the electronic density. Hydrogen atoms are omitted for clarity.

to study the reaction of tolan with  $(\text{PhAs})_6$ . Our results were closely similar to those obtained in previous studies<sup>2b,g</sup> when  $(\text{PhP})_5$  was reacted with tolan. As with the phosphorus compounds, we obtained mainly the expected four-membered ring 1 in ca. 15% maximum yield together with the triarsolene 4. The only characterized byproduct



was a monoxide derived from 4. The ratio of 1:4 was relatively insensitive to an increase in the temperature. The sharp influence of the substitution at the carbons of the ring was well put in evidence by conducting a similar experiment with 3-hexyne. In that case, only the five-membered ring 5 was obtained. Among the various



spectroscopic data collected on 1, the most significant appeared to be the shielding of the carbons of the  $\text{As}_2\text{C}_2$  ring by comparison with that of the  $\text{As}_3\text{C}_2$  ring of 4 [ $\delta(^{13}\text{C}(\text{ring}))$  151.4; 4  $\delta(^{13}\text{C}(\text{ring}))$ , 157.3 ( $\text{CDCl}_3$ , internal  $\text{Me}_4\text{Si}$ )]. This shielding is probably related to the cyclic strain of the four-membered ring.

**Crystal Structure of Compound 1.** Table I gives the atomic positional and thermal parameters with their estimated standard deviations for all non-hydrogen atoms.

The crystal structure of  $\text{C}_{26}\text{H}_{20}\text{As}_2$  (1) consists of discrete molecules only linked by van der Waals contacts. There are two  $\text{As}_2\text{C}_2\text{H}_{20}$  moieties in the crystallographic asymmetric unit, one of them is shown in Figure 1. The two molecules are not significantly different. Table II gives the least-squares mean planes of interest and selected torsional angles. Table III gives selected bond lengths and bond angles with averages and estimated standard deviations.

The overall crystal structure of 1 is close to that of the corresponding 1,2,3,4-tetraphenyl-1,2-diphosphetene but without the crystallographic twofold axis through the middle of each of the C1-C2 and As1-As2 vectors.<sup>2g</sup>

The  $\text{As}_2\text{C}_2$  rings are not planar, and the lone pairs of the As atoms are trans with respect to the four-membered rings as seen from the data of Table II. Together with the localization of the C=C double bond in the rings (1.353 (4) Å (mean)) this conformation reveals a lack of aromaticity also supported by the comparison of the As-C intracyclic bond lengths of 1.962 (2) Å (mean), close to the sum of the covalent radii of As and C (1.98 Å) and the As-C(phenyl) bond length (1.948 (2) Å (mean)).

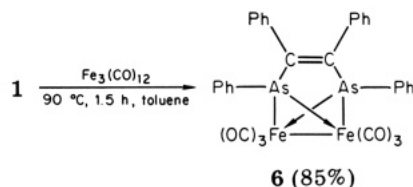
The geometry of the C=C bond is distorted when compared to normal  $\text{sp}^2$  geometry as shown by the C=C-C phenyl and C=C-As bond angles of, respectively, 129.9 (2) and 105.1 (1)° (average); these deformations are not as great as in the corresponding  $\text{P}_2\text{C}_2$  ring (131.2 (3) and 102.1 (2)°, respectively)<sup>2g</sup> due to the greater size of the arsenic atoms.

The As-As bond length of 2.4715 (7) Å (mean) also reflects the strain of the ring: it is significantly longer than the As-As bond length found in  $(\text{PhAs})_6$  (2.456 (5) Å<sup>4</sup>); in fact it appears to be the longest As-As bond ever recorded for either a free or a complexed polyarsine.<sup>5</sup>

The bond angles around each As atom are also considerably strained as around the carbon atoms of the C=C moiety, with As-As-C phenyl, C ring-As-C phenyl, and As-C ring-C phenyl bond angles of, respectively, 102.30 (1), 102.79 (9), and 124.8 (1)° while the mean value of the As-As-C ring bond angle is 72.67 (6)°, showing an important decrease with respect to the normal value.

In order to explain the stability of such a strained ring, we suggest the existence of a bent bond between the two arsenic atoms as we did in the case of the 1,2-diphosphetene ring.<sup>2g</sup>

**Reaction of 1 with Iron Carbonyls.** At 90 °C in toluene, 1 reacts rather rapidly with  $\text{Fe}_3(\text{CO})_{12}$  to give complex 6 in which a  $\text{Fe}_2(\text{CO})_6$  moiety has been inserted within the As-As bond. As expected the cleavage of the As-As bond appears to be easier than the cleavage of the P-P bond in the corresponding 1,2-diphosphetene.<sup>2g</sup>



The proposed structure for complex 6 is very likely on the basis of C, H, and Fe elemental analysis, mass spectroscopy, and comparison of the IR spectrum with the closely similar spectrum of the analogous phosphorus complex.<sup>2g</sup> The opening of the ring does not affect the ring carbon chemical shift ( $\delta^{13}\text{C}(\text{ring})$  151.5 in 6 vs. 151.4 in 1), showing once more the lack of aromaticity of the ring in 1.

The reaction of 1 with  $\text{Fe}_2(\text{CO})_9$  afforded more complicated complexes that were not identified.

## Experimental Section

NMR spectra were recorded on a Bruker WP 80 instrument at 80 and 20.15 MHz. Chemical shifts are reported in parts per million from internal  $\text{Me}_4\text{Si}$  for  $^1\text{H}$  and  $^{13}\text{C}$ ; products were in solution in  $\text{CDCl}_3$  unless otherwise stated. IR spectra were recorded on a Perkin-Elmer Model 217 spectrometer. Mass spectra

(4) K. Hedberg, E. W. Hughes, and J. Waser, *Acta Crystallogr.*, 14, 369 (1961).

(5) P. S. Elmes, B. M. Gatehouse, D. J. Lloyd, and B. O. West, *J. Chem. Soc., Chem. Commun.*, 953 (1974); E. Röttinger, A. Trenkle, R. Müller, and H. Vahrenkamp, *Chem. Ber.*, 113, 1280 (1980), and references cited herein.

Table I  
Positional and Thermal Parameters and Their Estimated Standard Deviations<sup>a</sup>

atom	x	y	z	B(1,1)	B(2,2)	B(3,3)	B(1,2)	B(1,3)	B(2,3)
As1	0.52904 (3)	-0.06606 (3)	0.33015 (4)	0.00570 (3)	0.00670 (3)	0.01093 (4)	-0.00266 (4)	0.00063 (6)	0.00186 (5)
As2	0.57888 (3)	0.05900 (3)	0.23992 (4)	0.00665 (3)	0.00605 (3)	0.00953 (4)	-0.00146 (4)	-0.00060 (6)	0.00177 (5)
As3	0.03341 (3)	0.41474 (3)	0.28751 (4)	0.00639 (3)	0.00641 (3)	0.01024 (4)	-0.00172 (5)	0.00072 (6)	0.00122 (5)
As4	0.07199 (3)	0.45991 (3)	0.13204 (4)	0.00605 (3)	0.00571 (2)	0.01176 (4)	-0.00158 (4)	0.00112 (6)	0.00377 (5)
C1	0.6756 (3)	-0.0778 (3)	0.3431 (3)	0.0061 (2)	0.0068 (2)	0.0086 (3)	-0.0026 (4)	0.0006 (5)	0.0035 (4)
C2	0.6951 (3)	0.0087 (3)	0.3235 (3)	0.0062 (2)	0.0062 (2)	0.0088 (3)	-0.0011 (4)	0.0009 (5)	0.0022 (4)
C3	0.5146 (3)	-0.1712 (3)	0.1973 (4)	0.0070 (3)	0.0060 (2)	0.0111 (4)	-0.0021 (4)	0.0013 (5)	0.0039 (5)
C4	0.4212 (4)	-0.2007 (3)	0.1786 (5)	0.0091 (3)	0.0085 (3)	0.0148 (5)	-0.0079 (5)	-0.0051 (7)	0.0043 (6)
C5	0.4047 (4)	-0.2693 (4)	0.0807 (6)	0.0139 (4)	0.0109 (4)	0.0227 (7)	-0.0126 (6)	-0.0170 (9)	0.0096 (8)
C6	0.4804 (5)	-0.3096 (4)	0.0047 (5)	0.0215 (6)	0.0096 (4)	0.0145 (6)	-0.0100 (8)	-0.0132 (10)	-0.0003 (8)
C7	0.5730 (5)	-0.2819 (4)	0.0222 (5)	0.0166 (6)	0.0102 (4)	0.0105 (5)	-0.0029 (8)	-0.0021 (9)	0.0000 (7)
C8	0.5900 (4)	-0.2126 (3)	0.1175 (4)	0.0096 (3)	0.0071 (3)	0.0108 (4)	-0.0026 (5)	-0.0019 (6)	0.0032 (5)
C9	0.7440 (3)	-0.1620 (3)	0.3696 (3)	0.0057 (2)	0.0057 (2)	0.0088 (3)	-0.0031 (4)	0.0000 (5)	0.0020 (4)
C10	0.7139 (3)	-0.2176 (3)	0.4380 (4)	0.0065 (2)	0.0080 (3)	0.0115 (4)	-0.0041 (4)	0.0009 (5)	0.0048 (5)
C11	0.7785 (3)	-0.2997 (3)	0.4600 (4)	0.0086 (3)	0.0076 (2)	0.0121 (4)	-0.0041 (4)	-0.0011 (6)	0.0075 (5)
C12	0.8723 (3)	-0.3281 (3)	0.4143 (4)	0.0085 (3)	0.0067 (2)	0.0112 (4)	-0.0023 (5)	-0.0026 (6)	0.0037 (5)
C13	0.9036 (3)	-0.2750 (3)	0.3458 (4)	0.0069 (3)	0.0077 (2)	0.0117 (4)	-0.0010 (5)	0.0012 (6)	0.0021 (6)
C14	0.8404 (3)	-0.1925 (3)	0.3231 (4)	0.0070 (3)	0.0069 (2)	0.0104 (4)	-0.0025 (4)	0.0010 (5)	0.0036 (5)
C15	0.7855 (3)	0.0551 (3)	0.3509 (3)	0.0055 (2)	0.0058 (2)	0.0091 (3)	-0.0020 (4)	0.0006 (5)	0.0028 (4)
C16	0.8327 (3)	0.0558 (3)	0.4531 (4)	0.0081 (3)	0.0086 (3)	0.0109 (4)	-0.0053 (5)	-0.0009 (6)	0.0053 (5)
C17	0.9138 (3)	0.1016 (4)	0.4816 (4)	0.0083 (3)	0.0105 (3)	0.0106 (4)	-0.0070 (5)	-0.0037 (6)	0.0044 (6)
C18	0.9509 (3)	0.1479 (4)	0.4095 (4)	0.0093 (3)	0.0096 (3)	0.0131 (5)	-0.0064 (5)	-0.0021 (7)	0.0029 (6)
C19	0.9063 (4)	0.1478 (3)	0.3072 (4)	0.0099 (3)	0.0098 (3)	0.0144 (5)	-0.0088 (5)	0.0005 (7)	0.0081 (6)
C20	0.8224 (3)	0.1019 (3)	0.2785 (4)	0.0079 (3)	0.0091 (3)	0.0111 (4)	-0.0059 (5)	-0.0029 (6)	0.0054 (5)
C21	0.5245 (3)	0.1885 (3)	0.3363 (3)	0.0058 (2)	0.0062 (2)	0.0094 (3)	-0.0032 (4)	-0.0002 (5)	0.0022 (4)
C22	0.5517 (3)	0.2214 (3)	0.4470 (4)	0.0066 (3)	0.0079 (3)	0.0102 (4)	-0.0011 (5)	-0.0004 (6)	0.0021 (5)
C23	0.5095 (4)	0.3163 (4)	0.5073 (4)	0.0078 (3)	0.0110 (4)	0.0112 (4)	-0.0049 (5)	-0.0005 (6)	-0.0041 (7)
C24	0.4404 (3)	0.3781 (3)	0.4585 (5)	0.0066 (3)	0.0073 (3)	0.0164 (5)	-0.0023 (5)	0.0018 (7)	-0.0017 (7)
C25	0.4117 (3)	0.3456 (3)	0.3501 (4)	0.0073 (3)	0.0062 (2)	0.0165 (5)	-0.0001 (5)	0.0021 (7)	0.0052 (6)
C26	0.4532 (3)	0.2510 (3)	0.2865 (4)	0.0069 (3)	0.0066 (2)	0.0116 (4)	-0.0027 (4)	-0.0009 (6)	0.0045 (5)
C27	0.0589 (3)	0.3001 (3)	0.1573 (3)	0.0057 (2)	0.0051 (2)	0.0099 (3)	-0.0014 (4)	0.0016 (5)	0.0022 (4)
C28	-0.0166 (3)	0.3165 (3)	0.0855 (3)	0.0061 (2)	0.0056 (2)	0.0097 (3)	-0.0017 (4)	0.0017 (5)	0.0026 (4)
C29	0.1457 (3)	0.4829 (3)	0.2801 (4)	0.0061 (2)	0.0057 (2)	0.0116 (4)	-0.0008 (4)	-0.0025 (5)	0.0020 (5)
C30	0.1729 (4)	0.5468 (3)	0.3761 (4)	0.0078 (3)	0.0075 (3)	0.0146 (5)	-0.0028 (5)	-0.0028 (7)	0.0028 (6)
C31	0.2492 (4)	0.5994 (4)	0.3735 (5)	0.0091 (3)	0.0083 (3)	0.0169 (6)	-0.0041 (5)	-0.0081 (7)	-0.0002 (7)
C32	0.2995 (4)	0.5883 (4)	0.2747 (5)	0.0086 (3)	0.0087 (3)	0.0218 (6)	-0.0067 (5)	-0.0082 (8)	0.0106 (7)
C33	0.2750 (4)	0.5257 (3)	0.1778 (5)	0.0079 (3)	0.0091 (3)	0.0166 (5)	-0.0039 (5)	-0.0012 (7)	0.0100 (6)
C34	0.1980 (3)	0.4718 (3)	0.1801 (4)	0.0066 (3)	0.0077 (3)	0.0133 (4)	-0.0024 (4)	-0.0033 (6)	0.0048 (6)
C35	0.1419 (3)	0.2145 (3)	0.1493 (4)	0.0059 (2)	0.0056 (2)	0.0105 (3)	-0.0024 (4)	0.0004 (5)	0.0035 (4)
C36	0.1802 (3)	0.1849 (3)	0.2460 (4)	0.0073 (3)	0.0068 (2)	0.0115 (4)	-0.0038 (4)	-0.0011 (6)	0.0028 (5)
C37	0.2592 (4)	0.1049 (3)	0.2377 (5)	0.0079 (3)	0.0079 (3)	0.0162 (5)	-0.0014 (5)	-0.0042 (7)	0.0081 (6)
C38	0.3006 (4)	0.0558 (3)	0.1357 (5)	0.0075 (3)	0.0062 (3)	0.0212 (6)	-0.0009 (5)	-0.0002 (8)	0.0045 (7)
C39	0.2656 (4)	0.0841 (4)	0.0403 (5)	0.0091 (3)	0.0077 (3)	0.0146 (5)	0.0009 (5)	0.0062 (7)	0.0023 (6)
C40	0.1866 (3)	0.1629 (3)	0.0467 (4)	0.0079 (3)	0.0077 (3)	0.0116 (4)	-0.0005 (5)	0.0040 (6)	0.0029 (6)

atom	B(1,1)	B(2,2)	B(3,3)	B(1,2)	B(1,3)	B(2,3)	B <sub>equiv</sub> , Å <sup>2</sup>
C41	-0.0513 (3)	0.2474 (3)	0.0061 (2)	0.0064 (2)	0.0092 (3)	-0.0011 (4)	0.0034 (4)
C42	-0.0848 (3)	0.2790 (3)	0.0087 (3)	0.0067 (2)	0.0098 (4)	-0.0021 (4)	0.0041 (5)
C43	-0.1178 (4)	0.2131 (4)	0.0106 (4)	0.0091 (3)	0.0101 (4)	-0.0024 (6)	0.0067 (5)
C44	-0.1191 (4)	0.1175 (4)	0.0104 (3)	0.0092 (3)	0.0107 (4)	-0.0052 (5)	0.0033 (6)
C45	-0.0888 (4)	0.0845 (3)	0.0127 (4)	0.0074 (3)	0.0131 (5)	-0.0036 (7)	0.0049 (6)
C46	-0.0550 (4)	0.1487 (3)	0.0107 (3)	0.0076 (3)	0.0111 (4)	-0.0057 (5)	0.0066 (5)
C47	-0.2073 (3)	0.4601 (3)	0.0061 (2)	0.0060 (2)	0.0096 (3)	-0.0017 (4)	0.0018 (5)
C48	-0.2799 (3)	0.5418 (3)	0.0068 (3)	0.0072 (3)	0.0123 (4)	-0.0012 (4)	0.0050 (5)
C49	-0.3770 (3)	0.5469 (4)	0.0070 (3)	0.0082 (3)	0.0162 (5)	0.0004 (5)	0.0046 (6)
C50	-0.4021 (3)	0.4724 (4)	0.0073 (3)	0.0091 (3)	0.0129 (4)	-0.0041 (5)	0.0000 (6)
C51	-0.3302 (4)	0.3928 (4)	0.0095 (3)	0.0095 (3)	0.0176 (5)	-0.0070 (5)	0.0076 (6)
C52	-0.2338 (4)	0.3853 (3)	0.0082 (3)	0.0079 (3)	0.0179 (5)	-0.0019 (5)	0.0087 (6)

General Temperature Factor Expressions—B's<sup>b</sup>

atom	B(1,1)	B(2,2)	B(3,3)	B(1,2)	B(1,3)	B(2,3)	B <sub>equiv</sub> , Å <sup>2</sup>
As1	4.03 (2)	4.80 (2)	6.14 (2)	-0.95 (2)	0.20 (2)	0.59 (2)	5.08 (1)
As2	4.71 (2)	4.34 (2)	5.35 (2)	-0.52 (2)	-0.19 (2)	0.56 (2)	4.94 (1)
Cl	4.3 (2)	4.8 (2)	4.8 (2)	-0.9 (1)	0.2 (1)	1.1 (1)	4.65 (9)
C2	4.4 (2)	4.4 (2)	5.0 (2)	-0.4 (1)	0.3 (2)	0.7 (1)	4.72 (9)
C3	4.9 (2)	4.3 (2)	6.2 (2)	-0.7 (1)	-0.4 (2)	1.2 (1)	5.2 (1)
C4	6.5 (2)	6.1 (2)	8.3 (3)	-2.8 (2)	-1.6 (2)	1.4 (2)	6.8 (1)
C5	9.9 (3)	7.8 (3)	12.8 (4)	-4.5 (2)	-5.4 (3)	3.0 (3)	9.8 (2)
C6	15.2 (5)	6.9 (3)	8.1 (3)	-3.6 (3)	-4.1 (3)	-0.1 (3)	10.3 (2)
C7	11.7 (4)	7.3 (3)	5.9 (3)	-1.0 (3)	-0.7 (3)	0.0 (2)	8.7 (2)
C8	6.8 (2)	5.1 (2)	6.1 (2)	-0.9 (2)	-0.6 (2)	1.0 (2)	6.1 (1)
C9	4.1 (2)	4.1 (1)	4.9 (2)	-1.1 (1)	0.0 (1)	0.6 (1)	4.38 (9)
C10	4.6 (2)	5.7 (2)	6.5 (2)	-1.5 (1)	0.3 (2)	1.5 (2)	5.5 (1)
C11	6.1 (2)	5.4 (2)	6.8 (2)	-1.5 (2)	-0.3 (2)	2.4 (2)	5.9 (1)
C12	6.0 (2)	4.8 (2)	6.3 (2)	-0.8 (2)	-0.8 (2)	1.2 (2)	5.8 (1)
C13	4.9 (2)	5.5 (2)	6.6 (2)	-0.3 (2)	0.4 (2)	0.7 (2)	5.9 (1)
C14	5.0 (2)	4.9 (2)	5.8 (2)	-0.9 (1)	0.3 (2)	1.2 (2)	5.2 (1)
C15	3.9 (2)	4.1 (2)	5.1 (2)	-0.7 (1)	0.2 (1)	0.9 (1)	4.42 (9)
C16	5.7 (2)	6.2 (2)	6.1 (2)	-1.9 (2)	-0.3 (2)	1.7 (2)	5.9 (1)
C17	5.9 (2)	7.5 (2)	6.0 (2)	-2.5 (2)	-1.2 (2)	1.4 (2)	6.3 (1)
C18	5.9 (2)	6.9 (2)	7.4 (3)	-2.3 (2)	-0.7 (2)	0.9 (2)	6.7 (1)
C19	7.0 (2)	7.0 (2)	8.1 (3)	-3.1 (2)	0.2 (2)	2.6 (2)	7.0 (1)
C20	5.6 (2)	6.5 (2)	6.2 (2)	-2.1 (2)	-0.9 (2)	1.7 (2)	6.0 (1)
C21	4.1 (2)	4.5 (2)	5.3 (2)	-1.2 (1)	-0.1 (1)	0.7 (1)	4.62 (9)
C22	4.7 (2)	5.7 (2)	5.7 (2)	-0.4 (2)	-0.1 (2)	0.7 (2)	5.6 (1)
C23	5.5 (2)	7.9 (3)	6.3 (2)	-1.7 (2)	-0.2 (2)	-1.3 (2)	7.0 (1)
C24	4.7 (2)	5.2 (2)	9.2 (3)	-0.8 (2)	0.6 (2)	-0.5 (2)	6.8 (1)
C25	5.2 (2)	4.4 (2)	9.2 (3)	-0.0 (2)	0.7 (2)	1.7 (2)	6.4 (1)
C26	4.9 (2)	4.7 (2)	6.5 (2)	-0.9 (1)	-0.3 (2)	1.4 (2)	5.4 (1)
As3	4.52 (2)	4.59 (2)	5.75 (2)	-0.61 (2)	0.23 (2)	0.39 (2)	5.12 (1)
As4	4.28 (2)	4.10 (2)	6.61 (2)	-0.56 (1)	0.35 (2)	1.20 (2)	5.02 (1)
C27	4.1 (2)	3.6 (1)	5.6 (2)	-0.5 (1)	0.5 (1)	0.7 (1)	4.51 (9)
C28	4.3 (2)	4.0 (2)	5.5 (2)	-0.6 (1)	0.5 (2)	0.8 (1)	4.65 (9)
C29	4.4 (2)	4.1 (2)	6.5 (2)	-0.3 (1)	-0.8 (2)	0.6 (2)	5.2 (1)
C30	5.5 (2)	5.4 (2)	8.2 (3)	-1.0 (2)	-0.9 (2)	0.9 (2)	6.5 (1)

Table I (Continued)

atom	B(1,1)	B(2,2)	B(3,3)	B(1,2)	B(1,3)	B(2,3)	$B_{\text{equiv}}, \text{Å}^2$
C31	6.4 (2)	5.9 (2)	9.5 (3)	1.4 (2)	-2.6 (2)	-0.1 (2)	7.6 (1)
C32	6.1 (2)	6.3 (2)	12.3 (3)	-2.4 (2)	-2.6 (2)	3.4 (2)	7.9 (1)
C33	5.6 (2)	6.5 (2)	9.3 (3)	-1.4 (2)	-0.4 (2)	3.2 (2)	6.9 (1)
C34	4.7 (2)	5.5 (2)	7.5 (2)	-0.9 (2)	-1.0 (2)	1.5 (2)	5.9 (1)
C35	4.0 (2)	4.2 (2)	5.9 (2)	-0.9 (1)	0.1 (2)	1.1 (1)	4.67 (9)
C36	5.1 (2)	4.9 (2)	6.4 (2)	-1.3 (2)	-0.3 (2)	0.9 (2)	5.5 (1)
C37	5.6 (2)	5.7 (2)	9.1 (3)	-0.5 (2)	-1.3 (2)	2.6 (2)	6.7 (1)
C38	5.3 (2)	4.4 (2)	11.9 (4)	-0.3 (2)	-0.1 (2)	1.4 (2)	7.4 (1)
C39	6.5 (2)	5.5 (2)	8.2 (3)	0.3 (2)	1.9 (2)	0.7 (2)	7.0 (1)
C40	5.6 (2)	5.5 (2)	6.5 (2)	-0.2 (2)	1.3 (2)	0.9 (2)	6.0 (1)
C41	4.3 (2)	4.6 (2)	5.2 (2)	-0.4 (1)	0.7 (2)	1.1 (1)	4.76 (9)
C42	6.1 (2)	4.8 (2)	5.5 (2)	-0.7 (2)	0.2 (2)	1.3 (2)	5.5 (1)
C43	7.5 (3)	6.5 (2)	5.7 (2)	-0.9 (2)	-0.8 (2)	2.1 (2)	6.5 (1)
C44	7.3 (2)	6.6 (2)	6.0 (2)	-1.9 (2)	-0.8 (2)	1.0 (2)	6.7 (1)
C45	9.0 (3)	5.3 (2)	7.4 (3)	-2.6 (2)	-1.1 (2)	1.5 (2)	7.1 (1)
C46	7.5 (2)	5.5 (2)	6.3 (2)	-2.0 (2)	-0.9 (2)	2.1 (2)	6.2 (1)
C47	4.3 (2)	4.3 (2)	5.4 (2)	-0.6 (1)	-0.2 (2)	0.6 (1)	4.8 (1)
C48	4.8 (2)	5.2 (2)	6.9 (2)	-0.4 (2)	0.4 (2)	1.6 (2)	5.7 (1)
C49	4.9 (2)	5.9 (2)	9.1 (3)	0.1 (2)	1.1 (2)	1.5 (2)	6.8 (1)
C50	5.2 (2)	6.5 (2)	7.3 (3)	-1.5 (2)	0.7 (2)	0.0 (2)	6.5 (1)
C51	6.7 (2)	6.8 (2)	9.9 (3)	-2.5 (2)	1.0 (2)	2.4 (2)	7.5 (1)
C52	5.8 (2)	5.6 (2)	10.0 (3)	-0.7 (2)	1.0 (2)	2.8 (2)	7.0 (1)

Positional and Thermal Parameters and Their Estimated Standard Deviations<sup>c</sup>

atom	x	y	z	atom	x	y	z
H4	0.3688 (0)	-0.1736 (0)	0.2330 (0)	H30	0.1386 (0)	0.5546 (0)	0.4452 (0)
H5	0.3405 (0)	-0.2882 (0)	0.0669 (0)	H31	0.2669 (0)	0.6435 (0)	0.4404 (0)
H6	0.4692 (0)	-0.3578 (0)	-0.0617 (0)	H32	0.3523 (0)	0.6245 (0)	0.2735 (0)
H7	0.6253 (0)	-0.3109 (0)	-0.0318 (0)	H33	0.3099 (0)	0.5189 (0)	0.1094 (0)
H8	0.6539 (0)	-0.1929 (0)	0.1289 (0)	H34	0.1811 (0)	0.4274 (0)	0.1132 (0)
H10	0.6483 (0)	-0.1994 (0)	0.4703 (0)	H36	0.1522 (0)	0.2197 (0)	0.3179 (0)
H11	0.7567 (0)	-0.3366 (0)	0.5077 (0)	H37	0.2843 (0)	0.0845 (0)	0.3038 (0)
H12	0.9159 (0)	-0.3845 (0)	0.4299 (0)	H38	0.3546 (0)	0.0011 (0)	0.1308 (0)
H13	0.9692 (0)	-0.2947 (0)	0.3134 (0)	H39	0.2954 (0)	0.0496 (0)	-0.0307 (0)
H14	0.8632 (0)	-0.1563 (0)	0.2752 (0)	H40	0.1626 (0)	0.1822 (0)	-0.0203 (0)
H16	0.8082 (0)	0.0239 (0)	0.5045 (0)	H42	-0.0851 (0)	0.3461 (0)	-0.1138 (0)
H17	0.9449 (0)	0.1014 (0)	0.5526 (0)	H43	-0.1397 (0)	0.2351 (0)	-0.2681 (0)
H18	1.0073 (0)	0.1799 (0)	0.4303 (0)	H44	-0.1415 (0)	0.0730 (0)	-0.2612 (0)
H19	0.9322 (0)	0.1788 (0)	0.2559 (0)	H45	0.0907 (0)	0.0176 (0)	-0.1017 (0)
H20	0.7906 (0)	0.1030 (0)	0.2080 (0)	H46	-0.0339 (0)	0.1253 (0)	0.0537 (0)
H22	0.5990 (0)	0.1792 (0)	0.4818 (0)	H48	-0.2631 (0)	0.5946 (0)	0.1503 (0)
H23	0.5286 (0)	0.3390 (0)	0.5834 (0)	H49	-0.4268 (0)	0.6031 (0)	0.2097 (0)
H24	0.4129 (0)	0.4434 (0)	0.5003 (0)	H50	-0.4691 (0)	0.4760 (0)	0.2794 (0)
H25	0.3627 (0)	0.3878 (0)	0.3173 (0)	H51	-0.3468 (0)	0.3418 (0)	0.2947 (0)
H26	0.4335 (0)	0.2292 (0)	0.2104 (0)	H52	-0.1850 (0)	0.3279 (0)	0.2287 (0)

<sup>a</sup> The form of the anisotropic thermal parameter is  $\exp[-(B(1,1)h^2 + B(2,2)k^2 + B(3,3)l^2 + B(1,2)hk + B(1,3)hl + B(2,3)kl)]$ . Estimated standard deviations in the least significant digits are shown in parentheses. <sup>b</sup> The form of the anisotropic thermal parameter is  $\exp[-0.25h^2a^2B(1,1) + k^2b^2B(2,2) + l^2c^2B(3,3) + 2hlacB(1,3) + 2klbcB(2,3)]$  where  $a$ ,  $b$ , and  $c$  are reciprocal lattice constants. <sup>c</sup> Estimated standard deviations in the least significant digits are shown in parentheses.  $B = 7.0000 (0) \text{Å}^2$ .

Table II. Mean Planes<sup>a</sup> and Selected Torsional Angles (deg)

planes	atoms	dist
PL1	C1*	0
	C2*	0
	As1*	0
PL2	C3	1.733 (4)
	C1*	0
	C2*	0
PL3	As2*	0
	C21	-1.639 (4)
	C27*	0
PL4	C28*	0
	As3*	0
	C29	1.750 (4)
	C27*	0
	C28*	0
	As4*	0
	C47	-1.740 (4)
Torsional Angles		
	C1-As1-As2-C2	-12.0
	C28-As4-As3-C27	-10.5
	As1-C1-C2-As2	-21.7
	As4-C28-C27-As3	-19.1
	C3-As1-C1-C9	-66.7
	C21-As2-C2-C15	-63.5
	C35-C27-As3-C29	-69.8
	C41-C28-As4-C47	-68.9

<sup>a</sup> Dihedral angles: PL1/PL2 = 21.7°; PL3/PL4 = 19.1°. Atoms labeled with an asterisk have been used for computing the mean plane.

Table III. Bond Lengths (Å) and Angles (deg) with Estimated Standard Deviations

Bond Lengths			
As1-As2	2.475 (1)	As1-C3	1.944 (5)
As3-As4	2.468 (1)	As2-C21	1.943 (4)
mean	2.471 (1)	As3-C29	1.950 (4)
C1-C2	1.361 (6)	As4-C47	1.955 (4)
C27-C28	1.346 (6)	mean	1.948 (2)
mean	1.353 (4)	C1-C9	1.455 (6)
As1-C1	1.963 (4)	C2-C15	1.477 (6)
As2-C2	1.959 (4)	C27-C35	1.475 (6)
As3-C27	1.960 (4)	C28-C41	1.478 (6)
As4-C28	1.965 (4)	mean	1.47 (2)
mean	1.962 (2)	C(phenyl)-	1.377 (1)
		C(phenyl)(mean)	
Bond Angles			
As1-As2-C2	72.5 (1)	As1-As2-C21	105.7 (1)
As2-As1-C1	72.7 (1)	As2-As1-C3	100.1 (1)
As3-As4-C28	72.5 (1)	As3-As4-C47	102.2 (1)
As4-As3-C27	72.9 (1)	As4-As3-C29	101.1 (1)
mean	72.67 (6)	mean	102.0 (4)
As1-C1-C2	104.5 (3)	C1-As1-C3	102.4 (2)
As2-C2-C1	105.2 (3)	C2-As2-C21	103.8 (2)
As3-C27-C28	105.1 (3)	C27-As3-C29	102.6 (2)
As4-C28-C27	105.6 (3)	C28-As4-C47	102.3 (2)
mean	105.1 (1)	mean	102.8 (1)
C1-C2-C15	129.3 (4)	As1-C1-C9	125.5 (3)
C2-C1-C9	129.9 (4)	As2-C2-C15	125.3 (3)
C27-C28-C41	130.1 (4)	As3-C27-C35	124.5 (3)
C28-C27-C35	130.2 (4)	As4-C28-C41	124.2 (3)
mean	129.9 (2)	mean	124.8 (1)

were recorded on a Nermag R10-10 spectrometer at 70 eV by M. Charré (SNPE). All reactions were carried out under argon. Chromatographic separations were performed on silicagel columns (70–230 mesh Merck) under argon.

**Reaction of Tolan with (PhAs)<sub>6</sub>.** A mixture of (PhAs)<sub>6</sub> (22.8 g, 25 mmol) and tolan (14.75 g, 83 mmol) was heated overnight at 160 °C. The resulting product was chromatographed with hexane–benzene (90:10). 1,2,3,4-Tetraphenyl-1,2-diarsetene (1) was obtained first: *R<sub>f</sub>* ~0.2; yield, 4.9 g (13.5%); mp 122 °C; <sup>13</sup>C

NMR δ 127.76–133.33 (CH), 138.91 and 139.10 (Ph, substituted C), 151.46 (ring C); mass spectrum (130–140 °C), *m/e* (relative intensity) 482 (M, 87), 304 (M – C<sub>2</sub>Ph<sub>2</sub>, 93%), 253 (M – AsPh<sub>2</sub>, 100), 227 (304 – Ph, 100), 178 (C<sub>2</sub>Ph<sub>2</sub>, 73). Anal. Calcd for C<sub>28</sub>H<sub>20</sub>As<sub>2</sub>: C, 64.75; H, 4.18; As, 31.07. Found: C, 64.38; H, 4.16; As, 29.86.

Then, 1,2,3,4,5-pentaphenyl-1,2,3-triazolene (4) was recovered: *R<sub>f</sub>* ~0.1; yield, 13.8 g (43.5%); mp 126 °C; <sup>13</sup>C NMR δ 126.59–134.59 (CH), 139.87 and 140.74 (Ph, substituted C), 157.32 (ring C); mass spectrum (140 °C), *m/e* (relative intensity) 634 (M, 63), 482 (M – AsPh, 10), 306 (34), 253 (16), 227 (PhAs<sub>2</sub>, 100), 178 (C<sub>2</sub>Ph<sub>2</sub>, 27), 152 (AsPh, 45). Anal. Calcd for C<sub>32</sub>H<sub>25</sub>As<sub>3</sub>: C, 60.59; H, 3.97; As, 35.43. Found: C, 60.28; H, 3.85; As, 34.73.

**Reaction of 3-Hexyne with (PhAs)<sub>6</sub>.** A mixture of (PhAs)<sub>6</sub> (1.82 g, 2 mmol) and 3-hexyne (0.5 g, 6 mmol) was heated overnight at 160 °C. The resulting product was chromatographed with pentane–benzene (96:4). 1,2,3-Triphenyl-4,5-diethyl-1,2,3-triazolene (5) was thus recovered as a colorless oil: yield, 0.3g (14%); <sup>1</sup>H NMR (external Me<sub>4</sub>Si) δ 1.13 (t, 6 H, CH<sub>3</sub>), 2.37 (m, 4 H, CH<sub>2</sub>), 7.23 (m, 15 H, Ph); mass spectrum (150 °C), *m/e* (relative intensity) 538 (M, 37), 402 (20), 386 (M – AsPh, 15), 306 (27), 304 (As<sub>2</sub>Ph<sub>2</sub>, 25), 229 (100), 227 (As<sub>2</sub>Ph, 75), 152 (AsPh, 55).

**Reaction of 1 with Fe<sub>3</sub>(CO)<sub>12</sub>.** A mixture of 1 (0.241 g, 0.5 mmol) and Fe<sub>3</sub>(CO)<sub>12</sub> (0.301 g, 0.6 mmol) was heated at 90 °C for 1.5 h in degassed toluene (20 mL). After filtration and evaporation, the organic residue was chromatographed with hexane–benzene (60:40). Complex 6 was thus recovered: yield, 0.35 g (86%); mp 189 °C; <sup>13</sup>C NMR δ 126.82–135.72 (Ph), 151.54 (C ring), 213.15 (CO); IR ν(CO) 2050, 2010, 1985, 1970, 1960 cm<sup>-1</sup>; mass spectrum (150–170 °C), *m/e* (relative intensity) 762 (M, 6), 706 (M – 2CO, 37), 594 (M – 6CO, 46), 439 (92), 178 (C<sub>2</sub>Ph<sub>2</sub>, 100). Anal. Calcd for C<sub>32</sub>H<sub>20</sub>As<sub>2</sub>Fe<sub>2</sub>O<sub>6</sub>: C, 50.43; H, 2.64; Fe, 14.65. Found: C, 51.54; H, 2.74; Fe, 14.60.

**X-ray Data Collection and Processing.** Suitable single crystals of 1 were obtained by slow evaporation at room temperature of EtOH solutions under inert atmosphere. A systematic search in reciprocal space using a Philips PW1100/16 automatic single crystal diffractometer showed that crystals of 1 belong to the triclinic system; on the basis of a Nz cumulative test on observed structure factor, the space group is P $\bar{1}$ .

The unit cell dimensions and their standard deviations were obtained and refined at room temperature with Cu K $\alpha$  radiation ( $\lambda = 1.5418$  Å) by using 25 carefully selected reflections and the standard Philips software. The experimental density was measured by flotation. Final results: C<sub>28</sub>H<sub>20</sub>As<sub>2</sub>, mol wt 482, *a* = 13.526 (5) Å, *b* = 14.004 (5) Å, *c* = 12.200 (4) Å,  $\alpha = 103.76$  (2)°,  $\beta = 91.98$  (2)°,  $\gamma = 79.60$  (2)°, *V* = 2207 Å<sup>3</sup>, *d*<sub>obsd</sub> = 1.42 ± 0.03 g·cm<sup>-3</sup>, *Z* = 4, *d*<sub>calcd</sub> = 1.451 g·cm<sup>-3</sup>, P $\bar{1}$ ,  $\mu = 21.01$  cm<sup>-1</sup>.

A parallelepiped crystal 0.012 × 0.012 × 0.020 cm was sealed in a Lindemann glass capillary and mounted on a rotation-free goniometer head. All intensity data were obtained with a Philips PW1100/16 four-circle diffractometer controlled by a P852M computer, using graphite-monochromated radiation and standard software.

The vertical and horizontal apertures in front of the scintillation counter were adjusted so as to minimize the background counts without loss of net peak intensity at the 2 $\sigma$  levels. The total scan width in the flying step-scan  $\omega/2\theta$  mode was  $\Delta\omega = 0.90^\circ + (\text{Cu } K\alpha_1, \alpha_2 \text{ splitting})$ , with a step width of 0.04° and a scan speed of 0.020 deg·s<sup>-1</sup>; 6122 reflections were measured (3.5° <  $\theta$  < 57°).

Three standard reflections measured every 2 h during the entire data collection period showed a mean loss of 15% in intensity which was corrected by a linear time-dependent function.

The resulting data set was transferred to a PDP11/60 computer; the raw step-scan measurements were converted to intensities by using the Lehmann–Larsen<sup>6</sup> algorithm and a local program. For all subsequent computation, the Enraf-Nonius SDP/V18 package<sup>7</sup> was used.

Intensities were corrected for Lorentz, polarization, and absorption factors, the last being computed by numerical integration<sup>8</sup>

(6) M. S. Lehmann and F. K. Larsen, *Acta Crystallogr. Sect. A*, **A30**, 508 (1974).

(7) B. A. Frenz in "Computing in Crystallography", H. Schenk, R. Olthoff-Hazekamp, H. Van Koningsveld, and G. C. Bassi, Eds., Delft University Press, Delft, Holland, 1978, pp 64–71.



(transmission factors between 0.64 and 0.75). All reflections having  $\sigma(F^2)/F^2 > 0.33$  were considered unobserved, leading to a unique data set of 4452 observations which were used to refine the structure.

The structure was solved by direct methods using MULTAN.<sup>9</sup> All non-hydrogen atoms could be located in the *E* map computed with the phases of the most probable set of MULTAN. Hydrogen atoms were introduced in structure factor calculation by their computed coordinates (C-H = 0.95 Å) and isotropic temperature

factors ( $B_H = 7 \text{ \AA}^2$ ) but not refined. The full-matrix refinement converged to  $R(F) = 0.034$  and  $R_w(F) = 0.049$ . The unit-weight observation was 1.04 with a *p* factor of 0.08 in  $\sigma(F^2) = \sigma_{\text{count}}^2 + (pI)^2$ . The final difference map showed no maxima greater than  $0.5 \text{ e \AA}^{-3}$ . Table IV (supplementary material) gives *h*, *k*, *l*,  $F_0$ , and  $F_c$  ( $\times 10$ ) for all observed structure factors.

**Registry No.** 1, 83783-15-7; 4, 83801-87-0; 5, 64278-86-0; 6, 83815-89-8; (PhAs)<sub>6</sub>, 20738-31-2; PhC≡CPh, 501-65-5; Fe<sub>3</sub>(CO)<sub>12</sub>, 17685-52-8.

(8) P. Coppens, "Crystallographic Computing", F. R. Ahmed, Ed., Munksgaard, Copenhagen, 1970, p 255.

(9) G. Germain, P. Main, and M. H. Woolfson, *Acta Crystallogr. Sect. B*, **B26**, 274 (1970); *Acta Crystallogr., Sect. A*, **A27**, 368 (1971).

**Supplementary Material Available:** Table IV, observed and computed structure factors for all observed reflections (19 pages). Ordering information is given on any current masthead page.

## Tellurium-125 and selenium-77 NMR shifts for symmetric and unsymmetric diorganyl chalcogenides

D. H. O'Brien, N. Dereu, C. K. Huang, K. J. Irgolic, and F. F. Knapp Jr.

*Organometallics*, 1983, 2 (2), 305-307 • DOI: 10.1021/om00074a017 • Publication Date (Web): 01 May 2002

Downloaded from <http://pubs.acs.org> on April 24, 2009

### More About This Article

---

The permalink <http://dx.doi.org/10.1021/om00074a017> provides access to:

- Links to articles and content related to this article
- Copyright permission to reproduce figures and/or text from this article



# Tellurium-125 and Selenium-77 NMR Shifts for Symmetric and Unsymmetric Diorganyl Chalcogenides

D. H. O'Brien,\* N. Dereu, C.-K. Huang, and K. J. Irgolic

Department of Chemistry, Texas A&M University, College Station, Texas 77843

F. F. Knapp, Jr.

Nuclear Medicine Group, Health and Safety Research Division, Oak Ridge National Laboratory, Oak Ridge, Tennessee 37834

Received July 27, 1982

The proton-noise-decoupled  $^{125}\text{Te}$  NMR spectra of symmetric dialkyl tellurides  $\text{R}_2\text{Te}$  ( $\text{R} = \text{Me, Et, } n\text{-Pr, } i\text{-Pr, } n\text{-Bu, } i\text{-Bu, } sec\text{-Bu, } t\text{-Bu, and neo-Pent}$ ) and 36 unsymmetric dialkyl tellurides  $\text{RTeR}'$  ( $\text{R, R}' = \text{all alkyl isomers } \text{C}_1\text{-C}_4 \text{ and neopentyl}$ ) and the  $^{77}\text{Se}$  and  $^{125}\text{Te}$  spectra of phenyl alkyl chalcogenides  $\text{C}_6\text{H}_5\text{XR}$  ( $\text{R} = \text{all alkyl isomers } \text{C}_1\text{-C}_4, \text{X} = \text{Se or Te}$ ) are reported. The unsymmetric diorganyl chalcogenides were prepared from diorganyl dichalcogenides and Grignard reagents or organic lithium compounds. The effect of alkyl substitution on the  $^{125}\text{Te}$  chemical shifts of the diorganyl tellurides was found to be additive but smaller than the shift changes for the diorganyl ditellurides. The magnitude of the effect diminishes as the substitution site moves away from the tellurium atom and becomes negligible at the fourth atom. The  $^{77}\text{Se}$  shifts of phenyl alkyl selenides plotted against the corresponding  $^{125}\text{Te}$  shifts of phenyl alkyl tellurides produce a straight line with a slope of 1.71. These data suggest that  $^{77}\text{Se}$  shifts and shift change parameters for selenides and diselenides may be predicted by dividing the tellurium values by 1.71.

## Introduction

The number of recent publications<sup>1-20</sup> reporting  $^{125}\text{Te}$  nuclear magnetic resonance measurements for the characterization of tellurium compounds illustrates the usefulness of this method. The potential applications of  $^{125}\text{Te}$  NMR spectroscopy include the identification of unknown tellurium compounds, the determination of reaction mechanisms and the elucidation of catalytic properties of tellurium derivatives. The wider use of  $^{125}\text{Te}$  NMR will be realized only after the chemical shifts of a sufficient number of representative classes of tellurium derivatives have been measured. For instance, only very limited chemical shift data are available for dialkyl tellurides.

Dimethyl telluride is used as the  $^{125}\text{Te}$  shift reference ( $\delta$  0). Shifts have been reported for diethyl telluride ( $\delta$  392 and 380)<sup>10,17</sup> and for diisopropyl telluride ( $\delta$  707).<sup>17</sup> Comparison of these shifts suggests that  $\alpha$ -methyl substitution causes large downfield  $^{125}\text{Te}$  shift changes. The shifts for diethyl telluride and bis( $\gamma$ -(trimethylsilyl)propyl) telluride ( $\delta$  241)<sup>7</sup> indicate that  $\beta$ -alkyl substitution effects smaller, upfield shift changes. Tellurium-125 chemical shift data have not been reported for unsymmetric tellurides. Radiolabeled alkyltelluroalkanecarboxylic acids,<sup>21</sup> tellurium-containing steroids,<sup>22</sup> and alkyltelluroalkyl barbiturates<sup>23</sup> are attractive candidates for organ imaging. The potential use of radiolabeled tellurium agents in nuclear medicine has recently been reviewed.<sup>24</sup> Tellurium-125 NMR spectroscopy may therefore be a convenient method to investigate the fate of the unlabeled organic tellurium compounds in biological systems.

## Results and Discussion

We have previously reported  $^{125}\text{Te}$  chemical shift data for symmetric and unsymmetric dialkyl ditellurides.<sup>20</sup> The shift changes for ditellurides are additive and can be empirically related to the extent of  $\alpha$ -,  $\beta$ -, and  $\gamma$ -alkyl substitution. We report here the  $^{125}\text{Te}$  chemical shifts for a large number of symmetric and unsymmetric dialkyl tellurides. Similar to the changes for ditellurides, shift differences are due to the additive effects of alkyl substitution  $\alpha$ ,  $\beta$ , and  $\gamma$  to tellurium. We also report the  $^{77}\text{Se}$  chemical

(1) D. B. Denney, D. Z. Denney, P. J. Hammond, and Y. F. Hsu, *J. Am. Chem. Soc.*, **103**, 2340 (1981).

(2) P. Granger, S. Chapelle, W. R. McWhinnie, and A. Al-Rubaie, *J. Organomet. Chem.*, **220**, 149 (1981).

(3) P. Granger, S. Chapelle, and C. Brevard, *J. Magn. Reson.*, **42**, 203 (1981).

(4) H. J. Gysling, N. Zumbulyadis, and J. A. Robertson, *J. Organomet. Chem.*, **209**, C41 (1981).

(5) W. Lohner and K. Praefcke, *J. Organomet. Chem.*, **208**, 43 (1981).

(6) W. Lohner and K. Praefcke, *J. Organomet. Chem.*, **208**, 39 (1981).

(7) N. Zumbulyadis and H. J. Gysling, *J. Organomet. Chem.*, **192**, 183 (1980).

(8) P. Granger and S. Chapelle, *J. Magn. Reson.*, **39**, 329 (1980).

(9) B. Kohn, W. Lohner, K. Praefcke, H. J. Jakobsen, and B. Villadsen, *J. Organomet. Chem.*, **166**, 373 (1979).

(10) G. V. Fazakerley and M. Celotti, *J. Magn. Reson.*, **33**, 219 (1979).

(11) T. Drakenberg, A.-B. Hornfeldt, S. Gronowitz, J.-M. Talbot, and J.-L. Piette, *Chem. Ser.*, **13**, 152 (1978-1979).

(12) W. Koch, O. Lutz, and A. Nolle, *Z. Phys. A*, **289**, 17 (1978).

(13) C. R. Lassigne and E. J. Wells, *J. Chem. Soc., Chem. Commun.*, 956 (1978).

(14) G. J. Schrobilgen, R. C. Burns, and P. Granger, *J. Chem. Soc., Chem. Commun.*, 957 (1978).

(15) K. U. Buckler, J. Kronenbitter, O. Lutz, and A. Nolle, *Z. Naturforsch., A*, **32A**, 1263 (1977).

(16) P. L. Goggin, R. J. Goodfellow, and S. R. Haddock, *J. Chem. Soc., Chem. Commun.*, 176 (1975).

(17) H. C. E. McFarlane and W. McFarlane, *J. Chem. Soc., Dalton Trans.*, 2416 (1973).

(18) C. Rodger, N. Sheppard, C. McFarlane, and W. McFarlane, in "NMR and the Periodic Table", R. K. Harris and B. E. Mann, Eds., Academic Press, New York, 1978, p 383-419.

(19) W. McFarlane, F. J. Berry, and B. C. Smith, *J. Organomet. Chem.*, **113**, 139 (1976).

(20) D. H. O'Brien, N. Dereu, R. A. Grigsby, K. J. Irgolic, and F. F. Knapp, Jr., *Organometallics*, **1**, 513 (1982).

(21) F. F. Knapp, Jr., K. R. Ambrose, A. P. Callahan, R. A. Grigsby, and K. J. Irgolic, in "Radiopharmaceuticals II, Society of Nuclear Medicine", New York, 1979. F. F. Knapp, Jr., K. R. Ambrose, A. P. Callahan, L. A. Ferren, R. A. Grigsby, and K. J. Irgolic, *J. Nucl. Med.*, **22**, 988 (1981); D. R. Elmaleh, F. F. Knapp, Jr., T. Yasuda, J. L. Coffey, S. Kapiwoda, R. Okada, and H. W. Strauss, *ibid.*, **22**, 994 (1981); R. Okada, F. F. Knapp, Jr., D. R. Elmaleh, T. Yasuda, C. A. Boucher, and H. W. Strauss, *Circulation*, **65**, 305 (1981).

(22) F. F. Knapp, Jr., K. R. Ambrose and A. P. Callahan, *J. Nucl. Med.*, **21**, 251 (1980); F. F. Knapp, Jr., K. R. Ambrose and A. P. Callahan, *ibid.*, **21**, 258 (1980).

(23) F. F. Knapp, Jr., K. R. Ambrose and A. P. Callahan, *J. Med. Chem.*, **24**, 794 (1981); F. F. Knapp, Jr., *J. Org. Chem.*, **44**, 1007 (1981).

(24) F. F. Knapp, Jr., in "Radiopharmaceuticals: Structure Activity Relationships", R. P. Spencer, Ed., Grune & Stratton, New York, 1981, Chapter 16, pp 345-391.

Table I. Tellurium-125 Chemical Shifts for Dialkyl Tellurides R<sub>1</sub>-Te-R<sub>2</sub><sup>a</sup>

R <sub>1</sub>	R <sub>2</sub>								
	Me	neo-Pent	<i>i</i> -Bu	<i>n</i> -Pr	<i>n</i> -Bu	Et	<i>s</i> -Bu	<i>i</i> -Pr	<i>t</i> -Bu
Me	0								
neo-Pent	25	45							
<i>i</i> -Bu	64	92	133						
<i>n</i> -Pr	115	140	183	233					
<i>n</i> -Bu	123	148	191	242	248				
Et	185	211	254	305	312	376			
<i>s</i> -Bu	276	307	352	401	408	469	578		
<i>i</i> -Pr	342	371	414	465	471	532	638	696	
<i>t</i> -Bu	497	524	574	622	628	690	806	866	999

<sup>a</sup> Chemical shifts are downfield relative to dimethyl telluride.

Table II. Tellurium-125 Chemical Shift Changes Caused by  $\alpha$ -Methyl Substitution,  $\alpha_1$ , in Dialkyl Tellurides R<sub>1</sub>-Te-R<sub>2</sub>

R <sub>1</sub>	R <sub>2</sub>	$\delta$	$\Delta\delta$	R <sub>1</sub>	R <sub>2</sub>	$\delta$	$\Delta\delta$
Me	Me	0		Me	Et	185	
Et	Me	185	+185	Et	Et	376	+191
Me	neo-Pent	25		Me	<i>sec</i> -Bu	276	
Et	neo-Pent	211	+186	Et	<i>sec</i> -Bu	469	+193
Me	<i>i</i> -Bu	64		Me	<i>i</i> -Pr	342	
Et	<i>i</i> -Bu	254	+190	Et	<i>i</i> -Pr	532	+190
Me	<i>n</i> -Pr	115		Me	<i>t</i> -Bu	504	
Et	<i>n</i> -Pr	305	+190	Et	<i>t</i> -Bu	690	+186
Me	<i>n</i> -Bu	123					
Et	<i>n</i> -Bu	312	+189				av +189 $\pm$ 2

shift data for a series of alkyl phenyl selenides and compare these data with values obtained by <sup>125</sup>Te NMR studies of the analogous alkyl phenyl tellurides.

The unsymmetric diorganyl tellurides and selenides were prepared by the reaction of organometallic compounds with diorganyl dichalcogenides just prior to shift determination (eq 1). Aqueous quenching followed by ether

$$R-X-X-R + R'M \rightarrow R-X-R' + R-X-M \rightarrow R-X-X-R \quad (1)$$

R = alkyl, phenyl; R' = alkyl; X = Se, Te; M =

MgCl, Li

extraction, drying, and solvent evaporation of these small scale preparations gave NMR samples that were immediately analyzed by <sup>77</sup>Se or <sup>125</sup>Te NMR. These samples always contained small quantities of the original symmetric dichalcogenide formed through oxidation of the selenols or tellurols during workup. These byproducts served as convenient internal chemical shift references.

The <sup>125</sup>Te chemical shifts for symmetric and unsymmetric dialkyl tellurides are presented in Table I. The effect of the first  $\alpha$ -methyl substitution may be obtained by comparing the shifts of the methyl alkyl tellurides to the shifts for the ethyl alkyl tellurides (Table II). These results demonstrate that methyl substitution causes a large downfield shift change of 189 ppm. Subsequent  $\alpha$ -methyl substitutions (ethyl to isopropyl, *n*-propyl to *sec*-butyl, and isopropyl to *tert*-butyl) result in slightly smaller downfield shift changes (Table III). Alkyl substitution  $\beta$  to the tellurium atom causes smaller upfield shift changes while substitution  $\gamma$  to the tellurium atom causes very small downfield shift changes. Structural changes more remote to tellurium than the  $\gamma$ -carbon have little or no effect on the <sup>125</sup>Te chemical shift. For example, the <sup>125</sup>Te shift for di-*n*-butyl telluride is  $\delta$  248 while the shift for dineopentyl telluride is  $\delta$  250. The additive shift change parameters for dialkyl tellurides are all slightly smaller than those for the tellurium atom closest to the substitution site in the corresponding ditellurides (Table III).<sup>20</sup>

The additive effect of alkyl substitutions on <sup>125</sup>Te chemical shifts is expressed in terms of methyl substitutions in Table III. However, the effect of the substitution

Table III. Tellurium-125 Chemical Shift Changes Due to Methyl Substitution for Dialkyl Tellurides

substituent	$\Delta\delta$		comparison
	telluride	ditelluride <sup>a</sup>	
$\alpha_1$	+189 $\pm$ 2	+211 $\pm$ 3	Me to Et
$\alpha_{2-1}$	+162 $\pm$ 5	+171 $\pm$ 2	Et to <i>i</i> -Pr
$\alpha_{2-2}$	+170 $\pm$ 5	+187 $\pm$ 3	<i>n</i> -Pr to <i>sec</i> -Bu
$\alpha_3$	+160 $\pm$ 4	+170 $\pm$ 4	<i>i</i> -Pr to <i>t</i> -Bu
$\beta_1$	-70 $\pm$ 1	-77 $\pm$ 2	Et to <i>n</i> -Pr
$\beta_{2-1}$	-50 $\pm$ 1	-51 $\pm$ 2	<i>n</i> -Pr to <i>i</i> -Bu
$\beta_{2-2}$	-62 $\pm$ 2	-61 $\pm$ 3	<i>i</i> -Pr to <i>s</i> -Bu
$\beta_3$	-44 $\pm$ 2	-61 $\pm$ 3	<i>i</i> -Bu to neo-Pent
$\gamma$	+8 $\pm$ 1	+7 $\pm$ 1	<i>n</i> -Pr to <i>n</i> -Bu

<sup>a</sup> Reference 20.

of larger alkyl groups is also additive and is the sum of the methyl substitution shift changes that make up the larger alkyl substitution. For example, the effect of  $\alpha$ -ethyl substitution, obtained by comparing methyl alkyl telluride shifts to *n*-propyl alkyl telluride shifts, is a downfield shift change of 120 ppm. This shift change is the sum of the changes for  $\alpha$ -methyl substitution,  $\alpha_1$ , and  $\beta$ -methyl substitution,  $\beta_1$ : +189 + (-70) = 119 ppm. Similarly, the effect of  $\alpha$ -isopropyl substitution (methyl to isobutyl, +70 ppm) is the sum of one  $\alpha$ -methyl substitution and two  $\beta$ -methyl substitutions:  $\alpha_1 + \beta_1 + \beta_{2-1}$ , +189 + (-70) + (-50) = 69 ppm.

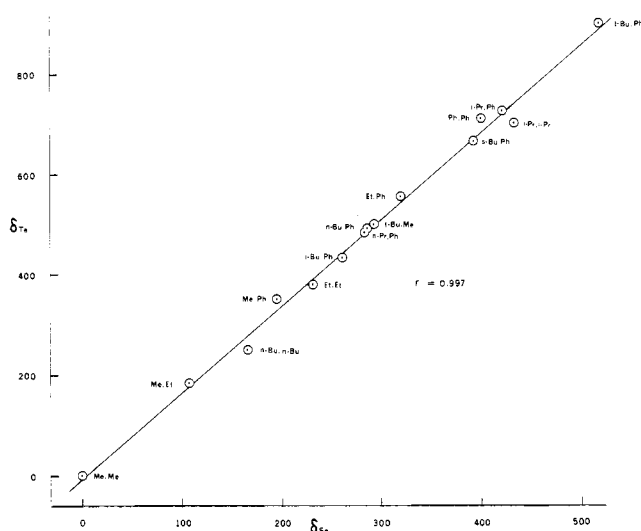
These shift changes parameters may be used to predict shifts for other organic tellurium compounds. For example, the <sup>125</sup>Te shift for 1,1-dimethylbutyl telluride is obtained from the shift for di-*n*-butyl telluride ( $\delta$  248) by adding two  $\alpha$ -methyl shift changes,  $2 \times \alpha_{2-2} = 340$  ppm, to give a predicted shift of  $\delta$  588. The observed chemical shift is  $\delta$  584. Similarly, these shift changes may be used to predict shifts for phenyl alkyl tellurides. The calculated shift values in Table IV were obtained by applying the shift change parameters to the observed shift for phenyl ethyl telluride. The predicted values agree well with the observed values.

For a large number of structurally similar organic tellurium and selenium compounds, the <sup>125</sup>Te shifts parallel the <sup>77</sup>Se shifts.<sup>17</sup> Chemical shifts of alkyl selenides depend

**Table IV.** Tellurium-125 and Selenium-77 Chemical Shifts for Phenyl Alkyl Compounds Ph-X-R (X = Te or Se)

R	$\delta^{125}\text{Te}$		$\delta^{77}\text{Se}$	ref
	calcd	obsd		
Me	363	349	197	202 <sup>a</sup>
<i>i</i> -Bu	432	429	264	
<i>n</i> -Pr	482	480	285	
<i>n</i> -Bu	490	488	288	
Et	552	552	322	327 <sup>a</sup>
<i>sec</i> -Bu	652	660	394	
<i>i</i> -Pr	714	720	424	
<i>t</i> -Bu	874	893	521	

<sup>a</sup> Reference 25.



**Figure 1.** The <sup>125</sup>Te and <sup>77</sup>Se chemical shifts for diorganyl chalcogenides. The <sup>77</sup>Se shifts for methyl ethyl, diethyl, methyl isobutyl, and diphenyl selenide are from ref 25.

upon the extent of  $\alpha$ -branching but the shift change parameters and additivity for  $\beta$ - and  $\gamma$ -alkyl substitutions for selenium have not been demonstrated.<sup>25,26</sup> We have determined the <sup>77</sup>Se shifts for eight phenyl alkyl selenides that differ by  $\alpha$ -,  $\beta$ -, and  $\gamma$ -methyl substitutions (Table IV). When these shifts and the shifts of other organic selenium compounds are plotted against the <sup>125</sup>Te shifts for the corresponding organic tellurium compounds, a straight line is obtained (Figure 1,  $r = 0.997$ ). The slope of 1.71 reflects the greater sensitivity of the electron distribution around tellurium toward substituent changes. In view of this very good linear relationship, it is reasonable that <sup>77</sup>Se shifts may be predicted by dividing the tellurium shifts by 1.71. Further, shift change parameters for methyl substitutions in selenides and diselenides may be obtained by dividing the corresponding tellurium shift changes for tellurides and ditellurides by 1.71.

### Experimental Section

Dimethyl telluride and diethyl telluride were obtained commercially. The symmetric ditellurides were prepared by the reaction  $\text{Te}_2^{2-}$  with alkyl halides. The symmetric dialkyl tellurides were obtained as byproducts in the preparations of the dialkyl ditellurides. In a typical preparation of a symmetric dialkyl ditelluride, absolute ethanol (200 mL) was placed into a 500 mL, three-necked flask equipped with a magnetic stirring bar, a reflux condenser, and a nitrogen inlet. Tellurium powder (12.7 g, 0.1 mol) was added followed by small pieces of sodium (3.5 g, 0.15

mol). After all the sodium had reacted, sodium borohydride (1.89 g, 0.05 mol) was introduced. The mixture was refluxed for 2 h under a nitrogen atmosphere. After the mixture had been cooled in an ice-water bath, the neat alkyl halide (0.1 mol) was added slowly. After all the halide had been added, the mixture was stirred for 30 min at room temperature, filtered to remove tellurium, and poured into distilled water (100 mL). The ethanol-water solution was extracted with two portions of diethyl ether (25 mL each). The extract was filtered and dried with anhydrous calcium chloride. The ether was removed under water aspirator vacuum. The red residue was distilled rapidly under pump vacuum to yield as first fraction the yellowish dialkyl tellurides and as second fraction the deep red dialkyl ditellurides.

Unsymmetric dialkyl tellurides, phenyl alkyl tellurides, and phenyl alkyl selenides were prepared from the reaction of ditellurides or diphenyl diselenide with organometallic reagents. Ethylmagnesium bromide, *n*-propylmagnesium chloride, isopropylmagnesium chloride, *n*-butyllithium, isobutylmagnesium chloride, *sec*-butyllithium, and *tert*-butylmagnesium chloride were obtained commercially. In a typical preparation, approximately 100 mg of a symmetric dialkyl ditelluride was dissolved in 30 mL of diethyl ether. The orange solution was titrated to a colorless end point by stepwise addition of the organolithium or organomagnesium reagent. The ether solution was washed with 10 mL of water, decanted, and dried over anhydrous sodium sulfate. The solvent was evaporated and the oily product dissolved in 2 mL of deuteriochloroform for NMR analysis. Samples of the phenyl alkyl tellurides and phenyl alkyl selenides were prepared in a similar manner except that 200 mg of diphenyl ditelluride or 300 mg of diphenyl diselenide was used.

All <sup>125</sup>Te and <sup>77</sup>Se spectra were obtained with a Varian Associates Model FT80 NMR spectrometer equipped with a broadband probe tuned to 25.104 MHz for <sup>125</sup>Te and to 15.17 MHz for <sup>77</sup>Se. About 2000–5000 average transients at a pulse repetition rate of 0.5 s with proton-noise decoupling were required to obtain satisfactory signal to noise ratios by using sweep widths of either 8 or 4 KHz stored in 8K data points. The <sup>125</sup>Te shifts are referenced to dimethyl telluride at 25 094 885 Hz. The <sup>77</sup>Se shifts are referenced to dimethyl selenide ( $\delta$  0) by using diphenyl diselenide at 15 176 912 Hz and the relationship:  $\delta = \delta_{\text{Ph}_2\text{Se}_2} + 460.25$ . Chemical shifts are believed to be precise to at least  $\pm 1$  ppm.

**Acknowledgment.** Support of this work by the Robert A. Welch Foundation of Houston, TX, is gratefully acknowledged. The work at the Oak Ridge National Laboratory is sponsored by the Office of Health and Environmental Research, U.S. Department of Energy, under Contract W-7405-eng-26 with the Union Carbide Corp.

**Registry No.** Me<sub>2</sub>Te, 593-80-6; MeTe(*neo*-pent), 83816-97-1; (*neo*-pent)<sub>2</sub>Te, 83816-98-2; MeTe(*i*-Bu), 83816-99-3; (*i*-Bu)Te(*neo*-pent), 83817-00-9; (*i*-Bu)<sub>2</sub>Te, 83817-01-0; (*n*-Pr)TeMe, 83817-02-1; (*n*-Pr)Te(*neo*-pent), 83817-03-2; (*n*-Pr)Te(*i*-Bu), 83817-04-3; (*n*-Pr)<sub>2</sub>Te, 64501-17-3; (*n*-Bu)TeMe, 83817-05-4; (*n*-Bu)Te(*neo*-pent), 83817-06-5; (*n*-Bu)Te(*i*-Bu), 83817-07-6; (*n*-Bu)Te(*n*-Pr), 83817-08-7; (*n*-Bu)<sub>2</sub>Te, 38788-38-4; EtTeMe, 83817-09-8; EtTe(*neo*-pent), 83817-10-1; EtTe(*i*-Bu), 83817-11-2; EtTe(*n*-Pr), 83817-12-3; EtTe(*n*-Bu), 83817-13-4; Et<sub>2</sub>Te, 627-54-3; (*sec*-Bu)TeMe, 83817-14-5; (*sec*-Bu)Te(*neo*-pent), 83817-15-6; (*sec*-Bu)Te(*i*-Bu), 83817-16-7; (*sec*-Bu)Te(*n*-Pr), 83817-17-8; (*sec*-Bu)Te(*n*-Bu), 83817-18-9; (*sec*-Bu)TeEt, 83817-19-0; (*sec*-Bu)<sub>2</sub>Te, 83817-20-3; (*i*-Pr)TeMe, 83817-21-4; (*i*-Pr)Te(*neo*-pent), 83817-22-5; (*i*-Pr)Te(*i*-Bu), 83817-23-6; (*i*-Pr)Te(*n*-Pr), 83817-24-7; (*i*-Pr)Te(*n*-Bu), 83817-25-8; (*i*-Pr)TeEt, 83817-26-9; (*i*-Pr)Te(*sec*-Bu), 83817-27-0; (*i*-Pr)<sub>2</sub>Te, 51112-72-2; (*t*-Bu)TeMe, 83817-28-1; (*t*-Bu)Te(*neo*-pent), 83817-29-2; (*t*-Bu)Te(*i*-Bu), 83817-30-5; (*t*-Bu)Te(*n*-Pr), 83831-14-5; (*t*-Bu)Te(*n*-Bu), 83817-31-6; (*t*-Bu)Te(Et), 83817-32-7; (*t*-Bu)Te(*sec*-Bu), 83817-33-8; (*t*-Bu)Te(*i*-Pr), 83817-34-9; (*t*-Bu)<sub>2</sub>Te, 83817-35-0; PhTeMe, 872-89-9; PhTe(*i*-Bu), 83817-36-1; PhTe(*n*-Pr), 55776-35-7; PhTe(*n*-Bu), 32343-98-9; PhTe(*sec*-Bu), 83817-37-2; PhTe(*i*-Pr), 32343-99-0; PhTe(*t*-Bu), 83817-38-3; PhTeEt, 55776-34-6; PhSe(*i*-Bu), 22233-92-7; PhSe(*n*-Pr), 22351-63-9; PhSe(*n*-Bu), 28622-61-9; PhSeEt, 17774-38-8; PhSe(*sec*-Bu), 42066-63-7; PhSe(*i*-Pr), 22233-89-2; PhSe(*t*-Bu), 22233-90-5; PhSeMe, 4346-64-9; <sup>77</sup>Se, 14681-72-2; <sup>125</sup>Te, 14390-73-9.

(25) W. McFarlane and R. J. Wood, *J. Chem. Soc., Dalton Trans.*, 1397 (1972).

(26) Reference 18, p 408.

## Cluster condensation reactions. 3. The synthesis and crystal and molecular structures of three hydride-rich hexaosmium clusters formed by the decarbonylation of $\text{HOs}_3(\text{CO})_9(\mu_3\text{-S})(\mu\text{-HC:NPh})$ under hydrogen

Richard D. Adams, Donald F. Foust, and Brigitte E. Segmueller

*Organometallics*, 1983, 2 (2), 308-314 • DOI: 10.1021/om00074a018 • Publication Date (Web): 01 May 2002

Downloaded from <http://pubs.acs.org> on April 24, 2009

### More About This Article

---

The permalink <http://dx.doi.org/10.1021/om00074a018> provides access to:

- Links to articles and content related to this article
- Copyright permission to reproduce figures and/or text from this article



ACS Publications  
High quality. High impact.

# Cluster Condensation Reactions. The Synthesis and Crystal and Molecular Structures of Three Hydride-Rich Hexaosmium Clusters Formed by the Decarbonylation of $\text{HOs}_3(\text{CO})_9(\mu_3\text{-S})(\mu\text{-HC=NPh})$ under Hydrogen

Richard D. Adams,\* Donald F. Foust, and Brigitte E. Segmüller

Department of Chemistry, Yale University, New Haven, Connecticut 06511

Received August 9, 1982

The thermolytic decarbonylation of  $\text{HOs}_3(\text{CO})_9(\mu_3\text{-S})(\mu\text{-HC=NPh})$ , I, under an atmosphere of hydrogen has been investigated. Three products,  $\text{H}_4\text{Os}_6(\text{CO})_{15}(\mu_4\text{-S})(\mu_3\text{-S})(\mu\text{-HC=NPh})_2$ , II,  $\text{H}_6\text{Os}_6(\text{CO})_{14}(\mu_4\text{-S})(\mu_3\text{-S})(\mu\text{-HC=NPh})_2$ , III, and  $\text{H}_4\text{Os}_6(\text{CO})_{15}(\mu_4\text{-S})(\mu_3\text{-S})(\mu\text{-HC=NPh})_2$ , IV, formed by the condensation of 2 mol of I and the addition of 1 or 2 mol of  $\text{H}_2$ , have been isolated and characterized by IR,  $^1\text{H}$  NMR, and single-crystal X-ray diffraction analyses. For II: space group  $P\bar{1}$ , No. 2,  $a = 10.762$  (4) Å,  $b = 14.850$  (5) Å,  $c = 15.843$  (9) Å,  $\alpha = 63.76$  (4)°,  $\beta = 87.35$  (4)°,  $\gamma = 82.04$  (3)°,  $V = 2249$  (2) Å<sup>3</sup>,  $Z = 2$ ,  $\rho_{\text{calcd}} = 2.78$  g/cm<sup>3</sup>. The structure was solved by a combination of Patterson and difference Fourier techniques. Full-matrix least-squares refinement on 4195 reflections yielded the final residuals  $R = 0.045$  and  $R_w = 0.052$ . The molecule consists of two open triangular units of I which are joined by a metal-sulfur donor-acceptor bond and one hydride bridged metal-metal bond. The molecule has four hydride ligands which bridge four of the five metal-metal bonds. For III: space group  $P\bar{1}$ , No. 2,  $a = 10.926$  (5) Å,  $b = 14.150$  (6) Å,  $c = 15.752$  (4) Å,  $\alpha = 72.48$  (3)°,  $\beta = 80.92$  (3)°,  $\gamma = 66.12$  (4)°,  $V = 2122$  Å<sup>3</sup>,  $Z = 2$ ,  $\rho_{\text{calcd}} = 2.88$  g/cm<sup>3</sup>. The structure was solved by a combination of Patterson and difference Fourier techniques. Full-matrix least-squares refinement on 2789 reflections yielded the final residuals  $R = 0.051$  and  $R_w = 0.049$ . The structure of III is analogous to that of II except that one carbonyl ligand has been substituted with two hydride ligands. III has six hydride ligands. One hydride ligand bridges each of the five metal-metal interactions and one is a terminal ligand. For IV: space group  $P\bar{1}$ , No. 2,  $a = 9.549$  (3) Å,  $b = 10.150$  (3) Å,  $c = 26.495$  (12) Å,  $\alpha = 89.29$  (3)°,  $\beta = 81.17$  (4)°,  $\gamma = 64.38$  (3)°,  $V = 2284$  (2) Å<sup>3</sup>,  $Z = 2$ ,  $\rho_{\text{calcd}} = 2.67$  g/cm<sup>3</sup>. This structure was solved by a combination of Patterson and difference Fourier techniques. Full-matrix least-squares refinement on 3644 reflections yielded the final residuals  $R = 0.043$  and  $R_w = 0.051$ . IV is an isomer of III. It contains six metal atoms arranged into groups of four and two. The two groups are held together by bridging sulfido ligands. The isomerization involves a repositioning of two of the hydride-bridged metal-metal bonds and a shift of one carbonyl ligand between two metal atoms. When thermolyzed in refluxing nonane solvent, IV loses all its hydride ligands and is converted into the known  $\text{Os}_6(\text{CO})_{15}(\mu_4\text{-S})_2(\mu\text{-HC=NPh})_2$ , V.

## Introduction

The syntheses of high nuclearity transition-metal cluster compounds is a subject that has received considerable attention in recent years.<sup>1-4</sup> We have been investigating the importance of heteroatoms in the syntheses of high nuclearity cluster compounds and have recently demonstrated the value of sulfido ligands in some cluster condensation reactions.<sup>5-8</sup>

The activation of hydrogen and the chemistry of hydride-containing cluster compounds is of fundamental importance to the development of cluster compounds as hydrogenation catalysts.<sup>9-12</sup> In the course of our investigations of self-condensation reactions of the cluster compound  $\text{HOs}_3(\text{CO})_9(\mu_3\text{-S})(\mu\text{-HC=NPh})$ ,<sup>5</sup> we have found

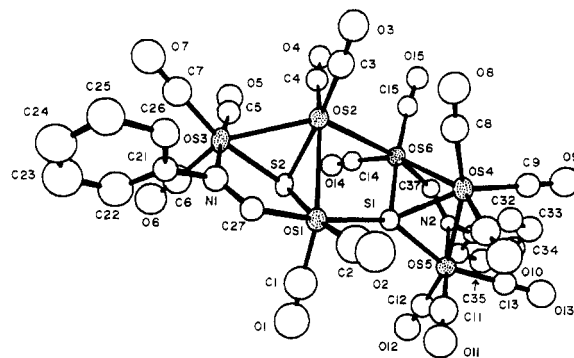


Figure 1. A perspective ORTEP diagram of  $\text{H}_4\text{Os}_6(\text{CO})_{15}(\mu_4\text{-S})(\mu_3\text{-S})(\mu\text{-HC=NPh})_2$ , II, showing 50% thermal-motion probability ellipsoids.

that hydrogen activation can occur in conjunction with condensation when the reactions are carried out under an atmosphere of hydrogen. A series of hydride-rich hexanuclear clusters which shows an intimate sequence of condensation and cluster growth processes has been obtained. A description of these reactions and the crystal and molecular structures of three of the products are reported here.

## Results

The principal product formed in 47% yield when  $\text{HOs}_3(\text{CO})_9(\mu_3\text{-S})(\mu\text{-HC=NPh})$ , I, is refluxed 1.75 h. in octane solvent under an atmosphere of  $\text{H}_2$  is  $\text{H}_4\text{Os}_6(\text{CO})_{15}(\mu_4\text{-S})(\mu_3\text{-S})(\mu\text{-HC=NPh})_2$ , II. Its formula and

- (1) Chini, P. *Gazz. Chim. Ital.* **1979**, *109*, 225.
- (2) Chini, P. *J. Organomet. Chem.* **1980**, *200*, 37.
- (3) Chini, P.; Longoni, G.; Albano, V. G. *Adv. Organomet. Chem.* **1976**, *14*, 285.
- (4) Lewis, J.; Johnson, B. F. G. *Pure Appl. Chem.* **1982**, *54*, 97.
- (5) Adams, R. D.; Dawoodi, Z.; Foust, D. F. *Organometallics* **1982**, *1*, 411.
- (6) Adams, R. D.; Horvath, I. T.; Yang, L. W. *J. Am. Chem. Soc.*, in press.
- (7) Adams, R. D.; Dawoodi, Z.; Foust, D. F.; Segmüller, B. E. *J. Am. Chem. Soc.*, in press.
- (8) Adams, R. D.; Männig, D.; Segmüller, B. E. *Organometallics*, **1983**, *2*, 149.
- (9) Whyman, R. In "Transition Metal Clusters"; Johnson, B. F. G., Ed.; Wiley: New York, 1980; Chapter 8.
- (10) Bau, R. "Transition Metal Hydrides"; American Chemical Society: Washington, DC, 1978; *Adv. Chem. Ser. No.* 167.
- (11) Humphries, A. P.; Kesz, H. D. *Prog. Inorg. Chem.* **1979**, *25*, 145.
- (12) Teller, R. G.; Bau, R. *Struc. Bonding (Berlin)* **1981**, *44*, 1.

Table I. Spectroscopic and Physical Data

compd	mp, °C	<sup>1</sup> H NMR δ	IR ν <sub>CO</sub> , cm <sup>-1</sup>
H <sub>4</sub> Os <sub>6</sub> (CO) <sub>15</sub> (μ <sub>4</sub> -S)(μ <sub>3</sub> -S)(μ-HCNPh) <sub>2</sub> , II	160 dec	10.80 (s, 1 H), 10.74 (s, 1 H), 7.3, 6.8 (m, 10 H), -14.31 (s, 1 H), -15.31 (d, 1 H, J <sub>H-H</sub> = 3 Hz), -16.68 (s, 1 H), -17.20 (d, 1 H, J <sub>H-H</sub> = 3 Hz) <sup>a</sup>	2110 m, 2085 m, 2052 vs, 2040 s, 2036 sh, 2027 w, 2007 m, 1995 s, 1993 sh, 1984 m, 1973 w, 1950 w <sup>b</sup>
H <sub>6</sub> Os <sub>6</sub> (CO) <sub>14</sub> (μ <sub>4</sub> -S)(μ <sub>3</sub> -S)(μ-HCNPh) <sub>2</sub> , III	190 dec	10.80 (s, 1 H), 10.75 (s, 1 H), 7.3, 6.8 (m, 10 H), -9.70 (d, 1 H, J <sub>H-H</sub> = 8 Hz), -12.88 (d, 1 H, J <sub>H-H</sub> = 8 Hz), -14.81 (d, 1 H, J <sub>H-H</sub> = 2 Hz), -15.41 (d, 1 H, J <sub>H-H</sub> = 3 Hz), -17.17 (s, 1 H), -18.19 (s, 1 H) <sup>a</sup>	2110 sh, 2106 s, 2094 w, 2063 sh, 2050 vs, 2045 sh, 2038 s, 2024 s, 2014 sh, 1993 w, 1984 m, 1978 sh, 1958 w <sup>b</sup>
H <sub>4</sub> Os <sub>6</sub> (CO) <sub>15</sub> (μ <sub>4</sub> -S)(μ <sub>3</sub> -S)(μ-HCNPh) <sub>2</sub> , IV	190 dec	10.75 (s, 1 H), 10.34 (s, 1 H), 7.3, 6.9 (m, 10 H), -11.65 (s, 1 H), -12.19 (s, 1 H), -15.03 (s, 1 H), -16.67 (s, 1 H) <sup>a</sup>	2104 s, 2071 m, 2048 sh, 2042 vs, 2031 m, 2023 m, 2019 sh, 2004 w, 1997 m, 1979 m, 1971 sh, 1942 w <sup>b</sup>

<sup>a</sup> CDCl<sub>3</sub>, room temperature. <sup>b</sup> Hexane.

Table II. Interatomic Distances (Å) with Esds for H<sub>4</sub>Os<sub>6</sub>(CO)<sub>15</sub>(μ<sub>4</sub>-S)(μ<sub>3</sub>-S)(μ-HC=NPh)<sub>2</sub>, II

Os(1)-Os(2)	3.011 (1)	N(1)-C(21)	1.51 (2)
Os(2)-Os(3)	2.957 (1)	C(21)-C(22)	1.40 (2)
Os(2)-Os(6)	3.166 (1)	C(21)-C(26)	1.37 (2)
Os(4)-Os(5)	2.837 (1)	C(22)-C(23)	1.38 (3)
Os(4)-Os(6)	3.019 (1)	C(23)-C(24)	1.25 (3)
Os(1)-S(1)	2.530 (4)	C(24)-C(25)	1.31 (2)
Os(1)-S(2)	2.423 (4)	C(25)-C(26)	1.41 (2)
Os(2)-S(2)	2.413 (5)	N(2)-C(31)	1.42 (2)
Os(3)-S(2)	2.416 (5)	C(31)-C(32)	1.37 (2)
Os(4)-S(1)	2.371 (4)	C(31)-C(36)	1.33 (2)
Os(5)-S(1)	2.412 (4)	C(32)-C(33)	1.44 (3)
Os(6)-S(1)	2.393 (4)	C(33)-C(34)	1.33 (3)
Os(1)-C(1)	1.85 (3)	C(34)-C(35)	1.29 (2)
Os(1)-C(2)	1.92 (2)	C(35)-C(36)	1.44 (3)
Os(1)-C(27)	2.00 (2)	C(1)-O(1)	1.15 (2)
Os(2)-C(3)	1.91 (2)	C(2)-O(2)	1.20 (2)
Os(2)-C(4)	1.91 (2)	C(3)-O(3)	1.17 (2)
Os(3)-C(5)	1.86 (2)	C(4)-O(4)	1.13 (2)
Os(3)-C(6)	1.96 (2)	C(5)-O(5)	1.12 (2)
Os(3)-C(7)	1.86 (2)	C(6)-O(6)	1.13 (2)
Os(3)-N(1)	2.15 (1)	C(7)-O(7)	1.20 (2)
Os(4)-C(8)	1.93 (2)	C(8)-O(8)	1.14 (2)
Os(4)-C(9)	1.93 (2)	C(9)-O(9)	1.11 (2)
Os(4)-C(10)	1.90 (2)	C(10)-O(10)	1.20 (2)
Os(5)-C(11)	1.87 (2)	C(11)-O(11)	1.16 (2)
Os(5)-C(12)	1.88 (2)	C(12)-O(12)	1.16 (2)
Os(5)-C(13)	1.86 (2)	C(13)-O(13)	1.17 (2)
Os(5)-N(2)	2.17 (1)	C(14)-O(14)	1.13 (2)
Os(6)-C(14)	1.90 (2)	C(15)-O(15)	1.15 (2)
Os(6)-C(15)	1.88 (2)	Os(1)···Os(3)	3.767 (1)
Os(6)-C(37)	2.07 (2)	Os(5)···Os(6)	3.765 (1)
N(1)-C(27)	1.30 (2)	Os(2)···Os(4)	4.578 (1)
N(2)-C(37)	1.29 (2)	Os(2)···C(8)	3.97 (3)

molecular structure were established by a combination of IR, <sup>1</sup>H NMR, and single-crystal X-ray diffraction analyses. IR and <sup>1</sup>H NMR spectra are listed in Table I. An ORTEP diagram of the molecular structure of II is shown in Figure 1. Bond distances and angles are listed in Tables II and III. The molecule can be visualized as a combination of two open triangular clusters of I, Os(1)-Os(2)-Os(3) and Os(4)-Os(5)-Os(6) joined by the Os(1)-S(1) and Os(2)-Os(6) bonds. There are five metal-metal interactions which are short enough to imply some degree of metal-metal bonding. These are Os(1)-Os(2) = 3.011 (1) Å, Os(2)-Os(3) = 2.957 (1) Å, Os(2)-Os(6) = 3.166 (1) Å, Os(4)-Os(5) = 2.837 (1) Å, and Os(4)-Os(6) = 3.019 (1) Å. Four of these are significantly longer than the Os-Os separation found of 2.877 (3) Å in Os<sub>3</sub>(CO)<sub>12</sub><sup>13</sup> while one, Os(4)-Os(5), is significantly shorter. The <sup>1</sup>H NMR spectrum of II indicates the presence of four bridging hydride

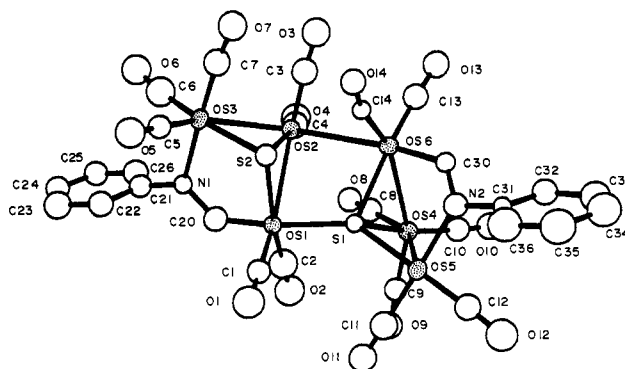


Figure 2. A perspective ORTEP diagram of H<sub>6</sub>Os<sub>6</sub>(CO)<sub>14</sub>(μ<sub>4</sub>-S)(μ<sub>3</sub>-S)(μ-HC=NPh)<sub>2</sub>, III, showing 50% thermal-motion probability ellipsoids.

ligands. Since bridging hydride ligands are known to produce significant lengthening effects on metal-metal bonds,<sup>14</sup> we conclude that there is one hydride ligand bridging each of the four elongated metal-metal bonds. There are two sulfido ligands. S(1) is a quadruply bridging, six-electron donor, serving as a triple bridge in the group Os(4)-Os(5)-Os(6) with an additional donor bond to Os(1). The latter plays a key role in linking the trinuclear groups. The Os-S(1) distances to the Os(4)-Os(5)-Os(6) group range from 2.371 to 2.412 Å and are similar to those found for triply bridging sulfido ligands in I<sup>15</sup> and several other triosmium clusters,<sup>16</sup> however, the S(1)-Os(1) donor bond at 2.530 (4) Å is significantly longer. S(2) serves as a triple bridge in the Os(1)-Os(2)-Os(3) group with Os-S distances, 2.413-2.423 Å, that are not unusual.<sup>15,16</sup> Formimidoyl ligands (HC=NPh) bridge the "open" edges Os(1)···Os(3) and Os(5)···Os(6) of the trinuclear groupings and do not show any unusual distortions.<sup>7,15</sup> There are 15 linear terminal carbonyl ligands distributed as shown in Figure 1. C(2)-O(2) is slightly bent, Os(1)-C(2)-O(2) = 163 (2)°. The reason for this is not apparent. The shortest intermolecular contact is between carbonyl oxygen atoms, O(4)···O(15) = 2.85 Å.

A minor product isolated (12% yield) from this reaction has been identified as H<sub>6</sub>Os<sub>6</sub>(CO)<sub>14</sub>(μ<sub>4</sub>-S)(μ<sub>3</sub>-S)(μ-HC=

(14) Churchill, M. R. In "Transition Metal Hydrides"; Bau, R., Ed.; American Chemical Society: Washington DC, 1978; *Adv. Chem. Ser. No. 167*, p 36.

(15) Adams, R. D.; Dawoodi, Z. *J. Am. Chem. Soc.* 1981, 103, 6510.  
 (16) (a) Adams, R. D.; Golembeski, N. M.; Selegue, J. P. *J. Am. Chem. Soc.* 1981, 103, 546. (b) Johnson, B. F. G.; Lewis, J.; Pippard, D.; Raithby, P. R.; Sheldrick, G. M.; Rouse, K. D. *J. Chem. Soc., Dalton Trans.* 1979, 616. (c) Johnson, B. F. G.; Lewis, J.; Pippard, D.; Raithby, P. R. *Acta Crystallogr., Sect. B* 1978, B34, 3767.



Table III. Selected Interatomic Angles (deg) with Esds for  $H_4Os_6(CO)_{15}(\mu_4-S)(\mu_3-S)(\mu-HC=NPh)_2$ , II

Os(1)-Os(2)-Os(3)	78.26 (3)	Os(4)-Os(5)-S(1)	53.0 (1)	C(22)-C(23)-C(24)	122 (2)
Os(1)-Os(2)-Os(6)	83.71 (3)	Os(4)-Os(5)-N(2)	87.8 (3)	C(23)-C(24)-C(25)	123 (2)
Os(3)-Os(2)-Os(6)	131.94 (3)	Os(4)-Os(5)-C(11)	92.0 (6)	C(24)-C(25)-C(26)	120 (2)
Os(5)-Os(4)-Os(6)	79.94 (3)	Os(4)-Os(5)-C(12)	165.0 (6)	C(25)-C(26)-C(21)	117 (2)
Os(2)-Os(6)-Os(4)	95.45 (3)	Os(4)-Os(5)-C(13)	99.2 (6)	Os(6)-C(37)-N(2)	124 (1)
Os(2)-Os(1)-S(1)	81.1 (1)	Os(2)-Os(6)-S(1)	79.9 (1)	Os(5)-N(2)-C(37)	127 (1)
Os(2)-Os(1)-S(2)	51.3 (1)	Os(2)-Os(6)-C(37)	167.2 (4)	Os(5)-N(2)-C(31)	117.5 (9)
Os(2)-Os(1)-C(27)	91.5 (4)	Os(2)-Os(6)-C(14)	81.1 (5)	C(37)-N(2)-C(31)	116 (1)
Os(2)-Os(1)-C(1)	150.4 (7)	Os(2)-Os(6)-C(15)	96.8 (5)	N(2)-C(31)-C(32)	117 (2)
Os(2)-Os(1)-C(2)	130.0 (7)	Os(4)-Os(6)-S(1)	50.4 (1)	N(2)-C(31)-C(36)	122 (2)
Os(1)-Os(2)-S(2)	51.7 (1)	Os(4)-Os(6)-C(37)	87.9 (4)	C(32)-C(31)-C(36)	121 (2)
Os(1)-Os(2)-C(3)	116.3 (5)	Os(4)-Os(6)-C(14)	155.1 (5)	C(31)-C(32)-C(33)	115 (2)
Os(1)-Os(2)-C(4)	152.8 (6)	Os(4)-Os(6)-C(15)	118.7 (5)	C(32)-C(33)-C(34)	124 (2)
Os(3)-Os(2)-S(2)	52.3 (1)	Os(1)-S(1)-Os(4)	119.0 (2)	C(33)-C(34)-C(35)	119 (2)
Os(3)-Os(2)-C(3)	117.9 (6)	Os(1)-S(1)-Os(5)	142.7 (2)	C(34)-C(35)-C(36)	121 (2)
Os(3)-Os(2)-C(4)	94.4 (5)	Os(1)-S(1)-Os(6)	113.7 (2)	C(35)-C(36)-C(31)	120 (2)
Os(6)-Os(2)-S(2)	81.7 (1)	Os(4)-S(1)-Os(5)	72.8 (1)	Os(1)-C(1)-O(1)	179 (2)
Os(6)-Os(2)-C(3)	110.0 (6)	Os(4)-S(1)-Os(6)	78.7 (1)	Os(1)-C(2)-O(2)	163 (2)
Os(6)-Os(2)-C(4)	82.0 (5)	Os(5)-S(1)-Os(6)	103.2 (2)	Os(2)-C(3)-O(3)	177 (2)
Os(2)-Os(3)-S(2)	52.2 (1)	Os(1)-S(2)-Os(2)	77.0 (1)	Os(2)-C(4)-O(4)	173 (2)
Os(2)-Os(3)-N(1)	90.3 (4)	Os(1)-S(2)-Os(3)	102.2 (2)	Os(3)-C(5)-O(5)	174 (2)
Os(2)-Os(3)-C(5)	84.9 (5)	Os(2)-S(2)-Os(3)	75.5 (1)	Os(3)-C(6)-O(6)	175 (2)
Os(2)-Os(3)-C(6)	149.1 (7)	S(1)-Os(1)-S(2)	86.3 (1)	Os(3)-C(7)-O(7)	177 (2)
Os(2)-Os(3)-C(7)	114.0 (6)	Os(1)-C(27)-N(1)	129 (1)	Os(4)-C(8)-O(8)	174 (2)
Os(5)-Os(4)-S(1)	54.3 (1)	Os(3)-N(1)-C(27)	124 (1)	Os(4)-C(9)-O(9)	178 (2)
Os(5)-Os(4)-C(8)	163.2 (5)	Os(3)-N(1)-C(21)	116.7 (9)	Os(4)-C(10)-O(10)	172 (2)
Os(5)-Os(4)-C(9)	91.4 (5)	C(27)-N(1)-C(21)	119 (1)	Os(5)-C(11)-O(11)	178 (2)
Os(5)-Os(4)-C(10)	90.0 (6)	N(1)-C(21)-C(22)	122 (2)	Os(5)-C(12)-O(12)	177 (2)
Os(6)-Os(4)-S(1)	51.0 (1)	N(1)-C(21)-C(26)	118 (2)	Os(5)-C(13)-O(13)	179 (1)
Os(6)-Os(4)-C(8)	91.1 (2)	C(22)-C(21)-C(26)	120 (2)	Os(6)-C(14)-O(14)	171 (2)
Os(6)-Os(4)-C(9)	114.4 (5)	C(21)-C(22)-C(23)	118 (2)	Os(6)-C(15)-O(15)	175 (1)
Os(6)-Os(4)-C(10)	153.2 (6)				

NPh)<sub>2</sub>, III, on the basis of IR, <sup>1</sup>H NMR, and a single-crystal X-ray diffraction analysis. An ORTEP diagram of the molecular structure of III is shown in Figure 2. Lists of bond distances and angles are given in Tables IV and V. The molecule is structurally very similar to II and is also readily visualized as a combination of two open trinuclear clusters joined by a metal-sulfur donor bond, Os(1)-S(1), and a metal-metal bond, Os(2)-Os(6). The <sup>1</sup>H NMR spectrum of III shows six hydride resonances, cf. Table I. Five of these lie in the region δ -12 to -19 indicative of bridging ligands while one at lower field (δ -9.70) could be indicative of a terminal hydride ligand. In support of this, the structural analysis shows that the five principal metal-metal interactions Os(1)-Os(2) = 2.996 (2), Os(2)-Os(3) = 2.969 (2), Os(2)-Os(6) = 3.159 (2), Os(4)-Os(5) = 3.032 (2), and Os(4)-Os(6) = 3.039 (2) Å are all significantly longer than the Os-Os distances in Os<sub>3</sub>(CO)<sub>12</sub>, 2.877 (3) Å.<sup>13</sup> Thus, it is believed that each of these bonds contains one bridging hydride ligand.<sup>14</sup> The Os(4)-Os(5) separation is 0.196 Å longer than the corresponding non-hydride-bridged distance in II. The coordination of Os(5) in III differs from Os(5) in II by the conspicuous absence of one carbonyl ligand. It is believed that this "empty" site is occupied by a terminal hydride ligand. Like II, III contains one quadruply bridging sulfido ligand S(1) and one triply bridging sulfido ligand S(2). The S(1)-Os(1) and S(1)-Os(4) bonds in III at 2.471 (7) and 2.468 (7) Å, respectively, are 0.06 Å shorter and 0.10 Å longer than the corresponding distances in II. As in II, there are formimidoyl ligands which bridge the open edges of each trinuclear group. Overall, there are 14 terminal carbonyl ligands distributed as shown in Figure 2. All of these are linear except C(14)-O(14) which could be semibringing to Os(2), Os(2)···C(14) = 3.32 (4) Å, Os(2)-Os(6)-C(14) = 77.5 (8)°, and Os(6)-C(14)-O(14) = 166 (2)°. The shortest intermolecular contact is between carbonyl oxygen atoms, O(1)···O(1) = 2.86 (4) Å.

The third product obtained in 21% yield is an isomer of II, H<sub>4</sub>Os<sub>6</sub>(CO)<sub>15</sub>(μ<sub>4</sub>-S)(μ<sub>3</sub>-S)(μ-HC=NPh)<sub>2</sub>, IV. An OR-

Table IV. Interatomic Distances (Å) with Esds for H<sub>6</sub>Os<sub>6</sub>(CO)<sub>14</sub>(μ<sub>4</sub>-S)(μ<sub>3</sub>-S)(μ-HC=NPh)<sub>2</sub>, III

Os(1)-Os(2)	2.996 (2)	Os(6)-C(13)	1.73 (3)
Os(2)-Os(3)	2.969 (2)	Os(6)-C(14)	1.90 (3)
Os(2)-Os(6)	3.159 (2)	N(1)-C(20)	1.42 (3)
Os(4)-Os(5)	3.033 (2)	N(1)-C(21)	1.43 (3)
Os(4)-Os(6)	3.039 (2)	C(21)-C(22)	1.41 (4)
Os(1)···Os(3)	3.761 (2)	C(21)-C(26)	1.39 (4)
Os(1)···Os(4)	4.249 (2)	C(22)-C(23)	1.43 (4)
Os(1)···Os(6)	4.111 (2)	C(23)-C(24)	1.38 (4)
Os(1)-S(1)	2.471 (7)	C(24)-C(25)	1.43 (4)
Os(1)-S(2)	2.417 (7)	C(25)-C(26)	1.40 (4)
Os(2)-S(2)	2.410 (8)	N(2)-C(30)	1.31 (3)
Os(3)-S(2)	2.389 (8)	N(2)-C(31)	1.45 (3)
Os(4)-S(1)	2.468 (7)	C(31)-C(32)	1.39 (4)
Os(5)-S(1)	2.406 (8)	C(31)-C(36)	1.38 (4)
Os(6)-S(1)	2.450 (7)	C(32)-C(33)	1.47 (4)
Os(1)-C(20)	1.77 (3)	C(33)-C(34)	1.30 (4)
Os(1)-C(1)	1.84 (3)	C(34)-C(35)	1.44 (4)
Os(1)-C(2)	1.89 (4)	C(35)-C(36)	1.50 (5)
Os(2)-C(3)	1.78 (3)	C(1)-O(1)	1.20 (3)
Os(2)-C(4)	1.77 (4)	C(2)-O(2)	1.15 (4)
Os(2)···C(14)	3.32 (4)	C(3)-O(3)	1.19 (3)
Os(3)-N(1)	2.13 (2)	C(4)-O(4)	1.26 (4)
Os(3)-C(5)	1.80 (3)	C(5)-O(5)	1.19 (3)
Os(3)-C(6)	1.75 (4)	C(6)-O(6)	1.23 (4)
Os(3)-C(7)	1.83 (3)	C(7)-O(7)	1.24 (3)
Os(4)-C(8)	1.99 (4)	C(8)-O(8)	1.13 (4)
Os(4)-C(9)	1.86 (3)	C(9)-O(9)	1.20 (3)
Os(4)-C(10)	1.86 (3)	C(10)-O(10)	1.20 (3)
Os(5)-N(2)	2.13 (2)	C(11)-O(11)	1.14 (3)
Os(5)-C(11)	1.88 (3)	C(12)-O(12)	1.23 (3)
Os(5)-C(12)	1.79 (3)	C(13)-O(13)	1.26 (3)
Os(6)-C(30)	2.08 (3)	C(14)-O(14)	1.17 (3)

TEP diagram of IV is shown in Figure 3. Interatomic distances and angles are listed in Tables VI and VII. The six metal atoms in IV are divided into groups of four and two, and the two groups are joined by the bridging sulfido ligands. The group of four can be visualized as an open cluster of three, Os(4)-Os(5)-Os(6), with the fourth metal atom Os(3) bridging the Os(5)-Os(6) edge. The <sup>1</sup>H NMR spectrum of IV (Table I) shows resonances which can be

Table V. Selected Interatomic Angles (deg) with Esds for  $H_4Os_6(CO)_{15}(\mu_4-S)(\mu_3-S)(\mu-HC=NPh)_2$ , III

Os(1)-Os(2)-Os(3)	78.17 (4)	Os(6)-Os(4)-C(10)	115.8 (9)	C(22)-C(23)-C(24)	115 (3)
Os(1)-Os(2)-Os(6)	83.76 (4)	Os(4)-Os(5)-S(1)	52.4 (2)	C(23)-C(24)-C(25)	121 (3)
Os(3)-Os(2)-Os(6)	131.04 (6)	Os(4)-Os(5)-N(2)	88.1 (7)	C(24)-C(25)-C(26)	121 (3)
Os(5)-Os(4)-Os(6)	77.78 (4)	Os(4)-Os(5)-C(11)	95.0 (10)	C(25)-C(26)-C(21)	121 (3)
Os(2)-Os(6)-Os(4)	98.80 (5)	Os(4)-Os(5)-C(12)	123.7 (10)	Os(6)-C(30)-N(2)	126 (2)
Os(2)-Os(1)-S(1)	82.8 (2)	Os(2)-Os(6)-S(1)	79.7 (2)	Os(5)-N(2)-C(30)	127 (2)
Os(2)-Os(1)-S(2)	51.5 (2)	Os(2)-Os(6)-C(30)	160.7 (7)	Os(5)-N(2)-C(31)	121 (2)
Os(2)-Os(1)-C(20)	91.9 (10)	Os(2)-Os(6)-C(13)	99.8 (10)	C(30)-N(2)-C(31)	112 (2)
Os(2)-Os(1)-C(1)	152.4 (8)	Os(2)-Os(6)-C(14)	77.5 (8)	N(2)-C(31)-C(32)	119 (3)
Os(2)-Os(1)-C(2)	112.5 (11)	Os(4)-Os(6)-S(1)	52.1 (2)	N(2)-C(31)-C(36)	120 (3)
Os(1)-Os(2)-S(2)	51.7 (2)	Os(4)-Os(6)-C(30)	88.3 (7)	C(32)-C(31)-C(36)	121 (3)
Os(1)-Os(2)-C(3)	151.6 (11)	Os(4)-Os(6)-C(13)	116.6 (9)	C(31)-C(32)-C(33)	118 (3)
Os(1)-Os(2)-C(4)	113.8 (10)	Os(4)-Os(6)-C(14)	153.5 (8)	C(32)-C(33)-C(34)	124 (3)
Os(3)-Os(2)-S(2)	51.5 (2)	Os(1)-S(1)-Os(4)	118.7 (3)	C(33)-C(34)-C(35)	118 (4)
Os(3)-Os(2)-C(3)	92.1 (10)	Os(1)-S(1)-Os(5)	142.4 (3)	C(34)-C(35)-C(36)	119 (3)
Os(3)-Os(2)-C(4)	118.6 (11)	Os(1)-S(1)-Os(6)	113.3 (3)	C(35)-C(36)-C(31)	119 (3)
Os(6)-Os(2)-S(2)	81.8 (2)	Os(4)-S(1)-Os(5)	76.9 (2)	Os(1)-C(1)-O(1)	177 (2)
Os(6)-Os(2)-C(3)	82.9 (11)	Os(4)-S(1)-Os(6)	76.3 (2)	Os(1)-C(2)-O(2)	171 (3)
Os(6)-Os(2)-C(4)	110.4 (11)	Os(5)-S(1)-Os(6)	103.4 (3)	Os(2)-C(3)-O(3)	173 (3)
Os(2)-Os(3)-S(2)	52.1 (2)	Os(1)-S(2)-Os(2)	76.7 (2)	Os(2)-C(4)-O(4)	174 (3)
Os(2)-Os(3)-N(1)	90.1 (6)	Os(1)-S(2)-Os(3)	103.0 (3)	Os(3)-C(5)-O(5)	178 (3)
Os(2)-Os(3)-C(5)	147.2 (9)	Os(2)-S(2)-Os(3)	76.4 (3)	Os(3)-C(6)-O(6)	174 (3)
Os(2)-Os(3)-C(6)	117.1 (12)	S(1)-Os(1)-S(2)	84.6 (3)	Os(3)-C(7)-O(7)	172 (3)
Os(2)-Os(3)-C(7)	88.6 (10)	Os(1)-C(20)-N(1)	138 (2)	Os(4)-C(8)-O(8)	178 (3)
Os(5)-Os(4)-S(1)	50.6 (2)	Os(3)-N(1)-C(20)	116 (2)	Os(4)-C(9)-O(9)	176 (3)
Os(5)-Os(4)-C(8)	147.5 (9)	Os(3)-N(1)-C(21)	115 (2)	Os(4)-C(10)-O(10)	175 (3)
Os(5)-Os(4)-C(9)	84.5 (9)	C(20)-N(1)-C(21)	129 (2)	Os(5)-C(11)-O(11)	177 (3)
Os(5)-Os(4)-C(10)	117.7 (10)	N(1)-C(21)-C(22)	124 (3)	Os(5)-C(12)-O(12)	176 (3)
Os(6)-Os(4)-S(1)	51.6 (2)	N(1)-C(21)-C(26)	121 (3)	Os(6)-C(13)-O(13)	174 (3)
Os(6)-Os(4)-C(8)	90.7 (8)	C(22)-C(21)-C(26)	115 (3)	Os(6)-C(14)-O(14)	166 (2)
Os(6)-Os(4)-C(9)	150.0 (9)	C(21)-C(22)-C(23)	127 (3)		

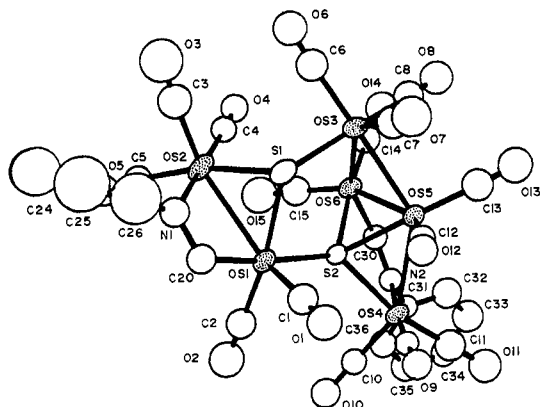


Figure 3. A perspective diagram of  $H_4Os_6(CO)_{15}(\mu_4-S)(\mu_3-S)(\mu-HC=NPh)_2$ , IV, showing 50% thermal-motion probability ellipsoids.

assigned to four bridging hydride ligands. Accordingly, it is believed that four of the five significant metal-metal interactions  $Os(1)-Os(2) = 2.950(1)$ ,  $Os(3)-Os(6) = 3.090(1)$ ,  $Os(4)-Os(5) = 2.972(1)$ , and  $Os(5)-Os(6) = 2.894(1)$  Å which are longer than the  $Os-Os$  distances in  $Os_3(CO)_{12}$ ,  $2.877(3)$  Å,<sup>13</sup> probably contain the hydride bridges, while the one short interaction  $Os(3)-Os(5) = 2.817(1)$  Å probably does not.<sup>14</sup> There are two sulfido ligands. S(2) is a quadruple bridge and has a geometry and bonding similar to the quadruple bridges S(1) in both II and III. It serves to link the two atom group to the four atom group through the  $Os(1)-S(2)$  bond. S(1) is a triple bridge bonded to both osmium atoms of the two atom group and one from the four atom group. Thus, it also serves as a bridge between the two clusters. A similarly coordinated sulfido ligand was observed in the compound  $HOs_3(CO)_8(PMe_2Ph)(\mu_3-S)(\mu_3-\eta^2-SCH_2)Cl$ .<sup>17</sup> There are two bridging formimidoyl ligands. One bridges the two atom

Table VI. Interatomic Distances (Å) with Esds for  $H_4Os_6(CO)_{15}(\mu_4-S)(\mu_3-S)(\mu-HC=NPh)_2$ , IV

Os(1)-Os(2)	2.950 (1)	Os(1)-C(2)	1.88 (2)
Os(3)-Os(5)	2.817 (1)	Os(2)-C(3)	1.95 (2)
Os(3)-Os(6)	3.090 (1)	Os(2)-C(4)	1.98 (2)
Os(4)-Os(5)	2.972 (1)	Os(2)-C(5)	1.94 (2)
Os(5)-Os(6)	2.894 (1)	Os(3)-C(6)	1.99 (2)
Os(1)-S(1)	2.402 (5)	Os(3)-C(7)	1.94 (2)
Os(1)-S(2)	2.489 (4)	Os(3)-C(8)	1.92 (2)
Os(2)-S(1)	2.435 (5)	Os(4)-C(9)	1.83 (2)
Os(3)-S(1)	2.520 (5)	Os(4)-C(10)	1.84 (2)
Os(4)-S(2)	2.412 (4)	Os(4)-C(11)	1.81 (2)
Os(5)-S(2)	2.381 (5)	Os(5)-C(12)	1.94 (2)
Os(6)-S(2)	2.427 (4)	Os(5)-C(13)	1.89 (2)
Os(1)-C(20)	2.04 (2)	Os(6)-C(14)	1.86 (2)
Os(1)-N(1)	2.13 (1)	Os(6)-C(15)	1.75 (2)
Os(4)-N(2)	2.15 (1)	C(1)-O(1)	1.13 (2)
Os(6)-C(30)	2.05 (2)	C(2)-O(2)	1.15 (2)
N(1)-C(20)	1.34 (2)	C(3)-O(3)	1.13 (2)
N(1)-C(21)	1.50 (2)	C(4)-O(4)	1.11 (2)
N(2)-C(30)	1.30 (2)	C(5)-O(5)	1.11 (2)
N(2)-C(31)	1.48 (2)	C(6)-O(6)	1.11 (2)
C(21)-C(22)	1.35 (3)	C(7)-O(7)	1.09 (2)
C(21)-C(26)	1.48 (3)	C(8)-O(8)	1.14 (2)
C(22)-C(23)	1.42 (3)	C(9)-O(9)	1.20 (2)
C(23)-C(24)	1.25 (4)	C(10)-O(10)	1.18 (2)
C(24)-C(25)	1.21 (4)	C(11)-O(11)	1.20 (2)
C(25)-C(26)	1.48 (4)	C(12)-O(12)	1.14 (2)
C(31)-C(32)	1.36 (2)	C(13)-O(13)	1.12 (2)
C(31)-C(36)	1.34 (2)	C(14)-O(14)	1.19 (2)
C(32)-C(33)	1.40 (2)	C(15)-O(15)	1.22 (2)
C(33)-C(34)	1.34 (2)	Os(1)···Os(3)	4.219 (1)
C(34)-C(35)	1.40 (3)	Os(2)···Os(3)	4.186 (1)
C(35)-C(36)	1.47 (3)	Os(4)···Os(6)	3.780 (1)
Os(1)-C(1)	1.83 (2)		

group,  $Os(1)-Os(2)$ , and the other bridges the "open" edge,  $Os(4)···Os(6)$ , in the four atom group. There are 15 linear terminal carbonyl ligands arranged as shown in Figure 3. The shortest intermolecular contact was between carbonyl oxygen atoms,  $O(1)···O(5) = 2.98(2)$  Å.

The formation of II is reversible. When heated to reflux in octane solvent under an atmosphere of CO, I is reformed in 78% yield. It is believed that II is a precursor both to

(17) Adams, R. D.; Golembeski, N. M. Selegue, J. P. *Organometallics* 1982, 1, 240.

Table VII. Selected Interatomic Angles (deg) with Esds for  $H_4Os_6(CO)_{15}(\mu_4-S)(\mu_3-S)(\mu-HCNPh)_2, IV$ 

Os(4)-Os(5)-Os(6)	80.24 (3)	Os(4)-Os(5)-C(12)	98.7 (5)	N(1)-C(21)-C(26)	117 (2)
Os(3)-Os(5)-Os(4)	136.46 (4)	Os(4)-Os(5)-C(13)	123.0 (6)	C(22)-C(21)-C(26)	118 (2)
Os(5)-Os(3)-Os(6)	58.45 (2)	Os(6)-Os(5)-S(2)	53.7 (1)	C(21)-C(22)-C(23)	119 (2)
Os(3)-Os(5)-Os(6)	65.49 (3)	Os(6)-Os(5)-C(12)	147.8 (5)	C(22)-C(23)-C(24)	123 (3)
Os(3)-Os(6)-Os(5)	56.06 (2)	Os(6)-Os(5)-C(13)	118.8 (6)	C(23)-C(24)-C(25)	122 (3)
Os(2)-Os(1)-S(1)	52.9 (1)	Os(3)-Os(6)-S(2)	78.6 (1)	C(24)-C(25)-C(26)	124 (4)
Os(2)-Os(1)-S(2)	107.6 (1)	Os(3)-Os(6)-C(30)	151.8 (5)	C(25)-C(26)-C(21)	113 (3)
Os(2)-Os(1)-C(20)	68.3 (5)	Os(3)-Os(6)-C(14)	98.1 (6)	N(2)-C(31)-C(32)	121 (2)
Os(2)-Os(1)-C(1)	143.6 (6)	Os(3)-Os(6)-C(15)	117.6 (6)	N(2)-C(31)-C(36)	113 (2)
Os(2)-Os(1)-C(12)	118.2 (6)	Os(5)-Os(6)-S(2)	52.3 (1)	C(32)-C(31)-C(36)	125 (2)
Os(1)-Os(2)-S(1)	51.9 (1)	Os(5)-Os(6)-C(30)	96.3 (5)	C(31)-C(32)-C(33)	113 (2)
Os(1)-Os(2)-N(1)	65.9 (4)	Os(5)-Os(6)-C(14)	121.5 (7)	C(32)-C(33)-C(34)	126 (2)
Os(1)-Os(2)-C(3)	144.4 (7)	Os(5)-Os(6)-C(15)	149.4 (6)	C(33)-C(34)-C(35)	122 (2)
Os(1)-Os(2)-C(4)	114.0 (5)	Os(1)-S(1)-Os(2)	75.2 (1)	C(34)-C(35)-C(36)	112 (2)
Os(1)-Os(2)-C(5)	116.3 (5)	Os(1)-S(1)-Os(3)	118.0 (2)	C(35)-C(36)-C(31)	122 (2)
Os(5)-Os(3)-S(1)	95.4 (1)	Os(2)-S(1)-Os(3)	115.3 (2)	Os(1)-C(1)-O(1)	174 (2)
Os(5)-Os(3)-C(6)	176.7 (6)	Os(1)-S(2)-Os(4)	130.9 (2)	Os(1)-C(2)-O(2)	177 (2)
Os(5)-Os(3)-C(7)	83.9 (6)	Os(1)-S(2)-Os(5)	119.5 (2)	Os(2)-C(3)-O(3)	176 (2)
Os(5)-Os(3)-C(8)	83.3 (6)	Os(1)-S(2)-Os(6)	125.9 (2)	Os(2)-C(4)-O(4)	178 (2)
Os(6)-Os(3)-S(1)	98.9 (1)	Os(4)-S(2)-Os(5)	76.7 (1)	Os(2)-C(5)-O(5)	174 (2)
Os(6)-Os(3)-C(6)	118.2 (6)	Os(4)-S(2)-Os(6)	102.8 (1)	Os(3)-C(6)-O(6)	176 (2)
Os(6)-Os(3)-C(7)	142.2 (6)	Os(5)-S(2)-Os(6)	74.0 (1)	Os(3)-C(7)-O(7)	173 (2)
Os(6)-Os(3)-C(8)	81.5 (6)	Os(1)-C(20)-N(1)	113 (1)	Os(3)-C(8)-O(8)	175 (2)
Os(5)-Os(4)-S(2)	51.2 (1)	Os(2)-N(1)-C(20)	112 (1)	Os(4)-C(9)-O(9)	175 (1)
Os(5)-Os(4)-N(2)	92.7 (4)	Os(2)-N(1)-C(21)	126 (1)	Os(4)-C(10)-O(10)	171 (2)
Os(5)-Os(4)-C(9)	84.4 (5)	C(20)-N(1)-C(21)	122 (1)	Os(4)-C(11)-O(11)	179 (2)
Os(5)-Os(4)-C(10)	147.8 (5)	Os(4)-N(2)-C(30)	127 (1)	Os(5)-C(12)-O(12)	173 (2)
Os(5)-Os(4)-C(11)	116.8 (7)	Os(4)-N(2)-C(31)	117 (1)	Os(5)-C(13)-O(13)	178 (2)
Os(3)-Os(5)-S(2)	85.20 (9)	Os(6)-C(30)-N(2)	126 (1)	Os(6)-C(14)-O(14)	169 (2)
Os(3)-Os(5)-C(12)	96.9 (5)	C(30)-N(2)-C(31)	116 (1)	Os(6)-C(15)-O(15)	177 (2)
Os(3)-Os(5)-C(13)	97.6 (6)	N(1)-C(21)-C(22)	125 (2)	Os(6)-C(15)-O(15)	177 (2)
Os(4)-Os(5)-S(2)	52.14 (9)				

III and IV. In support of this, it was found that octane solutions of II refluxed under a hydrogen atmosphere yielded significant amounts of III (17% yield) and IV (13% yield). By a similar treatment under an inert atmosphere, the yield of the isomer IV was greatly enhanced (58% yield).

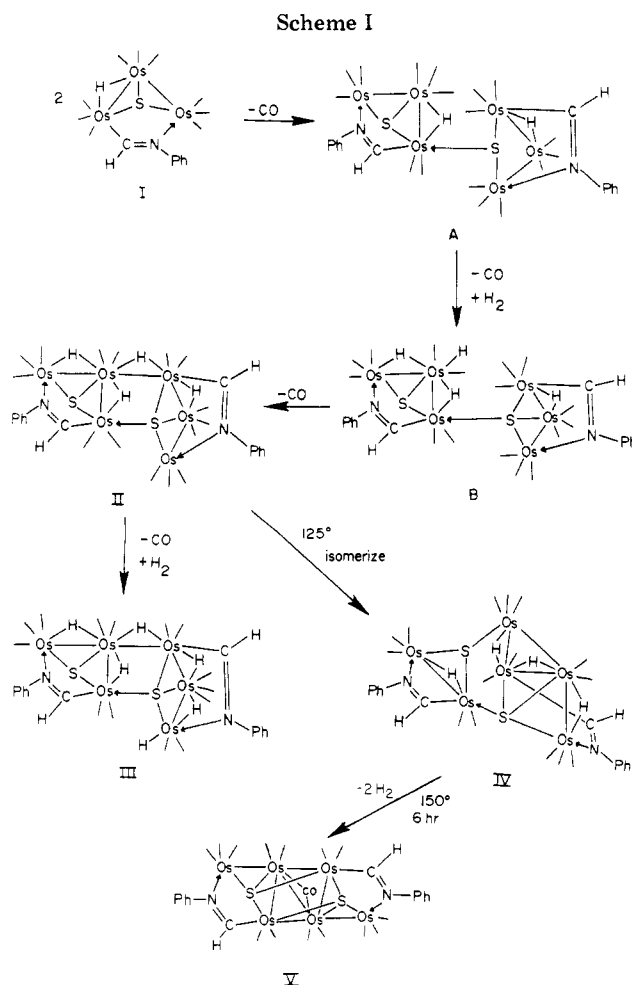
When thermolyzed in refluxing nonane, IV was converted to  $Os_6(CO)_{15}(\mu_4-S)_2(\mu-HC=NPh)_2, V$ , via the elimination of all the hydride ligands. V has been characterized previously.<sup>7</sup>

### Discussion

As reported previously, the thermal decarbonylation of I in refluxing octane under an inert atmosphere yields a series of disulfidohexaosmium carbonyl products.<sup>5,7</sup> These compounds consist of two clusters of I which are joined initially by a sulfido ligand and then by the formation of metal-metal bonds.

A cluster condensation reaction also occurs upon decarbonylation of I at octane reflux under a hydrogen atmosphere. However, the reaction is accompanied by the addition of 1 and 2 mol of hydrogen, yielding II and III, respectively, and IV, an isomer of II.

A variety of mechanisms for the formation of these compounds can be proposed. One we consider very attractive is shown in Scheme I. CO is lost from the osmium atom in I which is bonded to the carbon atom of the formimidoyl ligand. The vacant site is then filled by formation of a donor-acceptor bond to a second mole of I by utilizing the lone pair of electrons of the sulfido ligand. This would yield the intermediate A. We have proposed a similar process in the cyclotrimerization of  $[(\mu-H)(\mu_4-S)Ru_3(CO)_8]_3$ .<sup>8</sup> Loss of another mole of CO followed by an  $H_2$  addition could lead to an intermediate like B containing a terminal hydride ligand on the central osmium atom of the first trinuclear group. Finally, loss of a CO from the osmium atom bonded to the carbon atom of the formimidoyl ligand in the second trinuclear group could



be followed by an Os-H addition which could lead to the hydride-bridged metal-metal bond that links the two trinuclear groups.

Table VIII. Crystallographic Data for X-ray Diffraction Studies

	II	III	IV
(A) Crystal Data			
formula	Os <sub>6</sub> S <sub>2</sub> O <sub>15</sub> N <sub>2</sub> C <sub>29</sub> H <sub>32</sub> ·0.5CH <sub>2</sub> Cl <sub>2</sub>	Os <sub>6</sub> S <sub>2</sub> O <sub>15</sub> N <sub>2</sub> C <sub>29</sub> H <sub>18</sub>	Os <sub>6</sub> S <sub>2</sub> O <sub>15</sub> N <sub>2</sub> C <sub>29</sub> H <sub>16</sub>
temp, ± 5 °C	25	23	26
space group	$P\bar{1}$ , No. 2	$P\bar{1}$ , No. 2	$P\bar{1}$ , No. 2
a, Å	10.762 (4)	10.926 (5)	9.549 (3)
b, Å	14.850 (5)	14.150 (6)	10.150 (3)
c, Å	15.843 (9)	15.752 (4)	26.495 (12)
α, deg	63.76 (4)	72.48 (3)	89.29 (3)
β, deg	87.35 (4)	80.92 (3)	81.17 (4)
γ, deg	82.04 (3)	66.12 (4)	64.38 (3)
V, Å <sup>3</sup>	2249 (2)	2122 (1)	2284 (2)
M <sub>r</sub>	1880.25	1839.8	1837.8
Z	2	2	2
ρ <sub>calcd</sub> , g/cm <sup>3</sup>	2.78	2.88	2.67
(B) Measurement of Intensity Data			
radiation	Mo Kα (0.710 73 Å)	Mo Kα (0.710 73 Å)	Mo Kα (0.710 73 Å)
monochromator	graphite	graphite	graphite
detector aperture, mm			
horizontal (A + B tan θ)			
A	3.0	3.0	3.0
B	1.0	1.0	1.0
vertical	4.0	4.0	4.0
cryst faces	011, 0 $\bar{1}\bar{1}$ , 110, $\bar{1}\bar{1}0$	0 $\bar{1}\bar{1}$ , 011, $\bar{1}\bar{1}0$ , 110	100, $\bar{1}00$ , 00 $\bar{1}$
	$\bar{1}\bar{1}0$ , 010, 0 $\bar{1}0$	$\bar{1}\bar{1}0$ , 011	001, 120, $\bar{1}\bar{2}0$
cryst size	0.29 × 0.21 × 0.33	0.19 × 0.15 × 0.22	0.042 × 0.32 × 0.17
crystal orientatn direction;	normal to $\bar{1}\bar{1}\bar{1}$ ; 7.5°	normal to $\bar{1}\bar{1}\bar{2}$ ; 7.2°	normal to $\bar{1}\bar{2}0$ ; 13.6°
deg from φ axis			
reflections measd	<i>h</i> , ± <i>k</i> , ± <i>l</i>	<i>h</i> , ± <i>k</i> , ± <i>l</i>	<i>h</i> , ± <i>k</i> , ± <i>l</i>
max 2θ, deg	50	45	45
scan type			
ω scan width	moving crystal-	moving crystal-	moving crystal-
	stationary counter	stationary counter	stationary counter
A + 0.347 tan θ	0.95	1.50	1.00
bkgd			
ω scan rate (variable)	1/4 additional scan at	1/4 additional scan at	1/4 additional scan at
	each end of scan	each end of scan	each end of scan
max/min, deg	10.0	10.0	10.0
min/min, deg	1.7	2.0	1.7
no. of reflctns measd	7777	5473	5867
data used (F <sup>2</sup> ≥ 3.0σ(F) <sup>2</sup> )	4195	2789	3644
(C) Treatment of Data			
absorption corrections			
coeff, cm <sup>-1</sup>	171.2	180.8	178.3
grid	10 × 8 × 12	10 × 8 × 12	4 × 24 × 10
transmission coeff			
max	0.2963	0.419	0.5195
min	0.0881	0.186	0.0696
decay correction			
max	1.072		1.025
min	0.994		0.966
P factor	0.005	0.010	0.010
final residuals R	0.045	0.051	0.043
R <sub>w</sub>	0.052	0.049	0.051
esd of unit weight	2.989	1.96	2.86
largest shift/error value	0.21	0.30	0.21
on final cycle			

III is most likely formed by loss of CO from and addition of H<sub>2</sub> to osmium Os(5) in II.

The mechanism of the isomerization of II to IV is difficult to predict. Overall, the transformation involves a cleavage of the Os(1)–Os(2) and Os(2)–Os(3) bonds in II, a formation of bonds between Os(2) and Os(4) and Os(1) and Os(3), and a shift of a CO ligand from Os(4) to Os(2); see Figure 1.

Finally, under more forcing conditions IV can be transformed into V via the loss of 2 equiv of H<sub>2</sub>. We do not wish to advance speculation about the mechanism of this transformation at this time. V is also obtained in the decarbonylation of I in the absence of H<sub>2</sub>.<sup>7</sup>

The sequence of products II, III, and IV formed by the decarbonylation of I under hydrogen provides another

example of a stepwise formation of the high nuclearity cluster V. In these and other reactions which we have studied, the sulfido ligands have been instrumental in initiating the condensation reactions via the formation of donor–acceptor S→M bonds.<sup>5–8</sup>

### Experimental Section

**General Remarks.** Although the cluster complexes were air stable, reactions were routinely performed under a prepurified nitrogen atmosphere. Solvents were purified by distillation from sodium benzophenone (hexane, octane) or by storage over 4-Å molecular sieves and purging with nitrogen through a gas dispersion tube before use. HOs<sub>3</sub>(μ<sub>3</sub>-S)(μ-η<sup>2</sup>-HCNC<sub>6</sub>H<sub>5</sub>)(CO)<sub>9</sub> was prepared according to a published procedure.<sup>15</sup>

Melting points were determined by using a Thomas-Hoover apparatus and are uncorrected. Infrared spectra were recorded

on a Nicolet 7199 FT-IR. Fourier transform  $^1\text{H}$  NMR spectra were obtained at 270 MHz on a Bruker HX270. IR and  $^1\text{H}$  NMR spectra and melting points of all the products are listed in Table I.

**Thermolysis of  $\text{HOs}_3(\text{CO})_9(\mu_3\text{-S})(\mu\text{-}\eta^2\text{-HCNC}_6\text{H}_5)$  (I) in the Presence of Hydrogen.** A bright yellow solution of I (150 mg, 0.156 mmol) in octane (40 mL) was heated to reflux for 1.75 h while hydrogen was bubbled through the mixture. The solvent was then removed from the golden yellow reaction mixture in vacuo. Chromatographic separation of the residue on thin-layer silica plates with hexane/methylene chloride (4/1) solvent produced three major yellow bands. The top bright yellow band,  $\text{H}_4\text{Os}_6(\text{CO})_{15}(\mu_4\text{-S})(\mu_3\text{-S})(\mu\text{-}\eta^2\text{-HC=NC}_6\text{H}_5)_2$  (II; 68 mg, 47%), followed by a faint yellow band,  $\text{H}_6\text{Os}_6(\text{CO})_{14}(\mu_4\text{-S})(\mu_3\text{-S})(\mu\text{-}\eta^2\text{-HCNC}_6\text{H}_5)_2$  (III; 17 mg, 12%), an orange-yellow band (unknown compound, 11 mg), and another bright yellow band,  $\text{H}_4\text{Os}_6(\text{CO})_{15}(\mu_4\text{-S})(\mu_3\text{-S})(\mu\text{-}\eta^2\text{-HCNC}_6\text{H}_5)_2$  (IV; 31 mg, 21%). Compound II seems to be somewhat light sensitive.

**Thermolysis of  $\text{H}_4\text{Os}_6(\text{CO})_{15}(\mu_4\text{-S})(\mu\text{-}\eta^2\text{-HCNC}_6\text{H}_5)_2$  (II).** An octane solution (25 mL) of II (50 mg, 0.027 mmol) was heated to reflux for 6 h in an argon atmosphere. The yellow solution turned orange in color. The solvent was removed in vacuo, and the mixture was chromatographed on thin-layer silica plates with hexane/methylene chloride (5/1). Isolated from the mixture were II (3 mg, 6%), IV (14 mg, 28%), and a trace (<1 mg) of green  $\text{Os}_6(\text{CO})_{15}(\mu_4\text{-S})_2(\mu\text{-}\eta^2\text{-HCNC}_6\text{H}_5)_2$  (V). A similar thermolysis of II (19 mg) in octane (15 mL) for 4.5 h while argon was bubbled through the mixture afforded IV (11 mg, 58%) and V (<1 mg).

**Thermolysis of  $\text{H}_4\text{Os}_6(\text{CO})_{15}(\mu_4\text{-S})(\mu_3\text{-S})(\mu\text{-}\eta^2\text{-HCNC}_6\text{H}_5)$  (II) in the Presence of Hydrogen.** A yellow solution of II (63 mg, 0.034 mmol) in octane (30 mL) was heated to reflux for 3 h while hydrogen was bubbled through the mixture. The solvent was removed in vacuo, and the reaction mixture was purified on thin-layer silica plates using hexane/methylene chloride (4/1) as the eluent. Isolated from the plates were II (8 mg, 13%), III (11 mg, 17%), and IV (8 mg, 13%).

**Thermolysis of  $\text{H}_4\text{Os}_6(\text{CO})_{15}(\mu_4\text{-S})(\mu_3\text{-S})(\mu\text{-}\eta^2\text{-HCNC}_6\text{H}_5)_2$  (II) in the Presence of Carbon Monoxide.** Carbon monoxide was bubbled for 45 min through an octane solution (40 mL) of II (50 mg, 0.027 mmol) that was heated to reflux. The yellow solution became bright yellow in color. The solvent was removed in vacuo. The residue was applied to thin-layer silica plates and eluted with hexane/methylene chloride (5/1). A large yellow band,  $\text{HOs}_3(\text{CO})_9(\mu_3\text{-S})(\mu\text{-}\eta^2\text{-HCNC}_6\text{H}_5)$  (I; 39 mg, 78%), was isolated from the top of the plates.

**Thermolysis of  $\text{H}_4\text{Os}_6(\text{CO})_{15}(\mu_4\text{-S})(\mu_3\text{-S})(\mu\text{-}\eta^2\text{-HCNC}_6\text{H}_5)_2$  (IV).** A yellow solution of IV (20 mg, 0.011 mmol) in nonane (15 mL) was heated to reflux for 6 h. The solution turned brown-orange in color. The solvent was removed by vacuum and the residue chromatographed with hexane/methylene chloride (2/1) on thin-layer silica plates, and green  $\text{Os}_6(\text{CO})_{15}(\mu_4\text{-S})_2(\mu\text{-}\eta^2\text{-HCNC}_6\text{H}_5)_2$  (V) (1 mg, 5%) was taken from the bottom of the plates.

**Thermolysis of  $\text{H}_4\text{Os}_6(\text{CO})_{15}(\mu_4\text{-S})(\mu_3\text{-S})(\mu\text{-}\eta^2\text{-HCNC}_6\text{H}_5)_2$  (IV) in the Presence of Carbon Monoxide.** A solution of IV (60 mg, 0.033 mmol) in octane (25 mL) was heated to reflux for 6 h while carbon monoxide was bubbled through the mixture. The solvent was removed in vacuo and the residue applied to thin-layer silica plates. A hexane/methylene chloride mixture (4/1) eluted two yellow bands. The top yellow band consisted of I (25 mg, 40%), and the bottom band consisted of IV (30 mg, 50%).

**Crystallographic Analyses.** Crystals of II suitable for diffraction analysis were obtained by slow evaporation of hex-

ane/methylene chloride solutions at room temperature. Crystals of III were grown by slow crystallization of solutions of hexane/methylene chloride at  $-20^\circ\text{C}$ . Crystals of IV were obtained by allowing benzene solutions to evaporate at  $5^\circ\text{C}$ .

All crystals were mounted in thin-walled glass capillaries. Diffraction measurements were made on Enraf-Nonius CAD-4 fully automated four-circle diffractometer using graphite-monochromatized Mo  $K\alpha$  radiation. Unit cells were determined and refined from 25 randomly selected reflections obtained by using the CAD-4 automatic search, center, index, and least-squares routines. Crystal data and data collection parameters are listed in Table VIII. All data processing was performed on a Digital PDP 11/45 computer using the Enraf-Nonius SDP program library (Version 18). Absorption corrections of a Gaussian integration type were done for each structure. Neutral atom scattering factors were calculated by the standard procedures.<sup>18a</sup> Anomalous dispersion corrections were applied to all non-hydrogen atoms.<sup>18b</sup> Full-matrix least-squares refinements minimized the function  $\sum_{hkl} w(|F_o| - |F_c|)^2$  where  $w = 1/\sigma(F)^2$ ,  $\sigma(F) = \sigma(F_o^2)/2F_o$ , and  $\sigma(F_o^2) = [\sigma(I_{\text{raw}})^2 + (PF_o^2)^2]^{1/2}/Lp$ .

For all three analyses the space group  $P\bar{1}$  was assumed and subsequently confirmed by the successful solution and refinement of the structure. All three structures were solved by a combination of Patterson and difference Fourier analyses. For each structure all the metal atoms were refined anisotropically. For II and IV the sulfur atoms were also refined anisotropically. All other non-hydrogen atoms were refined isotropically. Positions of hydrogen atoms were calculated by assuming idealized geometry. Their contributions were added to structure factor calculations, but their positions were not refined. Hydride ligands were not located in difference Fourier syntheses and were subsequently ignored in the analyses.

It was discovered during the structure analysis that I cocrystallized with 0.5 mol of  $\text{CH}_2\text{Cl}_2$  solvent per mol of I.

Tables II and III list interatomic distances and angles for II. Tables IV and V list interatomic distances and angles for III and Tables VI and VII list interatomic distances for angles for IV. Estimated standard deviations were obtained by using the inverse matrix obtained on the final cycle of refinement for each structure. Fractional atomic coordinates, thermal parameters, and structure factor amplitudes are available for all three structures; see supplementary material.

**Acknowledgment.** This work was supported by the Office of Basic Energy Sciences of the U.S. Department of Energy under Contract No. DE-AC02-78ER04900 and the Alfred P. Sloan Foundation through a fellowship to R.D.A. NMR studies were supported by Grant No. CHE-7916210 to the Northeast Regional NSF-NMR Facility from the National Science Foundation. We wish to thank Engelhard Industries for a loan of osmium tetroxide.

**Registry No.** I, 80399-46-8; II, 83746-83-2; III, 83731-67-3; IV, 83731-68-4; V, 83731-69-5;  $\text{H}_2$ , 1333-74-0; Os, 7440-04-2.

**Supplementary Material Available:** Tables of final fractional atomic coordinates, thermal parameters, and structure factor amplitudes for all three structures (58 pages). Ordering information is given on any current masthead page.

(18) "International Tables for X-ray Crystallography"; Kynoch Press: Birmingham, England, 1975; Vol. IV: (a) Table 2.2B, pp 99-101; (b) Table 2.3.1, pp 149-150.

# Polynuclear Coordination and Ligand Activation. The Structure, Bonding, and Desulfurization of Thioformamido Ligands about a Trinuclear Site

Richard D. Adams,\* Zain Dawoodi, Donald F. Foust, and Brigitte E. Segmüller

Department of Chemistry, Yale University, New Haven, Connecticut 06511

Received October 12, 1982

The reactions of  $\text{H}_2\text{Os}_3(\text{CO})_{10}$  with the organoisothonocyanates  $\text{RN}=\text{C}=\text{S}$ ,  $\text{R} = \text{C}_6\text{H}_5$ ,  $\text{C}_6\text{H}_4\text{-}p\text{-F}$ ,  $\text{C}_6\text{H}_4\text{-}p\text{-CH}_3$ , and  $\text{CH}_3$ , have been investigated. A sequence of products has been isolated and structurally characterized that shows the activation and desulfurization of an organothioformamido ligand about a trinuclear site. The initial products of the reactions are the compounds  $\text{HOs}_3[\mu\text{-}\eta^1\text{-SC(H)=NR}](\text{CO})_{10}$ , Ia-IVa ( $\text{R} = \text{C}_6\text{H}_5$ ,  $\text{C}_6\text{H}_4\text{-}p\text{-F}$ ,  $\text{C}_6\text{H}_4\text{-}p\text{-CH}_3$ , and  $\text{CH}_3$ ). Ia has been characterized by X-ray crystallographic methods. It contains a thioformamido ligand that bridges an edge of the cluster via the sulfur atom. The carbon-sulfur bond distance at 1.782 (12) Å is long while the carbon-nitrogen distance at 1.279 (13) Å is short and similar to a C-N double bond. Under irradiation, Ia-IVa lose 1 mol of CO to form the complexes  $\text{HOs}_3[\mu\text{-}\eta^2\text{-SC(H)=NR}](\text{CO})_9$ , Ib-IVb ( $\text{R} = \text{C}_6\text{H}_5$ ,  $\text{C}_6\text{H}_4\text{-}p\text{-F}$ ,  $\text{C}_6\text{H}_4\text{-}p\text{-CH}_3$ , and  $\text{CH}_3$ ), that contain triply bridging thioformamido ligands in which the sulfur atom bridges two metal atoms and the nitrogen atom is bonded to the third. IIB was characterized by X-ray crystallographic methods. When heated to 125 °C, Ib-IVb are transformed into the compounds  $\text{HOs}_3(\mu\text{-S})(\mu\text{-HC=NR})(\text{CO})_9$ , Ic-IVc, that contain an "open" cluster of three metal atoms with a triply bridging sulfido ligand and formimidoyl ligand which bridges the open edge of the cluster. Ic was characterized by X-ray crystallographic methods. Ib was found to add 1 mol of  $\text{P}(\text{CH}_3)_2\text{C}_6\text{H}_5$  to form the complex  $\text{HOs}_3[\mu\text{-}\eta^2\text{-SC(H)=NC}_6\text{H}_5](\text{CO})_9[\text{P}(\text{CH}_3)_2\text{C}_6\text{H}_5]$ , Id. An X-ray crystallographic analysis showed that it contains a *N*-phenylthioformamido ligand bridging an edge of the cluster, but unlike Ia-IVa the ligand is coordinated through both the sulfur and nitrogen atoms. The carbon-sulfur distance at 1.69 (1) Å is significantly shorter than that in Ia while the carbon-nitrogen distance at 1.32 (1) Å is longer. The effect of coordination on the bonding in the thioformamido ligand and its influence on the desulfurization reaction is described and discussed.

## Introduction

The activation of organic ligands at polynuclear metal sites is a topic that has received a great deal of attention because of the bearing it may have on the development of cluster compounds as catalysts and the similarities it may have to catalysis on metal surfaces.<sup>1-5</sup> Recently, we have been investigating the nature of the reactions of the osmium clusters  $\text{H}_2\text{Os}_3(\text{CO})_{10}$  and  $\text{H}_2\text{Os}_3(\text{CO})_9\text{PMe}_2\text{Ph}$  with the heteroallenes  $\text{RN}=\text{C}=\text{O}$ ,<sup>6</sup>  $\text{RN}=\text{C}=\text{NR}$ ,<sup>7</sup> and  $\text{CS}_2$ .<sup>8</sup> The reactions of  $\text{CS}_2$  with  $\text{H}_2\text{Os}_3(\text{CO})_9\text{PMe}_2\text{Ph}$  yielded cluster complexes containing dithioformate and thioformaldehyde ligands that were formed apparently by hydrogen transfer and desulfurization processes. We have now investigated the reactions of  $\text{H}_2\text{Os}_3(\text{CO})_{10}$  with alkyl and aryl isothiocyanates and have discovered a sequence of reactions and products that reveal in vivid detail the nature of the ligand activation that facilitates and ultimately produces the desulfurization of a thioformamido ligand and the role that trinuclear coordination plays in this process. A preliminary report of this work has been published.<sup>9</sup>

## Results

At 25 °C the cluster  $\text{H}_2\text{Os}_3(\text{CO})_{10}$  adds 1 mol of alkyl or aryl isothiocyanate to form the complexes  $\text{HOs}_3(\mu\text{-}\eta^1\text{-SCH=NR})(\text{CO})_{10}$ , Ia-IVa ( $\text{R} = \text{C}_6\text{H}_5$ ,  $\text{C}_6\text{H}_4\text{-}p\text{-F}$ ,  $\text{C}_6\text{H}_4\text{-}p\text{-CH}_3$ , and  $\text{CH}_3$ ). The transfer of one hydride ligand to the carbon atom of the isothiocyanate molecule is indicated by a low-field <sup>1</sup>H NMR signal ( $\delta \approx 8\text{ppm}$ ) that is characteristic of the proton on thioformamido ligands (cf. Table I).<sup>10</sup>

Details of the molecular structure of these compounds were established by an X-ray crystallographic analysis of Ia. An ORTEP diagram of Ia is shown in Figure 1. The molecule consists of a triangular cluster of three osmium atoms. The Os-Os distances range from 2.861 (1) to 2.870 (1) Å and are very similar to those observed in  $\text{Os}_3(\text{CO})_{12}$ , 2.877 (3) Å.<sup>11</sup> Complete lists of bond distances and angles are given in Tables II and III. The thioformamido ligand bridges an edge of the cluster via the sulfur atom. The Os-S distances at 2.424 (3) and 2.431 (3) Å are similar to those found in sulfido osmium carbonyl clusters.<sup>8,13</sup> Within the thioformamido ligand the carbon-sulfur bond distance at 1.782 (12) Å is similar in length to that of a carbon-sulfur single bond, 1.80-1.82 Å,<sup>13</sup> while the carbon-nitrogen bond length of 1.279 (13) Å is similar to that

- (1) Muettterties, E. L. *Bull. Soc. Chim. Belg.* 1976, 85, 451.  
 (2) Muettterties, E. L.; Stein, J. *Chem. Rev.* 1979, 79, 479.  
 (3) Muettterties, E. L. *Pure Appl. Chem.* 1978, 50, 941.  
 (4) Shriver, D. F. In "Catalytic Activation of Carbon Monoxide"; Ford, P. C., Ed.; American Chemical Society, Washington, DC, 1981; *Adv. Chem. Ser. No. 152*.  
 (5) (a) Muettterties, E. L. *Science (Washington, D.C.)* 1977, 196, 839.  
 (b) Muettterties, E. L. *Bull. Soc. Chim. Belg.* 1975, 84, 959. (c) Ugo, R. *Catal. Rev.* 1975, 11, 225.  
 (6) Adams, R. D.; Golembeski, N. M.; Selegue, J. P. *Inorg. Chem.* 1981, 20, 1242.  
 (7) Adams, R. D.; Katahira, D. A.; Selegue, J. P. *J. Organomet. Chem.* 1981, 213, 259.  
 (8) Adams, R. D.; Golembeski, N. M.; Selegue, J. P. *J. Am. Chem. Soc.* 1981, 103, 546.  
 (9) Adams, R. D.; Dawoodi, Z. *J. Am. Chem. Soc.* 1981, 103, 6510.

- (10) (a) Sahajpal, A.; Robinson, S. D. *Inorg. Chem.* 1979, 18, 3572. (b) Robinson, S. D.; Sahajpal, A. *Ibid.* 1977, 16, 2722. (c) Brown, L. D.; Robinson, S. D.; Sahajpal, A.; Ibers, J. A. *Ibid.* 1977, 16, 2728.  
 (11) Churchill, M. R.; DeBoer, B. G. *Inorg. Chem.* 1977, 16, 878.  
 (12) (a) Johnson, B. F. G.; Lewis, J.; Pippard, D.; Raithby, P. R. *Acta Crystallogr., Sect. B* 1978, B34, 3767. (b) Johnson, B. F. G.; Lewis, J.; Pippard, D.; Raithby, P. R.; Sheldrick, G. M.; Rouse, K. D. *J. Chem. Soc., Dalton Trans.* 1979, 616. (c) Broadhurst, P. V.; Johnson, B. F. G.; Lewis, J.; Orpen, A. G.; Raithby, P. R.; Thornback, J. R. *J. Organomet. Chem.* 1980, 187, 141.  
 (13) (a) Frank, G. W.; Degen, P. J. *Acta Crystallogr. Sect. B* 1973, B29, 1815. (b) Vallee, G.; Busetti, V.; Mammi, M.; Carrazolo, G. *Ibid.* 1969, B25, 1432. (c) Fleming, J. E.; Lynton, H. *Can. J. Chem.* 1967, 45, 353.

Table I. Spectroscopic and Physical Data

compd	mp, °C	<sup>1</sup> H NMR δ	IR ν <sub>CO</sub> , cm <sup>-1</sup>
Ia, HO <sub>3</sub> [μ-η <sup>1</sup> -SC(H)NC <sub>6</sub> H <sub>5</sub> ] <sub>10</sub> (CO) <sub>10</sub>	142.5-144	7.70 (s, 1 H), 7.26 (m, 3 H), 6.93 (m, 2 H), -17.50 (s, 1 H) <sup>a</sup>	2110 w, 2085 sh, 2070 vs, 2062 s, 2036 sh, 2026 vs, 2018 s, 2005 m, 1991 w, 1988 w <sup>b</sup>
IIa, HO <sub>3</sub> [μ-η <sup>1</sup> -SC(H)N- <i>p</i> -C <sub>6</sub> H <sub>4</sub> F](CO) <sub>10</sub>	158.5-159.5	7.79 (s, 1 H), 7.05 (m, 4 H), -17.42 (s, 1 H) <sup>a</sup>	2110 w, 2085 sh, 2071 vs, 2062 s, 2036 sh, 2027 vs, 2019 s, 2006 m, 1992 w, 1988 w <sup>b</sup>
IIIa, HO <sub>3</sub> [μ-η <sup>1</sup> -SC(H)N- <i>p</i> -C <sub>6</sub> H <sub>4</sub> CH <sub>3</sub> ](CO) <sub>10</sub>	96-98	7.50 (s, 1 H), 7.43 (m, 1 H), 7.27 (m, 1 H), 6.86 (d, 1 H), 6.60 (d, 1 H), 2.06 (s, 3 H), -17.70 (s, 1 H) <sup>a</sup>	2110 w, 2085 sh, 2070 vs, 2061 s, 2036 sh, 2025 vs, 2018 s, 2005 m, 1990 w, 1987 w <sup>b</sup>
IVa, HO <sub>3</sub> [μ-η <sup>1</sup> -SC(H)NCH <sub>3</sub> ](CO) <sub>10</sub>	102-106	7.49 (s, 1 H), 3.51 (s, 3 H), -17.52 (s, 1 H) <sup>a</sup>	2110 w, 2086 sh, 2069 vs, 2061 s, 2035 sh, 2024 vs, 2017 s, 2005 m, 1990 w, 1987 w <sup>b</sup>
Ib, HO <sub>3</sub> [μ <sub>3</sub> -η <sup>2</sup> -SC(H)NC <sub>6</sub> H <sub>5</sub> ](CO) <sub>9</sub>	167-167.5	10.22 (s, 1 H), 7.43 (m, 3 H), 6.90 (m, 2 H), -13.69 (s, 1 H) <sup>a</sup>	2089 m, 2056 s, 2035 vs, 2006 s, 1991 s, 1970 w, 1959 w <sup>b</sup>
IIb, HO <sub>3</sub> [μ <sub>3</sub> -η <sup>2</sup> -SC(H)N- <i>p</i> -C <sub>6</sub> H <sub>4</sub> F](CO) <sub>9</sub>	156.5-157.5	10.24 (s, 1 H), 7.13 (m, 2 H), 6.89 (m, 2 H), -13.66 (s, 1 H) <sup>a</sup>	2089 m, 2058 s, 2035 vs, 2006 s, 1992 s, 1971 w, 1960 w <sup>b</sup>
IIIb, HO <sub>3</sub> [μ <sub>3</sub> -η <sup>2</sup> -SC(H)N- <i>p</i> -C <sub>6</sub> H <sub>4</sub> CH <sub>3</sub> ](CO) <sub>9</sub>	155-156	10.18 (s, 1 H), 7.20 (2 H, d), 6.79 (2 H, d), 2.38 (s, 3 H), -13.74 (s, 1 H) <sup>a</sup>	2088 m, 2056 s, 2035 vs, 2006 s, 1991 s, 1970 w, 1959 w <sup>b</sup>
IVb, HO <sub>3</sub> [μ <sub>3</sub> -η <sup>2</sup> -SC(H)NCH <sub>3</sub> ](CO) <sub>9</sub>	149.5-150.5	10.12 (s, 1 H), 3.53 (s, 3 H), -14.08 (s, 1 H) <sup>a</sup>	2089 m, 2058 s, 2032 s, 2006 s, 1992 s, 1970 m, 1956 m <sup>b</sup>
Ic, HO <sub>3</sub> (μ <sub>3</sub> -S-(μ-η <sup>2</sup> -HCNC <sub>6</sub> H <sub>5</sub> ))(CO) <sub>9</sub>	152 dec	11.16 (s, 1 H), 7.20 (m, 3 H), 6.77 (m, 2 H), -16.15 (s, 1 H); <sup>a</sup> isomer A, 10.76 (s, 1 H), 7.20 (m, 3 H), 6.77 (m, 2 H), -16.91 (s, 1 H); <sup>c</sup> isomer B, 11.58 (s, 1 H), 7.20 (m, 3 H), 6.77 (m, 2 H), -15.47 (s, 1 H) <sup>c</sup>	2108 m, 2077 vs, 2047 vs, 2027 w, 2016 m, 2007 s, 1989 m, 1981 m, 1971 m <sup>b</sup>
IIc, HO <sub>3</sub> (μ <sub>3</sub> -S-(μ-η <sup>2</sup> -HCNC <sub>6</sub> H <sub>4</sub> - <i>p</i> -F))(CO) <sub>9</sub>	172.5-173.5	11.11 (s, 1 H), 7.04 (m, 2 H), 6.75 (m, 2 H), -16.28 (s, 1 H); <sup>a</sup> isomer A, 10.78 (s, 1 H), 7.04 (m, 2 H), 6.74 (m, 2 H), -16.93 (s, 1 H); <sup>c</sup> isomer B, 11.60 (s, 1 H), 7.04 (m, 2 H), 6.74 (m, 2 H), -15.46 (s, 1 H) <sup>c</sup>	2108 m, 2079 vs, 2048 vs, 2027 w, 2017 m, 2008 s, 1988 m, 1983 m, 1973 m <sup>b</sup>
IIIc, HO <sub>3</sub> (μ <sub>3</sub> -S-(μ-η <sup>2</sup> -HCN- <i>p</i> -C <sub>6</sub> H <sub>4</sub> CH <sub>3</sub> ))(CO) <sub>9</sub>	150.5-151.5	11.10 (s, 1 H), 7.13 (d, 2 H), 6.63 (d, 2 H), 2.36 (s, 3 H), -16.21 (s, 1 H); <sup>a</sup> isomer A, 10.72 (s, 1 H), 7.13 (d, 2 H), 6.65 (d, 2 H), 2.36 (s, 3 H), -16.91 (s, 1 H); <sup>c</sup> isomer B, 11.54 (s, 1 H), 7.13 (d, 2 H), 6.65 (d, 2 H), 2.36 (s, 3 H), -15.46 (s, 1 H) <sup>c</sup>	2108 m, 2078 vs, 2046 vs, 2029 w, 2015 m, 2008 s, 1988 m, 1981 m, 1971 m <sup>b</sup>
IVc, HO <sub>3</sub> (μ <sub>3</sub> -S-(μ-η <sup>2</sup> -HCNCH <sub>3</sub> ))(CO) <sub>9</sub>	126.5-128	10.85 (s, 1 H), 3.73 (s, 3 H), -16.75 (s, 1 H); <sup>a</sup> isomer A, 10.68 (s, 1 H), 3.76 (s, 3 H), -17.13 (s, 1 H); <sup>c</sup> isomer B, 11.40 (s, 1 H), 3.76 (s, 3 H), -15.86 (s, 1 H) <sup>c</sup>	2107 m, 2077 vs, 2047 vs, 2039 sh, 2015 m, 2006 s, 1986 m, 1981 m, 1970 m <sup>b</sup>
Id, HO <sub>3</sub> [μ-η <sup>2</sup> -SC(H)NC <sub>6</sub> H <sub>5</sub> ](CO) <sub>9</sub> [P(CH <sub>3</sub> ) <sub>2</sub> C <sub>6</sub> H <sub>5</sub> ]	168-168.5	9.17 (s, 1 H), 7.3 (m, 3 H), 6.7 (m, 2 H), 2.31 (d, 3 H, J <sub>P-H</sub> = 4.6 Hz), 2.27 (d, 3 H, J <sub>P-H</sub> = 4.6 Hz), -13.26 (d, 1 H, J <sub>P-H</sub> = 12.20 Hz) <sup>a</sup>	2086 w, 2055 s, 2042 w, 2030 s, 2016 w, 2003 vs, 1993 s, 1970 m, 1958 w, 1932 w <sup>b</sup>
IIIe, H <sub>2</sub> Os <sub>2</sub> (μ <sub>4</sub> -S)(μ <sub>3</sub> -S-(μ-HCN- <i>p</i> -C <sub>6</sub> H <sub>4</sub> CH <sub>3</sub> ))(CO) <sub>17</sub>		12.35 (s, 1 H), 11.20 (s, 1 H), 7.18 (d, 4 H), 6.76 (d, 4 H), 2.42 (s, 3 H), 2.40 (s, 3 H), -13.82 (s, 1 H), -17.46 (s, 1 H) <sup>a</sup>	2111 m, 2097 m, 2066 vs, 2047 sh, 2042 s, 2028 m, 2010 m, 2006 m, 1988 m, 1980 m, 1975 sh, 1959 w <sup>b</sup>
IVe, H <sub>2</sub> Os <sub>2</sub> (μ <sub>4</sub> -S)(μ <sub>3</sub> -S-(μ-HCNCH <sub>3</sub> ))(CO) <sub>17</sub>		12.15 (s, 1 H), 11.11 (s, 1 H), 4.17 (s, 3 H), 4.11 (s, 3 H), -13.98 (s, 1 H), -17.61 (s, 1 H) <sup>a</sup>	2112 m, 2096 m, 2065 vs, 2046 sh, 2043 s, 2027 s, 2022 sh, 2009 m, 2005 m, 1986 m, 1978 m, 1973 sh, 1957 w <sup>b</sup>

<sup>a</sup> CDCl<sub>3</sub>, room temperature. <sup>b</sup> Hexanes. <sup>c</sup> CDCl<sub>3</sub>, -60 °C.

of a carbon-nitrogen bond double bond.<sup>14</sup> There are ten linear carbonyl ligands disposed as shown in Figure 1. The

<sup>1</sup>H NMR spectrum indicates the presence of one hydride ligand. This was not observed crystallographically, but it is believed to bridge the Os(1)-Os(3) bond in the cavity circumscribed by the carbonyl ligands C(1)-O(1), C(2)-O(2), C(8)-O(8), and C(10)-O(10).

When irradiated, the compounds Ia-IVa lose 1 mol of

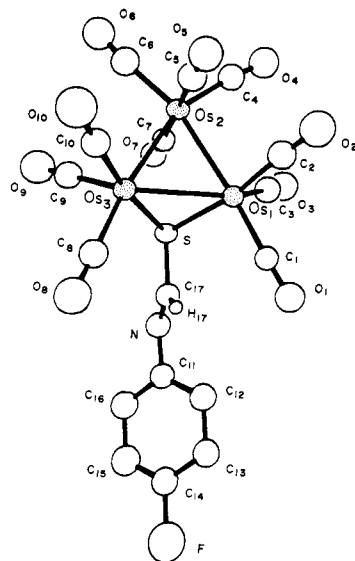


Figure 1. An ORTEP diagram of  $\text{HOs}_3[\mu\text{-}\eta^1\text{-SC(H)=NC}_6\text{H}_4\text{-p-F}](\text{CO})_{10}$ , Ib, showing 50% probability thermal-motion ellipsoids.

Table II. Interatomic Distances (Å) with Esds for  $\text{HOs}_3[\mu\text{-}\eta^1\text{-SC(H)N-}p\text{-C}_6\text{H}_4\text{F}](\text{CO})_{10}$ , Ia

Os(1)-Os(2)	2.861 (1)	C(11)-C(12)	1.382 (16)
Os(1)-Os(3)	2.870 (1)	C(12)-C(13)	1.399 (16)
Os(2)-Os(3)	2.868 (1)	C(13)-C(14)	1.346 (17)
Os(1)-S	2.424 (3)	C(14)-C(15)	1.307 (16)
Os(1)-C(1)	1.907 (11)	C(15)-C(16)	1.440 (17)
Os(1)-C(2)	1.871 (14)	C(16)-C(11)	1.377 (18)
Os(1)-C(3)	1.948 (14)	C(14)-F	1.416 (13)
Os(2)-C(4)	1.910 (15)	C(1)-O(1)	1.158 (12)
Os(2)-C(5)	1.987 (12)	C(2)-O(2)	1.169 (15)
Os(2)-C(6)	1.969 (14)	C(3)-O(3)	1.124 (14)
Os(2)-C(7)	1.922 (12)	C(4)-O(4)	1.130 (16)
Os(3)-S	2.431 (3)	C(5)-O(5)	1.149 (13)
Os(3)-C(8)	1.910 (13)	C(6)-O(6)	1.113 (14)
Os(3)-C(9)	1.863 (12)	C(7)-O(7)	1.168 (12)
Os(3)-C(10)	1.877 (13)	C(8)-O(8)	1.161 (14)
S-C(17)	1.782 (12)	C(9)-O(9)	1.170 (12)
C(17)-N	1.279 (13)	C(10)-O(10)	1.131 (14)
N-C(11)	1.425 (14)		

CO to form in high yield the compounds  $\text{HOs}_3[\mu_3\text{-}\eta^2\text{-SC(H)=NR}](\text{CO})_9$ , Ib-IVb (R =  $\text{C}_6\text{H}_5$ ,  $\text{C}_6\text{H}_4\text{-}p\text{-F}$ ,  $\text{C}_6\text{H}_4\text{-}p\text{-CH}_3$ , and  $\text{CH}_3$ ). The molecular structure of Ib was es-

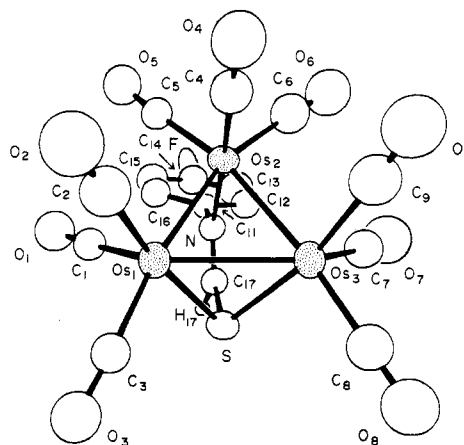


Figure 2. An ORTEP diagram of  $\text{HOs}_3[\mu_3\text{-}\eta^2\text{-SC(H)=NC}_6\text{H}_4\text{-}p\text{-F}](\text{CO})_9$ , IIb, showing 50% probability thermal-motion ellipsoids.

tablished by single-crystal X-ray diffraction methods, and an ORTEP diagram of it is shown in Figure 2. This molecule contains a triangular cluster of three metal atoms with a triply bridging thioformamido ligand. Two of the Os-Os distances Os(1)-Os(2) = 2.817 (1) Å and Os(2)-Os(3) = 2.824 (1) Å have shortened significantly from their values in Ia, but they are still only slightly shorter than those in  $\text{Os}_3(\text{CO})_{12}$ , 2.877 (3) Å.<sup>11</sup> The separation between the sulfur bridged metal atoms is similar to that in Ia: Complete lists of bond distance and angles are given in Tables IV and V. The thioformamido ligand serves as a triple bridge with the sulfur atom bonded to two metal atoms and the nitrogen atom bonded to the third, Os(2)-N = 2.193 (11) Å. The bonding within the thioformamido ligand is similar to that in Ia. The C-S distance at 1.774 (15) Å is similar to that of a carbon-sulfur single bond,<sup>13</sup> and the C-N distance at 1.250 (17) Å is similar to a carbon-nitrogen double bond.<sup>14</sup> Each metal atom contains three linear terminal carbonyl ligands. The hydride ligand is believed to bridge the Os(1)-Os(3) bond on the side of the cluster opposite the sulfur atom.

When octane solutions of the molecules Ib-IVb are refluxed for 15 min they are transformed into the products  $\text{HOs}_3(\mu_3\text{-S})(\mu\text{-HC=NR})(\text{CO})_9$ , Ic-IVc (R =  $\text{C}_6\text{H}_5$ ,  $\text{C}_6\text{H}_4\text{-}p\text{-F}$ ,  $\text{C}_6\text{H}_4\text{-}p\text{-CH}_3$ , and  $\text{CH}_3$ ). These molecules can also be made directly from Ia-IVa. The molecular structure of

Table III. Interatomic Angles (deg) with Esds for  $\text{HOs}_3[\mu\text{-}\eta^1\text{-SC(H)N-}p\text{-C}_6\text{H}_4\text{F}](\text{CO})_{10}$ , Ia

Os(1)-Os(2)-Os(3)	60.12 (2)	Os(3)-Os(2)-C(7)	90.9 (4)	Os(3)-S-C(17)	103.3 (4)
Os(2)-Os(1)-Os(3)	60.07 (2)	C(4)-Os(2)-C(5)	90.3 (6)	S-C(17)-N	119.7 (8)
Os(1)-Os(3)-Os(2)	59.80 (2)	C(4)-Os(2)-C(6)	101.1 (6)	C(17)-N-C(11)	115.8 (9)
Os(2)-Os(1)-S	83.03 (6)	C(4)-Os(2)-C(7)	94.8 (5)	N-C(11)-C(12)	123 (1)
Os(2)-Os(1)-C(1)	172.9 (3)	C(5)-Os(2)-C(6)	92.7 (5)	N-C(11)-C(16)	116 (1)
Os(2)-Os(1)-C(2)	87.9 (4)	C(5)-Os(2)-C(7)	174.3 (5)	C(16)-C(11)-C(12)	121 (1)
Os(2)-Os(1)-C(3)	92.2 (4)	C(6)-Os(2)-C(7)	88.9 (5)	C(11)-C(12)-C(13)	120 (1)
Os(3)-Os(1)-S	53.89 (7)	Os(1)-Os(3)-S	53.65 (7)	C(12)-C(13)-C(14)	117 (1)
Os(3)-Os(1)-C(1)	113.6 (4)	Os(1)-Os(3)-C(8)	112.9 (4)	C(13)-C(14)-C(15)	126 (1)
Os(3)-Os(1)-C(2)	116.6 (4)	Os(1)-Os(3)-C(9)	118.5 (4)	C(14)-C(15)-C(16)	118 (1)
Os(3)-Os(1)-C(3)	137.2 (4)	Os(1)-Os(3)-C(10)	135.4 (4)	C(15)-C(16)-C(11)	118 (1)
S-Os(1)-C(1)	95.6 (4)	Os(2)-Os(3)-S	82.73 (7)	C(13)-C(14)-F	116 (1)
S-Os(1)-C(2)	169.5 (4)	Os(2)-Os(3)-C(8)	172.6 (4)	C(15)-C(14)-F	117 (1)
S-Os(1)-C(3)	93.7 (4)	Os(2)-Os(3)-C(9)	91.6 (4)	Os(1)-C(2)-O(1)	177 (1)
C(1)-Os(1)-C(2)	92.7 (5)	Os(2)-Os(3)-C(10)	90.2 (4)	Os(1)-C(2)-O(2)	176 (1)
C(1)-Os(1)-C(3)	94.8 (5)	S-Os(3)-C(8)	93.6 (4)	Os(1)-C(3)-O(3)	178 (1)
C(2)-Os(1)-C(3)	92.0 (6)	S-Os(3)-C(9)	172.0 (4)	Os(2)-C(4)-O(4)	173 (1)
Os(1)-Os(2)-C(4)	96.2 (4)	S-Os(3)-C(10)	93.4 (4)	Os(2)-C(5)-O(5)	176 (1)
Os(1)-Os(2)-C(5)	86.0 (3)	C(8)-Os(3)-C(9)	91.4 (5)	Os(2)-C(6)-O(6)	174 (1)
Os(1)-Os(2)-C(6)	162.7 (4)	C(8)-Os(3)-C(10)	96.4 (6)	Os(2)-C(7)-O(7)	175 (1)
Os(1)-Os(2)-C(7)	90.8 (3)	C(9)-Os(3)-C(10)	92.3 (5)	Os(3)-C(8)-O(8)	177 (1)
Os(3)-Os(2)-C(4)	155.8 (4)	Os(1)-S-Os(3)	72.46 (8)	Os(3)-C(9)-O(9)	178 (1)
Os(3)-Os(2)-C(5)	83.4 (4)	Os(1)-S-C(17)	102.6 (4)	Os(3)-C(10)-O(10)	179 (1)
Os(3)-Os(2)-C(6)	102.6 (4)				



Table IV. Interatomic Distances (Å) with Esds for  $\text{HOs}_3[\mu_3\text{-}\eta^2\text{-SC(H)=N-}p\text{-C}_6\text{H}_4\text{F}](\text{CO})_9$ , IIb

Os(1)-Os(2)	2.817 (1)	C(17)-N	1.250 (17)
Os(1)-Os(3)	2.860 (1)	N-C(11)	1.46 (2)
Os(2)-Os(3)	2.824 (1)	C(11)-C(12)	1.37 (2)
Os(1)-C(1)	1.861 (14)	C(12)-C(13)	1.38 (3)
Os(1)-C(2)	1.924 (21)	C(13)-C(14)	1.33 (2)
Os(1)-C(3)	1.924 (17)	C(14)-F	1.40 (3)
Os(1)-S	2.456 (4)	C(14)-C(15)	1.39 (3)
Os(2)-C(4)	1.869 (18)	C(15)-C(16)	1.41 (2)
Os(2)-C(5)	1.904 (15)	C(16)-C(11)	1.38 (2)
Os(2)-C(6)	1.999 (23)	C(1)-O(1)	1.18 (2)
Os(2)-N	2.193 (11)	C(2)-O(2)	1.14 (2)
Os(3)-C(7)	1.948 (21)	C(3)-O(3)	1.20 (2)
Os(3)-C(8)	1.898 (18)	C(4)-O(4)	1.19 (2)
Os(3)-C(9)	1.933 (21)	C(5)-O(5)	1.14 (2)
Os(3)-S	2.449 (4)	C(6)-O(6)	1.11 (2)
S-C(17)	1.774 (15)	C(7)-O(7)	1.15 (2)
C(17)-H(17) <sup>a</sup>	1.19	C(8)-O(8)	1.15 (2)
		C(9)-O(9)	1.10 (2)

<sup>a</sup> H atom not refined.

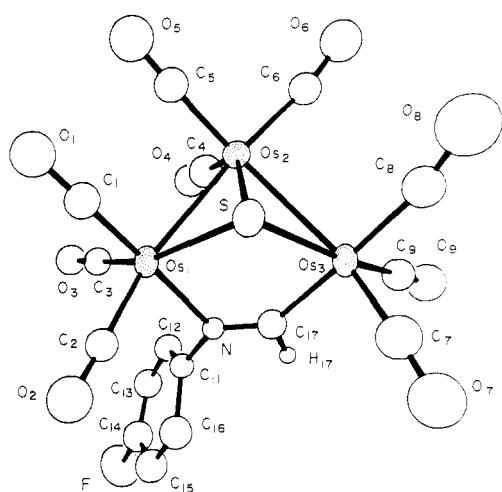
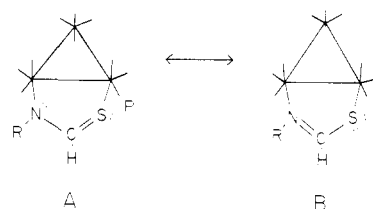


Figure 3. An ORTEP diagram of  $\text{HOs}_3(\mu_3\text{-S})(\mu\text{-HC=NC}_6\text{H}_4\text{-}p\text{-F})(\text{CO})_9$ , IIIb, showing 50% probability thermal-motion ellipsoids.

these compounds was established by an X-ray analysis of IIc and an ORTEP diagram of its structure is shown in Figure 3. This molecule contains an "open" triangular cluster of three metal atoms with only two metal-metal bonds. The Os(1)-Os(2) distance at 2.836 (1) Å is similar to the Os-Os separation of 2.877 (3) Å found in  $\text{Os}_3(\text{CO})_{12}$ .<sup>11</sup> However, the Os(2)-Os(3) distance of 2.988 (1) Å is significantly longer. Such elongations are characteristic of bridging hydride ligands and suggest that the hydride ligand in these molecules bridges this bond.<sup>15</sup> The Os(1)⋯Os(3) separation at 3.779 (1) Å is too long to permit a significant bonding interaction. There is a triply bridging sulfido ligand and a formimidoyl ligand ( $\text{HC=NC}_6\text{H}_4\text{-}p\text{-F}$ ) that bridges the "open" edge of the cluster. As expected, the short carbon-nitrogen bond distance, C(17)-N = 1.213 (14) Å, is indicative of a carbon-nitrogen double bond. The hydrogen atom on C(17), shown in an idealized position in the figure, was not observed crystallographically but was confirmed by its characteristic <sup>1</sup>H NMR shift ( $\delta$  11.11).<sup>16</sup> Each metal atom contains three linear, terminal carbonyl ligands. Complete lists of bond distance and angles are given in Tables VI and VII.

In solution IIc exists as a mixture of isomers that interconvert rapidly on the NMR timescale at room temperature. This process is slowed at -60 °C, and two isomers in a 1:2 ratio are observed. It is believed that the hydride ligand bridges different metal-metal bonds in the isomers.

Compound Ib adds 1 mol of  $\text{P}(\text{CH}_3)_2\text{C}_6\text{H}_5$  at room temperature in hexane-methylene chloride solutions to form the compound  $\text{HOs}_3[\mu\text{-}\eta^2\text{-SC(H)NC}_6\text{H}_5](\text{CO})_9[\text{P}(\text{CH}_3)_2\text{C}_6\text{H}_5]$ , Id. The molecular structure of Id was determined by X-ray crystallographic methods, and an ORTEP diagram of its structure is shown in Figure 4. This molecule contains a triangular cluster of three metal atoms with three significant metal-metal interactions. The unbridged metal-metal bonds Os(1)-Os(3) = 2.936 (1) Å and Os(2)-Os(3) = 2.909 (1) Å are longer than those in IIa. This could be due, in part, to the presence of the phosphine ligand. Such lengthening effects have been observed previously.<sup>17</sup> The long Os(1)-Os(2) bond at 2.963 (1) Å probably contains the bridging hydride ligand<sup>15</sup> and also contains a bridging *N*-phenylthioformamido ligand. The hydride ligand and the hydrogen atom on C(10) were not observed crystallographically, but their existence was confirmed by their characteristic <sup>1</sup>H NMR shifts (cf. Table I). Unlike the molecules Ia-IVa the *N*-phenylthioformamido ligand in Id is coordinated to the cluster through both the sulfur and nitrogen atoms. The carbon-sulfur bond distance at 1.69 (1) Å is significantly shorter than that in IIa or IIb but is similar to the C-S distances 1.65 (3) Å (average) and 1.661 (7) and 1.666 (7) Å found for bridging dithioformato ligands in  $\text{HOs}_3(\mu\text{-S}_2\text{CH})(\text{CO})_{10}$  and  $\text{HOs}_3(\mu\text{-S}_2\text{CH})(\text{CO})_9[\text{P}(\text{CH}_3)_2\text{C}_6\text{H}_5]$ , respectively.<sup>18</sup> Although the C(10)-N distance of 1.32 (1) Å is longer than that in IIa, it is still in the region that would be interpreted as multiple bonding. A delocalization of the  $\pi$ -electron density via an averaging of resonance forms such as A and B would account for the partial multiple bonding between



the C-N and C-S atoms as implied by these distances. There are nine linear terminal carbonyl ligands arranged such that Os(1) has two, Os(2) has three, and Os(3) has four. Since the molecules Ib-IVb have three carbonyl ligands on each metal atom, the addition of  $\text{P}(\text{CH}_3)_2\text{C}_6\text{H}_5$  to Ib has evidently induced a carbonyl shift between a pair of metal atoms. The phosphine ligand occupies an equatorial coordination position on Os(1) cis to the sulfur atom. Complete lists of bond distance and angles for Id are given in Tables VIII and IX.

## Discussion

$\text{H}_2\text{Os}_3(\text{CO})_{10}$  has been found to add 1 mol of organo-isothiocyanate and transfer one hydride ligand to the carbon atom to produce the compounds Ia-IVa in which the thioformamido ligand serves as a three-electron donor, bridging an edge of the cluster via the sulfur atom. The carbon-sulfur bond distance in IIa at 1.782 (12) Å implies

(15) Churchill, M. R.; DeBoer, B. G.; Rottela, F. J. *Inorg. Chem.* 1976, 15, 1843.

(16) (a) Adams, R. D.; Golembeski, N. M. *J. Am. Chem. Soc.* 1979, 101, 2579. (b) Ciriano, M.; Green, M.; Gregson, D.; Howard, J. A. K.; Spencer, J. L.; Stone, F. G. A.; Woodward, P. *J. Chem. Soc., Dalton Trans.* 1979, 1294.

(17) Benfield, R. E.; Johnson, B. F. G.; Raithby, P. R.; Sheldrick, G. M. *Acta Crystallogr., Sect. B* 1978, B34, 666.

(18) Adams, R. D.; Selegue, J. P. *J. Organomet. Chem.* 1980, 195, 223.

Table V. Interatomic Angles (deg) with Esds for  $\text{HOs}_3[\mu_3\text{-}\eta^2\text{-SC(H)N-}p\text{-C}_6\text{H}_4\text{F}](\text{CO})_9$ , IIb

Os(1)-Os(2)-Os(3)	60.92 (2)	N-Os(2)-C(4)	173.4 (7)	S-C(17)-H(17)	115 (1)
Os(1)-Os(3)-Os(2)	59.42 (2)	N-Os(2)-C(5)	90.7 (5)	N-C(17)-H(17)	122 (1)
Os(2)-Os(1)-Os(3)	59.66 (2)	N-Os(2)-C(6)	93.3 (6)	C(17)-N-C(11)	118 (1)
Os(2)-Os(1)-S	80.2 (1)	C(4)-Os(2)-C(5)	91.4 (7)	C(17)-N-Os(2)	123 (1)
Os(2)-Os(1)-C(1)	84.5 (5)	C(4)-Os(2)-C(6)	92.8 (8)	C(11)-N-Os(2)	119 (1)
Os(2)-Os(1)-C(2)	96.6 (6)	C(5)-Os(2)-C(6)	94.8 (7)	N-C(11)-C(12)	119 (1)
Os(2)-Os(1)-C(3)	171.3 (5)	Os(1)-Os(3)-S	54.5 (1)	N-C(11)-C(16)	117 (1)
Os(3)-Os(1)-S	54.21 (9)	Os(1)-Os(3)-C(7)	138.2 (5)	C(13)-C(14)-F	116 (2)
Os(3)-Os(1)-C(1)	134.3 (5)	Os(1)-Os(3)-C(8)	115.1 (6)	C(15)-C(14)-F	118 (2)
Os(3)-Os(1)-C(2)	115.5 (6)	Os(1)-Os(3)-C(9)	113.7 (6)	C(16)-C(11)-C(12)	123 (1)
Os(3)-Os(1)-C(3)	113.6 (4)	Os(2)-Os(3)-S	80.18 (9)	C(11)-C(12)-C(13)	119 (2)
S-Os(1)-C(1)	95.3 (5)	Os(2)-Os(3)-C(7)	89.6 (5)	C(12)-C(13)-C(14)	118 (2)
S-Os(1)-C(2)	169.5 (6)	Os(2)-Os(3)-C(8)	174.0 (5)	C(13)-C(14)-C(15)	126 (2)
S-Os(1)-C(3)	91.4 (5)	Os(2)-Os(3)-C(9)	89.4 (5)	C(14)-C(15)-C(16)	116 (2)
C(1)-Os(1)-C(2)	94.3 (7)	S-Os(3)-C(7)	96.0 (5)	C(15)-C(16)-C(11)	118 (2)
C(1)-Os(1)-C(3)	98.5 (7)	S-Os(3)-C(8)	94.5 (5)	Os(1)-C(1)-O(1)	175 (1)
C(2)-Os(1)-C(3)	91.4 (8)	S-Os(3)-C(9)	167.2 (6)	Os(1)-C(2)-O(2)	176 (2)
Os(1)-Os(2)-N	86.3 (3)	C(7)-Os(3)-C(8)	93.8 (8)	Os(1)-C(3)-O(3)	174 (1)
Os(1)-Os(2)-C(4)	87.1 (6)	C(7)-Os(3)-C(9)	91.2 (8)	Os(2)-C(4)-O(4)	177 (2)
Os(1)-Os(2)-C(5)	104.4 (5)	C(8)-Os(3)-C(9)	95.5 (7)	Os(2)-C(5)-O(5)	176 (1)
Os(1)-Os(2)-C(6)	160.7 (5)	Os(1)-S-Os(3)	71.3 (1)	Os(2)-C(6)-O(6)	173 (2)
Os(3)-Os(2)-N	86.3 (3)	Os(1)-S-C(17)	104.5 (5)	Os(3)-C(7)-O(7)	174 (2)
Os(3)-Os(2)-C(4)	89.1 (5)	Os(3)-S-C(17)	104.8 (5)	Os(3)-C(8)-O(8)	178 (2)
Os(3)-Os(2)-C(5)	165.3 (5)	S-C(17)-N	122 (1)	Os(3)-C(9)-O(9)	171 (2)
Os(3)-Os(2)-C(6)	99.8 (5)				

Table VI. Interatomic Distances (Å) with Esds for  $\text{HOs}_3(\mu_3\text{-S})(\mu\text{-HC=N-}p\text{-C}_6\text{H}_4\text{F})(\text{CO})_9$ , IIc

Os(1)-Os(2)	2.836 (1)	N-C(11)	1.36 (2)
Os(2)-Os(3)	2.988 (1)	C(11)-C(12)	1.37 (2)
Os(1)-S	2.422 (3)	C(12)-C(13)	1.40 (2)
Os(1)-N	2.205 (11)	C(13)-C(14)	1.36 (2)
Os(1)-C(1)	1.80 (2)	C(14)-C(15)	1.33 (2)
Os(1)-C(2)	1.92 (2)	C(15)-C(16)	1.40 (2)
Os(1)-C(3)	1.92 (1)	C(16)-C(11)	1.45 (2)
Os(2)-S	2.386 (4)	C(14)-F	1.38 (2)
Os(2)-C(4)	1.85 (2)	C(1)-O(1)	1.21 (2)
Os(2)-C(5)	1.88 (2)	C(2)-O(2)	1.16 (2)
Os(2)-C(6)	1.88 (1)	C(3)-O(3)	1.15 (1)
Os(3)-S	2.464 (4)	C(4)-O(4)	1.17 (2)
Os(3)-C(7)	1.84 (2)	C(5)-O(5)	1.14 (2)
Os(3)-C(8)	1.92 (2)	C(6)-O(6)	1.17 (2)
Os(3)-C(9)	1.91 (2)	C(7)-O(7)	1.20 (2)
Os(3)-C(17)	2.05 (1)	C(8)-O(8)	1.22 (2)
N-C(17)	1.213 (14)	C(9)-O(9)	1.14 (2)
Os(1)···Os(3)	3.779 (1)		

a bond order close to 1 while the carbon-nitrogen bond distance at 1.279 (13) Å implies a bond order of close to 2.

These molecules contrast structurally with the molecules  $\text{HOs}_3[\mu\text{-}\eta^2\text{-OC(H)NR}](\text{CO})_{10}$  formed by the reaction of  $\text{H}_2\text{Os}_3(\text{CO})_{10}$  with organoisonocyanates.<sup>6,19</sup> In these compounds the formamido ligand serves as a bridge across an edge of the cluster, but it is coordinated through both the oxygen and nitrogen atoms in a manner similar to the thioformamido ligand in Id (vide infra).

Compounds Ia-IVa lose 1 mol of CO upon photolysis from the unique metal atom of the cluster. The thioformamido ligand then becomes a triple bridge and five-electron donor when the lone pair of electrons on the nitrogen atom forms a coordinate bond to that metal atom. However, the coordination of this  $\sigma$ -lone pair of electrons does not significantly influence the  $\pi$  bonding in the thioformamido ligand. Thus, the  $\pi$ -electrons remain localized largely between the carbon and nitrogen atoms.

Addition of  $\text{P}(\text{CH}_3)_2\text{C}_6\text{H}_5$  to Ib converts the triply bridging thioformamido ligand into an edge bridging three electron donor in Id. However, in this compound the

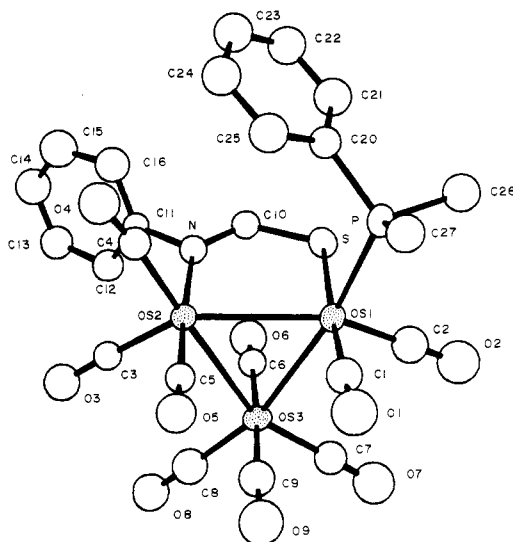


Figure 4. An ORTEP diagram of  $\text{HOs}_3[\mu\text{-}\eta^2\text{-SC(H)=NC}_6\text{H}_5](\text{CO})_9[\text{P}(\text{CH}_3)_2\text{C}_6\text{H}_5]$ , Id, showing 50% probability thermal-motion ellipsoids.

thioformamido ligand is coordinated via both the sulfur and nitrogen atoms and the sulfur atom is bonded to only one metal atom; see Scheme I. A shift of a carbonyl ligand between a pair of metal atoms has also accompanied the phosphine addition. The mechanism of the CO transfer was not established, but an intramolecular bridge-terminal process would seem to be the most probable.<sup>20</sup> In this coordination form the carbon-sulfur distance in the thioformamido ligand is shorter (1.69 (1) Å) than where the sulfur atom is coordinated to two metal atoms. At the same time, the carbon-nitrogen distance is longer. The bonding in this coordination form can be described as a mixture of the two resonance forms A and B and implies simply that the  $\pi$ -electron density is distributed across the three atoms S, C, and N. This was prevented in the S-

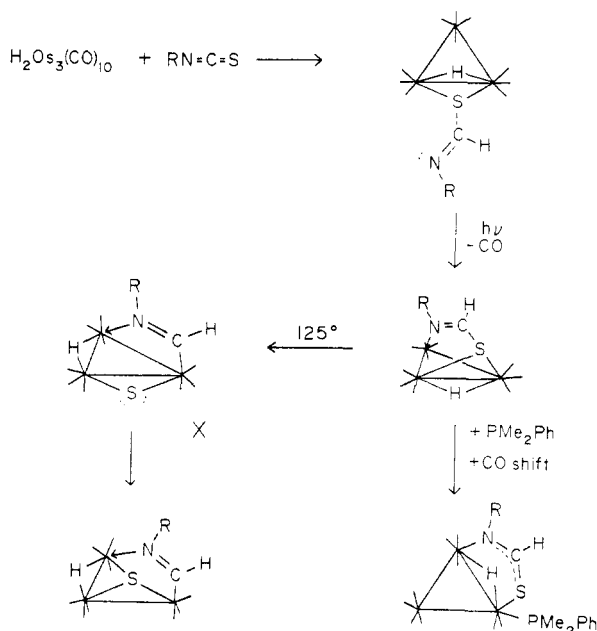
(20) (a) Band, E.; Muetterties, E. L. *Chem. Rev.* 1978, 78, 639. (b) Adams, R. D.; Cotton, F. A. In "Dynamic Nuclear Magnetic Resonance Spectroscopy"; Jackman, L. M., Cotton, F. A., Eds.; Academic Press: New York, 1975.

(19) Lin, Y. C.; Knobler, C. B.; Kaez, H. D. *J. Am. Chem. Soc.* 1981, 103, 1216.

Table VII. Interatomic Angles (deg) with Esds for  $\text{HOs}_3(\mu_3\text{-S})(\mu\text{-HC}=\text{N-}p\text{-C}_6\text{H}_4\text{F})(\text{CO})_9$ , IIc

Os(1)-Os(2)-Os(3)	80.88 (2)	S-Os(2)-C(4)	138.6 (5)	N-C(11)-C(12)	123 (1)
Os(2)-Os(1)-S	53.3 (1)	S-Os(2)-C(5)	99.4 (5)	C(11)-C(12)-C(13)	122 (1)
Os(2)-Os(1)-N	90.4 (2)	S-Os(2)-C(6)	113.2 (5)	C(12)-C(13)-C(14)	119 (2)
Os(2)-Os(1)-C(1)	91.0 (5)	C(4)-Os(2)-C(5)	96.3 (7)	C(13)-C(14)-C(15)	123 (2)
Os(2)-Os(1)-C(2)	158.0 (4)	C(4)-Os(2)-C(6)	104.1 (7)	C(14)-C(15)-C(16)	119 (2)
Os(2)-Os(1)-C(3)	103.6 (4)	C(5)-Os(2)-C(6)	92.5 (7)	C(15)-C(16)-C(11)	120 (1)
S-Os(1)-N	91.0 (2)	Os(2)-Os(3)-S	50.79 (9)	C(16)-C(11)-C(12)	116 (1)
S-Os(1)-C(1)	89.0 (4)	Os(2)-Os(3)-C(7)	150.5 (6)	N-C(11)-C(16)	120 (1)
S-Os(1)-C(2)	104.8 (4)	Os(2)-Os(3)-C(8)	90.6 (5)	F-C(14)-C(13)	117 (2)
S-Os(1)-C(3)	156.8 (4)	Os(2)-Os(3)-C(9)	117.4 (5)	F-C(14)-C(15)	119 (2)
N-Os(1)-C(1)	178.2 (5)	Os(2)-Os(3)-C(17)	86.9 (4)	Os(3)-C(17)-N	136 (1)
N-Os(1)-C(2)	88.7 (6)	S-Os(3)-C(7)	99.7 (6)	Os(1)-S-Os(2)	72.3 (1)
N-Os(1)-C(3)	89.3 (5)	S-Os(3)-C(8)	91.5 (6)	Os(1)-S-Os(3)	101.3 (1)
C(1)-Os(1)-C(2)	89.6 (7)	S-Os(3)-C(9)	168.2 (5)	Os(2)-S-Os(3)	76.0 (1)
C(1)-Os(1)-C(3)	91.5 (6)	S-Os(3)-C(17)	88.0 (4)	Os(1)-C(1)-O(1)	176 (1)
C(2)-Os(1)-C(3)	98.4 (6)	C(7)-Os(3)-C(8)	90.7 (7)	Os(1)-C(2)-O(2)	174 (1)
Os(1)-Os(2)-S	54.45 (8)	C(7)-Os(3)-C(9)	92.2 (7)	Os(1)-C(3)-O(3)	176 (1)
Os(1)-Os(2)-C(4)	87.4 (5)	C(7)-Os(3)-C(17)	92.3 (6)	Os(2)-C(4)-O(4)	179 (1)
Os(1)-Os(2)-C(5)	90.9 (5)	C(8)-Os(3)-C(9)	88.4 (7)	Os(2)-C(5)-O(5)	175 (1)
Os(1)-Os(2)-C(6)	167.6 (5)	C(8)-Os(3)-C(17)	177.1 (7)	Os(2)-C(6)-O(6)	171 (1)
Os(3)-Os(2)-S	53.17 (9)	C(9)-Os(3)-C(17)	91.5 (6)	Os(3)-C(7)-O(7)	176 (1)
Os(3)-Os(2)-C(4)	111.2 (6)	Os(1)-N-C(17)	118 (1)	Os(3)-C(8)-O(8)	169 (2)
Os(3)-Os(2)-C(5)	150.7 (5)	Os(1)-N-C(11)	114 (1)	Os(3)-C(9)-O(9)	178 (2)
Os(3)-Os(2)-C(6)	90.4 (5)				

Scheme I



bridged compounds because the lone pair of electrons on the sulfur atom, used to form the C-S double bond in A, was bonded to a second metal atom.

When heated, the compounds Ib-IVb are converted into the "open" cluster compounds Ic-IVc that contain triply bridging sulfido and edge bridging formimidoyl ligands. Their formation clearly involves the cleavage of the carbon-sulfur bond in the thioformamido ligand and one metal-metal bond in the cluster. A plausible sequence is shown in Scheme I. Cleavage of the carbon-sulfur bond is accompanied by formation of a metal-carbon bond to one of the adjacent osmium atoms. This could yield an intermediate like X containing edge bridging sulfido and formimidoyl ligands. Nucleophilic attack of the sulfido ligand on the third metal atom would then produce the triply bridging sulfido ligand and also induce cleavage of one of the metal-metal bonds.

It is important to recognize that it is the *trinuclear coordination* of the thioformamido ligand as found in compounds Ib-IVb that produces precisely the effects

Table VIII. Interatomic Distances with Esds for  $\text{HOs}_3[\mu\text{-SC}(\text{H})\text{NC}_6\text{H}_5](\text{CO})_9[\text{P}(\text{CH}_3)_2\text{C}_6\text{H}_5]_2$ , Id

Os(1)-Os(2)	2.963 (1)	C(14)-C(15)	1.33 (2)
Os(1)-Os(3)	2.936 (1)	C(15)-C(16)	1.37 (2)
Os(2)-Os(3)	2.909 (1)	C(16)-C(11)	1.38 (2)
Os(1)-S	2.446 (4)	P-C(20)	1.83 (1)
Os(1)-P	2.366 (4)	P-C(26)	1.82 (1)
Os(1)-C(1)	1.87 (2)	P-C(27)	1.84 (1)
Os(1)-C(2)	1.83 (2)	C(20)-C(21)	1.40 (2)
Os(2)-N	2.16 (1)	C(21)-C(22)	1.37 (2)
Os(2)-C(3)	1.89 (1)	C(22)-C(23)	1.37 (2)
Os(2)-C(4)	1.92 (2)	C(23)-C(24)	1.40 (2)
Os(2)-C(5)	1.91 (1)	C(24)-C(25)	1.38 (2)
Os(3)-C(6)	1.91 (2)	C(25)-C(20)	1.39 (2)
Os(3)-C(7)	1.90 (2)	C(1)-O(1)	1.17 (2)
Os(3)-C(8)	1.89 (1)	C(2)-O(2)	1.22 (2)
Os(3)-C(9)	1.89 (2)	C(3)-O(3)	1.15 (1)
C(10)-S	1.69 (1)	C(4)-O(4)	1.13 (2)
C(10)-N	1.32 (1)	C(5)-O(5)	1.14 (1)
N-C(11)	1.45 (1)	C(6)-O(6)	1.15 (2)
C(11)-C(12)	1.47 (2)	C(7)-O(7)	1.18 (2)
C(12)-C(13)	1.38 (2)	C(8)-O(8)	1.17 (1)
C(13)-C(14)	1.34 (2)	C(9)-O(9)	1.22 (2)

necessary to remove the sulfur atom from the thioformamido ligand. The two principal effects are (1) the lowering of the carbon-sulfur bond order toward 1 that is caused by the dinuclear coordination of the sulfur atom (the difference between the compounds IIb and Id reveals this effect most clearly) and (2) the coordination of the nitrogen atom to the third metal atom that brings the thioformamido ligand into a position where metal-carbon bond formation can occur immediately following or perhaps in concert with the carbon-sulfur bond cleavage. Since the bond distances and angles around the sulfur atom are similar both in IIa and IIb, the reactivity enhancement found in IIb may be largely entropic in nature. Ic-IVc lose CO and/or hydrogen when they are heated to reflux in octane solution for 1-3 h. A series of hexanuclear metal complexes formed by the combination two trinuclear species is produced.<sup>21</sup>

Recently, it was reported that the reaction of  $\text{Co}_2(\text{CO})_8$  with thioamides yields cluster complexes of the form  $\text{Co}_3(\mu_3\text{-S})(\mu\text{-R}^1\text{C}=\text{NR}^2)(\text{CO})_7$  ( $\text{R}^1 = \text{CH}_3, \text{C}_6\text{H}_5$ ;  $\text{R}^2 = \text{c}$

(21) Adams, R.; Dawoodi, Z.; Foust, D.; Segmuller, B. *J. Am. Chem. Soc.*, in press.

Table IX. Interatomic Angles (deg) with Esds for  $\text{HOs}_3[\mu\text{-SC}(\text{H})\text{NC}_6\text{H}_5](\text{CO})_9[\text{P}(\text{CH}_3)_2\text{C}_6\text{H}_5]_2$ , Id

Os(2)-Os(1)-Os(3)	59.09 (2)	N-Os(2)-C(5)	174.9 (4)	C(12)-C(13)-C(14)	122 (1)
Os(1)-Os(2)-Os(3)	60.00 (2)	C(3)-Os(2)-C(4)	94.9 (5)	C(13)-C(14)-C(15)	120 (2)
Os(1)-Os(3)-Os(2)	60.92 (2)	C(3)-Os(2)-C(5)	92.1 (5)	C(14)-C(15)-C(16)	123 (2)
Os(2)-Os(1)-S	86.72 (7)	C(4)-Os(2)-C(5)	92.2 (5)	C(15)-C(16)-C(11)	118 (1)
Os(2)-Os(1)-P	111.72 (9)	Os(1)-Os(3)-C(6)	90.6 (4)	Os(1)-P-C(20)	114.7 (4)
Os(2)-Os(1)-C(1)	95.1 (4)	Os(1)-Os(3)-C(7)	94.3 (4)	Os(1)-P-C(26)	115.7 (5)
Os(2)-Os(1)-C(2)	151.7 (4)	Os(1)-Os(3)-C(8)	161.7 (5)	Os(1)-P-C(27)	113.8 (5)
Os(3)-Os(1)-S	93.51 (8)	Os(1)-Os(3)-C(9)	91.0 (4)	C(20)-P-C(26)	105.1 (7)
Os(3)-Os(1)-P	170.71 (10)	Os(2)-Os(3)-C(6)	87.0 (4)	C(20)-P-C(27)	104.9 (7)
Os(3)-Os(1)-C(1)	91.0 (4)	Os(2)-Os(3)-C(7)	155.2 (4)	C(26)-P-C(27)	101.3 (6)
Os(3)-Os(1)-C(2)	93.7 (4)	Os(2)-Os(3)-C(8)	100.9 (5)	P-C(20)-C(21)	121 (1)
S-Os(1)-P	84.2 (1)	Os(2)-Os(3)-C(9)	91.2 (4)	P-C(20)-C(25)	119 (1)
S-Os(1)-C(1)	175.5 (4)	C(6)-Os(3)-C(7)	91.8 (6)	C(21)-C(20)-C(25)	120 (1)
S-Os(1)-C(2)	87.5 (5)	C(6)-Os(3)-C(8)	89.9 (16)	C(20)-C(21)-C(22)	119 (1)
P-Os(1)-C(1)	91.2 (4)	C(6)-Os(3)-C(9)	176.6 (5)	C(21)-C(22)-C(23)	121 (2)
P-Os(1)-C(2)	95.2 (5)	C(7)-Os(3)-C(8)	103.9 (6)	C(22)-C(23)-C(24)	121 (2)
C(1)-Os(1)-C(2)	92.8 (6)	C(7)-Os(3)-C(9)	91.0 (6)	C(23)-C(24)-C(25)	118 (1)
Os(1)-Os(2)-N	87.1 (2)	C(8)-Os(3)-C(9)	87.7 (6)	C(24)-C(25)-C(20)	121 (1)
Os(1)-Os(2)-C(3)	147.2 (4)	Os(1)-S-C(10)	108.9 (5)	Os(1)-C(1)-O(1)	177 (1)
Os(1)-Os(2)-C(4)	117.9 (3)	Os(2)-N-C(10)	127.1 (8)	Os(1)-C(2)-O(2)	178 (1)
Os(1)-Os(2)-C(5)	89.4 (3)	Os(2)-N-C(11)	118.0 (7)	Os(2)-C(3)-O(3)	175 (1)
Os(3)-Os(2)-N	94.2 (3)	N-C(10)-S	129 (1)	Os(2)-C(4)-O(4)	173 (1)
Os(3)-Os(2)-C(3)	87.3 (4)	C(10)-N-C(11)	115 (1)	Os(2)-C(5)-O(5)	175 (1)
Os(3)-Os(2)-C(4)	177.8 (4)	N-C(11)-C(12)	118 (1)	Os(3)-C(6)-O(6)	172 (1)
Os(3)-Os(2)-C(5)	87.2 (4)	N-C(11)-C(16)	123 (1)	Os(3)-C(7)-O(7)	178 (1)
N-Os(2)-C(3)	92.9 (5)	C(12)-C(11)-C(16)	119 (1)	Os(3)-C(8)-O(8)	174 (1)
N-Os(2)-C(4)	86.2 (5)	C(11)-C(12)-C(13)	116 (1)	Os(3)-C(9)-O(9)	175 (1)

$\text{C}_6\text{H}_{11}$ ).<sup>22</sup> However, since no intermediates were observed, the state of aggregation of the cluster that existed when the desulfurization occurred is not known.

The desulfurization of organic molecules is a reaction of particular interest in the purification of fossil fuels.<sup>23</sup> The most effective desulfurization catalysts are heterogeneous in nature. It is possible that a form of polynuclear coordination of the sulfur-containing molecules is an important component of the desulfurization reaction. Finally, organometallic complexes have recently attracted attention as desulfurization agents.<sup>24</sup>

### Experimental Section

**General Remarks.** Although the cluster complexes were generally air stable, reactions were routinely performed under a prepurified nitrogen atmosphere. Solvents were purified by distillation from sodium benzophenone (hexane, octane) or by storage over 4-Å molecular sieves and purging with nitrogen through a gas dispersion tube. *p*-Tolyl isothiocyanate and dimethylphenylphosphine were purchased, vacuum distilled, and stored under nitrogen before use.  $\text{H}_2\text{Os}_3(\text{CO})_{10}$ <sup>25</sup> was prepared by the reaction of  $\text{Os}_3(\text{CO})_{12}$ <sup>26</sup> with  $\text{H}_2$ .

Melting points were determined by using a Thomas-Hoover apparatus and are uncorrected. Infrared spectra were recorded on a Nicolet 7199 FT-IR spectrophotometer. Fourier transform <sup>1</sup>H NMR spectra were obtained at 270 MHz on a Bruker HX270 spectrometer. Photochemical reactions were run in Pyrex glassware utilizing a 100-W high-pressure mercury arc lamp. IR and <sup>1</sup>H NMR spectra and melting points of all the products are listed in Table I.

**Preparation of  $\text{HOs}_3[\mu\text{-}\eta^1\text{-SC}(\text{H})\text{NC}_6\text{H}_5](\text{CO})_{10}$  (Ia).** To a purple solution of  $\text{H}_2\text{Os}_3(\text{CO})_{10}$  (274 mg, 0.288 mmol) in hexane (25 mL) was added an excess (0.10 mL) of phenyl isothiocyanate over the course of 1 h. The solution turned yellow with the formation of a yellow precipitate. Following the addition, the

reaction mixture was stirred for an additional hour. The volume of the reaction mixture was reduced in vacuo to 5 mL and cooled to -20 °C. The mother liquor was decanted, and the yellow solid was washed with 2 × 10 mL of pentane at -20 °C. Following vacuum drying,  $\text{HOs}_3[\mu\text{-}\eta^1\text{-SC}(\text{H})\text{NC}_6\text{H}_5](\text{CO})_{10}$  (Ia) (251 mg, 81%) was obtained as a yellow powder.

**Preparation of  $\text{HOs}_3[\mu\text{-}\eta^1\text{-SC}(\text{H})\text{NR}](\text{CO})_{10}$  (R = *p*- $\text{C}_6\text{H}_4\text{F}$ , IIa; *p*- $\text{C}_6\text{H}_4\text{CH}_3$ , IIIa;  $\text{CH}_3$ , IVa).** Compounds IIa, IIIa, and IVa were prepared in a manner analogous to Ia by adding the appropriate organoisothoniocyanate to a hexane solution of  $\text{H}_2\text{Os}_3(\text{CO})_{10}$ . Compounds IIIa and IVa are slightly air sensitive: yields, IIa (86%), IIIa (64%), IVa (86%).

**Preparation of  $\text{HOs}_3[\mu_3\text{-}\eta^2\text{-SC}(\text{H})\text{NC}_6\text{H}_5](\text{CO})_9$  (Ib).** A yellow solution of Ia (106 mg, 0.107 mmol) in 60 mL of hexane was photolyzed with a mercury arc lamp for 1 h. The solution turned to an orange color with the evolution of gas. The solvent was removed in vacuo and the residue chromatographed on 12 thin silica plates, using a hexane/methylene chloride (9/1) eluent. Recrystallization of the orange band at -20 °C from a hexane/methylene chloride solution gave red, crystalline  $\text{HOs}_3[\mu_3\text{-}\eta^2\text{-SC}(\text{H})\text{NC}_6\text{H}_5](\text{CO})_9$  (63 mg, 61%). The reaction occurs similarly in a well-lit room over a period of days.<sup>9</sup> The reaction does not proceed in the dark.

**Preparation of  $\text{HOs}_3[\mu_3\text{-}\eta^2\text{-SC}(\text{H})\text{NR}](\text{CO})_9$  (R = *p*- $\text{C}_6\text{H}_4\text{F}$ , IIb; *p*- $\text{C}_6\text{H}_4\text{CH}_3$ , IIIb;  $\text{CH}_3$ , IVb).** The title compounds were prepared in photochemical reactions analogous to the preparation of Ib: yields, IIb (69%), IIIb (68%), IVb (63%).

**Preparation of  $\text{HOs}_3(\mu_3\text{-S})(\mu\text{-}\eta^2\text{-HCNC}_6\text{H}_5)(\text{CO})_9$  (Ic).** (a) **Thermolysis of  $\text{HOs}_3[\mu_3\text{-}\eta^2\text{-SC}(\text{H})\text{NC}_6\text{H}_5](\text{CO})_9$  (Ib).** An orange solution of  $\text{HOs}_3[\mu_3\text{-}\eta^2\text{-SC}(\text{H})\text{NC}_6\text{H}_5](\text{CO})_9$  (61 mg, 0.064 mmol) in octane (30 mL) was heated to reflux for 15 min and turned bright yellow in color. The solvent was removed in vacuo and the residue applied to six thin silica plates. Elution with hexane/methylene chloride (9/1) gave a large bright yellow band followed by two faint yellow bands. The first band was recrystallized from hexane/methylene chloride at -20 °C to yield yellow  $\text{HOs}_3(\mu_3\text{-S})(\mu\text{-}\eta^2\text{-HCNC}_6\text{H}_5)(\text{CO})_9$  (Ic) (25 mg, 41%). The two faint yellow bands were found to consist of two isomers of  $\text{H}_2\text{Os}_6(\mu_4\text{-S})(\mu_3\text{-S})(\mu\text{-HCNC}_6\text{H}_5)_2(\text{CO})_{17}$ . When the mixture was refluxed for longer periods, hexanuclear species formed from Ic become the principal products.<sup>21</sup>

(b) **Thermolysis of  $\text{HOs}_3[\mu\text{-}\eta^1\text{-SC}(\text{H})\text{NC}_6\text{H}_5](\text{CO})_{10}$  (Ia).** A solution of  $\text{HOs}_3[\mu\text{-}\eta^1\text{-SC}(\text{H})\text{NC}_6\text{H}_5](\text{CO})_{10}$  (111 mg, 0.114 mmol) in octane (25 mL) was heated to reflux for 3 h. The solvent was removed in vacuo, and the reaction mixture was chromatographed on silica gel plates. Hexane/methylene chloride (9/1) eluted a bright yellow band of Ic (70 mg, 65%).

(22) Patin, H.; Mignani, G.; Mahe, C.; LeMarouille, J. Y.; Benoit, A.; Grandjean, D.; Levesque, G. *J. Organomet. Chem.* 1981, 208, C39.

(23) Schuman, S. C.; Shalit, H. *Catal. Rev.* 1970, 4, 245.

(24) (a) DuBois, M. R.; VanDerveer, M. C.; DuBois, D. L.; Halthiwanger, R. C.; Miller, W. R. *J. Am. Chem. Soc.* 1980, 102, 7456. (b) Alper, H.; Paik, H. *J. Org. Chem.* 1977, 42, 3522.

(25) Knox, S. A. R.; Koepke, J. W.; Andrews, M. A.; Kaesz, H. D. *J. Am. Chem. Soc.* 1975, 97, 3942.

(26) Johnson, B. F. G.; Lewis, J.; Kilty, P. A. *J. Chem. Soc. A* 1968, 2859.

Table X. Crystallographic Data for X-ray Diffraction Studies

	IIa	IIb	IIc	Id
(A) Crystal Data				
formula	Os <sub>3</sub> SFO <sub>10</sub> NC <sub>17</sub> H <sub>6</sub>	Os <sub>3</sub> SFO <sub>9</sub> NC <sub>16</sub> H <sub>6</sub>	Os <sub>3</sub> SFO <sub>9</sub> NC <sub>16</sub> H <sub>6</sub>	Os <sub>3</sub> SPO <sub>9</sub> NC <sub>24</sub> H <sub>18</sub>
temp, ± 5 °C	28	25	25	25
space group	<i>P</i> 2 <sub>1</sub> / <i>n</i>	<i>P</i> 2 <sub>1</sub> / <i>c</i>	<i>P</i> 2 <sub>1</sub> / <i>n</i>	<i>P</i> <i>bca</i>
<i>a</i> , Å	13.068 (4)	12.545 (4)	11.562 (2)	8.140 (1)
<i>b</i> , Å	12.230 (3)	10.345 (2)	16.879 (3)	20.711 (3)
<i>c</i> , Å	14.517 (4)	17.906 (6)	11.952 (4)	34.150 (4)
β, deg	100.67 (2)	110.21 (3)	111.65 (3)	
<i>V</i> , Å <sup>3</sup>	2279.9 (19)	2181 (2)	2168 (2)	5757 (2)
<i>M<sub>r</sub></i>	1005.9	977.9	977.89	1098.1
ρ <sub>calcd</sub> , g/cm <sup>3</sup>	2.93	2.98	3.00	2.53
<i>Z</i>	4	4	4	8
(B) Measurement of Intensity Data				
radiation	Mo Kα (0.71073 Å)	Mo Kα	Mo Kα	Mo Kα
monochromator	graphite	graphite	graphite	graphite
detector aperture, mm				
horizontal ( <i>A</i> + <i>B</i> tan θ)				
<i>A</i>	3.0	3.0	3.0	3.0
<i>B</i>	1.0	1.0	1.0	1.0
vertical	4.0	4.0	4.0	4.0
cryst faces	101, $\bar{1}0\bar{1}$ , 12 $\bar{1}$ $\bar{1}\bar{2}\bar{1}$ , $\bar{1}\bar{1}\bar{1}$ , 1 $\bar{1}\bar{1}$	100, $\bar{1}00$ , 0 $\bar{1}\bar{1}$ 0 $\bar{1}\bar{1}$ , 011, 0 $\bar{1}\bar{1}$	$\bar{1}0\bar{1}$ , 10 $\bar{1}$ , $\bar{1}\bar{1}0\bar{1}$ 010, 101	0 $\bar{2}\bar{1}$ , 02 $\bar{1}$ , 0 $\bar{2}\bar{1}$ 021, $\bar{1}0\bar{2}$ , 20 $\bar{1}$
cryst size, mm	0.17 × 0.36 × 0.25	0.21 × 0.15 × 0.21	0.30 × 0.08 × 0.45	0.64 × 0.08 × 0.26
cryst orientatn, direction;	normal to 111;	normal to 101;	normal to 101;	normal to 201;
deg from φ axis	1.75	5.1	4.7	3.6
reflectns measd	<i>h, k, ±l</i>	<i>h, k, ±l</i>	<i>h, k, ±l</i>	<i>h, k, l</i>
max 2θ, deg	50	50	49	50
scan type		moving crystal-stationary counter		
ω scan width, <i>A</i> + 0.347	0.90	0.90	0.95	1.00
tan θ				
<i>A</i> , deg				
bkgnd		one-fourth additional scan at each end of scan		
ω scan rate (variable)				
max/min, deg	10.0	10.0	10.0	10.0
min/min, deg	1.3	1.3	1.4	1.7
no. of reflectns measd	4367	4207	3864	5640
data used ( <i>F</i> <sup>2</sup> ≥ 3.0σ( <i>F</i> ) <sup>2</sup> )	2968	2252	2314	2556
(C) Treatment of Data				
abs correctn				
coeff, cm <sup>-1</sup>	178.9	186.9	188.0	134.0
grid	10 × 10 × 10	8 × 8 × 12	14 × 4 × 16	14 × 8 × 8
transmission coeff				
max	0.10	0.20	0.340	0.51
min	0.01	0.07	0.015	0.13
decay correctn				
max	1.06			
min	0.99			
av	1.02			
<i>P</i> factor	0.01	0.02	0.005	0.01
final residuals <i>R</i>	0.042	0.051	0.063	0.036
<i>R<sub>w</sub></i>	0.046	0.056	0.067	0.033
esd of unit weight	2.74	2.49	4.21	1.72
largest shift/error	0.14	0.20	0.04	0.01
value on final cycle				
largest peaks in final	0.68	1.49		1.55
difference fourier, e/Å <sup>3</sup>				

**Preparation of HO<sub>3</sub>(μ<sub>3</sub>-S)(μ-η<sup>2</sup>-HCNR)(CO)<sub>9</sub> (R = *p*-C<sub>6</sub>H<sub>4</sub>F, IIc; *p*-C<sub>6</sub>H<sub>4</sub>CH<sub>3</sub>, IIIc; CH<sub>3</sub>, IVc).** The title compounds were prepared by using methods analogous to those utilized in the synthesis of Ic. Yields from the thermolysis of HO<sub>3</sub>[μ<sub>3</sub>-η<sup>2</sup>-SC(H)NR](CO)<sub>9</sub>: IIc (62%), IIIc (75%), IVc (55%). Yields from the thermolysis of HO<sub>3</sub>[μ-η<sup>1</sup>-SC(H)NR](CO)<sub>10</sub>: IIc (43%); IIIc (26%), IVc (46%). In addition to IIIc and IVc, compounds of the type H<sub>2</sub>Os<sub>8</sub>(μ<sub>4</sub>-S)(μ<sub>3</sub>-S)(μ-HCNR)<sub>2</sub>(CO)<sub>17</sub> (R = *p*-C<sub>6</sub>H<sub>4</sub>CH<sub>3</sub>, IIIe; CH<sub>3</sub>, IVe) were obtained in yields of approximately 5%. Thermolysis of IIb (136 mg, 0.139 mmol) in refluxing hexane (40 mL) for 22 h followed by chromatographic separation on thin silica plates resulted in IIc (73 mg, 54%).

**Preparation of HO<sub>3</sub>[μ-η<sup>2</sup>-SC(H)NC<sub>6</sub>H<sub>5</sub>](CO)<sub>9</sub>[P-(CH<sub>3</sub>)<sub>2</sub>C<sub>6</sub>H<sub>5</sub>] (Id).** To an orange solution of HO<sub>3</sub>[μ<sub>3</sub>-η<sup>2</sup>-SC(H)NC<sub>6</sub>H<sub>5</sub>](CO)<sub>9</sub> (120 mg, 0.125 mmol) in hexane/methylene chloride (9/1, 40 mL) was added dimethylphenylphosphine (50

μL). The solution was stirred for 15 min. The solvent was removed in vacuo, and the reaction mixture was separated (T1C) on silica plates. During this time it became yellow and a heavy yellow precipitate formed. Elution with hexane/methylene chloride (1/1) produced one bright yellow band. Recrystallization from hexane/methylene chloride at -20 °C gave HO<sub>3</sub>[μ-η<sup>2</sup>-SC(H)NC<sub>6</sub>H<sub>5</sub>](CO)<sub>9</sub>[P(CH<sub>3</sub>)<sub>2</sub>C<sub>6</sub>H<sub>5</sub>] (120 mg, 81%).

**Crystallographic Analysis.** Crystals of IIa suitable for diffraction analyses were obtained by slow evaporation of hexane/methylene chloride solutions at room temperature. Crystals of IIb were grown by slowly cooling hot hexane solutions. Crystals of IIIb were formed by slow crystallization of hexane solutions at 5 °C. Suitable crystals of Id were obtained by slow evaporation of hexane/methylene chloride solutions at 5 °C. The crystals were mounted in thin-walled glass capillaries. Diffraction measurements were made on an Enraf-Nonius CAD-4 fully automated

four-circle diffractometer using graphite-monochromatized Mo  $K\alpha$  radiation. Unit cells were determined and refined from 25 randomly selected reflections obtained by using the CAD-4 automatic search, center, index, and least-squares routines. The space groups for all the structures were identified uniquely from systematic absences observed during data collection. Crystal data and data collection parameters are listed in Table X. All data processing was performed on a Digital PDP 11/45 computer using the Enraf-Nonius SDP program library (Version 16). Absorption corrections of a Gaussian integration type were done for both structures. Neutral atom scattering factors were calculated by the standard procedures.<sup>27a</sup> Anomalous dispersion corrections were applied to all non-hydrogen atoms.<sup>27b</sup> Full-matrix least-squares refinements minimized the function  $\sum_{hkl} w(|F_o| - |F_c|)^2$ , where  $w = 1/\sigma(F)^2$ ,  $\sigma(F) = \sigma(F_o^2)/2F_o$ , and  $\sigma(F_o^2) = [\sigma(I_{raw})^2 + (PF_o^2)^2]^{1/2}/Lp$ . For all structures the positions of hydrogen atoms bonded to carbon atoms were calculated. Contributions from scattering by these atoms were included in structure factor calculations, but their positions were not refined. Hydride ligands were not observed and were ignored.

The structure of IIa was solved by a combination of Patterson and difference Fourier techniques. Only the osmium, sulfur, and fluorine atoms were refined anisotropically. Interatomic distances and angles with errors obtained from the inverse matrix obtained from the final cycle of least-squares refinement are listed in Tables II and III. Fractional atomic coordinates, thermal parameters, and structure factor amplitudes are available.<sup>28</sup>

The structure of IIb was solved by a combination of direct methods and difference Fourier techniques. The three metal atoms were located in an electron-density map based on the phasing (MULTAN) of 178 reflections ( $E_{min} \geq 1.70$ ). Only the osmium, sulfur, and fluorine atoms were refined anisotropically.

(27) "International Tables for X-ray Crystallography", Kynoch Press: Birmingham, England, 1975; Vol. IV: (a) Table 2.2B, pp 99-101; (b) Table 2.3.1, pp 149-150.

(28) See supplementary material.

Tables IV and V list interatomic distance and angles with estimated standard deviations. Fractional atomic coordinates, thermal parameters, and structure factor amplitudes are available.<sup>28</sup>

The structure of Ic was solved by a combination of Patterson and difference Fourier techniques. Only the osmium, sulfur, and fluorine atoms were refined anisotropically. Interatomic distances and angles with estimated standard deviations are listed in Tables VI and VII. Fractional atomic coordinates, thermal parameters, and structure factor amplitudes are available.<sup>28</sup>

The structure of Id was solved by a combination of direct methods and difference Fourier techniques. The three metal atoms were located in an electron-density map based on the phasing (MULTAN) of 256 reflections ( $E_{min} \geq 1.53$ ). All atoms heavier than oxygen were refined anisotropically. Tables VIII and IX list interatomic distances and angles with estimated standard deviations. Fractional atomic coordinates, thermal parameters, and structure factor amplitudes are available.<sup>28</sup>

**Acknowledgment.** This work was supported by the Office of Basic Energy Sciences of the U.S. Department of Energy under Contract No. DE-AC-2-78ER04900 and the Alfred P. Sloan Foundation through a fellowship to R.D.A. NMR studies were supported in part under Grant No. CHE-7916210 from the Chemistry Division of the National Science Foundation. We also wish to thank Engelhard Industries for a loan of osmium tetroxide.

**Registry No.** Ia, 84027-35-0; Ib, 84040-46-0; Ic, 84027-40-7; Id, 84027-43-0; IIa, 79737-56-7; IIb, 79994-14-2; IIc, 84027-41-8; IIIa, 84027-36-1; IIIb, 84027-38-3; IIIc, 84027-42-9; IVa, 84027-37-2; IVb, 84027-39-4; IVc, 84027-44-1;  $H_2Os_3(CO)_{10}$ , 41766-80-7;  $PhN=C=S$ , 103-72-0;  $FC_6H_4-p-N=C=S$ , 1544-68-9;  $MeC_6H_4-p-N=C=S$ , 622-59-3;  $MeN=C=S$ , 556-61-6.

**Supplementary Material Available:** Final fractional atomic coordinates, thermal parameters, and structure factor amplitudes for all four structures (49 pages). Ordering information is given on any current masthead page.

## Quadruply Bridging Sulfido Ligands. The Crystal and Molecular Structure of $Os_6(CO)_{18}(\mu_4-S)_2(\mu-HC=NPh)_2$

Richard D. Adams\* and Donald F. Foust

Department of Chemistry, Yale University, New Haven, Connecticut 06511

Received September 13, 1982

The crystal and molecular structure of the compound  $Os_6(CO)_{18}(\mu_4-S)_2(\mu-HC=NPh)_2$  has been determined by single-crystal X-ray diffraction methods: space group  $P2_1/c$ , No. 14,  $a = 9.504$  (1) Å,  $b = 23.440$  (5) Å,  $c = 19.538$  (3) Å,  $\beta = 92.10$  (1)°,  $V = 4349$  (2) Å<sup>3</sup>,  $Z = 4$ ,  $\rho_{calcd} = 2.93$  g/cm<sup>3</sup>. The structure was solved by a combination of direct methods and difference Fourier techniques. Full-matrix least-squares refinement on 2848 reflections ( $F_o \geq 3.0\sigma(F^2)$ ) yielded the final residuals  $R = 0.032$  and  $R_w = 0.028$ . The molecule consists of six osmium atoms arranged into three groups of two. Each pair contains a metal-metal bond. The three Os-Os bonding distances are 2.752 (1), 2.752 (1), and 2.756 (1) Å. Two quadruply bridging sulfido ligands each bridge two groups of two metal atoms. They have distorted tetrahedral (approximate  $D_{2d}$ ) geometries and serve as six-electron donors. Two  $\eta^2-N$ -phenylformimidoyl ligands bridge two pairs of metal atoms. Each metal atom contains three linear terminal carbonyl ligands.

### Introduction

Due to its ability to serve as a multicoordinate, multielectron donor, the bridging sulfido ligand has been of great value in the synthesis of transition-metal cluster compounds.<sup>1-10</sup> When bonded to four metal atoms, it can

serve either as a four-electron donor, I, or a six-electron donor, II. In the latter case the sulfido ligand has tetra-

(2) (a) Richter, F.; Vahrenkamp, H. *Angew. Chem., Int. Ed. Engl.* 1980, 19, 65. (b) Richter, F.; Vahrenkamp, H. *Ibid.* 1979, 18, 531. (c) Vahrenkamp, H.; Wucherer, E. J. *Ibid.* 1981, 20, 680.

(3) Nelson, L. L.; Lo, F. Y.; Rae, A. D.; Dahl, L. F. *J. Organomet. Chem.* 1982, 225, 309.

(1) Vahrenkamp, H. *Angew. Chem., Int. Ed. Engl.* 1975, 14, 322.

## Quadruply bridging sulfido ligands. The crystal and molecular structure of $\text{Os}_6(\text{CO})_{18}(\mu_4\text{-S})_2(\mu\text{-HC:NPh})_2$

Richard D. Adams, and Donald F. Foust

*Organometallics*, **1983**, 2 (2), 323-327 • DOI: 10.1021/om00074a020 • Publication Date (Web): 01 May 2002

Downloaded from <http://pubs.acs.org> on April 24, 2009

### More About This Article

---

The permalink <http://dx.doi.org/10.1021/om00074a020> provides access to:

- Links to articles and content related to this article
- Copyright permission to reproduce figures and/or text from this article



**ACS Publications**  
High quality. High impact.

four-circle diffractometer using graphite-monochromatized Mo  $K\alpha$  radiation. Unit cells were determined and refined from 25 randomly selected reflections obtained by using the CAD-4 automatic search, center, index, and least-squares routines. The space groups for all the structures were identified uniquely from systematic absences observed during data collection. Crystal data and data collection parameters are listed in Table X. All data processing was performed on a Digital PDP 11/45 computer using the Enraf-Nonius SDP program library (Version 16). Absorption corrections of a Gaussian integration type were done for both structures. Neutral atom scattering factors were calculated by the standard procedures.<sup>27a</sup> Anomalous dispersion corrections were applied to all non-hydrogen atoms.<sup>27b</sup> Full-matrix least-squares refinements minimized the function  $\sum_{hkl} w(|F_o| - |F_c|)^2$ , where  $w = 1/\sigma(F)^2$ ,  $\sigma(F) = \sigma(F_o^2)/2F_o$ , and  $\sigma(F_o^2) = [\sigma(I_{raw})^2 + (PF_o^2)^2]^{1/2}/Lp$ . For all structures the positions of hydrogen atoms bonded to carbon atoms were calculated. Contributions from scattering by these atoms were included in structure factor calculations, but their positions were not refined. Hydride ligands were not observed and were ignored.

The structure of IIa was solved by a combination of Patterson and difference Fourier techniques. Only the osmium, sulfur, and fluorine atoms were refined anisotropically. Interatomic distances and angles with errors obtained from the inverse matrix obtained from the final cycle of least-squares refinement are listed in Tables II and III. Fractional atomic coordinates, thermal parameters, and structure factor amplitudes are available.<sup>28</sup>

The structure of IIb was solved by a combination of direct methods and difference Fourier techniques. The three metal atoms were located in an electron-density map based on the phasing (MULTAN) of 178 reflections ( $E_{min} \geq 1.70$ ). Only the osmium, sulfur, and fluorine atoms were refined anisotropically.

(27) "International Tables for X-ray Crystallography", Kynoch Press: Birmingham, England, 1975; Vol. IV: (a) Table 2.2B, pp 99-101; (b) Table 2.3.1, pp 149-150.

(28) See supplementary material.

Tables IV and V list interatomic distance and angles with estimated standard deviations. Fractional atomic coordinates, thermal parameters, and structure factor amplitudes are available.<sup>28</sup>

The structure of Ic was solved by a combination of Patterson and difference Fourier techniques. Only the osmium, sulfur, and fluorine atoms were refined anisotropically. Interatomic distances and angles with estimated standard deviations are listed in Tables VI and VII. Fractional atomic coordinates, thermal parameters, and structure factor amplitudes are available.<sup>28</sup>

The structure of Id was solved by a combination of direct methods and difference Fourier techniques. The three metal atoms were located in an electron-density map based on the phasing (MULTAN) of 256 reflections ( $E_{min} \geq 1.53$ ). All atoms heavier than oxygen were refined anisotropically. Tables VIII and IX list interatomic distances and angles with estimated standard deviations. Fractional atomic coordinates, thermal parameters, and structure factor amplitudes are available.<sup>28</sup>

**Acknowledgment.** This work was supported by the Office of Basic Energy Sciences of the U.S. Department of Energy under Contract No. DE-AC-2-78ER04900 and the Alfred P. Sloan Foundation through a fellowship to R.D.A. NMR studies were supported in part under Grant No. CHE-7916210 from the Chemistry Division of the National Science Foundation. We also wish to thank Engelhard Industries for a loan of osmium tetroxide.

**Registry No.** Ia, 84027-35-0; Ib, 84040-46-0; Ic, 84027-40-7; Id, 84027-43-0; IIa, 79737-56-7; IIb, 79994-14-2; IIc, 84027-41-8; IIIa, 84027-36-1; IIIb, 84027-38-3; IIIc, 84027-42-9; IVa, 84027-37-2; IVb, 84027-39-4; IVc, 84027-44-1; H<sub>2</sub>O<sub>3</sub>(CO)<sub>10</sub>, 41766-80-7; PhN=C=S, 103-72-0; FC<sub>6</sub>H<sub>4</sub>-*p*-N=C=S, 1544-68-9; MeC<sub>6</sub>H<sub>4</sub>-*p*-N=C=S, 622-59-3; MeN=C=S, 556-61-6.

**Supplementary Material Available:** Final fractional atomic coordinates, thermal parameters, and structure factor amplitudes for all four structures (49 pages). Ordering information is given on any current masthead page.

## Quadruply Bridging Sulfido Ligands. The Crystal and Molecular Structure of Os<sub>6</sub>(CO)<sub>18</sub>(μ<sub>4</sub>-S)<sub>2</sub>(μ-HC=NPh)<sub>2</sub>

Richard D. Adams\* and Donald F. Foust

Department of Chemistry, Yale University, New Haven, Connecticut 06511

Received September 13, 1982

The crystal and molecular structure of the compound Os<sub>6</sub>(CO)<sub>18</sub>(μ<sub>4</sub>-S)<sub>2</sub>(μ-HC=NPh)<sub>2</sub> has been determined by single-crystal X-ray diffraction methods: space group  $P2_1/c$ , No. 14,  $a = 9.504$  (1) Å,  $b = 23.440$  (5) Å,  $c = 19.538$  (3) Å,  $\beta = 92.10$  (1)°,  $V = 4349$  (2) Å<sup>3</sup>,  $Z = 4$ ,  $\rho_{calcd} = 2.93$  g/cm<sup>3</sup>. The structure was solved by a combination of direct methods and difference Fourier techniques. Full-matrix least-squares refinement on 2848 reflections ( $F_o \geq 3.0\sigma(F^2)$ ) yielded the final residuals  $R = 0.032$  and  $R_w = 0.028$ . The molecule consists of six osmium atoms arranged into three groups of two. Each pair contains a metal-metal bond. The three Os-Os bonding distances are 2.752 (1), 2.752 (1), and 2.756 (1) Å. Two quadruply bridging sulfido ligands each bridge two groups of two metal atoms. They have distorted tetrahedral (approximate  $D_{2d}$ ) geometries and serve as six-electron donors. Two η<sup>2</sup>-*N*-phenylformimidoyl ligands bridge two pairs of metal atoms. Each metal atom contains three linear terminal carbonyl ligands.

### Introduction

Due to its ability to serve as a multicoordinate, multi-electron donor, the bridging sulfido ligand has been of great value in the synthesis of transition-metal cluster compounds.<sup>1-10</sup> When bonded to four metal atoms, it can

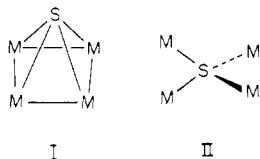
serve either as a four-electron donor, I, or a six-electron donor, II. In the latter case the sulfido ligand has tetra-

(1) Vahrenkamp, H. *Angew. Chem., Int. Ed. Engl.* 1975, 14, 322.

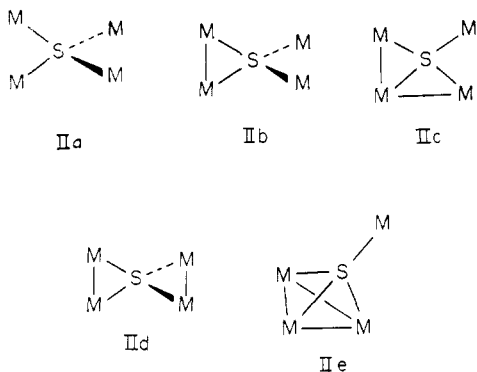
(2) (a) Richter, F.; Vahrenkamp, H. *Angew. Chem., Int. Ed. Engl.* 1980, 19, 65. (b) Richter, F.; Vahrenkamp, H. *Ibid.* 1979, 18, 531. (c) Vahrenkamp, H.; Wucherer, E. J. *Ibid.* 1981, 20, 680.

(3) Nelson, L. L.; Lo, F. Y.; Rae, A. D.; Dahl, L. F. *J. Organomet. Chem.* 1982, 225, 309.





hedral geometry<sup>1</sup> or slightly distorted tetrahedral geometry when accompanied by various degrees of metal-metal bonding IIb,<sup>11,12</sup> IIc,<sup>8,13,14</sup> IId,<sup>11,15</sup> IIe.<sup>16</sup> At least one example of each of the forms IIa–IIe has now been reported. In the presence of a metal-metal bond the M–S–M angle is fairly acute and lies generally in the range 65–75°. In these cases the remaining unsupported M–S–M angles are then fairly large and lie in the range 125–140°.



Recently we have been investigating the role of sulfido ligands in synthesis of high nuclearity metal carbonyl cluster compounds via cluster condensation reactions.<sup>11,14,17,18</sup> We have found that the thermolysis of  $\text{HO}_3(\text{CO})_9(\mu_3\text{-S})(\mu\text{-HC=NPh})$ , III, in octane yields a number of high nuclearity sulfido osmium carbonyl cluster compounds through a sequence of decarbonylations and cluster condensation processes.<sup>11,17</sup> A minor product, formed by the combination of 2 equiv of III and a loss of 1 equiv of  $\text{H}_2$ , is  $\text{Os}_6(\text{CO})_{18}(\mu_4\text{-S})_2(\mu\text{-HC=NPh})_2$ , IV, which contains two sulfido ligands of the structural type IId. The crystal and molecular structure of IV is reported herein.

(4) Vidal, J. L.; Fiato, R. A.; Cosby, L. A.; Pruett, R. L. *Inorg. Chem.* 1978, 17, 2574.

(5) Ghilardi, C. A.; Midollini, S.; Sacconi, L. *J. Chem. Soc., Chem. Commun.* 1981, 47.

(6) Gullevic, J.; Bars, O.; Grandjean, P. *Acta Crystallogr., Sect. B* 1976, B32, 1338, 1342.

(7) Bor, G.; Dietler, U. K.; Stanghellini, P. L.; Gervasio, G.; Rossetti, R.; Sbrignadello, G.; Battiston, G. *J. Organomet. Chem.* 1981, 213, 277.

(8) Vergamini, P. J.; Vahrenkamp, J.; Dahl, L. F. *J. Am. Chem. Soc.* 1971, 93, 6327.

(9) (a) Müller, A.; Bögge, J.; Schimanski, U. *J. Chem. Soc., Chem. Commun.* 1980, 91. (b) Müller, A.; Bögge, H.; Tolle, H. G.; Jostes, R.; Schimanski, U.; Dartmann, M. *Angew. Chem., Int. Ed. Engl.* 1980, 19, 654.

(10) Wolff, T. E.; Berg, J. M.; Power, P. P.; Hodgson, K. O.; Holm, R. H. *Inorg. Chem.* 1980, 19, 430.

(11) Adams, R. D.; Dawoodi, Z.; Foust, D. F. *Organometallics* 1982, 1, 411.

(12) Kullmer, V.; Rottinger, E.; Vahrenkamp, H. *J. Chem. Soc., Chem. Commun.* 1977, 782.

(13) Seyferth, D.; Henderson, R. S.; Fackler, J. P.; Mazany, A. M. *J. Organomet. Chem.* 1981, 213, C21.

(14) Adams, R. D.; Foust, D. F.; Segmüller, B. E. *Organometallics*, preceding article in this issue.

(15) Coleman, J. M.; Wojcicki, A.; Pollick, P. J.; Dahl, L. F. *Inorg. Chem.* 1967, 6, 1236.

(16) Adams, R. D.; Männig, D.; Segmüller, B. E. *Organometallics* 1983, 2, 149.

(17) Adams, R. D.; Dawoodi, Z.; Foust, D. F.; Segmüller, B. E. *Organometallics*, preceding article in this issue.

(18) Adams, R. D.; Horvath, I. T.; Yang, L. W. *J. Am. Chem. Soc.*, in press.

Table I. Crystallographic Data for X-ray Diffraction Study

(A) Crystal Data	
formula	$\text{Os}_6\text{S}_2\text{O}_{18}\text{N}_2\text{C}_{32}\text{H}_{14}$
temp, $\pm 5^\circ\text{C}$	25
space group	$P2_1/c$
a, Å	9.504 (1)
b, Å	23.440 (5)
c, Å	19.538 (3)
$\beta$ , deg	92.10 (1)
V, Å <sup>3</sup>	4349 (2)
$M_r$	1919.8
Z	4
$\rho_{\text{calcd}}$ , g/cm <sup>3</sup>	2.93
(B) Measurement of Intensity Data	
radiation	Mo $K\alpha$ (0.710 73 Å)
monochromator	graphite
detector aperture, mm	
horizontal (A + B tan $\theta$ )	
A	3.0
B	1.0
vertical	4.0
cryst faces	010, 0 $\bar{1}$ 0, 01 $\bar{1}$ , 0 $\bar{1}$ 1
	021, 0 $\bar{2}$ 1, 100, 100
cryst size, mm	0.340 × 0.033 × 0.096
cryst orientatn	normal to 100; 4.46
directn; deg from $\phi$ axis	
reflectns measd	–h, k, $\pm$ l
max 2 $\theta$ , deg	45
scan type	moving
	crystal-stationary
	counter
$\omega$ scan width:	A = 0.85
A + 0.347 tan $\theta$	
background	one-fourth additional scan at each end of scan
$\omega$ scan rate (variable)	
max/min, deg	10.0
min/min, deg	1.4
no. of reflectns	2848
( $F^2 \geq 3.0\sigma(F^2)$ )	
(C) Treatment of Data	
absorption correctn	
coeff, cm <sup>-1</sup>	187.2
grid	14 × 10 × 6
transmissn coeff	
max	0.5815
min	0.2445
P factor	0.010
final residuals R	0.032
$R_w$	0.028
esd of unit weight	1.355
largest shift/error	0.04
value on final cycle	
largest peaks in final difference fourier, e/Å <sup>3</sup>	0.50

## Experimental Section

The synthesis of IV was reported previously.<sup>17</sup> Yellow crystals of IV, suitable for X-ray diffraction measurements, were grown by slow evaporation of a hexane/methylene chloride solution at room temperature. The data crystal was mounted in a thin-walled glass capillary. Diffraction measurements were made on Enraf-Nonius CAD-4 fully automated four-circle diffractometer using graphite-monochromatized Mo  $K\alpha$  radiation. The unit cell was determined and refined from 25 randomly selected reflections obtained by using the CAD-4 automatic search, center, index, and least-squares routines. Crystal data and data collection parameters are listed in Table I. All data processing was performed on a Digital Equipment Corp. PDP 11/45 computer using the Enraf-Nonius SDP program library (Version 16). An absorption correction of a Gaussian integration type was applied to all the data. Neutral atom scattering factors were calculated by the

Table II. Positional and Thermal Parameters and Their Estimated Standard Deviations for  $\text{Os}_6(\text{CO})_{18}(\mu_4\text{-S})_2(\mu\text{-HC=NPh})_2$ , IV<sup>a</sup>

atom	x	y	z	B(1,1)	B(2,2)	B(3,3)	B(1,2)	B(1,3)	B(2,3)
Os1	0.13792 (8)	0.38420 (4)	0.03287 (4)	2.75 (4)	2.63 (4)	2.66 (3)	0.44 (4)	0.35 (3)	0.24 (4)
Os2	0.22723 (8)	0.27282 (4)	0.04446 (4)	2.75 (4)	2.44 (4)	3.30 (3)	0.38 (4)	0.49 (3)	-0.12 (4)
Os3	0.48931 (8)	0.38030 (4)	0.18637 (4)	2.17 (3)	3.81 (5)	3.53 (4)	0.13 (4)	0.34 (4)	-0.06 (4)
Os4	0.26156 (9)	0.33615 (4)	0.25140 (4)	2.87 (4)	2.83 (4)	2.71 (3)	0.07 (4)	0.29 (3)	0.40 (4)
Os5	0.36509 (9)	0.50368 (4)	0.33580 (4)	3.33 (4)	3.74 (5)	3.21 (3)	-0.76 (4)	-0.04 (3)	-0.50 (4)
Os6	0.16939 (9)	0.52136 (4)	0.23031 (4)	3.85 (4)	2.79 (5)	2.76 (3)	0.11 (4)	0.30 (3)	-0.11 (4)
S1	0.2760 (5)	0.3464 (2)	0.1284 (2)	2.7 (2)	2.9 (3)	2.9 (2)	0.1 (2)	0.4 (2)	0.3 (2)
S2	0.3149 (5)	0.4364 (2)	0.2440 (2)	3.0 (2)	3.5 (3)	2.8 (2)	-0.7 (2)	0.1 (2)	-0.3 (2)

atom	x	y	z	B, Å <sup>2</sup>	atom	x	y	z	B, Å <sup>2</sup>
O1	-0.020 (2)	0.3678 (7)	-0.1020 (7)	6.5 (4)	C13	0.522 (2)	0.5351 (11)	0.2927 (10)	5.8 (6)
O2	-0.130 (2)	0.3714 (7)	0.1156 (7)	7.4 (4)	C14	0.478 (2)	0.4689 (11)	0.4027 (11)	6.2 (6)
O3	0.165 (1)	0.5149 (7)	0.0230 (6)	4.3 (3)	C15	0.341 (2)	0.5731 (10)	0.3823 (10)	5.4 (6)
O4	0.398 (2)	0.1652 (8)	0.0808 (8)	7.5 (4)	C16	0.007 (2)	0.5089 (9)	0.1730 (9)	4.3 (5)
O5	-0.022 (1)	0.2323 (7)	0.1251 (7)	5.9 (4)	C17	0.296 (2)	0.5470 (10)	0.1601 (10)	5.1 (6)
O6	0.085 (1)	0.2345 (6)	-0.0887 (6)	5.0 (3)	C18	0.116 (2)	0.5919 (10)	0.2534 (9)	4.9 (5)
O7	0.640 (2)	0.2690 (7)	0.1599 (7)	6.9 (4)	C20	0.325 (2)	0.3703 (8)	-0.0180 (8)	3.2 (4)
O8	0.705 (2)	0.4123 (7)	0.2979 (7)	7.8 (5)	C21	0.492 (2)	0.3026 (9)	-0.0542 (9)	4.1 (5)
O9	0.595 (2)	0.4556 (8)	0.0721 (8)	8.4 (5)	C22	0.492 (2)	0.3145 (10)	-0.1224 (10)	4.6 (5)
O10	-0.054 (2)	0.3309 (7)	0.2725 (7)	6.3 (4)	C23	0.613 (2)	0.2913 (11)	-0.1606 (11)	6.4 (6)
O11	0.367 (1)	0.3358 (7)	0.4007 (6)	5.2 (3)	C24	0.708 (3)	0.2631 (12)	-0.1271 (12)	8.0 (8)
O12	0.298 (2)	0.2080 (7)	0.2362 (7)	7.4 (4)	C25	0.709 (3)	0.2526 (12)	-0.0608 (12)	8.1 (7)
O13	0.616 (2)	0.5495 (8)	0.2643 (8)	8.0 (5)	C26	0.592 (3)	0.2709 (12)	-0.0190 (11)	7.4 (7)
O14	0.548 (2)	0.4434 (7)	0.4447 (7)	6.1 (4)	C30	0.072 (2)	0.4877 (9)	0.3165 (8)	3.1 (4)
O15	0.315 (2)	0.6156 (7)	0.4062 (7)	6.7 (4)	C31	0.115 (2)	0.4505 (9)	0.4288 (9)	3.4 (5)
O16	-0.097 (1)	0.5014 (6)	0.1414 (6)	5.1 (3)	C32	0.008 (2)	0.4117 (10)	0.4311 (10)	4.9 (5)
O17	0.383 (2)	0.5607 (7)	0.1232 (7)	6.6 (4)	C33	-0.025 (2)	0.3887 (11)	0.4943 (11)	6.1 (6)
O18	0.081 (2)	0.6404 (8)	0.2677 (8)	8.2 (5)	C34	0.043 (2)	0.4043 (10)	0.5531 (10)	5.4 (6)
N1	0.373 (1)	0.3213 (7)	-0.0138 (7)	2.9 (3)	C35	0.152 (2)	0.4438 (10)	0.5515 (10)	5.2 (6)
N2	0.163 (2)	0.4758 (7)	0.3660 (7)	3.3 (4)	C36	0.192 (2)	0.4660 (9)	0.4898 (9)	3.9 (5)
C1	0.048 (2)	0.3777 (9)	-0.0502 (9)	4.2 (5)	H20	0.3706	0.3998	-0.0425	6.0
C2	-0.034 (2)	0.3769 (11)	0.0846 (10)	5.9 (6)	H30	-0.0274	0.4818	0.3189	6.0
C3	0.156 (2)	0.4662 (9)	0.0301 (9)	3.5 (4)	H22	0.4194	0.3369	-0.1437	6.0
C4	0.340 (2)	0.2053 (10)	0.0649 (10)	5.3 (6)	H23	0.6176	0.2968	-0.2084	6.0
C5	0.076 (2)	0.2467 (9)	0.0958 (9)	4.3 (5)	H24	0.7850	0.2489	-0.1523	6.0
C6	0.139 (2)	0.2497 (9)	-0.0373 (9)	3.5 (5)	H25	0.7855	0.2316	-0.0400	6.0
C7	0.583 (2)	0.3139 (10)	0.1655 (10)	5.1 (6)	H26	0.5871	0.2624	0.0283	6.0
C8	0.622 (2)	0.3986 (11)	0.2535 (10)	6.2 (6)	H32	-0.0421	0.4006	0.3900	6.0
C9	0.564 (2)	0.4295 (11)	0.1152 (10)	5.9 (6)	H33	-0.0983	0.3611	0.4963	6.0
C10	0.067 (2)	0.3332 (10)	0.2641 (9)	4.7 (5)	H34	0.0150	0.3885	0.5955	6.0
C11	0.327 (2)	0.3326 (9)	0.3411 (9)	3.5 (5)	H35	0.2010	0.4546	0.5928	6.0
C12	0.281 (2)	0.4584 (9)	0.2419 (9)	4.3 (5)	H36	0.2690	0.4919	0.4882	6.0

<sup>a</sup> The form of the anisotropic thermal parameter is  $\exp[-1/4 \{h^2 a^{*2} B(1,1) + k^2 b^{*2} B(2,2) + l^2 c^{*2} B(3,3) + 2hka^* b^* B(1,2) + 2hla^* c^* B(1,3) + 2kib^* c^* B(2,3)\}]$ . Hydrogen atoms were not refined.

standard procedures.<sup>19a</sup> Anomalous dispersion corrections were applied to all nonhydrogen atoms.<sup>19b</sup> Full-matrix least-squares refinements minimized the function  $\sum_{hkl} w(|F_o| - |F_c|)^2$ , where  $w = 1/\sigma(F)^2$ ,  $\sigma(F) = \sigma(F_o^2)/2F_o$ , and  $\sigma(F_o^2) = [(I_{\text{raw}})^2 + (PF_o^2)^2]^{1/2}/Lp$ .

The space group  $P2_1/c$ , No. 14, was established from the systematic absences  $0k0$ ,  $k = 2n + 1$ , and  $h0l$ ,  $l = 2n + 1$ . The structure was solved by a combination of direct methods and difference Fourier techniques. The coordinates of the six independent osmium atoms were obtained from an electron-density map based on the phasing (MULTAN) of 176 reflections ( $E_{\text{min}} \geq 1.90$ ). The coordinates of all remaining non-hydrogen atoms were obtained from difference Fourier syntheses. Positions of hydrogen atoms were calculated by assuming idealized geometry. Their contributions were added to structure factor calculations, but their positions were not refined. All atoms heavier than oxygen were refined anisotropically. All other nonhydrogen atoms were refined isotropically. Table II lists final fractional atomic coordinates and thermal parameters. Tables III and IV list interatomic distances and angles, respectively, with estimated standard deviations, obtained by using the inverse matrix obtained on the final cycle of refinement. Structure factor amplitudes are available; see supplementary material.

### Results and Discussion

An ORTEP diagram of the molecular structure of IV is shown in Figure 1. Fractional atomic coordinates and thermal parameters are listed in Table II. Interatomic distances and angles are listed in Tables III and IV, respectively. The six metal atoms are arranged into three groups of two. In each pair the metal atoms are joined by a metal-metal bond: Os(1)-Os(2) = 2.752 (1) Å, Os(3)-Os(4) = 2.752 (1) Å, and Os(5)-Os(6) = 2.756 (1) Å. These distances are considerably shorter than the Os-Os separation found in  $\text{Os}_3(\text{CO})_{12}$  of 2.877 (3) Å.<sup>20</sup> This shortening could be due to the presence of the bridging sulfido and formimidoyl ligands. The three pairs of metal atoms are linked by the tetracoordinate quadruply bridging sulfido ligands S(1) and S(2). The sulfido ligands are chemically equivalent and have the geometry II d analogous to that observed in the molecules  $[\text{Fe}_2(\text{CO})_6(\mu\text{-SMe})]_2(\mu_4\text{-S})$ ,<sup>15</sup>  $\text{Fe}_4(\text{CO})_{12}(\mu_4\text{-S})(\mu\text{-SCH}_2\text{C}_5\text{H}_4\text{FeCp})(\mu\text{-SMe})$ ,<sup>16</sup>  $\text{Fe}_4(\text{CO})_{12}$ -

(20) Churchill, M. R.; DeBoer, B. G. *Inorg. Chem.* 1977, 16, 878.

(21) Patin, H.; Mignani, G.; Mahe, C.; Le Marouille, J.-Y.; Benoit, A.; Grandjean, D. *J. Organomet. Chem.* 1981, 210, C1.

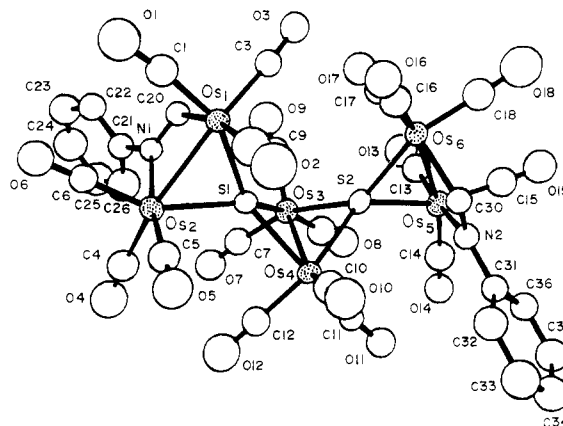
(22) Le Borgen, G.; Grandjean, D. *J. Organomet. Chem.* 1975, 92, 381.

(23) Dean, W. K.; Vanderveer, D. G. *J. Organomet. Chem.* 1978, 146, 143.

(19) "International Tables for x-ray Crystallography"; Kynoch Press: Birmingham, England, 1975; Vol. IV, (a) Table 2.2B, pp 99-101; (b) Table 2.3.1, pp 149-150.

Table III. Interatomic Distances (Å) with Esds for  $\text{Os}_6(\text{CO})_{18}(\mu_4\text{-S})_2(\mu\text{-HC=NPh})_2$ , IV

Os(1)-Os(2)	2.752 (1)	N(2)-C(30)	1.30 (2)
Os(3)-Os(4)	2.752 (1)	N(1)-C(21)	1.47 (2)
Os(5)-Os(6)	2.756 (1)	C(21)-C(22)	1.36 (2)
Os(1)-S(1)	2.411 (4)	C(21)-C(26)	1.37 (3)
Os(2)-S(1)	2.413 (5)	C(22)-C(23)	1.50 (3)
Os(3)-S(1)	2.420 (4)	C(23)-C(24)	1.28 (3)
Os(3)-S(2)	2.426 (5)	C(24)-C(25)	1.32 (3)
Os(4)-S(1)	2.424 (4)	C(25)-C(26)	1.47 (3)
Os(4)-S(2)	2.411 (5)	N(2)-C(31)	1.45 (2)
Os(5)-S(2)	2.421 (4)	C(31)-C(32)	1.37 (2)
Os(6)-S(2)	2.433 (5)	C(31)-C(36)	1.42 (2)
Os(1)-C(20)	2.09 (2)	C(32)-C(33)	1.39 (2)
Os(1)-C(1)	1.81 (2)	C(33)-C(34)	1.35 (2)
Os(1)-C(2)	1.96 (2)	C(34)-C(35)	1.39 (3)
Os(1)-C(3)	1.93 (2)	C(35)-C(36)	1.38 (2)
Os(2)-N(1)	2.15 (1)	C(1)-O(1)	1.20 (2)
Os(2)-C(4)	1.95 (2)	C(2)-O(2)	1.12 (2)
Os(2)-C(5)	1.88 (2)	C(3)-O(3)	1.15 (2)
Os(2)-C(6)	1.86 (2)	C(4)-O(4)	1.13 (2)
Os(3)-C(7)	1.85 (2)	C(5)-O(5)	1.17 (2)
Os(3)-C(8)	1.84 (2)	C(6)-O(6)	1.17 (2)
Os(3)-C(9)	1.96 (2)	C(7)-O(7)	1.19 (2)
Os(4)-C(10)	1.88 (2)	C(8)-O(8)	1.19 (2)
Os(4)-C(11)	1.84 (2)	C(9)-O(9)	1.09 (2)
Os(4)-C(12)	1.84 (2)	C(10)-O(10)	1.16 (2)
Os(5)-N(2)	2.14 (1)	C(11)-O(11)	1.22 (2)
Os(5)-C(13)	1.89 (2)	C(12)-O(12)	1.20 (2)
Os(5)-C(14)	1.85 (2)	C(13)-O(13)	1.12 (2)
Os(5)-C(15)	1.88 (2)	C(14)-O(14)	1.20 (2)
Os(6)-C(30)	2.11 (2)	C(15)-O(15)	1.13 (2)
Os(6)-C(16)	1.89 (2)	C(16)-O(16)	1.17 (2)
Os(6)-C(17)	1.96 (2)	C(17)-O(17)	1.16 (2)
Os(6)-C(18)	1.79 (2)	C(18)-O(18)	1.22 (2)
N(1)-C(20)	1.24 (2)		

Figure 1. An ORTEP diagram of  $\text{Os}_6(\text{CO})_{18}(\mu_4\text{-S})_2(\mu\text{-HC=NPh})_2$ , IV, showing 50% probability thermal-motion ellipsoids. Hydrogen atoms have been omitted.

The Os-S-Os bond angles are acute, 69.2 (1)–69.6 (1)°, where the metal atoms are bonded, and are fairly large, 125.3 (2)–142.0 (2)°, where they are not bonded. The local environment of each sulfido ligand deviates slightly from  $D_{2d}$  symmetry since the dihedral angles between the planes Os(1)-Os(2)-S(1) and Os(3)-Os(4)-S(1) and the planes Os(3)-Os(4)-S(2) and Os(5)-Os(6)-S(2) are 81.4° and 83.5°, respectively. This slight twisting from 90° could be due to steric interactions between the carbonyl ligands on Os(1) and Os(6). For example, the intramolecular non-bonding distances between O(3) and C(17)-O(17) are O(3)···C(17) = 3.01 (2) Å and O(3)···O(17) = 2.99 (2) Å. The

Table IV. Selected Interatomic Angles (deg) with Esds for  $\text{Os}_6(\text{CO})_{18}(\mu_4\text{-S})_2(\mu\text{-HC=NPh})_2$ , IV

Os(2)-Os(1)-S(1)	55.3 (1)	Os(5)-Os(6)-C(17)	98.8 (5)	C(30)-N(2)-C(31)	120 (1)
Os(2)-Os(1)-C(20)	68.1 (5)	Os(5)-Os(6)-C(18)	98.1 (6)	Os(6)-C(30)-N(2)	112 (1)
Os(2)-Os(1)-C(1)	97.3 (6)	Os(1)-S(1)-Os(2)	69.6 (1)	N(2)-C(31)-C(32)	124 (2)
Os(2)-Os(1)-C(2)	97.8 (7)	Os(1)-S(1)-Os(3)	131.7 (2)	N(2)-C(31)-C(36)	116 (2)
Os(2)-Os(1)-C(3)	156.9 (5)	Os(1)-S(1)-Os(4)	139.0 (2)	C(32)-C(31)-C(36)	120 (2)
Os(1)-Os(2)-S(1)	55.2 (1)	Os(2)-S(1)-Os(3)	133.6 (2)	C(31)-C(32)-C(33)	119 (2)
Os(1)-Os(2)-N(1)	70.0 (4)	Os(2)-S(1)-Os(4)	125.9 (2)	C(32)-C(33)-C(34)	122 (2)
Os(1)-Os(2)-C(4)	162.7 (6)	Os(3)-S(1)-Os(4)	69.2 (1)	C(33)-C(34)-C(35)	120 (2)
Os(1)-Os(2)-C(5)	96.5 (6)	Os(3)-S(2)-Os(4)	69.4 (1)	C(34)-C(35)-C(36)	120 (2)
Os(1)-Os(2)-C(6)	94.5 (6)	Os(3)-S(2)-Os(5)	125.3 (2)	C(35)-C(36)-C(31)	119 (2)
Os(4)-Os(3)-S(1)	55.5 (1)	Os(3)-S(2)-Os(6)	142.0 (2)	Os(1)-C(1)-O(1)	172 (2)
Os(4)-Os(3)-S(2)	55.1 (1)	Os(4)-S(2)-Os(5)	128.8 (2)	Os(1)-C(2)-O(2)	178 (2)
Os(4)-Os(3)-C(7)	100.3 (6)	Os(4)-S(2)-Os(6)	133.2 (2)	Os(1)-C(3)-O(3)	175 (2)
Os(4)-Os(3)-C(8)	106.9 (6)	Os(5)-S(2)-Os(6)	69.2 (1)	Os(2)-C(4)-O(4)	174 (2)
Os(4)-Os(3)-C(9)	149.3 (6)	Os(1)-C(20)-N(1)	115 (1)	Os(2)-C(5)-O(5)	176 (2)
Os(3)-Os(4)-S(1)	55.3 (1)	Os(2)-N(1)-C(20)	107 (1)	Os(2)-C(6)-O(6)	179 (2)
Os(3)-Os(4)-S(2)	55.6 (1)	Os(2)-N(1)-C(21)	131 (1)	Os(3)-C(7)-O(7)	172 (2)
Os(3)-Os(4)-C(10)	150.5 (6)	C(20)-N(1)-C(21)	122 (2)	Os(3)-C(8)-O(8)	177 (2)
Os(3)-Os(4)-C(11)	102.4 (5)	N(1)-C(21)-C(22)	119 (2)	Os(3)-C(9)-O(9)	174 (2)
Os(3)-Os(4)-C(12)	104.0 (6)	N(1)-C(21)-C(26)	115 (2)	Os(4)-C(10)-O(10)	179 (2)
Os(6)-Os(5)-S(2)	55.6 (1)	C(22)-C(21)-C(26)	125 (2)	Os(4)-C(11)-O(11)	174 (2)
Os(6)-Os(5)-N(2)	70.3 (3)	C(21)-C(22)-C(23)	116 (2)	Os(4)-C(12)-O(12)	178 (2)
Os(6)-Os(5)-C(13)	97.4 (6)	C(22)-C(23)-C(24)	118 (2)	Os(5)-C(13)-O(13)	174 (2)
Os(6)-Os(5)-C(14)	162.3 (7)	C(23)-C(24)-C(25)	125 (3)	Os(5)-C(14)-O(14)	176 (2)
Os(6)-Os(5)-C(15)	98.1 (6)	C(24)-C(25)-C(26)	121 (2)	Os(5)-C(15)-O(15)	173 (2)
Os(5)-Os(6)-S(2)	55.2 (1)	C(25)-C(26)-C(21)	114 (2)	Os(6)-C(16)-O(16)	176 (2)
Os(5)-Os(6)-C(30)	69.5 (4)	Os(5)-N(2)-C(30)	108 (1)	Os(6)-C(17)-O(17)	173 (2)
Os(5)-Os(6)-C(16)	158.6 (6)	Os(5)-N(2)-C(31)	132 (1)	Os(6)-C(18)-O(18)	178 (2)

$(\mu_4\text{-S})(\mu\text{-NC}_5\text{H}_4)(\mu\text{-SC}_5\text{H}_4\text{N})$ ,<sup>17</sup>  $\text{Fe}_4(\text{CO})_{12}(\mu_4\text{-S})(\mu\text{-CSNMe}_2)(\mu\text{-CNMe}_2)$ ,<sup>18</sup>  $\text{H}_2\text{Os}_6(\text{CO})_{17}(\mu_4\text{-S})(\mu_3\text{-S})(\mu\text{-HC=NPh})_2$ ,<sup>11</sup> and  $\text{H}_2\text{Os}_6(\text{CO})_{16}(\mu_4\text{-S})(\mu_3\text{-S})(\mu\text{-HC=NPh})_2$ .<sup>11</sup> The eight Os-S bond distances are not significantly different and span the small range 2.411 (4) Å to 2.433 (5) Å. These distances are very similar to the Os-S distances observed for triply bridging sulfido ligands found in a variety of triosmium cluster complexes.<sup>24</sup>

O(3)···C(16) distance is slightly larger at 3.34 (2) Å.

The outer pairs of metal atoms are each bridged by  $\eta^2$ -N-phenylformimidoyl ligands (HC=NPh) in which the

(24) (a) Adams, F. D.; Golembeski, N. M.; Selegue, J. P. *J. Am. Chem. Soc.* 1981, 103, 546. (b) Johnson, B. F. G.; Lewis, J.; Pippard, D.; Raithby, P. R.; Sheldrick, G. M.; Rouse, K. D. *J. Chem. Soc., Dalton Trans.* 1979, 616. (c) Johnson, B. F. G.; Lewis, J.; Pippard, D.; Raithby, P. R. *Acta Crystallogr., Sect. B* 1978, B34, 3767.

iminyl carbon and nitrogen atoms are bonded to different metal atoms. Structurally, these ligands show no unusual distortions.<sup>25</sup> Each metal atom contains three linear terminal carbonyl ligands.

The central  $S_2Os_2(CO)_6$  unit contains a "sawhorse" structure similar to that of  $(\mu-SEt)_2Fe_2(CO)_6$ .<sup>26</sup> The dihedral angle between the Os(3)-Os(4)-S(1) and Os(3)-Os(4)-S(2) planes is 102.4°. Overall, the molecule contains  $C_2$  symmetry although this is not crystallographically imposed.

The shortest intermolecular contacts were between the carbonyl oxygen atoms O(8)...O(10) = 3.04 (2) Å and O(5)...O(18) = 3.07 (2) Å.

In order that all the metal atoms can achieve 18-electron configurations, the sulfido ligands must serve as six-electron donors. This would include a formal donation of two electrons to both Os(1) and Os(6) and one electron to both Os(2) and Os(5).

It has been shown that sulfido ligands can play an important role in the synthesis of high nuclearity metal

carbonyl cluster compounds.<sup>1-13,16-18</sup> This is made possible to a large degree by their ability to serve as multicoordinate, multielectron bridging ligands and also engage in the wide variety of coordination environments I and IIa-IIe.

**Acknowledgment.** This work was supported by the Office of Basic Energy Sciences of the U.S. Department of Energy under Contract No. DE-AC02-78ER04900 and the Alfred P. Sloan Foundation through a fellowship to R.D.A. We wish to thank Engelhard Industries for a loan of osmium tetroxide and Drs. I. T. Horvath and B. E. Segmüller for helpful discussions.

**Registry No.** IV, 84000-57-7.

**Supplementary Material Available:** A listing of structure factor amplitudes (13 pages). Ordering information is given on any current masthead page.

(25) Adams, R. D.; Golembeski, N. M. *J. Am. Chem. Soc.* 1979, 101, 2579.

(26) Dahl, L. F.; Wei, C. H. *Inorg. Chem.* 1963, 2, 328.

## Crystal and Molecular Structure of Hexaphenylcyclohexaarsine, *cyclo-(AsPh)<sub>6</sub>*

Arnold L. Rheingold\* and Patrick J. Sullivan

Department of Chemistry, University of Delaware, Newark, Delaware 19711

Received September 10, 1982

The crystal and molecular structure of hexaphenylcyclohexaarsine (1) has been determined in order to establish a standard for a "normal" As-As bond distance. The new structural determination represents a many-fold improvement in precision over a study performed 22 years ago. 1 crystallizes in the monoclinic space group  $P2_1/n$  with  $a = 12.172$  (1) Å,  $b = 6.234$  (1) Å,  $c = 22.884$  (3) Å,  $\beta = 99.67$  (1)°,  $V = 1711.6$  (3) Å<sup>3</sup>, and  $Z = 2$ . The final residuals are  $R = 4.45\%$  and  $R_w = 4.76\%$ . The average As-As distance is 2.459 Å. A discussion of trends in As-As bond distances in 26 compounds is included.

### Introduction

The extreme adaptability of arsenic, both naked and combined, as a bridging element in transition-metal cluster structures has prompted us recently to prepare and characterize crystallographically a series of novel structures containing arsenic-arsenic bonds. The wide range in the As-As bond distances that we observed, 2.3-2.8 Å, caused us to search the existing literature for a reliable standard for a "normal" As-As single bond. The values most often cited as standards are (1) gaseous  $As_4$ , 2.45 Å,<sup>1</sup> (2)  $c-(CH_3As)_6$ , (av) 2.428 (5) Å,<sup>2</sup> and (3)  $c-(C_6H_5As)_6$ , (av) 2.456 (5) Å.<sup>3</sup> All of these standards have factors which limit their reliability: (1) the bond distance was determined 47 years ago by electron diffraction and the effects of strain caused by the 60° tetrahedral face angles is uncertain; (2) determined 25 years ago by X-ray crystallography with a 12.3% residual (all atoms isotropic, no absorption correction); and (3) determined 33 years ago by X-ray crystallography, no final residual reported, all atoms isotropic, no carbon atom parameters refined, and data limited to 482 observed reflections.

We wish now to report the results of a redetermination of the crystallographic structure of  $c-(C_6H_5As)_6$  (1) and to

Table I. Crystal and Refinement Data for I

formula	$As_6C_{36}H_{30}$
cryst system	monoclinic
space group	$P2_1/n$
$a$ , Å	12.172 (1)
$b$ , Å	6.234 (1)
$c$ , Å	22.884 (3)
$\beta$ , deg	99.67 (1)
$V$ , Å <sup>3</sup>	1711.6 (3)
$Z$	2
temp, °C	24
cryst dimens, mm	0.05 × 0.15 × 0.37
radiant	graphite-monochromated Mo K $\alpha$ ( $\lambda = 0.71073$ Å)
diffractometer	Nicolet R3
abs coeff, cm <sup>-1</sup>	58.0
scan speed, deg/min	variable 3-15
$2\theta$ scan range, deg	$3 < 2\theta < 55$
scan technique	$\theta/2\theta$
data collected	$\pm h, +k, +l$
scan width, deg	$1.7 + \Delta(\alpha_1 - \alpha_2)$
weighting factor, $g^a$	0.0012
unique data	3472 rflns (3931 collected)
unique data with $(F_o)^2 > 3\sigma(F_o)^2$	2584
std rflns	3/97 (no decay observed)
GOF	1.070
$R(F)$ , %	4.45
$R(wF)$ , %	4.76

$$^a w = [\sigma^2(F) + gF^2]^{-1}.$$

relate the new average As-As distance, 2.459 Å, to others found in the literature.

(1) Maxwell, L. R.; Hendricks, S. B.; Moseley, V. M. *J. Chem. Phys.* 1935, 3, 699.

(2) Burns, J. H.; Waser, J. *J. Am. Chem. Soc.* 1957, 79, 859.

(3) Hedberg, K.; Hughes, E. W.; Waser, J. *Acta Crystallogr.* 1961, 14, 369. An 11-year delay occurred between data collection and refinement.

## Crystal and molecular structure of hexaphenylcyclohexaarsine, $c\text{-(AsPh)}_6$

Arnold L. Rheingold, and Patrick J. Sullivan

*Organometallics*, **1983**, 2 (2), 327-331 • DOI: 10.1021/om00074a021 • Publication Date (Web): 01 May 2002

Downloaded from <http://pubs.acs.org> on April 24, 2009

### More About This Article

---

The permalink <http://dx.doi.org/10.1021/om00074a021> provides access to:

- Links to articles and content related to this article
- Copyright permission to reproduce figures and/or text from this article



ACS Publications  
High quality. High impact.

iminyl carbon and nitrogen atoms are bonded to different metal atoms. Structurally, these ligands show no unusual distortions.<sup>25</sup> Each metal atom contains three linear terminal carbonyl ligands.

The central  $S_2Os_2(CO)_6$  unit contains a "sawhorse" structure similar to that of  $(\mu-SEt)_2Fe_2(CO)_6$ .<sup>26</sup> The dihedral angle between the Os(3)-Os(4)-S(1) and Os(3)-Os(4)-S(2) planes is 102.4°. Overall, the molecule contains  $C_2$  symmetry although this is not crystallographically imposed.

The shortest intermolecular contacts were between the carbonyl oxygen atoms O(8)...O(10) = 3.04 (2) Å and O(5)...O(18) = 3.07 (2) Å.

In order that all the metal atoms can achieve 18-electron configurations, the sulfido ligands must serve as six-electron donors. This would include a formal donation of two electrons to both Os(1) and Os(6) and one electron to both Os(2) and Os(5).

It has been shown that sulfido ligands can play an important role in the synthesis of high nuclearity metal

carbonyl cluster compounds.<sup>1-13,16-18</sup> This is made possible to a large degree by their ability to serve as multicoordinate, multielectron bridging ligands and also engage in the wide variety of coordination environments I and IIa-IIe.

**Acknowledgment.** This work was supported by the Office of Basic Energy Sciences of the U.S. Department of Energy under Contract No. DE-AC02-78ER04900 and the Alfred P. Sloan Foundation through a fellowship to R.D.A. We wish to thank Engelhard Industries for a loan of osmium tetroxide and Drs. I. T. Horvath and B. E. Segmüller for helpful discussions.

**Registry No.** IV, 84000-57-7.

**Supplementary Material Available:** A listing of structure factor amplitudes (13 pages). Ordering information is given on any current masthead page.

(25) Adams, R. D.; Golembeski, N. M. *J. Am. Chem. Soc.* 1979, 101, 2579.

(26) Dahl, L. F.; Wei, C. H. *Inorg. Chem.* 1963, 2, 328.

## Crystal and Molecular Structure of Hexaphenylcyclohexaarsine, *cyclo*-(AsPh)<sub>6</sub>

Arnold L. Rheingold\* and Patrick J. Sullivan

Department of Chemistry, University of Delaware, Newark, Delaware 19711

Received September 10, 1982

The crystal and molecular structure of hexaphenylcyclohexaarsine (1) has been determined in order to establish a standard for a "normal" As-As bond distance. The new structural determination represents a many-fold improvement in precision over a study performed 22 years ago. 1 crystallizes in the monoclinic space group  $P2_1/n$  with  $a = 12.172$  (1) Å,  $b = 6.234$  (1) Å,  $c = 22.884$  (3) Å,  $\beta = 99.67$  (1)°,  $V = 1711.6$  (3) Å<sup>3</sup>, and  $Z = 2$ . The final residuals are  $R = 4.45\%$  and  $R_w = 4.76\%$ . The average As-As distance is 2.459 Å. A discussion of trends in As-As bond distances in 26 compounds is included.

### Introduction

The extreme adaptability of arsenic, both naked and combined, as a bridging element in transition-metal cluster structures has prompted us recently to prepare and characterize crystallographically a series of novel structures containing arsenic-arsenic bonds. The wide range in the As-As bond distances that we observed, 2.3-2.8 Å, caused us to search the existing literature for a reliable standard for a "normal" As-As single bond. The values most often cited as standards are (1) gaseous As<sub>4</sub>, 2.45 Å,<sup>1</sup> (2)  $c$ -(CH<sub>3</sub>As)<sub>6</sub>, (av) 2.428 (5) Å,<sup>2</sup> and (3)  $c$ -(C<sub>6</sub>H<sub>5</sub>As)<sub>6</sub>, (av) 2.456 (5) Å.<sup>3</sup> All of these standards have factors which limit their reliability: (1) the bond distance was determined 47 years ago by electron diffraction and the effects of strain caused by the 60° tetrahedral face angles is uncertain; (2) determined 25 years ago by X-ray crystallography with a 12.3% residual (all atoms isotropic, no absorption correction); and (3) determined 33 years ago by X-ray crystallography, no final residual reported, all atoms isotropic, no carbon atom parameters refined, and data limited to 482 observed reflections.

We wish now to report the results of a redetermination of the crystallographic structure of  $c$ -(C<sub>6</sub>H<sub>5</sub>As)<sub>6</sub> (1) and to

Table I. Crystal and Refinement Data for I

formula	As <sub>6</sub> C <sub>36</sub> H <sub>30</sub>
cryst system	monoclinic
space group	$P2_1/n$
$a$ , Å	12.172 (1)
$b$ , Å	6.234 (1)
$c$ , Å	22.884 (3)
$\beta$ , deg	99.67 (1)
$V$ , Å <sup>3</sup>	1711.6 (3)
$Z$	2
temp, °C	24
cryst dimens, mm	0.05 × 0.15 × 0.37
radiant	graphite-monochromated Mo K $\alpha$ ( $\lambda = 0.71073$ Å)
diffractometer	Nicolet R3
abs coeff, cm <sup>-1</sup>	58.0
scan speed, deg/min	variable 3-15
$2\theta$ scan range, deg	$3 < 2\theta < 55$
scan technique	$\theta/2\theta$
data collected	$\pm h, +k, +l$
scan width, deg	$1.7 + \Delta(\alpha_1 - \alpha_2)$
weighting factor, $g^a$	0.0012
unique data	3472 rflns (3931 collected)
unique data with ( $F_o$ ) <sup>2</sup> > $3\sigma(F_o)$ <sup>2</sup>	2584
std rflns	3/97 (no decay observed)
GOF	1.070
$R(F)$ , %	4.45
$R(wF)$ , %	4.76

$$^a w = [\sigma^2(F) + gF^2]^{-1}.$$

relate the new average As-As distance, 2.459 Å, to others found in the literature.

(1) Maxwell, L. R.; Hendricks, S. B.; Moseley, V. M. *J. Chem. Phys.* 1935, 3, 699.

(2) Burns, J. H.; Waser, J. *J. Am. Chem. Soc.* 1957, 79, 859.

(3) Hedberg, K.; Hughes, E. W.; Waser, J. *Acta Crystallogr.* 1961, 14, 369. An 11-year delay occurred between data collection and refinement.

Table II. Fractional Non-Hydrogen Atomic Coordinates for  $c\text{-(AsC}_6\text{H}_5)_6$ 

atom	x	y	z
As(1)	0.08499 (5)	0.55289 (12)	0.09139 (3)
As(2)	-0.11624 (5)	0.51001 (12)	0.05552 (3)
As(3)	-0.11971 (5)	0.75289 (12)	-0.02925 (3)
C(11)	0.0899 (5)	0.4087 (12)	0.1683 (3)
C(12)	0.1345 (5)	0.2075 (13)	0.1819 (3)
C(13)	0.1432 (6)	0.1264 (14)	0.2381 (3)
C(14)	0.1108 (7)	0.2455 (17)	0.2818 (4)
C(15)	0.0664 (6)	0.4461 (16)	0.2698 (3)
C(16)	0.0552 (6)	0.5279 (14)	0.2129 (3)
C(21)	-0.1715 (5)	0.7177 (11)	0.1079 (3)
C(22)	-0.2598 (5)	0.6477 (13)	0.1347 (3)
C(23)	-0.3035 (5)	0.7787 (15)	0.1741 (4)
C(24)	-0.2598 (7)	0.9739 (16)	0.1876 (4)
C(25)	-0.1717 (6)	1.0479 (14)	0.1617 (3)
C(26)	-0.1298 (6)	0.9207 (12)	0.1214 (3)
C(31)	-0.2836 (5)	0.7612 (11)	-0.0490 (3)
C(32)	-0.3305 (6)	0.9595 (15)	-0.0530 (5)
C(33)	-0.4450 (7)	0.9813 (15)	-0.0664 (5)
C(34)	-0.5120 (6)	0.8104 (16)	-0.0759 (4)
C(35)	-0.4649 (7)	0.6157 (19)	-0.0726 (5)
C(36)	-0.3511 (6)	0.5884 (15)	-0.0589 (5)

### Experimental Section

**Preparation of Sample.** **1** was prepared by the hypophosphorous acid reduction of benzene arsonic acid.<sup>4</sup> Various techniques were attempted to grow diffraction grade crystals from a range of organic solvents, but all failed to yield either large enough crystals or ones with a melting point about 195 °C. Crystals of high quality were finally obtained by accident; cooling a partially reacted solution of **1** with  $\text{CpMn(CO)}_3$  in toluene in a sealed reaction tube from 140 °C to room temperature over a period of 2 days resulted in the formation of large, well-formed single crystals of **1**, mp 210 °C.

**Collection of Diffraction Data.** The parameters used during the collection of diffraction data are given in Table I. Epoxy cement was used to affix the crystal to the tip of a fine glass fiber. The original structural determination of **1** was carried out in the monoclinic space group  $P2_1/c$ ,<sup>3</sup> but in order to take advantage of a less obtuse  $\beta$  angle, the nonstandard setting  $P2_1/n$  was used in the present analysis. The unit-cell dimensions were derived from the angular settings of 50 reflections with  $28^\circ \leq 2\theta \leq 35^\circ$ . The data were corrected for absorption by an empirical procedure that employs six refined parameters to define a pseudoellipsoid used to calculate the corrections.<sup>5</sup> A profile fitting procedure was applied to all intensity data to improve the precision of the measurement of weak reflections.

**Solution and Refinement of the Structure.** A satisfactory structure solution was obtained from the atomic coordinates of the original determination<sup>3</sup> after application of the transformation matrix to convert  $P2_1/c$  to  $P2_1/n$ . An all-isotropic model for the non-hydrogen atoms converged at  $R = 11.8\%$ . With all non-hydrogen atoms refined anisotropically employing idealized hydrogen atom positions ( $d(\text{C-H}) = 0.96 \text{ \AA}$ , thermal parameters equal 1.2 times the isotropic equivalent for the carbon atom to which it was attached) and a riding model that updated hydrogen atom positions after each cycle, the final residuals  $R(F) = 4.45\%$  and  $R(wF) = 4.76\%$  were obtained. A final difference Fourier synthesis showed only a diffuse background (maximum  $0.37 \text{ e/\AA}^3$ ). An inspection of  $F_o$  vs.  $F_c$  values and trends based upon  $\sin \theta$ , Miller index, or parity group failed to reveal any systematic errors in the data.

A listing of atomic coordinates is provided in Table II. Tables III–VS (supplementary material) list the anisotropic thermal parameter, hydrogen atom coordinates, and the structure factors ( $F_o$  vs.  $F_c$ ), respectively.

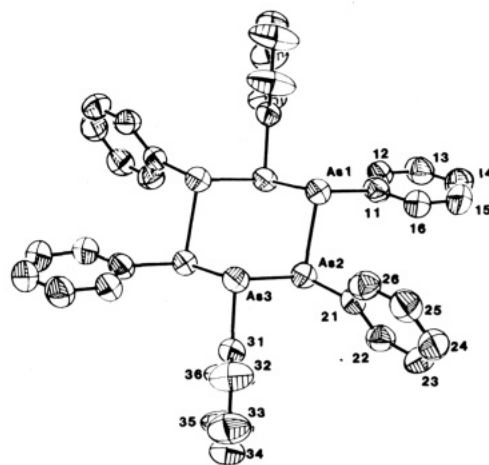


Figure 1. Thermal ellipsoid drawing of  $c\text{-(AsPh)}_6$ , **1**, with the current labeling scheme as viewed with the molecular orientation perpendicular to the crystallographic  $b$  axis.

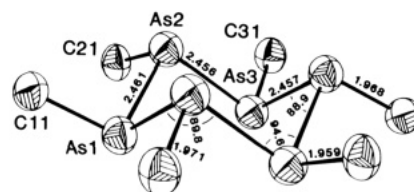


Figure 2. Details of the  $\text{As}_6$  ring environment in **1** revealing the highly puckered ring structure, [ $\langle \text{av} \rangle \text{As-As-As angle} = 91.0^\circ$ ], and the all-equatorial phenyl ring configuration.

### Results and Discussion

As is now well-known, **1** crystallizes as a discrete cyclohexamer containing an all-arsenic ring framework in a chair conformation with the phenyl groups in equatorial positions. Many aspects of the structure have been thoroughly described in earlier publications.<sup>3,6</sup> A thermal ellipsoid drawing is shown in Figure 1 with the current labeling scheme. The  $\text{As}_6$  ring environment is more clearly seen in Figure 2. The packing of molecules in the crystalline lattice (Figure 3) produces a short intermolecular  $\text{As}\cdots\text{As}$  contact [ $\text{As}(3)\cdots\text{As}(3)' = 4.297(1) \text{ \AA}$ ]<sup>7</sup> which is shorter than the  $\text{As}(3)\cdots\text{As}(3)'$  intramolecular, transannular distance  $4.349(1) \text{ \AA}$ . A space-filling stereo diagram (Figure 4) reveals an absence of crowding not visible in "ball-and-stick" depictions. A table of selected bond distances and angles including torsional angles is provided in Table VI.

Of primary interest are the AsAs bond distances, both bonded and nonbonded. The three independent As-As distances are (1-2) =  $2.464(1)$ , (2-3) =  $2.456(1)$ , and (1-3) =  $2.457(1) \text{ \AA}$  [ $\langle \text{av} \rangle = 2.459 \text{ \AA}$ ]; the previous determination of these parameters produced the values  $2.457(6)$ ,  $2.456(8)$ , and  $2.456(9) \text{ \AA}$  [ $\langle \text{av} \rangle = 2.456(5) \text{ \AA}$ ]. The previous observation that the As-As distances are all equal (within experimental error) should now be revised to take account of the current result that one As-As distance is slightly longer than the other two. The nonbonded, transannular As-As distances are of interest in an assessment of the role that across-ring, lone pair-lone pair interactions play in ring stabilization.<sup>8</sup> The "1-3" distances are (1-3)' =  $3.616$

(4) Reesor, J. W. B.; Wright, G. F. *J. Org. Chem.* **1957**, *22*, 382.

(5) This program and all others used in the data collection and refinement are contained in the Nicolet program packages P3, SHELXTL (version 3.0), and XP and were executed on our in-house Data General Nova 4 computer.

(6) Donohue, J. *Acta Crystallogr.* **1962**, *15*, 708.

(7) Generated by the transformation  $-x, 2-y, -z$ .

(8) (a) Cowley, A. H.; Dewar, M. J. S.; Lattman, J.; Mills, J. L.; McKee, M. *J. Am. Chem. Soc.* **1978**, *100*, 3349. (b) Cowley, A. H. In "Homoatomic Rings, Chains and Macromolecules of Main-Group Elements"; Rheingold, A. L., Ed.; Elsevier: Amsterdam, 1977; p 59.

Table VI. Selected Bond Distances, Bond Angles, and Torsion Angles for *c*-(AsC<sub>6</sub>H<sub>5</sub>)<sub>6</sub>.

(A) Bond Distances (Å)			
As(1)-As(2)	2.464 (1)	As(1)-C(11)	1.968 (7)
As(2)-As(3)	2.456 (1)	As(2)-C(21)	1.959 (7)
As(3)-As(1')	2.457 (1)	As(3)-C(31)	1.971 (6)
(av) As-As	2.459	(av) As-C	1.966
(B) Bond Angles (deg)			
As(2)-As(1)-As(3')	88.92 (4)	As(3)'-As(1)-C(11)	100.4 (2)
As(1)-As(2)-As(3)	94.59 (4)	As(1)-As(2)-C(21)	98.5 (2)
As(2)-As(3)-As(1')	89.82 (4)	As(3)-As(2)-C(21)	96.6 (2)
(av) As-As-As	91.1	As(2)-As(3)-C(31)	94.5 (2)
As(2)-As(1)-C(11)	97.3 (2)	As(1)'-As(3)-C(31)	98.9 (2)
		(av) As-As-C	97.7
(C) Torsion Angles (deg)			
As(1)-As(2)-As(3)-As(1')	91.08 (4)	C(11)-As(1)-As(2)-As(3)	169.4 (2)
As(2)-As(3)-As(1)'-As(2)'	85.4 (2)	C(11)-As(1)-As(3)'-As(2)'	-177.4 (2)
As(3)-As(2)-As(1)-As(3)'	-90.31 (4)	C(21)-As(2)-As(3)-As(1)'	-169.7 (2)
(av) As-As-As-As	188.9	C(21)-As(2)-As(1)-As(3)'	172.4 (2)
C(11)-As(1)-As(2)-C(21)	72.0 (3)	C(31)-As(3)-As(2)-As(1)'	-180.0 (2)
C(21)-As(2)-As(3)-C(31)	-70.9 (3)	C(31)-As(3)-As(2)-As(1)'	-170.0 (2)
C(31)-As(3)-As(1)-C(11)'	-82.8 (3)	(av) C-As-As-As	173.2
(av) C-As-As-C	175.2		

(1), (2-3') = 3.446 (1), and (1-2') = 3.468 (1) Å. The "1-4" distances are considerably longer: (1-1') = 4.393 (1), (2-2') = 4.110 (1), and (3-3') = 4.349 (1) Å.

The As-C distances were found to vary considerably in the earlier determination,<sup>3</sup> 1.92-2.01 Å [(av) = 1.97 (2) Å], a result surely due to the lack of refinement of carbon atom parameters. We find the range 1.959 (7)-1.971 (6) Å [(av) = 1.966 Å] more reasonable and it in agreement with other aryl-As bond distances. The As-As-As bond angles agree almost identically to their earlier found values.

Table VII provides least-squares planes with interrelating dihedral angles. An inspection of these data reveals a considerable variation in the dihedral angle relating the plane of the phenyl ring to the plane formed by the three arsenic atoms on which the phenyl ring is centered (and to the "best-fit" plane for all six As atoms). Whereas the rings attached to As(2) and As(3) are arranged very nearly perpendicularly, 91.5 and 88.4°, respectively, the ring-As plane angle for As(1) shows a considerable tilt for perpendicularity, 75.4°. Since a minimization of steric crowding would be achieved by an all-perpendicular arrangement, it is reasonable to conclude that intramolecular steric factors are not prominent in determining the phenyl-ring tilt angle. The unusual tilt of the phenyl ring attached to As(1) is particularly evident in Figure 4 and is likely attributable to packing phenomena.

A review of available As-As bond distance data reveals trends useful in correlating bond orders with bond distances. The Pauling covalent radius for arsenic is 1.21 Å (Dahl estimates its value as 1.22 Å<sup>9</sup>), suggesting a "normal" As-As single bond might fall in the range of 2.42-2.44 Å. A table of representative As-As bond distances obtained from a survey of the literature is provided in Table VIII. The values quoted range from 2.27 to 2.75 Å and would roughly correspond to a range of bond orders from 2.0 to 0.5. It is interesting to note that all of the shortest As-As bond distances (<2.4 Å) are found in transition-metal complexes in which bond orders greater than 1 may presumably be stabilized. Dahl has proposed that the apparent As=As bonds in I-III are the result of a back-donation of electrons from metal to the π\* levels of As≡As.<sup>10</sup> The trend seen in these four compounds is exactly what

Table VII. Least-Squares Planes<sup>a, b</sup> for *c*-(C<sub>6</sub>H<sub>5</sub>As)<sub>6</sub>.

atoms	dev	atoms	dev
Plane I: 0.4934X - 0.8678Y - 0.0592Z - 2.7048 = 0			
As(1)	0.6757	As(3)'	-0.6845
As(2)	-0.7232	C11	-0.1784
As(3)	0.6845	C21	-0.0044
As(1)'	-0.6757	C31	-0.2340
As(2)'	0.7232		
Plane II: 0.9145X + 0.3984Y + 0.0704Z - 2.2583 = 0			
C(11)	0.0017	C(14)	0.0050
C(12)	0.0064	C(15)	0.0032
C(13)	-0.0098	C(16)	-0.0064
Plane III: 0.6510X - 0.3885Y + 0.6521Z + 1.2449 = 0			
C(21)	0.0073	C(24)	0.0030
C(22)	0.0039	C(25)	0.0084
C(23)	-0.0091	C(26)	-0.0135
Plane IV: -0.0587X - 0.0362Y + 0.9976Z + 0.5149 = 0			
C(31)	0.0040	C(34)	0.0054
C(32)	-0.0043	C(35)	-0.0057
C(33)	-0.0004	C(36)	0.0010
Plane V: -0.1885X + 0.7711Y + 0.6081Z - 3.6317 = 0			
As(1)	0	As(3)	0
As(2)	0	C(21)	1.9215
Plane VI: 0.9854X + 0.1438Y + 0.0914Z + 0.7794 = 0			
As(2)	0	As(1)'	0
As(3)	0	C(31)	-1.9412
Plane VII: 0.0630X + 0.6239Y - 0.7790Z - 0.7208 = 0			
As(2)	0	As(3)'	0
As(1)	0	C(11)	-1.9203

## Dihedral Angles between Planes

	II	III	IV	V	VI	VII
I	37.6	93.1	96.9	57.3	52.7	51.8
II		60.9	89.9	79.8	15.2	75.4
III			51.2	91.5	49.8	135.2
IV				53.9	88.4	143.5
V					91.1	90.3
VI						85.4

<sup>a</sup> Orthonormal coordinates. <sup>b</sup> Italicized atoms used to construct plane.

would be expected for the increasing basicity of the transition-metal moiety present in each.

In IV and VII, a metal carbonyl group forms a three-membered ring with a RAsAsR group, Cr(CO)<sub>5</sub> in IV, and

(9) Campana, C. F.; Lo, F. Y.-K.; Dahl, L. F. *Inorg. Chem.* 1979, 18, 3060.

(10) Foust, A. S.; Campana, C. F.; Sinclair, J. D.; Dahl, L. F. *Inorg. Chem.* 1979, 18, 3047.



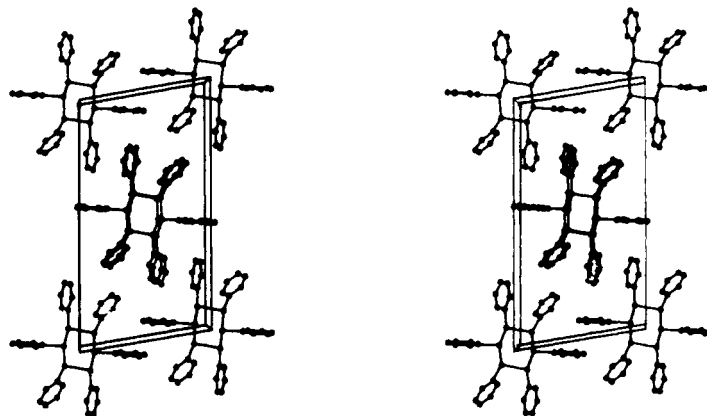


Figure 3. Stereoview of the unit-cell packing in 1 as viewed along the *b* axis.

Table VIII. Representative Arsenic-Arsenic Bond Distances

	compd	$d(\text{As}-\text{As})$ , Å	structural comment	ref
I	$[\mu-(\eta^2-\text{As})_2][\text{Co}_3(\text{CO})_5\text{PPh}_3]$	2.273 (3)	$\sim \text{As}=\text{As}$	10, 12
II	$[\mu_3-(\eta^2-\text{As}_2)][\text{W}(\text{CO})_5]_3$	2.279 (4)	$\sim \text{As}=\text{As}$	13
III	$[\mu-(\eta^2-\text{As}_2)][\text{CpM}(\text{CO})_2]_2$	2.312 (3), M = Mo 2.323 (3), M = W	$\sim \text{As}=\text{As}$	14
IV	$[\mu_3-(\eta^2-\text{AsPh})_2][\text{Cr}(\text{CO})_5]_3$	2.371	one of the $\text{Cr}(\text{CO})_5$ groups is between and perpendicular to the As-As bond	15
V	$(\eta^3\text{-c-As}_3)[\text{Co}(\text{CO})_3]$	2.372 (5)		16
VI	$[\mu-(\eta^4\text{-c-As}_5)][\text{CpMo}]_2$	2.385 (3) 2.397 (3) 2.563 (2) 2.726 (3) 2.752 (3)	$\mu-(\eta^2-\text{As}_3)$ $\mu-(\eta^2-\text{As}_2)$	17
VII	$[\eta^2-(\text{AsC}_6\text{F}_5)_2][\text{Fe}(\text{CO})_4]$	2.388 (7)	$\text{As}_2\text{Fe}$ ring	18
VIII	$\{\mu-[\eta^2\text{-catena}(\text{AsMe})_4]\}[\text{Fe}(\text{CO})_3]_2$	2.391 (7) [1,2]	4-membered chain bridging $\text{Fe}(\text{CO})_3$ groups	19
IX	$\text{Ba}_3\text{As}_{14}$	2.399 2.432 2.498	tricyclic $\text{As}_7^{3-}$	20
X	$\text{CH}_3\text{C}(\text{CH}_2\text{As})_3$	2.405 (5) 2.422 (5)	$\text{As}_3$ ring	21
XI	$[\mu-(\eta^1-\text{AsMe})][\mu-\text{AsMe}][\text{Mn}(\text{CO})_4]_2$	2.422 (3)		22
XII	$\text{c}-(\text{AsMe})_5$	2.428 (5) (av)		2
XIII	$\{\mu-[\eta^4\text{-catena}(\text{AsPr})_8]\}[\text{Mo}(\text{CO})_3]_2$	2.434 (7) (av)	$\text{As}_8$ chain bridging two $\text{Mo}(\text{CO})_3$ groups	23
XIV	$\{\mu-[\eta^2\text{-catena}(\text{AsMe})_5]\}[\text{CpMo}(\text{CO})_3]_2$	2.434 (2) (av int) 2.449 (2) (av term)	$\text{As}_5$ chain bridging two $\text{CpMo}(\text{CO})_3$ groups	24
XV	$[\mu-(\eta^1-\text{AsMe})_2][\text{Cr}(\text{CO})_4]_2$	2.442 (1)		25
XVI	$[\mu-\eta^6\text{-c}-(\text{AsMe})_9][\text{Cr}(\text{CO})_3]_2$	2.445 (8) (av)	$\text{As}_9$ ring bridging two $\text{Cr}(\text{CO})_3$ groups	26
XVII	$[(\mu-\eta^3\text{-c-As}_3)(\text{triphos Co})_2]^{2+}$	2.45 (1) (av)	$\text{As}_3$ ring	27
XVIII	$\text{c}-(\text{CF}_3\text{As})_4$	2.454 (1)		28
XIX	$[\mu-(\eta^1-\text{AsPh})_2][\text{CpFe}(\text{CO})_2]_2$	2.456 (2)	a tetrasubstituted diarsine	29
XX	$\text{c}-(\text{AsPh})_6$	2.459 (av)		this work
XXI	$[\mu-(\eta^1-\text{AsHPh})_2][\text{CpMn}(\text{CO})_2]_2$	2.460 (1)		30
XXII	$\text{CoAs}_3$ (skutterudite)	2.464 (2) 2.572 (2)		31
XXIII	$(\text{PhC-AsPh})_2$	2.475 (1)	substituted 1,2-diarsacyclobutene	32
XXIV	$(\text{As})_\infty$ ( $\alpha$ -arsenic)	2.516 (1)	two-dimensional nets of $\text{As}_6$ rings	33
XXV	$\text{As}_4\text{S}_4$	2.519 (3) 2.550 (3)		34

$\text{Fe}(\text{CO})_4$  in VII. It is uncertain whether the best description for these complexes is as a three-membered heterocycle or as a  $\eta^2(\pi)$  interaction; the former description requires an As-As single bond shortened by the effects of small ring formation and the latter, an As=As double bond elongated by the synergic combination of a  $\sigma$  donor/ $\pi$  acceptor metal-ligand interaction.<sup>10</sup> In IV, R =  $\text{C}_6\text{H}_5$ , and in VII, R =  $\text{C}_6\text{F}_5$ . The effect of a more electron-withdrawing organic substituent in VII is to lengthen the As-As bond (2.371 Å in IV and 2.388 (7) Å in VII) and to restrict the donor capability of As in VII; in IV, but not in VII, two additional 16-electron  $\text{Cr}(\text{CO})_5$  groups are coordinated to the As atoms.

In V and VI "naked" atoms form planar rings which in V are bonded to one  $\text{Co}(\text{CO})_3$  group and in VI, to two  $\text{CpMo}$  groups. In V the ring atoms form a single, symmetrical  $\eta^3\text{-As}_3$  ligand, whereas in VI, the  $\text{As}_5$  ring may be partitioned into  $\eta^2\text{-As}_3$  and  $\eta^2\text{-As}_2$  ligands. The two longest As-As bonds in VI (2.726 (3) and 2.752 (3) Å) connect the two ligands. These bond distances correspond to a bond order of  $\sim 0.5$  and are the longest accurately determined As-As distances we have been able to locate.

Compounds VIII, XI, and XIII-XVI contain chains of RAs units bonded in various bridging geometries to metal carbonyl groups. The longest bonds in these As chain complexes are found at the termini, but since bond lengths



Figure 4. Stereoview of a space-filling depiction of 1.

of uncoordinated As chains are not available for comparison, it is difficult to assess the full impact of coordination on As-As bond lengths in chains. It might be noted, however, that the terminal S-S bond distances in  $S_4^{2-}$  are longer than the interior distance, 2.074 vs. 2.061 Å,<sup>11</sup> by

(11) Abrahams, S. C.; Bernstein, J. L. *Acta Crystallogr., Sect. B* 1969, B25, 2365. Tegman, R. *Ibid.* 1973, B29, 1463.

(12) Foust, A. S.; Foster, M. S.; Dahl, L. F. *J. Am. Chem. Soc.* 1969, 91, 5633.

(13) Sigwarth, F.; Zsolnai, L.; Berke, H.; Huttner, G. *J. Organomet. Chem.* 1982, 226, C5.

(14) Sullivan, P. J.; Rheingold, A. L. *Organometallics* 1982, 1, 1547.

(15) Huttner, G.; Schmid, H.-G.; Frank, A.; Orama, O. *Angew. Chem., Int. Ed. Engl.* 1976, 15, 234.

(16) Foust, A. S.; Foster, M. S.; Dahl, L. F. *J. Am. Chem. Soc.* 1976, 91, 5631.

(17) Rheingold, A. L.; Foley, M. J.; Sullivan, P. J. *J. Am. Chem. Soc.* 1982, 104, 4727.

(18) Elmes, P. S.; Leverett, P.; West, B. O. *J. Chem. Soc., Chem. Commun.* 1971, 747.

(19) Gatehouse, B. M. *J. Chem. Soc., Chem. Commun.* 1969, 948.

(20) Schmettow, W.; von Schnering, H.-G. *Angew. Chem., Int. Ed. Engl.* 1977, 16, 857.

(21) Ellerman, J.; Schössner, H. *Angew. Chem., Int. Ed. Engl.* 1974, 13, 601.

(22) Röttinger, E.; Trenkle, A.; Müller, R.; Vahrenkamp, H. *Chem. Ber.* 1980, 113, 1280.

(23) Elmes, P. S.; Gatehouse, B. M.; Lloyd, D. J.; West, B. O. *J. Chem. Soc., Chem. Commun.* 1974, 953.

(24) Rheingold, A. L.; Churchill, M. R. *J. Organomet. Chem.*, in press.

(25) Cotton, F. A.; Webb, T. R. *Inorg. Chim. Acta* 1974, 10, 127.

(26) Elmes, P. S.; Gatehouse, B. M.; Lloyd, D. J.; West, B. O. *J. Chem. Soc., Chem. Commun.* 1974, 953.

(27) Di Vaira, M.; Midollini, S.; Sacconi, L. *J. Am. Chem. Soc.* 1979, 101, 1756.

(28) Mandel, N.; Donohue, J. *Acta Crystallogr., Sect. B* 1971, B27, 476.

(29) Rheingold, A. L.; Sullivan, P. J. *Organometallics* 1982, 1, 1429.

(30) Huttner, G.; Schmid, H.-G.; Lorenz, H. *Chem. Ber.* 1976, 109, 3741.

a difference similar to that found in the As chain complexes.

Compounds XII, XVIII, and XX contain single rings of monoorganoarsenic units. Because ring size and substitution varies so much among the rings, little value could derive from making comparisons. It is unusual that the stable allotrope of elemental arsenic ( $\alpha$ -arsenic, XXIV) contains a "long" As-As bond, 2.516 (1) Å. This may be attributed to interlayer bonding of the two-dimensional nets of  $As_8$  rings found in  $\alpha$ -arsenic.

A full consideration of representative data suggests that the range of a "normal" As-As single bond should be established as 2.43–2.46 Å and that for an As-As double bond as 2.27–2.32 Å. Distances outside these ranges are found in compounds in which special circumstances exert substantial bond compression or elongation effects.

**Acknowledgment.** This work was funded, in part, by a grant from the National Science Foundation, No. CHE 7911330. We are indebted to the authors of ref 32 who have allowed us to quote their work prior to its publication.

**Registry No.** 1, 20738-31-2.

**Supplementary Material Available:** Table IIIS, anisotropic thermal parameters, Table IVS, hydrogen atom coordinates, and Table VS,  $F_o$  vs.  $F_c$  (26 pages). Ordering information is given on any current masthead page.

(31) Mandel, N.; Donohue, J. *Acta Crystallogr., Sect. B* 1971, B27, 2288.

(32) Sennyey, G.; Mathey, F.; Fischer, J.; Mitschler, A., submitted for publication.

(33) Schiferl, D.; Barrett, C. S. *J. Appl. Cryst.* 1969, 2, 30.

(34) Kutoglu, A. *Z. Anorg. Allg. Chem.* 1976, 419, 176.

# Synthesis and Spectroscopic Studies of $\beta$ -Trimethylsilyl-Substituted, $\alpha,\beta$ -Unsaturated Carbonyl Compounds

Junzo Otera,\* Tadakatsu Mandai, Makio Shiba, Toshiaki Saito, Koichi Shimohata, Keiji Takemori, and Yuzuru Kawasaki

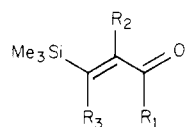
Okayama University of Science, Ridai-cho, Okayama 700, Japan

Received August 10, 1982

A new synthetic method for  $\beta$ -trimethylsilyl-substituted,  $\alpha,\beta$ -unsaturated carbonyl compounds **1** has been developed. The procedures consist of the following sequence of reactions: silylation at  $\alpha$ -phenylsulfonyl carbon of **3** and a facile elimination of benzenesulfonic acid in **5** under mild conditions. UV spectra of **1** exhibited characteristic bathochromic shifts of  $\pi-\pi^*$  bands as compared with the corresponding parent compounds. The magnitude of the shift varied from 5 to 21 nm depending on the methyl substituent. The shift was interpreted in terms of the stabilization of the LUMO of  $\alpha,\beta$ -unsaturated carbonyl chromophores induced by the interaction with the 3d orbital of silicon.

## Introduction

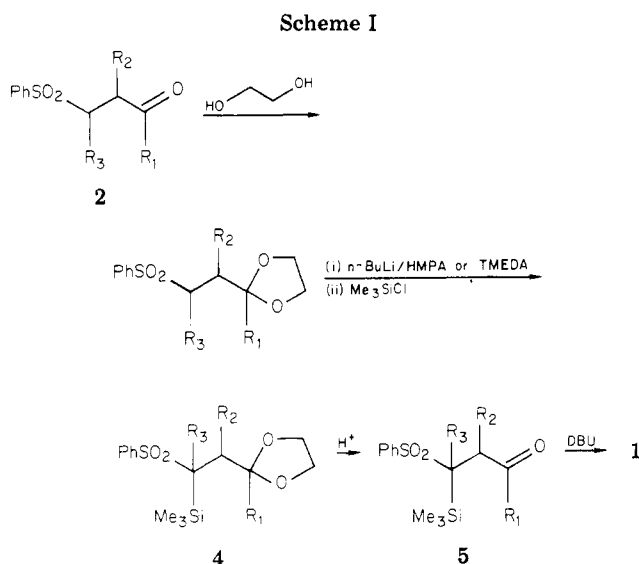
In connection with synthetically useful vinylsilanes, considerable attention has been paid to silyl-substituted,  $\alpha,\beta$ -unsaturated carbonyl compounds **1**, which are versatile precursors for silyl-substituted dienes<sup>1-5</sup> or dienones,<sup>6</sup> and highly substituted,  $\alpha,\beta$ -unsaturated ketones.<sup>7</sup>



**1**,  $R_1, R_2, R_3 = \text{H or CH}_3$

Moreover, another interesting aspect of **1** is their spectral properties. Since  $\alpha,\beta$ -unsaturated carbonyl chromophores exhibit  $\pi-\pi^*$  absorption maxima in the ultraviolet region and the effect of alkyl substitution in these chromophores is well understood,<sup>8</sup> the effect of the silyl substitution on an adjacent ethylenic chromophore can be elucidated on the basis of UV spectra of **1**. For the vinyl ketone derivative **1d**, Brook et al. have observed a bathochromic effect of  $\beta$ -trimethylsilyl substitution.<sup>9</sup> A similar effect has been put forth for the  $n-\pi^*$  transition.<sup>10</sup>

Usually compounds **1** are derived from functionally substituted vinylsilanes,<sup>9,11,12</sup> allenylsilanes,<sup>13,14</sup> or alkenylsilanes.<sup>3,5,7</sup> The methods of hydrosilylation of acetylenes<sup>15,16</sup> and dehydrogenation of the saturated  $\gamma$ -keto-



**a**,  $R_1, R_2, R_3 = \text{H}$ ; **b**,  $R_1, R_2 = \text{H}, R_3 = \text{Me}$ ; **c**,  $R_1, R_3 = \text{H}, R_2 = \text{Me}$ ; **d**,  $R_2, R_3 = \text{H}, R_1 = \text{Me}$ ; **e**,  $R_1, R_3 = (\text{CH}_2)_{3/2}, R_2 = \text{H}$

silanes<sup>10</sup> have also been reported. However, these methods are not always satisfactory with respect to generality, selectivity, and availability of starting materials.

Here we report a new general method for preparing compounds of type **1**, employing readily available reagents, and the spectral properties of **1** thus obtained will be described.

## Results and Discussion

**Synthesis.** Our basic route for **1** is depicted in Scheme I. The present procedures are based on facile carbanion formation at the  $\alpha$ -phenylsulfonyl carbon and a smooth elimination of benzenesulfonic acid  $\beta$  to the carbonyl group under mild conditions.<sup>17-20</sup>

(1) Carter, M. J.; Fleming, I. *J. Chem. Soc., Chem. Commun.* **1976**, 679.

(2) Fleming, I.; Percival, A. *J. Chem. Soc., Chem. Commun.* **1978**, 178.

(3) Carter, M. J.; Fleming, I.; Percival, A. *J. Chem. Soc., Perkin Trans. 1*, **1981**, 2415.

(4) Garland, R. B.; Palmer, J. R.; Schulz, J. A.; Sollman, P. B.; Rappo, R. *Tetrahedron Lett.* **1978**, 3669.

(5) Jung, M. E.; Gaede, B. *Tetrahedron* **1979**, *35*, 621.

(6) Pillot, J.-P.; Dunogues, J.; Calas, R. *J. Chem. Res., Synop.* **1977**, 268.

(7) Fleming, I.; Perry, D. A. *Tetrahedron* **1981**, *37*, 4027.

(8) Jaffé, H. H.; Orchin, M. "Theory and Application of Ultraviolet Spectroscopy"; Wiley: New York, 1962.

(9) Brook, A. G.; Duff, J. M. *Can. J. Chem.* **1973**, *51*, 2024.

(10) Felix, R. A.; Weber, W. P. *J. Org. Chem.* **1972**, *37*, 2323.

(11) Pillot, J.-P.; Dunogues, J.; Calas, R. *Bull. Soc. Chim. Fr.* **1975**, 2143.

(12) Cunico, R. F.; Clayton, F. J. *J. Org. Chem.* **1976**, *41*, 1480.

(13) Mantione, R.; Leroux, Y. *J. Organomet. Chem.* **1971**, *31*, 5.

(14) Merault, G.; Picard, J.-P.; Bourgeois, P.; Dunogues, J.; Duffaut, N. *J. Organomet. Chem.* **1972**, *42*, C80.

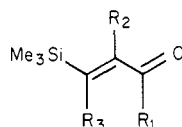
(15) Mashlyakovskii, L. N.; Chelpanova, L. F. *Zh. Obshch. Khim.* **1965**, *35*, 2009.

(16) Kamarov, N. V.; Puchnarevich, V. B.; Suschinskaya, S. P.; Kalabin, G. A.; Sakharovskii, V. G. *Izv. Akad. Nauk SSSR, Soc. Khim.* **1968**, 803.

(17) Julia, M.; Paris, J.-M. *Tetrahedron Lett.* **1973**, 4833.

(18) Kondo, K.; Tunemoto, D. *Tetrahedron Lett.* **1975**, 1007.

(19) Mandai, T.; Yamaguchi, H.; Nishikawa, K.; Kawada, M.; Otera, J. *Tetrahedron Lett.* **1981**, *22*, 763.

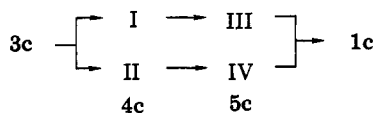
Table I. <sup>1</sup>H NMR Spectral Parameters of 1<sup>a</sup>

compd	R			δ (pattern, J)				
	R <sub>1</sub>	R <sub>2</sub>	R <sub>3</sub>	CH <sub>3</sub> Si	R <sub>1</sub>	R <sub>2</sub>	R <sub>3</sub>	
1a	H	H	H	0.19 (s)	9.47 (d, J = 7.0)	6.43 (ABX, J <sub>AB</sub> = 19, J <sub>AX</sub> = 7.0)	7.18 (AB, J = 19)	
1b	H	H	CH <sub>3</sub>	0.07 (s)	9.89 (d, J = 7.2)	6.01 (dq, J = 7.2 and 2.0)	2.06 (d, J = 2.0)	
1c	H	CH <sub>3</sub>	H	E isomer	0.16 (s)	9.10 (d, J = 7.6)	6.19 (dq, J = 7.6 and 1.2)	1.99 (d, J = 1.2)
					0.24 (s)	9.34 (s)	1.93 (d, J = 0.9)	6.69 (q, J = 0.9)
1d	CH <sub>3</sub>	H	H	Z isomer	0.18 (s)	2.18 (s)	6.27 and 6.85 (AB, J = 19)	
					0.05 (s)	1.70-2.40 (m)	5.95 (s)	1.70-2.40 (m)

<sup>a</sup> δ in ppm and J in Hz in CDCl<sub>3</sub>.

The starting sulfones 2 were conveniently prepared by 1,4 addition of benzenesulfonic acid to α,β-unsaturated carbonyl compounds.<sup>21</sup> However, the α-carbon of the ketalized sulfones 3 could not be silylated by a simple addition of Me<sub>3</sub>SiCl to the *n*-butyllithium-generated anions. This is rather unexpected since the α-phenylsulfonyl carbanion undergoes alkylation easily under similar conditions.<sup>17-20</sup> The most successful results were obtained when the reactions were run in the presence of 3 molar equiv of hexamethylphosphoramide (HMPA) for 3b, 3d, and 3e or tetramethylethylenediamine (TMEDA) for 3a and 3c. Then, after removal of the protecting group, 4 was treated with 1,8-diazabicyclo[5,4,0]undec-7-ene (DBU) in dichloromethane to yield 1. Interestingly, treatment of the cyclohexenone derivative 4e with HCl in aqueous acetone resulted in not only deketalization but also desulfonylation, thus affording 1e directly.<sup>22</sup>

The procedures for the methacrolein derivative require further comment. Silylation of 3c yielded 4c as two unseparable diastereomers I and II as shown in Figure 1. When the protecting group of 4c was removed, in 5 N HCl-acetone at 0 °C I was deketalized smoothly to afford 5c (isomer III), while II remained almost intact after 24 h. Prolonged treatment initiated deketalization of II,



requiring 80 h for the complete conversion to 5c (isomer IV), but the formation of (*E*)-β-(phenylsulfonyl)methacrolein (6) derived by elimination of Me<sub>3</sub>SiH from 5c was a competing side reaction. Once 6 had been formed, the presence of this compound prevented the isolation of III in pure form by column chromatography. Therefore, it was desirable to increase the ratio of I because the silylation in the presence of HMPA yielded I and II in 3:7 ratio. Improvement was achieved by employing TMEDA in place of HMPA, the ratio being reversed to 8:2. Either of the isomers III or IV provided 1c on treatment with DBU.

The <sup>1</sup>H NMR spectral parameters of 1 are summarized in Table I. It is evident for 1a and 1d that only trans isomers were formed on the basis of the vicinal coupling

(20) Mandai, T.; Nishikawa, K.; Yamaguchi, H.; Kawada, M.; Otera, J. *Chem. Lett.* 1981, 473.

(21) Gilman, H.; Cason, L. F. *J. Am. Chem. Soc.* 1950, 72, 3469.

(22) After this study has completed, acid-catalyzed desulfonylation to give β-substituted α,β-unsaturated carbonyl compounds has been reported: Yoshida, T.; Saito, S. *Chem. Lett.* 1982, 165.

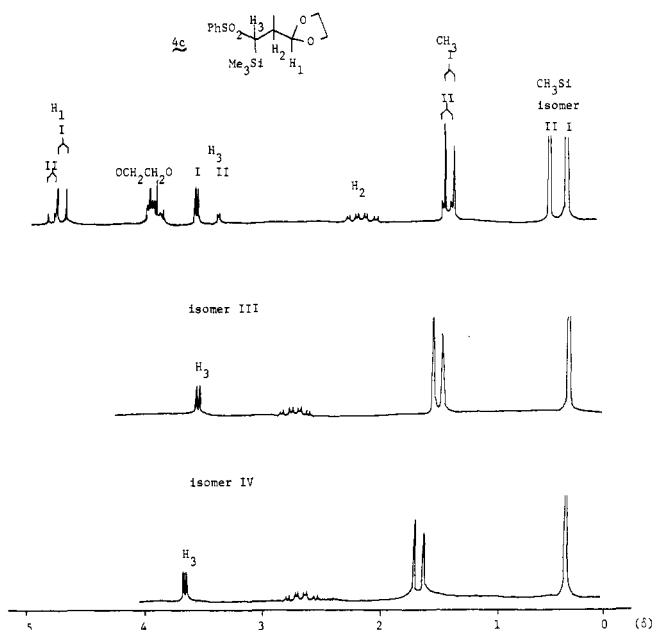


Figure 1. <sup>1</sup>H NMR spectra of 4c and 5c (isomer III and IV).

constants of olefinic protons (19 Hz for both 1a and 1d), together with the GLC analysis that gave rise to a single peak. The GLC of 1b showed *E* and *Z* isomers in a 4:1 ratio. In line with this result, the <sup>1</sup>H NMR spectrum of 1b exhibited a pair of signals for each proton with the expected integral ratio. The GLC of 1c also showed two peaks in a 18:1 ratio. The major component is ascribed to the *E* isomer by analogy with 2-methyl-2-pentenal for which the *E* form was found to be much more thermodynamically favored than the *Z* form.<sup>23</sup> This is confirmed with <sup>1</sup>H NMR spectra. In the isomeric 2-methyl-2-pentenal, the *Z* aldehyde proton exhibits its signal at a 0.73-ppm lower field than the *E* isomer. Similarly, <sup>1</sup>H NMR spectrum of 1c gave rise to a weak signal at δ 9.70 in addition to a main signal at δ 9.34 for the aldehydic proton.<sup>24</sup>

(23) Chan, K. C.; Jewell, R. A.; Nutting, W. H.; Rapoport, H. *J. Org. Chem.* 1968, 33, 3382.

(24) It should be noted that this difference is diagnostic of α-substituted enals. In the case of β-substituted enals, *E* isomer exhibits its aldehydic proton signal usually at lower field than the corresponding *Z* isomer. Cf. Ishida, A.; Mukaiyama, T. *Chem. Lett.* 1975, 1167. "The Aldrich Library of NMR Spectra"; Aldrich Chemical Co. Ltd.: 1974; Vol. II, p 101. The assignments of *E/Z* designation to 1b and 1c given in Table I are also consistent with the GLC analysis, in which both compounds gave rise to a minor peak at a shorter retention time characteristic of the *Z* form.

Table II.  $\pi-\pi^*$  Absorption Maxima of 1 and Their Parent Compounds<sup>a</sup>

compd	$\lambda_{\max}$ , nm	$\Delta^b$
1a	217 (212)	5
1b	235 (214)	21
1c	232 (213)	19
1d	220 (210)	10
1e	230 (218)	12

<sup>a</sup>  $\lambda_{\max}$  of parent compounds are given in parentheses.

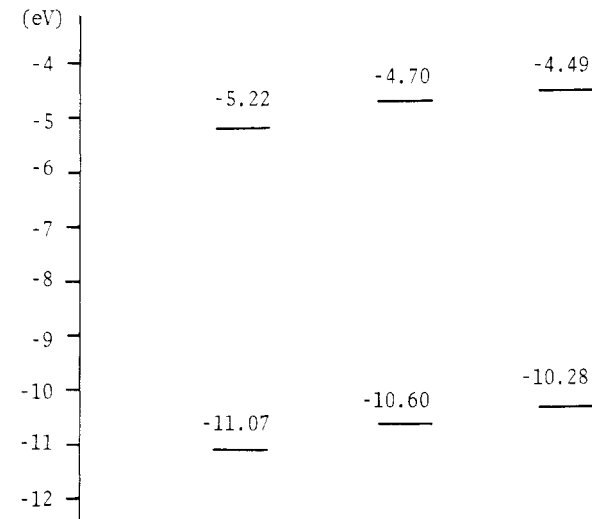
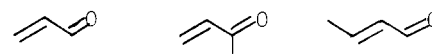
<sup>b</sup>  $\Delta = \lambda_{\max}(\text{silyl derivative}) - \lambda_{\max}(\text{parent compound})$ .

**UV Spectra.** In the study of  $\pi-\pi^*$  bands in  $\alpha,\beta$ -unsaturated carbonyl compounds, an appropriate solvent should be carefully employed on account of the solvent dependence of the band. With a change of the solvent from *n*-hexane to ethanol, which is most frequently used, Woodward predicted a bathochromic shift by 7 nm, while Fieser proposed a shift by 11 nm.<sup>8</sup> By contrast, only a slight red shift (2 nm) was found for 1d when the solvent was changed from cyclohexane to ethanol. Analogous results have been reported with a change from cyclohexane to methanol.<sup>9</sup> Accordingly, cyclohexane was selected as a solvent in this study since this solvent is believed to give rise to the least interaction with the solute.

In Table II are shown the comparison of  $\pi-\pi^*$  bands of 1 and their parent compounds. Although  $\beta$ -trimethylsilyl substitution in general caused a bathochromic shift, a marked difference was observed, depending on the methyl substituent; that is, the magnitude of the shift is 5 nm for acrolein, 10–12 nm for the ketones, and 19–21 nm for the  $\alpha$ - and  $\beta$ -methyl-substituted aldehydes. If the inductive electron release of the trimethylsilyl group is responsible for these shifts, the magnitude of the shift should be comparable for all compounds. The present results seem to lend promising support to the previously suggested explanation<sup>9,10</sup> that a lowering of LUMO of the  $\alpha,\beta$ -unsaturated carbonyl chromophore induced by the interaction with the 3d orbital in silicon is responsible for the bathochromic shift. In Figure 2, the relative energy levels of HOMO and LUMO for acrolein, methyl vinyl ketone, and crotonaldehyde are illustrated schematically. In this scheme, the energy levels of the HOMO were determined on the basis of reported photoelectron spectra,<sup>25</sup> and addition of  $\pi-\pi^*$  excitation energy (calculated from UV spectra) to HOMO led to the energy levels of LUMO. Obviously, the LUMO levels are raised in the same order as the magnitude of bathochromic shifts caused by the silyl substitution. It may be suggested, therefore, that the higher the LUMO level, the more effectively the  $d\pi-p\pi^*$  interaction takes place, resulting in stabilization of the LUMO level. Brook et al. have suggested that HOMO is also lowered by the interaction with the d orbital in silicon, but to a lesser extent.<sup>9</sup> It is reasonably assumed that the upper-lying empty 3d orbital can interact more strongly with LUMO than HOMO.

### Experimental Section

Reactions requiring anhydrous conditions were carried out under a nitrogen atmosphere. Commercially available reagents were distilled before use. Solvents were purified by standard methods. <sup>1</sup>H NMR spectra were obtained with a Hitachi R-24B spectrometer operating at 60 MHz and with a Jeol FX-100 spectrometer operating at 100 MHz. <sup>13</sup>C and <sup>29</sup>Si NMR spectra were also measured with this spectrometer. Chemical shifts are related to internal tetramethylsilane in parts per million for all cases, positive signs indicating downfield shifts from the reference.



**Figure 2.** Schematic representation of relative energy levels of HOMO and LUMO of  $\alpha,\beta$ -unsaturated carbonyl compounds.

UV spectra were recorded by using a Hitachi Model 285 spectrophotometer equipped with 1-cm quartz cells. The GLC analyses were run on a Hitachi 163 gas chromatograph with 3 mm  $\times$  3 m column packed with 10% PEG 20 M on Uniport B. Melting points were uncorrected.

**Preparation of 2.** To an acetic acid solution (100 mL) of sodium benzenesulfinate dihydrate (15.0 g, 75 mmol) was added acrolein (2.80 g, 50 mmol). After being stirred overnight at room temperature, the reaction mixture was shaken with an aqueous sodium bicarbonate solution and extracted with benzene–water. Drying the benzene layer on magnesium sulfate and evaporation yielded synthetically pure 3-(phenylsulfonyl)propionaldehyde (**2a**) as an oil (6.80 g, 68%). The product was used in the next step without further purification. Other sulfones were prepared by the same method. Yield: **2b**, 90%; **2c**, 66%; **2d**, 99%; **2e**, 85%.

**Preparation of 3.** A benzene solution containing **2a** (6.80 g, 34 mmol), a large excess of ethylene glycol, and a catalytic amount of *p*-toluenesulfonic acid was refluxed to remove water azeotropically. After the removal of water was complete, the reaction mixture was poured into an aqueous sodium bicarbonate solution. The organic layer was washed with water and dried followed by evaporation to give the ketalized sulfone **3a** (7.24 g, 87%) that was found pure enough for further use. Other ketalizations were carried out analogously in 95–99% yields.

**Preparation of 4.** In 100 mL of THF was dissolved **3a** (4.11 g, 17 mmol) and TMEDA (5.93 g, 51 mmol) under nitrogen. *n*-Butyllithium in pentane (1.5 N, 13.6 mL, 20.4 mmol) was added dropwise to this solution at  $-78^\circ\text{C}$  and stirred for 1 h at this temperature. To this solution was added  $\text{Me}_3\text{SiCl}$  (3.69 g, 34 mmol). The solution was stirred for 1 h at  $-78^\circ\text{C}$  and for additional 1 h at room temperature. Then the reaction mixture was extracted with benzene–water. Drying and evaporation of the organic layer gave a crude product that was chromatographed on silica gel (hexane–ether, 10:1) to afford pure **4a** as white crystals: yield 5.0 g (94%); mp  $85\text{--}86^\circ\text{C}$ .

The methacrolein derivative **4c** was obtained by the same method in 95% yield: column chromatography (hexane–ether, 10:1); mp  $75\text{--}76^\circ\text{C}$ .

Other silylated compounds were prepared by an analogous method employing HMPA in place of TMEDA. **4b**: yield 98%; column chromatography (hexane–ether, 5:1); mp  $70\text{--}73^\circ\text{C}$ . **4d**: yield 97%; column chromatography (hexane–ether, 5:1); oil. **4e**: yield 90%; column chromatography (hexane–ether, 10:1), mp  $86\text{--}88^\circ\text{C}$ . Anal. Calcd for  $\text{C}_{17}\text{H}_{26}\text{O}_4\text{Si}$ : C, 57.59; H, 7.39. Found: C, 57.47; H, 7.29.

**Preparation of 5a.** In acetone (100 mL) and 5 N aqueous HCl (100 mL) was dissolved **4a** (4.50 g, 14.3 mmol), and the solution was stirred for 17 h at room temperature. The reaction mixture was extracted with benzene–water and usual workup gave a crude

product that was chromatographed on silica gel (hexane-ether, 10:1) to yield white crystals: yield 2.91 g (75%); mp 50–53 °C. Anal. Calcd for C<sub>19</sub>H<sub>18</sub>O<sub>3</sub>SSi: C, 53.30; H, 6.71. Found: C, 53.19; H, 6.75.

**Preparation of 5b.** This compound was prepared by the analogous method for 5a except that the reaction time was 6 h in 78% yield: white crystals after column chromatography (hexane-ether, 10:1); mp 61–64 °C. Anal. Calcd for C<sub>19</sub>H<sub>20</sub>O<sub>3</sub>SSi: C, 54.89; H, 7.09. Found: C, 54.77; H, 7.14.

**Preparation of 5c.** In acetone (5 mL) and 5 N aqueous HCl (5 mL), 4c (110 mg, 0.34 mmol) was stirred at 0 °C. After 24 h, TLC monitoring exhibited two spots at R<sub>f</sub> = 0.5 and 0.6, respectively (hexane-ether, 1:2). Careful column chromatography on silica gel (hexane-ether, 15:1) revealed the former spot derived from III: yield 51.5 mg (60%); mp 48–50 °C. Anal. Calcd for C<sub>13</sub>H<sub>20</sub>O<sub>3</sub>SSi: C, 54.89; H, 7.09. Found: C, 54.64; H, 7.38. The NMR spectrum showed that another component of R<sub>f</sub> = 0.6 consisted of unreacted 4c (isomer II) and a small amount of IV. When the reaction was stirred for more than 24 h, (E)-β-(phenylsulfonyl)methacrolein (6) (R<sub>f</sub> = 0.55–0.6) was formed that could not be separated from III by column chromatography. Nevertheless, when the same reaction was run for 80 h, the isomer IV could be obtained in 10% yield: mp 45–47 °C. Anal. Calcd for C<sub>13</sub>H<sub>20</sub>O<sub>3</sub>SSi: C, 54.89; H, 7.09. Found: C, 54.51; H, 6.98.

**Preparation of 5d.** This compound was prepared by the analogous method for 5b in 95% yield: colorless oil after column chromatography (hexane-ether, 10:1). Anal. Calcd for C<sub>13</sub>H<sub>20</sub>O<sub>3</sub>SSi: C, 54.89; H, 7.09. Found: C, 54.58; H, 7.18.

**Preparation of 1a.** In 7 mL of dichloromethane, 5a (200 mg, 0.74 mmol) and DBU (225 mg, 1.48 mmol) were stirred under nitrogen at 0 °C for 2 h. Since evaporation of dichloromethane from the reaction mixture was found to result in a loss of 1a due to its relatively low boiling point, the solvent was replaced with *n*-pentane column chromatographically by using *n*-pentane as an eluent. Careful distillation of *n*-pentane from the solution thus obtained under reduced pressure induced no loss of 1a, leaving a colorless liquid. This liquid was distilled in the presence of hydroquinone with Kugelrohr: bath temperature 60 °C at 30 mmHg (lit.<sup>5</sup> 53–54 °C at 30 mmHg). However, the sample after *n*-pentane was distilled off was pure enough: yield 86 mg (91%); mass spectrum, *m/e* (P) 128.0649 (calcd 128.0657).

**Preparation of 1b.** A dichloromethane solution (10 mL) of 5b (300 mg, 1.06 mmol) and DBU (322 mg, 2.12 mmol) was refluxed for 2 h under nitrogen. Workup as described for 1a afforded a colorless liquid of 1b: yield 143 mg (95%); mass spectrum, *m/e* (P) 142.0874 (calcd 142.0813).

**Preparation of 1c.** A dichloromethane solution (5 mL) of 5c<sup>26</sup> (120 mg, 0.42 mmol) and DBU (129 mg, 0.85 mmol) was refluxed for 2 h under nitrogen. Workup as described for 1a afforded a colorless liquid of 1c: yield 40 mg (67%); mass spectrum, *m/e* (P) 142.0831 (calcd 142.0813).

**Preparation of 1d.** A dichloromethane solution (10 mL) of 5d (300 mg, 1.06 mmol) and DBU (322 mg, 2.12 mmol) was refluxed for 50 min under nitrogen. Workup as described for 1a afforded a colorless liquid of 1d: yield 140 mg (93%); mass spectrum *m/e* (P) 142.0820 (calcd 142.0813).

**Preparation of 1e.** In 350 mL of a 1:1 mixture of 4 N aqueous HCl and acetone, 4e (2.47 g, 6.97 mmol) was stirred at room temperature for overnight. The reaction mixture was extracted with benzene, and the benzene layer was washed with water. Usual workup gave a crude product that was subjected to column chromatography on silica gel to afford 1e as an oil: yield 0.95 g (81%); mass spectrum, *m/e* (P) 168.0998 (calcd 168.0970).

**NMR and UV Spectral Data.** 2a: <sup>1</sup>H NMR (CCl<sub>4</sub>) δ 2.65–2.90 (m, 2 H, CH<sub>2</sub>SO<sub>2</sub>Ph), 3.17–3.45 (m, 2 H, CH<sub>2</sub>CO), 7.37–7.85 (m, 5 H, Ph), 9.56 (s, 1 H, CHO).

2b: <sup>1</sup>H NMR (CCl<sub>4</sub>) δ 1.21 (d, 3 H, CH<sub>3</sub>, *J* = 6.6 Hz), 2.30–3.34 (m, 2 H, CH<sub>2</sub>CO), 3.45–3.91 (m, 1 H, CHSO<sub>2</sub>Ph), 7.45–7.90 (m, 5 H, Ph), 9.69 (s, 1 H, CHO).

2c: <sup>1</sup>H NMR (CCl<sub>4</sub>) δ 1.37 (d, 3 H, CH<sub>3</sub>, *J* = 7.0 Hz), 2.75–3.10 (m, 2 H, CH<sub>2</sub>SO<sub>2</sub>Ph), 3.40–3.70 (m, 1 H, CH), 7.50–8.02 (m, 5 H, Ph), 9.52 (s, 1 H, CHO).

2d: <sup>1</sup>H NMR (CCl<sub>4</sub>) δ 2.06 (s, 3 H, CH<sub>3</sub>), 2.65–2.91 (m, 2 H,

CH<sub>2</sub>SO<sub>2</sub>Ph), 3.17–3.41 (m, 2 H, CH<sub>2</sub>CO), 7.45–7.90 (m, 5 H, Ph).

2e: <sup>1</sup>H NMR (CCl<sub>4</sub>) δ 1.50–2.40 (m, 8 H, CH<sub>2</sub>), 3.05–3.35 (m, 1 H, CHSO<sub>2</sub>Ph), 7.50–7.90 (m, 5 H, Ph).

3a: <sup>1</sup>H NMR (CCl<sub>4</sub>) δ 1.73–2.06 (m, 2 H, CCH<sub>2</sub>C), 2.86–3.30 (m, 2 H, CH<sub>2</sub>SO<sub>2</sub>Ph), 3.74 (s, 4 H, OCH<sub>2</sub>CH<sub>2</sub>O), 4.77 (t, 1 H, CH, *J* = 4.0 Hz), 7.37–7.85 (m, 5 H, Ph).

3b: <sup>1</sup>H NMR (CCl<sub>4</sub>) δ 1.27 (d, 3 H, CH<sub>3</sub>, *J* = 6.6 Hz), 1.55–2.45 (m, 2 H, CCH<sub>2</sub>C), 3.0–3.55 (m, 1 H, CHSO<sub>2</sub>Ph), 3.80 (s, 4 H, OCH<sub>2</sub>CH<sub>2</sub>O), 4.89 (t, 1 H, CH, *J* = 5.0 Hz), 7.45–7.91 (m, 5 H, Ph).

3c: <sup>1</sup>H NMR (CCl<sub>4</sub>) δ 0.94 (d, 3 H, CH<sub>3</sub>, *J* = 6.6 Hz), 1.77–2.35 (m, 1 H, CCHC), 2.35–3.14 (m, 2 H, CH<sub>2</sub>SO<sub>2</sub>Ph), 3.58 (s, 4 H, OCH<sub>2</sub>CH<sub>2</sub>O), 4.41 (d, 1 H, CH, *J* = 3.0 Hz), 7.28–7.75 (m, 5 H, Ph).

3d: <sup>1</sup>H NMR (CCl<sub>4</sub>) δ 1.12 (s, 3 H, CH<sub>3</sub>), 1.70–1.96 (m, 2 H, CH<sub>2</sub>), 2.77–3.03 (m, 2 H, CH<sub>2</sub>SO<sub>2</sub>Ph), 3.70 (s, 4 H, OCH<sub>2</sub>CH<sub>2</sub>O), 7.36–7.82 (m, 5 H, Ph).

3e: <sup>1</sup>H NMR (CCl<sub>4</sub>) δ 1.20–2.10 (m, 8 H, CH<sub>2</sub>), 2.70–3.20 (m, 1 H, CHSO<sub>2</sub>Ph), 3.67 (s, 4 H, OCH<sub>2</sub>CH<sub>2</sub>O), 7.40–7.85 (m, 5 H, Ph).

4a: <sup>1</sup>H NMR (CCl<sub>4</sub>) δ 0.19 (s, 9 H, CH<sub>3</sub>Si), 1.80 (dd, 2 H, CCH<sub>2</sub>C), 2.67 (t, 1 H, CHSO<sub>2</sub>Ph, *J* = 5.0 Hz), 3.48 (s, 4 H, OCH<sub>2</sub>CH<sub>2</sub>O), 4.07 (t, 1 H, CH, *J* = 4.8 Hz), 7.35–7.80 (m, 5 H, Ph).

4b: <sup>1</sup>H NMR (CCl<sub>4</sub>) δ 0.25 (s, 9 H, CH<sub>3</sub>Si), 1.22 (s, 3 H, CH<sub>3</sub>), 1.70–1.92 (m, 2 H, CCH<sub>2</sub>C), 3.65–3.75 (b d, 4 H, OCH<sub>2</sub>CH<sub>2</sub>O), 4.70 (t, 1 H, CH, *J* = 4.4 Hz), 7.45–7.85 (m, 5 H, Ph).

4c: <sup>1</sup>H NMR (CCl<sub>4</sub>) δ 0.29 and 0.41 (s, 9 H, CH<sub>3</sub>Si), 1.26 and 1.29 (d, 3 H, CH<sub>3</sub>, *J* = 7.1 and 6.6 Hz), 1.89–2.16 (m, 1 H, CCHC), 3.24 and 3.43 (d, 1 H, CHSO<sub>2</sub>Ph, *J* = 1.1 and 1.8 Hz), 3.56–3.83 (m, 4 H, OCH<sub>2</sub>CH<sub>2</sub>O), 4.55 and 4.62 (d, 1 H, CH, *J* = 7.0 and 7.6 Hz), 7.50–8.16 (m, 5 H, Ph); <sup>13</sup>C NMR (CDCl<sub>3</sub>) δ 0.0 and 1.5 (CH<sub>3</sub>Si), 12.9 and 13.6 (CH<sub>3</sub>C), 37.7 and 38.0 (CCC), 56.3 and 57.7 (SiCSO<sub>2</sub>Ph), 64.5, 64.9, and 64.2, 64.6 (OCH<sub>2</sub>CH<sub>2</sub>O), 104.7 and 105.4 (CH), 127.5, 127.8, 128.7, 132.7 (Ph).

4d: <sup>1</sup>H NMR (CCl<sub>4</sub>) δ 0.16 (s, 9 H, CH<sub>3</sub>Si), 0.78 (s, 3 H, CH<sub>3</sub>), 1.88–2.01 (m, 2 H, CCH<sub>2</sub>C), 2.54 (t, 1 H, CHSO<sub>2</sub>Ph, *J* = 4.4 Hz), 3.35–3.56 (m, 4 H, OCH<sub>2</sub>CH<sub>2</sub>O), 7.26–7.78 (m, 5 H, Ph).

4e: <sup>1</sup>H NMR (CCl<sub>4</sub>) δ 0.26 (s, 9 H, CH<sub>3</sub>Si), 0.80–2.10 (m, 8 H, CH<sub>2</sub>), 3.70 (b s, 4 H, OCH<sub>2</sub>CH<sub>2</sub>O), 7.20–7.70 (m, 5 H, Ph).

5a: <sup>1</sup>H NMR (CCl<sub>4</sub>) δ 0.27 (s, CH<sub>3</sub>Si), 2.86 (dd, 2 H, CH<sub>2</sub>CO), 3.58 (t, 1 H, CHSO<sub>2</sub>Ph, *J* = 5.0 Hz), 7.55–8.05 (m, 5 H, Ph), 9.53 (s, 1 H, CHO).

5b: <sup>1</sup>H NMR (CCl<sub>4</sub>) δ 0.38 (s, 9 H, CH<sub>3</sub>Si), 1.31 (s, 3 H, CH<sub>3</sub>), 2.48 (d, 2 H, CH<sub>2</sub>CO, *J* = 2.8 Hz), 7.52–7.93 (m, 5 H, Ph), 9.83 (t, 1 H, CHO, *J* = 2.8 Hz).

5c. Isomer III: <sup>1</sup>H NMR (CDCl<sub>3</sub>) δ 0.29 (s, 9 H, CH<sub>3</sub>Si), 1.37 (d, 3 H, CH<sub>3</sub>, *J* = 7.6 Hz), 2.59 (dq, 1 H, CCHC), 3.41 (d, 1 H, CHSO<sub>2</sub>Ph, *J* = 2.0 Hz), 7.51–7.97 (m, 5 H, Ph), 9.63 (s, 1 H, CHO); <sup>13</sup>C NMR (CDCl<sub>3</sub>) δ 0.2 (CH<sub>3</sub>Si), 12.9 (CH<sub>3</sub>), 44.8 (CCC), 58.2 (SiCSO<sub>2</sub>Ph), 127.9, 129.2, 133.4 (Ph), 202.5 (CHO). Isomer IV: <sup>1</sup>H NMR (CDCl<sub>3</sub>) δ 0.31 (s, 9 H, CH<sub>3</sub>Si), 1.55 (d, 3 H, CH<sub>3</sub>, *J* = 7.7 Hz), 2.57 (dq, 1 H, CCHC), 3.54 (d, 1 H, CHSO<sub>2</sub>Ph, *J* = 1.7 Hz), 7.48–7.91 (m, 5 H, Ph), 9.42 (s, 1 H, CHO); <sup>13</sup>C NMR (CDCl<sub>3</sub>) δ 0.9 (CH<sub>3</sub>Si), 12.4 (CH<sub>3</sub>), 45.6 (CCC), 55.5 (SiCSO<sub>2</sub>Ph), 127.8, 129.3, 133.3 (Ph), 201.1 (CHO).

5d: <sup>1</sup>H NMR (CCl<sub>4</sub>) δ 0.26 (s, 9 H, CH<sub>3</sub>Si), 1.95 (s, 3 H, CH<sub>3</sub>CO), 2.80 (m, 2 H, CCH<sub>2</sub>C), 3.66 (t, 1 H, CHSO<sub>2</sub>Ph, *J* = 5.5 Hz), 7.50–8.00 (m, 5 H, Ph).

1a: <sup>13</sup>C NMR (CDCl<sub>3</sub>) δ -2.0 (CH<sub>3</sub>Si), 144.2 (SiCH=), 158.2 (=CHCO), 194.4 (CHO); <sup>29</sup>Si NMR (CDCl<sub>3</sub>) δ -4.81; UV spectrum (cyclohexane) λ<sub>max</sub> (ε) 217 (7800), 340 (31), 354 (31), 371 (22), 390 (8).

1b: <sup>13</sup>C NMR (CDCl<sub>3</sub>) δ 1.94 (CH<sub>3</sub>Si), 18.6 (CH<sub>3</sub>), 134.7 (SiC=), 153.9 (=CHCO), 193.8 (CHO); <sup>29</sup>Si NMR (CDCl<sub>3</sub>) δ 7.30; UV spectrum (cyclohexane) λ<sub>max</sub> (ε) 235 (15800), 335 (46), 347 (52), 362 (56), 377 (43), 395 (17).

1c: <sup>13</sup>C NMR (CDCl<sub>3</sub>) δ -0.88 (CH<sub>3</sub>Si), 13.3 (CH<sub>3</sub>), 152.2 (=CCO), 153.2 (SiCH=), 195.7 (CHO); <sup>29</sup>Si NMR (CDCl<sub>3</sub>) δ -7.63; UV spectrum (cyclohexane) λ<sub>max</sub> (ε) 232 (6300), 335 (31), 348 (29), 363 (20), 380 (7).

1d: <sup>13</sup>C NMR (CDCl<sub>3</sub>) δ -1.88 (CH<sub>3</sub>Si), 26.2 (CH<sub>3</sub>), 143.0 (SiCH=), 147.5 (=CHCO), 198.5 (COCH<sub>3</sub>); <sup>29</sup>Si NMR (CDCl<sub>3</sub>) δ -4.96; UV spectrum (cyclohexane) λ<sub>max</sub> (ε) 220 (13800), 338 (48), 350 (43), 365 (27).

1e: <sup>13</sup>C NMR (CDCl<sub>3</sub>) δ -2.76 (CH<sub>3</sub>Si), 23.5, 27.8, 38.0 (CH<sub>2</sub>), 135.6 (CH=), 167.4 (SiC=), 198.1 (CO); <sup>29</sup>Si NMR (CDCl<sub>3</sub>) δ -2.96;

UV spectrum (cyclohexane)  $\lambda_{\max}$  ( $\epsilon$ ) 230 (14 300), 340 (58), 353 (64), 368 (47).

**Registry No.** 1a, 33755-86-1; (*E*)-1b, 33755-87-2; (*Z*)-1b, 33755-88-3; (*E*)-1c, 83802-83-9; (*Z*)-1c, 83802-84-0; 1d, 49750-09-6; 1e, 66085-04-9; 2a, 83802-85-1; 2b, 83802-86-2; 2c, 83802-87-3; 2d, 24731-39-3; 2e, 83802-88-4; 3a, 56161-51-4; 3b, 56161-52-5; 3c,

56161-53-6; 3d, 56161-54-7; 3e, 83802-89-5; 4a, 83802-90-8; 4b, 83802-91-9; 4c, 83802-92-0; 4d, 83802-93-1; 4e, 83802-94-2; 5a, 83802-95-3; 5b, 83802-96-4; 5c (isomer III), 83802-97-5; 5c (isomer IV), 83802-99-7; 5d, 83802-98-6; 6, 83803-00-3; Me<sub>3</sub>SiCl, 75-77-4; sodium benzenesulfinate, 873-55-2; ethylene glycol, 107-21-1; 2-propenal, 107-02-8; 2-butenal, 4170-30-3; 2-methyl-2-propenal, 78-85-3; 3-buten-2-one, 78-94-4; 2-cyclohexen-1-one, 930-68-7.

## Synthesis and Reactivity of 1-Silaadamantyl Systems<sup>1,2</sup>

Philip Boudjouk,\* Craig A. Kapfer, and Robert F. Cunico<sup>†</sup>

Department of Chemistry, North Dakota State University, Fargo, North Dakota 58105

Received October 13, 1982

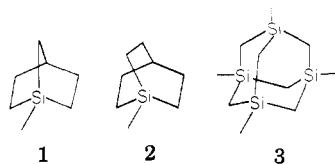
Six derivatives of the 1-silaadamantyl cage system were prepared and characterized. The key step in the synthesis of this new cage system is the Lewis acid catalyzed redistribution of *cis*-1,3,5-tris(trimethylsilyl)cyclohexane to give 1-methyl-1-silaadamantane in 67% yield. The relative reactivities of 1-chloro-1-silaadamantane, 1-chloro-1-silabicyclo[2.2.1]heptane, 1-chloro-1-silabicyclo[2.2.2]octane, and 1-chloro-3,5,7-trimethyl-1,3,5,7-tetrasilaadamantane toward nucleophilic reagents were determined. The 1-silaadamantyl system is much more reactive than the tetrasilaadamantyl system but only slightly less reactive than the 1-silabicyclo[2.2.2]octyl system. Of the four cage molecules, 1-chloro-1-silabicyclo[2.2.1]heptane is the most reactive. These results are in concert with S<sub>N</sub>2-Si mechanistic pathways and support the hypothesis that the reactivity of bridgehead silanes and their ground-state geometries are related: the closer the geometry around the silicon is to a trigonal bipyramid, the idealized transition state for S<sub>N</sub>2-Si reactions, the more reactive is the silane.

### Introduction

The reaction pathways of organosilanes have been postulated as proceeding through pentacoordinate transition states.<sup>3</sup> The mechanisms, which feature flank or backside attack, are derived largely from Sommer's stereochemical studies and have been widely accepted in the field of organosilicon chemistry.

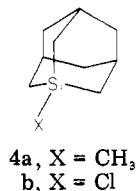
From structure-reactivity studies on bridgehead silanes it was postulated that reactivity was related to ground-state geometry; i.e., a bridgehead silane will exhibit enhanced reactivity to nucleophilic substitution the closer its ground-state geometry resembles that of the transition state.<sup>4</sup> Although these chemical studies could not discriminate between the two most likely transition-state geometries, tetragonal pyramid or trigonal bipyramid, recent structural work on bridgehead silanes strongly suggest that the latter is the favored geometry.<sup>5</sup>

The data available on the structure-reactivity relationships in silicon chemistry have been limited by the number of bridgehead silanes. Prior to the work discussed in this paper, the only bridgehead silicon compounds studied were the 1-silabicyclo[2.2.1]heptyl (1),<sup>4a</sup> the 1-silabicyclo[2.2.2]octyl (2),<sup>4b</sup> and the 3,5,7-trimethyl-1,3,5,7-tetrasilaadamantyl (3) systems.<sup>4c,d</sup>



Recently we reported the synthesis of the new bridgehead silanes 4a,b via a novel application of the Lewis acid redistribution reaction.<sup>6</sup> Redistribution reactions of or-

ganosilanes are well-known and have been investigated in considerable detail.<sup>7</sup> However, almost all of the systems studied were simple aliphatic silanes, comparatively little attention being given to cyclic or more complex molecules. The preparation of the tetrasilaadamantanes 3 by treating (Me<sub>2</sub>SiCH<sub>2</sub>)<sub>n</sub>, n = 2 and 3, with aluminum chloride is an unique example of a designed synthesis of a complex silane via the redistribution reaction.<sup>8</sup>



(1) Taken in part from the Ph.D. thesis of Craig A. Kapfer, North Dakota State University, 1979.

(2) The IUPAC nomenclature for 1-silaadamantane is 1-silatricyclo-[3.3.1.1<sup>3,7</sup>]decane.

(3) (a) Sommer, L. H. "Stereochemistry, Mechanism and Silicon"; McGraw-Hill: New York, 1965. (b) Sommer, L. H. *Intra-Sci. Chem. Rep.* 1973, 7, 1-38. (c) Corriu, R. J. P.; Guerin, C. *J. Organomet. Chem.* 1980, 198, 231-320. (d) Corriu, R. J. P.; Guerin, C. *Adv. Organomet. Chem.* 1982, 20, 265-312.

(4) (a) Sommer, L. H.; Bennett, O. F. *J. Am. Chem. Soc.* 1957, 79, 1008-1009. (b) *Ibid.* 1959, 81, 251-252. (c) Homer, G. D.; Sommer, L. H. *Ibid.* 1973, 95, 7700-7707. (d) Reactivity studies of bridgehead organosilanes with electrophilic and radical chlorinating agents have been reported: Homer, G. D.; Sommer, L. H. *J. Organomet. Chem.* 1975, 84, 297-304.

(5) (a) Hilderbrandt, R. L.; Homer, G. D.; Boudjouk, P. *J. Am. Chem. Soc.* 1976, 98, 7476-7480. (b) Shen, Q.; Kapfer, C. A.; Boudjouk, P.; Hilderbrandt, R. L. *J. Organomet. Chem.* 1979, 169, 147-154. (c) Schei, S. H.; Shen, Q.; Cunico, R. F.; Hilderbrandt, R. L. *J. Mol. Struct.* 1980, 63, 59-71.

(6) (a) Kapfer, C. A.; Boudjouk, P. Proceedings of the 174th National Meeting of the American Chemical Society, Chicago, IL, Aug 1977; American Chemical Society: Washington, DC, 1977; Abstract No. INOR 113. (b) Kapfer, C. A.; Boudjouk, P. *J. Organomet. Chem.* 1978, 144, C6-C8.

(7) For review of the reactions of organosilanes with Lewis acids, see: (a) O'Brien, D. H.; Hairston, T. J. *Organomet. Chem. Rev. A* 1971, 7, 95-157. (b) Weyenberg, D. R.; Mahone, L. G.; Atwell, W. H. *Ann. N. Y. Acad. Sci.* 1969, 159, 38-55.

\* Department of Chemistry, Northern Illinois University, DeKalb, IL 60115.

UV spectrum (cyclohexane)  $\lambda_{\max}$  ( $\epsilon$ ) 230 (14 300), 340 (58), 353 (64), 368 (47).

**Registry No.** 1a, 33755-86-1; (*E*)-1b, 33755-87-2; (*Z*)-1b, 33755-88-3; (*E*)-1c, 83802-83-9; (*Z*)-1c, 83802-84-0; 1d, 49750-09-6; 1e, 66085-04-9; 2a, 83802-85-1; 2b, 83802-86-2; 2c, 83802-87-3; 2d, 24731-39-3; 2e, 83802-88-4; 3a, 56161-51-4; 3b, 56161-52-5; 3c,

56161-53-6; 3d, 56161-54-7; 3e, 83802-89-5; 4a, 83802-90-8; 4b, 83802-91-9; 4c, 83802-92-0; 4d, 83802-93-1; 4e, 83802-94-2; 5a, 83802-95-3; 5b, 83802-96-4; 5c (isomer III), 83802-97-5; 5c (isomer IV), 83802-99-7; 5d, 83802-98-6; 6, 83803-00-3; Me<sub>3</sub>SiCl, 75-77-4; sodium benzenesulfinate, 873-55-2; ethylene glycol, 107-21-1; 2-propenal, 107-02-8; 2-butenal, 4170-30-3; 2-methyl-2-propenal, 78-85-3; 3-buten-2-one, 78-94-4; 2-cyclohexen-1-one, 930-68-7.

## Synthesis and Reactivity of 1-Silaadamantyl Systems<sup>1,2</sup>

Philip Boudjouk,\* Craig A. Kapfer, and Robert F. Cunico<sup>†</sup>

Department of Chemistry, North Dakota State University, Fargo, North Dakota 58105

Received October 13, 1982

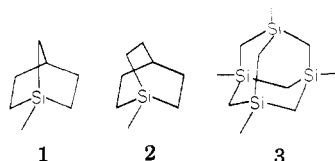
Six derivatives of the 1-silaadamantyl cage system were prepared and characterized. The key step in the synthesis of this new cage system is the Lewis acid catalyzed redistribution of *cis*-1,3,5-tris(trimethylsilyl)cyclohexane to give 1-methyl-1-silaadamantane in 67% yield. The relative reactivities of 1-chloro-1-silaadamantane, 1-chloro-1-silabicyclo[2.2.1]heptane, 1-chloro-1-silabicyclo[2.2.2]octane, and 1-chloro-3,5,7-trimethyl-1,3,5,7-tetrasilaadamantane toward nucleophilic reagents were determined. The 1-silaadamantyl system is much more reactive than the tetrasilaadamantyl system but only slightly less reactive than the 1-silabicyclo[2.2.2]octyl system. Of the four cage molecules, 1-chloro-1-silabicyclo[2.2.1]heptane is the most reactive. These results are in concert with S<sub>N</sub>2-Si mechanistic pathways and support the hypothesis that the reactivity of bridgehead silanes and their ground-state geometries are related: the closer the geometry around the silicon is to a trigonal bipyramid, the idealized transition state for S<sub>N</sub>2-Si reactions, the more reactive is the silane.

### Introduction

The reaction pathways of organosilanes have been postulated as proceeding through pentacoordinate transition states.<sup>3</sup> The mechanisms, which feature flank or backside attack, are derived largely from Sommer's stereochemical studies and have been widely accepted in the field of organosilicon chemistry.

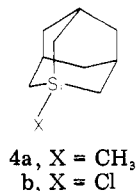
From structure-reactivity studies on bridgehead silanes it was postulated that reactivity was related to ground-state geometry; i.e., a bridgehead silane will exhibit enhanced reactivity to nucleophilic substitution the closer its ground-state geometry resembles that of the transition state.<sup>4</sup> Although these chemical studies could not discriminate between the two most likely transition-state geometries, tetragonal pyramid or trigonal bipyramid, recent structural work on bridgehead silanes strongly suggest that the latter is the favored geometry.<sup>5</sup>

The data available on the structure-reactivity relationships in silicon chemistry have been limited by the number of bridgehead silanes. Prior to the work discussed in this paper, the only bridgehead silicon compounds studied were the 1-silabicyclo[2.2.1]heptyl (1),<sup>4a</sup> the 1-silabicyclo[2.2.2]octyl (2),<sup>4b</sup> and the 3,5,7-trimethyl-1,3,5,7-tetrasilaadamantyl (3) systems.<sup>4c,d</sup>



Recently we reported the synthesis of the new bridgehead silanes 4a,b via a novel application of the Lewis acid redistribution reaction.<sup>6</sup> Redistribution reactions of or-

ganosilanes are well-known and have been investigated in considerable detail.<sup>7</sup> However, almost all of the systems studied were simple aliphatic silanes, comparatively little attention being given to cyclic or more complex molecules. The preparation of the tetrasilaadamantanes 3 by treating (Me<sub>2</sub>SiCH<sub>2</sub>)<sub>n</sub>, n = 2 and 3, with aluminum chloride is an unique example of a designed synthesis of a complex silane via the redistribution reaction.<sup>8</sup>



(1) Taken in part from the Ph.D. thesis of Craig A. Kapfer, North Dakota State University, 1979.

(2) The IUPAC nomenclature for 1-silaadamantane is 1-silatricyclo-[3.3.1.1<sup>3,7</sup>]decane.

(3) (a) Sommer, L. H. "Stereochemistry, Mechanism and Silicon"; McGraw-Hill: New York, 1965. (b) Sommer, L. H. *Intra-Sci. Chem. Rep.* 1973, 7, 1-38. (c) Corriu, R. J. P.; Guerin, C. *J. Organomet. Chem.* 1980, 198, 231-320. (d) Corriu, R. J. P.; Guerin, C. *Adv. Organomet. Chem.* 1982, 20, 265-312.

(4) (a) Sommer, L. H.; Bennett, O. F. *J. Am. Chem. Soc.* 1957, 79, 1008-1009. (b) *Ibid.* 1959, 81, 251-252. (c) Homer, G. D.; Sommer, L. H. *Ibid.* 1973, 95, 7700-7707. (d) Reactivity studies of bridgehead organosilanes with electrophilic and radical chlorinating agents have been reported: Homer, G. D.; Sommer, L. H. *J. Organomet. Chem.* 1975, 84, 297-304.

(5) (a) Hilderbrandt, R. L.; Homer, G. D.; Boudjouk, P. *J. Am. Chem. Soc.* 1976, 98, 7476-7480. (b) Shen, Q.; Kapfer, C. A.; Boudjouk, P.; Hilderbrandt, R. L. *J. Organomet. Chem.* 1979, 169, 147-154. (c) Schei, S. H.; Shen, Q.; Cunico, R. F.; Hilderbrandt, R. L. *J. Mol. Struct.* 1980, 63, 59-71.

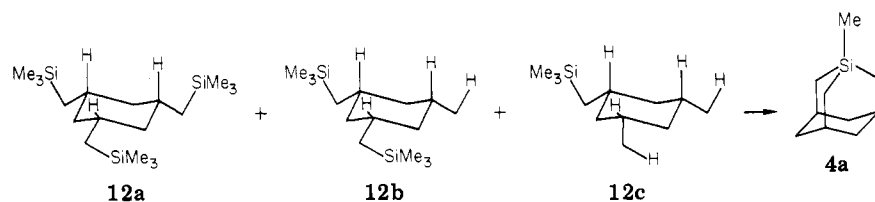
(6) (a) Kapfer, C. A.; Boudjouk, P. Proceedings of the 174th National Meeting of the American Chemical Society, Chicago, IL, Aug 1977; American Chemical Society: Washington, DC, 1977; Abstract No. INOR 113. (b) Kapfer, C. A.; Boudjouk, P. *J. Organomet. Chem.* 1978, 144, C6-C8.

(7) For review of the reactions of organosilanes with Lewis acids, see: (a) O'Brien, D. H.; Hairston, T. J. *Organomet. Chem. Rev. A* 1971, 7, 95-157. (b) Weyenberg, D. R.; Mahone, L. G.; Atwell, W. H. *Ann. N. Y. Acad. Sci.* 1969, 159, 38-55.

\* Department of Chemistry, Northern Illinois University, DeKalb, IL 60115.



Table I. Conditions for the Synthesis of 1-Methyl-1-Silaadamantane



run	silane(s)	amount of silane(s), g	% wt of AlCl <sub>3</sub>	amount of benzene, mL	time, h	% yield <sup>a</sup> of 4a
1	12a-c <sup>b</sup>	2	10	neat	1	15
2	12a-c	2	10	5	24	50
3	12a-c	2	10	100	24	c
4	12a-c	2	40	5	24	50 <sup>d</sup>
5	12a	8	50	25	6	67 <sup>d</sup>
6	12b	1	50	5	6	10 <sup>e</sup>

<sup>a</sup> % yield of runs 1-5 based on pure 12a; % yield of run 6 based on pure 12b. <sup>b</sup> % composition of 12a, 12b, and 12c mixture is 85.4%, 13.7%, and 0.9%, respectively. <sup>c</sup> 4a not detected by GLC. <sup>d</sup> Contained traces of 4b. <sup>e</sup> 4a detected by GLC.

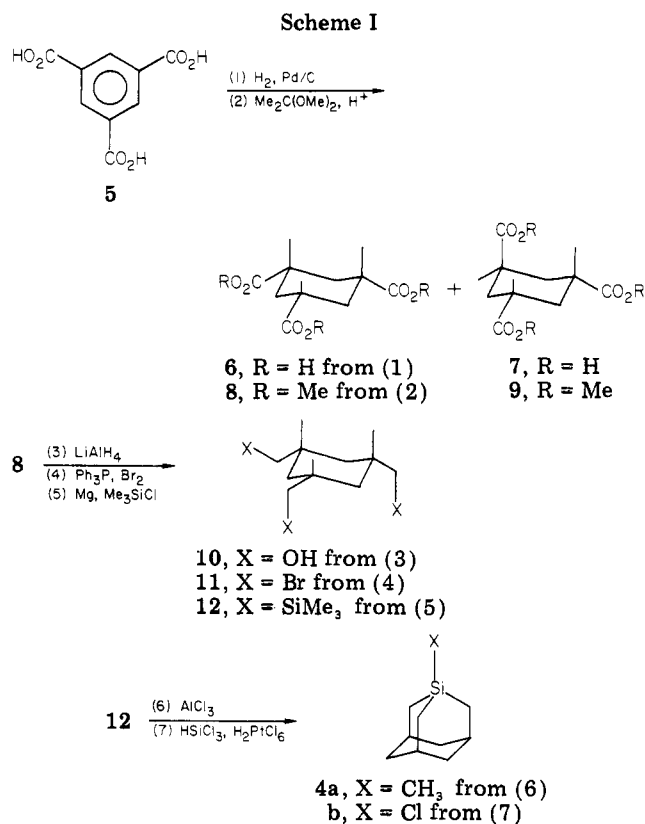
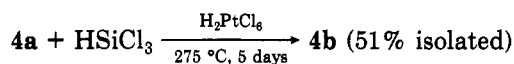
In this paper we present the details of the synthesis and some reactions of the 1-silaadamantyl system as well as a comparison of the reactivity of 4b to those of the chloro derivatives of 1-3 toward nucleophilic substitution.<sup>9</sup>

### Results and Discussion

The probe in our study, 1-chloro-1-silaadamantane (4b), was prepared by a seven-step synthesis from trimesic acid (Scheme I). Compounds 5-11 are the same intermediates prepared by Galik and co-workers for the synthesis of 1-azaadamantane.<sup>10</sup> However, in our hands, their conditions were not amenable to scale up and we had to develop new techniques for larger scale syntheses. These modifications are detailed in the Experimental Section.

The key step in the sequence is the preparation of the 1-silaadamantyl cage structure by the acid-promoted redistribution of *cis*-1,3,5-tris(trimethylsilyl)methylcyclohexane (12a). The effects of varying the reaction conditions are summarized in Table I. 1-Methyl-1-silaadamantane (4a) can be prepared from 12a, 12b, or the mixture 12a-c with AlCl<sub>3</sub>. The highest yield, 67%, of 4a was obtained in run 5 where pure 12a and a 50% by weight AlCl<sub>3</sub> loading were stirred together in refluxing benzene. Tetramethylsilane and small quantities of trimethylchlorosilane (Me<sub>3</sub>SiCl) were evolved from the reaction mixture and collected in a cold trap. The molar ratio of 4a: Me<sub>3</sub>SiCl was very close to 1:2. Although pure 12a gave the highest yield of 4a, the use of the mixture 12a-c also gave excellent yields (50%) of the product (runs 2 and 4). We employed the mixture in our preparations of 4a because the purification of 12a is tedious. It is noteworthy that pure 12b also produces 4a although the yield is only 10%.

Functionalization of 4a was achieved by using a high-temperature modification of the chlorodemethylation procedure of Beck and Benkeser.<sup>11</sup> This chlorosilane



proved to be surprisingly stable to isolation techniques that included washing with water and chromatography on silica gel. Typically, 4a was not purified for this reaction but used as part of the crude product mixture from the redistribution of 12a-c. Yields and purity of 4b were essentially the same as when pure 4a was employed. The conditions and yields of this reaction were not optimized.

### Structure-Reactivity Results

The compounds examined in the structure-reactivity studies were the 1-silabicyclo[2.2.1]heptyl (1), 1-silabicyclo[2.2.2]octyl (2), 3,5,7-trimethyl-1,3,5,7-tetrasilaadamantyl (3), and 1-silaadamantyl (4) systems. The results of these comparisons are summarized in Table II. These reagents, when used under the conditions in this study,

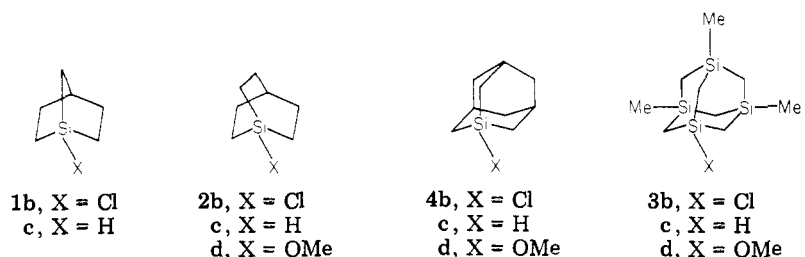
(8) (a) Frye, C. L.; Klosowski, J. M.; Weyenberg, D. R. *J. Am. Chem. Soc.* 1970, 92, 6379-6380.

(9) Preliminary accounts of some of the chemistry of 4b have been presented: (a) Boudjouk, P.; Kapfer, C. A.; Erickson, B. C. Organosilicon Symposium, Ft. Worth, TX, March, 1980. (b) Boudjouk, P.; Han, B.-H.; Kapfer, C. A. Proceedings of the 182nd National Meeting of the American Chemical Society, New York, August, 1981; American Chemical Society: Washington, DC, 1981; Abstract No. INOR 17.

(10) (a) Lukes, R.; Galik, V.; Bauer, J. *Collect. Czech. Chem. Commun.* 1954, 19, 712-715. (b) Galik, V.; Kafka, Z.; Safar, M.; Landa, S. *Ibid.* 1974, 39, 895-898.

(11) Beck, K. R.; Benkeser, R. A. *J. Organomet. Chem.* 1970, 21, P35-37.

Table II. Comparison of Nucleophilic Substitution Reactions at Bridgehead Silanes



		approx half-life at 25 °C			
solvent	reagent	1	2	4	3
diethyl ether	LiAlH <sub>4</sub>	instantaneous <sup>a</sup>	instantaneous <sup>b,c</sup>	4 min <sup>d</sup>	100 hs <sup>c</sup>
MeOH	MeOH	<sup>e</sup>	4 h <sup>d</sup>	10 h <sup>d</sup>	no reaction after 24 h <sup>c</sup>
diethyl ether	CH <sub>3</sub> Li	<sup>e</sup>	instantaneous <sup>d,f</sup>	4 min <sup>d</sup>	no reaction after 1 h <sup>c</sup>
diethyl ether	CH <sub>3</sub> MgX	reaction obtained in 24 h <sup>g</sup>	no reaction after 24 h <sup>h</sup>	no reaction after 24 h <sup>h</sup>	no reaction after 24 h <sup>h</sup>

<sup>a</sup> From ref 4a. <sup>b</sup> From ref 4b. <sup>c</sup> From ref 4c. <sup>d</sup> This work. <sup>e</sup> No data available on these reactions. However 1b reacts with H<sub>2</sub>O and C<sub>6</sub>H<sub>5</sub>Li instantaneously and exothermically to give the siloxane and phenyl derivatives in high yields.<sup>4c</sup> <sup>f</sup> Reaction 90% complete after 1 min. <sup>g</sup> X = Cl. <sup>h</sup> X = I.

are known to produce inversion of configuration of acyclic organosilanes by an S<sub>N</sub>2-Si mechanism.<sup>3</sup> The reduction of 1b in diethyl ether is instantaneous and exothermic.<sup>4a</sup> Qualitative observation indicates that the bridgehead chloride 2b is less reactive than 1b, but 2b also undergoes rapid reduction with LiAlH<sub>4</sub>. The same result was observed in the LiAlH<sub>4</sub> reduction of 4b. Here, the half-life could be measured owing to its lesser reactivity, yet the reduction is still fairly rapid. The greatest change in reactivity is seen in the reduction of 3b that has a half-life of ~100 h.<sup>4c</sup>

1-Chloro-1-silabicyclo[2.2.1]heptane (1b) was not available, and data on the methanolysis of 1b are not in the literature. Therefore, the bridgehead chlorosilanes studied for the methanolysis reaction were limited to systems 2b, 3b, and 4b. Compounds 2b, 3b, and 4b, showed the same general trend in reactivity toward methanolysis as was found with the LiAlH<sub>4</sub> reduction. The reactivity of 2b is more than twice that of 4b. A reaction does not occur with 3b in methanol within 24 h. Methanolysis of 3b will occur in the presence of sodium methoxide in methanol solvent. The half-life for this reaction was found by Homer and Sommer<sup>4c</sup> to be ~1 min. Plausible explanations for this dramatic increase in reactivity are the greater nucleophilicity of sodium methoxide as compared with methanol and the driving force provided by the lattice energy obtained from precipitation of sodium chloride.

The reaction of 4b with methyl lithium in diethyl ether exhibited a slight reduction in reactivity as compared with that of 2b. A methylation reaction does not occur with 3b after 1 h; however, a reaction does occur with a half-life of ~5 min when the methyl lithium is decomplexed with tetramethylethylenediamine (TMEDA).<sup>4c</sup> Methylations using Grignard reagents were also explored. Smith and Clark<sup>12</sup> have shown that methylmagnesium chloride fails to methylate 1,3,5,7-tetrachloro-1,3,5,7-tetrasiladamantane. We found that compounds 2b, 3b, and 4b were inert to reaction with methylmagnesium iodide within a 24-h period. On the other hand, 1b was methylated by methylmagnesium chloride to give 1-methyl-1-silabicyclo[2.2.1]heptane (1a) within 24 h.<sup>4c</sup>

The rate of the base-catalyzed solvolysis of 4c was obtained relative to triethylsilane,<sup>13</sup> the standard against

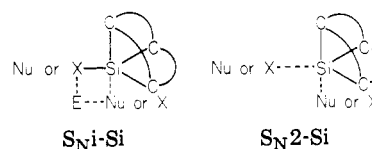


Figure 1. S<sub>N</sub>i-Si and S<sub>N</sub>2-Si retention mechanisms for bridgehead silanes.

which 1c and 2c were measured,<sup>3a</sup> permitting a comparison of the reactivities of these bridgehead silanes. The results of the solvolysis study show the relative reactivities to follow the same general trend as in nucleophilic substitution reactions: 1c ≫ 2c ≈ 4c with relative rates of 10<sup>3</sup>:10:3, respectively. Data for the solvolysis of 3c were not available from the literature. Silylamine derivatives of tetrasiladamantyl 3 systems have been prepared and were found to be sufficiently stable to aqueous HCl to be recovered from solution with the silicon-nitrogen bond still intact,<sup>14</sup> a rare occurrence in organosilicon chemistry.<sup>15</sup> The diethylamine derivative of 1-silaadamantane was prepared by treating 4b with the lithium salt of diethylamine in a diethyl ether-hexane solvent. The silylamine 4e is considerably less reactive toward methanolysis or hydrolysis than aliphatic silylamines but more reactive than amine derivatives of the tetrasiladamantyl system. Analysis of a solution of 4e in anhydrous methanol by GLC gave a half-life of ~11 h. The product of the reaction was 1-methoxy-1-silaadamantane (4d). The silylamine was also hydrolyzed by moisture to afford the disiloxane, bis(1-silaadamantyl)oxide (4f). 1-Amino-1-silaadamantanes serve as analogues to the well-known antiviral agent amantidine (1-aminoadamantane).<sup>16</sup> Efforts to prepare hydrolytically stable amine derivatives of siladamantane are still in progress.

### Mechanistic Considerations

The cage systems 1-4 cannot react by a S<sub>N</sub>2-Si inversion mechanism because reagents cannot approach the silicon centers from the backside. The S<sub>N</sub>i-Si retention mecha-

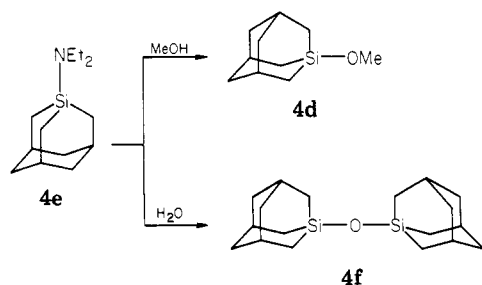
(14) (a) Frye, C. L.; Klosowski, J. M. *J. Am. Chem. Soc.* 1972, 94, 7186-7187. (b) Homer, G. D.; Sommer, L. H. *J. Organomet. Chem.* 1974, 67, C10-C11.

(15) The hydrochloride and hydrobromide salts of tri-*tert*-butylsilylamine, the only other examples of protonated silylamines, have also been reported: Nowakowski, P. M.; Sommer, L. H. *J. Organomet. Chem.* 1979, 95-103.

(16) Schwartz, A. R. "Annual Reports in Medicinal Chemistry"; Heinzelman, R. V., Ed.; Academic Press: New York, 1974.

(12) Smith, A. L.; Clark, H. A. *J. Am. Chem. Soc.* 1961, 83, 3345-3346.

(13) Sommer, L. H.; Bennett, O. F.; Campbell, P. G.; Weyenberg, D. R. *J. Am. Chem. Soc.* 1957, 79, 3295-3298.



nism (Figure 1) is probably not operable in these reactions because the electrophilic assistance needed for the mechanism to occur is not significant with the reagents used.

In order to explain the enhanced reactivity of **1**, Sommer postulated that the ground-state geometry of this molecule approached the transition-state geometry required (a trigonal bipyramid or a tetragonal pyramid) for an  $S_N2$ -Si retention mechanism to operate, allowing displacement to occur with very little movement of the groups attached to the silicon atom.<sup>3a</sup> Structural evidence in support of this hypothesis is seen in Table III. The molecular geometry at the silicon center of **1a** is close to that of a trigonal bipyramid. With use of the atom numbering system in Table III, the trigonal bipyramid is formed by using atom  $C_2$  as an apex and atoms  $C_1$ ,  $C_3$ , and  $C_4$  as the equatorial groups. It can then be visualized that with only slight distortion of the  $\angle C_1SiC_2$  and  $\angle C_2SiC_3$  valence angles which are already  $94.5^\circ$  in **1a**, a great deal of the required transition-state geometry is in a sense "built in" as a result of the strained bicyclic nature of the molecule.

The ground-state geometry of **2b** is less strained than that of **1a** and further removed from the geometry of a trigonal bipyramid as seen by the size of the valence angles given in Table III. Because the molecule has less strain involved in its ground-state geometry, it may be possible for **2b** to distort its valence angles to approach a trigonal-bipyramid transition state. The reactivity of **2b** would then depend on how close it could approach the desired transition state, i.e., closer would lead to more reactivity, further away would give less reactivity.

The angle strain present around the silicon atoms of 1-methyl-1-silabicyclo[2.2.1]heptane (**1a**), 1-chloro-1-silabicyclo[2.2.2]octane (**2b**), 1,3,5,7-tetramethyl-1,3,5,7-tetrasilaadamantane (**3a**), and 1-methyl-1-silaadamantane (**4a**) is found to increase in the order  $3a < 4a \approx 2b < 1a$ , as shown in Table III. The geometry for compounds **1a**, **2b**, and **4a** were measured by gas-phase electron diffraction.<sup>5a-c</sup> On the basis of accurate molecular models,<sup>1a</sup> compound **3a** is believed to have tetrahedral geometry about the silicon atoms.

The different reactivities of the silabicyclooctyl and silaadamantyl cage systems (**2** and **4**, respectively) are not explained by the local geometries about the silicon atoms because the bond angles are nearly identical. Thus our observations are consistent with, but not completely explained by, orbital hybridization arguments.<sup>3d</sup> Other more subtle factors must be involved. From the inspection of molecular models and preliminary molecular mechanics calculations<sup>17</sup> we find the 2.2.1 cage system more deformable than the silaadamantyl cage. From this we have drawn the tentative conclusion that the greater reactivity of **2b** relative to **4b** is because the former more readily distorts to the transition-state geometry.

Finally, it is pertinent to note that the ground-state geometries of these bridgehead silanes provide easier access for apical entry as opposed to equatorial attack by the

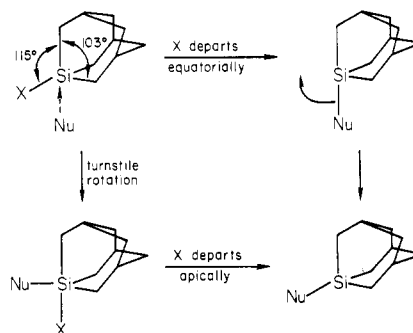


Figure 2.

nucleophile. With the assumption of apical attack, the retention of configuration can be achieved by the two pathways shown in Figure 2. Of these, the pathway of least motion involves equatorial departure of the leaving group followed by movement of the newly attached nucleophile to give the ground-state geometry of the product. The route requiring turnstile rotation of the five-coordinate intermediate followed by apical departure and adoption of the final configuration appears to be a higher energy and therefore less favorable pathway.<sup>18</sup>

### Experimental Section

All solvents were reagent grade and were purified by standard methods only if they were suspected of being contaminated. Tetrahydrofuran (THF) was refluxed over sodium metal and benzophenone until the blue color of benzophenone ketyl was observed, and then it was distilled just prior to use. Reactions requiring diethyl ether were carried out by using freshly opened cans of MC/B absolute ether. Chlorosilanes were from Dow-Corning Co. or Petrarch Systems, Inc., and were purified only if needed. The silica gel and alumina used were of activity 1. All specialty chemicals were from either Aldrich or Alfa. Before use, all glassware was oven dried for at least 4 h, assembled hot, and cooled under a stream of dry nitrogen.

NMR spectra were recorded on Varian EM-390 and Varian A60-A NMR spectrometers. The solvent and internal standard appear in each experimental write up as solvent and internal standard. All chemical shifts are reported as  $\delta$  values. IR spectra were recorded on a Perkin-Elmer 137 spectrophotometer (polystyrene calibration) and a Beckman IR 4240 spectrophotometer. Mass spectra were taken on Finnigan 1015D GC-MS and Varian CH-5 mass spectrometers at 70 eV. Melting points were obtained on a Thomas-Hoover Mel-Temp apparatus and are uncorrected. Boiling points are also uncorrected. Elemental analyses were performed by Galbraith Laboratories, Inc., and Chemalytics, Inc. Analytic and preparative GLC data were obtained on a Varian Aerograph Model 920 with thermal conductivity detectors.

**cis- and trans-1,3,5-Cyclohexanetricarboxylic Acid (6 and 7).** A slurry of trimesic acid (**5**) (35 g, 0.167 mol) in distilled water (300 mL) was hydrogenated by using 10% palladium on carbon (1 g) as catalyst. The hydrogenation was performed at 1000 psi in a Parr bomb with heating (heating tape at Variac setting 70) and stirring. After 24 h, the pressure had decreased by  $\sim 800$  psi. The catalyst was filtered from the otherwise homogeneous solution and the water removed under reduced pressure to give a white solid possessing a sweet odor. Drying at  $90^\circ\text{C}$  for 24 h gave 34.2 g (95%) of **6** and **7** as a white amorphous powder: mp  $170$ – $205^\circ\text{C}$  (lit.<sup>19</sup>  $175$ – $206^\circ\text{C}$ ); IR (KBr)  $2940$  (OH),  $1709\text{ cm}^{-1}$  (C=O), no out-of-plane C–H bending vibrations below  $900\text{ cm}^{-1}$ .

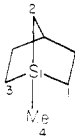
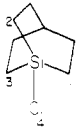

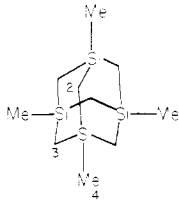
**cis-Trimethyl 1,3,5-Cyclohexanetricarboxylate (8).** A solution of a mixture of *cis*- and *trans*-1,3,5-cyclohexanetricarboxylic acid (**6** and **7**) (190.86 g, 0.884 mol) and an excess of 2,2-dimethoxypropane (393.86 g, 3.79 mol) in dry methanol (1 L) was added to a saturated solution of HCl gas (freshly prepared from sodium chloride and concentrated sulfuric acid) in dry

(18) For detailed discussions of the role of five-coordinate intermediates in reactions of silicon compounds see ref 3c,d.

(19) Seitz, A., Jr. *J. Org. Chem.* 1968, 33, 2978–2979.

(17) Hilderbrandt, R. L., private communication.

Table III. Valence Angles (deg) of the Silicon Cage Structures

				
	1a	2b	4a	3a
$\angle C1SiC2$	$94.5 \pm 0.6^a$	$103.9 \pm 0.2^b$	$103.2 \pm 0.5^c$	$109.5^d$
$\angle C2SiC3$	$94.5 \pm 0.6$	$103.9 \pm 0.2$	$103.2 \pm 0.5$	109.5
$\angle C1SiC3$	$99.1 \pm 1.5$	$103.9 \pm 0.2$	$103.2 \pm 0.5$	109.5
$\angle C1SiC4$	$122.9 \pm 1.0$	$114.6 \pm 0.2$	$115.2 \pm 0.4$	109.5
$\angle C3SiC4$	$122.9 \pm 1.0$	$114.6 \pm 0.2$	$115.2 \pm 0.4$	109.5
$\angle C2SiC4$	$116.0 \pm 2.0$	$114.6 \pm 0.2$	$115.2 \pm 0.4$	109.5

<sup>a</sup> Reference 5a. <sup>b</sup> Reference 5c. <sup>c</sup> Reference 5b. <sup>d</sup> Reference 3a.

methanol (1 L). The reaction turned dark red-brown after being stirred and refluxed under dry nitrogen for 44 h. The reaction mixture was concentrated to a volume of ~250 mL under reduced pressure and diethyl ether (500 mL) added. The ethereal solution was washed with saturated sodium chloride solution (2 × 250 mL), saturated sodium bicarbonate (2 × 250 mL), and finally with water (250 mL). The ethereal solution was then dried over MgSO<sub>4</sub>, filtered, and concentrated under reduced pressure to produce a yellow oil. Distillation of the oil at 135–140 °C (0.02 mm) gave 206.32 g (91%) of a pale yellow oil that partially crystallized upon standing. The oil (79.83 g) was separated from the solid (126.49 g) by suction filtration. Recrystallization of the oily solid from hot hexanes produced 104.17 g (46% based on total esterification) of 8 as long white needles: mp 48–50 °C (lit.<sup>10</sup> 46 °C); IR (KBr) 2924 (CH), 1730 (C=O), 1250 cm<sup>-1</sup>; NMR (CDCl<sub>3</sub>, Me<sub>3</sub>SiCl)  $\delta$  1.53 (br q, 3 H,  $J = 12$  Hz, CCH<sub>2</sub>C (axial)), 2.13–2.63 (br m, 6 H, CCHC and CCH<sub>2</sub>C (equatorial)), 3.72 (s, 9 H, OCH<sub>3</sub>); MS,  $m/e$  258 (parent), 227, 199, 198, 167, 166, 139, 138, 79. The oil (21.47 g) recovered from the mother liquor was combined with the original 79.83 g. The oil was a mixture of the *cis* and *trans* isomers and showed a higher concentration of the *trans* isomer when analyzed by GLC.

***cis*-1,3,5-Tris(hydroxymethyl)cyclohexane (10).** A solution of *cis*-trimethyl 1,3,5-cyclohexanetricarboxylate (8) (106.68 g, 0.414 mol) in dry THF (200 mL) was slowly added dropwise to a continuously stirred ice cold suspension of LiAlH<sub>4</sub> (31.14 g, 0.820 mol) in dry THF (1 L). The mixture was refluxed for 24 h and cooled to 0 °C, the salts were decomposed with a 1:4 mixture of water:95% ethanol (250 mL), and the suspension was refluxed for 4 h. The resulting precipitate was suction filtered hot, and the solids were washed with hot 95% ethanol (800 mL). The combine filtrates were concentrated under reduced pressure to give a solid residue that was extracted in a Soxhlet apparatus with *p*-dioxane (600 mL). Removal of the *p*-dioxane under reduced pressure gave white cubic crystals. The crystals were washed with ether (50 mL) and air-dried to afford 64.74 g (90%) of 10: mp 115–117 °C (lit.<sup>10</sup> 111–112 °C); IR (KBr) 3280 (OH), 2865 (CH), 1060 cm<sup>-1</sup> (CO). The reduction when performed on small quantities (15–20 g) of 8 produced yields of ~95%.

***cis*-1,3,5-Tris(bromomethyl)cyclohexane (11).** Triphenylphosphine (189.72 g, 0.724 mol) and *cis*-1,3,5-tris(hydroxymethyl)cyclohexane (10) (40 g, 0.230 mol) were dissolved in dry DMF (500 mL). Bromine (116 g, 0.725 mol) was added dropwise to the stirred mixture at 0–20 °C. The reaction temperature was maintained between 0–20 °C for 2 h after the addition was complete. The temperature was raised to ambient conditions and the mixture stirred for 18 h. Removal of the DMF under reduced pressure gave an orange-red syrup. The syrup was dissolved in benzene (800 mL), washed with a saturated sodium chloride solution (2 × 100 mL) and H<sub>2</sub>O (1 × 100 mL), and dried over MgSO<sub>4</sub>. Removal of the MgSO<sub>4</sub> by filtration, followed by concentration of the benzene solution under reduced pressure, gave a pale yellow solid. The solid was stirred with ether (250 mL) for 15–20 min and filtered by gravity to remove the triphenylphosphine oxide. The filtrate was concentrated under reduced pressure to a solid and the above procedure repeated two

more times with decreasing amounts of ether (150 mL and then 100 mL). The above method removes about 70–80% of the triphenylphosphine oxide present. The last filtrate was concentrated to a volume of ~50 mL, the material preadsorbed onto neutral alumina (50 g), and placed on a neutral alumina column (5 cm × 30 cm). The product was eluted as one fraction by using a 1:9 ether–hexane solution (1.5 L). White crystals were obtained after removal of the solvent under reduced pressure. Recrystallization from hot methanol gave 68.76 g (82%) of 11 as cubic crystals: mp 55–57 °C (lit.<sup>10</sup> 56–57 °C); IR (KBr) no OH absorption at 3279 cm<sup>-1</sup>; NMR (CDCl<sub>3</sub>, Me<sub>3</sub>SiCl)  $\delta$  0.82 (q, 3 H,  $J = 12$  Hz, CCH<sub>2</sub>C (axial)), 1.48–2.20 (br m overlapping an apparent br d at  $\delta$  2.05 ( $J = 11.3$  Hz), 6 H, CCHC and CCH<sub>2</sub>C (equatorial)), 3.37 (d, 6 H,  $J = 5.7$  Hz, CCH<sub>2</sub>Br); MS,  $m/e$  365, 363 (parent), 361, 359, 285, 283, 281, 203, 201 121.

***cis*-1,3,5-Tris(trimethylsilyl)methylcyclohexane (12a).** *cis*-1,3,5-Tris(bromomethyl)cyclohexane (11) (70 g, 0.193 mol) in dry THF (200 mL) was slowly added dropwise to a chilled (0 °C), stirred mixture of magnesium turnings (29.52 g, 1.215 mol), which were cleaned with 1,2-dibromoethane (10.9 g, 58 mmol) in dry THF (100 mL), and trimethylchlorosilane (128.71 g, 1.186 mol) in dry THF (900 mL). The reaction mixture was refluxed for 20 h, and then 825 mL of a mixture of THF and trimethylchlorosilane was removed from the reaction by distillation. Trimethylchlorosilane (50 mL) was added to the concentrated reaction mixture, and this was refluxed for 5 h to ensure complete Grignard reagent coupling. Another 100 mL of THF and trimethylchlorosilane mixture was removed by distillation and the reaction mixture hydrolyzed slowly with a saturated NH<sub>4</sub>Cl solution (200 mL). Diethyl ether (250 mL) was added, the liquid portions were decanted from the excess magnesium turnings, and the turnings were washed with ether (50 mL). The diethyl ether was separated and the aqueous portion extracted with ether (2 × 100 mL). The combined ethereal extracts were washed with water (2 × 100 mL), dried (MgSO<sub>4</sub>), and filtered. The solvent was removed under reduced pressure, leaving 94.31 g of a yellow oil which was deposited on 100 g of silica gel. The adsorbed product mixture was divided into two equal portions and each portion placed on a silica gel column measuring 5 cm × 25 cm. Elution with pentane (1 L), 5% ether–pentane (1.5 L), and ether (1 L) afforded 42.16 g of a water white liquid, 13.87 g of a water-white oil, and 27.84 g of a yellow oil, respectively. The only fraction to contain the product was that eluted with pentane. The other fractions contained material possessing SiO bonds by IR spectroscopy. Evaluation of the product by GLC (6 ft × 0.25 in. 10% SE-30 on Chromosorb W) revealed three peaks corresponding to 0.37 g of *cis*-1,3-dimethyl-5-((trimethylsilyl)methyl)cyclohexane (12c), 5.76 g of *cis*-1-methyl-3,5-bis((trimethylsilyl)methyl)cyclohexane (12b), and 36.01 g (55%) of *cis*-1,3,5-tris((trimethylsilyl)methyl)cyclohexane (12a). This mixture may be used in subsequent reactions, or 12a may be separated from the other two components by spinning band distillation at 92–93 °C (0.03 mm). This procedure gave 12a in >99% purity by GLC, but the isolated yield was only 34% of theoretical. A 71% yield of 12a was obtained in one run on a 68.7-mmol scale. Analytical samples of 12b and 12a were obtained by preparative GLC.

*cis*-1-Methyl-3,5-bis(trimethylsilyl)methylcyclohexane (**12b**): IR (CCl<sub>4</sub>) 2860 (CH), 1250 cm<sup>-1</sup> (SiCH<sub>3</sub>); NMR (CCl<sub>4</sub>, benzene)  $\delta$  0.07 (s, 18 H, SiCH<sub>3</sub>), 0.3–0.83 and 1.16–1.93 (2 m, 13 H, mixture of SiCH<sub>2</sub>C, CCHC, and CCH<sub>2</sub>C), 0.92 (d, 3 H, CCH<sub>3</sub>); MS, *m/e* 270 (parent), 255, 240, 183, 181, 167, 73. Anal. Calcd for C<sub>15</sub>H<sub>34</sub>Si<sub>2</sub>: C, 66.58; H, 12.66. Found: C, 66.77; H, 12.36.

*cis*-1,3,5-Tris(trimethylsilyl)methylcyclohexane (**12a**): IR (neat) 2880 and 2930 (CH), 1250 cm<sup>-1</sup> (SiCH<sub>3</sub>); NMR (CCl<sub>4</sub>, benzene)  $\delta$  0.03 (s, 27 H, SiCH<sub>3</sub>) 0.33–0.82 and 1.20–1.88 (2 m, 15 H, CCH<sub>2</sub>CHCH<sub>2</sub>SI); MS, *m/e* 342 (parent), 268, 253, 165, 73 (base). Anal. Calcd for C<sub>18</sub>H<sub>42</sub>Si<sub>3</sub>: C, 63.07; H, 12.35. Found: C, 62.94; H, 12.55.

**1-Methyl-1-silaadamantane (4a)**. A mixture of *cis*-1,3,5-tris(trimethylsilyl)methylcyclohexane (**12a**) (8.0 g, 23.4 mmol) and anhydrous aluminum chloride (4.0 g, 30 mmol) in dry benzene (120 mL) was refluxed for 6 h with rapid stirring in a dry nitrogen atmosphere. The reaction mixture was cooled to room temperature, wet acetone (20 mL) added, and the mixture stirred for 1.5 h. The benzene solution was washed with 10% HCl (2 × 50 mL) and with distilled H<sub>2</sub>O (2 × 50 mL). Drying of the benzene solution over anhydrous Na<sub>2</sub>SO<sub>4</sub>, followed by filtration and concentration under reduced pressure gave 4.8 g of a very pale yellow liquid. The liquid was preadsorbed onto silica gel (15 g) and placed on a 4 cm × 18 cm silica gel column. Elution with pentane (1 L) as one fraction gave 3.24 g of a clear, water-white oil. GLC analysis (6 ft × 0.25 in. 10% SE-30 on Chromosorb W) of the oil showed it contained ~80% 1-methyl-1-silaadamantane (**4a**). This corresponds to an overall yield of ~67% of theoretical. An analytical sample of **4a** was obtained by preparative GLC: mp (sealed tube) 35.5–36.5 °C; IR (CCl<sub>4</sub>) 2865 (CH), 1250 cm<sup>-1</sup> (SiCH<sub>3</sub>); NMR (CCl<sub>4</sub>, benzene)  $\delta$  0.00 (s, 3 H, SiCH<sub>3</sub>), 0.84 (d, 6 H, *J* = 4.4 Hz), SiCH<sub>2</sub>C, 1.70 (apparent singlet with small broad signals located at  $\delta$  1.52 and 1.87, 6 H, CHCH<sub>2</sub>CH), 2.40 (broad apparent singlet, 3 H, CCHC); MS, *m/e* 166 (parent), 165, 151, 123, 109, 97, 95. Anal. Calcd for C<sub>10</sub>H<sub>18</sub>Si: C, 72.21; H, 10.91. Found: C, 72.08; H, 11.06.

**1-Chloro-1-silaadamantane (4b)**. 1-Methyl-1-silaadamantane (**4a**) (1.0 g, 6.0 mmol), trichlorosilane (4.03 g, 29.7 mmol), and chloroplatinic acid (~10 mg) were heated at 275–280 °C in a stainless steel bomb for 5 days. The contents of the bomb were filtered through a cotton plug under a dry nitrogen atmosphere, and the excess trichlorosilane was removed under reduced pressure to afford a dark brown oil. GLC analysis (6 ft × 0.25 in. 10% SE-30 on Chromosorb W) of the oil showed it to contain 1-chloro-1-silaadamantane (**4b**) and some higher molecular weight material. The oil was preadsorbed onto silica gel (1 g) and placed on a silica gel column measuring 2 cm × 15 cm. Elution with pentane (200 mL) as one fraction gave 800 mg of a slightly oily white solid. 1-Chloro-1-silaadamantane (**4b**) (507 mg, 51%) was obtained as a white crystalline material by standard preparative GLC methods: mp (sealed tube) 129–130.5 °C; IR (CCl<sub>4</sub>) 2860, 1428, 1390, 1180, 905, 878 cm<sup>-1</sup>; NMR (CCl<sub>4</sub>, benzene)  $\delta$  1.20 (d, 6 H, *J* = 4.4 Hz, ClSiCH<sub>2</sub>), 1.69 (apparent singlet with small broad signals located at  $\delta$  1.52 and 1.83, 6 H, CHCH<sub>2</sub>CH), 2.55 (broad apparent singlet, 3 H, CCHC); MS, *m/e* 186 (parent), 185 (base), 117, 63. Anal. Calcd for C<sub>9</sub>H<sub>15</sub>SiCl: C, 57.88; H, 8.10. Found: C, 57.59; H, 8.29.

**1-Silaadamantane (4c)**. 1-Chloro-1-silaadamantane (**4b**) (91.8 mg, 0.49 mmol) was added in one portion to a stirred suspension of 95% LiAlH<sub>4</sub> (78.8 mg, 2.07 mmol) in anhydrous diethyl ether (3.5 mL) at 25 °C in a dry nitrogen atmosphere. The reaction mixture was stirred for 20 h and then carefully hydrolyzed with distilled H<sub>2</sub>O (2 mL). The organic layer was removed and the aqueous residue extracted with ether (3 × 5 mL). The combined ethereal solutions were filtered through anhydrous Na<sub>2</sub>SO<sub>4</sub>. Analysis of the ethereal solution by GLC (6 ft × 0.25 in. 10% SE-30 on Chromosorb W) showed the absence of starting material. Removal of the solvent under reduced pressure gave a white solid. 1-Silaadamantane was purified by standard preparative GLC methods and obtained in 86% (64 mg) yield: mp (sealed tube) 243–245 °C; IR (CCl<sub>4</sub>) 2870, 2108 (Si-H), 1188, 1024, 888 cm<sup>-1</sup>; NMR (CCl<sub>4</sub>, benzene)  $\delta$  1.01 (d, 6 H, *J* = 4.3 Hz, SiCH<sub>2</sub>C), 1.74 (apparent singlet with small broad signals located at  $\delta$  1.63 and 1.92, 6 H, CHCH<sub>2</sub>CH), 2.43 (broad apparent singlet, 3 H, CCHC), 4.11 (q, 1 H, *J* = 2.3, SiH); MS, *m/e* 152 (parent), 151, 124, 123, 109, 110, 111, 93, 95, 96, 97, 83, 69, 67, 55, 43. Anal. Calcd for

C<sub>9</sub>H<sub>16</sub>Si: C, 70.97; H, 10.59. Found: C, 70.94; H, 10.43.

During the course of the reaction, the reaction mixture was analyzed by GLC (6 ft × 0.25 in. 10% SE-30 on Chromosorb W). The reaction had a half-life of ~4 min and was complete in 30 min.

**1-Methoxy-1-silaadamantane (4d)**. 1-Chloro-1-silaadamantane (**4b**) (200 mg, 1.07 mmol) was stirred in anhydrous methanol (4 mL) at 25 °C for 72 h in a dry nitrogen atmosphere. Removal of the excess methanol under reduced pressure gave a pale yellow oil. 1-Methoxy-1-silaadamantane (**4d**) (170 mg, 87%) was obtained as a clear oil by standard preparative GLC methods: IR (CCl<sub>4</sub>) 2880, 1188, 1074, 890 cm<sup>-1</sup>; NMR (CCl<sub>4</sub>, benzene)  $\delta$  0.99 (d, 6 H, *J* = 4.5 Hz, SiCH<sub>2</sub>), 1.67 (apparent singlet with small broad signals located at  $\delta$  1.49 and 1.81, 6 H, CHCH<sub>2</sub>CH), 2.54 (broad apparent singlet, 3 H, CCHC), 3.42 (s, 3 H, OCH<sub>3</sub>); MS, *m/e* 183 (parent and base), 167, 142, 115. Anal. Calcd. for C<sub>10</sub>H<sub>18</sub>SiO: C, 65.87; H, 9.95. Found: C, 65.71; H, 9.96.

A half-life of ~10 h was obtained for the reaction by NMR analysis at 25 °C. The difference in chemical shift between the six ring protons adjacent to the silicon atom in the starting chlorosilane ( $\delta$  1.20) and the corresponding six ring protons of the product ( $\delta$  0.99) allowed for the time study by NMR. The reaction was performed on 15 mg of **4b** in anhydrous methanol (0.5 mL), which was sealed in an NMR tube under a dry nitrogen atmosphere.

**1-Methyl-1-silaadamantane (4a) from 1-Chloro-1-silaadamantane (4b) and Methyllithium**. To a stirred solution of 1-chloro-1-silaadamantane (84.3 mg, 0.45 mmol) in anhydrous ether (3 mL) under a nitrogen atmosphere at 25 °C was added 1 mL of a 1.8 M diethyl ether solution of methyllithium–lithium bromide complex (1.81 mmol) in one portion. A white precipitate formed immediately. The reaction mixture was stirred for 20 h and then carefully hydrolyzed with distilled H<sub>2</sub>O (2 mL). The organic portion was separated and the aqueous layer washed with ether (3 × 5 mL). The combined ethereal solutions were filtered through anhydrous Na<sub>2</sub>SO<sub>4</sub> and concentrated under reduced pressure. Analysis of the concentrate by GLC (6 ft × 0.25 in. 10% SE-30 on Chromosorb W) showed the absence of starting material. Purification of the reaction product by standard GLC techniques gave 66.5 mg (89%) of a clear white solid, mp (sealed tube) 35.5–36.5 °C. All spectra were consistent with a known sample of **4a**.

Periodic sampling of the reaction mixture and analysis by GLC (6 ft × 0.25 in. 10% SE-30 on Chromosorb W) showed the reaction to have a half-life of ~4 min.

**Attempted Methylation of 1-Chloro-1-silaadamantane (4b) by Methylmagnesium Iodide**. 1-Chloro-1-silaadamantane (100 mg, 0.54 mmol) was added in one portion to a stirred solution of methylmagnesium iodide at 25 °C under a dry nitrogen atmosphere. Methylmagnesium iodide was prepared by the slow addition of methyl iodide (337 mg, 2.38 mmol) to stirred magnesium turnings (50 mg, 2.16 mmol) in anhydrous ether (4 mL) under a dry nitrogen atmosphere at 25 °C. Periodic analysis of the reaction by GLC (6 ft × 0.25 in. 10% SE-30 on Chromosorb W) revealed no reaction after 24 h. The reaction mixture was slowly hydrolyzed with distilled H<sub>2</sub>O (2 mL), the ether solution removed, and the aqueous layer extracted with ether (2 × 5 mL). The combined ethereal solutions were filtered through anhydrous Na<sub>2</sub>SO<sub>4</sub>, and the solvent was removed under reduced pressure to afford 95 mg (95%) of 1-chloro-1-silaadamantane as a very pale yellow crystalline solid. All spectra were consistent with those of the starting material. Pure 1-chloro-1-silaadamantane was obtained by standard preparative GLC (6 ft × 0.25 in. 10% SE-30 on Chromosorb W) techniques.

**1-(Diethylamino)-1-silaadamantane (4e)**. *n*-Butyllithium (1.6 M) in hexane (1 mL, 1.6 mmol) was slowly added dropwise to a stirred solution of diethylamine (134 mg, 1.84 mmol) in dry hexane (3 mL) at 0 °C under a dry nitrogen atmosphere. The mixture was stirred for 1 h to ensure complete salt formation. 1-Chloro-1-silaadamantane (**4b**) (200 mg, 1.07 mmol) in dry hexane (1 mL) was added to the lithium salt at room temperature. GLC (6 ft × 0.25 in. 10% SE-30 on Chromosorb W) analysis showed the reaction to be ~75% complete after 48 h. Dry diethyl ether (3 mL) was added and the reaction mixture stirred at room temperature for another 48 h. The mixture was filtered under a dry nitrogen atmosphere. The salts were washed with dry

hexane (5 × 5 mL), filtered, and combined with the original filtrate. Removal of the solvents under reduced pressure gave a yellow oil. The oil was purified by standard preparative GLC techniques (the 6 ft × 0.25 in. 10% SE-30 on Chromosorb W column was sited with hexamethyldisilazane at 120 °C prior to use). 1-(diethylamino)-1-silaadamantane (**4e**) was obtained in 88% (210 mg) yield as a clear, water white oil: IR (CCl<sub>4</sub>) 2940 and 2860 (CH), 1425, 1360, 1190, 1180, 1165, 1080, 1015, 910, 880, 710, 685 cm<sup>-1</sup>; the R<sub>2</sub>N-Si frequency is located in the 975–600-cm<sup>-1</sup> region; NMR (CCl<sub>4</sub>, benzene) δ 0.91 and 0.97 (d (*J* = 4.8 Hz), and t (*J* = 6.9 Hz) with 12 H present for the overlapping signals of SiCH<sub>2</sub>C and CCH<sub>3</sub>, respectively), 1.64 (apparent singlet with small broad signals located at δ 1.47 and 1.81, 6 H, CHCH<sub>2</sub>CH), 2.46 (broad apparent singlet, 3 H, CCHC), 2.73 (q, 4 H, *J* = 6.9 Hz, NCH<sub>2</sub>C). Anal. Calcd for C<sub>13</sub>H<sub>25</sub>NSi: C, 69.88; H, 11.28. Found: C, 69.57; H, 11.09.

**Hydrolysis of 1-(Diethylamino)-1-silaadamantane (4e).** A sample of **4e** was left open to the moisture present in the atmosphere. A white solid forms within 24 h. Analysis of the solid showed it to be bis(1-silaadamantyl) oxide (**4f**): mp (sealed tube) 226–228 °C; IR (CCl<sub>4</sub>) 2890 (CH), 1185, 1090, 1040 (SiOSi), 885 cm<sup>-1</sup>; NMR (CCl<sub>4</sub>, benzene) δ 0.92 (d, 12 H, *J* = 4.4 Hz, SiCH<sub>2</sub>C), 1.60 (apparent singlet with small broad signals located at δ 1.39 and 1.71, 12 H, CCH<sub>2</sub>C), 2.41 (broad apparent singlet, 6 H, CCHC); MS, *m/e* 318 (parent), 195, 167, 151. Anal. Calcd for C<sub>18</sub>H<sub>30</sub>O<sub>2</sub>Si<sub>2</sub>: C, 67.86; H, 9.49. Found: C, 67.75; H, 9.62.

**Methanolysis of 1-(Diethylamino)-1-silaadamantane (4e).** 1-(Diethylamino)-1-silaadamantane (**4e**) (50 mg, 0.22 mmol) was stirred in anhydrous methanol (0.3 mL) at 25 °C under a dry nitrogen atmosphere. Periodic GLC (6 ft × 0.25 in. 10% SE-30 on Chromosorb W) analysis of the reaction mixture gave a half-life of ~11 h. The product of the reaction was shown to be 1-methoxy-1-silaadamantane (**4d**) by comparison of its GLC retention time with that of a known sample.

**1-Methyl-1-silabicyclo[2.2.2]octane (2a) from 1-Chloro-1-silabicyclo[2.2.2]octane (2b) and Methylolithium.** To a stirred solution of 1-chloro-1-silabicyclo[2.2.2]octane<sup>20</sup> (**2b**) (250 mg, 1.56 mmol) in anhydrous ether (1.5 mL) under a dry nitrogen atmosphere at 25 °C was added 3.5 mL of 1.8 M ether solution of methylolithium–lithium bromide complex (6.23 mmol) in one portion. A white precipitate formed immediately. The reaction mixture was stirred for 20 h and then carefully hydrolyzed with distilled H<sub>2</sub>O (2 mL). The organic portion was separated and the aqueous layer washed with ether (3 × 3 mL). The combined ethereal solutions were filtered through anhydrous Na<sub>2</sub>SO<sub>4</sub> and concentrated under reduced pressure. Analysis of the concentrate by GLC (10 ft × 0.25 in. 25% SE-30 on Chromosorb W) showed the absence of starting material. Purification of the reaction product by standard preparative GLC techniques gave a clear, water-white oil (187.8 mg, 86%): IR (CCl<sub>4</sub>) 2860, 1430, 1395, 1240 (SiCH<sub>3</sub>), 1155, 910 cm<sup>-1</sup>; NMR (CCl<sub>4</sub>, benzene) δ 0.04 (s, 3 H, SiCH<sub>3</sub>), 0.51–0.88 (m, 6 H, SiCH<sub>2</sub>C), 1.47 (m – 6 lines resolved, 1 H, *J* = 3.4 Hz, CCHC), 1.73–2.07 (m, 6 H, CCH<sub>2</sub>C); MS, *m/e* 140 (parent), 112, 97, 84. Anal. Calcd for C<sub>8</sub>H<sub>16</sub>Si: C, 68.49; H, 11.49. Found: C, 68.20; H, 11.59. The reaction was found to be approximately 90% complete after 1 min by GLC (10 ft × 0.25 in. 25% SE-30 on Chromosorb W) analysis.

**Attempted Methylation of 1-Chloro-1-silabicyclo[2.2.2]octane (2b) by Methylmagnesium Iodide.** A solution of 1-chloro-1-silabicyclo[2.2.2]octane (200 mg, 1.25 mmol) in anhydrous ether (2 mL) was added in one portion to a stirred solution of methylmagnesium iodide at 25 °C under a dry nitrogen atmosphere. Methylmagnesium iodide was prepared by the slow addition of methyl iodide (707 mg, 5 mmol) to a stirred magnesium turnings (121 mg, 4.98 mmol) in anhydrous ether (2 mL) under a dry nitrogen atmosphere at 25 °C. Periodic analysis of the reaction mixture by GLC (10 ft × 0.25 in. 25% SE-30 on Chromosorb W) revealed no reaction after 24 h. The reaction mixture was concentrated under reduced pressure and the solid residue washed with anhydrous pentane (3 × 5 mL). The pentane was removed under reduced pressure, and 180 mg (90%) of 1-chloro-1-silabicyclo[2.2.2]octane was obtained after purification by standard preparative GLC techniques. All spectra were matched

with those of a known sample of 1-chloro-1-silabicyclo[2.2.2]octane (**2b**).

**1-Methoxy-1-silabicyclo[2.2.2]octane (2d).** 1-Chloro-1-silabicyclo[2.2.2]octane (**2b**) (250 mg, 1.56 mmol) was stirred in anhydrous methanol (5 mL) at 25 °C for 48 h in a dry nitrogen atmosphere. Removal of the excess methanol under reduced pressure gave a pale yellow oil. 1-Methoxy-1-silabicyclo[2.2.2]octane (**2c**) (205 mg, 86%) was obtained as a clear, water-white oil by standard preparative GLC (10 ft × 0.25 in. 25% SE-30 on Chromosorb W) techniques: IR (CCl<sub>4</sub>) 2875, 1435, 1400, 1155, 1065 (SiOCH<sub>3</sub>), 910 cm<sup>-1</sup>; NMR (CCl<sub>4</sub>, benzene) δ 0.63–0.97 (m, 6 H, SiCH<sub>2</sub>C), 1.42 (m – 6 lines resolved, 1 H, *J* = 3.4 Hz, CCHC), 1.80–2.13 (m, 6 H, CCH<sub>2</sub>C), 3.38 (s, 3 H, SiOCH<sub>3</sub>). Anal. Calcd for C<sub>8</sub>H<sub>16</sub>O<sub>2</sub>Si: C, 61.48; H, 10.32. Found: C, 61.19; H, 10.58.

During the course of the reaction, aliquot samples were quenched by removal of the methanol under reduced pressure and analyzed by NMR. The reaction was found to have a half-life of ~4 h. The following formula was used to obtain the percent reaction:

$$100 \frac{4.33}{\frac{\text{(total area of ring protons)}}{\text{(area of methoxyl protons)}}} = \text{percent reaction}$$

The value of 4.33 represents the ratio of ring protons to methoxyl protons at 100% reaction.

**Attempted Methylation of 1-Chloro-3,5,7-trimethyl-1,3,5,7-tetrasilaadamantane (3b) by Methylmagnesium Iodide.** 1-Chloro-3,5,7-trimethyl-1,3,5,7-tetrasilaadamantane (**3b**) (100 mg, 0.36 mmol) prepared by the method of Homer and Sommer<sup>2</sup> was added in one portion to a stirred solution of methylmagnesium iodide at 25 °C under a dry nitrogen atmosphere. Methylmagnesium iodide was prepared by the slow addition of methyl iodide (247 mg, 1.75 mmol) to stirred magnesium turnings (34 mg, 1.45 mmol) in anhydrous diethyl ether (4 mL) under a dry nitrogen atmosphere at 25 °C. Periodic analysis of the reaction mixture by GLC (6 ft × 0.25 in. 10% SE-30 on Chromosorb W) revealed no reaction after 24 h. The reaction mixture was slowly hydrolyzed with distilled H<sub>2</sub>O (2 mL), the ether solution removed, and the aqueous layer extracted with ether (2 × 5 mL). The combined ethereal solutions were filtered through anhydrous Na<sub>2</sub>SO<sub>4</sub>, and the solvent was removed under reduced pressure to afford 97 mg (97%) of **3b**. All spectra were consistent with those of the starting material. Pure **3b** was obtained by standard preparative GLC methods.

**Competitive Solvolysis Study of 1-Silaadamantane (4c) and Triethylsilane.** 1-Silaadamantane (**4c**) (18.3 mg, 0.12 mmol) in anhydrous ethanol (0.7 mL) and 1 mL of a 0.12 M anhydrous ethanol solution of triethylsilane were placed in a 5-mL round-bottom flask under a dry nitrogen atmosphere. The mixture of silanes was placed in a thermostatically controlled water bath at 35 ± 0.1 °C and stirred for 1 h. A separate flask containing a standardized 1.6776 M aqueous solution of NaOH was also placed in the water bath for 1 h. At the end of this time period, 0.3 mL of the NaOH solution was rapidly added and mixed with the ethanol solution of the silanes. The reaction was monitored periodically by GLC (10 ft × 0.25 in. 25% SE-30 on Chromosorb W). The decreasing peak areas of **4c** and triethylsilane were compared. A relative rate for the solvolysis of **4c** of ~3 was obtained by setting the solvolysis rate of triethylsilane equal to one.

**1-Methyl-1-silaadamantane (4a) from 1-Methyl-3,5-bis-((trimethylsilyl)methyl)cyclohexane (12b).** A mixture of *cis*-1-methyl-3,5-bis-((trimethylsilyl)methyl)cyclohexane (**12b**) (250 mg, 0.93 mmol) and anhydrous AlCl<sub>3</sub> (80 mg, 0.60 mmol) in dry benzene (2 mL) was refluxed for 20 h under a dry nitrogen atmosphere. The reaction was cooled to room temperature, and wet acetone (0.5 mL) and a solution of 10% HCl (5 mL) were added. The benzene layer was separated from the aqueous portion, washed with distilled H<sub>2</sub>O (5 mL), and dried over anhydrous MgSO<sub>4</sub>. A yellow-brown oil (150 mg) was obtained after removal of the benzene under reduced pressure. GLC (6 ft × 0.25 in. 10% SE-30 on Chromosorb W) showed 1-methyl-1-silaadamantane (**4a**) to have been formed in ~10% yield. The starting silane **12b** had undergone ~50% reaction by GLC analysis. 1-Methyl-1-silaadamantane (**4a**) from this reaction was identified

by comparison of its GLC retention time with that of an authentic sample.

**Acknowledgment** is made to the donors of The Petroleum Research Fund, administered by the American Chemical Society, for partial support of this research. Financial support from the National Science Foundation, through Grant CHE-7911812, is also gratefully acknowledged. We also wish to thank Vern Feil, Frank Farris, and

John S. Kiely for help in obtaining mass spectral data and Richard L. Hilderbrandt and G. David Homer for helpful discussions.

**Registry No.** 1b, 18135-81-4; 2a, 81500-59-6; 2b, 18379-57-2; 2c, 280-37-5; 2d, 84010-93-5; 3b, 30038-39-2; 4a, 65672-54-0; 4b, 65672-61-9; 4c, 65957-76-8; 4d, 84010-94-6; 4e, 84010-95-7; 4f, 84010-96-8; 5, 554-95-0; 6, 16526-68-4; 7, 16526-69-5; 8, 6998-83-0; 10, 30363-89-4; 11, 65672-58-4; 12a, 65672-56-2; 12b, 65672-57-3; 12c, 84010-92-4.

## Communications

### Reactions of 1,1-Dimethylsilene with Alkynes

Robert T. Conlin,\* Young-Woo Kwak, and Holly B. Huffaker

Department of Chemistry, North Texas State University  
Denton, Texas 76203

Received July 28, 1982

**Summary:** Dimethylsilene, generated by pyrolysis of 1,1-dimethylsilacyclobutane, reacts with alkynes to give silacyclobutenes or acyclic products. The temperature dependence of product ratios has been determined, and the relative reactivities of three alkynes toward the 1,1-dimethylsilene are reported.

The ability of conjugated dienes to intercept silenes appears unaffected by the nature of the substituents<sup>1</sup> at either end of the silicon-carbon  $\pi$  bond and by changes in reaction conditions<sup>2</sup> such as temperature or medium. Brook and co-workers<sup>3</sup> have shown that silenes, generated from photolysis or thermolysis of acyldisilanes in condensed media, readily add to phenylpropyne to give exclusively silacyclobutenes in good yield. In contrast, Wiberg's group<sup>4</sup> has recently reported that a silene, 1,1-dimethyl-2,2-bis(trimethylsilyl)silene, produced in solution by thermal elimination of lithium salts from substituted  $\alpha$ -lithiosilyl phosphates, does not react with alkynes such as tolane or bis(trimethylsilyl)acetylene. Instead, only dimers of the silene are produced. In this communication we report that thermal gas-phase reactions of 1,1-dimethylsilene with three alkynes leads to new products not observed in solution.

(1) For examples of reactions between dienes and silenes bearing a wide variety of substituents see: (a) Nametkin, N. S.; Gusel'nikov, L. E.; Ushakova, R. L.; Vdovin, V. M. *Dokl. Akad. Nauk SSSR* 1971, 201, 1365. (b) Brook, A. G.; Harris, J. W. *J. Am. Chem. Soc.* 1976, 98, 381. (c) Wiberg, N.; Preiner, G. *Angew. Chem., Int. Ed. Engl.* 1977, 16, 328. (d) Ando, W.; Sekiguchi, A.; Rothschild, A. J.; Gallucci, R. R.; Jones, M., Jr.; Barton, T. J.; Kilgour, J. A. *J. Am. Chem. Soc.* 1977, 99, 6995. (e) Ishikawa, M.; Fuchikama, T.; Kumada, M. *J. Organomet. Chem.* 1978, 149, 37. (f) Barton, T. J.; Hoekman, S. K. *J. Am. Chem. Soc.* 1980, 102, 1584. (g) Jones, P. R.; Lim, T. F. O.; Pierce, R. A. *Ibid.* 1980, 102, 4970. (h) Barton, T. J.; Burns, S. A.; Burns, G. T. *Organometallics* 1982, 1, 210.

(2) Reaction conditions in ref 1 vary from temperatures of -100 to +600 °C and include condensed as well as gas phase processes.

(3) Brook, A. G.; Harris, J. W.; Lennon, J.; El Sheikh, M. *J. Am. Chem. Soc.* 1979, 101, 83.

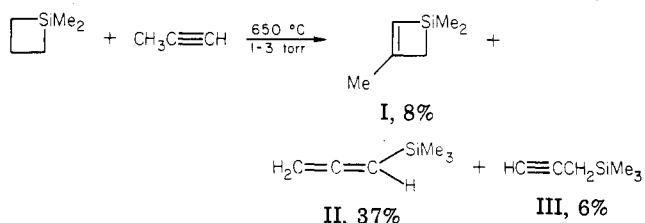
(4) Wiberg, N.; Preiner, G.; Schieda, O. *Chem. Ber.* 1981, 114, 3518.

Table I. Pyrolysis of Dimethylsilacyclobutane and Propyne. Dependence of Product Ratio on Temperature

temp, °C	II/III	(II + III)/I
600	16.0	7.2
650	6.2	5.1
700	5.5	4.6

Copyrolysis<sup>5</sup> of 1,1-dimethylsilacyclobutane and a tenfold excess of acetylene in a vacuum flow system at 650 °C gave 1,1-dimethylsilacyclobutene (22% yield)<sup>6</sup> along with ethylene and the 1,1,3,3-tetramethyl-1,3-disilacyclobutane (56% yield). Formation of the dimethylsilacyclobutene is consistent with a 2 + 2 cycloaddition between 1,1-dimethylsilene and acetylene while the disilacyclobutane is that product expected from the usual silene dimerization.

When propyne was used to trap the silene under otherwise identical reaction conditions, three new products are observed: 1,1,3-trimethylsilacyclobutene, I, allenyltrimethylsilane, II, and propargyltrimethylsilane, III, in yields indicated below. In addition, formation of tetramethyldisilacyclobutane (28% yield) is noted. The pos-



sibility that both allenyl- and propargyltrimethylsilanes might arise from secondary decomposition of the 1,1,3-trimethylsilacyclobutene has been eliminated as follows. Pyrolysis of the neat trimethylsilacyclobutene<sup>7</sup> at temperatures from 600 to 700 °C gave quantitative recovery of starting material. Furthermore, when a tenfold excess of propyne was used to trap the 1,1,3-trimethyl-1-silabutadiene anticipated from electrocyclic ring opening<sup>8</sup> of the

(5) Pyrolyses were carried out in a seasoned hot zone consisting of a 10-mm i.d.  $\times$  30 cm quartz tube. Residence times in the hot zone were on the order of tenths of seconds and pressures in the hot zone were 1-5 torr. Both residence time and pressure were controlled by a 0.8-mm aperture placed at the end of the pyrolysis chamber.

(6) Products yields were based on the quantity of 1,1-dimethylsilacyclobutane decomposed. At 650 °C decomposition of dimethylsilacyclobutane is  $\approx$ 70% and mass balances are typically 80%. Products were characterized by comparison of their spectral and chromatographic properties with those of authentic samples.

(7) Block, E.; Revelle, L. K. *J. Am. Chem. Soc.* 1978, 100, 1630.

(8) Tzeng, D.; Fong, R. H.; Soysa, H. S. D.; Weber, W. P. *J. Organomet. Chem.* 1981, 219, 153.

## Reactions of 1,1-dimethylsilene with alkynes

Robert T. Conlin, Young Woo Kwak, and Holly B. Huffaker

*Organometallics*, **1983**, 2 (2), 343-344 • DOI: 10.1021/om00074a024 • Publication Date (Web): 01 May 2002

Downloaded from <http://pubs.acs.org> on April 24, 2009

### More About This Article

---

The permalink <http://dx.doi.org/10.1021/om00074a024> provides access to:

- Links to articles and content related to this article
- Copyright permission to reproduce figures and/or text from this article





by comparison of its GLC retention time with that of an authentic sample.

**Acknowledgment** is made to the donors of The Petroleum Research Fund, administered by the American Chemical Society, for partial support of this research. Financial support from the National Science Foundation, through Grant CHE-7911812, is also gratefully acknowledged. We also wish to thank Vern Feil, Frank Farris, and

John S. Kiely for help in obtaining mass spectral data and Richard L. Hilderbrandt and G. David Homer for helpful discussions.

**Registry No.** 1b, 18135-81-4; 2a, 81500-59-6; 2b, 18379-57-2; 2c, 280-37-5; 2d, 84010-93-5; 3b, 30038-39-2; 4a, 65672-54-0; 4b, 65672-61-9; 4c, 65957-76-8; 4d, 84010-94-6; 4e, 84010-95-7; 4f, 84010-96-8; 5, 554-95-0; 6, 16526-68-4; 7, 16526-69-5; 8, 6998-83-0; 10, 30363-89-4; 11, 65672-58-4; 12a, 65672-56-2; 12b, 65672-57-3; 12c, 84010-92-4.

## Communications

### Reactions of 1,1-Dimethylsilene with Alkynes

Robert T. Conlin,\* Young-Woo Kwak, and Holly B. Huffaker

Department of Chemistry, North Texas State University  
Denton, Texas 76203

Received July 28, 1982

**Summary:** Dimethylsilene, generated by pyrolysis of 1,1-dimethylsilacyclobutane, reacts with alkynes to give silacyclobutenes or acyclic products. The temperature dependence of product ratios has been determined, and the relative reactivities of three alkynes toward the 1,1-dimethylsilene are reported.

The ability of conjugated dienes to intercept silenes appears unaffected by the nature of the substituents<sup>1</sup> at either end of the silicon-carbon  $\pi$  bond and by changes in reaction conditions<sup>2</sup> such as temperature or medium. Brook and co-workers<sup>3</sup> have shown that silenes, generated from photolysis or thermolysis of acyldisilanes in condensed media, readily add to phenylpropyne to give exclusively silacyclobutenes in good yield. In contrast, Wiberg's group<sup>4</sup> has recently reported that a silene, 1,1-dimethyl-2,2-bis(trimethylsilyl)silene, produced in solution by thermal elimination of lithium salts from substituted  $\alpha$ -lithiosilyl phosphates, does not react with alkynes such as tolane or bis(trimethylsilyl)acetylene. Instead, only dimers of the silene are produced. In this communication we report that thermal gas-phase reactions of 1,1-dimethylsilene with three alkynes leads to new products not observed in solution.

(1) For examples of reactions between dienes and silenes bearing a wide variety of substituents see: (a) Nametkin, N. S.; Gusel'nikov, L. E.; Ushakova, R. L.; Vdovin, V. M. *Dokl. Akad. Nauk SSSR* 1971, 201, 1365. (b) Brook, A. G.; Harris, J. W. *J. Am. Chem. Soc.* 1976, 98, 381. (c) Wiberg, N.; Preiner, G. *Angew. Chem., Int. Ed. Engl.* 1977, 16, 328. (d) Ando, W.; Sekiguchi, A.; Rothschild, A. J.; Gallucci, R. R.; Jones, M., Jr.; Barton, T. J.; Kilgour, J. A. *J. Am. Chem. Soc.* 1977, 99, 6995. (e) Ishikawa, M.; Fuchikama, T.; Kumada, M. *J. Organomet. Chem.* 1978, 149, 37. (f) Barton, T. J.; Hoekman, S. K. *J. Am. Chem. Soc.* 1980, 102, 1584. (g) Jones, P. R.; Lim, T. F. O.; Pierce, R. A. *Ibid.* 1980, 102, 4970. (h) Barton, T. J.; Burns, S. A.; Burns, G. T. *Organometallics* 1982, 1, 210.

(2) Reaction conditions in ref 1 vary from temperatures of -100 to +600 °C and include condensed as well as gas phase processes.

(3) Brook, A. G.; Harris, J. W.; Lennon, J.; El Sheikh, M. *J. Am. Chem. Soc.* 1979, 101, 83.

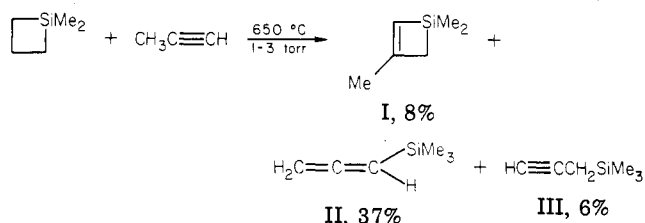
(4) Wiberg, N.; Preiner, G.; Schieda, O. *Chem. Ber.* 1981, 114, 3518.

Table I. Pyrolysis of Dimethylsilacyclobutane and Propyne. Dependence of Product Ratio on Temperature

temp, °C	II/III	(II + III)/I
600	16.0	7.2
650	6.2	5.1
700	5.5	4.6

Copyrolysis<sup>5</sup> of 1,1-dimethylsilacyclobutane and a tenfold excess of acetylene in a vacuum flow system at 650 °C gave 1,1-dimethylsilacyclobutene (22% yield)<sup>6</sup> along with ethylene and the 1,1,3,3-tetramethyl-1,3-disilacyclobutane (56% yield). Formation of the dimethylsilacyclobutene is consistent with a 2 + 2 cycloaddition between 1,1-dimethylsilene and acetylene while the disilacyclobutane is that product expected from the usual silene dimerization.

When propyne was used to trap the silene under otherwise identical reaction conditions, three new products are observed: 1,1,3-trimethylsilacyclobutene, I, allenyl-trimethylsilane, II, and propargyltrimethylsilane, III, in yields indicated below. In addition, formation of tetramethyldisilacyclobutane (28% yield) is noted. The pos-



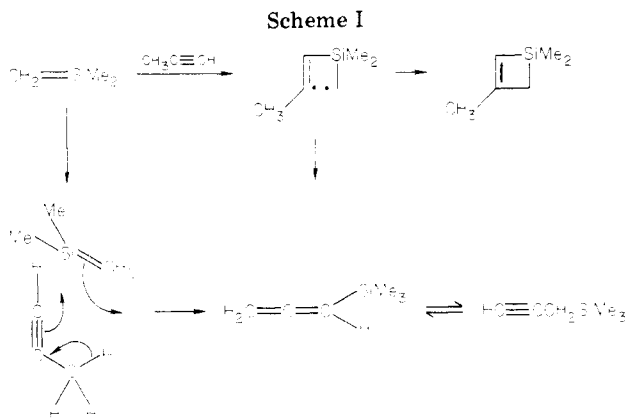
sibility that both allenyl- and propargyltrimethylsilanes might arise from secondary decomposition of the 1,1,3-trimethylsilacyclobutene has been eliminated as follows. Pyrolysis of the neat trimethylsilacyclobutene<sup>7</sup> at temperatures from 600 to 700 °C gave quantitative recovery of starting material. Furthermore, when a tenfold excess of propyne was used to trap the 1,1,3-trimethyl-1-silabutadiene anticipated from electrocyclic ring opening<sup>8</sup> of the

(5) Pyrolyses were carried out in a seasoned hot zone consisting of a 10-mm i.d. × 30 cm quartz tube. Residence times in the hot zone were on the order of tenths of seconds and pressures in the hot zone were 1-5 torr. Both residence time and pressure were controlled by a 0.8-mm aperture placed at the end of the pyrolysis chamber.

(6) Product yields were based on the quantity of 1,1-dimethylsilacyclobutane decomposed. At 650 °C decomposition of dimethylsilacyclobutane is  $\approx$  70% and mass balances are typically 80%. Products were characterized by comparison of their spectral and chromatographic properties with those of authentic samples.

(7) Block, E.; Revelle, L. K. *J. Am. Chem. Soc.* 1978, 100, 1630.

(8) Tzeng, D.; Fong, R. H.; Soysa, H. S. D.; Weber, W. P. *J. Organomet. Chem.* 1981, 219, 153.

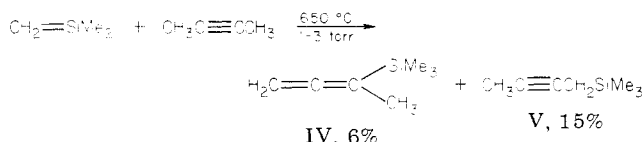


trimethylsilacyclobutene, no reaction products were observed.

The temperature dependence of the product distribution, shown in Table I, suggests that propargyltrimethylsilane is formed by isomerization of the initially produced allenyltrimethylsilane. At 600 °C the ratio of II/III was 16.0. With increasing temperatures of 650 and 700 °C the ratio of II/III decreased to 6.2 and 5.5, respectively, in close agreement with the equilibrium value 6.1 reported by Slutsky and Kwart<sup>9</sup> for the reversible isomerization of allenyltrimethylsilane and propargyltrimethylsilane. Increasing reaction temperature also favors formation of the 1,1,3-trimethylsilacyclobutene (I) over acyclic silanes II and III. In the absence of any secondary decomposition, the temperature dependence of product ratios suggests that the composite activation barrier for the 2 + 2 cycloaddition is higher than that leading to the acyclic (or ene) products.

A reasonable reaction pathway (Scheme I) leading to all three observed products involves approach of the silicon atom of the silene to the *less* substituted carbon atom of the triple bond. The absence of 1,1,2-trimethylsilacyclobutene or any other products resulting from silicon approach to the *more* substituted sp-carbon atom may be rationalized in terms of steric congestion in the transition state or electronic factors in a biradical or zwitterionic intermediate. In principle, the allenylsilane may be formed by a hydrogen shift from the hypothetical biradical or by an intermolecular ene reaction. The data in Table I do not allow us to distinguish between the two pathways.

Reaction between 1,1-dimethylsilene and 2-butyne at 650 °C gave two acyclic products 1-methyl-1-trimethylsilyllallene<sup>10</sup> (6% yield) and 2-butynyltrimethylsilane<sup>11</sup> (15% yield). The remaining silene products are accounted for by dimerization to tetramethyldisilacyclobutane (52% yield). At the lowest pyrolysis temperature, 600 °C, the



ratio of the allenylsilane to the butynylsilane was 2.8, but at 650 and 700 °C the product ratios dropped to 0.40 and

0.42, respectively, where the butynylsilane predominates. We suggest that the higher reaction temperatures establish an equilibrium ratio which favors the less sterically crowded isomer 2-butynyltrimethylsilane.

Conspicuous by its absence from the butyne reaction products is the 2 + 2 cycloaddition product 1,1,2,3-tetramethylsilacyclobutene. In the gas phase at high temperatures, alkyl substitution at both sp-carbon atoms apparently eliminates the pathway leading to cycloaddition. Nevertheless, allenyl- and butynyltrimethylsilanes are obtained, and we suggest that they derive in part, if not exclusively, from an intermolecular pericyclic ene reaction.<sup>12,13</sup> We add, however, that the absence of cycloadduct from 2-butyne might also be ascribed to an unusually high barrier for ring closure of the biradical adduct.

Lastly, we report relative reactivities of the three alkynes toward 1,1-dimethylsilene. Competition experiments in the gas phase at 650 °C indicate the following order propyne (2.4) > 2-butyne (1.0)  $\approx$  acetylene (1.0).<sup>14</sup> Relative reactivities were determined from total product yields for pairs of reacting alkynes. The ratios of product isomers from either propyne or 2-butyne were the same in both the competition studies and the copyrolyses. Two interesting features of the relative reactivities emerge. The first is that the intermolecular silene ene products are formed more rapidly from propyne than from butyne despite the statistical advantage of two allylic methyl groups on the latter alkyne. Secondly, we note that the 1,1-dimethylsilene cycloaddition to acetylene proceeds about three times as fast as cycloaddition to propyne.

It appears that substituents on both the alkyne and the silene can significantly influence the energetics of possible reaction pathways. Experiments designed to reveal this effect of substituents on the cycloaddition and ene pathways are currently in progress.

**Acknowledgment.** We gratefully acknowledge the Robert A. Welch Foundation and the North Texas State University Faculty Research Fund for support of this work.

**Registry No.** I, 66222-36-4; II, 14657-22-8; III, 13361-64-3; IV, 74542-82-8; V, 18825-29-1; 1,1-dimethylsilacyclobutane, 2295-12-7; acetylene, 74-86-2; 1,1-dimethylsilacyclobutene, 66222-35-3; ethylene, 74-85-1; 1,1,3,3-tetramethyl-1,3-disilacyclobutane, 1627-98-1; propyne, 74-99-7; 1,1-dimethylsilene, 4112-23-6; 2-butyne, 503-17-3.

(12) Wiberg, N.; Preiner, G.; Schieda, O.; Fischer, G. *Chem. Ber.* **1981**, *114*, 3505.

(13) Conlin, R. T.; Bessellieu, M. P.; Jones, P. R.; Pierce, R. A. *Organometallics* **1982**, *1*, 396.

(14) The estimated error in these measurements is  $\pm 15\%$ .

### Facile Reduction of Tricyclopentadienyluranium(IV) Alkyl to Corresponding Anionic Uranium(III) Complexes: A Novel Route to Remarkably Stable f Element-Alkyl Systems

Lucile Arnaudet, Gérard Folcher,\* and Hubert Marquet-Ellis

Département de Physico-Chimie, Section Chimie Moléculaire CEN Saclay, F-91191 Gif sur Yvette, France

Eberhard Klähne, Kenan Yünlü, and R. Dieter Fischer\*

Institut für Anorganische und Angewandte Chemie Universität Hamburg, D-2000 Hamburg 13, West Germany

Received March 26, 1982

**Summary:** Exposure of Cp<sub>3</sub>U<sup>IV</sup>R (R = CH<sub>3</sub>, *i*-C<sub>3</sub>H<sub>7</sub>, *i*-C<sub>4</sub>H<sub>9</sub>, and *n*-C<sub>4</sub>H<sub>9</sub>; **1a-d**) to excess LiR (R = CH<sub>3</sub> or *n*-

(9) Slutsky, J.; Kwart, H. *J. Am. Chem. Soc.* **1973**, *95*, 8678.

(10) <sup>1</sup>H NMR:  $\delta$  (neat) 3.96 (2 H, q,  $J = 3.0$  Hz, H<sub>2</sub>C=C), 1.50 (3 H, t,  $J = 3.0$  Hz, H<sub>3</sub>CC=C), 0.02 (9 H, s, (CH<sub>3</sub>)<sub>3</sub>Si). <sup>13</sup>C NMR:  $\delta$  (neat) 208.9 (s, =C=), 127.7 (s, =CSi), 66.9 (t, H<sub>2</sub>C=), 14.4 (q, H<sub>3</sub>C), -2.6 (q, (CH<sub>3</sub>)<sub>3</sub>Si). Mass spectrum:  $m/e$  126 (14), 111 (29), 73 (100).

(11) <sup>1</sup>H NMR:  $\delta$  (neat) 1.72 (3 H, t,  $J = 3.0$  Hz, H<sub>3</sub>CCC), 1.40 (2 H, q,  $J = 3.0$  Hz, CCH<sub>2</sub>), 0.18 (9 H, s, (CH<sub>3</sub>)<sub>3</sub>Si). <sup>13</sup>C NMR:  $\delta$  (neat) 75.4 (s, C), 73.0 (s, C), 6.6 (t, CH<sub>2</sub>Si), 2.7 (q, CH<sub>3</sub>), -2.7 (s, (CH<sub>3</sub>)<sub>3</sub>Si). Mass spectrum:  $m/e$  126 (18), 111 (12), 73 (100).

## Facile reduction of tricyclopentadienyluranium(IV) alkyl to corresponding anionic uranium(III) complexes: a novel route to remarkably stable f element-alkyl systems

Lucile Arnaudet, Gerard Folcher, Hubert Marquet-Ellis, Eberhard Klaehne, Kenan Yuenlue, and R. Dieter Fischer

*Organometallics*, 1983, 2 (2), 344-346 • DOI: 10.1021/om00074a025 • Publication Date (Web): 01 May 2002

Downloaded from <http://pubs.acs.org> on April 24, 2009

### More About This Article

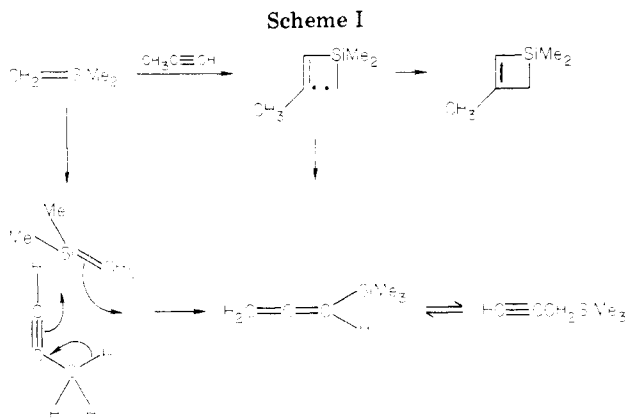
---

The permalink <http://dx.doi.org/10.1021/om00074a025> provides access to:

- Links to articles and content related to this article
- Copyright permission to reproduce figures and/or text from this article



ACS Publications  
High quality. High impact.

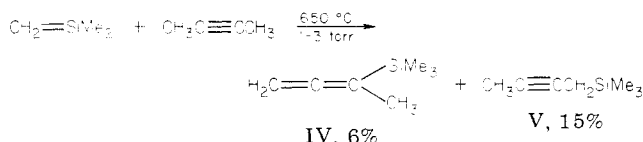


trimethylsilylacyclobutene, no reaction products were observed.

The temperature dependence of the product distribution, shown in Table I, suggests that propargyltrimethylsilane is formed by isomerization of the initially produced allenyltrimethylsilane. At 600 °C the ratio of II/III was 16.0. With increasing temperatures of 650 and 700 °C the ratio of II/III decreased to 6.2 and 5.5, respectively, in close agreement with the equilibrium value 6.1 reported by Slutsky and Kwart<sup>9</sup> for the reversible isomerization of allenyltrimethylsilane and propargyltrimethylsilane. Increasing reaction temperature also favors formation of the 1,1,3-trimethylsilylacyclobutene (I) over acyclic silanes II and III. In the absence of any secondary decomposition, the temperature dependence of product ratios suggests that the composite activation barrier for the 2 + 2 cycloaddition is higher than that leading to the acyclic (or ene) products.

A reasonable reaction pathway (Scheme I) leading to all three observed products involves approach of the silicon atom of the silene to the *less* substituted carbon atom of the triple bond. The absence of 1,1,2-trimethylsilylacyclobutene or any other products resulting from silicon approach to the *more* substituted sp-carbon atom may be rationalized in terms of steric congestion in the transition state or electronic factors in a biradical or zwitterionic intermediate. In principle, the allenylsilane may be formed by a hydrogen shift from the hypothetical biradical or by an intermolecular ene reaction. The data in Table I do not allow us to distinguish between the two pathways.

Reaction between 1,1-dimethylsilene and 2-butyne at 650 °C gave two acyclic products 1-methyl-1-trimethylsilyllallene<sup>10</sup> (6% yield) and 2-butynyltrimethylsilane<sup>11</sup> (15% yield). The remaining silene products are accounted for by dimerization to tetramethyldisilacyclobutane (52% yield). At the lowest pyrolysis temperature, 600 °C, the



ratio of the allenylsilane to the butynylsilane was 2.8, but at 650 and 700 °C the product ratios dropped to 0.40 and

0.42, respectively, where the butynylsilane predominates. We suggest that the higher reaction temperatures establish an equilibrium ratio which favors the less sterically crowded isomer 2-butynyltrimethylsilane.

Conspicuous by its absence from the butyne reaction products is the 2 + 2 cycloaddition product 1,1,2,3-tetramethylsilylacyclobutene. In the gas phase at high temperatures, alkyl substitution at both sp-carbon atoms apparently eliminates the pathway leading to cycloaddition. Nevertheless, allenyl- and butynyltrimethylsilanes are obtained, and we suggest that they derive in part, if not exclusively, from an intermolecular pericyclic ene reaction.<sup>12,13</sup> We add, however, that the absence of cycloadduct from 2-butyne might also be ascribed to an unusually high barrier for ring closure of the biradical adduct.

Lastly, we report relative reactivities of the three alkynes toward 1,1-dimethylsilene. Competition experiments in the gas phase at 650 °C indicate the following order propyne (2.4) > 2-butyne (1.0)  $\approx$  acetylene (1.0).<sup>14</sup> Relative reactivities were determined from total product yields for pairs of reacting alkynes. The ratios of product isomers from either propyne or 2-butyne were the same in both the competition studies and the copyrolyses. Two interesting features of the relative reactivities emerge. The first is that the intermolecular silene ene products are formed more rapidly from propyne than from butyne despite the statistical advantage of two allylic methyl groups on the latter alkyne. Secondly, we note that the 1,1-dimethylsilene cycloaddition to acetylene proceeds about three times as fast as cycloaddition to propyne.

It appears that substituents on both the alkyne and the silene can significantly influence the energetics of possible reaction pathways. Experiments designed to reveal this effect of substituents on the cycloaddition and ene pathways are currently in progress.

**Acknowledgment.** We gratefully acknowledge the Robert A. Welch Foundation and the North Texas State University Faculty Research Fund for support of this work.

**Registry No.** I, 66222-36-4; II, 14657-22-8; III, 13361-64-3; IV, 74542-82-8; V, 18825-29-1; 1,1-dimethylsilylacyclobutane, 2295-12-7; acetylene, 74-86-2; 1,1-dimethylsilylacyclobutene, 66222-35-3; ethylene, 74-85-1; 1,1,3,3-tetramethyl-1,3-disilacyclobutane, 1627-98-1; propyne, 74-99-7; 1,1-dimethylsilene, 4112-23-6; 2-butyne, 503-17-3.

(12) Wiberg, N.; Preiner, G.; Schieda, O.; Fischer, G. *Chem. Ber.* **1981**, *114*, 3505.

(13) Conlin, R. T.; Bessellieu, M. P.; Jones, P. R.; Pierce, R. A. *Organometallics* **1982**, *1*, 396.

(14) The estimated error in these measurements is  $\pm 15\%$ .

### Facile Reduction of Tricyclopentadienyluranium(IV) Alkyl to Corresponding Anionic Uranium(III) Complexes: A Novel Route to Remarkably Stable f Element-Alkyl Systems

Lucile Arnaudet, Gérard Folcher,\* and Hubert Marquet-Ellis

Département de Physico-Chimie, Section Chimie Moléculaire CEN Saclay, F-91191 Gif sur Yvette, France

Eberhard Klähne, Kenan Yünlü, and R. Dieter Fischer\*

Institut für Anorganische and Angewandte Chemie Universität Hamburg, D-2000 Hamburg 13, West Germany

Received March 26, 1982

**Summary:** Exposure of Cp<sub>3</sub>U<sup>IV</sup>R (R = CH<sub>3</sub>, *i*-C<sub>3</sub>H<sub>7</sub>, *i*-C<sub>4</sub>H<sub>9</sub>, and *n*-C<sub>4</sub>H<sub>9</sub>; **1a-d**) to excess LiR (R = CH<sub>3</sub> or *n*-

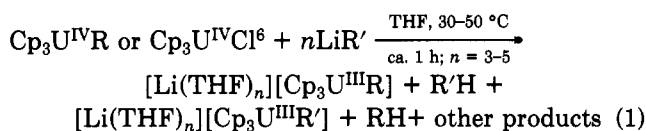
(9) Slutsky, J.; Kwart, H. *J. Am. Chem. Soc.* **1973**, *95*, 8678.

(10) <sup>1</sup>H NMR:  $\delta$  (neat) 3.96 (2 H, q,  $J = 3.0$  Hz, H<sub>2</sub>C=C), 1.50 (3 H, t,  $J = 3.0$  Hz, H<sub>3</sub>CC=C), 0.02 (9 H, s, (CH<sub>3</sub>)<sub>3</sub>Si). <sup>13</sup>C NMR:  $\delta$  (neat) 208.9 (s, =C=), 127.7 (s, =CSi), 66.9 (t, H<sub>2</sub>C=), 14.4 (q, H<sub>3</sub>C), -2.6 (q, (CH<sub>3</sub>)<sub>3</sub>Si). Mass spectrum:  $m/e$  126 (14), 111 (29), 73 (100).

(11) <sup>1</sup>H NMR:  $\delta$  (neat) 1.72 (3 H, t,  $J = 3.0$  Hz, H<sub>3</sub>CCC), 1.40 (2 H, q,  $J = 3.0$  Hz, CCH<sub>2</sub>), 0.18 (9 H, s, (CH<sub>3</sub>)<sub>3</sub>Si). <sup>13</sup>C NMR:  $\delta$  (neat) 75.4 (s, C), 73.0 (s, C), 6.6 (t, CH<sub>2</sub>Si), 2.7 (q, CH<sub>3</sub>), -2.7 (s, (CH<sub>3</sub>)<sub>3</sub>Si). Mass spectrum:  $m/e$  126 (18), 111 (12), 73 (100).

$C_4H_9$ ) in THF between 30 and 50 °C yields saturated hydrocarbons RH and, among other  $Cp_3U^{III}$  derivatives, the solvated species  $[Li(THF)_n][Cp_3U^{III}R]$  (6). GC/MS studies suggest hydrogen uptake from MR (M = coordinated U or Li) and not from the (deuterated) solvent.

According to the qualitative order of *thermal* stability of  $\sigma$ -bonded organouranium(IV) systems,<sup>1</sup> e.g.,  $Cp_3UR$  (1) >  $Cp^*_2UXR^{2a}$  (2) >  $Cp^*_2UR_2$  (3) >  $Li_nUR_{4+n}L_m$  (4) >> "UR<sub>4</sub>" (5) ( $Cp = \eta^5-C_5H_5$ ;  $Cp^* = \eta^5-C_5(CH_3)_5$ ; X = halide; L = Lewis base; R = alkyl), a distinct maximum arrived at is type 1. Facile *reduction* of the "halide precursors" of types 2 and 5,  $Cp^*_2UCl_2^{2a}$  and  $UCl_4$ ,<sup>3</sup> respectively, by alkyl lithium, presumably via labile uranium(IV) alkyl complexes,<sup>4</sup> has been observed. We now wish to report that even representatives of type 1 are readily reduced by additional LiR under comparatively mild conditions.<sup>5,6</sup> Equation 1 only specifies so far the best-identified products for  $3 \leq n \leq 5$ . Unlike reactions with Grignard reagents,<sup>5b</sup>



the complexes 1b and 1c are likewise reduced by  $LiCH_3$  mainly to the species 6a. However, the alkynyl complex 1e (R =  $C\equiv CH$ ) has been reported to react with  $Li(n-C_4H_9)$  simply by exchange of R.<sup>8</sup>  $(C_5H_4CH_3)_3UCl$  and  $(C_9H_7)_3UCl$  ( $C_9H_7$  = indenyl) react with  $LiCH_3$  (molar ratio  $\approx 1:4$ ) already at room temperature under rapid  $CH_4$  evolution and formation of dark suspensions.<sup>9</sup>

(1) Fagan, P. J.; Manriquez, J.; Marks, T. J. In "Organometallics of the f-Elements"; Marks, T. J.; Fischer, R. D., Eds.; D. Reidel Publishing Company: Dordrecht, Holland, 1979; p 131.

(2) (a) Manriquez, J. M.; Fagan, P. J.; Marks, T. J.; Vollmer, S. H.; Day, C. S.; Day, V. W. *J. Am. Chem. Soc.* **1979**, *101*, 5075. So far only  $Li(n-C_4H_9)$  has successfully been applied to reduce  $Cp^*_2U^{IV}Cl_2$  to  $[Cp^*_2U^{III}R]$ ; the only reportedly stable  $Cp^*_2U^{III}R$  system involves R =  $CH(SiMe_3)_2$ . (b) Fagan, P. J.; Manriquez, J. M.; Marks, T. J.; Day, C. S.; Vollmer, S. H.; Day, V. W. *Organometallics* **1982**, *1*, 170.

(3) (a) Marks, T. J.; Seyam, A. M. *J. Organomet. Chem.* **1974**, *67*, 61. (b) Evans, W. J.; Wink, D. J.; Stanley, D. R. *Inorg. Chem.* **1982**, *21*, 2565.

(4) (a) The so far adopted formulation of " $U^{IV}R_n$ "<sup>3a</sup> has most recently been questioned.<sup>3b</sup> (b) Most of the type 4 species probably undergo reduction too, as suggested from decomposition under gas evolution above -20 °C: Sigurdson, E.; Wilkinson, G. *J. Chem. Soc., Dalton Trans.* **1977**, 812.

(5) (a) This reaction is also initiated by light irradiation at room temperature. Actually, the observations described in this note derive from previous engagements in the convenient preparation, and photolysis, of various type 1 complexes.<sup>7</sup> (b) The lack of any previous observation of RH evolution and U(III) complexes in either of the original reports on type 1 complexes (for a literature survey, see ref 1) may be due to restriction to rather low temperatures and to final workup adopting non-polar solvents unlike THF. (c) It is worth noting here that reaction of  $Cp_3UCl$  with some Grignard reagents  $RMgBr$  in very large excess yields  $Cp_3U^{III}THF$  in very high yields.<sup>7b</sup>

(6) Preparation of dissolved  $[Li(THF)_n][Cp_3U(n-C_4H_9)]$ . A solution of 64 mg (1 mmol) of  $Li(n-C_4H_9)$  in 0.6 mL of *n*-hexane (Merck) is added to a frozen (liquid  $N_2$ ) solution of 113.6 mg (0.25 mmol) of  $Cp_3UCl$  in 5 mL of THF. The rapidly stirred reaction mixture is allowed to reach room temperature within ca. 5 min and kept in a water bath (35-40 °C) for another 30 min until the initially red-brown solution has changed to deep red and gas evolution has ended. Alternatively,  $Cp_3UR$  is reacted with LiR (1:4) starting immediately at room temperature.

(7) (a) Klähne, E.; Giannotti, C.; Marquet-Ellis, H.; Folcher, G.; Fischer, R. D. *J. Organomet. Chem.* **1980**, *201*, 399 and further references therein. (b) Burton, M.; Marquet-Ellis, H.; Folcher, G.; Giannotti, C. *J. Organomet. Chem.* **1982**, *229*, 21.

(8) Tsutsui, M.; Ely, N.; Gebala, A. *Inorg. Chem.* **1975**, *14*, 78.

Table I. <sup>1</sup>H NMR Shifts<sup>18</sup> (ppm) of A,  $Cp_3UCH_3$ , B,  $[Li(THF)_n][Cp_3UCH_3]$ , C,  $[Li\cdot 2.1.1][Cp_3UCH_3]$ , D,  $Cp_3U(n-C_4H_9)$ , and E,  $[Li(THF)_n][Cp_3U(n-C_4H_9)]^a$

sample	Cp protons	protons of R
A	9.7 s (15)	198.0 s (3)
B	21.7 s (15)	100.9 s (3)
C	20.5 s (15)	100.0 s (3)
		[protons of cryptand: 5.2 t, 4.2 m]
D	10.4 s (15)	200.0 t (2), 33.0 m (2), 27.6 m (2), 18.7 t (3)
E	21.3 s (15)	98.5 t (2), 15.8 m (2), 14.1 m (2), 11.8 t (3)

<sup>a</sup> Solvent: THF-*d*<sub>8</sub>. Cp proton shifts of  $Cp_3U\cdot THF/THF-d_8$ , 24.0 ppm, and of  $Cp_3U(\text{nicotine})/\text{toluene}-d_8$ , 22.3 ppm.

GC analysis<sup>10</sup> has confirmed noticeable evolution of  $CH_4$ , but only of traces of  $C_2H_6$ , for R = R' =  $CH_3$  (experiment A), and predominantly of  $CH_4$  and  $n-C_4H_{10}$  for R =  $CH_3$  and R' =  $n-C_4H_9$  (experiment B) as well as for R =  $n-C_4H_9$  and R' =  $CH_3$  (experiment C). In experiments B and C, variable  $CH_4/n-C_4H_{10}$  ratios  $\leq 1$  were found (experiment C: the ratio was 1:4 during the main reaction phase and almost 1:1 toward its end<sup>11</sup>). For R = R' =  $n-C_4H_9$  (experiment D) mainly  $n-C_4H_{10}$  was monitored. The observation of only minor amounts of butenes and octane in experiments B-D (throughout <10% relative to  $CH_4$ ) as well as the clear predominance of  $CH_4$  over  $CH_3D$  (>100:1) in experiment A' (solvent THF-*d*<sub>8</sub> and gas analysis by combined GC/MS techniques<sup>12</sup>) make the preferential formation of  $CH_3$  or  $n-C_4H_{10}$  radicals<sup>13</sup> with THF as their primary hydrogen source quite unlikely. Both <sup>1</sup>H NMR and near-IR/vis spectroscopic features (vide infra) suggest independently that only for  $n \geq 3$  (eq 1) optimal formation of type 6 species takes place. Interestingly, excess of LiR has most recently also been suspected to act as a primary hydrogen source during the reduction of  $UCl_4$ .<sup>3b</sup>

The necessity to adopt LiR in excess and to use THF as the "optimal" solvent,<sup>5</sup> has appeared to strongly hamper the isolation of pure products involving 6. While solvent evaporation from THF solutions of 6 yields extremely air-sensitive viscous oils, all attempts to arrive at saltlike precipitates  $A[Cp_3U^{III}R]$  from concentrated solutions involving A =  $[Li(\text{TMED})_2]^+$ ,  $[AsPh_4]^+$ , and  $[N(\text{PPh}_3)_2]^+$  have failed. Only addition of the lithiophilic cryptand [2.1.1]<sup>14</sup> to 6a/THF leads within 1-2 h to a brownish red precipitate,<sup>15</sup> solutions of which in THF display an es-

(9) (a)  $(\text{ind})_3UCl$  has already been reported to react with  $Li(p\text{-tolyl})$  to  $(\text{ind})_3U$  and bitolyl<sup>9</sup> (and probably some further products). (b) Unlike  $Cp_3UCl$ ,  $(\text{ind})_3UCl$  is likewise reduced even by  $NaBH_4$ . Cf. Goffart, J.; Kanellakopoulos, B.; Duyckaerts, G., quoted in: Goffart, M.; Michel, G.; Gilbert, B. P.; Duyckaerts, G. *J. Inorg. Nucl. Chem.* **1978**, *14*, 393.

(10) Instrumentation and technical details of the GC, EPR, near-IR/vis, IR, and <sup>1</sup>H NMR studies, respectively, were essentially the same as described in ref 7 and 16.

(11) Product analysis of experiment C by <sup>1</sup>H NMR has, on the other hand, indicated the formation of at least 90% of 1a relative to 1d.

(12) Mass spectroscopic studies were made on a double-focussed Finnigan T 311 A spectrometer (70 eV, source temperature 200 °C) allowing, e.g., clear differentiation between the fragments  $CH_3D^+$ ,  $CHD_2^+$ , and  $OH^+$ .

(13) (a) *n*-Butyl radicals are known to have a disproportionation/dimerization ratio of ca. 0.13: cf. Sheldon, R. A.; Kochi, J. K. *J. Am. Chem. Soc.* **1970**, *92*, 4395. (b) The absence of butene also rules out  $\beta$  elimination of coordinated  $n-C_4H_9$ .

(14) Kryptofix-2.1.1 = 4,7,13,18-tetraoxa-1,10-diazabicyclo[8.5.5]heptane (Merck, dried over  $P_2O_5$ ).

(15) The elemental analyses of four different samples (prepared from both  $Cp_3UCl$  and  $Cp_3U(n-C_4H_9)$ ) have resulted in unexpectedly high atomic ratios Li/U between 2 and 4, suggesting that the cryptand [2.1.1] coordinates rather unspecifically  $Li^+$  ions originating from both the anionic organouranium system and other organolithium compounds (C/U = 24-30, N/U  $\approx$  2).

Table II.  $^7\text{Li}$  NMR shifts<sup>19</sup> (ppm)<sup>a</sup>

	$[\text{Li}(\text{THF})_n]\text{-}[\text{Cp}_3\text{U}(\text{CH}_3)_3]$	$[\text{Li}\cdot 2.1.1]\text{[Cp}_3\text{U}(\text{CH}_3)_3]$
chemical shift	4.63	6.47, 1.16, -0.8
relative intensity		6.0, 1.0, 2.2
external standard	$\text{LiCH}_3/\text{THF}$	$[\text{Li}\cdot 2.1.1]\text{[ClO}_4/\text{H}_2\text{O}]$
corrected <sup>a</sup>	ca. 6.5	5.2
isotropic shift		

<sup>a</sup> Corrected for bulk paramagnetism; positive sign refers to high-field shift.

essentially unchanged  $^1\text{H}$  NMR spectrum of **6a** (Table I).

The presence of U(III) in **6a** is confirmed by the appearance of a broad EPR signal at  $g = 2.56$  (frozen THF, 7 K, 9.14 GHz) that lies very close to that of  $\text{Cp}_3\text{U}^{\text{III}}\cdot\text{THF}$ .<sup>16</sup> The f-f crystal field spectra (near-IR/vis range ca.  $7.000\text{--}17.000\text{ cm}^{-1}$ ) of both  $\text{Cp}_3\text{UCl}$  and  $\text{Cp}_3\text{U}\cdot\text{THF}$  coincide after reaction with  $\text{Li}(n\text{-C}_4\text{H}_9)$  (molar ratios 1:2 and 1:1, respectively; cf. curve b in Figure 1), almost ideally with the spectrum of  $\text{Cp}_3\text{U}$  dissolved in THF or  $\text{Et}_2\text{O}$ <sup>17</sup> but differ clearly from the near-IR/vis spectra of both purely isolated and in situ prepared  $\text{Cp}_3\text{U}(n\text{-C}_4\text{H}_9)$  (curve a). Yet, spectra of solutions involving predominantly **6d** obtained from  $\text{Cp}_3\text{U}(n\text{-C}_4\text{H}_9)$  or  $\text{Cp}_3\text{UCl}$  and excess  $\text{Li}(n\text{-C}_4\text{H}_9)$  (molar ratios 1:3 and 1:4, respectively; cf. curve c) differ notably from curves a and b. Reaction of  $\text{Cp}_3\text{U}\cdot\text{THF}$  with 3–4 equiv of  $\text{Li}(n\text{-C}_4\text{H}_9)$  results in deep red, concentrated solutions, the corresponding near-IR/vis spectra of which are dominated by intense charge-transfer bands above ca.  $8.500\text{ cm}^{-1}$  (curve d).

The facile formation of **6** from **1** and excess LiR is best reflected by significant changes of the  $^1\text{H}$  NMR spectra (Table I).<sup>18</sup> Similar high-field shifts (relative to type 1) of the Cp proton resonance have been noted previously<sup>7</sup> and are likewise typical of  $\text{Cp}_3\text{U}\cdot\text{THF}$  and  $\text{Cp}_3\text{U}(\text{nicotine})$  (Table I). The occurrence of appropriately intense  $\text{CH}_2$  and  $\text{CH}_3$  resonances of R, also in high-field positions, strongly confirms the presence of uranium(III)-coordinated alkyl groups. In accordance with near-IR/vis spectroscopic results, the  $^1\text{H}$  NMR spectra of  $\text{Cp}_3\text{U}\cdot\text{THF}$  reacted with LiR lack any of these alkyl proton resonances. By addition of a few crystals of iodine to an NMR sample of **6a** all resonances of this species are replaced by one singlet characteristic of  $\text{Cp}_3\text{UI}$  at 9.6 ppm. First tentative  $^7\text{Li}$  NMR studies of the suggested species  $[\text{Li}(\text{THF})_4]\text{-}[\text{Cp}_3\text{U}(\text{CH}_3)_3]$  and  $[\text{Li}\cdot 2.1.1]\text{[Cp}_3\text{U}(\text{CH}_3)_3]$  solvated in THF (Table II) indicate, also after correction for the paramagnetic bulk susceptibility of the solution,<sup>19</sup> nonnegligible magnetic dipolar and/or contact interactions of the  $^7\text{Li}$  nucleus with the paramagnetic U(III) ion.

While  $\text{Cp}_3\text{U}\cdot\text{THF}$  does not selectively react with 1 equiv of LiR to give **6**, **6a** has most recently also been obtained by electroreduction of **1a**.<sup>20</sup> The thermal reaction  $1 \rightarrow 6$

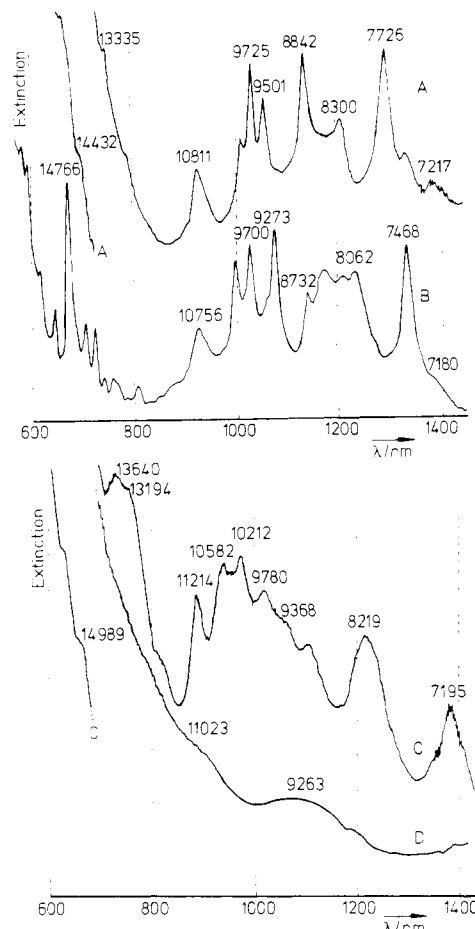


Figure 1. Near-IR/vis absorption spectra of THF solutions of (A)  $\text{Cp}_3\text{U}(n\text{-C}_4\text{H}_9)$ , (B)  $\text{Cp}_3\text{U}\cdot\text{THF}/\text{Li}(n\text{-C}_4\text{H}_9)$  (1:1), (C)  $\text{Cp}_3\text{UCl}$  reacted with 4 equiv of  $\text{Li}(n\text{-C}_4\text{H}_9)$ , and (D)  $\text{Cp}_3\text{U}\cdot\text{THF}$  reacted with  $\text{Li}(n\text{-C}_4\text{H}_9)$  (1:3).

is most likely to pass a number of individual steps with the hypothetical bimetallic species  $\{\text{Cp}_3\text{U}^{\text{IV}}(\mu\text{-R})(\mu\text{-R}')\text{-Li}(\text{THF})_n\}$  as a primary intermediate.<sup>21,22</sup>

**Acknowledgment.** This research was supported by the DAAD, Bonn, West Germany, the C.E.N., Saclay, France (by grants to E.K.), the DFG, Bonn, West Germany, and the Fonds der Chemischen Industrie, Frankfurt/M, West Germany. We also wish to thank Dipl.-Chem. K. D. Schrader for valuable GC/MS measurements and Prof. B. Kanellakopoulos for samples of the compounds  $\text{Cp}_3\text{U}\cdot\text{THF}$  and  $\text{Cp}_3\text{U}(\text{nicotine})$ .<sup>23</sup>

**Registry No.** **1a**, 37205-28-0; **1b**, 37298-79-6; **1c**, 82585-17-9; **1d**, 37298-84-3;  $\text{Li}[\text{Cp}_3\text{U}(\text{CH}_3)_3]$ , 82762-08-1;  $\text{Li}[\text{Cp}_3\text{U}(n\text{-C}_4\text{H}_9)]$ , 83999-88-6;  $[\text{Li}\cdot 2.1.1]\text{[Cp}_3\text{U}(\text{CH}_3)_3]$ , 83999-90-0;  $\text{LiCH}_3$ , 917-54-4;  $\text{Li}(n\text{-C}_4\text{H}_9)$ , 109-72-8; THF, 109-99-9.

(16) Cf. Soulié, E.; Folcher, G.; Marquet-Ellis, H. *Can. J. Chem.* **1982**, *60*, 1751.

(17) Zanella, P.; Rosetto, G.; de Paoli, G.; Traverso, O. *Inorg. Chim. Acta* **1980**, *44*, L 155.

(18) (a) See ref 7; a few studies were carried out independently on a Bruker WP 80 spectrometer using  $\text{THF-d}_6$  as solvent. (b) All resonances are referred to  $\text{C}_6\text{H}_6$ , a positive sign denoting high-field shifts. (c) In some instances, during the in situ preparation of samples of **1a** a fine green suspension was briefly observed. The clear, dark-red solution obtained after its disappearance displayed first two singlets at 46.8 and 30.2 ppm which were, after a short period of virtual nonresonance, replaced by the two final resonances of **6a** (Table I).

(19)  $^7\text{Li}$  NMR studies were made on a Bruker WH 90 spectrometer (35 MHz) with external standards (4 M  $\text{LiCl}/\text{H}_2\text{O}$ ). (b) The paramagnetic bulk susceptibility was accounted for by using Evans' method: Evans, D. F. *J. Chem. Soc.* **1959**, 2003, and assuming a molar susceptibility  $\chi_m$  of the U(III)-complex of  $2.300 \times 10^{-6}$ .

(20) Mugnier, Y.; Dormond, A.; Arnaudet, L.; Folcher, G. *J. Organomet. Chem.*, in press. For a successful electroreduction of  $\text{Cp}_3\text{UCl}$  see: Mugnier, Y.; Dormond, A.; Laviron, E. *J. Chem. Soc., Chem. Commun.* **1982**, 257. (b) We have found most recently that, unlike  $\text{Cp}_3\text{U}\cdot\text{THF}$ , the corresponding lanthanide complexes  $\text{Cp}_3\text{Ln}$  do react readily with LiR (1:1) in THF (but not in toluene) to form well-defined  $[\text{Li}(\text{THF})_n]\text{-}[\text{Cp}_3\text{LnR}]$  without any "unwanted" LiR consumption: Fischer, R. D.; Jahn, W., unpublished results.

(21) Similar intermediates  $\text{Cp}_3\text{U}(\mu\text{-R})(\mu\text{-R}')\text{AlR}_2$  have already been deduced from NMR experiments: Vasil'ev, B. K.; Sokolov, V. N.; Kondratenkov, G. P. *J. Organomet. Chem.* **1977**, *142*, C7; *Dokl. Akad. Nauk SSSR* **1977**, *236*, 360.

(22) Organozirconium complexes  $\text{Cp}_3\text{ZrR}'$  have also been shown to react with  $\text{AlR}_3$  both under exchange of R and elimination of  $\text{RH}$ : Kaminsky, W.; Sinn, H. J.; Vollmer, H.-J. unpublished results. Vollmer, H.-J. Dissertation, Universität Hamburg, 1979.

(23) Kanellakopoulos, B.; Fischer, E. O.; Dornberger, E.; Baumgärtner, F. *J. Organomet. Chem.* **1970**, *24*, 507.

**Multielectron-Transfer Electrochemistry.  
Two-Electron Reduction of  
Bis( $\eta^6$ -hexamethylbenzene)ruthenium(2+) and  
( $\eta^6$ -Hexamethylbenzene)( $\eta^6$ -cyclophane)ruthenium-  
(2+) Complexes**

Richard G. Finke,\* Richard H. Voegell,  
Evan D. Laganis,† and Virgil Boekelheide

Department of Chemistry, University of Oregon  
Eugene, Oregon 97403

Received October 26, 1982

**Summary:** Two-electron reductions of the bis(arene)ruthenium(2+) complexes bis( $\eta^6$ -hexamethylbenzene)ruthenium(2+), **1**, and the ( $\eta^6$ -hexamethylbenzene)([2<sub>n</sub>]-cyclophane)ruthenium(2+) complexes ([2<sub>n</sub>]cyclophane = [2<sub>6</sub>](1,2,3,4,5,6)cyclophane, **2**; [2<sub>4</sub>](1,2,3,5)cyclophane, **3**; [2<sub>4</sub>](1,2,4,5)cyclophane, **4**) are reported, results which provide an unprecedented opportunity to examine a two-electron reduction in a monometallic organotransition-metal complex as a function of ligand (cyclophane) structure.

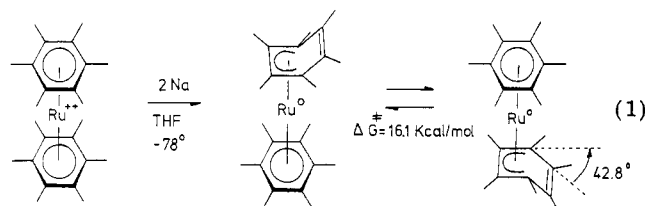
The simplest possible multielectron transfer,<sup>1</sup> a two-electron transfer,<sup>2-7</sup> is of fundamental significance. In a two-electron reduction, for example, an important question is how the thermodynamic condition necessary for a direct<sup>2a</sup> two-electron transfer is achieved where, by definition, the second electron transfer occurs at an easier, more positive potential than the first,  $E_2^{o'} \geq E_1^{o'}$ . Typically, Coulombic effects make  $E_2^{o'}$  more difficult (negative) of  $E_1^{o'}$  by 0.4–0.5 V<sup>2c,d</sup> under electrochemical conditions of solvent and electrolyte. Other important questions concerning two-electron transfers are whether any structural changes accompany charge transfer,<sup>2-8</sup> the significance of solvent<sup>2a-c,4a</sup> and ion-pairing effects,<sup>9</sup> and, ultimately, the

detailed mechanism of the two-electron transfer.

Previous studies of two-electron transfers in organic systems have appeared such as the classic COT (tub) + 2e = COT<sup>2-</sup> (flat) system<sup>3</sup> or, more recently, lucigenin,<sup>4</sup> bianthrone,<sup>5</sup> and related systems.<sup>4b,6</sup> It is noteworthy that stepwise mechanisms such as EE, ECE, EEC, and a geometry/conformational change as the C step are often observed (E = electrochemical step; C = chemical step). Although two-electron transfers involving simple inorganic complexes such as Pt<sup>4+</sup>/Pt<sup>2+</sup>, Ti<sup>3+</sup>/Ti<sup>+</sup>, or Sn<sup>4+</sup>/Sn<sup>2+</sup> are well-known,<sup>2g</sup> no well-studied, prototype example of a two-electron transfer to a monometallic, organotransition-metal complex has previously appeared, a surprising observation given the current interest in understanding nature's metal-containing multielectron redox systems<sup>10</sup> and in synthetic multielectron redox catalysts.<sup>11</sup>

Herein we report an electrochemical study of the two-electron reductions of ( $\eta^6$ -arene)( $\eta^6$ -arene or  $\eta^6$ -cyclophane)ruthenium(2+) complexes. The results establish the significance of an  $\eta^6 \rightarrow \eta^4$  geometry change in (a) achieving  $E_2^{o'} \geq E_1^{o'}$ ; (b) controlling the  $E^o$  (obsd) =  $(E_1^{o'} + E_2^{o'})/2$  in a direct, two-electron reduction, and (c) controlling the chemical stability of the Ru<sup>0</sup> product. The results also (d) illustrate the use of solvent effects to separate a single two-electron wave into two component one-electron waves (or vice versa), thereby proving the presence of a Ru<sup>+</sup> = (arene)(arene or cyclophane)Ru<sup>+</sup> intermediate and (e) provide considerable insight into the detailed electrochemical mechanism.

Previously, ( $\eta^6$ -hexamethylbenzene)( $\eta^4$ -hexamethylbenzene)ruthenium(0) was prepared<sup>12a</sup> by Na reduction and isolated and its X-ray crystal structure<sup>12b</sup> and fluxionality<sup>12c</sup> were determined (eq 1). The bis( $\eta^6$ -hexa-



methylbenzene)ruthenium(2+) (**1**) and the other analytically pure, fully characterized complexes<sup>13</sup> **2–4** (Figure 1) were examined by cyclic voltammetry and coulometry in CH<sub>3</sub>CN at Pt, using 0.3–1.0 mM compound, 0.1 M Bu<sub>4</sub>NPF<sub>6</sub>, ferrocene as an internal standard, PAR equipment, and a three-electrode cell equipped with a Luggin capillary and placed in a N<sub>2</sub>-filled, vacuum atmosphere drybox, all as previously described.<sup>13a,14</sup> As anticipated, the bis( $\eta^6$ -hexamethylbenzene)ruthenium(2+) complex (**1**) showed a two-electron ( $\Delta E_p = 35 \pm 9$  mV;  $n$ (coulometry)

† Present address: Central Research and Development, Experimental Station, E. I. du Pont de Nemours, Wilmington, DE 19898.

(1) (a) Polcyn, D. S.; Shain, I. *Anal. Chem.* **1966**, *38*, 370. (b) Nicholson, R. S.; Shain, I. *Ibid.* **1965**, *37*, 178. (c) *Ibid.* **1965**, *37*, 190. (d) Myers, R. L.; Shain, I. *Ibid.* **1969**, *41*, 980. (e) Amatore, C.; Savéant, J. M. *J. Electroanal. Chem.* **1977**, *85*, 27.

(2) (a) Ammar, F.; Savéant, J. M. *J. Electroanal. Chem. Interfacial Electrochem.* **1973**, *47*, 115. (b) Phelps, J.; Bard, A. J. *J. Electroanal. Chem.* **1976**, *68*, 313. (c) Bard, A. J. *Pure Appl. Chem.* **1971**, *25*, 379. (d) Kojima, H.; Bard, A. J.; Wong, H. C.; Sondheimer, F. *J. Am. Chem. Soc.* **1976**, *98*, 5560. (e) Flanagan, J. B.; Margel, S.; Bard, A. J.; Anson, F. C. *Ibid.* **1978**, *100*, 4248. (f) Garst, J. F., Jr.; Pacifici, J. G.; Zabolotny, E. R. *Ibid.* **1966**, *88*, 3872 and references therein. (g) A discussion of two-electron transfers involving simple inorganic systems can be found in: Sykes, A. G. *Adv. Inorg. Chem. Radiochem.* **1967**, *10*, 153 (see p 180).

(3) For studies of COT + 2e = COT<sup>2-</sup> see: (a) Allendoerfer, R. D.; Rieger, P. H. *J. Am. Chem. Soc.* **1965**, *87*, 2336. (b) Huebert, B. J.; Smith, D. E. *J. Electroanal. Chem. Interfacial Electrochem.* **1971**, *31*, 333. (c) Fry, A. J.; Hutchins, C. S.; Chung, L. L. *J. Am. Chem. Soc.* **1975**, *97*, 591. (d) Allendoerfer, R. D. *Ibid.* **1975**, *97*, 218. (e) Jensen, B. S.; Ronlán, A.; Parker, V. D. *Acta Chem. Scand., Ser. B* **1975**, *B29*, 394. (f) Smith, W. H.; Bard, A. J. *J. Electroanal. Chem.* **1977**, *76*, 19. (g) See also ref 2d.

(4) (a) Ahlberg, E.; Hammerich, O.; Parker, V. D. *J. Am. Chem. Soc.* **1981**, *103*, 844 and references therein. (b) See the discussion on p 848 of ref 4a and ref 42 and 43 cited therein. (c) See also ref 5b.

(5) (a) Olsen, B. A.; Evans, D. H. *J. Am. Chem. Soc.* **1981**, *103*, 839 and ref 5 and 6 therein. (b) Evans, D. H.; Busch, R. W. *Ibid.* **1982**, *104*, 5057.

(6) Kissinger, P. T.; Holt, P. T.; Reilly, C. N. *J. Electroanal. Chem.* **1971**, *33*, 1.

(7) (a) Wilson, G. S.; Swanson, D. D.; Klug, J. T.; Glass, R. S.; Ryan, M. D.; Musker, W. K. *J. Am. Chem. Soc.* **1979**, *101*, 1040. (b) Doi, J. T.; Musker, W. K. *Ibid.* **1981**, *103*, 1159. (c) Coleman, B. R.; Glass, R. S.; Setzer, W. N.; Prabhu, U. D. G.; Wilson, G. S. *Adv. Chem. Ser.* **1982**, No. 201.

(8) For a series on the structural consequences of electron transfer see: (a) Albright, T. A.; Geiger, W. E., Jr.; Moraczewski, J.; Tulyathan, B. J. *Am. Chem. Soc.* **1981**, *103*, 4787. (b) Moraczewski, J.; Geiger, W. E., Jr. *Ibid.* **1981**, *103*, 4779 (part 5) and the previous papers in this series. (c) See also ref 2 c and see ref 5 in Evan's paper.<sup>5b</sup>

(9) (a) Garst, J. F.; Zabolotny, E. R.; Cole, R. S. *J. Am. Chem. Soc.* **1964**, *86*, 2257. (b) Szwarc, M. "Ions and Ion Pairs in Organic Reactions"; Wiley: New York, 1972; Vol. I, 1974; Vol. II.

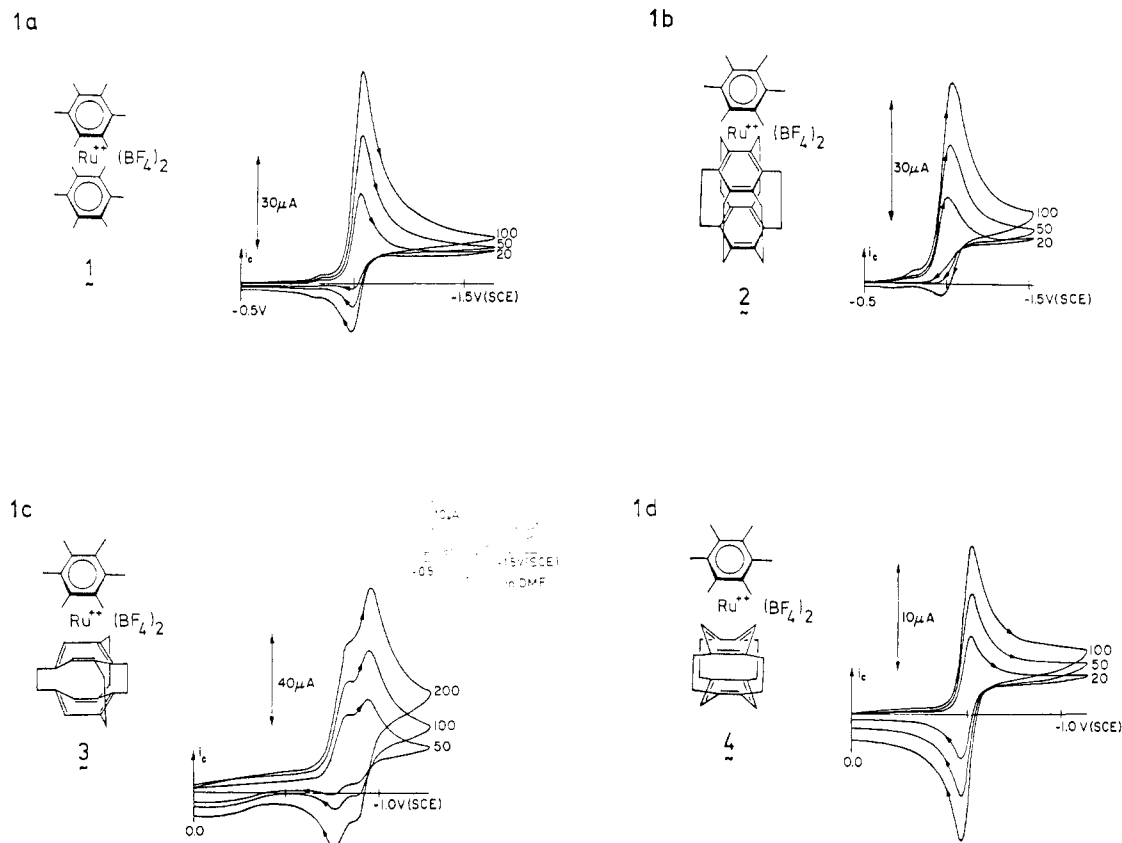
(10) (a) "Inorganic Biochemistry"; H. H. O. Hill, Ed.; The Chemical Society: Burlington House, London, 1979; *Spec. Period. Rep., Vol. I*. (b) Thomson, A. J.; Thorneley, R. N. F. *Chem. Brit.* **1982**, *18*, 176 and references therein.

(11) (a) Collman, J. P.; Denisevich, P.; Konai, Y.; Marrocco, M.; Koval, C.; Anson, F. C. *J. Am. Chem. Soc.* **1980**, *102*, 6027 and references therein. (b) Collman, J. P.; Chong, A. O.; Jameson, G. B.; Oakley, R. T.; Rose, E.; Schmittou, E. R.; Ibers, J. A. *J. Am. Chem. Soc.* **1981**, *103*, 516.

(12) (a) Fischer, E. O.; Elschenbroich, C. *Chem. Ber.* **1970**, *103*, 162. (b) Hüttner, G.; Lange, S. *Acta Crystallogr., Sect. B* **1972**, *B28*, 2049. (c) Darenbourg, M. Y.; Muetterties, E. L. *J. Am. Chem. Soc.* **1979**, *100*, 7425.

(13) (a) Laganis, E. D.; Voegeli, R. H.; Swann, R. T.; Finke, R. G.; Hopf, H.; Boekelheide, V. *Organometallics* **1982**, *1*, 1415. (b) Laganis, E. D.; Finke, R. G.; Boekelheide, V. *Tetrahedron Lett.* **1980**, *21*, 4405. (c) Laganis, E. D.; Finke, R. G.; Boekelheide, V. *Proc. Natl. Acad. Sci. U.S.A.* **1981**, *78*, 2657.

(14) Finke, R. G.; Gaughan, G.; Voegeli, R. *J. Organomet. Chem.* **1982**, *229*, 179.



**Figure 1.** Cyclic voltammograms of 1-4 in  $\text{CH}_3\text{CN}$ , with the numerical data summarized below (all  $\Delta E_p$  values are at 20 mV/s and are corrected, assuming the ferrocene internal standard should have  $\Delta E_p = 59$  mV;  $i_{pa}/i_{pc}$  values are at 100 mV/s;  $i_{pc}/\nu_{1/2}$  was a constant from 20 to 200 mV/s unless noted otherwise and all waves were diffusion controlled and absorption free;  $n$  values were obtained by coulometry): complex 1,  $E_{1/2} = -1.02 \pm 0.01$  V (SCE),  $\Delta E_p = 35 \pm 9$  mV,  $i_{pa}/i_{pc} = 0.36 \pm 0.05$ ,  $n = 2.04 \pm 0.08$ ; complex 2,  $E_{1/2} = 0.95 \pm 0.01$  V (SCE),  $\Delta E_p = 32 \pm 6$  mV,  $i_{pa}/i_{pc} = 0.27 \pm 0.02$ ,  $n = 1.49 \pm 0.09$  (due to a follow-up chemical reaction<sup>18</sup>); complex 3,  $E_{1/2}(1) = -0.83 \pm 0.01$  V,  $E_{1/2}(2) = -0.95 \pm 0.01$  V,  $\Delta E_p(1) = 45 \pm 13$  mV,  $\Delta E_p(2) = 41 \pm 12$  mV,  $i_{pa}/i_{pc}(\text{total}) = 0.38 \pm 0.02$  (increases to 1.0 at 25 V/s),  $n(\text{total}) = 2.04 \pm 0.04$ ; complex 4,  $E_{1/2} = -0.50 \pm 0.01$  V,  $\Delta E_p = 36 \pm 5$  mV,  $i_{pa}/i_{pc} = 0.96 \pm 0.01$ ,  $n = 2.02 \pm 0.04$ .

$= 2.04 \pm 0.08$ ), partially chemically reversible ( $i_{pa}/i_{pc} = 0.36$  at 100 mV/s), diffusion-controlled wave at  $E_{1/2} (= (E_{pc} + E_{pa})/2) = -1.02 \pm 0.01$  V (SCE). The  $i_{pa}/i_{pc}$  value increased to  $\approx 1.0$  at a scan rate,  $\nu$ ,  $\approx 1.0$  V/s but then decreased again past 20 V/s to  $i_{pa}/i_{pc} \approx 0.55$  at 100 V/s.

Using the cyclophane<sup>15</sup> ligands shown in complexes 2-4 and in Figure 1b-d, we were able to probe the importance of the relatively rigid, crystallographically characterized<sup>16</sup> cyclophane structure upon these two-electron reductions. In particular, the  $[2_6](1,2,3,4,5,6)$ cyclophane<sup>16b</sup> in 2 rigorously cannot adopt the  $\eta^4$  geometry of the  $\text{Ru}^0$  product (eq 1), the  $[2_4](1,2,3,5)$ cyclophane<sup>16c</sup> in 3 is partially preformed toward an  $\eta^4$  geometry, while the  $[2_4](1,2,4,5)$ cyclophane<sup>16d</sup> in 4 has a fully preformed, near-optimum geometry to bind  $\eta^4$ . The electrochemical response to the cyclophane structure is striking (Figure 1b-d). The ease of reduction and chemical reversibility ( $\text{Ru}^0$  product stability) increased by over 0.45 V and 3-fold, respectively, along the series  $2 < 3 < 4$  with  $E_{1/2}$  and  $i_{pa}/i_{pc}$  of  $-0.95$  V and 0.27,  $-0.89$  V (average) and 0.38 (average), and  $-0.50$  V and 0.96, each complex exhibiting an overall two-electron reduction. Also distinctive are the two closely spaced, overlapping one-electron waves rather than a single, two-electron wave

observed for 3 (Figure 1c). This observation suggests that each of the other overall two-electron reductions (Figure 1a,b,d) may actually consist of two discrete, one-electron steps hidden because  $E_2^{o'} (\sim E_{1/2}(2)) \geq E_1^{o'} (\sim E_{1/2}(1))$ .<sup>17</sup>

Based on the literature,<sup>2a-c,4a</sup> it appeared possible to separate the waves, if two existed, by a  $\text{CH}_3\text{CN}$  to  $\text{CH}_2\text{Cl}_2$  solvent change, thereby decreasing the relative  $\text{Ru}^{2+}$  vs.  $\text{Ru}^+$  solvation energy and thus increasing the relative ease of  $\text{Ru}^{2+}$  vs.  $\text{Ru}^+$  reduction. Conversely, a  $\text{CH}_3\text{CN}$  to DMF or  $\text{Me}_2\text{SO}$  change should have the opposite effect, moving the two waves for 3 (Figure 1c) closer together and toward more negative potentials. As anticipated, 3 in DMF shows only a single wave at a more negative potential,  $E_{1/2} = -1.03$  V (SCE) (Figure 1c (insert)). Furthermore, both 1 and 2 separate into two, one-electron ( $n_1 = 0.97 \pm 0.08$ ;  $n(\text{total}) = 1.94 \pm 0.08$ ), overlapping waves on changing to  $\text{CH}_2\text{Cl}_2$  (Figure 2a,b), while the two waves for 3 move even further apart, from  $\Delta E_{1/2} (= E_{1/2}(1) - E_{1/2}(2)) = 120$  mV in  $\text{CH}_3\text{CN}$  to 180 mV in  $\text{CH}_2\text{Cl}_2$ . Even 4, with its estimated<sup>1d</sup> negative  $\Delta E_{1/2} \approx -20 \pm 20$  mV in  $\text{CH}_3\text{CN}$ , shows a noticeable peak broadening in  $\text{CH}_2\text{Cl}_2$  (Figure 2d). The IR drop corrected  $E_p - E_{p/2} = 68$  mV implies<sup>1d</sup> that two closely spaced,  $\Delta E_{1/2} \approx +50$  mV, waves are present.

The observation of two waves—the direct electrochemical detection of the  $\text{Ru}^+$  intermediate—is significant as it limits possible mechanisms yet establishes a minimum of two steps (two one-electron E steps) in any viable

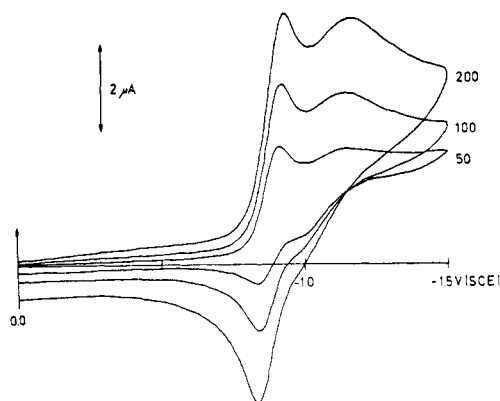
(15) For recent overviews of the  $[2_n]$ cyclophanes see: (a) Boekelheide, V. *Acc. Chem. Res.* 1980, 13, 65. (b) Kleinschroth, J.; Hopf, H. *Angew. Chem., Int. Engl. Ed.* 1982, 21, 469.

(16) (a) The single-crystal, X-ray diffraction structures of the  $[2_6](1,2,3,4,5,6)$ ,<sup>16b</sup>  $[2_4](1,2,3,5)$ ,<sup>16c</sup> and  $[2_4](1,2,4,5)$ <sup>16d</sup> cyclophanes are available. (b) Hanson, A. W.; Cameron, T. S. *J. Chem. Res., Synop.* 1980, 336. (c) Irrgartinger, H.; Hekeler, J.; Lang, B. M. *Chem. Ber.*, in press. (d) Hanson, A. W. *Acta Crystallogr., Sect. B* 1977, B33, 2003.

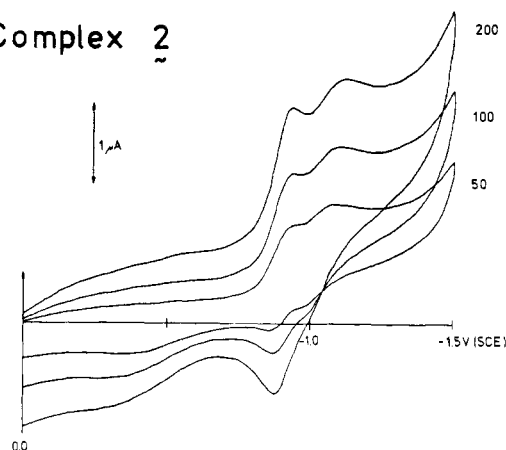
(17) (a)  $E_{1/2}$  is usually a close approximation to the formal potential  $E^{o'}$ , for a reversible couple.<sup>17b</sup> (b) Bard, A. J.; Faulkner, L. R. "Electrochemical Methods"; Wiley: New York, 1980; p 60.



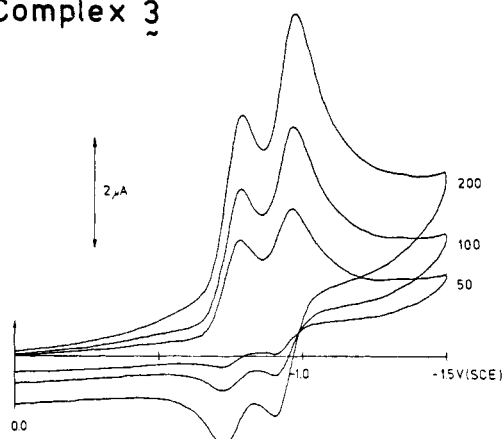
## 2a Complex 1



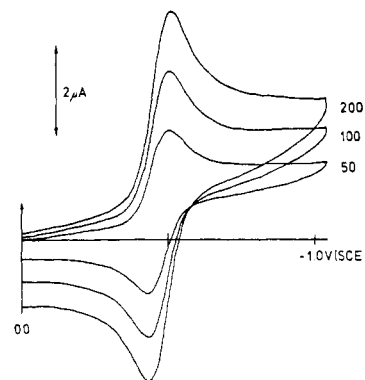
## 2b Complex 2



## 2c Complex 3



## 2d Complex 4



**Figure 2.** Cyclic voltammograms of 1–4 in  $\text{CH}_2\text{Cl}_2$  with the numerical data summarized below (all  $\Delta E_p$  values are at 50 mV/s and are corrected, assuming the ferrocene internal standard should have  $\Delta E_p = 59$  mV;  $i_{pa}/i_{pc}$  values are at 100 mV/s): complex 1,  $E_{1/2}(1) = -0.89 \pm 0.01$  V (SCE),  $E_{pc}(2) = -1.15 \pm 0.01$  V to  $-1.20 \pm 0.01$  V (SCE) at scan rates 50 mV/s up to 500 mV/s, respectively;  $\Delta E_p(1) = 54 \pm 7$  mV,  $i_{pa}/i_{pc}(\text{total}) = 0.66 \pm 0.03$ ; complex 2,  $E_{1/2}(1) = -0.84 \pm 0.01$  V (SCE),  $E_{pc}(2) = -1.01 \pm 0.01$  V to  $-1.07 \pm 0.01$  V (SCE),  $\Delta E_p(1) = 57 \pm 5$  mV,  $i_{pa}/i_{pc}(\text{total}) = 0.51 \pm 0.04$ ; complex 3,  $E_{1/2}(1) = -0.76 \pm 0.01$  V (SCE),  $E_{1/2}(2) = 0.94 \pm 0.01$  V (SCE),  $\Delta E_p(1) = 55 \pm 4$  mV,  $\Delta E_p(2) = 59 \pm 4$  mV,  $i_{pa}/i_{pc}(\text{total}) = 0.44 \pm 0.03$ ; complex 4,  $E_{1/2}(\text{calcd})(1) = -0.41 \pm 0.02$  V (SCE),  $E_{1/2}(\text{calcd})(2) = -0.46 \pm 0.02$  V (SCE),  $E_{1/2}(\text{measd}) = -0.47 \pm 0.01$  V (SCE),  $\Delta E_p = 63 \pm 5$  mV,  $(E_{pc} - E_{p/2}) = 68$  mV,  $i_{pa}/i_{pc} = 0.90 \pm 0.03$ .

mechanism. Upon including the observed  $\eta^6 \rightarrow \eta^4$ , geometry change C step, the simplest possible mechanisms become CEE, ECE, EEC, or possibly  $E_C E$ ,  $EE_C$ , or  $E_C E_C$ , where the latter notation indicates the geometry change occurs concomitant with the first, second, or partially with both charge transfers, respectively. Ultimately, these mechanisms are distinguished by the timing of the geometry change and the exact structure of the  $\text{Ru}^+$  intermediate.

The close similarity in their voltammograms ( $E_{1/2}$ ,  $i_{pa}/i_{pc}$  data in  $\text{CH}_2\text{Cl}_2$ ) strongly suggests that 1 and 2 have similar mechanisms, as expected since they have similar  $\text{Ru}^0$  products where only the hexamethylbenzene ligand can distort  $\eta^6 \rightarrow \eta^4$ . Their voltammograms in  $\text{CH}_2\text{Cl}_2$  (Figure 2a,b) show somewhat surprisingly that the second electron transfer in 1 and 2 is slow, probably due to a major geometry change occurring concerted with the  $\text{Ru}^+$  to  $\text{Ru}^0$  reduction,<sup>13</sup> an overall  $EE_C$  mechanism (at least in  $\text{CH}_2\text{Cl}_2$ ), where the key implied feature is that the  $\text{Ru}^+$  geometry is closer to that of  $\text{Ru}^{2+}$  than to the  $\text{Ru}^0$  product.<sup>4</sup>

The ca. 0.5 V easier reduction and high reversibility of the second wave in  $\text{CH}_2\text{Cl}_2$  require a different mechanism for 4 as does the different product, where only the cyclo-

phane bonds  $\eta^4$  to  $\text{Ru}^0$ —a point we have confirmed by a preliminary variable-temperature NMR study.<sup>18</sup> The electrochemical data on 4 as well as rapid scan data<sup>19a</sup> are not easily understood in terms of EEC or CEE mechanisms<sup>19b</sup> but suggest, instead, an  $E_C E$  or possibly an ECE mechanism, where the essential feature is that the  $\text{Ru}^+$  intermediate should have a structure closer to that of the  $\text{Ru}^0$  product.<sup>4</sup>

The results presented herein offer an unprecedented opportunity to examine a two-electron reduction in a monometallic organotransition-metal complex as a function of ligand structure. Complexes of five additional, crys-

(18) Finke, R. G.; Voegeli, R. H.; Laganis, E. D.; Boekelheide, V., unpublished results.

(19) (a) Rapid scan experiments in  $\text{CH}_3\text{CN}$  on 4 showed an ca. constant  $i_{pa}/i_{pc}$  from 0.05 to  $10^2$  V/s scan rate. The  $i_{pa}/i_{1/2}$  was constant until 2 V/s and then declined linearly. (b) Besides producing high-energy 19- and 20-electron intermediates, the EEC mechanism does not explain why 4 is reduced 0.45 V easier, why a single two-electron wave is seen in  $\text{CH}_3\text{CN}$ , nor does it take into account the preformed geometry ("preaccomplished C step") in 4. An CEE mechanism appears inconsistent with the normal, undiminished  $i$  value observed, the two-electron,  $E_2^{o'} > E_1^{o'}$ , wave seen in  $\text{CH}_3\text{CN}$ , and with the similar electrochemistry of 4 observed both in  $\text{CH}_2\text{Cl}_2$  and in the more coordinating  $\text{CH}_3\text{CN}$ .

tallographically characterized cyclophanes have been prepared as part of this work, and their electrochemical behavior will be reported in due course.<sup>13a,18</sup>

**Acknowledgment.** Financial support was provided by NSF Grants CHE-8018199 (R.G.F.) and CHE-7901763 (V.B.). It is a pleasure to acknowledge the receipt of the [2<sub>4</sub>](1,2,3,5)cyclophane used to prepare **3** from Professor H. Hopf and helpful electrochemical consultation from Professor C. Michael Elliott. R.G.F. is a Dreyfus Teacher-Scholar (1982-1987) and an Alfred P. Sloan Foundation Fellow (1982-1984).

**Registry No.** **1**, 71861-31-9; **2**, 82871-67-8; **3**, 82880-39-5; **4**, 82871-65-6; ( $\eta^6$ -hexamethylbenzene)( $\eta^4$ -hexamethylbenzene)ruthenium, 83927-89-3; ( $\eta^6$ -hexamethylbenzene)([2<sub>6</sub>](1,2,3,4,5,6)-cyclophane)ruthenium, 83927-87-1; ( $\eta^6$ -hexamethylbenzene)-([2<sub>4</sub>](1,2,3,5)cyclophane)ruthenium, 83927-88-2; ( $\eta^6$ -hexamethylbenzene)([2<sub>4</sub>](1,2,4,5)cyclophane)ruthenium, 83927-90-6.

### Synthesis, Structure, and Properties of [(CH<sub>3</sub>)<sub>5</sub>C<sub>5</sub>]<sub>2</sub>VS<sub>2</sub>

Stephen A. Koch\* and Venkatasuryanarayana Chebolu

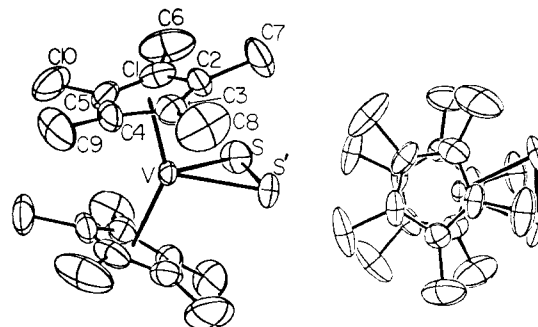
Department of Chemistry  
State University of New York at Stony Brook  
Stony Brook, New York 11794

Received September 8, 1982

**Summary:** The preferred metallo polysulfide chelate ring size in [(CH<sub>3</sub>)<sub>5</sub>C<sub>5</sub>]<sub>2</sub>VS<sub>2</sub> (**1**) is dramatically altered from that in the previously reported [C<sub>5</sub>H<sub>5</sub>]<sub>2</sub>VS<sub>2</sub> (**2**).

The metallo polysulfide chelate ring size of [C<sub>5</sub>H<sub>5</sub>]<sub>2</sub>MS<sub>n</sub> compounds of the early transition elements is strongly metal dependent. In the case of Ti,<sup>1</sup> Zr,<sup>2</sup> Hf,<sup>2</sup> and V,<sup>3,4</sup> the MS<sub>5</sub> ring is the exclusive product while for Mo<sup>5</sup> and W<sup>6</sup> the MS<sub>4</sub> ring is the most stable.<sup>7</sup> We wish to report that substitution of the cyclopentadienyl rings by pentamethylcyclopentadienyl groups dramatically alters the ring size preference from Cp<sub>2</sub>VS<sub>5</sub> (**2**) to [(CH<sub>3</sub>)<sub>5</sub>C<sub>5</sub>]<sub>2</sub>VS<sub>2</sub> (**1**). The chemistry of polychalcogenide ligands, particularly S<sub>2</sub><sup>2-</sup> and Se<sub>2</sub><sup>2-</sup>, is of considerable interest both for homogenous metal complexes and in solid-state materials.<sup>8</sup>

Decamethylvanadocene (**3**) is transformed quantitatively to [(CH<sub>3</sub>)<sub>5</sub>C<sub>5</sub>]<sub>2</sub>VCl<sub>2</sub> (**4**) by reaction with PCl<sub>5</sub> in diethyl ether.<sup>9</sup> The reaction of a solution of **4** in acetone with aqueous (NH<sub>4</sub>)<sub>2</sub>S<sub>5</sub> for 2 h at 60 °C, followed by hot filtration, produces black crystals of **1** in 50% yield. These



**Figure 1.** Ortep diagrams of **1**. Selected distances (Å) and angles (deg) for **1**; corresponding parameters for **2** are given in the square brackets: V-S = 2.390 (1) [2.457]; V-C<sub>av</sub> = 2.349 (6) [2.300]; S-S' = 2.053 (3); V-(CH<sub>3</sub>)<sub>5</sub>C<sub>5</sub> = 2.023 [1.959]; S-V-S' = 50.86 (8) [89.3 (1)]; ((CH<sub>3</sub>)<sub>5</sub>C<sub>5</sub>)-V-((CH<sub>3</sub>)<sub>5</sub>C<sub>5</sub>) = 140.2 [134.1].

reaction conditions are similar to those used to prepare [C<sub>5</sub>H<sub>5</sub>]<sub>2</sub>VS<sub>2</sub> (**2**).<sup>3</sup> Alternately **1** can be prepared by the reaction of **4** with Na<sub>2</sub>S<sub>2</sub>.

An X-ray diffraction study of **1** has revealed that the molecule crystallizes in the orthorhombic space group *Fdd*2 with *a* = 17.514 (4) Å, *b* = 26.221 (4) Å, *c* = 8.661 (4) Å, *V* = 3973 (4) Å<sup>3</sup>, and *Z* = 8. Diffraction data was collected on an Enraf-Nonius diffractometer using Mo K $\alpha$  radiation. The structure was solved by using Patterson and difference Fourier methods. Final least-squares refinement of all the non-hydrogen atoms gave *R* = 0.047 and *R*<sub>w</sub> = 0.064 using 1369 unique reflections with *I* > 3 $\sigma$ (*I*). The molecule (Figure 1) possesses a crystallographically imposed C<sub>2</sub> axis which passes through the vanadium atom and the midpoint of the S-S bond. The S-S distance of 2.053 (3) Å is typical for a coordinated disulfide,<sup>8</sup> compound **1** is best formulated as V<sup>4+</sup>(S<sub>2</sub><sup>2-</sup>). Important bond distances and angles of **1** are compared with those of **2** in Figure 1.

The change in the size of the VS<sub>n</sub> ring going from **2** to **1** is likely dominated by steric considerations.<sup>10</sup> The smaller VS<sub>2</sub> ring lessens sulfur-methyl steric interactions. The recent report of the structure of [(CH<sub>3</sub>)<sub>5</sub>C<sub>5</sub>]<sub>2</sub>TiS<sub>3</sub> provides another example of the stability of smaller rings in the (CH<sub>3</sub>)<sub>5</sub>C<sub>5</sub> series of compounds.<sup>11</sup> In both the [C<sub>5</sub>H<sub>5</sub>]<sub>2</sub>MS<sub>n</sub> and the [(CH<sub>3</sub>)<sub>5</sub>C<sub>5</sub>]<sub>2</sub>MS<sub>n</sub> series, a decrease in MS<sub>n</sub> ring size correlates with an increase in the number of *d* electrons.<sup>12</sup> The decrease in the X-M-X angle in [C<sub>5</sub>H<sub>5</sub>]<sub>2</sub>MX<sub>2</sub> compounds as a function of increasing *d* electron count is well documented and well understood.<sup>13,14</sup> Smaller X-M-X angles should favor smaller MS<sub>n</sub> rings.

Compound **1** gives a characteristic sharp intense IR band at 552 cm<sup>-1</sup> that is assigned to the S-S stretch. The small vanadium hyperfine splitting value (45 G) in the ESR spectrum of **1** is also distinctive. The hyperfine coupling constant for **4** (75 G) is close to the value found for [C<sub>5</sub>H<sub>5</sub>]<sub>2</sub>VCl<sub>2</sub>,<sup>13</sup> which is a typical value (60-75 G) for [C<sub>5</sub>H<sub>5</sub>]<sub>2</sub>VX<sub>2</sub> compounds including **2**.<sup>4</sup> The reduced splitting constant for **1** is nearly identical with those reported for [C<sub>5</sub>H<sub>5</sub>]<sub>2</sub>VL where L is a  $\eta^2$  ligand such as an alkene or alkyne.<sup>15</sup>

(10) The steric interactions among the ligands is reflected in the displacements of the methyl groups from the least squares plane of the cyclopentadienyl rings: C6 (0.136 Å), C7 (0.250 Å), C8 (0.021 Å), C9 (0.390 Å), C10 (0.266 Å).

(11) Bird, P. H.; McCall, J. M.; Shaver, A.; Siriwardane, U. *Angew. Chem., Int. Ed. Engl.* **1982**, *21*, 384.

(12) (a) C<sub>5</sub>H<sub>5</sub> series: d<sup>0</sup> [C<sub>5</sub>H<sub>5</sub>]<sub>2</sub>MS<sub>5</sub>, M = Ti,<sup>4</sup> Zr,<sup>12b</sup> Hf<sup>12b</sup> (S-Ti-S = 95.0 (1)°); d<sup>1</sup> [C<sub>5</sub>H<sub>5</sub>]<sub>2</sub>VS<sub>5</sub> (S-V-S = 89.3 (1)°); d<sup>2</sup> [C<sub>5</sub>H<sub>5</sub>]<sub>2</sub>MS<sub>4</sub> (S-M-S (M = Mo) = 88.2 (2)°, (M = W) = 89.1 (1)°),<sup>5,6</sup> [C<sub>5</sub>H<sub>5</sub>]<sub>2</sub>MoS<sub>2</sub>,<sup>12b</sup> (CH<sub>3</sub>)<sub>5</sub>C<sub>5</sub> series: d<sup>0</sup> [(CH<sub>3</sub>)<sub>5</sub>C<sub>5</sub>]<sub>2</sub>TiS<sub>3</sub><sup>11</sup> (S-Ti-S = 84.44 (9)°); d<sup>1</sup> **1** (S-V-S = 50.86 (8)°). (b) No crystallographic information.

(13) Petersen, J. L.; Dahl, L. F. *J. Am. Chem. Soc.* **1975**, *97*, 6422.

(14) Lauher, J. W.; Hoffmann, R. *J. Am. Chem. Soc.* **1976**, *98*, 1729.

- (1) Köpf, H.; Kahl, W. *J. Organomet. Chem.* **1974**, *64*, C37.  
 (2) McCall, J. M.; Shaver, A. *J. Organomet. Chem.* **1980**, *193*, C37.  
 (3) Köpf, H.; Wirl, A.; Kahl, W. *Angew. Chem., Int. Ed. Engl.* **1971**, *10*, 137.  
 (4) Müller, E. G.; Petersen, J. L.; Dahl, L. F. *J. Organomet. Chem.* **1976**, *111*, 91.  
 (5) Block, H. D.; Allmann, R. *Cryst. Struct. Commun.* **1975**, *4*, 53.  
 (6) Davis, B. R.; Bernal, I. *J. Cryst. Mol. Struct.* **1972**, *2*, 135.  
 (7) (C<sub>5</sub>H<sub>5</sub>)<sub>2</sub>MoS<sub>2</sub> has been reported, but it readily converts into the more stable (C<sub>5</sub>H<sub>5</sub>)<sub>2</sub>MoS<sub>4</sub>: Köpf, H.; Hazari, S. K. S.; Leitner, M. Z. *Naturforsch., B: Anorg. Chem., Org. Chem.* **1978**, *33B*, 1398.  
 (8) Müller, A.; Jaegermann, W. *Inorg. Chem.* **1979**, *18*, 2631. Rakowski Dubois, M.; Dubois, D. L.; VanDerveer, M. C.; Haltiwanger, R. C. *Ibid.* **1981**, *20*, 3064. Seyferth, D.; Henderson, R. S.; Song, L.-C. *Organometallics* **1982**, *1*, 125. Bolinger, C. M.; Hoots, J. E.; Rauchfuss, T. B. *Ibid.* **1982**, *1*, 223. Hoffmann, R.; Shaik, S.; Scott, J. C.; Whangbo, M.-H.; Foshie, M. J. *J. Solid State Chem.* **1980**, *34*, 263. Rouxel, J. *Mol. Cryst. Liq. Cryst.* **1982**, *81*, 31.  
 (9) Morán, M. *Transition Met. Chem. (Weinheim, Ger.)* **1981**, *6*, 42.

tallographically characterized cyclophanes have been prepared as part of this work, and their electrochemical behavior will be reported in due course.<sup>13a,18</sup>

**Acknowledgment.** Financial support was provided by NSF Grants CHE-8018199 (R.G.F.) and CHE-7901763 (V.B.). It is a pleasure to acknowledge the receipt of the [2<sub>4</sub>](1,2,3,5)cyclophane used to prepare **3** from Professor H. Hopf and helpful electrochemical consultation from Professor C. Michael Elliott. R.G.F. is a Dreyfus Teacher-Scholar (1982-1987) and an Alfred P. Sloan Foundation Fellow (1982-1984).

**Registry No.** **1**, 71861-31-9; **2**, 82871-67-8; **3**, 82880-39-5; **4**, 82871-65-6; ( $\eta^6$ -hexamethylbenzene)( $\eta^4$ -hexamethylbenzene)ruthenium, 83927-89-3; ( $\eta^6$ -hexamethylbenzene)([2<sub>6</sub>](1,2,3,4,5,6)-cyclophane)ruthenium, 83927-87-1; ( $\eta^6$ -hexamethylbenzene)-([2<sub>4</sub>](1,2,3,5)cyclophane)ruthenium, 83927-88-2; ( $\eta^6$ -hexamethylbenzene)([2<sub>4</sub>](1,2,4,5)cyclophane)ruthenium, 83927-90-6.

### Synthesis, Structure, and Properties of [(CH<sub>3</sub>)<sub>5</sub>C<sub>5</sub>]<sub>2</sub>VS<sub>2</sub>

Stephen A. Koch\* and Venkatasuryanarayana Chebolu

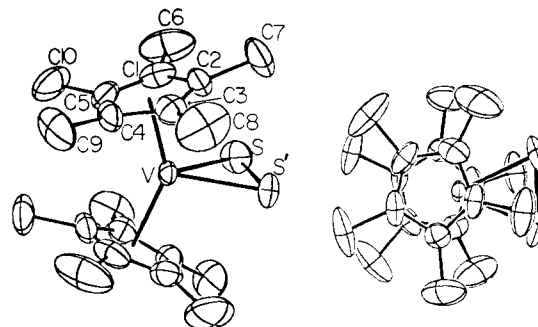
Department of Chemistry  
State University of New York at Stony Brook  
Stony Brook, New York 11794

Received September 8, 1982

**Summary:** The preferred metallo polysulfide chelate ring size in [(CH<sub>3</sub>)<sub>5</sub>C<sub>5</sub>]<sub>2</sub>VS<sub>2</sub> (**1**) is dramatically altered from that in the previously reported [C<sub>5</sub>H<sub>5</sub>]<sub>2</sub>VS<sub>2</sub> (**2**).

The metallo polysulfide chelate ring size of [C<sub>5</sub>H<sub>5</sub>]<sub>2</sub>MS<sub>n</sub> compounds of the early transition elements is strongly metal dependent. In the case of Ti,<sup>1</sup> Zr,<sup>2</sup> Hf,<sup>2</sup> and V,<sup>3,4</sup> the MS<sub>5</sub> ring is the exclusive product while for Mo<sup>5</sup> and W<sup>6</sup> the MS<sub>4</sub> ring is the most stable.<sup>7</sup> We wish to report that substitution of the cyclopentadienyl rings by pentamethylcyclopentadienyl groups dramatically alters the ring size preference from Cp<sub>2</sub>VS<sub>5</sub> (**2**) to [(CH<sub>3</sub>)<sub>5</sub>C<sub>5</sub>]<sub>2</sub>VS<sub>2</sub> (**1**). The chemistry of polychalcogenide ligands, particularly S<sub>2</sub><sup>2-</sup> and Se<sub>2</sub><sup>2-</sup>, is of considerable interest both for homogenous metal complexes and in solid-state materials.<sup>8</sup>

Decamethylvanadocene (**3**) is transformed quantitatively to [(CH<sub>3</sub>)<sub>5</sub>C<sub>5</sub>]<sub>2</sub>VCl<sub>2</sub> (**4**) by reaction with PCl<sub>5</sub> in diethyl ether.<sup>9</sup> The reaction of a solution of **4** in acetone with aqueous (NH<sub>4</sub>)<sub>2</sub>S<sub>5</sub> for 2 h at 60 °C, followed by hot filtration, produces black crystals of **1** in 50% yield. These



**Figure 1.** Ortep diagrams of **1**. Selected distances (Å) and angles (deg) for **1**; corresponding parameters for **2** are given in the square brackets: V-S = 2.390 (1) [2.457]; V-C<sub>av</sub> = 2.349 (6) [2.300]; S-S' = 2.053 (3); V-(CH<sub>3</sub>)<sub>5</sub>C<sub>5</sub> = 2.023 [1.959]; S-V-S' = 50.86 (8) [89.3 (1)]; ((CH<sub>3</sub>)<sub>5</sub>C<sub>5</sub>)-V-((CH<sub>3</sub>)<sub>5</sub>C<sub>5</sub>) = 140.2 [134.1].

reaction conditions are similar to those used to prepare [C<sub>5</sub>H<sub>5</sub>]<sub>2</sub>VS<sub>2</sub> (**2**).<sup>3</sup> Alternately **1** can be prepared by the reaction of **4** with Na<sub>2</sub>S<sub>2</sub>.

An X-ray diffraction study of **1** has revealed that the molecule crystallizes in the orthorhombic space group *Fdd*2 with *a* = 17.514 (4) Å, *b* = 26.221 (4) Å, *c* = 8.661 (4) Å, *V* = 3973 (4) Å<sup>3</sup>, and *Z* = 8. Diffraction data was collected on an Enraf-Nonius diffractometer using Mo K $\alpha$  radiation. The structure was solved by using Patterson and difference Fourier methods. Final least-squares refinement of all the non-hydrogen atoms gave *R* = 0.047 and *R*<sub>w</sub> = 0.064 using 1369 unique reflections with *I* > 3 $\sigma$ (*I*). The molecule (Figure 1) possesses a crystallographically imposed C<sub>2</sub> axis which passes through the vanadium atom and the midpoint of the S-S bond. The S-S distance of 2.053 (3) Å is typical for a coordinated disulfide;<sup>8</sup> compound **1** is best formulated as V<sup>4+</sup>(S<sub>2</sub><sup>2-</sup>). Important bond distances and angles of **1** are compared with those of **2** in Figure 1.

The change in the size of the VS<sub>n</sub> ring going from **2** to **1** is likely dominated by steric considerations.<sup>10</sup> The smaller VS<sub>2</sub> ring lessens sulfur-methyl steric interactions. The recent report of the structure of [(CH<sub>3</sub>)<sub>5</sub>C<sub>5</sub>]<sub>2</sub>TiS<sub>3</sub> provides another example of the stability of smaller rings in the (CH<sub>3</sub>)<sub>5</sub>C<sub>5</sub> series of compounds.<sup>11</sup> In both the [C<sub>5</sub>H<sub>5</sub>]<sub>2</sub>MS<sub>n</sub> and the [(CH<sub>3</sub>)<sub>5</sub>C<sub>5</sub>]<sub>2</sub>MS<sub>n</sub> series, a decrease in MS<sub>n</sub> ring size correlates with an increase in the number of *d* electrons.<sup>12</sup> The decrease in the X-M-X angle in [C<sub>5</sub>H<sub>5</sub>]<sub>2</sub>MX<sub>2</sub> compounds as a function of increasing *d* electron count is well documented and well understood.<sup>13,14</sup> Smaller X-M-X angles should favor smaller MS<sub>n</sub> rings.

Compound **1** gives a characteristic sharp intense IR band at 552 cm<sup>-1</sup> that is assigned to the S-S stretch. The small vanadium hyperfine splitting value (45 G) in the ESR spectrum of **1** is also distinctive. The hyperfine coupling constant for **4** (75 G) is close to the value found for [C<sub>5</sub>H<sub>5</sub>]<sub>2</sub>VCl<sub>2</sub>,<sup>13</sup> which is a typical value (60-75 G) for [C<sub>5</sub>H<sub>5</sub>]<sub>2</sub>VX<sub>2</sub> compounds including **2**.<sup>4</sup> The reduced splitting constant for **1** is nearly identical with those reported for [C<sub>5</sub>H<sub>5</sub>]<sub>2</sub>VL where L is a  $\eta^2$  ligand such as an alkene or alkyne.<sup>15</sup>

(10) The steric interactions among the ligands is reflected in the displacements of the methyl groups from the least squares plane of the cyclopentadienyl rings: C6 (0.136 Å), C7 (0.250 Å), C8 (0.021 Å), C9 (0.390 Å), C10 (0.266 Å).

(11) Bird, P. H.; McCall, J. M.; Shaver, A.; Siriwardane, U. *Angew. Chem., Int. Ed. Engl.* **1982**, *21*, 384.

(12) (a) C<sub>5</sub>H<sub>5</sub> series: d<sup>0</sup> [C<sub>5</sub>H<sub>5</sub>]<sub>2</sub>MS<sub>5</sub>, M = Ti,<sup>4</sup> Zr,<sup>12b</sup> Hf<sup>12b</sup> (S-Ti-S = 95.0 (1)°); d<sup>1</sup> [C<sub>5</sub>H<sub>5</sub>]<sub>2</sub>VS<sub>2</sub> (S-V-S = 89.3 (1)°); d<sup>2</sup> [C<sub>5</sub>H<sub>5</sub>]<sub>2</sub>MS<sub>4</sub> (S-M-S (M = Mo) = 88.2 (2)°, (M = W) = 89.1 (1)°),<sup>5,6</sup> [C<sub>5</sub>H<sub>5</sub>]<sub>2</sub>MoS<sub>2</sub>,<sup>12b</sup> (CH<sub>3</sub>)<sub>5</sub>C<sub>5</sub> series: d<sup>0</sup> [(CH<sub>3</sub>)<sub>5</sub>C<sub>5</sub>]<sub>2</sub>TiS<sub>3</sub><sup>11</sup> (S-Ti-S = 84.4 (9)°); d<sup>1</sup> **1** (S-V-S = 50.86 (8)°). (b) No crystallographic information.

(13) Petersen, J. L.; Dahl, L. F. *J. Am. Chem. Soc.* **1975**, *97*, 6422.

(14) Lauher, J. W.; Hoffmann, R. *J. Am. Chem. Soc.* **1976**, *98*, 1729.

- (1) Köpf, H.; Kahl, W. *J. Organomet. Chem.* **1974**, *64*, C37.  
 (2) McCall, J. M.; Shaver, A. *J. Organomet. Chem.* **1980**, *193*, C37.  
 (3) Köpf, H.; Wirl, A.; Kahl, W. *Angew. Chem., Int. Ed. Engl.* **1971**, *10*, 137.  
 (4) Müller, E. G.; Petersen, J. L.; Dahl, L. F. *J. Organomet. Chem.* **1976**, *111*, 91.  
 (5) Block, H. D.; Allmann, R. *Cryst. Struct. Commun.* **1975**, *4*, 53.  
 (6) Davis, B. R.; Bernal, I. *J. Cryst. Mol. Struct.* **1972**, *2*, 135.  
 (7) (C<sub>5</sub>H<sub>5</sub>)<sub>2</sub>MoS<sub>2</sub> has been reported, but it readily converts into the more stable (C<sub>5</sub>H<sub>5</sub>)<sub>2</sub>MoS<sub>4</sub>: Köpf, H.; Hazari, S. K. S.; Leitner, M. Z. *Naturforsch., B: Anorg. Chem., Org. Chem.* **1978**, *33B*, 1398.  
 (8) Müller, A.; Jaegermann, W. *Inorg. Chem.* **1979**, *18*, 2631. Rakowski Dubois, M.; Dubois, D. L.; VanDerveer, M. C.; Haltiwanger, R. C. *Ibid.* **1981**, *20*, 3064. Seyferth, D.; Henderson, R. S.; Song, L.-C. *Organometallics* **1982**, *1*, 125. Bolinger, C. M.; Hoots, J. E.; Rauchfuss, T. B. *Ibid.* **1982**, *1*, 223. Hoffmann, R.; Shaik, S.; Scott, J. C.; Whangbo, M.-H.; Foshie, M. J. *J. Solid State Chem.* **1980**, *34*, 263. Rouxel, J. *Mol. Cryst. Liq. Cryst.* **1982**, *81*, 31.  
 (9) Morán, M. *Transition Met. Chem. (Weinheim, Ger.)* **1981**, *6*, 42.

The electrochemistry of **1** shows a reversible one-electron oxidation at 0.19 V (vs. SCE) and two irreversible reductions at -0.84 and -1.49 V.<sup>16</sup> Refluxing a solution of **1** in acetonitrile in the presence of added sulfur results in its transformation into  $[(\text{CH}_3)_5\text{C}_5]_2\text{V}_2\text{S}_5$ .<sup>17,18</sup> Further reactivity studies of the coordinated  $\text{S}_2$  are in progress.

**Acknowledgment.** Partial financial support was provided by a Dow Chemical U.S.A. Grant of Research Corp.

**Registry No.** **1**, 84174-74-3; **2**, 11077-28-4; **3**, 74507-60-1; **4**, 83617-50-9.

**Supplementary Material Available:** Tables of crystallographic data, positional and thermal parameters, least-squares planes, and bond distances and angles and a listing of structure factor amplitudes (11 pages). Ordering information is given on any current masthead page.

(15) Petersen, J. L.; Griffith, L. *Inorg. Chem.* **1980**, *19*, 1852.

(16) DC polarography, DMF solvent, 0.1 M  $\text{Et}_4\text{BF}_4$  supporting electrolyte, platinum electrode. The slope of the plot of  $\log(i_d - i)/i$  vs.  $E$ : 57 mV [0/1+], 89 mV [0/1-], 95 mV [1-/2-].

(17)  $^1\text{H}$  NMR ( $\text{CDCl}_3$ )  $\delta$  2.17 (s); mass spectrum,  $m/e$  (relative intensity) 532 (20,  $\text{M}^+$ ), 500 (40,  $(\text{M} - \text{S})^+$ ), 468 (100,  $(\text{M} - 2\text{S})^+$ ).

(18)  $(\text{C}_5\text{H}_5)_2\text{V}_2\text{S}_5$  has been reported: ref 4. Schunn, R. A.; Fritchie, C. J.; Prewitt, C. T. *Inorg. Chem.* **1966**, *5*, 892. Bolinger, C. M.; Rauchs, T. B.; Rheingold, A. L. *Organometallics* **1982**, *1*, 1551.

## Chemistry of Siloles.

### 1-Methyldibenzosilacyclopentadienide Anion

Mitsuo Ishikawa,\*<sup>1a</sup> Tatsuru Tabohashi,<sup>1a</sup>  
Hakubun Ohashi,<sup>1a</sup> Makoto Kumada,\*<sup>1a</sup> and Jun Iyoda<sup>1b</sup>

Department of Synthetic Chemistry, Faculty of Engineering  
Kyoto University, Kyoto 606, Japan

Government Industrial Research Institute Osaka  
Ikeda, Osaka 563, Japan

Received September 8, 1982

**Summary:** The reaction of 1-methyl-1-(trimethylsilyl)dibenzosilole with (methyldiphenylsilyl)lithium in THF afforded the 1-methyldibenzosilacyclopentadienide anion in high yield. Similar reaction of 1-methyl-3,4-diphenyl-1,2,5-tris(trimethylsilyl)silole with (methyldiphenylsilyl)lithium gave a lithium compound as the sole product, which formed two isomers of 1-methyl-3,4-diphenyl-2,2,5-tris(trimethylsilyl)-1-(methyldiphenylsilyl)-1-silacyclopent-3-ene in high yield on hydrolysis.

The silacyclopentadienide anion is an attractive compound for theoreticians as well as silicon chemists. However, all attempts to prepare this species have been unsuccessful to date. In this paper we report the successful synthesis of the anion of dibenzosilole and its behavior. Recently, we found that the reaction of 1-methyl-1-(trimethylsilyl)dibenzosilole (**1**) with an excess of an alkyl-lithium such as methyl- or butyllithium afforded the corresponding 1,1-dialkyldibenzosilole in almost quantitative yield.<sup>2</sup> In marked contrast, the reaction with a silyllithium has been found to produce the 1-methyldibenzosilacyclopentadienide anion (**2**). The  $^1\text{H}$  NMR

spectrum of anion **2** revealed a sharp resonance at  $\delta$  0.24, due to methylsilyl protons. The UV spectrum of **2** in THF exhibits characteristic absorptions at 377 ( $\epsilon$  5700) and 546 nm (1200), while dibenzosilole **1** shows absorptions at 234 ( $\epsilon$  25 000), 242 (24 000), 278 (14 000), 288 (13 000), 304 (1700), and 318 nm (170).

In a typical experiment, 3.0 mL of (methyldiphenylsilyl)lithium, prepared from 0.9546 g (2.42 mmol) of 1,2-dimethyltetraphenyldisilane in 10 mL of THF, was added to 0.3466 g (1.29 mmol) of **1** in 2 mL of THF at  $-78^\circ\text{C}$  under a dry argon atmosphere. The mixture was warmed to room temperature and hydrolyzed with dilute hydrochloric acid. The organic layer was separated, washed with water, and dried over potassium carbonate. GC analysis of the resulting solution using nonadecane as an internal standard showed the presence of 1-hydro-1-methyldibenzosilole<sup>3</sup> (**3**) and siloxane<sup>4</sup> (**4**) in 23 and 46% yield, respectively, in addition to a 65% yield of 1,1,1,2-tetramethyldiphenyldisilane (**5**). Compounds **3** and **4** were isolated by preparative GC analysis. That siloxane **4** is a secondary product was shown by the fact that compound **3** could readily be transformed into **4** under the conditions used. The formation of **3** clearly indicates that the silicon-silicon bond in dibenzosilole **1** was cleaved by the silyllithium reagent to give the dibenzosilacyclopentadienide anion **2**.

The reaction of **1** with 1 equiv of (methyldiphenylsilyl)lithium in THF at  $-78^\circ\text{C}$ , followed by treatment of the solution with ethyldimethylchlorosilane at room temperature, gave tetramethyldiphenyldisilane **5** and 1-(ethyldimethylsilyl)-1-methyldibenzosilole<sup>5</sup> (**6**) in 68 and 64% yield, respectively, as shown in Scheme I. Interestingly, in this reaction, no 1-ethyl-1,1,2-trimethyldiphenyldisilane, which might be expected to form from (methyldiphenylsilyl)lithium and ethyldimethylchlorosilane, was detected by either spectroscopic or GC analysis, indicating that the equilibrium lies far to the formation of anion **2**.

1-Methyl-3,4-diphenyl-1,2,5-tris(trimethylsilyl)silole<sup>6</sup> (**7**) reacts with (methyldiphenylsilyl)lithium in a manner different from dibenzosilole **1**. Thus, treatment of 0.2303 g (0.50 mmol) of **7** in 6 mL of THF with 1.7 mL (0.77 mmol) of (methyldiphenylsilyl)lithium-THF solution at  $-78^\circ\text{C}$  gave a dark green solution. After a 15-h reaction time at room temperature, analysis of the resulting solution by  $^1\text{H}$  NMR showed the presence of anion **8** [ $^1\text{H}$  NMR  $\delta$  -0.43 (9 H, s,  $\text{Me}_3\text{Si}$ ), -0.17 (9 H, s,  $\text{Me}_3\text{Si}$ ), 0.34 (9 H, s,  $\text{Me}_3\text{Si}$ ), 0.15 (3 H, s,  $\text{MeSi}$ ), 0.85 (3 H, s,  $\text{MeSi}$ ), 6.4-8.0 (20 H, m, ring protons)] as the sole product. After hydrolysis of the mixture with dilute hydrochloric acid, the organic layer was separated and the solvent was evaporated. The residue was chromatographed to give white crystals (82% yield). The  $^1\text{H}$  NMR spectrum of the crystals that were gas chromatographically homogeneous showed the presence of the two isomers of 1-methyl-3,4-diphenyl-2,2,5-tris(trimethylsilyl)-1-(methyldiphenylsilyl)-1-silacyclo-

(3) Compound **3**:  $^1\text{H}$  NMR  $\delta$  0.57 (3 H, d,  $J = 4$  Hz,  $\text{MeSi}$ ), 4.92 (1 H, q,  $J = 4$  Hz, HSi), 7.2-7.9 (8 H, m, ring protons); IR 2125  $\text{cm}^{-1}$ ; exact mass calcd for  $\text{C}_{13}\text{H}_{12}\text{Si}$  196.0708, found 196.0713.

(4) Compound **4**:  $^1\text{H}$  NMR  $\delta$  0.36 (6 H, s,  $\text{MeSi}$ ), 7.0-7.7 (16 H, m, ring protons); IR 1076  $\text{cm}^{-1}$ ; mass spectrum,  $m/e$  406 ( $\text{M}^+$ ). Anal. Calcd for  $\text{C}_{26}\text{H}_{22}\text{Si}_2\text{O}$ : C, 76.80; H, 5.45. Found: C, 76.70; H, 5.34.

(5) Compound **6**:  $^1\text{H}$  NMR  $\delta$  0.04 (6 H, s,  $\text{Me}_2\text{SiEt}$ ), 0.48 (3 H, s,  $\text{MeSi}$ ), 0.52-0.68 (2 H, m,  $\text{CH}_2\text{Si}$ ), 0.68-1.00 (3 H, m,  $\text{CH}_3\text{C}$ ), 7.1-7.8 (8 H, m, ring protons); mass spectrum,  $m/e$  344 ( $\text{M}^+$ ). Anal. Calcd for  $\text{C}_{17}\text{H}_{22}\text{Si}$ : C, 72.27; H, 7.85. Found: C, 72.46; H, 8.07.

(6) Ishikawa, M.; Sugisawa, H.; Harata, O.; Kumada, M. *J. Organomet. Chem.* **1981**, *217*, 43.

(1) (a) Department of Synthetic Chemistry. (b) Government Industrial Research Institute Osaka.

(2) Ishikawa, M.; Nishimura, N.; Sugisawa, H.; Kumada, M. *J. Organomet. Chem.* **1981**, *218*, C21.

## Chemistry of siloles. 1-Methyldibenzosilacyclopentadienide anion

Mitsuo Ishikawa, Tatsuru Tabohashi, Hakubun Ohashi, Makoto Kumada, and Jun Iyoda

*Organometallics*, **1983**, 2 (2), 351-352 • DOI: 10.1021/om00074a028 • Publication Date (Web): 01 May 2002

Downloaded from <http://pubs.acs.org> on April 24, 2009

### More About This Article

---

The permalink <http://dx.doi.org/10.1021/om00074a028> provides access to:

- Links to articles and content related to this article
- Copyright permission to reproduce figures and/or text from this article



The electrochemistry of **1** shows a reversible one-electron oxidation at 0.19 V (vs. SCE) and two irreversible reductions at -0.84 and -1.49 V.<sup>16</sup> Refluxing a solution of **1** in acetonitrile in the presence of added sulfur results in its transformation into  $[(\text{CH}_3)_5\text{C}_5]_2\text{V}_2\text{S}_5$ .<sup>17,18</sup> Further reactivity studies of the coordinated  $\text{S}_2$  are in progress.

**Acknowledgment.** Partial financial support was provided by a Dow Chemical U.S.A. Grant of Research Corp.

**Registry No.** **1**, 84174-74-3; **2**, 11077-28-4; **3**, 74507-60-1; **4**, 83617-50-9.

**Supplementary Material Available:** Tables of crystallographic data, positional and thermal parameters, least-squares planes, and bond distances and angles and a listing of structure factor amplitudes (11 pages). Ordering information is given on any current masthead page.

(15) Petersen, J. L.; Griffith, L. *Inorg. Chem.* **1980**, *19*, 1852.

(16) DC polarography, DMF solvent, 0.1 M  $\text{Et}_4\text{BF}_4$  supporting electrolyte, platinum electrode. The slope of the plot of  $\log(i_d - i)/i$  vs.  $E$ : 57 mV [0/1+], 89 mV [0/1-], 95 mV [1-/2-].

(17)  $^1\text{H}$  NMR ( $\text{CDCl}_3$ )  $\delta$  2.17 (s); mass spectrum,  $m/e$  (relative intensity) 532 (20,  $\text{M}^+$ ), 500 (40,  $(\text{M} - \text{S})^+$ ), 468 (100,  $(\text{M} - 2\text{S})^+$ ).

(18)  $(\text{C}_5\text{H}_5)_2\text{V}_2\text{S}_5$  has been reported: ref 4. Schunn, R. A.; Fritchie, C. J.; Prewitt, C. T. *Inorg. Chem.* **1966**, *5*, 892. Bolinger, C. M.; Rauffuss, T. B.; Rheingold, A. L. *Organometallics* **1982**, *1*, 1551.

## Chemistry of Siloles.

### 1-Methyldibenzosilacyclopentadienide Anion

Mitsuo Ishikawa,<sup>\*1a</sup> Tatsuru Tabohashi,<sup>1a</sup>  
Hakubun Ohashi,<sup>1a</sup> Makoto Kumada,<sup>\*1a</sup> and Jun Iyoda<sup>1b</sup>

Department of Synthetic Chemistry, Faculty of Engineering  
Kyoto University, Kyoto 606, Japan  
Government Industrial Research Institute Osaka  
Ikeda, Osaka 563, Japan

Received September 8, 1982

**Summary:** The reaction of 1-methyl-1-(trimethylsilyl)dibenzosilole with (methyldiphenylsilyl)lithium in THF afforded the 1-methyldibenzosilacyclopentadienide anion in high yield. Similar reaction of 1-methyl-3,4-diphenyl-1,2,5-tris(trimethylsilyl)silole with (methyldiphenylsilyl)lithium gave a lithium compound as the sole product, which formed two isomers of 1-methyl-3,4-diphenyl-2,2,5-tris(trimethylsilyl)-1-(methyldiphenylsilyl)-1-silacyclopent-3-ene in high yield on hydrolysis.

The silacyclopentadienide anion is an attractive compound for theoreticians as well as silicon chemists. However, all attempts to prepare this species have been unsuccessful to date. In this paper we report the successful synthesis of the anion of dibenzosilole and its behavior. Recently, we found that the reaction of 1-methyl-1-(trimethylsilyl)dibenzosilole (**1**) with an excess of an alkyl-lithium such as methyl- or butyllithium afforded the corresponding 1,1-dialkyldibenzosilole in almost quantitative yield.<sup>2</sup> In marked contrast, the reaction with a silyllithium has been found to produce the 1-methyldibenzosilacyclopentadienide anion (**2**). The  $^1\text{H}$  NMR

spectrum of anion **2** revealed a sharp resonance at  $\delta$  0.24, due to methylsilyl protons. The UV spectrum of **2** in THF exhibits characteristic absorptions at 377 ( $\epsilon$  5700) and 546 nm (1200), while dibenzosilole **1** shows absorptions at 234 ( $\epsilon$  25 000), 242 (24 000), 278 (14 000), 288 (13 000), 304 (1700), and 318 nm (170).

In a typical experiment, 3.0 mL of (methyldiphenylsilyl)lithium, prepared from 0.9546 g (2.42 mmol) of 1,2-dimethyltetraphenyldisilane in 10 mL of THF, was added to 0.3466 g (1.29 mmol) of **1** in 2 mL of THF at  $-78^\circ\text{C}$  under a dry argon atmosphere. The mixture was warmed to room temperature and hydrolyzed with dilute hydrochloric acid. The organic layer was separated, washed with water, and dried over potassium carbonate. GC analysis of the resulting solution using nonadecane as an internal standard showed the presence of 1-hydro-1-methyldibenzosilole<sup>3</sup> (**3**) and siloxane<sup>4</sup> (**4**) in 23 and 46% yield, respectively, in addition to a 65% yield of 1,1,1,2-tetramethyldiphenyldisilane (**5**). Compounds **3** and **4** were isolated by preparative GC analysis. That siloxane **4** is a secondary product was shown by the fact that compound **3** could readily be transformed into **4** under the conditions used. The formation of **3** clearly indicates that the silicon-silicon bond in dibenzosilole **1** was cleaved by the silyllithium reagent to give the dibenzosilacyclopentadienide anion **2**.

The reaction of **1** with 1 equiv of (methyldiphenylsilyl)lithium in THF at  $-78^\circ\text{C}$ , followed by treatment of the solution with ethyldimethylchlorosilane at room temperature, gave tetramethyldiphenyldisilane **5** and 1-(ethyldimethylsilyl)-1-methyldibenzosilole<sup>5</sup> (**6**) in 68 and 64% yield, respectively, as shown in Scheme I. Interestingly, in this reaction, no 1-ethyl-1,1,2-trimethyldiphenyldisilane, which might be expected to form from (methyldiphenylsilyl)lithium and ethyldimethylchlorosilane, was detected by either spectroscopic or GC analysis, indicating that the equilibrium lies far to the formation of anion **2**.

1-Methyl-3,4-diphenyl-1,2,5-tris(trimethylsilyl)silole<sup>6</sup> (**7**) reacts with (methyldiphenylsilyl)lithium in a manner different from dibenzosilole **1**. Thus, treatment of 0.2303 g (0.50 mmol) of **7** in 6 mL of THF with 1.7 mL (0.77 mmol) of (methyldiphenylsilyl)lithium-THF solution at  $-78^\circ\text{C}$  gave a dark green solution. After a 15-h reaction time at room temperature, analysis of the resulting solution by  $^1\text{H}$  NMR showed the presence of anion **8** [ $^1\text{H}$  NMR  $\delta$  -0.43 (9 H, s,  $\text{Me}_3\text{Si}$ ), -0.17 (9 H, s,  $\text{Me}_3\text{Si}$ ), 0.34 (9 H, s,  $\text{Me}_3\text{Si}$ ), 0.15 (3 H, s,  $\text{MeSi}$ ), 0.85 (3 H, s,  $\text{MeSi}$ ), 6.4-8.0 (20 H, m, ring protons)] as the sole product. After hydrolysis of the mixture with dilute hydrochloric acid, the organic layer was separated and the solvent was evaporated. The residue was chromatographed to give white crystals (82% yield). The  $^1\text{H}$  NMR spectrum of the crystals that were gas chromatographically homogeneous showed the presence of the two isomers of 1-methyl-3,4-diphenyl-2,2,5-tris(trimethylsilyl)-1-(methyldiphenylsilyl)-1-silacyclo-

(3) Compound **3**:  $^1\text{H}$  NMR  $\delta$  0.57 (3 H, d,  $J = 4$  Hz,  $\text{MeSi}$ ), 4.92 (1 H, q,  $J = 4$  Hz,  $\text{HSi}$ ), 7.2-7.9 (8 H, m, ring protons); IR 2125  $\text{cm}^{-1}$ ; exact mass calcd for  $\text{C}_{13}\text{H}_{12}\text{Si}$  196.0708, found 196.0713.

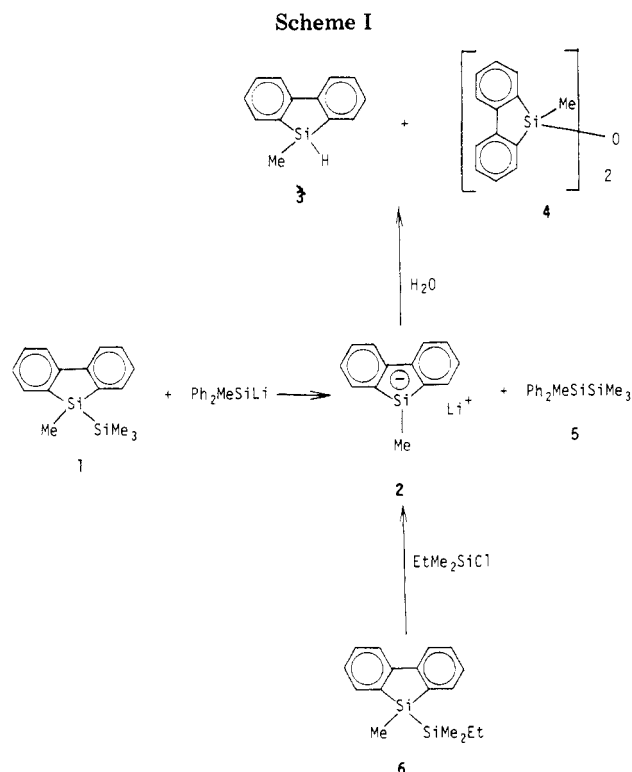
(4) Compound **4**:  $^1\text{H}$  NMR  $\delta$  0.36 (6 H, s,  $\text{MeSi}$ ), 7.0-7.7 (16 H, m, ring protons); IR 1076  $\text{cm}^{-1}$ ; mass spectrum,  $m/e$  406 ( $\text{M}^+$ ). Anal. Calcd for  $\text{C}_{26}\text{H}_{22}\text{Si}_2\text{O}$ : C, 76.80; H, 5.45. Found: C, 76.70; H, 5.34.

(5) Compound **6**:  $^1\text{H}$  NMR  $\delta$  0.04 (6 H, s,  $\text{Me}_2\text{SiEt}$ ), 0.48 (3 H, s,  $\text{MeSi}$ ), 0.52-0.68 (2 H, m,  $\text{CH}_2\text{Si}$ ), 0.68-1.00 (3 H, m,  $\text{CH}_3\text{C}$ ), 7.1-7.8 (8 H, m, ring protons); mass spectrum,  $m/e$  344 ( $\text{M}^+$ ). Anal. Calcd for  $\text{C}_{17}\text{H}_{22}\text{Si}$ : C, 72.27; H, 7.85. Found: C, 72.46; H, 8.07.

(6) Ishikawa, M.; Sugisawa, H.; Harata, O.; Kumada, M. *J. Organomet. Chem.* **1981**, *217*, 43.

(1) (a) Department of Synthetic Chemistry. (b) Government Industrial Research Institute Osaka.

(2) Ishikawa, M.; Nishimura, N.; Sugisawa, H.; Kumada, M. *J. Organomet. Chem.* **1981**, *218*, C21.



pent-3-ene (**9**<sup>7</sup> and **10**<sup>8</sup>) in a ratio of 1.5:1. Fractional recrystallization of the crystals gave **9** in a pure form, but pure **10** could not be obtained. Compound **10** thus obtained was always contaminated with a small amount of **9** (ca. 14%).

The production of anion **8** can be understood in terms of the transient formation of a pentacoordinate interme-

(7) Compound **9**: mp 172–173 °C; <sup>1</sup>H NMR δ -0.51 (9 H, s, Me<sub>3</sub>Si), -0.25 (9 H, s, Me<sub>3</sub>Si), 0.28 (9 H, s, Me<sub>3</sub>Si), 0.78 (3 H, s, MePh<sub>2</sub>Si), 0.90 (3 H, s, MeSi), 2.15 (1 H, s, HC), 6.70–7.00 and 7.15–7.70 (20 H, m, ring protons); mass spectrum, *m/e* 662 (M<sup>+</sup>). Anal. Calcd for C<sub>30</sub>H<sub>54</sub>Si<sub>5</sub>: C, 70.62; H, 8.21. Found: C, 70.48; H, 8.33.

(8) Compound **10**: <sup>1</sup>H NMR δ -0.60 (9 H, s, Me<sub>3</sub>Si), -0.18 (9 H, s, Me<sub>3</sub>Si), 0.21 (9 H, s, Me<sub>3</sub>Si), 0.68 (3 H, s, MePh<sub>2</sub>Si), 0.89 (3 H, s, MeSi), 2.15 (1 H, s, HC), 7.00–7.45 and 7.54–7.75 (20 H, m, ring protons); mass spectrum, *m/e* 662 (M<sup>+</sup>).

diate such as **A**, followed by rearrangement of a trimethylsilyl group attached to silicon to an adjacent unsaturated atom as shown in Scheme II.

**Acknowledgment.** The authors are grateful to Professors A. Nakamura and H. Yasuda, Department of Macromolecular Science, Faculty of Science, Osaka University, for useful discussions. We also express our appreciation to Toshiba Silicon Co., Ltd., and Shin-etsu Chemical Co., Ltd., for a gift of organochlorosilanes.

**Registry No.** 1, 80073-04-7; 2, 84081-97-0; 3, 53268-89-6; 4, 18766-02-4; 5, 1450-16-4; 6, 84081-98-1; 7, 79633-98-0; 8, 84081-99-2; 9, 84082-00-8; 10, 84082-01-9; Ph<sub>2</sub>MeSiLi, 3839-30-3; EtMe<sub>2</sub>SiCl, 6917-76-6; Ph<sub>2</sub>MeSiSiMePh<sub>2</sub>, 1172-76-5.

**Reactivity of Multisite-Bound Ligands. Nucleophilic Attack at Carbon in Cluster Acetylides by Isocyanides and Amination of the Products. X-ray Structures of HRu<sub>3</sub>(CO)<sub>9</sub>[C(CN-*t*-Bu)CPh] and Os<sub>3</sub>(CO)<sub>9</sub>[C(C(NH-*n*-Bu)(NH-*t*-Bu))CPh](PPh<sub>2</sub>)**

Shane A. MacLaughlin, James P. Johnson, Nicholas J. Taylor, and Arthur J. Carty\*  
Guelph-Waterloo Centre, Waterloo Campus  
Department of Chemistry, University of Waterloo  
Waterloo, Ontario N2L 3G1, Canada

**Enrico Sappa**

Istituto di Chimica Generale ed Inorganica  
Università di Torino, Corso M. D'Azeglio 48  
Turin, Italy

Received August 30, 1982

**Summary:** Regiospecific addition of the isocyanide *t*-BuNC at the α-carbon atoms of the multisite-bound acetylides in the trinuclear clusters HRu<sub>3</sub>(CO)<sub>9</sub>(μ<sub>3</sub>-η<sup>2</sup>-C≡CPh) and Os<sub>3</sub>(CO)<sub>9</sub>(μ<sub>3</sub>-η<sup>2</sup>-C≡CPh)(PPh<sub>2</sub>) generates carbon-carbon bonds via isocyanide-acetylide coupling. X-ray structural analysis of (μ-H)Ru<sub>3</sub>(CO)<sub>9</sub>[C(CN-*t*-Bu)CPh] has confirmed the synthesis of a new zwitterionic μ<sub>3</sub>-η<sup>2</sup> ligand via nucleophilic attack at carbocationic carbon. Derivatization of the isocyanide adduct Os<sub>3</sub>(CO)<sub>9</sub>[C(CN-*t*-Bu)CPh](PPh<sub>2</sub>) with *n*-BuNH<sub>2</sub> affords the carbenium zwitterion Os<sub>3</sub>(CO)<sub>9</sub>[C{C(NH-*t*-Bu)(NH-*n*-Bu)}CPh](PPh<sub>2</sub>) whose structure has been determined by X-ray analysis. Direct nucleophilic attack by uncharged carbon nucleophiles at carbocationic multisite-bound ligands in clusters may be a useful strategy for the elaboration of unsaturated ligands.

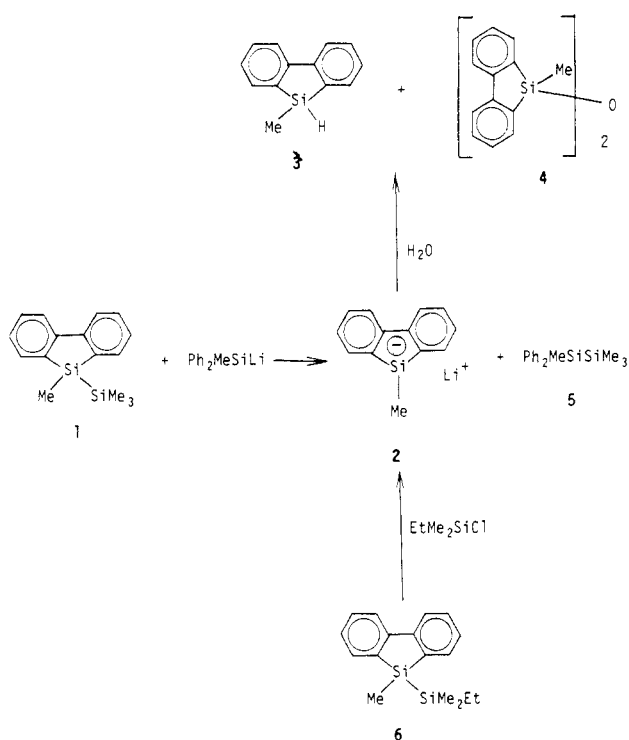
Multisite coordination on the edge or face of a metal cluster is a key step in the activation of small molecules such as CO, olefins, and acetylenes.<sup>1</sup> The simple reactivity patterns of μ-η-bound ligands are thus of fundamental significance to the design of strategies for the elaboration of these molecules. In the specific context of CO hydrogenation there is evidence for proton induced cleavage of μ<sub>4</sub>-η<sup>2</sup>-CO in HFe<sub>4</sub>(CO)<sub>13</sub><sup>-</sup> yielding an exposed carbide carbon atom that on subsequent protonation affords methane.<sup>2</sup> Our attention has focussed on the chemical behavior of cluster-bound acetylides,<sup>3</sup> ligands which are

(1) Muetterties, E. L.; Stein, J. *Chem. Rev.* 1979, 79, 479.

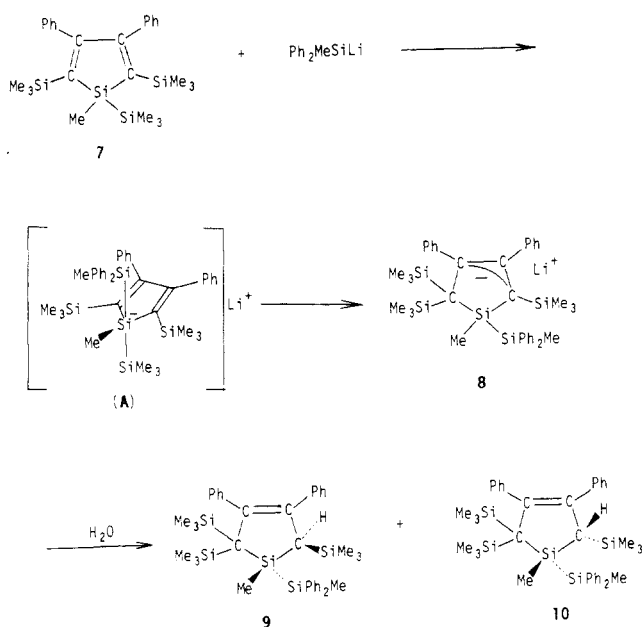
(2) Holt, E. M.; Whitmire, K. H.; Shriver, D. F. *J. Organomet. Chem.* 1981, 213, 125. See also: Tachikawa, M.; Muetterties, E. L. *J. Am. Chem. Soc.* 1980, 102, 4541.

(3) Carty, A. J. *Pure Appl. Chem.* 1982, 53, 113.

Scheme I



Scheme II



pent-3-ene (9<sup>7</sup> and 10<sup>8</sup>) in a ratio of 1.5:1. Fractional recrystallization of the crystals gave 9 in a pure form, but pure 10 could not be obtained. Compound 10 thus obtained was always contaminated with a small amount of 9 (ca. 14%).

The production of anion 8 can be understood in terms of the transient formation of a pentacoordinate interme-

diate such as A, followed by rearrangement of a trimethylsilyl group attached to silicon to an adjacent unsaturated atom as shown in Scheme II.

**Acknowledgment.** The authors are grateful to Professors A. Nakamura and H. Yasuda, Department of Macromolecular Science, Faculty of Science, Osaka University, for useful discussions. We also express our appreciation to Toshiba Silicon Co., Ltd., and Shin-etsu Chemical Co., Ltd., for a gift of organochlorosilanes.

**Registry No.** 1, 80073-04-7; 2, 84081-97-0; 3, 53268-89-6; 4, 18766-02-4; 5, 1450-16-4; 6, 84081-98-1; 7, 79633-98-0; 8, 84081-99-2; 9, 84082-00-8; 10, 84082-01-9;  $\text{Ph}_2\text{MeSiLi}$ , 3839-30-3;  $\text{EtMe}_2\text{SiCl}$ , 6917-76-6;  $\text{Ph}_2\text{MeSiSiMePh}_2$ , 1172-76-5.

**Reactivity of Multisite-Bound Ligands. Nucleophilic Attack at Carbon in Cluster Acetylides by Isocyanides and Amination of the Products. X-ray Structures of  $\text{HRu}_3(\text{CO})_9[\text{C}(\text{CN}-t\text{-Bu})\text{CPh}]$  and  $\text{Os}_3(\text{CO})_9[\text{C}(\text{CN}-n\text{-Bu})(\text{NH}-t\text{-Bu})\text{CPh}](\text{PPh}_2)$**

Shane A. MacLaughlin, James P. Johnson, Nicholas J. Taylor, and Arthur J. Carty\*  
Guelph-Waterloo Centre, Waterloo Campus  
Department of Chemistry, University of Waterloo  
Waterloo, Ontario N2L 3G1, Canada

**Enrico Sappa**

Istituto di Chimica Generale ed Inorganica  
Università di Torino, Corso M. D'Azeglio 48  
Turin, Italy

Received August 30, 1982

**Summary:** Regiospecific addition of the isocyanide  $t\text{-BuNC}$  at the  $\alpha$ -carbon atoms of the multisite-bound acetylides in the trinuclear clusters  $\text{HRu}_3(\text{CO})_9(\mu_3\text{-}\eta^2\text{-C}\equiv\text{CPh})$  and  $\text{Os}_3(\text{CO})_9(\mu_3\text{-}\eta^2\text{-C}\equiv\text{CPh})(\text{PPh}_2)$  generates carbon-carbon bonds via isocyanide-acetylide coupling. X-ray structural analysis of  $(\mu\text{-H})\text{Ru}_3(\text{CO})_9[\text{C}(\text{CN}-t\text{-Bu})\text{CPh}]$  has confirmed the synthesis of a new zwitterionic  $\mu_3\text{-}\eta^2$  ligand via nucleophilic attack at carbocationic carbon. Derivatization of the isocyanide adduct  $\text{Os}_3(\text{CO})_9[\text{C}(\text{CN}-t\text{-Bu})\text{CPh}](\text{PPh}_2)$  with  $n\text{-BuNH}_2$  affords the carbenium zwitterion  $\text{Os}_3(\text{CO})_9[\text{C}(\text{CN}-t\text{-Bu})(\text{NH}-n\text{-Bu})\text{CPh}](\text{PPh}_2)$  whose structure has been determined by X-ray analysis. Direct nucleophilic attack by uncharged carbon nucleophiles at carbocationic multisite-bound ligands in clusters may be a useful strategy for the elaboration of unsaturated ligands.

Multisite coordination on the edge or face of a metal cluster is a key step in the activation of small molecules such as CO, olefins, and acetylenes.<sup>1</sup> The simple reactivity patterns of  $\mu\text{-}\eta$ -bound ligands are thus of fundamental significance to the design of strategies for the elaboration of these molecules. In the specific context of CO hydrogenation there is evidence for proton induced cleavage of  $\mu_4\text{-}\eta^2\text{-CO}$  in  $\text{HFe}_4(\text{CO})_{13}^-$  yielding an exposed carbide carbon atom that on subsequent protonation affords methane.<sup>2</sup> Our attention has focussed on the chemical behavior of cluster-bound acetylides,<sup>3</sup> ligands which are

(7) Compound 9: mp 172-173 °C;  $^1\text{H NMR}$   $\delta$  -0.51 (9 H, s,  $\text{Me}_3\text{Si}$ ), -0.25 (9 H, s,  $\text{Me}_3\text{Si}$ ), 0.28 (9 H, s,  $\text{Me}_3\text{Si}$ ), 0.78 (3 H, s,  $\text{MePh}_2\text{Si}$ ), 0.90 (3 H, s,  $\text{MeSi}$ ), 2.15 (1 H, s, HC), 6.70-7.00 and 7.15-7.70 (20 H, m, ring protons); mass spectrum,  $m/e$  662 ( $\text{M}^+$ ). Anal. Calcd for  $\text{C}_{35}\text{H}_{54}\text{Si}_5$ : C, 70.62; H, 8.21. Found: C, 70.48; H, 8.33.

(8) Compound 10:  $^1\text{H NMR}$   $\delta$  -0.60 (9 H, s,  $\text{Me}_3\text{Si}$ ), -0.18 (9 H, s,  $\text{Me}_3\text{Si}$ ), 0.21 (9 H, s,  $\text{Me}_3\text{Si}$ ), 0.68 (3 H, s,  $\text{MePh}_2\text{Si}$ ), 0.89 (3 H, s,  $\text{MeSi}$ ), 2.15 (1 H, s, HC), 7.00-7.45 and 7.54-7.75 (20 H, m, ring protons); mass spectrum,  $m/e$  662 ( $\text{M}^+$ ).

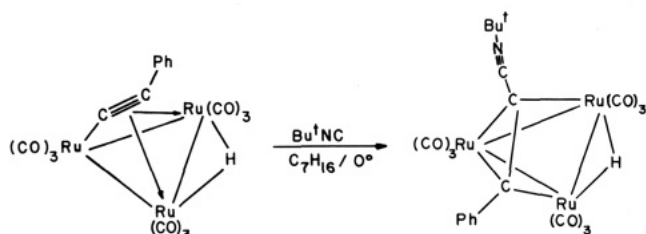
(1) Muettterties, E. L.; Stein, J. *Chem. Rev.* 1979, 79, 479.

(2) Holt, E. M.; Whitmire, K. H.; Shriver, D. F. *J. Organomet. Chem.* 1981, 213, 125. See also: Tachikawa, M.; Muettterties, E. L. *J. Am. Chem. Soc.* 1980, 102, 4541.

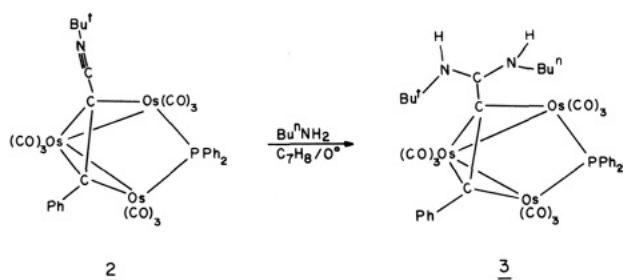
(3) Carty, A. *J. Pure Appl. Chem.* 1982, 53, 113.



## Scheme I

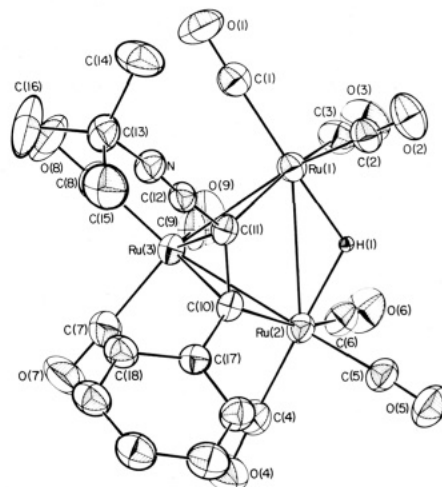


## Scheme II



structurally and electronically related to CO and the carbides. Previous work has shown that neutral binuclear<sup>4</sup> and trinuclear<sup>3,5</sup>  $\mu\text{-}\eta^2\text{-acetylides}$  are unusually sensitive to attack at  $\alpha$ - and  $\beta$ -carbon atoms by neutral nucleophiles. Very recently addition of phosphines to  $\text{HOs}_3(\text{CO})_9(\mu_3\text{-}\eta^2\text{-C}\equiv\text{CR})$  has been shown.<sup>6</sup> We describe herein the direct synthesis of carbon-carbon bonds via regioselective addition of the isocyanide  $t\text{-BuNC}$  to the  $\alpha$ -carbon atoms of the cluster bound  $\mu_3\text{-}\eta^2\text{-acetylides}$  in  $\text{HRu}_3(\text{CO})_9(\text{C}\equiv\text{CPh})$  and  $\text{Os}_3(\text{CO})_9(\text{C}\equiv\text{CPh})(\text{PPh}_2)$ , generating  $\text{HRu}_3(\text{CO})_9[\text{C}(\text{CN-}t\text{-Bu})\text{CPh}]$  (**1**, Scheme I) and  $\text{Os}_3(\text{CO})_9[\text{C}(\text{CN-}t\text{-Bu})\text{CPh}](\text{PPh}_2)$  (**2**). Facile amination of the latter with  $n\text{-BuNH}_2$  affords  $\text{Os}_3(\text{CO})_9[\text{C}(\text{CN-}t\text{-Bu})\text{CPh}](\text{PPh}_2)$  (**3**), a carbenium zwitterion (Scheme II). The addition of uncharged carbon nucleophiles to cluster-bound unsaturates may thus be a useful synthetic strategy. The similarity in ligand behavior of CO and the isocyanides also suggests that due consideration be given to the possibility of direct attack by CO on  $\mu\text{-}\eta$ -coordinated molecules as a mechanism of C-C bond formation in cluster chemistry.

Treatment of  $(\mu\text{-H})\text{Ru}_3(\text{CO})_9(\mu_3\text{-}\eta^2\text{-C}\equiv\text{CPh})$ <sup>7</sup> (0.21 g, 0.32 mmol) in  $n\text{-heptane}$  (10 mL) at  $0^\circ\text{C}$  with  $t\text{-BuNC}$  (35  $\mu\text{l}$ , 0.33 mmol) gave a yellow cloudy mixture. Florisil chromatography yielded three products. The last yellow band eluted was judged by its high frequency  $\nu(\text{C}\equiv\text{N})$  band to be the product of attack on the acetylide. Crystallization from  $n\text{-heptane}$  at  $-10^\circ\text{C}$  overnight afforded yellow crystals of an adduct,  $\text{HRu}_3(\text{CO})_9(\text{C}\equiv\text{CPh})(t\text{-BuNC})$  (**1**) ( $\sim 20\%$ ): IR ( $\text{C}_6\text{H}_{12}$ )  $\nu(\text{CO})$ , 2080 (m), 2054 (s), 2024 (vs), 2013 (s), 1997 (m), 1986 (m), 1970 (w), 1956 (w),



**Figure 1.** The molecular structure of  $\text{HRu}_3(\text{CO})_9[\text{C}(\text{CN-}t\text{-Bu})\text{CPh}]$  as drawn by ORTEP to illustrate the nature of the new ligand.

$\nu(\text{C}\equiv\text{N})$  2201  $\text{cm}^{-1}$ ;  $^1\text{H NMR}$  ( $\text{C}_6\text{D}_6$ )  $\delta$  -18.9 (s, Ru-H-Ru), 0.7 (s,  $\text{C}(\text{CH}_3)_3$ ), 7.0 (m, Ph).

Similarly, slow addition of  $t\text{-BuNC}$  (47 mg) in heptane (7 mL) to a solution of  $\text{Os}_3(\text{CO})_9(\mu_3\text{-}\eta^2\text{-C}\equiv\text{CPh})(\text{PPh}_2)$  (226 mg, 0.2 mmol) in toluene (10 mL) and heptane (7 mL) gave an orange solution. IR monitoring indicated complete consumption of starting material. Removal of solvent in vacuo and recrystallization of the orange solid from heptane-toluene containing a trace of  $t\text{-BuNC}$  gave orange crystals of **2** (94%): IR ( $\text{C}_7\text{H}_8$ )  $\nu(\text{CO})$  2068 (m), 2046 (vs), 2013 (s), 1994 (m), 1962 (m),  $\nu(\text{C}\equiv\text{N})$  2235 (w), 2190 (w)  $\text{cm}^{-1}$ ;  $^{31}\text{P NMR}$  ( $\text{C}_6\text{D}_6$ )  $\delta(\text{H}_3\text{PO}_4)$  -70.0;  $^1\text{H NMR}$  ( $\text{C}_6\text{D}_6$ )  $\delta$  0.60 (s,  $t\text{-Bu}$ ), 6.91-7.26 (m), 7.49 (t), 8.13 (dd, Ph). The high-field  $^{31}\text{P}$  chemical shift of the  $\text{PPh}_2$  group in **2** (-70.0 ppm) suggests the absence of a substantial Os...Os interaction along the edge of the cluster bridged by the phosphido group.<sup>9</sup> The location of the isocyanide in these adducts was established by a single-crystal X-ray structural study of **1**.<sup>10</sup> A perspective view of the adduct drawn so as to illustrate the isocyanide-acetylide interaction is shown in Figure 1. In the closed, triangular skeleton, there are two strong Ru-Ru bonds (Ru(1)-Ru(3) = 2.7372 (4) Å, Ru(2)-Ru(3) = 2.7497 (4) Å) with the third significantly longer (Ru(1)-Ru(2) = 2.9644 (5) Å) and bridged by a

(9) Carty, A. J. *Adv. Chem. Ser.* **1982**, No. 196, 163.

(10) Crystals, of  $\text{Ru}_3\text{O}_9\text{NC}_22\text{H}_{15}$ , are monoclinic of space group  $P2_1/c$  with  $a = 9.798$  (1) Å,  $b = 14.553$  (2) Å,  $c = 18.836$  (2) Å,  $\beta = 99.30$  (1) $^\circ$ ,  $V = 2650.5$  Å<sup>3</sup>,  $Z = 4$ ,  $\rho(\text{calcd}) = 1.856$  g·cm<sup>-3</sup>,  $\rho(\text{measd}) = 1.86$  g·cm<sup>-3</sup>, and  $\mu$  (Mo K $\alpha$ ) = 16.96 cm<sup>-1</sup>. Intensity data were collected on a crystal of dimensions 0.25 × 0.23 × 0.24 mm using  $\theta$ - $2\theta$  scans ( $3.2^\circ < 2\theta \leq 50.0^\circ$ ) with a variable scan speed of 2.0-29.3 $^\circ$  min<sup>-1</sup> and a scan width of +0.8 $^\circ$  below  $K\alpha_1$  to 0.8 $^\circ$  above  $K\alpha_2$  on a Syntex P2<sub>1</sub> diffractometer. From a total of 4709 measured reflections, 3695 had  $I \geq 3\sigma(I)$  and were used in the structure solution and refinement. Two standard reflections monitored after every 100 measurements showed no change in intensity over the course of data collection. With  $\mu = 16.96$  cm<sup>-1</sup> for these atoms no absorption correction was deemed necessary. Transmission factors varied between 0.59 and 0.74. The three ruthenium atoms were located in a Patterson synthesis and light atoms via a subsequent Fourier map. Refinement of all non-hydrogen atoms with isotropic parameters gave a value  $R$  ( $R = \sum |F_o| - |F_c| / \sum |F_o|$ ) of 0.067. Two cycles of refinement with anisotropic coefficients reduced  $R$  to 0.034. A difference map at this stage allowed the location of all hydrogen atoms. These were included in subsequent refinements. The converged  $R$  and  $R_w$  ( $R_w = [\sum w|F_o| - |F_c|]^2 / \sum w|F_o|^2]^{1/2}$ ) values were 0.024 and 0.027. A final difference map was featureless. Scattering factors were taken from the compilations of ref 11a and, for hydrogen, the data of Stewart et al.<sup>11b</sup> Both real and imaginary components of anomalous dispersion were applied to corrections for the ruthenium atoms. Computer programs used have been described in detail elsewhere.<sup>4d</sup>

(11) (a) "International Tables for X-ray Crystallography"; Kynoch Press: Birmingham, England, 1974; Vol. IV. (b) Stewart, R. F.; Davidson, E. R.; Simpson, W. T. *J. Chem. Phys.* **1965**, *42*, 3175.

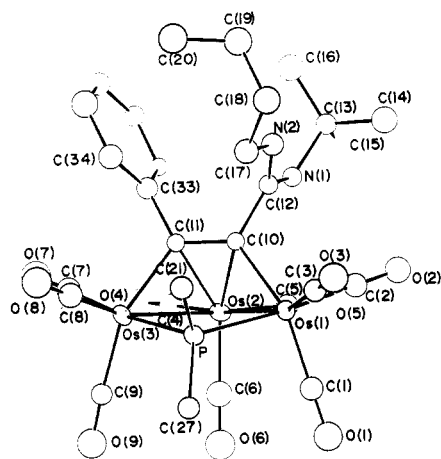
(4) (a) Wong, Y. S.; Paik, H. N.; Chieh, P. C.; Carty, A. J. *J. Chem. Soc. Chem. Commun.* **1975**, 309. (b) Carty, A. J.; Taylor, N. J.; Smith, W. F.; Paik, H. N.; Yule, J. E. *Ibid.* **1976**, 41. (c) Carty, A. J.; Mott, G. N.; Taylor, N. J.; Ferguson, G.; Khan, M. A.; Roberts, P. J. *J. Organomet. Chem.* **1978**, *149*, 345. (d) Carty, A. J.; Mott, G. N.; Taylor, N. J.; Yule, J. E. *J. Am. Chem. Soc.* **1978**, *100*, 3051.

(5) Deeming, A. J.; Hasso, S. *J. Organomet. Chem.* **1976**, *112*, C39.

(6) Henrick, K.; McPartlin, M.; Deeming, A. J.; Hasso, S.; Manning, P. *J. Chem. Soc., Dalton Trans.* **1982**, 899.

(7) This hydride was synthesized by a modification of the procedures described for the  $t$ -butyl analogue by Sappa and co-workers. See: Sappa, E.; Gambino, O.; Milone, L.; Cetini, G. *J. Organomet. Chem.* **1972**, *39*, 169.

(8) Satisfactory analyses are available for all compounds described herein.



**Figure 2.** An ORTEP plot of the structure of the zwitterionic carbenium species  $\text{Os}_3(\text{CO})_9[\text{C}(\text{C}(\text{NH}-t\text{-Bu})(\text{NH}-n\text{-Bu})\text{CPh})\text{PPh}_2$ . The open edge of the  $\text{Os}_3$  triangle is between Os(1) and Os(3).

hydride ( $\text{Ru}(1)\text{-H}(1) = 1.67(5) \text{ \AA}$ ,  $\text{Ru}(2)\text{-H}(1) = 1.73(5) \text{ \AA}$ ). The isocyanide is attached via C(12) to the original  $\alpha$ -carbon atom of the acetylide C(11). Thus nucleophilic attack on the  $\mu_3\text{-}\eta^2$ -acetylide by  $t\text{-BuNC}$  has resulted in the formation of a strong carbon-carbon bond ( $\text{C}(11)\text{-C}(12) = 1.400(5) \text{ \AA}$ ).<sup>12</sup> The "carbon-coordinated" isocyanide is essentially linear ( $\text{C}(11)\text{-C}(12)\text{-N} = 175.2(3)^\circ$ ,  $\text{C}(12)\text{-N}\text{-C}(13) = 174.6(2)^\circ$ ) but the acetylide, previously coordinated as a perpendicular acetylene<sup>13</sup> to Ru(1) and Ru(2), is now best described in terms of parallel interactions with Ru(1) and Ru(2) and an  $\eta^2$  bond to Ru(3). The  $\text{C}(10)\text{-C}(11)$  bond length ( $1.415(3) \text{ \AA}$ ) is considerably longer than in the *tert*-butyl analogue of the parent hydride ( $1.315(3) \text{ \AA}$ ).<sup>14</sup> On the basis of spectroscopic data and subsequent chemical behavior (vide infra) the osmium cluster  $\text{Os}_3(\text{CO})_9(\text{C}\equiv\text{CPh})(\text{PPh}_2)(t\text{-BuNC})$  has a closely related structure but with a three-electron donor  $\text{PPh}_2$  group replacing a metal-metal bond and  $\mu$ -hydride in 1.

Although carbon-carbon bond formation by nucleophilic attack on a coordinated ligand is a well-established principle of organometallic chemistry,<sup>15</sup> the *direct* synthesis of C-C bonds on the face of a neutral cluster via coupling of a neutral carbon nucleophile with a multisite-bound ligand has few precedents.<sup>16</sup> Direct coupling of surface bound carbide and carbon monoxide has been documented as a possible mechanism for C-C bond formation in carbon monoxide hydrogenation<sup>17</sup> and CO attack on a mononuclear manganese carbene generating a metalocyclopropanone has been reported.<sup>18</sup> The closest analogies are

(12) The covalent radius of an sp-hybridized carbon atom is  $0.70 \text{ \AA}$ . Thus a single bond between two sp carbon atoms should have a bond length of  $\sim 1.40 \text{ \AA}$ . If C(11) (Figure 1) is considered as close to  $\text{sp}^2$ , then a predicted  $\text{C}(11)\text{-C}(12)$  single bond would have a length of  $\sim 1.44 \text{ \AA}$ . The measured distance is compatible with a strong single bond.

(13) For a recent account of perpendicular and parallel metal-acetylene interactions see: Hoffman, D. M.; Hoffman, R.; Fisel, C. R. *J. Am. Chem. Soc.* 1982, 104, 3858.

(14) Catti, M.; Gervasio, G.; Mason, S. A. *J. Chem. Soc., Dalton Trans.* 1977, 2260.

(15) See for example: Collman, J. P.; Hegedus, L. S. "Principles and Applications of Organotransition Metal Chemistry"; University Science Books: Mill Valley, CA, 1980. For a recent discussion of metal acetylide reactivity see: Kostic, W. M.; Fenske, R. F. *Organometallics* 1982, 1, 974.

(16) We have briefly reported activation of edge bridging acetylides in binuclear complexes to attack by carbenes and isocyanides: (a) Carty, A. J.; Taylor, N. J.; Smith, W. F.; Lappert, M. F.; Pye, P. L. *J. Chem. Soc., Chem. Commun.* 1978, 1017. (b) Carty, A. J.; Mott, G. N.; Taylor, N. J. *J. Organomet. Chem.* 1981, 212, C54.

(17) See, for example, ref 1, p 487.

(18) Herrmann, W. A.; Plank, J.; Ziegler, M. L.; Weidenhammer, K. *J. Am. Chem. Soc.* 1979, 101, 3134.

the formation of C-C bonds in reactions of the neutral iron carbide cluster  $\text{Fe}_4(\text{CO})_{13}\text{C}$  with CO,<sup>19</sup> the generation of acylium species  $[\text{Co}_3(\text{CO})_9\text{CCO}]^+$  from  $\text{Co}_3(\text{CO})_9\text{CCl}$  in the presence of a Lewis acid,<sup>20</sup> and the synthesis of the ketenylidene complex  $\text{H}_2\text{Os}_3(\text{CO})_9(\text{CCO})$  via thermal loss of CO from  $\text{Os}_3(\text{CO})_{10}(\mu\text{-CO})(\mu\text{-CH}_2)$ .<sup>21</sup> Some of these reactions may however involve *intramolecular* CO migrations.<sup>19,21</sup>

The isolation of clusters 1 and 2 suggested the possibility of further derivatizing the unsaturated fragment derived from the acetylide and isocyanide. Treatment of 2 (63 mg, 0.053 mmol) in toluene at  $0^\circ\text{C}$  with  $n\text{-BuNH}_2$  (5 mL) and removal of volatiles in vacuo followed by recrystallization from heptane-toluene(1:1) afforded  $\text{Os}_3(\text{CO})_9[\text{C}(\text{C}(\text{NH}-t\text{-Bu})(\text{NH}-n\text{-Bu})\text{CPh})\text{PPh}_2$  (3) in 98% yield.<sup>22</sup> Analogous  $\text{CH}_3\text{NH}_2$  and  $\text{EtNH}_2$  derivatives have been characterized. The structure of 3<sup>23</sup> (Figure 2) confirms that the amine has added across the "carbon-coordinated" isocyanide converting the isocyanide to a carbene with retention of the C(11)-C(12) bond in 2. The new hydrocarbyl ligand is coordinated to Os(1) and Os(3) via  $\sigma$  bonds to C(10) and C(11) and as in 2 via an  $\eta^2$  interaction with Os(2). Within the aminocarbene moiety the C(12)-N(1) ( $1.327(22) \text{ \AA}$ ) and C(12)-N(2) ( $1.321(22) \text{ \AA}$ ) distances indicate substantial C-N multiple bonding; C(12) has strictly planar stereochemistry. The  $\text{Os}_3$  cluster is an open triangle with the  $\text{Os}(1)\cdots\text{Os}(3)$  distance of  $3.850(1) \text{ \AA}$  being nonbonding, and as expected from the  $^{31}\text{P}$  shift (see also 2) the  $\text{Os}(1)\text{-P-Os}(3)$  angle of  $105.0(0)^\circ$  is large.

Careful IR and NMR monitoring of the reactions leading to 1 and 2 shows that attack by RNC on the acetylide has a very high regioselectivity. Indeed we have been unable to detect any products derived from attack at  $\text{C}_\beta$  of the acetylide. This regioselectivity and the facility of subsequent amination suggests that the exposed  $\alpha$ -carbon atom in these multisite-bound acetylides is exceptionally electrophilic. Such electrophilicity and hence regioselectivity to nucleophilic attack should be open to exploitation in organometallic and organic synthesis.

**Acknowledgment.** We are grateful to NSERC (A.J.C.) and NATO (A.J.C. and E.S.) for financial support of this work.

(19) Bradley, J. S.; Ansell, G. B.; Hill, E. W. *J. Am. Chem. Soc.* 1979, 101, 7417.

(20) Seyferth, D.; Williams, G. H.; Nivert, C. L. *Inorg. Chem.* 1977, 16, 758.

(21) Sievert, A. C.; Strickland, D. S.; Shapley, J. R.; Steinmetz, G. R.; Geoffroy, G. L. *Organometallics* 1982, 1, 214.

(22) 3:  $\text{Ir}(\text{C}_6\text{H}_5) \nu(\text{CO})$  2065 (m), 2039 (s), 2005 (m), 1994 (s), 1969 (m), 1957 (m), 1950 (m), 1924 (w),  $\nu(\text{NH})$  3419 (w), 3354 (w)  $\text{cm}^{-1}$ ;  $^1\text{H NMR}$  ( $\text{CD}_2\text{Cl}_2\text{-CHCl}_3$ )  $\delta$  0.9-1.55 (m,  $\text{CH}_2\text{CH}_2\text{CH}_3$ ), 1.35 (s,  $t\text{-Bu}$ ), 3.10, 3.30 (m,  $\text{CH}_2\text{N}$ ), 7.00-8.00 (m, Ph),  $^{31}\text{P NMR}$  ( $\text{CD}_2\text{Cl}_2\text{-CHCl}_3$ )  $\delta$ -72.5.

(23) Crystals of  $\text{Os}_3\text{PO}_9\text{NC}_{38}\text{H}_{35}$  are monoclinic of space group  $\text{P}2_1/n$  with  $a = 12.012(5) \text{ \AA}$ ,  $b = 15.260(6) \text{ \AA}$ ,  $c = 20.937(7) \text{ \AA}$ ,  $\beta = 91.18(3)^\circ$ ,  $V = 3837(3) \text{ \AA}^3$ ,  $Z = 4$ ,  $\rho(\text{calcd}) 2.187 \text{ g}\cdot\text{cm}^{-3}$ ,  $\rho(\text{measd}) 2.19 \text{ g}\cdot\text{cm}^{-3}$ ,  $F(000) = 2360$ , and  $\mu(\text{Mo K}\alpha) = 106.40 \text{ cm}^{-1}$ . A prismatic crystal was rounded to a sphere of diameter 0.11 mm for data collection. From a total of 4159 measured intensities collected out to  $2\theta = 42.0^\circ$  with graphite-monochromated Mo K $\alpha$  radiation ( $\lambda = 0.71069 \text{ \AA}$ ) and  $\theta$ - $2\theta$  scans on a Syntex  $\text{P}2_1$  automatic diffractometer, 2875 reflections having  $I \geq 3\sigma(I)$  were considered as observed and used in the structure solution and refinement. Standard reflections monitored throughout the course of data collection varied in intensity by only  $\pm 2\%$ . A spherical absorption correction  $^{11a}(\mu R = 0.59)$  was applied to the observed data. The osmium and phosphorus atoms were located in a Patterson map and light atoms in subsequent Fourier syntheses. Refinement proceeded with isotropic temperature parameters to  $R = 0.059$ . With anisotropic coefficients for osmium and phosphorus and isotropic coefficient for C, N, and O atoms the final  $R$  and  $R_w$  values were 0.040 and 0.046. Since the data crystal was of poorer quality than for the ruthenium complex and the diffraction data less precise, no effort was made to locate hydrogen atoms. A final difference map was however featureless, with maximum peak heights at the level of  $1.2 \text{ e } \text{ \AA}^{-3}$  in the vicinity of the osmium atoms.

**Registry No.** 1, 82647-62-9; 2, 82647-60-7; 3, 84081-57-2; ( $\mu$ -H) $\text{Ru}_3(\text{CO})_9(\mu_3\text{-}\eta^2\text{-C}\equiv\text{CPh})$ , 82647-61-8;  $\text{Os}_3(\text{CO})_9(\mu_3\text{-}\eta^2\text{-C}\equiv\text{CPh})(\text{PPh}_2)$ , 82640-93-5; *t*-BuNC, 7188-38-7; *n*-BuNH<sub>2</sub>, 109-73-9; Ru, 7440-18-8; Os, 7440-04-2.

**Supplementary Material Available:** Table I, atomic positions, Table II, anisotropic thermal parameters, Table III, bond lengths and angles for ( $\mu$ -H) $\text{Ru}_3(\text{CO})_9[\text{C}(\text{CN-}t\text{-Bu})\text{CPh}]$ , Table IV, atomic positions and thermal parameters, Table V, bond lengths and angles for  $\text{Os}_3(\text{CO})_9[\text{C}(\text{CN-}t\text{-Bu})(\text{NH-}n\text{-Bu})\text{-CPh}](\text{PPh}_2)$ , and listings of structure factor amplitudes for both compounds (44 pages). Ordering information is given on any masthead page.

## Amides of Rhodium and Iridium Stabilized as Hybrid Multidentate Ligands

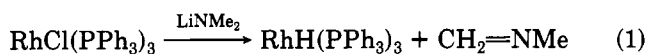
Michael D. Fryzuk\* and Patricia A. MacNeil

Department of Chemistry, University of British Columbia  
Vancouver, British Columbia, Canada V6T 1Y6

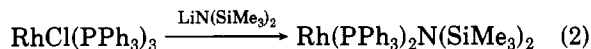
Received August 24, 1982

**Summary:** A variety of rhodium and iridium amido phosphine derivatives have been isolated and fully characterized. These complexes are exceptionally stable, a unique feature of group 8 transition-metal amides, owing to the incorporation of the amido function as a part of a "hybrid" ligand. The catalytic homogeneous hydrogenation activity of these rhodium and iridium species has also been investigated.

Although amides of the "hard" early transition metals are well-known, such complexes of the "soft" later metals are very rare. The paucity of amide derivatives of the group 8 metals may be ascribed to unfavorable hard/soft pair interactions as well as kinetic instability. Attempts to isolate rhodium alkylamides were unsuccessful,<sup>1</sup> owing to decomposition via  $\beta$  elimination of the metal-amide bond (eq 1). The incorporation of a ligand having no



$\beta$ -hydrogens resulted in the synthesis of the first rhodium amide<sup>2</sup> (eq 2). However, although this complex is stable



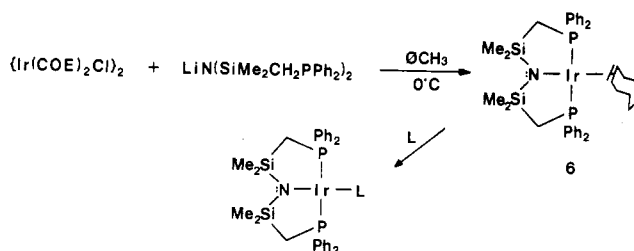
under inert atmospheres in the solid state, decomposition, with concomitant elimination of  $\text{HN}(\text{SiMe}_2)_2$ , occurs at 25 °C in benzene solution ( $t_{1/2} = 12$  h).

We have previously described<sup>3</sup> the use of the hybrid ligand strategy in the design of novel transition-metal amido phosphine complexes. The term "hybrid" refers to a ligand system that contains both "hard" and "soft" donors linked in a chelating manner. To date, we have used this approach to prepare amido phosphine derivatives of Ni(II), Pd(II), Pt(II),<sup>4,5</sup> Zr(IV), and Hf(IV),<sup>6,7</sup> illustrating the versatile coordinating ability of this ligand type.

We now wish to report the isolation and characterization

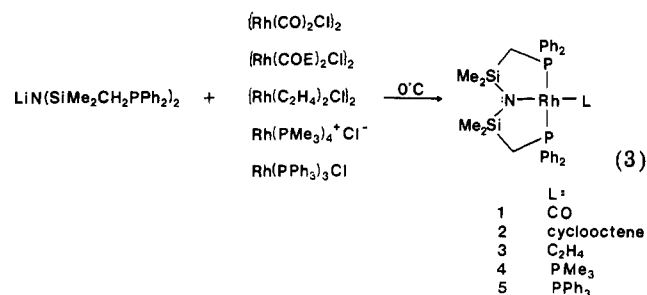
- (1) Diamond, S. E.; Mares, F. J. *Organomet. Chem.* 1977, 142, C55.  
 (2) Cetinkaya, B.; Lappert, M. F.; Torroni, S. J. *Chem. Soc., Chem. Commun.* 1979, 843.  
 (3) Fryzuk, M. D.; MacNeil, P. A. *J. Am. Chem. Soc.* 1981, 103, 3592.  
 (4) Fryzuk, M. D.; MacNeil, P. A. *Organometallics* 1982, 1, 918.  
 (5) Fryzuk, M. D.; MacNeil, P. A. *Organometallics* 1982, 1, 1540.  
 (6) Fryzuk, M. D.; Rettig, S. J.; Williams, H. D., submitted for publication in *Inorg. Chem.*  
 (7) Fryzuk, M. D.; Williams, H. D. *Organometallics* 1983, 2, 162.

### Scheme I



of a number of rhodium and iridium amides which not only may be readily prepared in high yields as crystalline solids but are thermally stable under inert atmosphere, both in the solid state and in solution. In addition, some of these complexes show unusual catalytic hydrogenation behavior with simple olefins under very mild reaction conditions.

Reaction of  $\text{LiN}(\text{SiMe}_2\text{CH}_2\text{PPh}_2)_2$  with a variety of rhodium precursors in cold toluene or ether solutions, followed by extraction with hexane, results in high yields of the rhodium(I) amido phosphines 1-5 (eq 3). All of these complexes are highly air- and moisture-sensitive crystalline solids; they are typically recrystallized from hexane at -30 °C to give analytically pure products in 70-80% yields.



In all of these complexes, the hybrid ligand is coordinated in a tridentate fashion, binding to the rhodium center through both phosphines and the amide nitrogen, resulting in a square-planar, 16-electron species. The exclusive trans disposition of the chelating phosphines was established by the presence of a virtual triplet<sup>8</sup> for the  $\text{CH}_2\text{P}$  protons at ~1.8 ppm in the <sup>1</sup>H NMR ( $J_{\text{app}} \approx 5$  Hz). Further support for this trans configuration was given by the chemical shift difference of 0.6-1.0 ppm between the ortho and para/meta protons of the *P*-phenyl substituents, when the spectrum is recorded in deuterated aromatic solvents.<sup>9</sup> Deuteriobenzene solutions of these complexes, sealed in NMR tubes under nitrogen, show no decomposition, even after several months at 25 °C.

The analogous iridium derivatives may be prepared in a similar manner or, more simply, via reaction of the iridium cyclooctene amide (6) with the desired neutral ligand at room temperature in toluene (Scheme I). In contrast to the previous preparation of the rhodium analogues, the solvent used in the synthesis of the iridium amides is crucial; when diethyl ether is employed, inseparable mixtures of products are formed whereas the use of toluene results in high yields of the pure complexes. Once again, the <sup>1</sup>H NMR spectra of these derivatives indicate that all are square-planar complexes with trans disposed phosphines. It should be noted that *only one* other iridium amide complex,  $\text{Ir}(\text{COD})\{\text{N}(\text{SiMe}_2)_2\}(\text{PEt}_3)$ , has been prepared to date.<sup>10</sup>

Rhodium and iridium amides have also been synthesized

- (8) Brookes, P. R.; Shaw, B. L. *J. Chem. Soc. A* 1967, 1079.  
 (9) Moore, D. S.; Robinson, S. D. *Inorg. Chim. Acta* 1981, 53, L171.

## Amides of rhodium and iridium stabilized as hybrid multidentate ligands

Michael D. Fryzuk, and Patricia A. MacNeil

*Organometallics*, 1983, 2 (2), 355-356 • DOI: 10.1021/om00074a030 • Publication Date (Web): 01 May 2002

Downloaded from <http://pubs.acs.org> on April 24, 2009

### More About This Article

---

The permalink <http://dx.doi.org/10.1021/om00074a030> provides access to:

- Links to articles and content related to this article
- Copyright permission to reproduce figures and/or text from this article



ACS Publications  
High quality. High impact.

**Registry No.** 1, 82647-62-9; 2, 82647-60-7; 3, 84081-57-2; ( $\mu$ -H) $\text{Ru}_3(\text{CO})_9(\mu_3\text{-}\eta^2\text{-C}\equiv\text{CPh})$ , 82647-61-8;  $\text{Os}_3(\text{CO})_9(\mu_3\text{-}\eta^2\text{-C}\equiv\text{CPh})(\text{PPh}_2)$ , 82640-93-5; *t*-BuNC, 7188-38-7; *n*-BuNH<sub>2</sub>, 109-73-9; Ru, 7440-18-8; Os, 7440-04-2.

**Supplementary Material Available:** Table I, atomic positions, Table II, anisotropic thermal parameters, Table III, bond lengths and angles for ( $\mu$ -H) $\text{Ru}_3(\text{CO})_9[\text{C}(\text{CN-}t\text{-Bu})\text{CPh}]$ , Table IV, atomic positions and thermal parameters, Table V, bond lengths and angles for  $\text{Os}_3(\text{CO})_9[\text{C}(\text{NH-}t\text{-Bu})(\text{NH-}n\text{-Bu})\text{-CPh}](\text{PPh}_2)$ , and listings of structure factor amplitudes for both compounds (44 pages). Ordering information is given on any masthead page.

## Amides of Rhodium and Iridium Stabilized as Hybrid Multidentate Ligands

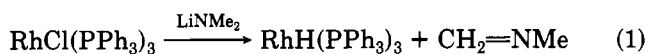
Michael D. Fryzuk\* and Patricia A. MacNeil

Department of Chemistry, University of British Columbia  
Vancouver, British Columbia, Canada V6T 1Y6

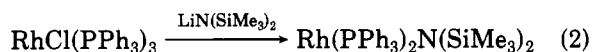
Received August 24, 1982

**Summary:** A variety of rhodium and iridium amido phosphine derivatives have been isolated and fully characterized. These complexes are exceptionally stable, a unique feature of group 8 transition-metal amides, owing to the incorporation of the amido function as a part of a "hybrid" ligand. The catalytic homogeneous hydrogenation activity of these rhodium and iridium species has also been investigated.

Although amides of the "hard" early transition metals are well-known, such complexes of the "soft" later metals are very rare. The paucity of amide derivatives of the group 8 metals may be ascribed to unfavorable hard/soft pair interactions as well as kinetic instability. Attempts to isolate rhodium alkylamides were unsuccessful,<sup>1</sup> owing to decomposition via  $\beta$  elimination of the metal-amide bond (eq 1). The incorporation of a ligand having no



$\beta$ -hydrogens resulted in the synthesis of the first rhodium amide<sup>2</sup> (eq 2). However, although this complex is stable



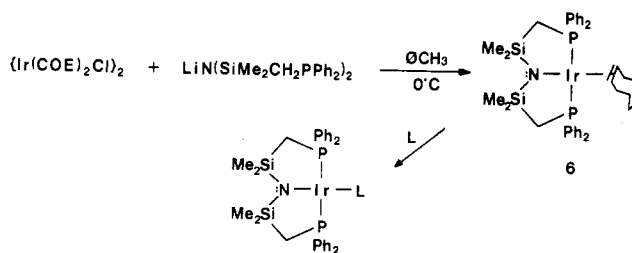
under inert atmospheres in the solid state, decomposition, with concomitant elimination of  $\text{HN}(\text{SiMe}_3)_2$ , occurs at 25 °C in benzene solution ( $t_{1/2} = 12$  h).

We have previously described<sup>3</sup> the use of the hybrid ligand strategy in the design of novel transition-metal amido phosphine complexes. The term "hybrid" refers to a ligand system that contains both "hard" and "soft" donors linked in a chelating manner. To date, we have used this approach to prepare amido phosphine derivatives of Ni(II), Pd(II), Pt(II),<sup>4,5</sup> Zr(IV), and Hf(IV),<sup>6,7</sup> illustrating the versatile coordinating ability of this ligand type.

We now wish to report the isolation and characterization

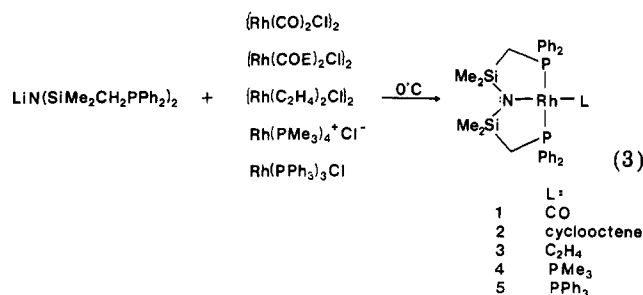
- (1) Diamond, S. E.; Mares, F. *J. Organomet. Chem.* 1977, 142, C55.  
(2) Cetinkaya, B.; Lappert, M. F.; Torroni, S. *J. Chem. Soc., Chem. Commun.* 1979, 843.  
(3) Fryzuk, M. D.; MacNeil, P. A. *J. Am. Chem. Soc.* 1981, 103, 3592.  
(4) Fryzuk, M. D.; MacNeil, P. A. *Organometallics* 1982, 1, 918.  
(5) Fryzuk, M. D.; MacNeil, P. A. *Organometallics* 1982, 1, 1540.  
(6) Fryzuk, M. D.; Rettig, S. J.; Williams, H. D., submitted for publication in *Inorg. Chem.*  
(7) Fryzuk, M. D.; Williams, H. D. *Organometallics* 1983, 2, 162.

## Scheme I



of a number of rhodium and iridium amides which not only may be readily prepared in high yields as crystalline solids but are thermally stable under inert atmosphere, both in the solid state and in solution. In addition, some of these complexes show unusual catalytic hydrogenation behavior with simple olefins under very mild reaction conditions.

Reaction of  $\text{LiN}(\text{SiMe}_2\text{CH}_2\text{PPh}_2)_2$ <sup>4</sup> with a variety of rhodium precursors in cold toluene or ether solutions, followed by extraction with hexane, results in high yields of the rhodium(I) amido phosphines 1-5 (eq 3). All of these complexes are highly air- and moisture-sensitive crystalline solids; they are typically recrystallized from hexane at -30 °C to give analytically pure products in 70-80% yields.



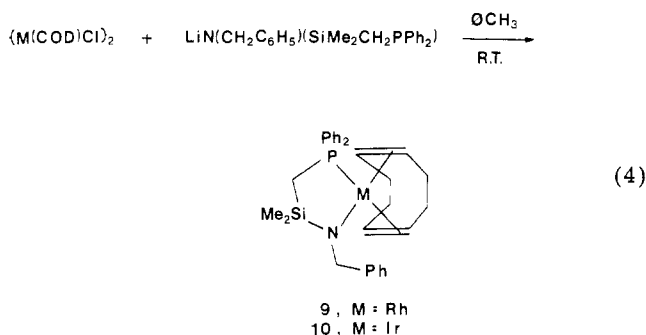
In all of these complexes, the hybrid ligand is coordinated in a tridentate fashion, binding to the rhodium center through both phosphines and the amide nitrogen, resulting in a square-planar, 16-electron species. The exclusive trans disposition of the chelating phosphines was established by the presence of a virtual triplet<sup>8</sup> for the  $\text{CH}_2\text{P}$  protons at ~1.8 ppm in the <sup>1</sup>H NMR ( $J_{\text{app}} \approx 5$  Hz). Further support for this trans configuration was given by the chemical shift difference of 0.6-1.0 ppm between the ortho and para/meta protons of the *P*-phenyl substituents, when the spectrum is recorded in deuterated aromatic solvents.<sup>9</sup> Deuteriobenzene solutions of these complexes, sealed in NMR tubes under nitrogen, show no decomposition, even after several months at 25 °C.

The analogous iridium derivatives may be prepared in a similar manner or, more simply, via reaction of the iridium cyclooctene amide (6) with the desired neutral ligand at room temperature in toluene (Scheme I). In contrast to the previous preparation of the rhodium analogues, the solvent used in the synthesis of the iridium amides is crucial; when diethyl ether is employed, inseparable mixtures of products are formed whereas the use of toluene results in high yields of the pure complexes. Once again, the <sup>1</sup>H NMR spectra of these derivatives indicate that all are square-planar complexes with trans disposed phosphines. It should be noted that *only one* other iridium amide complex,  $\text{Ir}(\text{COD})\{\text{N}(\text{SiMe}_3)_2\}(\text{PEt}_3)$ , has been prepared to date.<sup>10</sup>

Rhodium and iridium amides have also been synthesized

- (8) Brookes, P. R.; Shaw, B. L. *J. Chem. Soc. A* 1967, 1079.  
(9) Moore, D. S.; Robinson, S. D. *Inorg. Chim. Acta* 1981, 53, L171.

incorporating *bidentate* hybrid ligands. The preparation of the cyclooctadiene derivatives **9** and **10** is very straightforward (eq 4); carried out at room temperature,



the products are obtained in virtually quantitative yields as analytically pure crystals. Although exceptionally air and moisture sensitive, these complexes, either as solids or in solution, undergo no decomposition (via  $\beta$  elimination) under inert atmospheres.

As anticipated, some of these 16-electron Rh(I) and Ir(I) species are catalyst precursors for the homogeneous hydrogenation of simple olefins. For both the  $[\text{Rh}(\text{COE})\text{N}(\text{SiMe}_2\text{CH}_2\text{PPh}_2)_2]$  (COE  $\equiv$  cyclooctene) and  $[\text{Rh}(\text{PPh}_3)\text{N}(\text{SiMe}_2\text{CH}_2\text{PPh}_2)_2]$  systems, 1-hexene is efficiently hydrogenated to hexane under one atmosphere of hydrogen at 22 °C. Typical runs<sup>11</sup> were carried out in neat olefin, employing a substrate to catalyst ratio of approximately 1000:1. The hydrogenations were monitored by GLC<sup>12</sup> and indicate a rather unusual feature of these rhodium amido phosphines, that is, their surprisingly high isomerization activity. Assuming that hydrogenation proceeds through a dihydride intermediate (either via the well-established "hydride route" or "unsaturate route"<sup>13</sup>), only straightforward reduction of olefinic substrates would be expected, since most rhodium phosphine dihydride species show very little, if any, tendency toward olefin isomerization.<sup>14</sup> However, when either  $[\text{Rh}(\text{COE})\text{N}(\text{SiMe}_2\text{CH}_2\text{PPh}_2)_2]$  or  $[\text{Rh}(\text{PPh}_3)\text{N}(\text{SiMe}_2\text{CH}_2\text{PPh}_2)_2]$  is employed as catalyst precursor, the turnover number<sup>15</sup> for isomerization of 1-

hexene to *cis/trans*-2-hexene ( $\sim 70/\text{h}$ ) is higher than for hydrogenation to hexane ( $\sim 50/\text{h}$ ). Similar behavior obtains for the rhodium and iridium bidentate amido phosphines; with  $[\text{Ir}(\text{COD})\{(\text{CH}_2\text{C}_6\text{H}_5)(\text{SiMe}_2\text{CH}_2\text{PPh}_2)\}]$  the turnover number for hydrogenation is approximately 120/h as compared to  $\sim 40/\text{h}$  for isomerization (the Rh analogue is about 4 times slower).

Since *no* isomerization is observed in the absence of hydrogen, this process is clearly not occurring via oxidative addition of the olefin to form an allyl hydride intermediate (which can then reductively eliminate to produce internal olefins). Presumably then, for these systems,  $\beta$  elimination of the coordinated alkyl intermediate to form internal olefins is a competing process with reductive elimination of the saturated alkane. The anomalous reactivity of these rhodium catalysts is further demonstrated by the observation that internal olefins such as 2-hexene are hydrogenated as rapidly as terminal ones; this is in contrast to the pronounced preference of terminal vs. internal olefins exhibited by classical Wilkinson-type hydrogenation systems.<sup>16</sup>

To complicate matters further, the  $[\text{Ir}(\text{COE})\{N(\text{SiMe}_2\text{CH}_2\text{PPh}_2)_2\}]$  derivative shows no evidence of isomerization and only straightforward reduction of olefins to alkanes under identical hydrogenation conditions; the turnover number, using 1-hexene as substrate, is comparable to that of its rhodium congener ( $\sim 70/\text{h}$ ).

Although the origins of the unique catalytic activity of these rhodium and iridium hybrid ligand complexes are not fully understood, it is possible that it is a function of the ligand stereochemistry. It has been shown<sup>17</sup> that a facial coordination of the tridentate ligand is possible; therefore, it is conceivable that the rhodium complexes require a *fac*  $\leftrightarrow$  *mer* isomerism during the catalytic cycle which slows the reductive elimination step so that reversible  $\beta$  elimination can occur. Another possibility is that the dihydride intermediate undergoes reductive elimination of the metal-amide bond to form a *monohydride amino* phosphine species which then acts as the active catalyst. The olefin isomerization ability of rhodium monohydride complexes has been well documented.<sup>16</sup> We are at present further investigating these systems in order to gain more mechanistic information.

**Acknowledgment.** Financial support for this research was generously provided by the Department of Chemistry and the Natural Sciences and Engineering Research Council of Canada. We also thank Johnson Matthey for the loan of  $\text{RhCl}_3$  and  $\text{IrCl}_3$ . P.A.M. wishes to thank the Walter C. Sumner Memorial Foundation for a graduate scholarship.

**Registry No.** 1, 84074-25-9; 2, 84074-26-0; 3, 84074-27-1; 4, 84074-28-2; 5, 84074-29-3; 6, 84074-30-6; 7, 84074-31-7; 8, 84074-32-8; 9, 84074-33-9; 10, 84074-34-0.

**Supplementary Material Available:** Spectral data ( $^1\text{H}$  NMR,  $^{31}\text{P}$  NMR, IR), analytical data for compounds 1–10, and hydrogenation profile graphs (8 pages). Ordering information is given on any current masthead page.

(10) Kermode, N. J.; Lappert, M. F.; Samways, B. J., presented in part at the International Conference on the Chemistry of the Platinum Group Metals, Bristol, England, July 1981.

(11) (a) A typical run was carried out in a 250-mL heavy-walled flask, fitted with a Kontes 9-mm needle-valve inlet, attached directly to a vacuum line that had access to vacuum and purified hydrogen (passed through  $\text{MnO}$  on vermiculite and activated 4-Å molecular sieves<sup>11b</sup>). Reaction temperature was maintained at 22 °C through the use of a glass water-jacket attached to a Haake temperature-controlling unit. The substrates (1-hexene and *cis/trans*-2-hexene) were purchased from Aldrich (Gold Label) and dried over activated 4-Å molecular sieves, vacuum transferred, and freeze-pump-thawed several times. Any trace peroxides were removed by passing the dried olefins through a short column of activated alumina (Fisher 80–200 mesh). Samples were withdrawn via syringe and vacuum transferred away from the catalyst prior to GLC analysis. (b) Bafus, D. A.; Brown, T. L.; Dickerhoff, D. W.; Morgan, G. L. *Rev. Sci. Instrum.* **1962**, *33*, 491.

(12) Column specifications: 60/80 Chromosorb P(AW)/20% tri-*o*-cresyl phosphate, 20 ft  $\times$  1/8 in. SS; column temperature, 40 °C; sample size, 0.5  $\mu\text{L}$ ; detector, FID.

(13) Collman, J. P.; Hegedus, L. S. "Principles and Applications of Organotransition Metal Chemistry"; University Science: Mill Valley, CA, 1980; Chapter 6.

(14) Osborn, J. A.; Schrock, R. R. *J. Am. Chem. Soc.* **1976**, *98*, 2134.

(15) Turnover numbers given are those values averaged over a number ( $>5$ ) of experimental runs and were calculated by using the expression: Turnover number = (mol substrate converted/mol catalyst)/unit time.

(16) James, B. R. In "Comprehensive Organometallic Chemistry"; Wilkinson, G., Ed.; Pergamon Press: New York, 1982; Vol. 5, Chapter 51.

(17) Fryzuk, M. D.; MacNeil, P. A. *Organometallics*, in press.